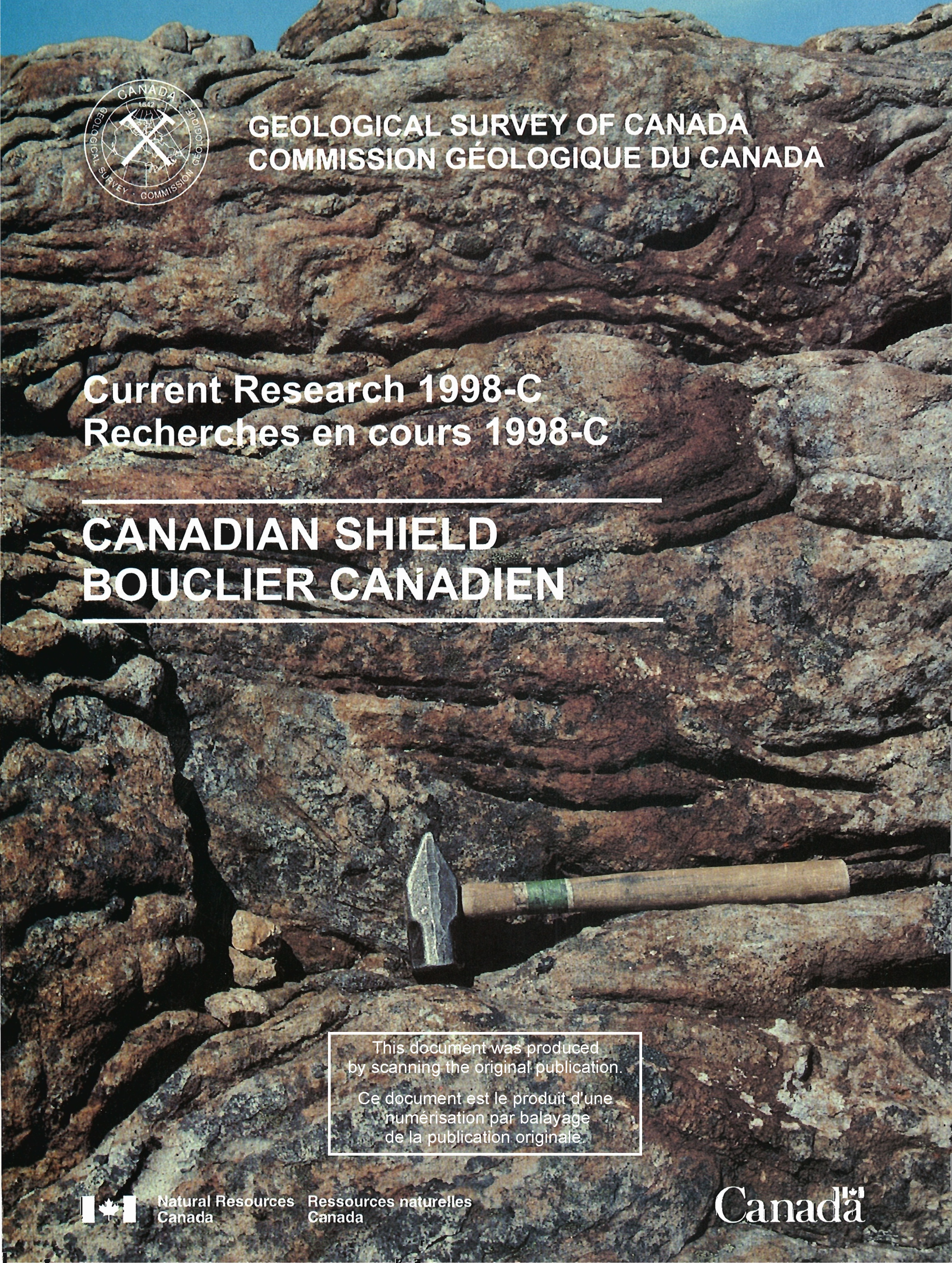

GEOLOGICAL SURVEY OF CANADA
COMMISSION GÉOLOGIQUE DU CANADA

Current Research 1998-C
Recherches en cours 1998-C

CANADIAN SHIELD
BOUCLIER CANADIEN

Natural Resources Canada | Ressources naturelles Canada

Canada

NOTICE TO LIBRARIANS AND INDEXERS

The Geological Survey's Current Research series contains many reports comparable in scope and subject matter to those appearing in scientific journals and other serials. Most contributions to Current Research include an abstract and bibliographic citation. It is hoped that these will assist you in cataloguing and indexing these reports and that this will result in a still wider dissemination of the results of the Geological Survey's research activities.

AVIS AUX BIBLIOTHÉCAIRES ET PRÉPARATEURS D'INDEX

La série Recherches en cours de la Commission géologique contient plusieurs rapports dont la portée et la nature sont comparables à ceux qui paraissent dans les revues scientifiques et autres périodiques. La plupart des articles publiés dans Recherches en cours sont accompagnés d'un résumé et d'une bibliographie, ce qui vous permettra, on l'espère, de cataloguer et d'indexer ces rapports, d'où une meilleure diffusion des résultats de recherche de la Commission géologique.

GEOLOGICAL SURVEY OF CANADA
COMMISSION GÉOLOGIQUE DU CANADA

CURRENT RESEARCH 1998-C

CANADIAN SHIELD

RECHERCHES EN COURS 1998-C

BOUCLIER CANADIEN

1998

Catalogue No. M44-1998/3E
ISBN 0-660-17300-X

Available in Canada from
Geological Survey of Canada offices:

601 Booth Street
Ottawa, Ontario K1A 0E8

3303-33rd Street N.W.
Calgary, Alberta T2L 2A7

101-605 Robson Street
Vancouver, B.C. V6B 5J3

or from

Canadian Government Publishing
Public Works and Government Services Canada
Ottawa, Ontario K1A 0S9

A deposit copy of this publication is also available for reference in selected public libraries across Canada

Price subject to change without notice

Cover illustration

D_3 (orogen-parallel) southwest-verging folds of sillimanite-biotite±garnet psammite (Lake Harbour Group), south Baffin Island, Northwest Territories. See paper by St-Onge et al., this volume. Photograph by M. St-Onge. GSC 1997-84

Photo en page couverture

Plis de déformation D_3 (parallèle à l'orogène) à vergence sud-ouest dans des psammites à sillimanite-biotite±grenat (Groupe de Harbour Lake), sud de l'île de Baffin, Territoires du Nord-Ouest. Cette photographie se rapporte à l'article de St-Onge et al. dans le présent volume. Photo : M. St-Onge, GSC 1997-84

Separates

A limited number of separates of the papers that appear in this volume are available by direct request to the individual authors. The addresses of the Geological Survey of Canada offices follow:

Geological Survey of Canada
601 Booth Street
Ottawa, Ontario
K1A 0E8
(FAX: 613-996-9990)

Geological Survey of Canada (Calgary)
3303-33rd Street N.W.
Calgary, Alberta
T2L 2A7
(FAX: 403-292-5377)

Geological Survey of Canada (Pacific)
101-605 Robson Street
Vancouver, British Columbia
V6B 5J3
(FAX: 604-666-1124)

Geological Survey of Canada (Pacific)
P.O. Box 6000
9860 Saanich Road
Sidney, British Columbia
V8L 4B2
(FAX: 604-363-6565)

Geological Survey of Canada (Atlantic)
Bedford Institute of Oceanography
P.O. Box 1006
Dartmouth, Nova Scotia
B2Y 4A2
(FAX: 902-426-2256)

Quebec Geoscience Centre/INRS
2535, boulevard Laurier
C.P. 7500
Sainte-Foy (Québec)
G1V 4C7
(FAX: 418-654-2615)

Tirés à part

On peut obtenir un nombre limité de «tirés à part» des articles qui paraissent dans cette publication en s'adressant directement à chaque auteur. Les adresses des différents bureaux de la Commission géologique du Canada sont les suivantes :

Commission géologique du Canada
601, rue Booth
Ottawa (Ontario)
K1A 0E8
(facsimilé : 613-996-9990)

Commission géologique du Canada (Calgary)
3303-33rd Street N.W.,
Calgary, Alberta
T2L 2A7
(facsimilé : 403-292-5377)

Commission géologique du Canada (Pacifique)
101-605 Robson Street
Vancouver, British Columbia
V6B 5J3
(facsimilé : 604-666-1124)

Commission géologique du Canada (Pacifique)
P.O. Box 6000
9860 Saanich Road
Sidney, British Columbia
V8L 4B2
(facsimilé : 604-363-6565)

Commission géologique du Canada (Atlantique)
Institut océanographique Bedford
P.O. Box 1006
Dartmouth, Nova Scotia
B2Y 4A2
(facsimilé : 902-426-2256)

Centre géoscientifique de Québec/INRS
2535, boulevard Laurier
C.P. 7500
Sainte-Foy (Québec)
G1V 4C7
(facsimilé : 418-654-2615)

CONTENTS

Detailed gravity profiles across the Sleepy Dragon Complex and adjacent parts of the Yellowknife Domain, Slave structural province, Northwest Territories: preliminary data
W. Bleeker, R.V. Cooper, M.E. Berrigan, W.R. Roest, and K.A.B. Hendry 1

Central Slave Basement Complex, Northwest Territories: its autochthonous cover, décollement, and structural topology
W. Bleeker and J. Ketchum 9

Surficial geology and implications for drift prospecting, Hope Bay volcanic belt area, Northwest Territories
D.E. Kerr and R.D. Knight 21

An update on the metallogeny of the Woodburn Lake Group, western Churchill Province, Northwest Territories
J.A. Kerswill, S.P. Goff, L. Wilkinson, G.A. Jenner, B.A. Kjarsgaard, R. Bretzlaff, and C. Samaras 29

Geology of the McKellar Bay-Wight Inlet- Frobisher Bay area, southern Baffin Island, Northwest Territories
M.R. St-Onge, D.J. Scott, N. Wodicka, and S.B. Lucas 43

Progress report: Precambrian geology, Angikuni Lake area, District of Keewatin, Northwest Territories
L.B. Aspler, J.R. Chiarenzelli, K.B. Powis, and B.L. Cousens 55

New insights into the geology of the Yathkyed Lake greenstone belt, western Churchill Province, Northwest Territories
C. Relf, D. Irwin, K. MacLachlan, and A. Mills 67

Field contributions to thematic studies related to the Kaminak greenstone belt, Kivalliq Region, Northwest Territories
S. Hanmer, R.H. Rainbird, H.A. Sandeman, T.D. Peterson, and J.J. Ryan 77

Geology of the Kaminak greenstone belt from Padlei to Quartzite Lake, Kivalliq Region, Northwest Territories
S. Hanmer, T.D. Peterson, H.A. Sandeman, R.H. Rainbird, and J.J. Ryan 85

Preliminary report on the geology and tectonic history of the Trans-Hudson Orogen in the northwestern Reindeer Zone, Saskatchewan
D. Corrigan, R.O. Maxeiner, A. Bashforth, and S.B. Lucas 95

Some notes on the assemblage boundaries and internal structure of the Uchi-Confederation greenstone belt, northwestern Ontario
C.R. van Staal 107

Tectonostratigraphy of central Sturgeon Lake, Ontario: deposition and deformation of submarine tholeiites and emergent calc-alkaline volcano-sedimentary sequences
M. Sanborn-Barrie, T. Skulski, and J.B. Whalen 115

Structural transect of the central Wabigoon subprovince between the Sturgeon Lake and Obonga Lake greenstone belts, Ontario
J.A. Percival 127

New observations on the French River alkaline syenite complex, Bigwood township, Ontario
K.L. Currie 137

Questions of correlation across the Grenville Front east of Sudbury, Ontario
A. Davidson 145

Sedimentology of the Oak Ridges Moraine, Humber River watershed, southern Ontario: a preliminary report
H.A.J. Russell, D.R. Sharpe, and R.W.C. Arnott 155

Data on the origin of the Kipawa syenite complex, northwestern Quebec
K.L. Currie 167

A note on the Obedjiwan nepheline syenite, central Quebec
K.L. Currie and J. Gittins 173

Geochemistry and petrogenesis of the Lapeyrère gabbronorite, south-central Grenville Province, Quebec
L. Nadeau, P. Brouillette, and J. Bédard 179

Author Index. 189

Detailed gravity profiles across the Sleepy Dragon Complex and adjacent parts of the Yellowknife Domain, Slave structural province, Northwest Territories: preliminary data

Wouter Bleeker, Roy V. Cooper[1], Mike E. Berrigan[1], Walter R. Roest, and Karen A.B. Hendry

Continental Geoscience Division, Ottawa

Bleeker, W., Cooper, R.V., Berrigan, M.E., Roest, W.R., and Hendry, K.A.B., 1998: Detailed gravity profiles across the Sleepy Dragon Complex and adjacent parts of the Yellowknife Domain, Slave structural province, Northwest Territories: preliminary data; in Current Research 1998-C; Geological Survey of Canada, p. 1-8.

Abstract: A detailed gravity survey was performed east of Yellowknife, across the Sleepy Dragon basement complex, its flanking greenstone belts and adjacent parts of the Yellowknife Domain. A total of 152 stations were recorded along three profiles that link up with Lithoprobe's high-resolution SNORCLE transect along the Ingraham Trail. Major gravity anomalies were recorded over the greenstone belts and over a variety of granitoid plutons that will help in constraining the deep structure of the area. In general, the gravity profiles show excellent correlation with the known geology. This short report presents general background information on the survey as well as the preliminary data.

Résumé : Un levé gravimétrique détaillé a été réalisé à l'est de Yellowknife, à travers le complexe de Sleepy Dragon, ses ceintures de roches vertes bordières et les parties adjacentes du Domaine de Yellowknife. Les données enregistrées proviennent de 152 stations situées le long de trois profils reliés au transect à haute résolution SNORCLE du projet Lithoprobe le long de la route Ingraham Trail. D'importantes anomalies gravimétriques ont été observées au-dessus des ceintures de roches vertes et de divers plutons granitoïdes, lesquelles aideront à déterminer la structure profonde de la région. En général, les profils gravimétriques sont en étroite corrélation avec la géologie connue. Ce bref rapport présente en outre des informations générales sur le levé ainsi que les données préliminaires.

[1] Geomatics Canada, Geodetic Survey Division, 615 Booth Street, Ottawa, Ontario K1A 0E9

INTRODUCTION

The Yellowknife Domain of the Archean Slave structural province is a typical Neoarchean granite-greenstone terrain that is among the most intensely studied and best documented examples of such terrains in the world (e.g. Henderson, 1985; Kusky, 1990; Lambert et al., 1992; Bleeker, 1996; Isachsen and Bowring, 1997). In addition to a variety of on-going structural, stratigraphic, isotopic, and general mapping studies, recent geophysical surveys have advanced our knowledge of the deep crust and lithosphere. These surveys, involving seismic reflection profiles extending from east of Yellowknife to the Pacific coast, deep probing magnetotelluric studies, and detailed gravity measurements (1 km spacing), are part of Lithoprobe's SNORCLE transect (e.g. Cook and Erdmer, 1997). Many of these studies are still in progress or in early stage of analysis.

To the east of Yellowknife, road-based geophysical surveys under the auspices of Lithoprobe's SNORCLE project were extended to the end of the Ingraham Trail, an all-weather road that extends about 50 km into the supracrustal domain east of Yellowknife (Fig. 1). Additional acquisition, extending along the winter road into the central portion of the Slave Province, may be carried out in a later phase of the SNORCLE programme, if technical and budgetary constraints allow such a follow up. In either case, some of the most critical and geologically best studied parts of the area, the Sleepy Dragon Complex and its flanking greenstone belts (Fig. 1), lie to the east of the present seismic reflection coverage and to the east of the potential winter road transect. It was thus decided, in conjunction with regional structural-stratigraphic studies (e.g. Bleeker, 1996), to acquire additional gravity profiles across the Sleepy Dragon Complex and adjacent parts of the Yellowknife Domain to help constrain the deeper structure of the area. Gravity measurements were made along three intersecting regional profiles that link up with the previously acquired Lithoprobe seismic reflection and gravity profiles along the Ingraham Trail. The new data extend SNORCLE's "reach" to east and south of the Sleepy Dragon Complex.

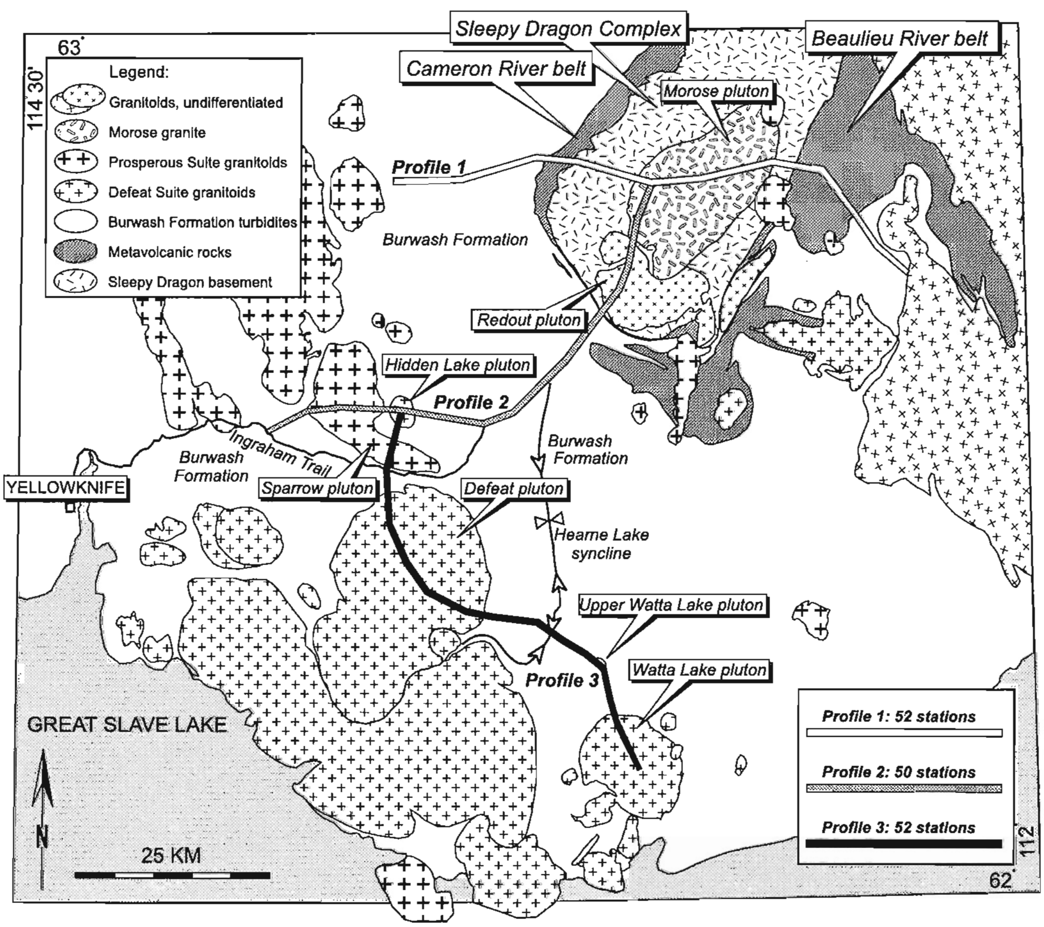

Figure 1. Simplified location and geological map of the southern Yellowknife Domain. The three gravity profiles are marked. Note also the Ingraham Trail along which 1-km-spaced gravity readings were recorded previously under the auspices of Lithoprobe's SNORCLE project.

METHODS

A total of 152 gravity stations were recorded over a 3-day period using a LaCoste and Romberg gravimeter (Fig. 2a) and a differential GPS continuous data logging system (Allan Osborne Associates Turbo Rogue SNR 8000) for post-processing of positions. Access was by means of a Hughes 500D helicopter (Fig. 2b), which allowed landings in relatively restricted clearings in the otherwise tree-covered terrain. The differential GPS logging system, with a base station at the Canadian seismic control station in Yellowknife, allows for spatial control better than 1.0 m. Final uncertainty in elevations is conservatively estimated at approximately $\pm$1.0 m, which translates into $\pm$0.3 mGal uncertainty in the final gravity data. Independent checks of the elevation data were provided by readings of two barometric altimeters (AIR Model HB-1A) that were recorded at each station, as well as twice daily at the base station.

The 152 stations were spaced at an average distance of 1-2 km along the profiles with first-order geological contacts generally covered by stations spaced at $\leq$1 km. The three profiles (Fig. 1) were strategically chosen to cover the Sleepy Dragon Complex basement complex, its flanking steeply dipping greenstone belts (e.g. the Cameron River and Beaulieu River greenstone belts), and various granitoid plutons, as well as the regional background gravity field over metasedimentary rocks of the Burwash Formation (Henderson, 1985). The three profiles intersect and connect with detailed gravity readings along the road, potentially allowing 3D modelling of the deep structure. Where possible, the profiles were acquired perpendicular to or at a high angle to the first-order geological structures.

To allow detailed gravity modelling, samples were collected along the profiles for density determinations of the major rock units. The same samples will also provide the basis for other rock properties studies such as acoustic velocities and heat generation data (U, Th, K), as well as for geochemical studies (e.g. Nd isotopes).

PREVIOUS GRAVITY STUDIES

Existing gravity data for the area (National Gravity Database, Fig. 3) comprise widely spaced (5-10 km) regional data acquired in the 1960s. A more detailed survey was performed over the southern extent of the Yellowknife greenstone belt and formed the basis of the first detailed gravity models for the area (Gibb and Thomas, 1980). McGrath et al. (1983) presented a gravity model for a profile across the Yellowknife greenstone belt, suggesting a very limited depth extent (2-3 km) for the volcanic rocks. However, neither of these studies were constrained by detailed geological sections, whereas both used the simplifying assumption of a uniform, regional granodiorite unit (2.64 g/cm^3) at depth.

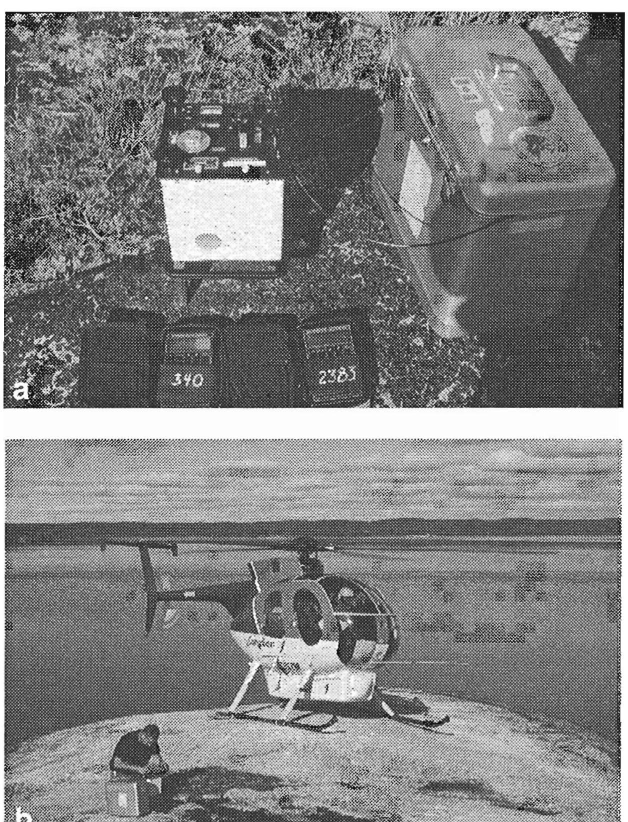

Figure 2.

a) *LaCoste and Romberg gravimeter at a measurement station with two altimeters visible in the foreground.* ***b)*** *Access along the profile was by means of a Hughes 500D helicopter. One person performed the gravity readings, a second person operated/checked the GPS data logger, while a third person performed detailed navigation to optimize the stations along the profiles and relative to geological structures. On average, gravity readings required about 5-8 minutes per station, with about 5 minutes travel between stations.*

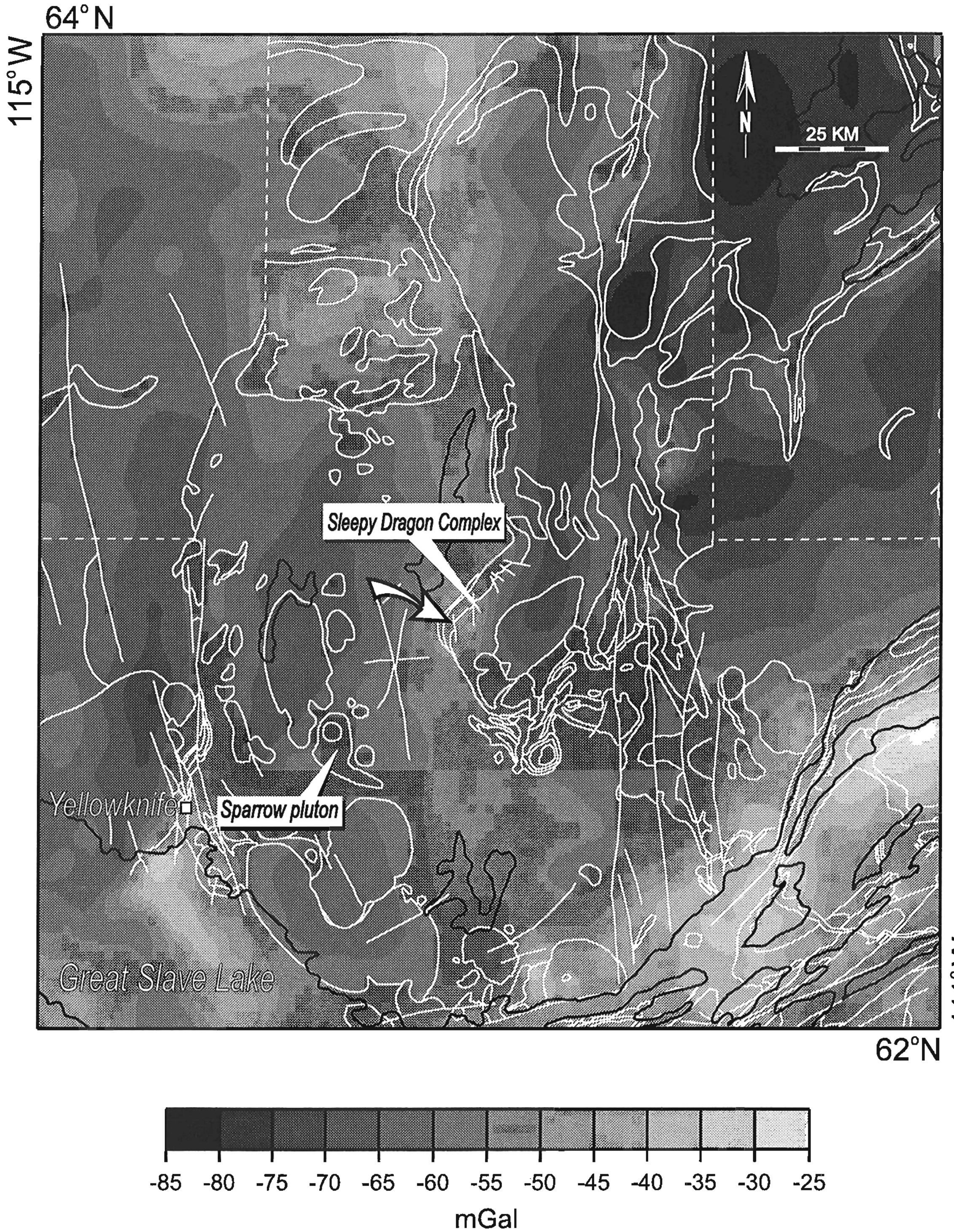

Figure 3. *Regional Bouguer gravity field (National Gravity Database). The Sleepy Dragon Complex and the Sparrow pluton are indicated for reference. Note also the gravity maximum (arrow) situated over the Cameron River basalts at the western fold closure (see Bleeker, 1996) of the Sleepy Dragon Complex. Geological contacts from Hoffman and Hall (1993).*

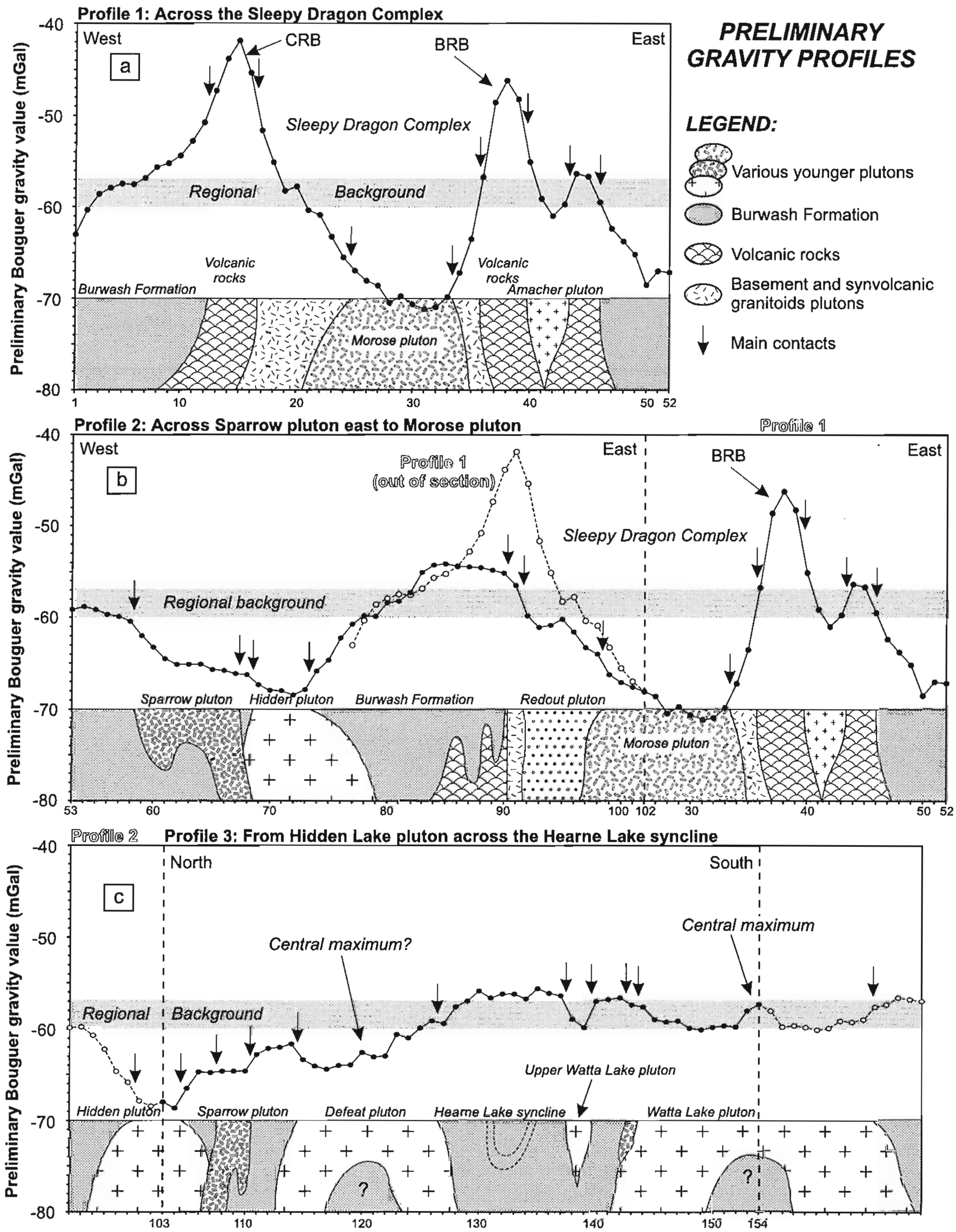

Figure 4. Preliminary gravity data for the three profiles, shown at a uniform arbitrary spacing. Preliminary free air and Bouguer corrections have been applied. Major geological contacts and structures are shown schematically below each profile. Neither scale nor modelling are implied. ***a)*** *Profile 1 from west to east across the Sleepy Dragon Complex. Abrreviations: CRB and BRB for Cameron River and Beaulieu River greenstone belts, respectively.* ***b)*** *Profile 2 from west of the Sparrow pluton to the core of the Sleepy Dragon Complex. Data of profile 1 are shown as well.* ***c)*** *Profile 3 from the core of the Hidden Lake pluton to the core of the Watta Lake pluton across the Defeat pluton and the Hearne Lake syncline. Profile 3 has been extended with parts of profile 2 (from the core of the Hidden Lake pluton to the end of the road) and by assuming radial symmetry of the data across the circular Watta Lake pluton. An approximate regional background of -57 to -60 mGal is estimated from the western shoulder of the Cameron River belt anomaly in profile 1.*

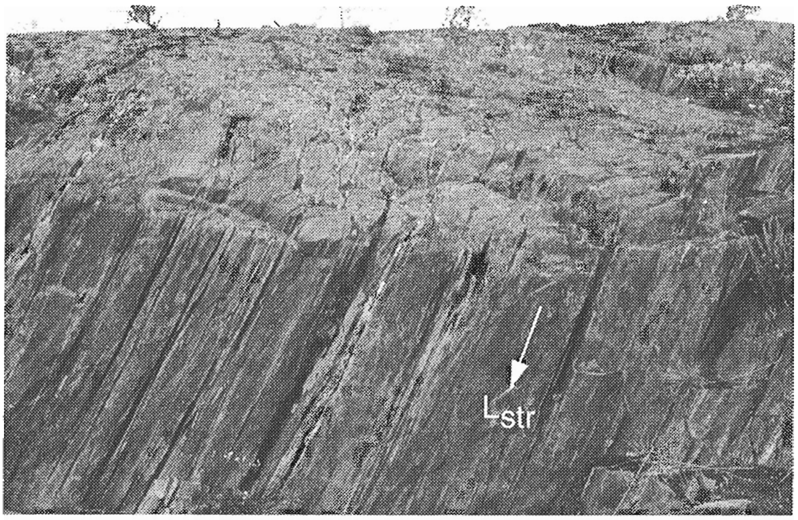

Figure 5.

Highly deformed pillow basalts of the Cameron River greenstone belt with strong down-dip stretching lineations (L_{str}). Note the extreme aspect ratios of the pillows, which are nearly parallel-sided in the sectional view (looking towards the north). Given that the greenstone belts are several kilometres wide at the surface, the typical mesoscopic structures shown here would suggest that the greenstones should project down to a depth of several times the surface widths of the belts.

GRAVITY PROFILES

Three regional profiles were acquired, each with about 50 gravity measurements spread out over a profile length of about 70 km (Fig. 1, 4).

Profile 1 (Fig. 1, 4a) extends from west to east across the Sleepy Dragon Complex basement-cored antiform and its flanking greenstone belts. It includes more detailed measurements across a previously recorded regional gravity high centred on the mafic volcanic rocks of the Cameron River belt west of Patterson Lake (see arrow in Fig. 3). The major question addressed by this profile is the depth extent of the steeply dipping Cameron River basalt package, which at surface is characterized by strong down-dip stretching lineations of pillows, amygdules, and other strain markers (Fig. 5). This profile also addresses the general correlation of low Bouguer values with older basement rocks (Fig. 6a) and it may help constrain the 3D geometry of the Morose Lake K-feldspar megacrystic granite pluton (Fig. 6b) in the core of the basement antiform. Towards its eastern end, the profile crosses the Beaulieu River volcanic belt and the Amacher Lake synvolcanic quartz porphyry intrusion.

Profile 2 (Fig. 1, 4b) extends from near the centre of the Morose Lake pluton, across the Redout biotite granite pluton (Fig. 6c) and the basement/cover contact on the southwestern flank of the Sleepy Dragon Complex, into Burwash Formation metaturbidites towards the end of the Ingraham Trail. From the end of the road, the profile extends further west across the Hidden Lake biotite granodiorite pluton and the two-mica granite of the Sparrow pluton (Fig. 6d), before reconnecting with the road. Along the profile, the Burwash Formation varies from well-preserved, lower greenschist facies metaturbidites to cordierite±andalusite porphyroblastic schists (Fig. 6e).

Profile 3 (Fig. 1, 4c) extends from northwest to southeast, from the centre of the Hidden Lake pluton to the core of the Watta Lake tonalite pluton of the Defeat Suite (Fig. 6f). The profile crosses the folded "tail" of the Sparrow pluton, the circular Defeat tonalite-granodiorite pluton (the type pluton of the Defeat Suite), and the regional-scale Hearne Lake syncline of low grade metaturbidites (Fig. 6g). The greatest depth extent of the metaturbidites is anticipated to underlie this synclinal structure. The southern half of profile 3 follows the structural cross-section of Bleeker and Beaumont-Smith (1995).

CONCLUSIONS

A total of 152 new gravity readings were made along three profiles extending from the end of the Ingraham Trail east of Yellowknife. Preliminary data along the three profiles are presented diagrammatically in Figure 4. Preliminary free air and Bouguer corrections have been applied to the data using raw elevation data and Bouguer corrections were made using an average density of 2.67 g/cm^3. The differential correction of the GPS data will result in minor changes in the final data. Terrain corrections will be applied prior to final modelling, as needed.

As shown in Figure 4, the profiles show an excellent correlation with the surface geology. Major positive anomalies (about 20 mGal) are recorded over the greenstone belts, whereas significant negative anomalies (about 10 mGal) are recorded over many of the granitoid plutons. An interesting aspect is that some of the plutons show a weak to pronounced W-shaped anomaly pattern with a central maximum (e.g. the Defeat and Watta Lake plutons), possibly suggesting that they are folded sheets rather than deeply rooted plutons. A regional minimum of -71 mGal is recorded over the Morose Lake granite in the core of the Sleepy Dragon Complex. The preliminary data set shows promise for future modelling to resolve such questions as the depth extent and attitude of the greenstone belts and the shapes of the various granitoid plutons.

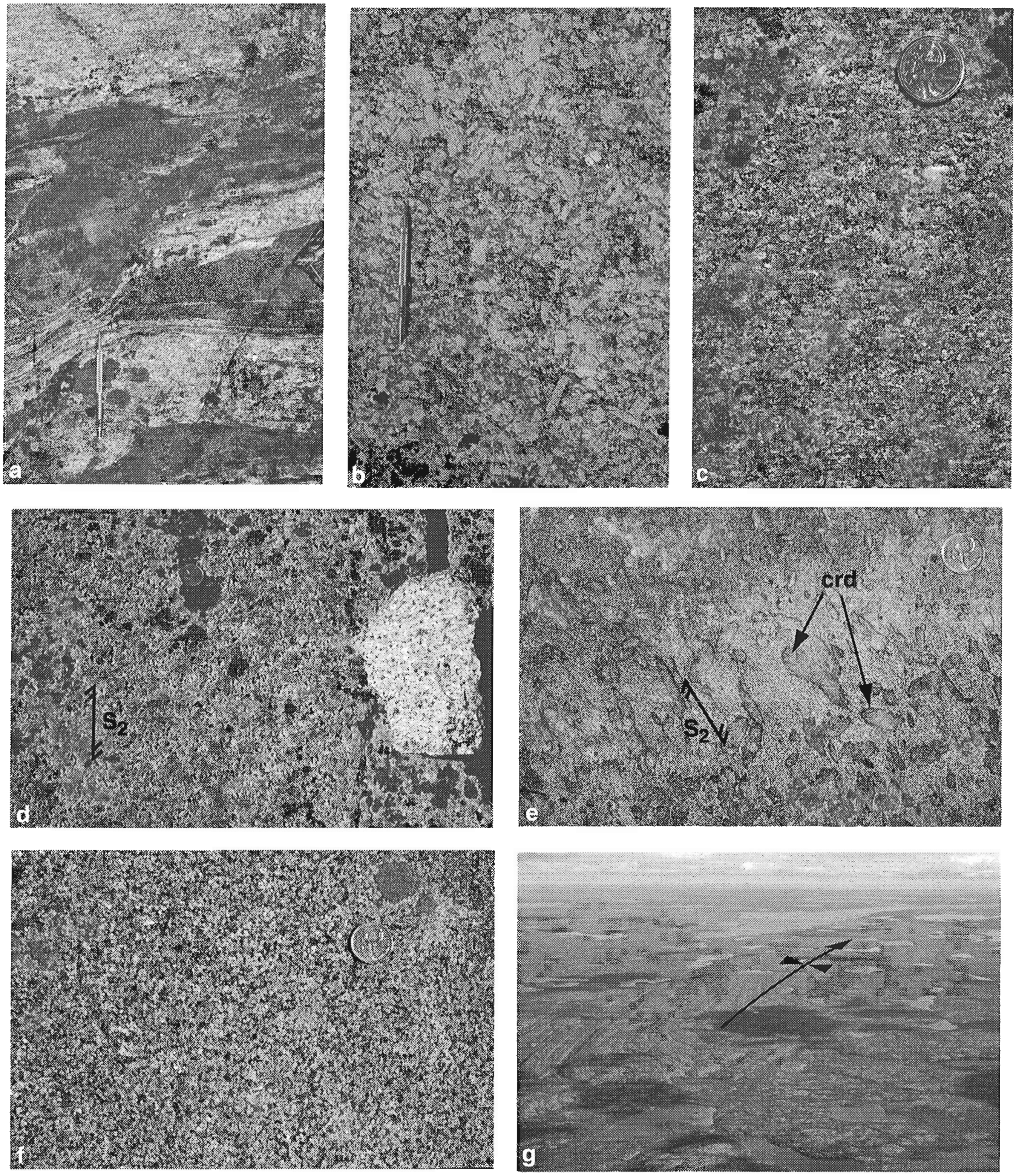

Figure 6. *Some of the important rock units along the profiles.* ***a)*** *Migmatitic tonalite-diorite gneisses typical for the basement assemblage of the Sleepy Dragon Complex.* ***b)*** *K-feldspar megacrystic biotite granite of the Morose Lake pluton in the core of the Sleepy Dragon Complex.* ***c)*** *Typical biotite granite of the Redout granite pluton.* ***d)*** *Prosperous Suite two-mica granite of Sparrow pluton.* ***e)*** *Typical cordierite (crd) grade metaturbidites of the Burwash Formation.* ***f)*** *Biotite tonalite representative of the Watta Lake and Upper Watta Lake tonalite plutons.* ***g)*** *Aerial view of the low grade metaturbidites of the Burwash Formation in the Hearne Lake syncline (trace shown by arrow). View towards the southeast across Hearne Lake.*

ACKNOWLEDGMENTS

The Indian and Northern Affairs Canada, Northwest Territories Geology Division is thanked for their cooperation throughout the summer and for helping out with fixed-wing support (the Beaver) for getting fuel cashes in place on time. Mike Pollock and Shane Wilkinson assisted with logistics in Yellowknife, whereas Curt Purdue from Canadian Helicopters is thanked for his expert flying skills. Eric de Kemp and Steve Lucas critically read the manuscript. K.A.B. Hendry is partially supported by a NSERC Lithoprobe Supporting Geoscience Grant WR Roest. Lithoprobe Contribution 907.

REFERENCES

Bleeker, W.
1996: Thematic structural studies in the Slave Province, Northwest Territories: the Sleepy Dragon Complex; in Current Research 1996-C; Geological Survey of Canada, p. 37-48.

Bleeker, W. and Beaumont-Smith, C.
1995: Thematic structural studies in the Slave Province: preliminary results and implications for the Yellowknife Domain, Northwest Territories; in Current Research 1995-C; Geological Survey of Canada, p. 87-96.

Cook, F. and Erdmer, P. (comp.)
1997: Slave-Northern Cordillera Lithospheric Evolution (SNORCLE) Transect and Cordilleran Workshop Meeting (March 7-9), University of Calgary, Lithoprobe Report No. 56, 245 p.

Gibb, R.A. and Thomas, M.D.
1980: Correlation of gravity anomalies with Yellowknife Supergroup rocks, North Arm, Great Slave Lake; Canadian Journal of Earth Sciences, v. 17, p. 1506-1516.

Henderson, J.B.
1985: Geology of the Yellowknife-Hearne Lake area, District of MacKenzie: a segment across an Archean basin; Geological Survey of Canada, Memoir 414, 135 p., scale 1:250 000.

Hoffman, P. and Hall, L.
1993: Geology, Slave cratons and environs, District of MacKenzie, Northwest Territories; Geological survey of Canada, Open File 2559, scale 1:1 000 000.

Isachsen, C.E. and Bowring, S.A.
1997: The Bell Lake Group and Anton Complex: a basement-cover sequence beneath the Archean Yellowknife greenstone belt revealed and implicated in greenstone belt formation; Canadian Journal of Earth Sciences, v. 34, p. 169-189.

Kusky, T.M.
1990: Evidence for Archean ocean opening and closing in the southern Slave province; Tectonics, v. 9, no. 6, p. 1533-1563.

Lambert, M.B., Ernst, R.E., and Dudás, F.Ö.
1992: Archean mafic dyke swarms near the Cameron River and Beaulieu River volcanic belts and their implications for tectonic modelling of the Slave Province, Northwest Territories; Canadian Journal of Earth Sciences, v. 29, p. 2226-2248.

McGrath, P.H., Henderson, J.B., and Lindia, F.M.
1983: Interpretation of a gravity profile over a contact zone between an Archean granodiorite and the Yellowknife Supergroup using an interactive computer program with partial automatic optimization; in Current Research, Part B; Geological Survey of Canada, Paper 83-1B, p. 189-194.

Geological Survey of Canada Projects 870008, 960023, and 960025

Central Slave Basement Complex, Northwest Territories: its autochthonous cover, décollement, and structural topology

Wouter Bleeker and John Ketchum[1]
Continental Geoscience Division, Ottawa

Bleeker, W. and Ketchum, J., 1998: Central Slave Basement Complex, Northwest Territories: its autochthonous cover, décollement, and structural topology; in Current Research 1998-C; Geological Survey of Canada, p. 9-19.

Abstract: A comprehensive and testable model is presented for basement/cover relationships in the south-central Slave Province. Basement rocks predating the Yellowknife Supergroup can be combined into a single basement block, the Central Slave Basement Complex. Its structural topology is described and preliminary U-Pb data are presented for a ca. 3.4-3.2 Ga gneiss below the Courageous Lake greenstone belt. All presently known occurrences of a distinctive quartzite and banded iron-formation assemblage occur immediately above the complex and are included in a new stratigraphic entity, the Central Slave Cover Group, which represents the autochthonous cover to the Central Slave Basement Complex. A regional décollement marks the contact of the basement complex and its cover with the overlying parautochthonous to allochthonous tholeiitic break-up sequence. Mutually consistent lineation data and kinematic indicators, at five widely spaced localities, suggest significant northeast-to-southwest transport of the tholeiite sequence over the basement complex and its cover sequence.

Résumé : Le présent article donne les grandes lignes d'un modèle global et testable des rapports substratum-couverture dans le centre sud de la Province des Esclaves. Les roches du substratum antérieures à la formation du Supergroupe de Yellowknife peuvent être regroupées en un bloc unique, appelé Complexe du substratum de la Province des Esclaves centrale (CSPEC). La topologie structurale de ce bloc est ensuite décrite et des données préliminaires de datation U/Pb présentées pour un gneiss d'environ 3,2-3,4 Ga, échantillonné au sud de la ceinture de roches vertes de Courageous Lake. Toutes les occurrences actuellement connues d'un assemblage distinctif de quartzite et de formation de fer rubanée s'observent directement au-dessus du CSPEC; elles sont associées à une nouvelle entité stratigraphique, le Groupe de couverture de la Province des Esclaves centrale, qui représente les roches autochtones sus-jacentes au CSPEC. Un décollement régional marque le contact entre, d'une part, le complexe du substratum et sa couverture et, d'autre part, la séquence de rupture sus-jacente (tholéiites parautochtones à allochtones). Des données de linéation et des indicateurs cinématiques provenant de cinq localités très espacées laissent supposer qu'il y a eu un important déplacement du nord-est vers le sud-ouest de la séquence tholéiitique par rapport au CSPEC et aux roches qui le recouvrent.

[1] Department of Earth Sciences, Memorial University of Newfoundland, St. John's, Newfoundland A1B 3X5

INTRODUCTION

The Slave craton of northwestern Laurentia (Fig. 1) has an extensive rock record (Mortensen et al., 1988; Bowring et al., 1989; van Breemen et al., 1992; Isachsen and Bowring, 1994, 1997; Villeneuve et al., 1994; Bleeker and Stern, 1997), with specific assemblages punctuating Earth's history from ca. 4.05 Ga to ca. 2.55 Ga. Although 2.73-2.58 Ga supracrustal assemblages and associated granitoid rocks dominate the craton, it has long been known that some of the Neoarchean supracrustal assemblages overlie considerably older basement rocks (Baragar, 1966; McGlynn and Henderson, 1970).

The Neoarchean supracrustal rocks traditionally have been lumped into a single lithostratigraphic entity, the Yellowknife Supergroup (Henderson, 1970), which was viewed as the product of a relatively simple, single-stage, ca. 2.7 Ga ensialic rifting event (e.g. Henderson, 1985). Much of this paradigm evolved prior to 1980, without precise U-Pb zircon geochronological data. Recently, with an ever increasing number of precise U-Pb ages becoming available, it has been shown that the Yellowknife Supergroup is a complex entity with spatially and temporally distinct assemblages of diverse tectonic origin including rift and local shelf assemblages, plume and break-up-type tholeiitic sequences, juvenile as well as crustally contaminated arc sequences, turbidite sequences of various ages, and late tectonic clastic basins. Uranium-lead geochronology has confirmed the prediction that parts of the Yellowknife Supergroup are underlain by sialic basement (e.g. Nikic et al., 1980; Henderson, 1985; Isachsen and Bowring, 1997). This prediction was first put forward by Baragar (1966) based on the observation that old mafic dyke swarms cut through subgreenstone belt granitoid terrains. Isotopic tracer studies (Pb, Nd) have provided further evidence for the widespread influence of evolved and significantly older sialic crust on younger volcanic rocks and plutons (e.g. Davis and Hegner, 1992; Yamashita et al., 1995), contributing to the notion that a single older basement block, the Anton terrane (Kusky, 1990), underlies much of the western part of the Slave Province.

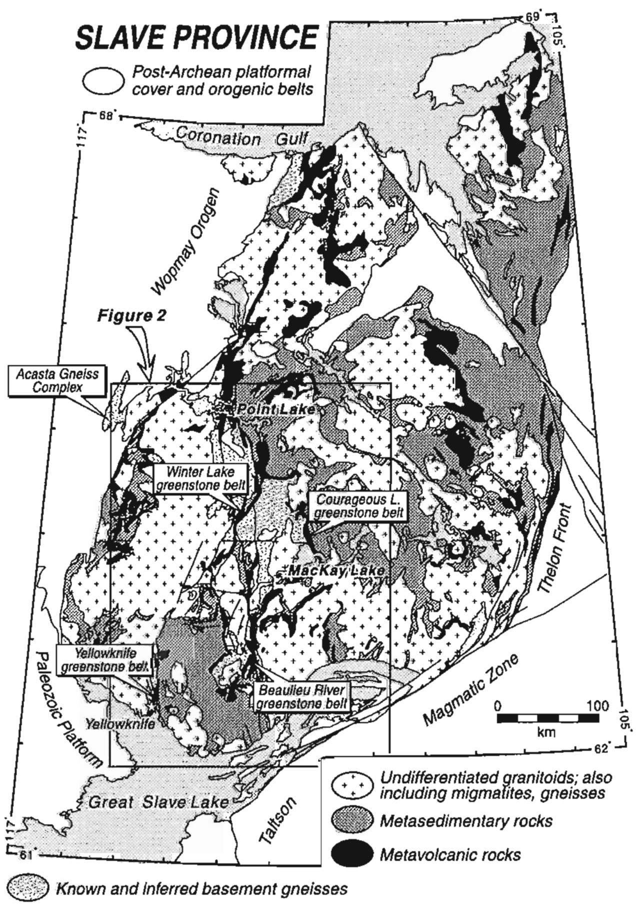

Figure 1. Simplified geological map of the Slave structural province. Area of Figure 2 is shown.

Nevertheless, the extent and geometry of the basement terrane have remained obscure. In this study we present the first definitive outline and structural topology of a large basement block in the south-central Slave Province (Fig. 2), and propose to call this the Central Slave Basement Complex.

The complex is overlain by a thin, generally highly deformed and locally imbricated autochthonous cover sequence (Fig. 2) consisting of conglomerate, mafic and ultramafic volcanic rocks, chromite-bearing quartzite, and banded iron-formation. We propose to include these cover rocks into a single lithostratigraphic unit, the Central Slave Cover Group. Significantly, all previously known and some new occurrences of this thin cover sequence, which is perhaps best typified by the fuchsitic chromite-bearing quartzites, are associated with the Central Slave Basement Complex.

The autochthonous cover sequence is overlain by a thick, parautochthonous to allochthonous tholeiitic basalt sequence. Everywhere where the original basement/cover relationship has been preserved and has not been cut out or reworked by younger granitoid complexes or truncated by younger unconformities, the top of the basement complex is represented by an impressive high strain zone that predates ca. 2686 Ma dykes (Bleeker et al., 1997a) and is best interpreted as a regional décollement. Mutually consistent lineation data and kinematic indicators have been found in several widely spaced localities along the décollement and suggest northeast-to-southwest transport of the tholeiitic break-up sequence over the basement complex.

CENTRAL SLAVE BASEMENT COMPLEX

In an on-going effort to better characterize and date basement rocks throughout the Slave Province and assess their role in the tectonic evolution of the craton, all previously known geochronology sample sites of basement rocks predating Yellowknife Supergroup of the south-central Slave were visited and re-evaluated. The following conclusions emerged from this survey:

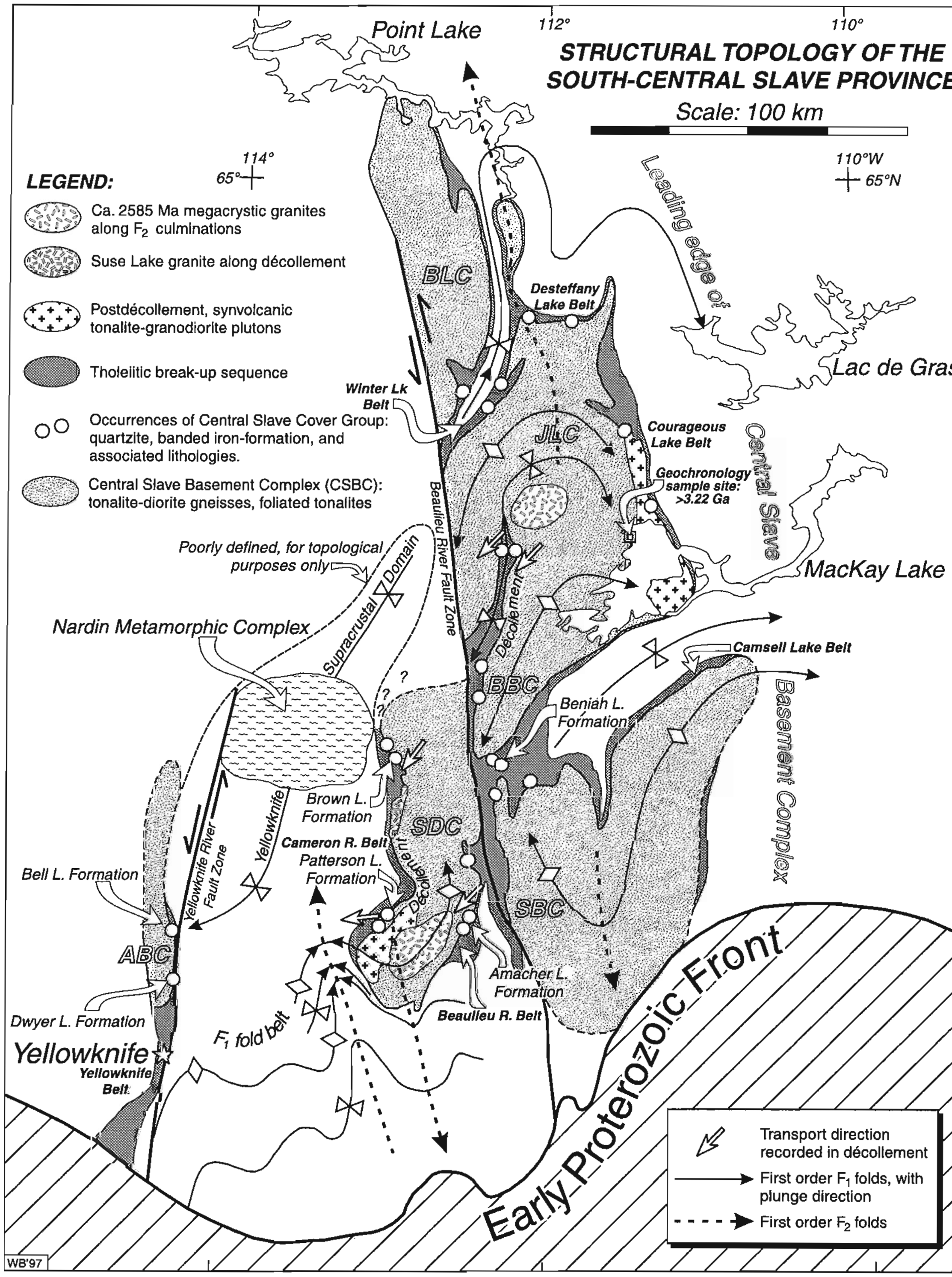

Figure 2. Topological map of the proposed Central Slave Basement Complex. The complex includes the previously defined Anton Basement Complex (ABC), the Sleepy Dragon Complex (SDC), the Jolly Lake Complex (JLC), and the newly defined Beniah Basement Complex (BBC), Step'nduck Basement Complex (SBC), and tentatively, the Big Lake Complex (BLC) of Thompson and Kerswill (1994). Inclusion of the Big Lake Complex in the Central Slave Basement Complex is contingent on a synclinal fold relationship across the Winter Lake greenstone belt, as is strongly suggested by the overall topology. Note also that the topology requires basement rocks to be present west of the northern extent of the Yellowknife supracrustal domain. However, we currently do not complete this part of the topology due to poor definition of the geology in this area. All known occurrences of the quartzite/banded iron-formation assemblage are indicated and are confined to the immediate cover of the Central Slave Basement Complex. Note also the geochronology sample site discussed in this paper, on the west shore of MacKay Lake.

1. The most common and widespread basement lithology is a heterogeneous assemblage of dioritic to tonalitic gneisses (Fig. 3a,b). These gneissic rocks commonly contain an old migmatitic layering that is truncated by one or more swarms of mafic dykes that are themselves deformed, metamorphosed, and intruded by younger granitoid rocks (e.g. Fig. 3d, e). In at least some localities, such gneisses are located unequivocally in the footwall of nearby, thin, quartzite/banded iron-formation assemblages at the base of the greenstone belts, and show a distinct metamorphic contrast with lower temperature mineral assemblages in the greenstones.
2. Also common are foliated, but nonmigmatized tonalites and granodiorites (Fig. 3c) that are intruded by multiple dyke swarms. Recent mapping of parts of the Sleepy Dragon Complex shows that foliated basement tonalite below the quartzite/banded iron-formation assemblage of the Patterson Lake Formation contains three distinct dyke swarms, the oldest of which is transposed in the regional décollement (Bleeker et al., 1997b).
3. Where the quartzite/banded iron-formation cover assemblage is expected but nevertheless absent, this absence generally can be explained by one of the following complications: the original basement/cover contact has been truncated by or incorporated into ca. 2690-2670 Ma plutons; the original basement/cover contact has been cut out by younger unconformities (e.g. Bleeker et al., 1997b); large segments of the basement/cover contact have been eliminated by intrusion of late orogenic, ca. 2585 Ma K-feldspar

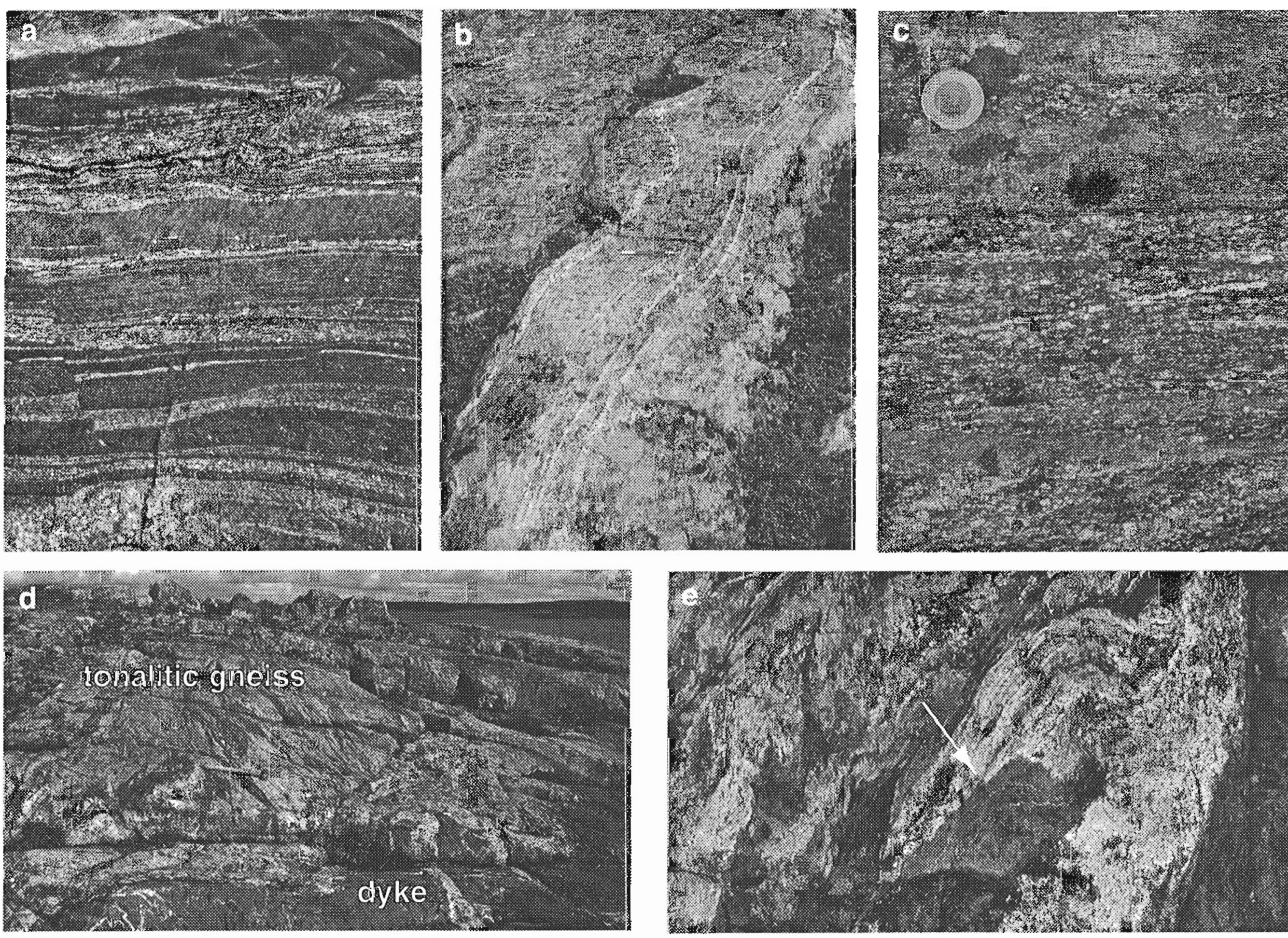

Figure 3. Typical basement lithologies of the Central Slave Basement Complex. ***a)*** *Migmatitic diorite-tonalite gneiss at Brown Lake at the northern end of the Beaulieu River greenstone belt.* ***b)*** *Foliated and layered tonalitic gneiss of the Jolly Lake Complex, Jolly Lake.* ***c)*** *Foliated and metamorphosed, but nonmigmatitic tonalite below the Patterson Lake Formation, Patterson Lake.* ***d)*** *Heterogeneous tonalite-diorite gneiss on western MacKay Lake cut by amphibolitized and deformed mafic dyke (in foreground). This gneiss unit has been dated at ca. 3.3 Ga and results are presented in Figure 4.* ***e)*** *Close-up of outcrop shown in Figure d, showing old migmatitic layering being truncated (at arrow) by the deformed mafic dyke. Both the gneiss and dyke are folded and cut by a younger granitoid dyke.*

granites; or segments of the basement/cover contact have been excised due to late stage dip-slip extensional faulting that accompanied K-feldspar granite intrusion (e.g. James and Mortensen, 1992). Examples of all four of these complications have been documented around the Sleepy Dragon Complex.

Using the above conclusions as criteria for establishing basement rocks beyond the handful of previously dated occurrences, the outline of the Central Slave Basement Complex as proposed in Figure 2 follows as a logical prediction. This prediction was further tested in the field and will be tested extensively by U-Pb zircon geochronology. Specifically, basement rock types as described above can be followed discontinuously from the southern end of the Sleepy Dragon Complex, to below the northern end of the Beaulieu River greenstone belt, into the Jolly Lake Complex and further northeast into the footwall of the Courageous Lake greenstone belt. Uranium-lead zircon data from a first sample of our regional sample suite are presented in Figure 4 and confirm a basement age (>3.2 Ga) for the diorite-tonalite migmatitic gneisses. The dated sample was collected along the western shore of MacKay Lake (Fig. 3d, e), within view of the overlying Courageous Lake greenstone belt. It represents "Unit 1" quartzofeldspathic gneiss of Thompson and Kerswill (1994). Although we stress the preliminary nature of the U-Pb results, they define a minimum age of 3218 Ma. The gneiss could be as old as ca. 3323 Ma, an upper intercept age defined by a discordia line through three colinear data points.

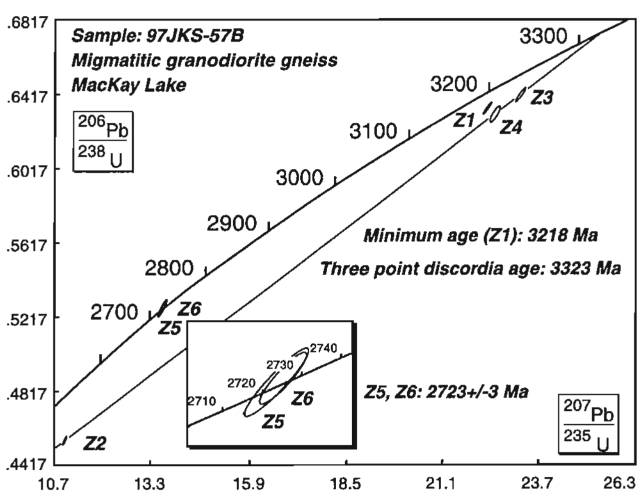

Figure 4. Uranium-lead concordia diagram showing preliminary results of six zircon fractions of a gneiss sample on the western shore of MacKay Lake. Brown prismatic grains (fractions Z1 to Z4) define the crystallization age of the gneiss. The $^{207}Pb/^{206}Pb$ age of fraction Z1 provides a minimum age of ca. 3218 Ma. Three of the fraction are colinear and possibly indicate an upper intercept age of ca. 3323 Ma. An even older age is also possible on the basis of these preliminary results. Colourless, equant, low U grains record a younger zircon growth event at ca. 2722 Ma.

Morphologically distinct, equant, colourless zircon grains of low U content define new zircon growth at ca. 2723 Ma, which is attributed to a cryptic metamorphic event.

Supporting evidence for the Central Slave Basement Complex as shown in Figure 2 is provided by the Bouguer gravity field of the Slave Province, which shows a broad negative anomaly over much of the complex. It is suggested that the broad negative Bouguer anomaly tracks older sialic crust at depth. The proposed outline of the complex is also in agreement with the regional variation in Pb-isotopic data for syngenetic ore leads (Thorpe et al., 1992; and R. Thorpe, unpub. data, 1997). Most if not all of the greenstone belts overlying the complex share a similar tectonostratigraphy, typically comprising a lower, rather monotonous tholeiite sequence disconformably to unconformably overlain by a younger calc-alkaline, dacite- and rhyolite-rich sequence, which itself is overlain by ca. 2665-2658 Ma Burwash Formation turbidites (e.g. compare the Courageous Lake belt and the Cameron River belt).

The proposed Central Slave Basement Complex encompasses the previously named Sleepy Dragon, Jolly Lake, and Anton basement complexes, which merely represent different parts of the Central Slave Basement Complex (Fig. 2). Furthermore, the Central Slave Basement Complex reappears to the east of Sleepy Dragon Complex as basement below the southeastern flank of the Beaulieu River greenstone belt, the southern flank of the Beniah Lake greenstone belt, and the Camsell Lake greenstone belt. It is proposed that this part of the Central Slave Basement Complex be named the Step'n-duck Complex after a dyke complex described by Lambert et al. (1992). Although this basement complex locally includes migmatitic diorite-tonalite gneisses, the full extent of old basement rocks relative to younger intrusive granitoid intrusions is poorly known. The eastern and southern limits of this complex are poorly constrained. In general, at least 50% of the Central Slave Basement Complex appears to be intruded by younger granitoid rocks.

CENTRAL SLAVE COVER GROUP: AUTOCHTHONOUS COVER OF THE CENTRAL SLAVE BASEMENT COMPLEX

The Central Slave Basement Complex is overlain by a thin, generally highly deformed and locally imbricated, volcanic and clastic cover sequence (Fig. 5). The typical stratigraphy of this cover sequence consists of mafic and ultramafic volcanic rocks at or near the base, overlain in succession by conglomerate, immature quartz-rich grit, chromite-bearing fuchsitic quartzite, and silicate or oxide facies banded iron-formation (e.g. Bleeker et al., 1997b). Ultramafic sills locally intrude the sequence. Felsic volcaniclastic rocks have been described from two localities (Dwyer Lake and Beniah Lake; Covello et al., 1988; Isachsen and Bowring, 1997). The entire succession is generally less than 200 m thick, although at Beniah Lake it attains a considerably greater thickness, perhaps as much as a 1000 m. In part, this greater thickness appears to result from several folds within the Beniah Lake area.

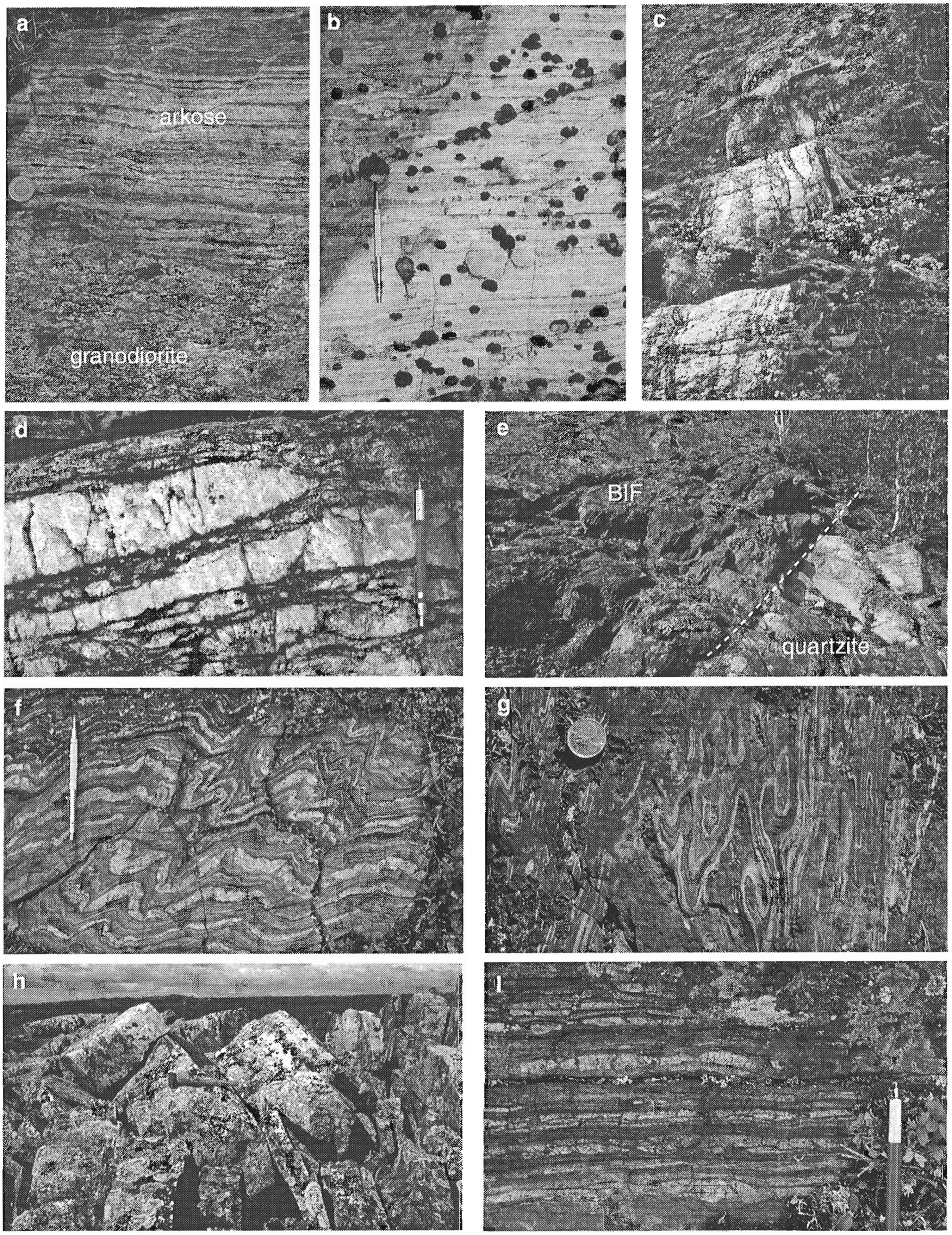
a
arkose
granodiorite
b
c
d
e
BIF
quartzite
f
g
h
i

Scattered occurrences of this cover sequence have been recognized by a number of workers over the last decade (Hauer, 1979; Helmstaedt and Padgham, 1986; Covello et al., 1988; Roscoe et al., 1989; Rice et al., 1990; Isachsen, 1992; Stubley, 1996; Bleeker et al., 1997b). These occurrences have been referred to informally or incorrectly under a variety of names at the formation or group rank. For instance, in several consecutive publications, Isachsen and coworkers referred to a thin quartzite/banded iron-formation package at Dwyer Lake, 25 km north of Yellowknife, as the Dwyer Formation (Isachsen et al., 1991), the Dwyer Group (Isachsen, 1992), the Dwyer group (Isachsen and Bowring, 1994), and the Bell Lake group (Isachsen and Bowring, 1997). Others have generally referred to these occurrences as local formations, such as the Patterson Lake Formation (at Patterson Lake: Bleeker et al., 1997b) and the Beniah Formation (at Beniah Lake: Roscoe et al., 1989). In the light of the present study it seems both timely and justified to simplify and formalize this nomenclature by defining this cover sequence as the Central Slave Cover Group, while maintaining formation names for each specific locality (e.g. Dwyer Lake Formation, Patterson Lake Formation, etc., see Fig. 2).

Although most contacts between the Central Slave Cover Group and underlying basement probably do represent highly sheared and faulted unconformities, the best evidence for an original unconformity has been found at Brown Lake on the northwestern flank of the Sleepy Dragon Complex. Along the west side of the lake a coarse quartz cobble conglomerate (Fig. 5c, d) directly overlies mylonitized, tonalitic basement gneiss that is intruded by multiple mafic dyke swarms. The mylonitized tonalite is very similar to foliated tonalites underneath the Patterson Lake Formation further south (Bleeker et al., 1997b) and is presumed to be ca. 2.9 Ga. Near the contact, the tonalite contains conspicuous amounts of aluminosilicates (both andalusite and sillimanite, up to 10-20 modal percent) while maintaining an overall granitoid texture. This provides strong evidence for a metamorphosed weathering profile underneath the quartz cobble conglomerate. The quartz cobble conglomerate is overlain by a highly deformed polymict conglomerate, an approximately 10 m thick quartzite unit with minor fuchsite (Fig. 5e; see Fig. 5b), and 1-5 m of banded iron-formation (Fig. 5f). A thin sulphidic chert is locally present at the contact between banded iron-formation and the overlying pillow basalts of the Cameron River belt.

The age of the Central Slave Cover Group is still poorly constrained. Detrital zircon data for a chromite-bearing quartzite with relict crossbedding at Dwyer Lake indicate a depositional age that is younger than 2924 Ma (Isachsen and Bowring, 1997). Eight detrital zircon grains from thin, graded, arkosic layers at the top of the Patterson Lake Formation show $^{207}Pb/^{206}Pb$ ages between 3147 and 2943 Ma (W. Bleeker and M. Villeneuve, unpub. data, 1997). The two youngest grains in the latter data set are concordant at 2943 Ma, providing an age constraint similar to that for the Dwyer Lake quartzite. Isachsen and Bowring (1997) report a 2835 ± 4 Ma age for a rhyolite ash flow tuff that overlies quartzite at Dwyer Lake, but the volcaniclastic nature of this unit together with the scatter among individual data points may cast some doubt on this result. Do the zircon data possibly reflect a detrital population? A conservative assessment of the existing data thus suggests that the Central Slave Cover Group is younger than ca. 2924 Ma and older than ca. 2730 Ma, the oldest recorded age for Yellowknife Supergroup volcanic rocks.

Figure 5. *Typical outcrops of the Central Slave Cover Group.* ***a)*** *Basal, slightly fuchsitic, arkosic quartzite of the Dwyer Lake Formation, overlying foliated basement granodiorite at Dwyer Lake. Isachsen and Bowring (1997) dated the granodiorite at 2.96 Ga or older (their preferred age being 3017 ± 1 Ma, "tonalitic gneiss" SP90-20).* ***b)*** *Fuchsitic quartzite of the Patterson Lake Formation on the western flank of the Sleepy Dragon Complex (see Bleeker et al., 1997b).* ***c)*** *Basal quartz cobble conglomerate (hammer for scale) overlying a metamorphosed weathering profile at Brown Lake.* ***d)*** *Close-up of the large, deformed vein quartz cobbles of the Brown Lake basal conglomerate. The quartz pebbles and cobbles occur in a slightly fuchsitic quartzite matrix.* ***e)*** *Quartzite overlain by banded iron-formation (BIF) at the top of the Brown Lake Formation, just underneath pillow basalts of the northern part of the Cameron River greenstone belt.* ***f)*** *Close-up of folded (F_2) oxide-chert banded iron-formation at the top of the Brown Lake Formation.* ***g)*** *Folded (F_1-F_2) oxide-chert banded iron-formation at the top of the Amacher Lake Formation on the eastern flank of the Sleepy Dragon Complex.* ***h)*** *Fuchsitic quartzite along the basement/cover contact on the southwestern flank of the Jolly Lake Complex.* ***i)*** *Silicate and oxide banded iron-formation overlying the quartzite unit shown in Figure h, on eastern limb of syncline southwest of the Jolly Lake Complex.*

DÉCOLLEMENT

In most places where the contact between Central Slave Basement Complex and cover rocks can be observed it is marked by a high strain zone that is one to several kilometres wide (Fig. 6). In this high strain zone, the basement rocks vary from strongly foliated protomylonitic granitoids or gneisses (e.g. Fig. 6a,b) to well-developed mylonites (e.g. Fig 6c). Early mafic dyke swarms, possibly related to initial rifting of the Central Slave Basement Complex, are transposed into parallelism with the mylonitic fabric (Bleeker et al., 1997b), whereas later dyke swarms cut the high strain fabric. Stretching lineations in the high strain zones typically pitch 20-65° within steeper dipping mylonitic foliations (Fig. 6a) and are distinct from younger down-dip stretching and intersection lineations in the overlying volcanic rocks. The obliquity of the stretching lineations in the mylonitic gneisses, together with the observation that the mylonitic fabrics are cut by some of the dyke swarms, negates the argument that they result from deformation associated with high-amplitude upright folding of the greenstone belts.

Compatible lineation directions and kinematic indicators in the high strain zones at five widely spaced localities allow the high strain zones along segments of the Central Slave Basement Complex basement/cover contact to be linked into a single, regional décollement along which the cover was translated from northeast to southwest. Presently, the preserved map width of this décollement parallel to the movement direction is about 300 km. If high-amplitude folding of the décollement is taken into account (e.g. over the Jolly Lake and Sleepy Dragon antiformal complexes), the preserved width must be considerably greater than 300 km. Hence, the extent of the Central Slave Basement Complex décollement is within the realm of widths of basal décollements underneath younger external thrust belts (e.g. the Cape Smith belt; St. Onge et al., 1992).

The total displacement along the décollement is unknown and is likely to have varied from place to place. Nevertheless, the gross displacement must be considerable given the

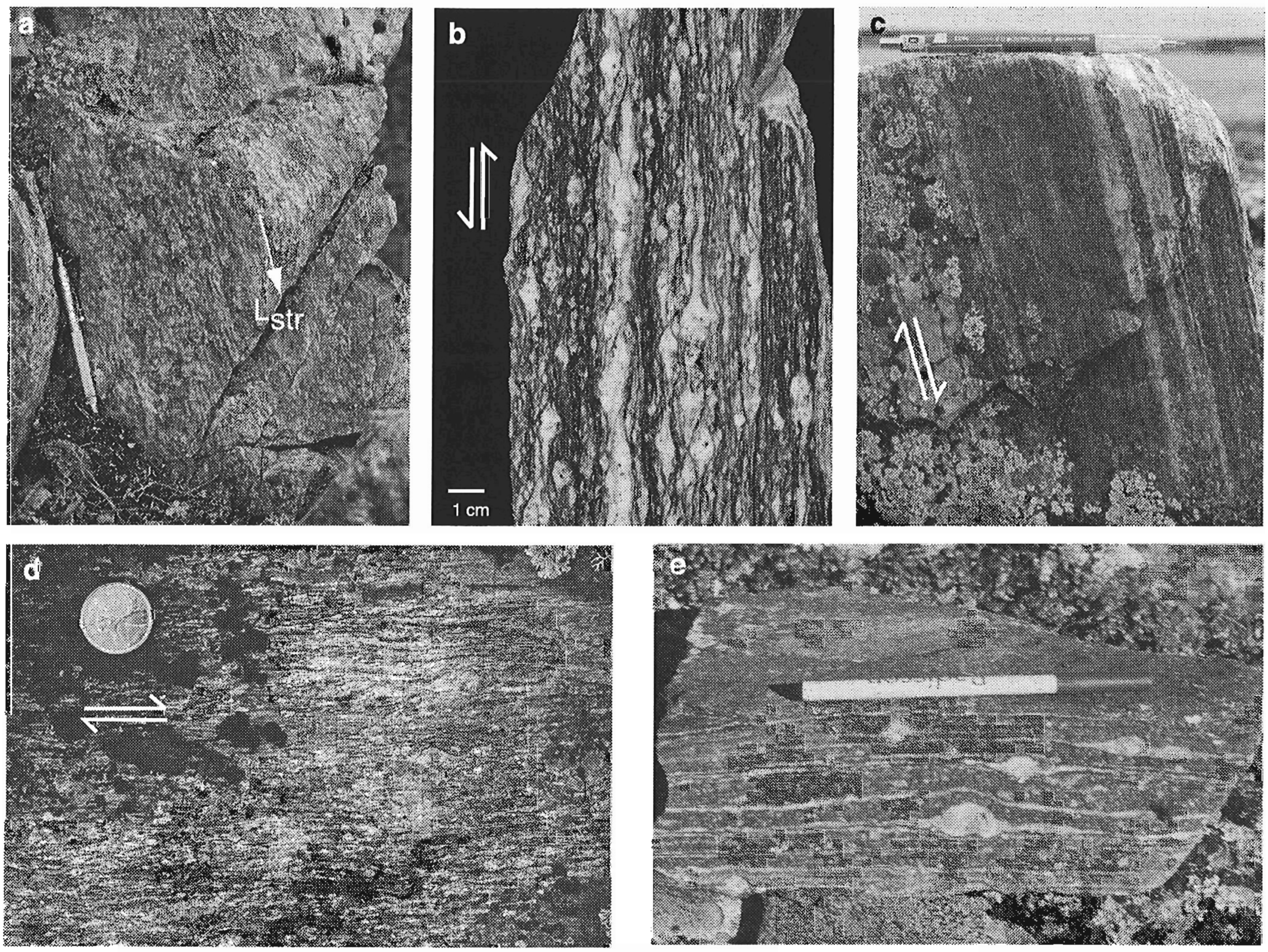

*Figure 6. Representative photographs of the décollement along the basement/cover contact of the Central Slave Basement Complex. **a)** Protomylonitic to mylonitic tonalites at Patterson Lake, western flank of the Sleepy Dragon Complex, with oblique, westerly plunging stretching lineations (L_{str}). **b)** Close-up of (proto)mylonitic gneisses on Patterson Lake, viewed in northeast-looking section parallel to the stretching lineation. C-S fabrics indicate a west-side-down sense of movement in the décollement on western flank of the Sleepy Dragon Complex. **c)** Mylonitic gneisses below the Central Slave Cover Group on the southwestern flank of the Jolly Lake Complex, on eastern limb of the synclinally folded greenstone belt. **d)** Basement-derived tonalitic S-C mylonite on eastern flank of the Sleepy Dragon Complex, west of Amacher Lake. View down onto outcrop surface, subparallel to shallowly northeast-plunging stretching lineation. The dextral sense of shear indicates that the Beaulieu River belt moved south and up relative to the basement of the Sleepy Dragon Complex. **e)** Mylonitic gneiss with rotated feldspar augen in the high strain zone below the Beniah Lake greenstone belt.*

general strain state and width of the shear zone. Given that the oldest dykes, currently represented by amphibolite sheets with strong L-S fabrics, are transposed into parallelism with the basement/cover contact and the mylonitic fabric over widths of more than 1 km, minimum displacements of more than 10 km are indicated (shear strains of about 10 or higher over 1 km width). This minimum estimate merely includes the distributed strain in the high strain zone and neglects the bulk of the displacement which more than likely was accommodated on discrete slip surfaces.

DISCUSSION AND CONCLUSIONS

A coherent and testable structural model is beginning to emerge for the south-central Slave Province. Our new data and a re-evaluation of previously published data allow a large basement block to be outlined (Fig. 2), which we define as the Central Slave Basement Complex. Our first critical test of the hypothesis to extend basement rocks into the structural footwall of the Courageous Lake greenstone belt has resulted in an age of ca. 3.4-3.2 Ga for a migmatitic gneiss at MacKay Lake (Fig. 4).

The Central Slave Basement Complex is overlain by a characteristic cover stratigraphy (Fig. 5), which we define and propose to formalize as the Central Slave Cover Group. This name is both simple and intuitive and links what presently appear to be spatially separate occurrences of the cover sequence into a single lithostratigraphic entity. On a local scale, these occurrences can continue to be referred to as formations such as the Dwyer Lake Formation, Patterson Lake Formation, or Beniah Lake Formation. The Central Slave Cover Group probably represents rifting (mafic and ultramafic volcanic rocks, conglomerates) of the Central Slave Basement Complex and subsequent development of small, local, shallow shelves (quartzites) where mixed detritus of basement and volcanic origin was abraded, sorted, and upgraded to an extent that only quartz, minor K-feldspar, and chromite survived. The top of the Central Slave Basement Complex is represented by a more than 300 km wide décollement along which the tholeiitic break-up sequence of the south-central Slave and parts the clastic cover sequence were translated to the southwest.

Although a central element of our proposal, that of a regional décollement, is shared with the model of Kusky (1990), there are many important differences. We disagree with the model and analysis of Kusky (1990) on the following points:

1. The tholeiite sequence in the hanging wall of the décollement does not represent oceanic crust, but rather a tholeiitic break-up sequence that likely formed on thinned continental crust of the Central Slave Basement Complex.
2. There are no exotic rocks in the high strain zone overlying the décollement, merely highly deformed Central Slave Basement Complex rocks, deformed and locally imbricated cover rocks, and disrupted and transposed mafic dykes. Serpentinite occurrences at or near the décollement represent the ultramafic flows and sills associated with the Central Slave Cover Group.
3. We restrict our lineation and kinematic indicator observations to the mylonitic gneisses in the décollement (Fig. 2, 6). Most lineations in the volcanic rocks, certainly those in the younger volcanic rocks along the southern flank of the Sleepy Dragon Complex (e.g. the <2683 Ma Tumpline basalts; Lambert, 1988), are related to younger deformation.

Consequently, our analysis proposes a southwesterly transport direction rather than east-to-west transport. We can constrain the displacement to more than 10 km, along a décollement more than 300 km wide (from northeast to southwest). Thrusting took place prior to deposition of the <2683 Ma Raquette Lake Formation, which overlies an unconformity that locally truncates the décollement (Bleeker et al., 1997b). Mafic dykes that cut the high strain fabric have been dated at 2686 ± 2 Ma (W. Bleeker and W.J. Davis, unpub. data, 1997). The topology as proposed in Figure 2 is internally consistent and incorporates the geometrical effects of the two major, postdécollement folding phases. The topology also suggest major, late stage, dextral strike-slip displacement along the Beaulieu River and Yellowknife River fault zones.

Future work will further test the proposed model. For instance, is our prediction correct that the quartzitic schists at the base of the Courageous Lake and Destaffaney Lake greenstone belts (see Fig. 3 in Thompson et al., 1995) are part of the Central Slave Cover Group? Will other potential basement samples collected for U-Pb work indeed produce ages older than ca. 2.9 Ga?

The next critical advance will likely come from a more detailed understanding of the Winter Lake greenstone belt on the northwestern flank of the Central Slave Basement Complex. If this complex greenstone belt (Hrabi et al., 1995) indeed represents a synclinal structure of the tectonostratigraphy, as strongly suggested by the regional structural topology (Fig. 2), then the Central Slave Basement Complex and overlying cover can be extended to the west side of the Winter Lake belt and from there to Point Lake. If so, the proposed basement on the northwestern side of the Winter Lake belt (the Big Lake Complex of Thompson and Kerswill, 1994; BLC in Fig. 2), would represent another fold-repeated part of the Central Slave Basement Complex. Furthermore, the complex would then also include the central Point Lake basement complex, whereas the highly deformed basement/cover contact at Point Lake could prove to be another segment of the same regional décollement as that exposed at the Sleepy Dragon Complex. Our analysis suggests that the key to these critical questions should be provided by an attempt to correlate basement and the Central Slave Cover Group across the Winter Lake belt.

ACKNOWLEDGMENTS

Our sincere thanks go to the Department of Indian Affairs and Northern Development, Northwest Territories Geology Division for their permission to make use of their float plane. This enabled us to visit more localities than would have been possible otherwise. We also would like to thank John Henderson, Peter Thompson, Maurice Lambert, Mike Stubley, Val Jackson, and countless other geologists who preceded us in the area and whose maps significantly contributed to the model presented in this paper. Shane Wilkinson assisted in the field. Steve Lucas reviewed the manuscript and provided constructive criticism. Lithoprobe Contribution 906.

REFERENCES

Baragar, W.R.A.
1966: Geochemistry of the Yellowknife volcanic rocks; Canadian Journal of Earth Sciences, v. 3, p. 9-30.

Bleeker, W. and Stern, R.A.
1997: The Acasta gneisses: an imperfect sample of Earth's oldest crust; Geological Association of Canada, Program with Abstracts Ottawa '97, p. A-13.

Bleeker, W., Davis, W.J., and Villeneuve, M.
1997a: The Slave Province: evidence for contrasting crustal domains and a complex, multistage tectonic evolution; in Slave-Northern Cordillera Lithospheric Evolution (SNORCLE) Transect and Cordilleran Tectonics Workshop Meeting, March 7-9, University of Calgary, (comp.) F. Cook, and P. Erdmer; Lithoprobe Report No. 56, p. 36-37.

Bleeker, W., Villeneuve, M., and Bethune, K.
1997b: Thematic structural studies in the Slave Province, Northwest Territories: contrasting basement/cover relationships on the western and southwestern flanks of the Sleepy Dragon Complex; in Current Research 1996-C; Geological Survey of Canada, p. 27-37.

Bowring, S.A., Williams, I.S., and Compston, W.
1989: 3.96 Ga gneisses from the Slave province, Northwest Territories, Canada; Geology, v. 17, p. 971-975.

Covello, L., Roscoe, S.M., Donaldson, J.A., Roach, D., and Fyson, W.K.
1988: Archean quartz arenite and ultramafic rocks at Beniah Lake, Slave structural province, N.W.T.; in Current Research, Part C; Geological Survey of Canada, Paper 88-1C, p. 223-232.

Davis, W.J. and Hegner, E.
1992: Neodymium isotopic evidence for the tectonic assembly of Late Archean crust in the Slave province, northwest Canada; Contributions to Mineralogy and Petrology, v. 111, p. 493-504.

Hauer, L.
1979: Preliminary geological map of the northern end of the Yellowknife greenstone belt; Compilation EGS 1979-10 sheets A and B, Department of Indian and Northern Development, Yellowknife, Northwest Territories.

Helmstaedt, H. and Padgham, W.A.
1986: A new look at the stratigraphy of the Yellowknife Supergroup at Yellowknife, NWT. Implications for the age of gold-bearing shear zones and Archean basin evolution; Canadian Journal of Earth Sciences, v. 23, p. 454-475.

Henderson, J.B.
1970: Stratigraphy of the Archean Yellowknife Supergroup, Yellowknife Bay-Prosperous Lake area, District of MacKenzie (85 J/8, J/9); Geological Survey of Canada, Paper 70-26, 12 p.
1985: Geology of the Yellowknife-Hearne Lake area, District of MacKenzie: a segment across an Archean basin; Geological Survey of Canada, Memoir 414, 135 p., scale 1:250 000.

Hrabi, R.B., Nelson, M.D., and Helmstaedt, H.
1995: Diverse metavolcanic sequences and late polymictic conglomerate-associated metasedimentary rocks in the Winter Lake supracrustal belt, Slave Province, Northwest Territories; in Current Research 1995-E; Geological Survey of Canada, p. 137-148.

Isachsen, C.E.
1992: U-Pb zircon geochronology of the Yellowknife volcanic belt and subjacent rocks, N.W.T., Canada: constraints on the timing, duration, and mechanics of greenstone belt formation; Ph.D. thesis, Washington University, St. Louis, Missouri, 164 p.

Isachsen, C.E. and Bowring, S.A.
1994: Evolution of the Slave craton; Geology, v. 22, p. 917-920.
1997: The Bell Lake group and Anton Complex: a basement-cover sequence beneath the Archean Yellowknife greenstone belt revealed and implicated in greenstone belt formation; Canadian Journal of Earth Sciences, v. 34, p. 169-189.

Isachsen, C.E., Bowring, S.A., and Padgham, W.A.
1991: U-Pb geochronology of the Yellowknife volcanic belt, N.W.T., Canada: New constraints on the timing and duration of greenstone belt magmatism; Journal of Geology, v. 99, p. 55-67.

James, D.T. and Mortensen, J.K.
1992: An Archean metamorphic core complex in the southern Slave Province: basement-cover structural relationships between the Sleepy Dragon Complex and the Yellowknife Supergroup; Canadian Journal of Earth Sciences, v. 29, p. 2133-2145.

Kusky, T.M.
1990: Evidence for Archean ocean opening and closing in the southern Slave Province; Tectonics, v. 9, no.6, p. 1533-1563.

Lambert, M.B.
1988: The Cameron River and Beaulieu River volcanic belts, District of MacKenzie, Northwest Territories; Geological Survey of Canada of Canada, Bulletin 382.

Lambert, M.B., Ernst, R.E., and Dudás, F.Ö.
1992: Archean mafic dyke swarms near the Cameron River and Beaulieu River volcanic belts and their implications for tectonic modelling of the Slave Province, Northwest Territories; Canadian Journal of Earth Sciences, v. 29, p. 2226-2248.

McGlynn, J.C. and Henderson, J.B.
1970: Archean volcanism and sedimentation in the Slave structural province; in Symposium on Basins and Geosynclines of the Canadian Shield, (ed.) A.J. Baer; Geological Survey of Canada, Paper 70-40, p. 31-44.

Mortensen, J.K., Thorpe, R.I., Padgham, W.A., King, J.E., and Davis, W.J.
1988: U-Pb zircon ages of felsic volcanism in Slave Province, N.W.T.; in Radiogenic Age and Isotopic Studies, Report 2, Geological Survey of Canada, Paper 88-2, p. 85-95.

Nikic, Z., Baadsgaard, H., Folinsbee, R.E., Krupicka, J., Payne Leech, A., and Sasaki, A.
1980: Boulders from the basement, the trace of ancient crust?; Geological Society of America, Special Paper 182, p. 169-175.

Rice, R.J., Long, D.G.F., Fyson, W.K., and Roscoe, S.M.
1990: Sedimentological evaluation of three Archean metaquartzite- and conglomerate-bearing sequences in the Slave Province, N.W.T.; in Current Research, Part C, Geological Survey of Canada, Paper 90-1C, p. 305-322.

Roscoe, M., Stubley, M., and Roach, D.
1989: Archean quartz arenites and pyritic paleoplacers in the Beaulieu River supracrustal blet, Slave structural province, N.W.T.; in Current Research, Part C; Geological Survey of Canada, Paper 89-1C, p. 199-214.

St. Onge, M.R., Lucas, S.B., and Parrish, R.R.
1992: Terrane accretion in the internal zone of the Ungava orogen, northern Quebec. Part I: Tectonostratigraphic assemblages and their tectonic implications; Canadian Journal of Earth Sciences, v. 29, p. 746-764.

Stubley, M.
1996: Carp Lakes (85P) - Preliminary geological compilation; EGS 1996-03 Carp Lakes (85P), Indian and Northern Affairs Canada, Yellowknife, Northwest Territories.

Thompson, P.H. and Kerswill, J.A.
1994: Preliminary geology of the Winter Lake - Lac de Gras area, District of MacKenzie, Northwest Territories; Geological Survey of Canada, Open File 2740, scale 1:250 000.

Thompson, P.H., Russel, I., Paul, D., Kerswill, J.A., and Froese, E.
1995: Regional geology and mineral potential of the Winter Lake – Lac de Gras area, central Slave Province, Northwest Territories; in Current Research 1995-C; Geological Survey of Canada, p. 107-119.

Thorpe, R.I., Cumming, G.L., and Mortensen, J.K.
1992: A significant Pb-isotope boundary in the Slave Province and its probable relation to ancient basement in the western Slave Province; in Project Summaries, Canada-Northwest Territories Mineral Development Subsidiary Agreement 1987-1991, (ed.) D.G. Richardson and M. Irving; Geological Survey of Canada, Open File 2484, p. 179-184.

van Breemen, O., Davis, W.J., and King, J.E.
1992: Temporal distribution of granitoid plutonic rocks in the Archean Slave Province, northwest Canadian Shield; Canadian Journal of Earth Sciences, v. 29, p. 2186-2199.

Villeneuve, M.E., Relf, C., Hrabi, B., and Jackson, V.
1994: Ages of detrital zircons from supracrustal sequences in the Slave Province, NWT, Canada: implications for age of basement; Geological Society of America 1994 Annual Meeting, Abstracts with Programs, v. 26, p. A-232.

Yamashita, K., Jensen, J.E., Creaser, R.A., and Gebert, J.S.
1995: Geology, geochemistry and Nd isotopic study of the Hanikahimajuk Lake area (NTS 86 I/2, 86 H/14,15), northern Point Lake belt, Slave structural province, NWT; Geological Association of Canada, Program with Abstracts, v. 20, p. A-112.

Geological Survey of Canada Project 870008

Surficial geology and implications for drift prospecting, Hope Bay volcanic belt area, Northwest Territories

D.E. Kerr and R.D. Knight
Terrain Sciences Division

Kerr, D.E. and Knight, R.D., 1998: Surficial geology and implications for drift prospecting, Hope Bay volcanic belt area, Northwest Territories; in Current Research 1998-A; Geological Survey of Canada, p. 21-28.

Abstract: Surficial geology mapping and till sampling in Rideout Island and Elu Inlet map areas provide regional baseline data for drift prospecting and integrated environmental assessment planning in the Hope Bay volcanic belt. Raised marine sediments are the most widespread surficial sediment, although wave-washed till is extensive. Eskers, glaciofluvial outwash, and marine beaches are potential aggregate resources, but may contain segregated and massive ground ice. Dominant ice flow directions from the last ice movement range from west-southwestward to northward. In the northeasternmost regions, a predominant westward flow is recorded; an older northwestward flow may also have occurred but crosscutting relationships are ambiguous. Near the Hope Bay volcanic belt, effects of the dominant northwestward flow on dispersal patterns of volcanic pebbles in till are evident; lithological distributions reflect the predominant northwestward flow and suggest limited glacial transport. Potential massive ground ice in fine-grained marine sediments warrants geotechnical investigations prior to major development.

Résumé : La cartographie des dépôts meubles et l'échantillonnage du till dans la région de l'île Rideout et de l'inlet Elu fournissent des données régionales de base pour la prospection glacio-sédimentaire et la planification intégrée des évaluations environnementales dans la ceinture volcanique de Hope Bay. Les matériaux superficiels les plus répandus sont des sédiments marins soulevés; du till délavé est également répandu. Les eskers, les dépôts fluvioglaciaires et les plages marines sont des sources d'agrégats éventuels mais peuvent contenir de la glace de ségrégation et de la glace de sol massive. Les directions prédominantes d'écoulement glaciaire varient d'ouest-sud-ouest à nord. Un écoulement vers l'ouest est reconnu dans l'extrême nord-est, où un écoulement plus ancien pourrait aussi avoir eu lieu vers le nord-ouest. Près de la ceinture volcanique de Hope Bay, la distribution des cailloux volcaniques dans le till reflète l'écoulement glaciaire prédominant vers le nord-ouest et indique que la distance de transport a été limitée. En raison de la présence éventuelle de glace de sol massive dans les sédiments marins à grain fin, on recommande d'effectuer des études géotechniques avant d'entreprendre des travaux d'aménagement.

INTRODUCTION

Ongoing mineral exploration and development in the central and north Slave Province have resulted in the need for a wide range of baseline information (Fig. 1). In response, Terrain Sciences Division initiated regional surficial mapping through the Slave NATMAP Project to provide data on surficial materials, ice flow history, and till geochemistry. As an extension to the Slave NATMAP Project, surficial mapping continued during July 1997, focusing on the Hope Bay volcanic belt area in the north half of the Rideout Island and southwest quadrant of the Elu Inlet map sheets, excluding Kent Peninsula (76O and 77A, Fig. 2). The regional glacial geology was first presented by Blake (1963), and as part of a larger regional overview by Aylsworth and Shilts (1989).

METHODS

In order to provide regional coverage, the area was mapped by helicopter-assisted traversing following interpretation of 1:60 000 scale airphotos. From a total of 169 stations, 95 two-kilogram till samples were collected for trace element geochemistry and grain size determinations. At these 95 sites, 50 pebbles (2 to 6 cm in diameter) were also collected for provenance and glacial transport investigations. Locally, extensive blankets of surficial marine sediments preclude till sampling. Till was collected at depths of 0.3 to 0.7 m from hand-dug pits in mudboils. Where bedrock was exposed, striae were measured and rock type noted. Permafrost features, observations on bedrock weathering, and other geomorphic processes were identified at each station location in the map area.

REGIONAL SETTING

The Rideout Island/Elu Inlet map area lies in the north-central District of Mackenzie. Elevations range from 0 m (present-day sea level) to 319 m in the Buchan and Naujaat hills in the northwestern regions. The terrain in the western half of the map area rises abruptly inland from the coast southward and eastward, and generally reaches elevations of 100-200 m. Much of the area in the eastern regions, including the Koignuk River valley, is at elevations between <50 m and 100 m, with the notable exception of the northeasternmost regions where elevations reach 160 m. Local relief is variable, commonly between <5 m and 15 m in areas of outcrop and marine sediments, although it reaches >100 m in rocky areas of the Buchan and Naujaat hills.

Regional drainage is northward, into Melville Sound, with a minor westward flow towards Bathurst Inlet. The Koignuk River comprises the largest drainage system, forming a long north-trending basin up to 40 km or more in width. Its catchment area extends southward beyond the map area and its northern outlet drains into Melville Sound. Numerous small lakes occupy glacially scoured bedrock in the west, as well as isolated depressions in marine sediments and wave-washed till in the east. Most drainageways are shallow; few streams and rivers have cut into bedrock or surficial sediments, with the exception of the Koignuk River, which has incised marine and glaciofluvial sediments, and a few smaller unnamed rivers near the coast. The map area lies north of the treeline; sparse clumps of tundra heath vegetation are found in rocky areas. In regions underlain by fine-grained marine

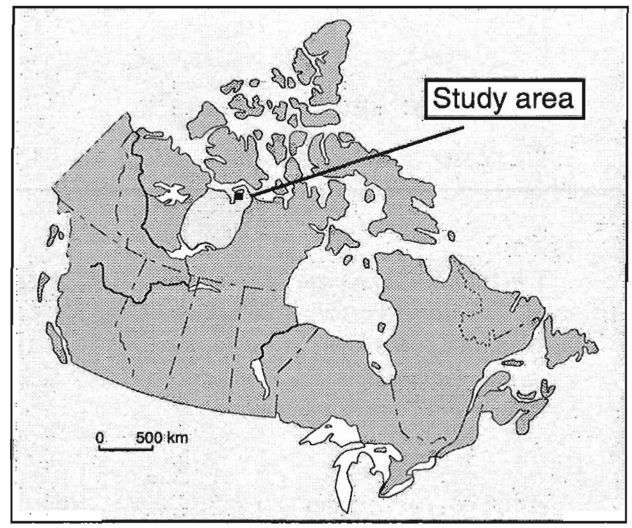

Figure 1. *Location of the study area within the northeast Slave Province (light gray shaded area).*

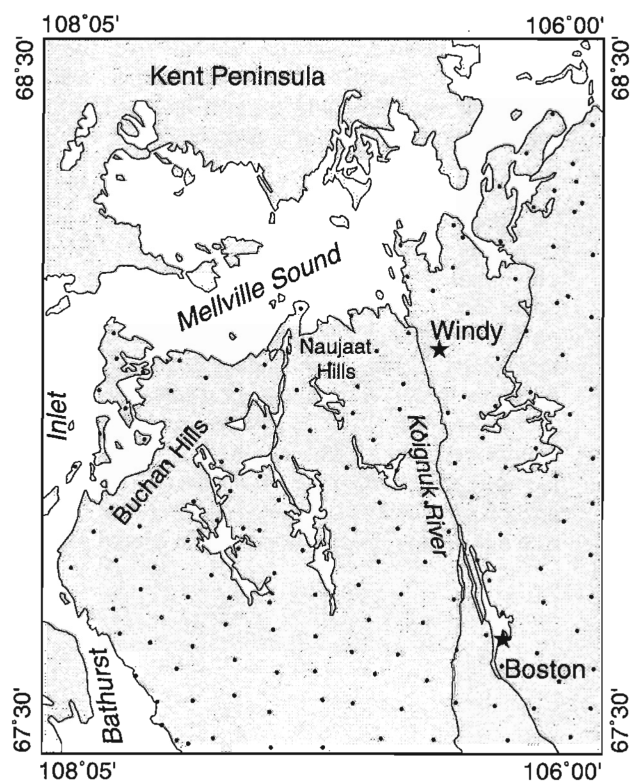

Figure 2. *Principal physiographic features and locations of field stations (black dots).*

sediments, low birch, alder, and peat predominate in areas of poor drainage. The Rideout Island/Elu Inlet region is within the zone of continuous permafrost (Brown, 1967). Climatic data from an Atmospheric Environment Service weather station operating at Cambridge Bay (120 km to the northeast) indicate an annual daily air temperature of -15°C (Atmospheric Environment Service, 1982).

BEDROCK GEOLOGY

The study area falls within the Bathurst Block of the northeastern Slave Province. Bedrock geology is generalized in Figure 3; material consists primarily of Archean volcanic and granitic rocks, Proterozoic sedimentary rocks and gabbro sills, and diabase dykes (Fraser, 1964; Roscoe, 1984). Economic interest is focused on the Hope Bay volcanic belt (Gebert, 1990, 1993), which is dominated by mafic volcanic rocks with minor felsic volcanic rocks, volcaniclastic rocks, metasedimentary rocks, and iron-formation that were metamorphosed from greenschist to amphibolite facies and intruded by widespread granite, granodiorite, and gneiss. Proterozoic sedimentary rocks include quartzite, siltstone, and minor conglomerate of the Burnside River Formation. Gabbro sills intrude the volcanic, granitic, and sedimentary rocks, as do the northwest-trending Mackenzie and Franklin diabase dykes. Many outcrops have been glacially sculptured and striated (Fig. 4a).

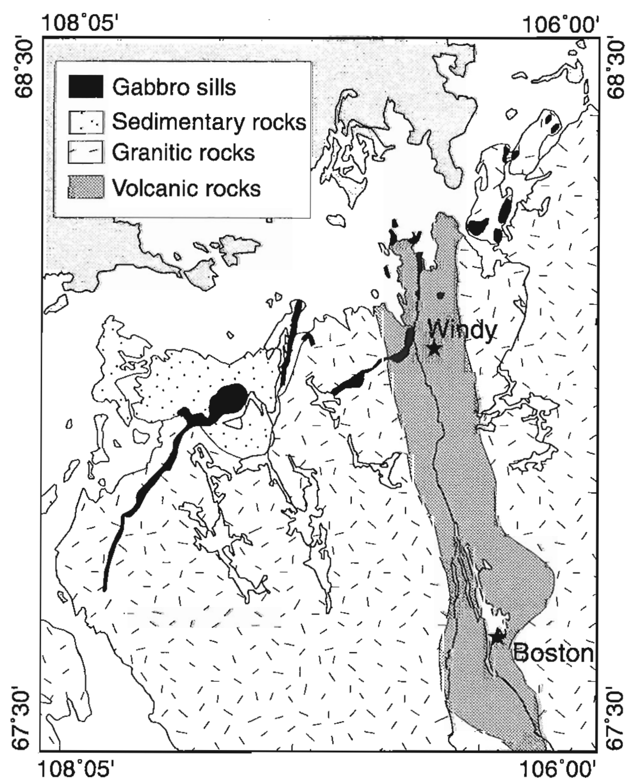

Figure 3. Generalized bedrock geology and selected mineral deposits, modified from Roscoe (1984) and Gebert (1993).

A number of mineral deposits associated with the Hope Bay belt occur in the study area, notably the Boston and Windy gold deposits, smaller gold showings associated with quartz veins in greenstone (Hope Bay, Brick, Lahti, Gunn), as well as copper prospects (Joe). The north end of the belt also hosts an abandoned silver mine where native silver ore was mined from veins.

SURFICIAL SEDIMENTS

Till

Till is a widespread Quaternary sediment in the map area but is not easily recognized on airphotos or in the field because of the effects of marine submergence following deglaciation, i.e., till was covered by marine sediments and/or reworked by marine processes. It consists of a silty to fine-grained sandy matrix-supported diamicton, and exhibits low to high compaction. It contains up to 50 per cent clasts, most exposures having between 10 and 30 per cent clasts, some of which are striated. Clasts range in size from small pebbles to large boulders, although medium to large pebbles predominate. Subangular to subrounded clasts are the most common.

Till veneers, generally <2 m thick, are common in more elevated, rocky areas with extensive bedrock outcrops such as the Buchan and Naujaat hills. They are generally loosely compact with high concentrations of cobbles and boulders at the surface; where the veneer is discontinuous, structural bedrock features are visible (Fig. 4b). In some areas, much of the fine-grained sediment in the matrix has been removed by meltwater and wave action, resulting in isolated lag deposits consisting of pebble- to boulder-sized clasts <2 m in diameter. Till veneers are the main surficial sediment above the limit of marine submergence (approximately 200-220 m a.s.l.). Till blankets are generally >2 m thick, form low- to moderate-relief drumlinoid and crag-and-tail features in the west-central and southeast regions (Fig. 4c), and tend to be relatively compact.

Glaciofluvial sediments

Glaciofluvial deposits consist of eskers, kames, and proglacial outwash. Eskers range from small sinuous ridges a few tens of metres long, to large, more linear features up to 15 km long. They generally trend northwest in the western regions and north-northwest to north in the eastern regions (Fig. 5). They are rare to absent in the northern half of the map area. Cobble and boulder lags, produced by wave action during postglacial marine regression, may cover eskers as well as bedrock surfaces between esker segments. Composition ranges from fine sand to cobbles, and may change rapidly over short distances. In the southern half of the map area, small outwash terraces are associated with the esker complexes. As with eskers, grain size in these terraces is varied. Esker-outwash complexes are generally parallel to the dominant glacial flow direction, and those within the Koignuk River valley may be characterized by raised beaches in their flanks (Fig. 4d). Such glaciofluvial deposits are potential sources for large volumes of granular material. However, the presence of permafrost typically results in the formation of ice-wedge

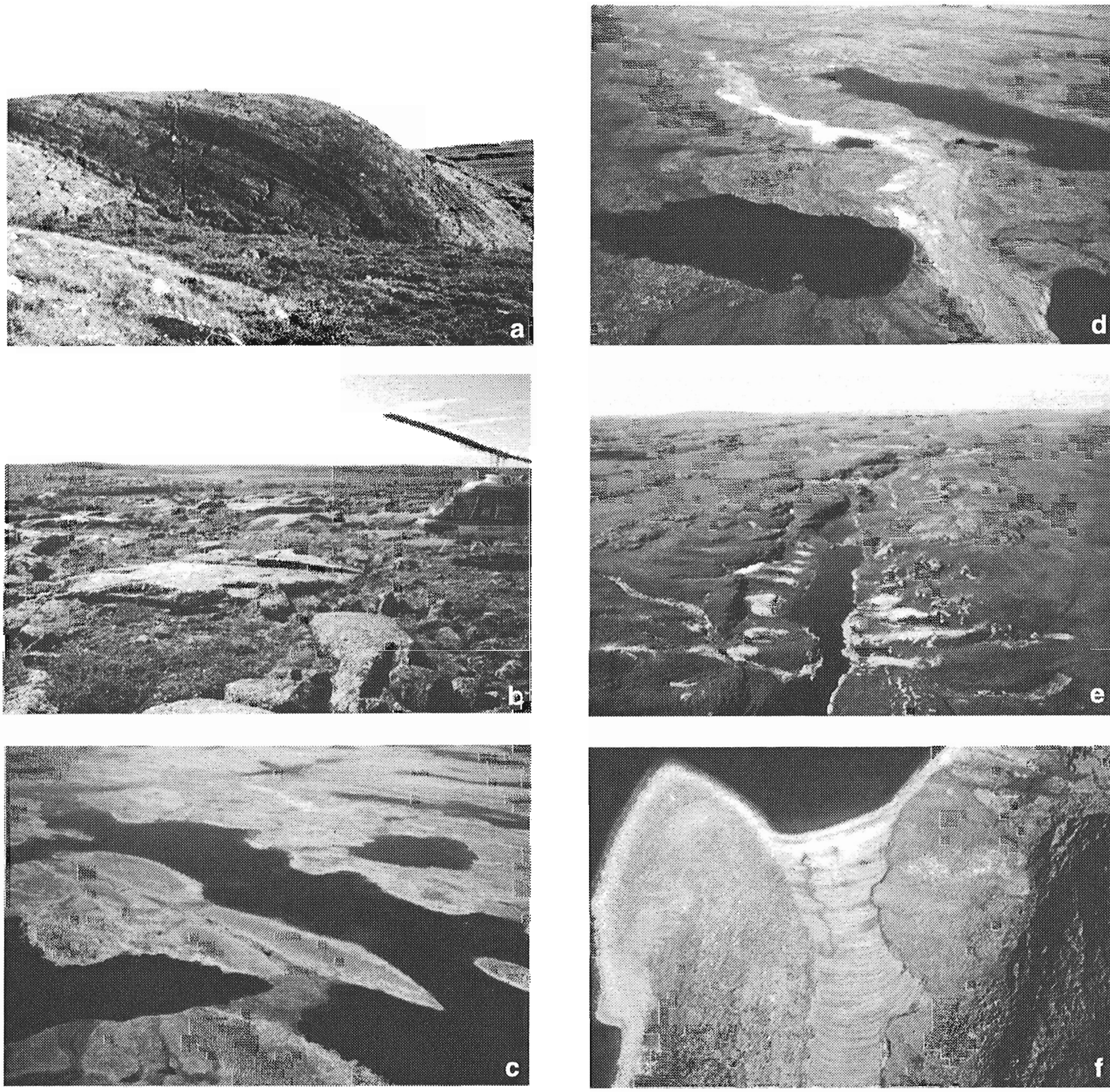

*Figure 4. (**a**) Glacially sculptured volcanic bedrock outcrop with grooves and striae, south of the Windy deposit (GSC 1997-67A). (**b**) Till veneer and granite bedrock outcrops west of the Koignuk River (GSC 1997-67C). (**c**) Northwest-trending fluted landform consisting of till blanket surrounded by till veneer (GSC 1997-67F). (**d**) Wave-washed northwest-trending esker with beach ridges (GSC 1997-67B). (**e**) Silty clay marine sediments along the Koignuk River. Note small thaw flowslides and unvegetated gullied exposures (GSC 1997-67D). (**f**) Sandy raised beaches (in centre) being covered by solifluction lobes creeping downslope (on left), south shore of Melville Sound (GSC 1997-67E)*

polygons in glaciofluvial sediments. Some eskers and outwash sediments are likely cored by massive ice, and geotechnical investigations should be conducted prior to any development.

Marine sediments

Marine sediments are the dominant surficial sediment in the map area. They are extensive along the coastal lowlands of Melville Sound, extending up to 75 km inland in the Koignuk River valley, and commonly occupy low bedrock areas along the coast of Bathurst Inlet. They provide evidence for postglacial marine inundation and subsequent emergence of approximately 220 m. They are primarily of three types: (1) undifferentiated, massive to well stratified clay and silt that may be overlain by a thin sand layer forming a blanket >2 m and up to 20 m or more thick; (2) a veneer ranging in composition from clay to sand and gravel <2 m thick that covers extensive regions below the marine limit; and (3) coarse sand, pebbles, and cobbles of littoral origin (raised beaches) found at various elevations from near marine limit to present sea level.

Permafrost has extensively affected marine sediments and evidence for this is widespread. In many areas along the coast, particularly within the Koignuk River valley, the fine-grained marine blanket deposits are gullied and devoid of vegetation. Retrogressive thaw flowslides are common along streams in this area, with active slides typically >10 m in diameter and headwalls 1-2 m high (Fig. 4e). Solifluction lobes are particularly active in fine-grained marine sediments. They show considerable sediment translocation, with lobes tens of metres long. Locally, significant downslope movement has occurred in recent times as evidenced by solifluction lobes encroaching on raised beaches near present sea level (Fig. 4f). Ice-wedge polygons are common on most raised beach and sandy littoral sediments. Where littoral sediments form laterally extensive veneers over marine silts or clays, tundra ponds and low-centre polygons are common.

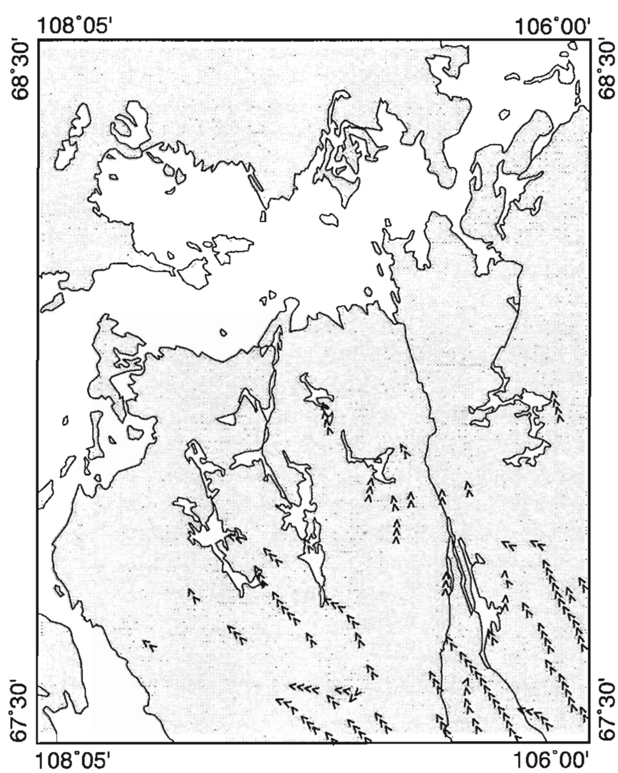

Figure 5. Glacial drainage system as defined by eskers and outwash sediments.

Alluvial sediments

Alluvial sediments comprise silt- to gravel-sized material deposited by postglacial streams and rivers. They range from massive to well stratified and vary in thickness from 1 to 5 m. They are associated with meandering and braided stream environments, as well as floodplains and alluvial fans.

Organic sediments

Organic sediments consist of peat formed by the accumulation of fibrous, woody, and mossy plant material up to 1 m or more in thickness, locally overlain by a dense grass cover. They occur predominantly in poorly drained topographic depressions and valley bottoms, and are most noticeable below the marine limit where they overlie fine-grained marine sediments. Ice-wedge polygons are common in organic sediments and are rooted in the underlying glaciofluvial or marine deposits. Frozen ground was encountered at depths as shallow as 0.10 m below the surface in peat in late summer.

ICE FLOW PATTERNS

Figure 6 is a summary diagram of ice flow direction based on airphoto identification of ice-streamlined landforms and 167 striae measurements, as well as on regional observations made by Blake (1963) in the Rideout Island/Elu Inlet map area. At a few locations in the northeast, crosscutting striae were noted, and their relationships record an early west-northwestward to north-northwestward flow (1 in Fig. 6), although the extent of this event is not known.

Throughout the southern and central study area, a strong pattern of ice flow radiating from the southeast (2 in Fig. 6) is apparent. Flow shifts clockwise from west-southwestward in the southwest region to westward, northwestward, and eventually north-northwestward in the northeastern region (2 in Fig. 6). This flow is responsible for the creation of all streamlined glacial landforms (drumlins and crag-and-tails) in the study area. Where Melville Sound meets Bathurst Inlet, the northwestward flow rotates anticlockwise to a westward flow. Westward flows were also recorded in the coastal zones of the northeastern region. Local variations in ice flow directions were encountered along the eastern edge of the Buchan Hills and are attributed to local topography that deflecting ice northward along major escarpments. Ice apparently flowed preferentially down the northwest-trending axis of the broad

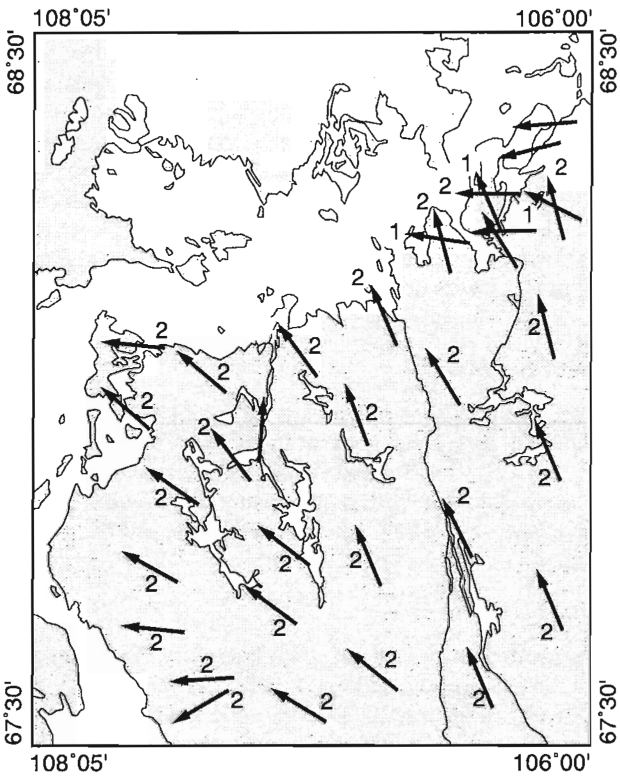

Figure 6. Summary ice flow diagram. 1=oldest flow, 2=youngest flow.

shallow valley containing the Koignuk River. A late focus of flow was also directed into Bathurst Inlet. The general radiating pattern for ice is reflected in the orientation of fluted landforms.

GLACIAL HISTORY

All glacial features in the study area relate to the Late Wisconsin glaciation. This region became ice-free by about 9000 BP (Dyke and Prest, 1987). The oldest reported striae (1 in Fig. 6) may represent a northwestward ice advance that occurred prior to the establishment of the dominant regional patterns, possibly during ice build-up. Alternatively, they may be related to early variations in the dominant, final, glacial ice flow (2 in Fig. 6). The youngest and most prominent westward to north-northwestward ice flow indicators (2 in Fig. 6) likely relate to the last phases prior to and during deglaciation, as shown by the distribution of eskers, which generally parallel this ice flow. The relative age of westward flows in the northeast and their relation to flows 1 and 2 are unclear.

During deglaciation, ice retreated rapidly from the study area; this ice retreat occurred simultaneously with the marine incursion across isostatically-depressed terrain. Little evidence exists in this region that can be used to precisely define marine limit elevation, but regional data suggest that the marine limit was approximately 220 m and was reached by 9000 BP (Kerr, 1994). The size and configuration of postglacial precursors of Bathurst Inlet and Melville Sound evolved as a function of isostatic uplift over the last 9000 years. As sea level dropped to successively lower elevations, numerous beaches were formed where suitable sediments for strandlines were present. It is believed that the region is still undergoing uplift.

PEBBLE LITHOLOGY PROVENANCE STUDIES

Because of their clearly defined source area, their economic importance, and the fact that they are easily distinguished from sedimentary and granitic clasts, volcanic rocks were chosen as indicators to illustrate patterns of glacial dispersal and estimate transport distances in aid to mineral exploration. Figure 7a shows the percentage (by count) and distribution of volcanic pebbles in till over the area. These pebbles occur at about 25 per cent of the 95 sites, most of which are underlain by volcanic rocks. Figure 7b shows the percentage of granitic pebbles that are found at all sample sites.

The expected distribution of volcanic pebbles involves a sharp decline in clast concentration down-ice from the source rock and bedrock contact, as illustrated by Shilts (1975) and others. This predicted pattern of clast-content attenuation is clearly evident. The pebble distribution map (Fig. 7a) shows that the dominant north-northwestward flow over the Hope Bay volcanic belt transported clasts northwestward onto granitic terrain to the west. The highest concentrations (up to 90 per cent) of volcanic clasts are found in areas underlain by volcanic bedrock. However, the number of clasts remains generally low (20-40 per cent) even over the volcanic belt itself. Concentrations decrease rapidly to <20-0 per cent approximately 10 km down-ice from the nearest source outcrops. Only 5 per cent of the sites record concentrations up to 8 per cent of volcanic clasts 45 km down-ice.

Granitic clasts are the dominant pebble lithology throughout most of the study area (Fig. 7b), with the majority of sites containing almost 90-100 per cent granite. They mask much of the volcanic belt and dilute the volcanic clast count. Only in the area underlain by sedimentary rocks do the granite clasts show any significant decrease in number, even though they are present as erratic boulders. The highest concentrations (up to 95-100 per cent) of granitic clasts are found east of the volcanic belt and in the south-central region. A slight decrease in concentration (to 80 per cent) east of Bathurst Inlet is the result of dilution by sedimentary clasts. These clasts may be associated with preexisting outcrops that were completely eroded during the last glaciation, or with unmapped bedrock covered by surficial sediments.

IMPLICATIONS FOR DRIFT PROSPECTING AND SUMMARY

Surficial geology mapping and till sampling in the Rideout Island/Elu Inlet map area (NTS 76O, north half; NTS 77A, southwest quadrant) provide regional baseline data for drift

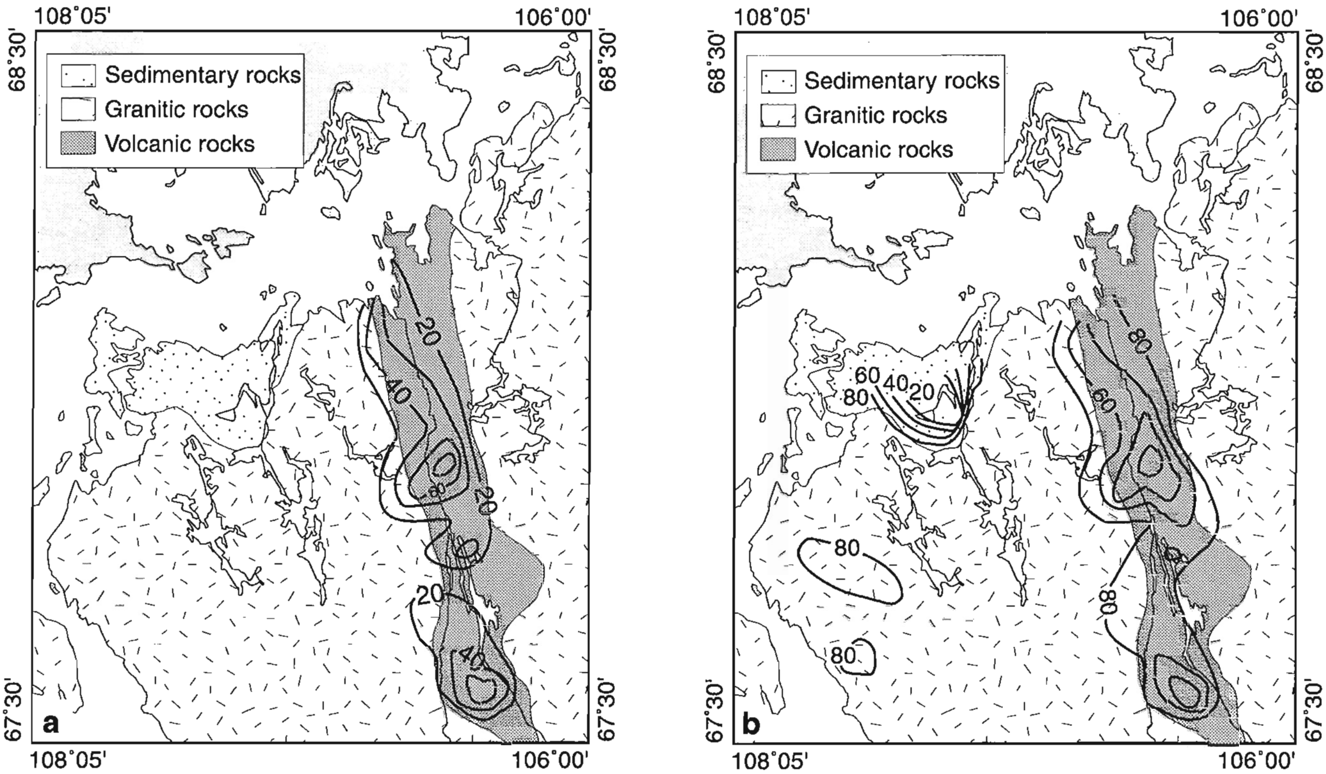

Figure 7. (a) Clast lithology map showing contoured percentages of volcanic pebbles in till with underlying bedrock geology. (b) Clast lithology map showing contoured percentages of granitic pebbles in till, with underlying bedrock geology.

prospecting and integrated environmental assessment planning. Marine sediments are the most widespread surficial deposit, although a till veneer also covers an extensive area. The similarity between the two units in this map area makes surficial geology mapping particularly difficult and poses a problem for drift prospecting. Both units can be represented by a wave-washed stony diamicton, which may or may not retain a geochemical signature indicative of underlying bedrock. The presence of thick fine-grained marine sediments masks much of the underlying till and bedrock. However, as noted by BHP Minerals Canada Ltd. geologists working in the area and by the authors of this study, it is possible in some cases to successfully sample till from these areas for geochemical purposes. In areas where bedrock protrudes from the marine blankets, a discontinuous ring of till can be found on the stoss and lee sides of some outcrops. With respect to infrastructure development, glaciofluvial deposits and certain raised beaches may serve as potential aggregate resources, but can contain significant thicknesses of massive ground ice. Dominant ice flow directions, corresponding to the last ice movement, range clockwise from west-southwestward to north-northwestward across the map area, and locally westward in certain coastal regions. The effects of the last ice flow (2) on the dispersal patterns of pebbles in till are evident since the distribution of pebble types reflects the predominant northwestward flow, with glacial transportation distances being generally less than 5 km except for far-travelled erratics (tens of kilometres). In addition, no evidence of the earlier flow (1) is found in the distribution of volcanic clasts west of the Koignuk River valley.

ACKNOWLEDGMENTS

The authors would like to thank the Polar Continental Shelf Project for providing helicopter support. Field accommodations and logistical support were provided by BHP Minerals Canada Ltd. at Wolverine and Windy camps. The authors would also like to thank Greg MacMaster, senior project geologist, BHP, for assisting with co-ordination, and D.A. Hodgson, GSC, for critical review.

REFERENCES

Atmospheric Environment Service
1982: Canadian climate normals, temperature and precipitation 1951-1980. The North: Yukon Territory and Northwest Territories; Environment Canada, Downsview, Ontario.

Aylsworth, J.M. and Shilts, W.W.
1989: Glacial features around the Keewatin Ice Divide: Districts of Mackenzie and Franklin; Geological Survey of Canada, Paper 88-24, 21 p.

Blake, W. Jr.
1963: Notes on glacial geology, northeastern District of Mackenzie; Geological Survey of Canada, Paper 63-28.

Brown, R.J.E.
1967: Permafrost in Canada; Geological Survey of Canada, Map 1246A (scale 1:7 603 200).

Dyke, A.S. and Prest, V.K.
1987: Paleogeography of northern North America 11 000–8400 years ago; Geological Survey of Canada, Map 1703A, 3 sheets (scale 1:12 500 000).

Fraser, J.A.
1964: Geological notes on Northeastern District of Mackenzie, Northwest Territories; Geological Survey of Canada, Paper 63-40.

Gebert, J.
1990: Geology of the Hope Bay and Elu Inlet metavolcanic belts, Bathurst Block, northeastern Slave province, Northwest Territories; in Exploration Overview 1990; Indian and Northern Affairs Canada, p. 26-27.

Gebert, J. (cont.)
1993: Geology and mineral potential of the Archean Hope Bay and Elu Inlet volcanic belts, northeastern Slave structural province, District of Mackenzie, Northwest Territories; part of NTS areas 76O/9, 10, 15, 16 and 77A/2, 3, 6, 7, 10; Indian and Northern Affairs Canada, Economic Geology Section, 1993-01.

Kerr, D.E.
1994: Late Quaternary stratigraphy and depositional history of the Parry Peninsula-Perry River area, District of Mackenzie, Northwest Territories; Geological Survey of Canada, Bulletin 465, 34 p.

Roscoe, S.M.
1984: Assessment of mineral resource potential in the Bathurst Inlet area, NTS 76J, K, N, O including the proposed Bathurst Inlet National Park; Geological Survey of Canada, Open File 788.

Shilts, W.W.
1975: Principles of geochemical exploration for sulphide deposits using shallow samples of glacial drift; Canadian Institute of Mining and Metallurgy Bulletin, v. 68, p. 73-80.

Geological Survey of Canada Project 920072

An update on the metallogeny of the Woodburn Lake Group, western Churchill Province, Northwest Territories[1]

J.A. Kerswill, S.P. Goff[2], L. Wilkinson[3], G.A. Jenner[4], B.A. Kjarsgaard, R. Bretzlaff, and C. Samaras[4]
Mineral Resources Division, Ottawa

Kerswill, J.A., Goff, S.P., Wilkinson, L., Jenner, G.A., Kjarsgaard, B.A., Bretzlaff, R., and Samaras, C., 1998: An update on the metallogeny of the Woodburn Lake Group, western Churchill Province, Northwest Territories; in *Current Research 1998-C; Geological Survey of Canada, p. 29-41.*

Abstract: The Woodburn Lake Group in the Third Portage and Pipedream lakes area (NTS 56E/4 and 66H/1) contains a spectrum of mineral occurrences including massive sulphide, polymetallic vein, vein gold and iron-formation-hosted gold, and several distinct varieties of sulphide-bearing iron-formation. Different types of occurrences are commonly found in the same area. Genetic links between massive sulphide and pyrrhotite-rich sulphide iron-formation, and between pyrite-rich oxide iron-formation and pyritic exhalite, are suggested by similarities in stratigraphic setting and lithogeochemical and geophysical signatures. Evidence in polymetallic vein occurrences for multiple generations of sulphide-bearing veins/fractures, and deformation of both veins and alteration zones, indicate that synvolcanic processes are likely to have contributed to metal concentration. Evidence in both pyrrhotite-rich and pyrite-rich varieties of gold-bearing sulphide iron-formation is consistent with synsedimentary/diagenetic sulphidation of oxide iron-formation at or just below the seafloor.

Résumé : Dans les régions de Third Portage et de Pipedream Lake (SNRC 56E/4 et 66H/1), le Groupe de Woodburn Lake renferme un large éventail d'indices minéralisés, notamment des sulfures massifs, des filons polymétalliques, de l'or filonien, de l'or encaissé dans des formations de fer rubanées et de nombreuses variétés distinctes de formations de fer rubanées à sulfures. Souvent, dans une même région, on observe différents types d'indices. Des liens génétiques entre les sulfures massifs et les formations de fer rubanées à sulfures riches en pyrrhotine de même qu'entre les formations de fer rubanées à oxydes riches en pyrite et les exhalites à pyrite sont suggérés par des similitudes quant à leur cadre stratigraphique et à leurs signatures lithogéochimique et géophysique. Les données sur les filons polymétalliques (qui permettent de supposer l'existence de plusieurs générations de filons/fractures à minéralisation sulfurée) et l'observation de la déformation des filons et des zones d'altération portent à croire que des processus synvolcaniques ont pu contribuer à la concentration des métaux. Les données relatives à deux variétés de formations de fer rubanées à sulfures minéralisées en or, soit celles riches en pyrrhotine et celles riches en pyrite, indiquent qu'elles dérivent de la sulfuration synsédimentaire/diagénétique de formations de fer rubanées à oxydes sur le plancher océanique ou à faible profondeur sous ce dernier.

[1] Contribution to the Western Churchill NATMAP Project
[2] Northwest Territories Geology Division, Department of Indian Affairs and Northern Development, Yellowknife, Northwest Territories
[3] Continental Geoscience Division, Ottawa
[4] Department of Earth Sciences, Memorial University, St. John's, Newfoundland

INTRODUCTION

The discovery of many gold occurrences in the Woodburn Lake Group in the 1980s (Laporte, 1987; Hearn, 1990), including iron-formation-hosted gold at the Meadowbank prospects (Davidson, 1996; Goff, 1997), has led to considerable interest in the economic geology of the area. This paper is a contribution to the mineral deposits/metallogenic component of the Western Churchill NATMAP program and is based on our work in the Third Portage and Pipedream lakes area. It presents highlights of petrographic and lithogeochemical investigations on rock samples collected during the 1996 field season, and additional information from field and laboratory work in 1997. A mineral occurrence map based on a compilation of mineral occurrence data for NTS sheets 56E/4 and 66H/1 is also provided. The overall objectives of this work are a) to identify metallogenic domains most favourable for the discovery of economic deposits within the Woodburn Lake Group; b) to develop better empirical exploration guides for these deposit types, through documentation of critical features of occurrences and their host environments; c) to help develop better genetic models for specific deposit types, e.g. iron-formation-hosted gold deposits; and, d) to help construct regional tectonostratigraphic models.

The geological and field context for the mineral deposit studies has been in part presented by Kjarsgaard et al. (1997) and Zaleski et al. (1997a, b). This contribution focuses on documenting gold, base-metal, and polymetallic occurrences, and several varieties of sulphide-bearing iron-formation. Metallogenic implications are also presented. A companion paper in preparation by Jenner at al. (unpub. data) will present more detailed information concerning the geology and mineral occurrences of the Pipedream Lake area. Previous detailed studies on iron-formation-hosted gold prospects in the Third Portage area were undertaken by Armitage et al. (1996) and Miller and Armitage (1992).

HIGHLIGHTS OF THE MINERAL OCCURRENCE COMPILATION

A compilation of public-domain information on mineral occurrences within the Woodburn Lake Group resulted in the capture of data for 118 occurrences in nine 1:50 000 topographic sheets. Eighty-three occurrences lie within 56E/4 and 66H/1 (Fig. 1), the area covered by Geological Survey of Canada Open File 3461 (Zaleski et al., 1997b) and this report. As noted by Hearn (1990), two northeasterly trending belts can be defined. The northern belt extends from Zing Lake to Hippo Lake; the southern belt extends from Third Portage Lake to the Ron gold occurrence. Three classes of mineral deposits have been identified by commodity. These are 1) gold occurrences containing 2000 ppb or more gold, but lacking anomalous concentrations of base metals, 2) base-metal occurrences containing about 1000 ppm or more copper and/or zinc and/or lead and/or nickel, but lacking in gold, and, 3) polymetallic vein occurrences containing significant gold, lead and/or zinc. The gold occurrences are widespread, and include structurally controlled vein-type gold in a variety of host rocks, as well as those hosted by sulphide-rich iron-formation (Third Portage, Goose Island and North Portage prospects in the Third Portage area, as well as the Moraine Lake and Herb Lake occurrences). The vein-type occurrences can be either arsenic-poor as at the Hippo and Lakeshore occurrences or arsenic-rich as at the Donna and Ron occurrences, whereas gold-rich sulphide iron-formation is typically arsenic-poor. The base-metal occurrences are fewest in number and include the volcanic-associated pyrrhotite-rich massive sulphide accumulations discovered in the Pipedream Lake area in 1996 (Kjarsgaard et al., 1997) and 1997 (Jenner et al., unpub. data). These are mostly stratiform accumulations in interlayered felsic and komatiitic volcanic rocks and associated volcaniclastic sedimentary rocks. Polymetallic veins (Sheba, Horace, Tern Lake, Cricket, Wally World, and Long Root occurrences) are more widely distributed than the massive sulphide showings and occur principally within felsic volcanic rocks or quartz-feldspar porphyry bodies of probable intrusive character. Molybdenite has been reported at five occurrences, including the Ron occurrence, and four on the Sheba property (two polymetallic vein, one base metal, and one gold).

HIGHLIGHTS OF FIELD INVESTIGATIONS

Sulphide-bearing iron-formation and related rocks

Several varieties of sulphide-bearing iron-formation recognized during field work in 1996 (Kjarsgaard et al., 1997) and 1997 are located on Figure 1. These include a) cherty, pyrrhotite-rich, iron-formation in which laterally extensive pyrrhotite is spatially associated with iron-silicate-rich bands (i.e. Drizzle Bay, South Sheba, West BIF, and Farside Lake), b) pyrrhotite-rich, oxide iron-formation in which pyrrhotite is dominantly intergrown with magnetite in well laminated, cherty, oxide iron-formation (i.e. Third Portage, Goose Island, and North Portage), and, c) cherty, pyrite-rich, oxide iron-formation in which pyrite dominantly replaces magnetite adjacent to both discordant quartz veins and bedding-parallel quartz veins and/or cherty layers (i.e. Pipedream Lake area). For the pyrrhotite-rich occurrences (a and b) the distribution of pyrrhotite is not controlled in any consistent way by late structures (veins or shear zones). In addition, locales of pyritic exhalite (well laminated, thin, but laterally continuous units containing alternating layers of quartz and pyrite) were identified in the Pipedream Lake area. Photographs of representative slabs of sulphide iron-formation and pyritic exhalite are presented in Figures 2 through 5.

Polymetallic vein occurrences

Quartz-sericite schist with disseminated to fracture-filling pyrite hosts or occurs in the immediate vicinity of polymetallic veins at Sheba, Horace, and Long Root occurrences. Similar rocks were noted in the vicinity of arsenopyrite-bearing quartz veins at the Donna occurrence. Several small patches of rusty quartz-sericite schist show tight folds on Donna and sericite is intensely crenulated in samples from the Sheba and Donna occurrences.

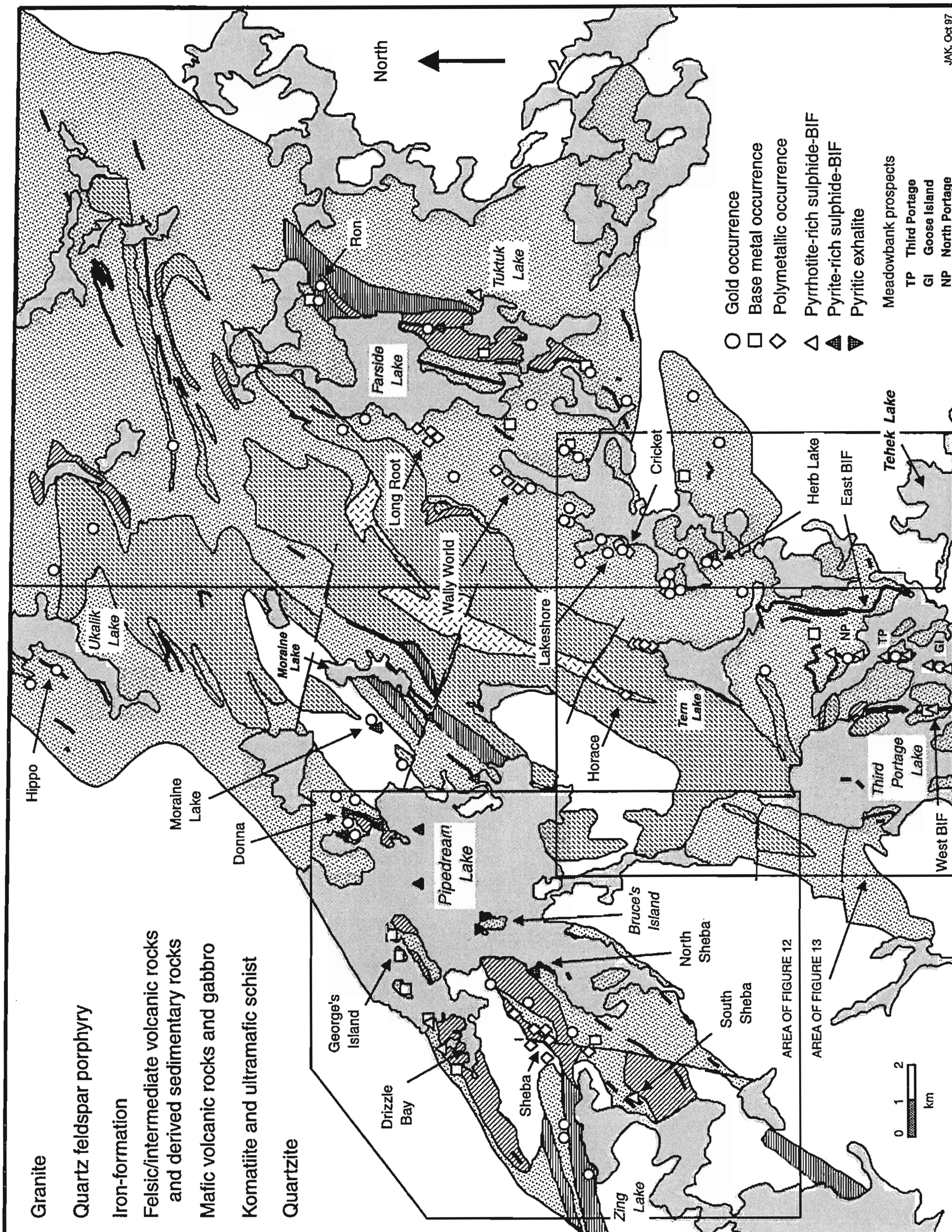

Figure 1. Mineral occurrence map for NTS sheets 56 E/4 and 66 H/1.

At the Horace occurrence, the mineralized zone is about 50 m long and 5 m wide, and is best described as an enigmatic sulphide-bearing siliceous zone within altered intermediate to felsic tuffs near quartzite. The siliceous zone contains mostly layer/foliation-parallel pyrite-rich accumulations, with minor galena, chalcopyrite, and fluorite, that are spatially associated with boudinaged cherty bands and/or layer-parallel quartz veins as well as some later discordant quartz veins. The occurrence might represent a deformed stringer zone that was once beneath a massive sulphide deposit.

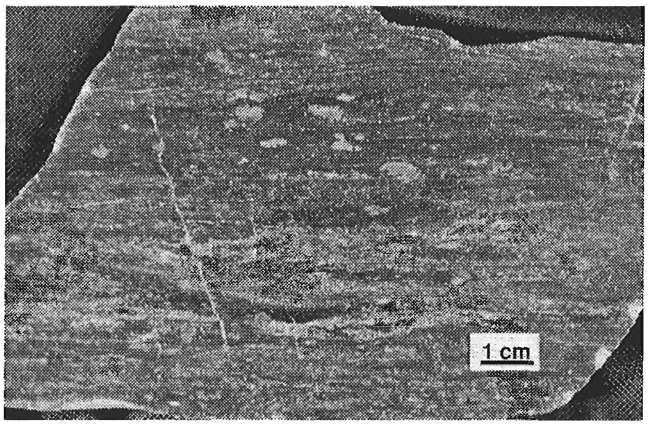

Figure 2. Cherty pyrrhotite-rich oxide-poor iron-formation from the Drizzle Bay area in which pyrrhotite occurs in garnetiferous bands.

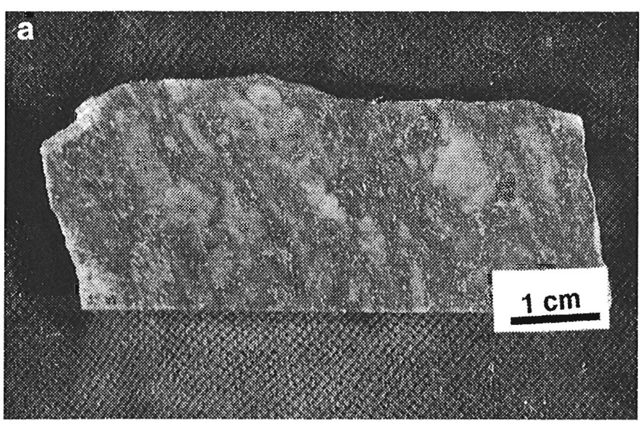

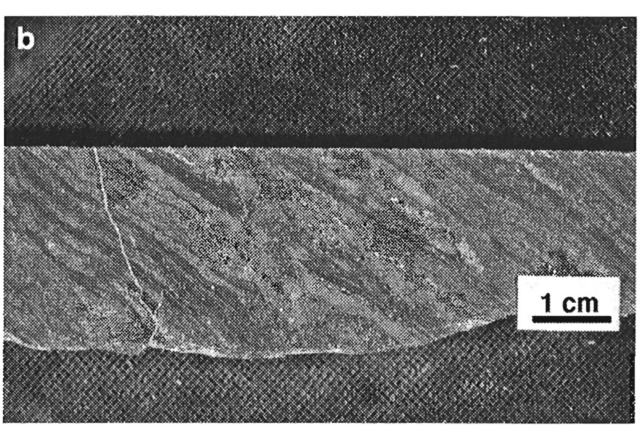

***Figure 3.** Pyrrhotite-rich oxide iron-formation from the Goose Island prospect (**a** and **b**) in which magnetite (medium grey) is replaced by pyrrhotite (light grey).*

A brief visit to the occurrences near the north end of Tern Lake indicated that the mineralization is spatially associated with one or more, largely layer/foliation-parallel, boudinaged, sulphide-bearing quartz veins that are 15 to 20 cm thick. Although exposure north of the lake is poor, the veins might be continuous over a distance of about 1 km. The veins are hosted by biotite-chlorite schist (possible intermediate tuff) that has interbeds of cherty carbonate-magnetite banded iron-formation and talc-bearing schist (possible mafic to ultramafic flow or sill). Pyrite is the principal sulphide, but chalcopyrite, sphalerite, galena, and arsenopyrite are locally abundant.

HIGHLIGHTS OF PETROGRAPHIC INVESTIGATIONS

Extensive examination of slabs cut from sulphide-bearing iron-formation and pyritic exhalite reveals several important observations. In all three varieties of sulphide-bearing iron-formation,

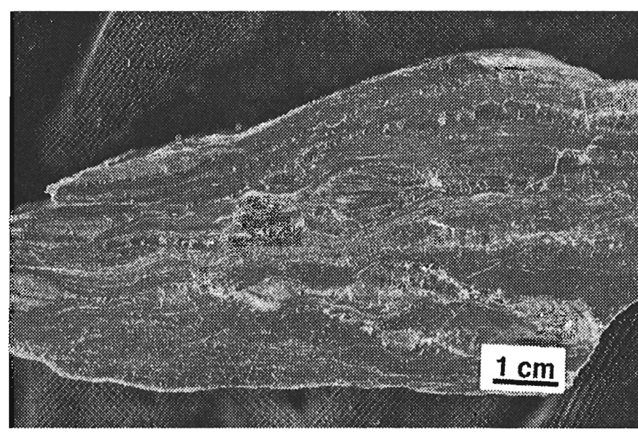

***Figure 4.** Pyritic oxide iron-formation from the Pipedream Lake area.*

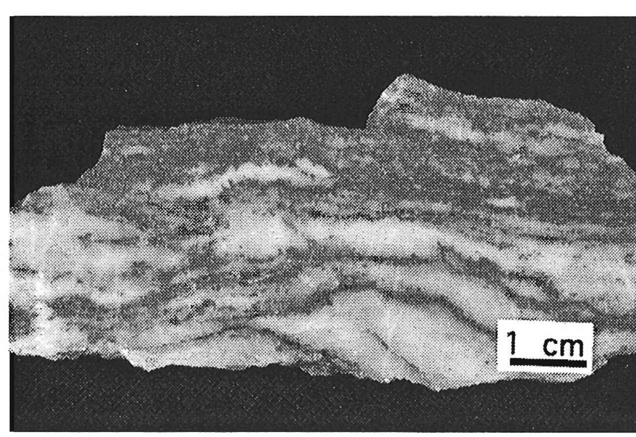

***Figure 5.** Typical pyritic exhalite from Pipedream Lake area.*

cherty layers and/or largely layer-parallel quartz veins commonly contain significant disseminated sulphide, and these sulphide-bearing layers/veins are typically tightly folded. We interpret this to imply that significant sulphide was present before folding in all varieties and in the two varieties developed in oxide iron-formation, sulphide distribution is not restricted to sulphidized magnetite-rich layers. In some samples of pyritic oxide iron-formation, both discordant quartz veins and bedding-parallel veins/cherty layers are tightly folded (Fig. 6), indicating that at least some discordant veins predate a folding event. Numerous slabs of pyritic exhalite contain thin to wispy bands of magnetite that appear to have been replaced by pyrite (Fig. 7).

In slabs of drill core and surface samples from The Sheba occurrence, some of the veins and fractures which contain galena and/or sphalerite are tightly folded (Fig. 8). Some samples show several generations of veins and fractures and several different styles of alteration.

Kjarsgaard et al. (1997) reported that during the 1996 field season grunerite/cummingtonite was identified at numerous locales of sulphide-bearing iron-formation beyond the area of the Meadowbank prospects. Reconnaissance studies of polished thin sections from all locations sampled in 1996 confirm that grunerite/cummingtonite is present in silicate-rich bands associated with pyrrhotite-rich iron-formation at South Sheba, Drizzle Bay, Farside Lake, and the West BIF occurrences. A green amphibole, tentatively identified as hornblende, was observed to be intergrown with, or to rim grunerite/cummingtonite in these samples. Grunerite/cummingtonite appears to be less common in occurrences of

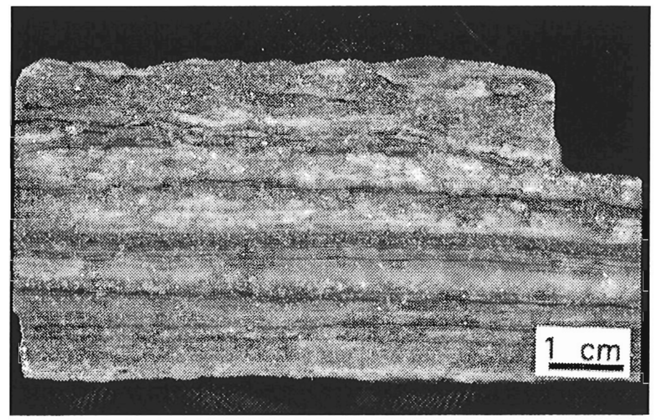

Figure 7. *Pyritic exhalite from Pipedream Lake area showing apparent replacement of magnetite bands by pyrite.*

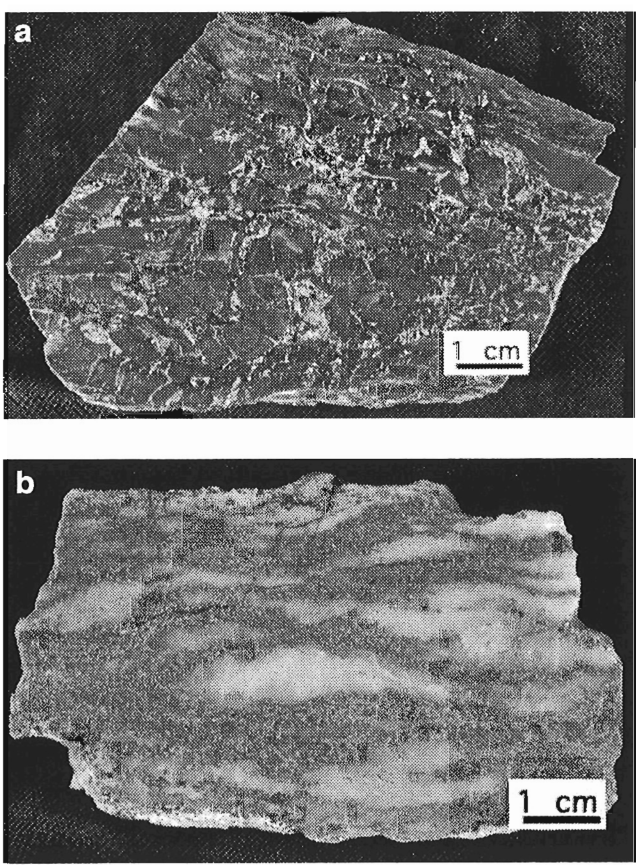

Figure 6. ***a)*** *Pyritic oxide iron-formation and* ***b)*** *pyritic exhalite from the Pipedream Lake area containing tightly folded pyritic chert layers or layer-parallel quartz veins.*

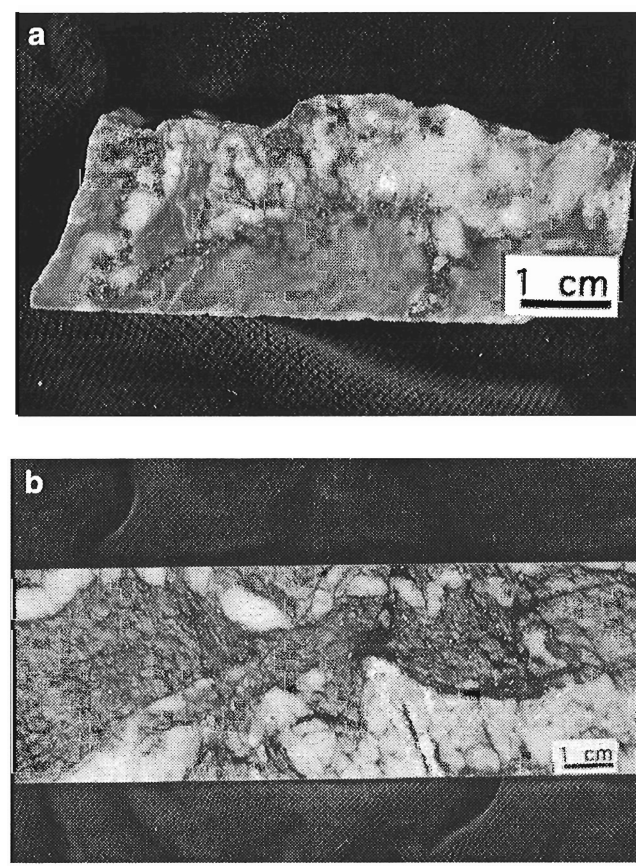

Figure 8. *Samples from Sheba polymetallic vein occurrence showing presence of deformed veins in quartz-sericite schist (**a** and **b**).*

pyritic oxide iron-formation, possibly because silicate-rich bands are rare to absent in such rock. No correlation was apparent between the distribution of gold and the distribution of grunerite/cummingtonite/hornblende.

HIGHLIGHTS OF LITHOGEOCHEMICAL INVESTIGATIONS

Visual inspection of whole-rock data on 32 elements obtained by ICP-MS on 135 samples collected in 1996 indicates significant lithogeochemical differences and similarities among the principal sulphide-bearing rock types of the study area. Nine elements were identified that are particularly useful in characterizing the different rock types: gold, nickel, zinc, silver, lead, copper, manganese, chromium, and vanadium. Several groups of interrelated elements were also identified. These include silver-gold with or without arsenic, nickel-cobalt-manganese with or without chromium and vanadium, and zinc-silver-lead with or without copper. Table 1 is an attempt to summarize the lithogeochemical character of the different sulphide-bearing rock types. Average and highest values for each of the nine elements are provided as indications of relative strength of the different element groups.

Samples from the massive sulphide occurrence discovered on George's Island, as well as from several similar occurrences in the vicinity, are gold-poor, but contain

Table 1. Means and highest values for Au, Ag, Cu, Zn, Pb, Ni, Co, Cr, Mn, V, Fe, and S for the seven principal sulphide-bearing rock types of the study area (<u>see</u> text) and for sulphide-poor oxide iron-formation from nine locales across the region (Fig. 1).

Rock Type	*Po[1]-rich massive sulphide*	*Po-rich S-BIF[2]*	*Po-rich mudstone/BIF*	*Po-rich oxide-BIF*	*Pyritic oxide-BIF*	*Pyritic exhalite*	*Pyritic quartz vein*	*S-poor oxide-BIF*
Locale[3]	PD	DB and SS	WBIF	TP	PD, ML and HL	PD	ML and TK	PD, ML, HL, TP, EBIF
Samples[4]	9	11	3	3	25	12	2	8
Au (Mean)	0.5	0.5	1	12173	2949	122	3145	2.3
Au (Highest)	0.5	0.5	2	17300	43800	634	3440	7
Ag (Mean)	2.0	0.5	1.9	2.9	1.7	2.8	2.0	0.6
Ag (Highest)	3.5	0.8	2.7	4.8	13.6	6.2	2.4	0.8
Cu (Mean)	409	390	373	25	126	61	239	24
Cu (Highest)	670	1010	598	29	602	157	353	48
Zn (Mean)	245	90	1585	30	42	50	36	61
Zn (Highest)	319	146	2990	32	84	450	71	146
Pb (Mean)	15	3.9	35	20	23	101	30	14
Pb (Highest)	26	11	54	22	257	567	54	16
Ni (Mean)	1126	1246	74	72	23	118	40	5
Ni (Highest)	2580	4420	95	113	50	486	48	12
Co (Mean)	116	109	44	9	11	18	33	4
Co (Highest)	168	250	57	10	47	71	58	7
Cr (Mean)	128	1222	264	171	109	183	129	93
Cr (Highest)	244	2600	342	244	206	278	137	150
Mn (Mean)	4747	1364	138	794	782	179	405	509
Mn (Highest)	6210	2530	272	983	2240	657	527	986
V (Mean)	58	144	139	37	47	20	52	37
V (Highest)	80	248	207	40	119	26	62	63
Fe (Mean)	22.1	11.4	15.8	25.2	16.8	16.0	19.1	25.7
Fe (Highest)	29.3	17.3	18.6	26.3	26.4	25.1	23.0	30.2
S (Mean)	13.5	3.7	10.0	6.4	3.0	16.0	7.0	0.2
S (Highest)	20.7	7.5	12.9	10.0	19.5	29.6	12.1	0.3
Au-Ag[5]	-	-	-	+++	+ to +++	+	++	-
Ni-Co-Mn	+++	+++	-	-	-	-	-	-
Zn-Pb-Ag	+	-	+++	-	-	++	-	-

1 Pyrrhotite.
2 Iron formation.
3 PD, Pipedream Lake; DB, Drizzle Bay; SS, South Sheba; WBIF, West BIF; TP, Third Portage gossan; ML, Moraine Lake occurrence; HL, Herb Lake occurrence; TK, Tuktuk Lake; EBIF, East BIF.
4 Au is expressed in ppb, Fe and S in wt.%, all others in ppm.
5 Information is also presented on the three principal geochemical associations that were identified. The presence of anomalous values for the elements that constitute a particular association is indicated by a +. The presence of moderately and strongly anomalous values is indicated by ++ and +++, respectively. Background values for the elements that constitute a particular association are indicated by a -. For example, sulphide-poor oxide iron formation contains background values for all three associations.

anomalous concentrations of nickel, cobalt, manganese, copper, and zinc. Samples of the pyrrhotite-rich sulphide iron-formation from South Sheba and Drizzle Bay occurrences are also gold-poor and enriched in nickel, cobalt, copper, and manganese. Contents of chromium and vanadium are significantly greater than in the massive sulphide samples. The nickel contents at both locales exceed those reported by Laporte (1987, p. 112) from his samples of iron-formation in the Drizzle Bay area (400, 700, and 1200 ppm). In contrast, the three samples collected from the pyrrhotite-rich oxide iron-formation at the Third Portage prospect are gold-rich, but poor in nickel, cobalt, chromium, manganese, copper, zinc, and vanadium.

Samples of finely banded, cherty, pyrrhotite-rich rock (Fig. 9) that were collected from the western boundary of the West BIF occurrence, about 1 km west of the Goose Island prospect, contain less than 5 ppb gold, anomalous concentrations of zinc, lead, silver, copper, and vanadium, and sufficient iron (more than 15 wt. % Fe) to qualify as iron-formation. Contents of nickel, cobalt, manganese, and chromium are low. This locale is plotted on Figure 1 as a base-metal occurrence hosted by sulphide iron-formation. The rocks might be described as pyrrhotite-rich 'exhalite'.

Several samples of pyritic 'exhalite' from the Pipedream Lake area contained anomalous concentrations of one or more of gold, lead, silver, and zinc. Iron contents consistently greater than 15 wt. % indicate that these rocks can be interpreted as a variety of sulphide iron-formation.

Samples collected from two already-known iron-formation-hosted gold showings outside the Meadowbank area returned assays equal to or greater than previously reported values. Pyritic and locally arsenopyrite-bearing oxide iron-formation from just west of Moraine Lake ranged from 27 to 43 800 ppb and included values of 32, 288, 307, 313, 333, 349, 552, 1170, 1260, 1420, 2140, 2280, 3080, 5520, and 5790 ppb Au. A pyrite-rich quartz vein assayed 3440 ppb Au. Previously reported values were 240 and 4600 ppb Au (DIAND Assessment Report 082906). Pyritic oxide iron-formation near Herb Lake returned values of 17,

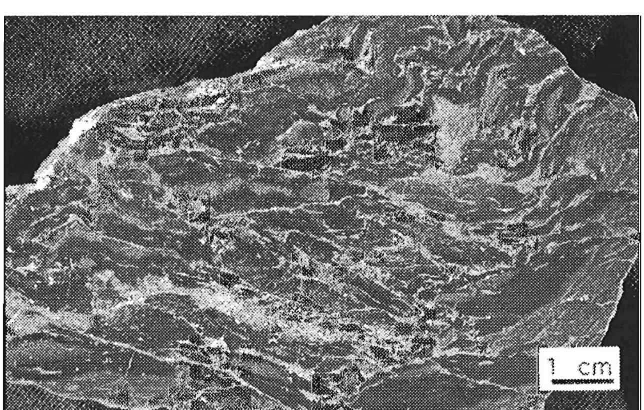

Figure 9. *Pyrrhotite-rich cherty mudstone/iron-formation from the West BIF occurrence.*

19, 321, 367, 1090, and 3020 ppb Au. Previously reported values included 7, 15, 19, 23, 82, 270, 790, and 1700 ppb Au (DIAND Assessment Report 082906).

Samples from iron-formation reported to have low gold values generally confirmed the previous assays. All nine samples from three sites along the East BIF occurrence (about 1.0 to 1.5 km east of Third Portage and North Portage prospects) returned values of less than 20 ppb Au. Seven of eight samples of variably sulphidic iron-formation from the West BIF occurrence returned assays of less than 1 ppb Au. The single anomalous sample from the West BIF occurrence returned an assay of 392 ppb Au. It was collected near the gold-poor samples, but was from a massive, coarse-grained, silicate iron-formation with disseminated pyrrhotite, rather than a cherty, well laminated, mixed silicate/oxide/sulphide iron-formation. This sample also contained anomalous concentrations of nickel, cobalt, chromium, and manganese.

Eleven samples were collected just north of Tuktuk Lake in the vicinity of a previous sample that returned an anomalous assay of 230 ppb Au (DIAND Assessment Report 082906). Seven samples of pyrite-bearing iron-formation returned gold contents of less than 1, 27, 29, 89, 100, 104, and 147 ppb; four samples of pyrrhotite-bearing iron-formation assayed 6, 12, 14, and 20 ppb Au. Further to the north, about midway between Farside and Tuktuk lakes, two samples of variably sulphidic mixed carbonate/oxide iron-formation returned quite variable results. One sample, which included a pyrite-rich quartz vein cutting locally pyritized oxide iron-formation, assayed 2850 ppb Au. The other sample, which did not include pyritic vein material, assayed 43 ppb Au.

Figure 10 illustrates the relationship between gold, nickel, and zinc for all samples from 56E/4 and 66H/1. The pyrrhotite-rich massive sulphide samples from the Pipedream Lake area and pyrrhotite-rich sulphide iron-formation samples from the Drizzle Bay and South Sheba occurrences overlap in composition, but are clearly distinct from pyrrhotite-rich oxide iron-formation at the Third Portage prospect, pyritic, oxide iron-formation and pyritic exhalite. Pyritic oxide iron-formation and pyritic exhalite samples plot in the central portions of both scattergrams. It is particularly noteworthy that some samples of pyritic oxide iron-formation are gold-rich (greater than 2000 ppb). These samples are from the Moraine Lake and Herb Lake locales (see above). The two samples of pyritic quartz veins from the Moraine Lake and Farside/Tuktuk lake areas (see above) overlap the gold-rich pyritic oxide iron-formation samples. Pyrrhotite-rich mudstone/iron-formation from the West BIF occurrence is most similar to the pyrrhotite-rich iron-formation from Drizzle Bay and South Sheba occurrences, and the pyrrhotite-rich massive sulphide occurrences in Pipedream Lake. Two of these samples contain the highest zinc contents (1610 and 2990 ppm) of all samples analyzed. As might be expected, sulphide-poor oxide iron-formation from across the region (small black dots, Fig. 10), as well as the two sulphide-poor samples from the Third Portage gossan, contain less than 10 ppb Au, 20 ppm Ni, and 100 ppb Zn.

HIGHLIGHTS OF GIS-RELATED WORK

Superimposed mineral occurrences and bedrock geology on Geological Survey of Canada regional (800 m line spacing) total field magnetic data reveal a number of interesting features. For example, the polymetallic occurrences in both northeast-trending belts lie within domains of low magnetic response that correspond dominantly with rocks mapped as intermediate or felsic to intermediate tuffs, crystal tuffs, lapilli tuffs, and breccias that are locally bedded and transitional to reworked volcaniclastic deposits (Fig. 11). Furthermore, the domain that hosts the polymetallic occurrences in the Wally World and Long Root areas appears to extend southwesterly to include the iron-formation-hosted gold prospects in the Third Portage area.

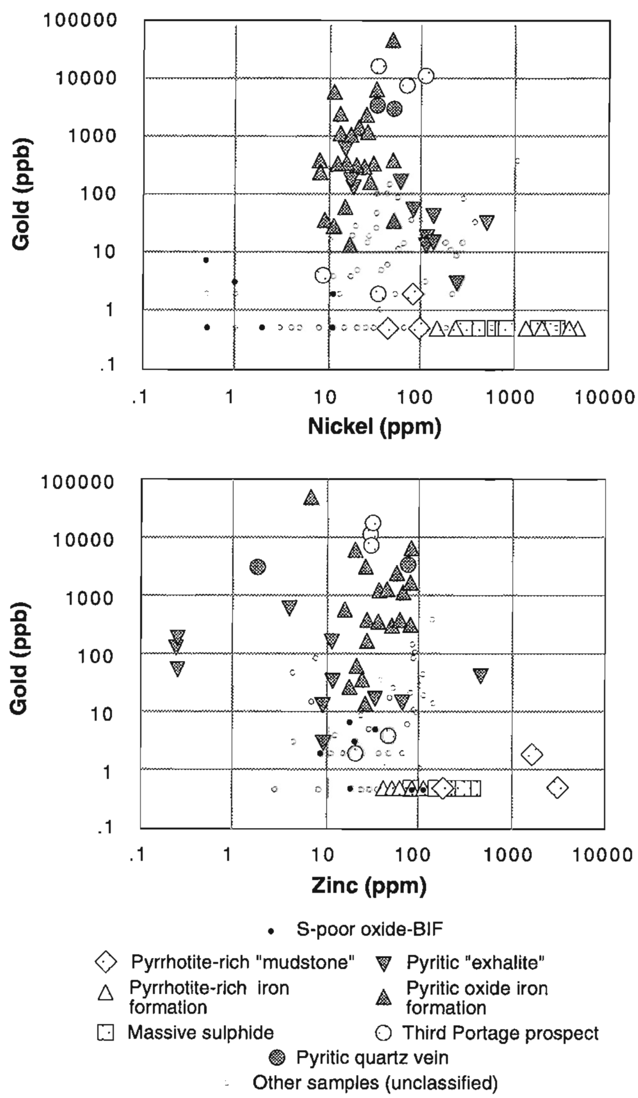

Figure 10. *Gold versus nickel and gold versus zinc scattergrams for all samples. The three samples from the Third Portage prospect that contain the high gold contents are pyrrhotite rich (see Table 1). The two samples from the Third Portage prospect that contain low gold contents are pyrrhotite poor and part of the sulphide-poor, oxide iron-formation population of Table 1.*

Examination of Figure 11 also indicates that areas of magnetic highs generally correspond with areas of known iron-formation although the magnetic anomalies are commonly much broader than the extent of mapped iron-formation. Conversely, some areas of known oxide iron-formation, including the gold-rich oxide iron-formation at Moraine and Herb lakes do not show up as magnetic anomalies on maps derived from widely spaced data. This is due to a scale problem related to the wide line spacing which can prevent detection of thin units, particularly those that are parallel to flight lines.

In the Pipedream Lake area, Geological Survey of Canada regional data merged with a high-resolution magnetic survey (100 m line spacing) by McChip Resources (Fig. 12) revealed that most of the occurrences of pyritic oxide iron-formation and pyritic exhalite are associated with a narrow, but pronounced and continuous northeast-trending magnetic anomaly that extends from the southern limit of coverage to southwest of the Donna property. In marked contrast, the pyrrhotite-rich sulphide iron-formation in the Drizzle Bay area falls within a smaller, much broader northeast-trending anomaly that is more diffuse and less continuous. The differences in the two magnetic anomalies are consistent with differences in the character of the iron-formation (weakly magnetic, pyrrhotite-rich, oxide-poor iron-formation near Drizzle Bay, versus highly magnetic, pyritic, oxide-rich iron-formation and pyritic exhalite to the south). There is only a weak magnetic response from the massive sulphide occurrence on George's Island.

Shaded relief maps of high-resolution data, in which differences in magnetic values are exaggerated, suggest the presence of complex fold-like patterns in the Third Portage area (Fig. 13) and enhance the sigmoidal geometry within the southern magnetic anomaly in the Pipedream Lake area that is suggested in Figure 12. In the latter, high resolution Geological Survey of Canada data (200 m line spacing) and Cumberland Resources high-resolution (nominal 50 m line spacing) gridded to 20 m were merged.

The gold-rich prospects at Third Portage, Goose Island, and North Portage occur within iron-formation that has a somewhat subdued magnetic response with respect to gold-poor iron-formation to the south and east (Fig. 13). The magnetic response associated with the gold occurrences is lower, narrower, and less continuous than that from the gold-poor iron-formation to the south and east. Indeed, the response over the occurrences is similar to the response over the West BIF occurrence.

METALLOGENIC IMPLICATIONS

The two mineralized belts contain representatives of all three deposit types as well as occurrences of sulphide iron-formation. The different deposit types are commonly found within the same geographical area and can be considered co-regional in the sense of Hutchinson (1993). This co-regionality suggests the possibility of genetic links between the different styles of mineralization.

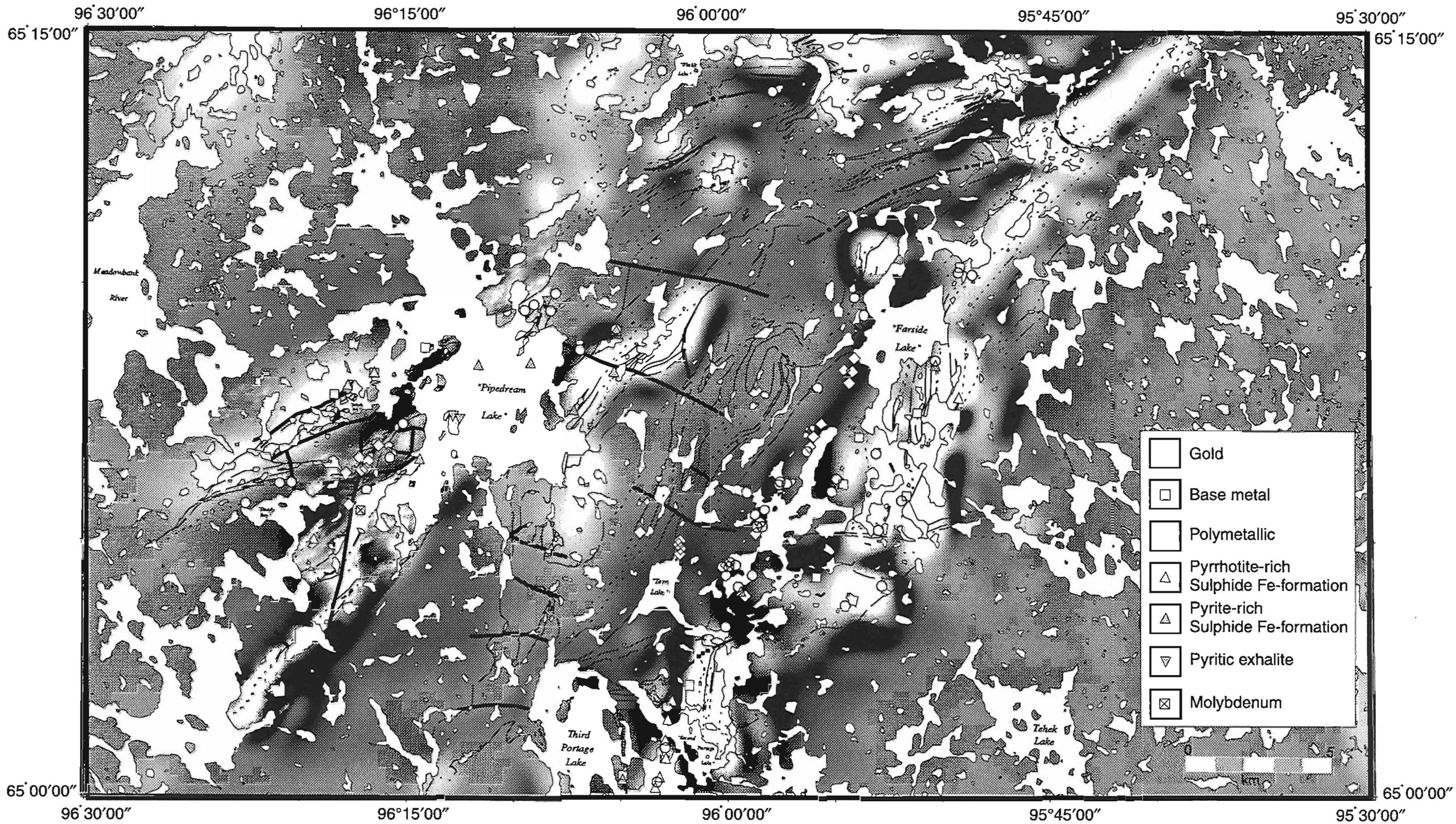

Figure 11. Total magnetic field map for the study area based on Geological Survey of Canada regional data.

Spatial, lithogeochemical, and geophysical linkages established between pyrrhotite-rich but gold-poor sulphide iron-formation, and base-metal-bearing pyrrhotite-rich massive sulphide in the Pipedream Lake area can be interpreted to indicate deposition of both rock types by synvolcanic/synsedimentary processes. A contribution by komatiitic volcanism is suggested by the anomalous concentrations of nickel and cobalt. Similarly, the spatial link between base-metal-bearing, pyrrhotite-rich, but gold-poor sulphide iron-formation, and gold-rich, pyrrhotite-rich sulphide iron-formation in the Third Portage area is consistent with deposition of at least some sulphide iron-formation by synvolcanic/synsedimentary processes.

There appears to be a continuum between many of the sulphide-rich rocks that occur in the study area, including pyrrhotite-rich massive sulphide, pyrrhotite-rich iron-formation, base-metal-rich pyrrhotite iron-formation, pyritic exhalite, pyritic oxide iron-formation and possibly gold-rich pyrrhotite-rich sulphide iron-formation. All these rocks may qualify as stratafers using the terminology developed by Gross (1986), who recognized spatial and genetic links between the processes that have concentrated a variety of metals in siliceous, iron- and sulphide-rich, largely stratiform sedimentary rocks.

The anomalous concentrations of zinc, lead, silver, and gold in some pyritic exhalites in the vicinity of known massive sulphide accumulations and polymetallic veins is consistent with a chemical sedimentary origin for these exhalites. The presence of very thin wisps/bands of magnetite in some samples suggests a genetic link between exhalites and cherty, oxide-rich, chemical sedimentary rocks. A primary synsedimentary origin is also consistent with the

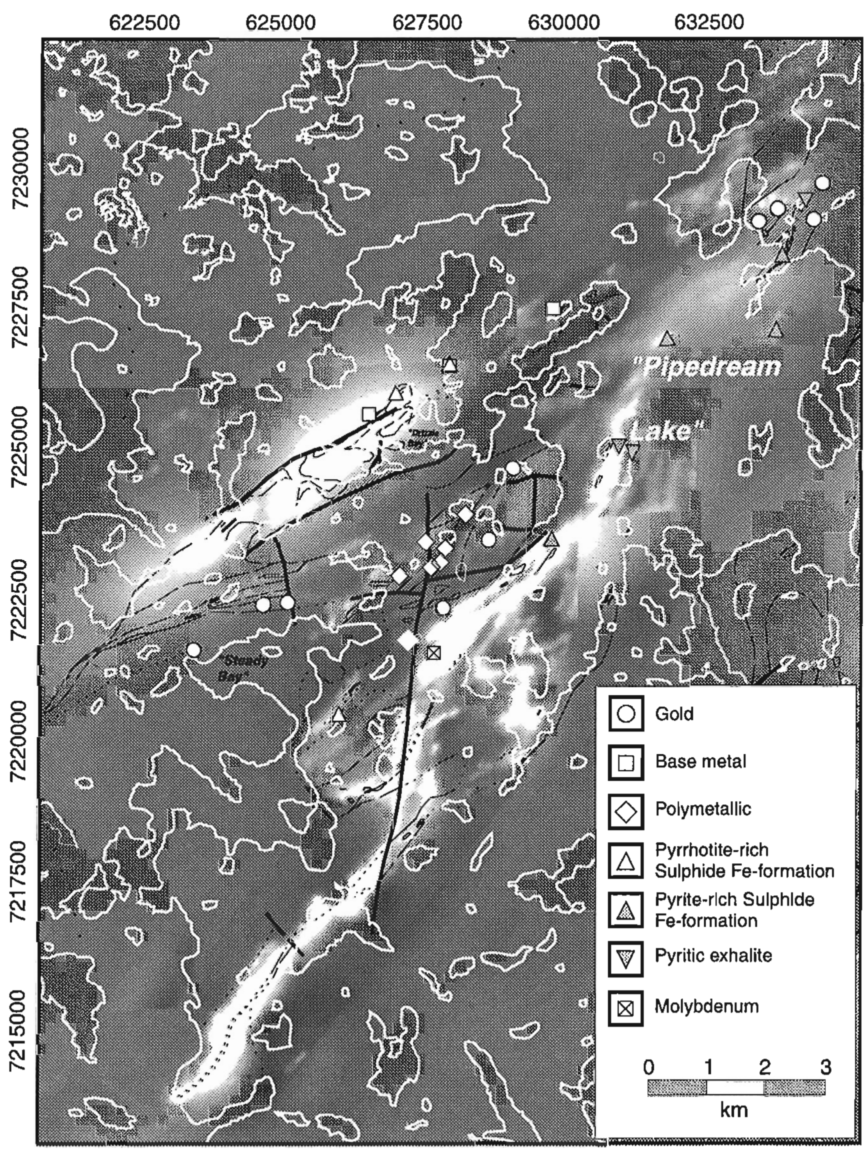

__Figure 12.__ Total magnetic field map for the Pipedream Lake area based on merged Geological Survey of Canada and McChip data.

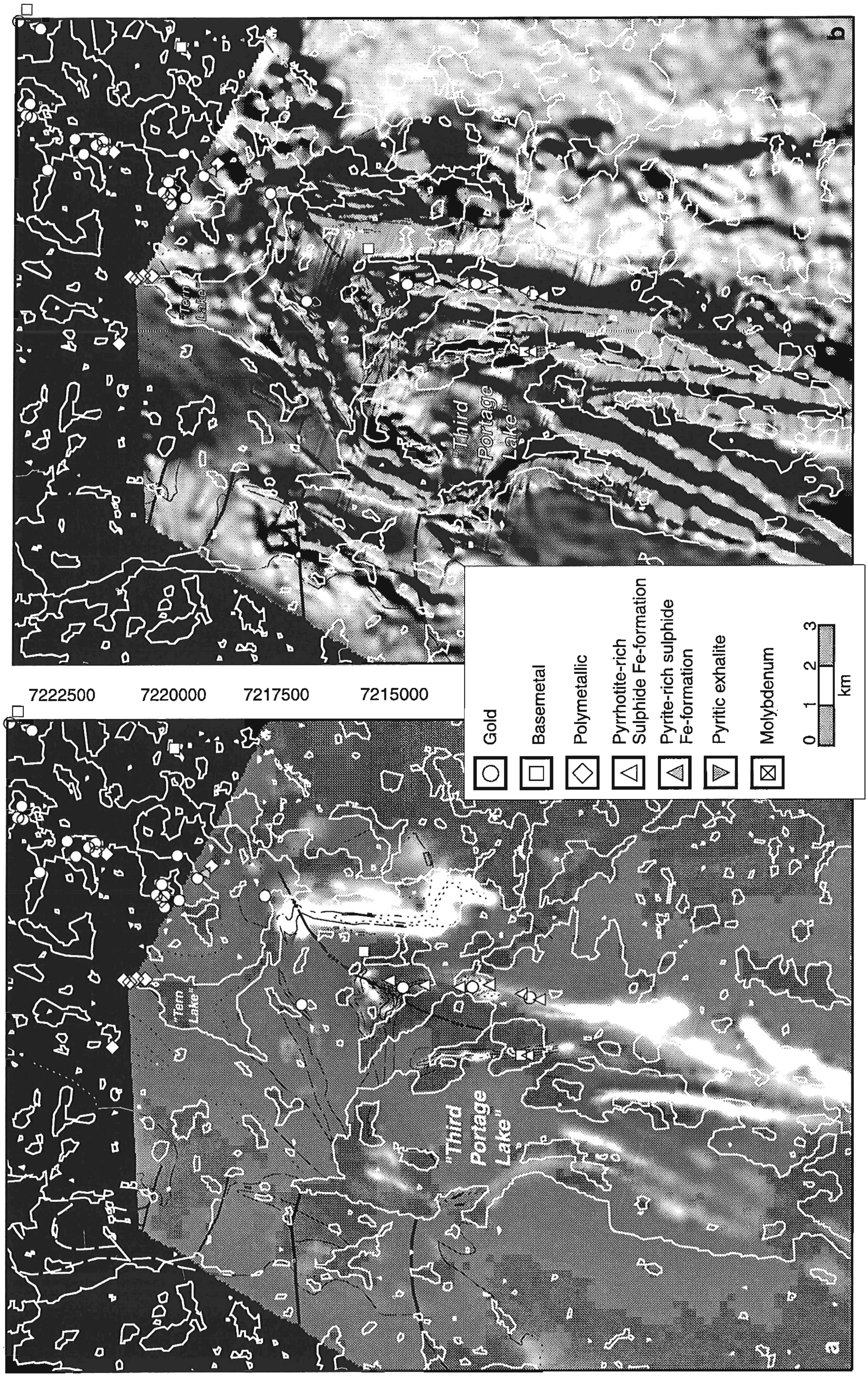

***Figure 13. a)** Total magnetic field map for the Meadowbank area based on merged Geological Survey of Canada and **b)** Cumberland data versus shaded relief total magnetic field map.*

presence of folded pyrite-bearing cherty bands/early bedding-parallel quartz veins and discordant quartz veins in pyritic oxide iron-formation. The apparent lack of control on the distribution of significant pyrite by late structures suggests that direct chemical precipitation and/or early sulphidation of iron oxide contributed to deposition of the contained metals (gold, silver, copper, lead, and zinc). This is in contrast to our previous suggestion that occurrences of pyrite-rich sulphide iron-formation were 'late' relative to occurrences of pyrrhotite-rich sulphide iron-formation (Kjarsgaard et al., 1997). However, both pyrrhotite and pyrite may have been concentrated by synsedimentary/diagenetic processes, possibly at different times.

The widespread distribution of grunerite/cummingtonite in gold-poor iron-formation suggests that at least some grunerite/cummingtonite is related to regional metamorphism rather than localized gold-related metasomatism. Armitage et al. (1996) interpreted all the grunerite/cummingtonite in the Third Portage area as a product of late structurally controlled sulphidation of oxide iron-formation.

Ongoing work on the Meadowbank prospects indicates that the deposits have features typical of both stratiform and non-stratiform iron-formation-hosted gold deposits as described by Kerswill (1993, 1996). The laterally extensive pyrrhotite-rich iron-formation and the absence of late structural control on the distributions of sulphur and gold are characteristic of Lupin-like stratiform ores. However, the abundance of oxide iron-formation and the ubiquitous textural evidence of magnetite replaced by pyrrhotite are essential features of non-stratiform ores. Our favoured model for the Meadowbank deposits includes synsedimentary/diagenetic sulphidation of permeable oxide-rich chemical sediments on or near the seafloor accompanied by deposition of significant gold. Our observations thus far do not support widespread direct precipitation of continuous layers of pyrrhotite-rich sulphide iron-formation onto the seafloor and do not preclude several stages of introduction of gold. Contrary to the suggestion of Armitage et al. (1996), no evidence has been seen to suggest that all the gold and sulphur at Meadowbank are spatially or genetically linked to Proterozoic shear zones. As noted earlier, the early sulphidation model may also be appropriate for the gold-bearing pyritic oxide iron-formation and pyritic exhalite occurrences in the study area.

EXPLORATION GUIDELINES

The relatively high gold contents of some pyritic oxide iron-formation samples indicates that exploration for iron-formation-hosted gold deposits need not be restricted to the search for pyrrhotite-rich Meadowbank-like targets.

The anomalous concentrations of zinc, lead, silver, and gold in some pyritic 'exhalites' in the vicinity of known massive sulphide accumulations, polymetallic veins, and iron-formation-hosted gold occurrences suggests that exhalites may be useful guides to mineralization.

Total field magnetic maps, particularly those based on relatively closely spaced flight lines, are useful in identifying and tracing units that are favourable hosts for various styles of mineralization. This has been demonstrated for many of the gold-rich polymetallic vein occurrences throughout the study area and for the gold-bearing pyritic oxide iron-formation in the Pipedream Lake area. Shaded relief maps can enhance complex structures as indicated in the area of Third Portage Lake.

The co-regionality of different styles of mineralization suggests that the presence of one type may be a useful exploration guide for another type. For example, massive sulphide and polymetallic vein occurrences may indicate potential for iron-formation-hosted gold deposits. The presence of gold-rich pyritic oxide iron-formation may be a favourable indicator for Meadowbank-like occurrences and vice versa. Pyrrhotite-rich base-metal occurrences, such as the zinc-rich but gold-poor mudstone/iron-formation associated with the West BIF occurrence, may indicate potential for nearby pyrrhotite-rich gold-rich oxide iron-formation, as at Meadowbank.

In view of the probable involvement of synsedimentary/diagenetic processes in the deposition of some gold in iron-formation, explorationists should consider documenting critical features of the sedimentary environment, including the distribution of all varieties of sulphide iron-formation, in their search for ore.

CONCLUSIONS

The Woodburn Lake Group is host to a spectrum of mineral occurrences including massive sulphide accumulations, polymetallic vein gold, vein gold, and iron-formation-hosted gold. Several distinct styles of sulphide iron-formation have been identified, including pyrrhotite-rich and pyrite-rich varieties (pyritic oxide iron-formation and pyritic exhalite).

Lithogeochemical data can discriminate between varieties of sulphide iron-formation in the Woodburn Lake Group, including gold-rich pyrrhotite-bearing iron-formation as at Third Portage, Goose Island, and North Portage; gold-poor pyrrhotite-bearing iron-formation with anomalous concentrations of nickel, cobalt, chromium, and manganese, as at South Sheba and Drizzle Bay occurrences; auriferous to gold-rich pyritic oxide iron-formation without anomalous concentrations of nickel, cobalt, chromium, and manganese, as in the Pipedream Lake area; and pyrrhotite-rich, but gold-poor sulphide iron-formation with anomalous concentrations of zinc, lead, silver, and copper, as in the West BIF occurrence near the Meadowbank prospects.

Much work must be done to better constrain the timing of the different styles of mineralization within the Woodburn Lake Group. Although it is clear that Archean synvolcanic/synsedimentary processes contributed directly to the accumulation of gold-poor massive sulphide and probably the gold-poor pyrrhotite-rich sulphide iron-formation in the Pipedream Lake and West BIF occurrence areas, the timing of gold introduction in the pyrrhotite-rich and pyrite-rich varieties of gold-rich sulphide iron-formation is still unresolved. Evidence to date suggests that synsedimentary/diagenetic sulphidation was responsible for concentration of at least some pyrrhotite, pyrite, and gold. A growing body of data suggests that the gold-rich polymetallic vein occurrences may be synvolcanic, but the timing of this mineralization relative to deposition of massive sulphide and sulphide-rich iron-formation is unclear. Evidence of several stages of gold introduction and remobilization in polymetallic vein and sulphide iron-formation occurrences complicates the building of valid genetic models.

ACKNOWLEDGMENTS

We would like to thank McChip Resources and Cumberland Resources for their support of our work. Access to their helicopters was essential for visiting mineral occurrences throughout the study area. Both companies provided high-resolution total field magnetic data that was merged with Geological Survey of Canada data from more widely spaced flight lines. We would also like to thank B. and L. Kotelewetz of Baker Lake Lodge for their extra efforts in providing for us and our rock pails. M. Henderson and E. Zaleski are thanked for their timely and constructive comments.

REFERENCES

Armitage, A.E., James, R.S., and Goff, S.P.
1996: Gold mineralization in Archean banded iron-formation, Third Portage Lake area, Northwest Territories, Canada; Exploration and Mining Geology, v. 5, no. 1, p. 1-15.

Davidson, G.I.
1996: Meadowbank gold project, an update; in Exploration Overview 1996; Northwest Territories, NWT Geology Division, Department of Indian Affairs and Northern Development, Yellowknife, p. 3-12 - 3-13.

Goff, S.P.
1997: Active advanced exploration projects in Nunavut; Canadian Miner, Flagship Edition, Vancouver, p. 13-33.

Gross, G.A.
1986: The metallogenic significance of iron-formation and related stratafer rocks; Journal of the Geological Society of India, v. 28 (2/3), p. 92-108.

Hearn, K.
1990: Baker Lake Project; in Mineral Industry report 1986-87; Northwest Territories, NWT Geology Division, Indian and Northern Affairs Canada, p. 88-93.

Hutchinson, R.W.
1993: A multi-stage, multi-process genetic hypothesis for greenstone-hosted gold lodes; Ore Geology Reviews, v. 8, p. 349-382.

Kerswill, J.A.
1993: Models for iron-formation-hosted gold deposits; in Mineral Deposit Modeling, (ed.) R.V. Kirkham, W.D. Sinclair, R.I. Thorpe, and J.M. Duke; Geological Association of Canada, Special Paper 40, p. 171-199.
1996: Iron-formation-hosted stratabound gold; in Geology of Canadian Mineral Deposit Types, (ed.) O.R. Eckstrand, W.D. Sinclair, and R.I. Thorpe; Geological Survey of Canada, Geology of Canada, no. 8, p. 367-382 (also Geological Society of America, The Geology of North America, v. F-1, p. 367-382).

Kjarsgaard, B.A., Kerswill, J.A., and Jenner, G. A.
1997: Lithostratigraphy and metallogenic implications of komatiite-banded iron-formation felsic volcanic rocks of the Archean Woodburn Lake group, Pipedream lake, central Churchill Province, Northwest Territories; in Current Research 1997-C; Geological Survey of Canada, p. 101-110.

Laporte, P.J.
1987: Tehek Lake Project; in Mineral Industry report 1984-85; Northwest Territories, NWT Geology Division, Indian and Northern Affairs Canada, p. 110-113.

Miller, A.R. and Armitage, A.
1992: Comparison of iron-formation-hosted gold mineralization at the Meliadine (Discovery Zone) and Meadowbank projects, District of Keewatin, NWT; in Exploration Overview 1992; Northwest Territories; NWT Geology Division, Department of Indian Affairs and Northern Development, Yellowknife, p. 35-36.

Zaleski, E., Corrigan, D., Kjarsgaard, B.A., Jenner, G., Kerswill, J.A., and Henderson, J.R.
1997: Preliminary results of mapping and structural interpretation from the Woodburn Project, western Churchill Province, Northwest Territories; in Current Research 1997-C, Geological Survey of Canada, p. 91-100.

Zaleski, E., Corrigan, D., Kjarsgaard, B.A., Kerswill, J.A., Jenner, G.A. and Henderson, J.R.
1997: Geology, Woodburn Lake Group, Meadowbank River to Tehek Lake (66H/1, 56E/4), District of Keewatin (Nunavut), Northwest Territories; Geological Survey of Canada, Open file 3461, scale 1:50 000.

Geological Survey of Canada Project 840003 wc

Geology of the McKellar Bay-Wight Inlet-Frobisher Bay area, southern Baffin Island, Northwest Territories

M.R. St-Onge, D.J. Scott, N. Wodicka, and S.B. Lucas
Continental Geoscience Division, Ottawa

St-Onge, M.R., Scott, D.J., Wodicka, N., and Lucas, S.B., 1998: Geology of the McKellar Bay-Wight Inlet-Frobisher Bay area, southern Baffin Island, Northwest Territories; in Current Research 1998-C; Geological Survey of Canada, p. 43-53.

Abstract: Metasedimentary rocks and orthogneiss of the McKellar Bay-Wight Inlet-Frobisher Bay area (southern Baffin Island) occur in recumbently folded and imbricated panels of a southwest-verging fold-thrust belt exposed along the hinge zone and southeastern limb of a regional crossfold antiform. Three principal tectonostratigraphic assemblages are recognized. At the lowest structural levels, in the hinge of the antiform, are layered monzogranite-granodiorite-tonalite orthogneiss with diorite and rare anorthosite (Narsajuaq arc) dated at 1.84-1.82 Ga. Marble, psammite, and semipelite of the 1.93-1.86 Ga Lake Harbour Group tectonically overlie this orthogneiss. A ca. 1.95 Ga dominantly monzogranite-tonalite orthogneiss (Ramsay River orthogneiss) occurs at the highest structural levels preserved on the limbs of the regional antiform, where it is imbricated with the structurally underlying Lake Harbour Group. Both the Lake Harbour Group and Ramsay River orthogneiss are intruded by the ca. 1.86-1.85 Ga Cumberland batholith.

Résumé : Dans la région de la baie McKellar-inlet Wight-baie Frobisher (partie sud de l'île de Baffin), des roches métasédimentaires et de l'orthogneiss se rencontrent dans des panneaux imbriqués et déformés en plis couchés d'une zone de plissement et de chevauchement à vergence sud-ouest qui est visible le long de la zone charnière et du flanc sud-est d'une antiforme majeure. Trois assemblages tectonostratigraphiques principaux sont reconnus. Aux niveaux structuraux les plus bas, dans la zone charnière de l'antiforme, un gneiss de composition monzogranitique, granodioritique et tonalitique avec diorite et anorthosite rare (arc de Narsajuaq) remonte à 1,84-1,82 Ga. Du marbre, de la psammite et de la semipélite du Groupe de Lake Harbour (1,93-1,86 Ga) sont séparés de l'orthogneiss sous-jacent par un contact tectonique. Aux niveaux structuraux les plus élevés sur les flancs de l'antiforme, sont imbriqués un gneiss de composition principalement monzogranitique et tonalitique (orthogneiss de Ramsay River), qui remonte à environ 1,95 Ga, et le groupe sous-jacent de Lake Harbour. Le batholite de Cumberland (environ 1,86-1,85 Ga) recoupe le Groupe de Lake Harbour et l'orthogneiss de Ramsay River.

INTRODUCTION

The third season of fieldwork for the South Baffin project focused on the Lake Harbour (NTS 25K) and southern Armshow River (NTS 25N) map areas, Meta Incognita Peninsula (Fig. 1, 2). Systematic bedrock mapping at 1:100 000 scale (1-2 km traverse spacing) has now been completed for the four NTS sheets (25K, L, M, N) in the project area. In addition, key areas first examined during the 1995 and 1996 field seasons were revisited for updated/enhanced additional field observations and sampling for geochemistry/geochronology. Bedrock geological investigations from the two previous field seasons (Hanmer et al., 1996a, b; Scott et al., 1996; St-Onge et al., 1996b, 1997a, b, c) are summarized in St-Onge et al. (1996a) and Scott et al. (1997). Mapping of the surficial deposits at 1:250 000 scale continued. The second phase of a regional aeromagnetic survey of the South Baffin–Hudson Strait area was completed in 1997.

This report presents an overview of the bedrock geology in the portion of the project area studied in 1997 and integrates observations with those made in previous years. The accompanying bedrock geology maps are GSC Open File maps 3536, 3537, and 3538 (St-Onge et al., 1998a,b,c). The results of ongoing supporting geochronological studies are reported by Wodicka and Scott (1997) and Scott and Wodicka (in press). Related thematic studies include a regional Nd-isotopic investigation (R. Thériault, GSC), a metamorphic study of the siliciclastic rocks in the area (I. Russell, Queen's University), a regional structural study of Big Island (D. Copeland, University of New Brunswick), and a detailed mapping project in the Lake Harbour Group north of Kimmirut (E. Piper, Memorial University).

GEOLOGICAL FRAMEWORK

The metasedimentary rocks and orthogneiss in the project area (Fig. 1, 2) are part of the northeastern (Quebec-Baffin) segment of the Paleoproterozoic Trans-Hudson Orogen (Lewry and Stauffer, 1990), which comprises tectonostratigraphic assemblages accumulated on, or accreted to, the northern margin of the Archean Superior Province during >200 Ma of tectonic activity (Lucas and St-Onge, 1992; Lucas et al., 1992; Scott et al., 1992, 1997; St-Onge et al., 1992, 1996a, in press; Scott, 1997, in press). Southern Baffin Island is characterized by three orogen-scale stacked tectonic elements (St-Onge et al., 1997d; Wodicka and Scott, 1997), which include the following map units (from lowest to highest structural level) (Table 1): Level 1, Superior Province basement and Povungnituk Group (St-Onge et al., 1996a); Level 2, Narsajuaq arc (Scott, 1997); Level 3, Lake Harbour Group (Jackson and Taylor, 1972), Ramsay River orthogneiss (see below), and Blandford Bay assemblage (Scott et al., 1997). The Cumberland batholith (Blackadar, 1967) has intruded all units in Level 3.

The map pattern on Meta Incognita Peninsula is largely controlled by interference between late orogenic, orogen-parallel folds (north- to northwest-trending) and crossfolds (northeast-trending). In the McKellar Bay-Wight Inlet-Frobisher Bay area (Fig. 2), at the lowest structural levels exposed along the antiformal hinge zone of a northeast-trending crossfold between Kimmirut and Barrier Inlet (Fig. 2), Level 2 comprises layered monzogranite-granodiorite-tonalite gneiss with diorite and rare anorthosite sheets. These units, dated at 1.84-1.82 Ga (Scott, 1997; Wodicka and Scott, 1997), have been correlated with the Narsajuaq arc in northern

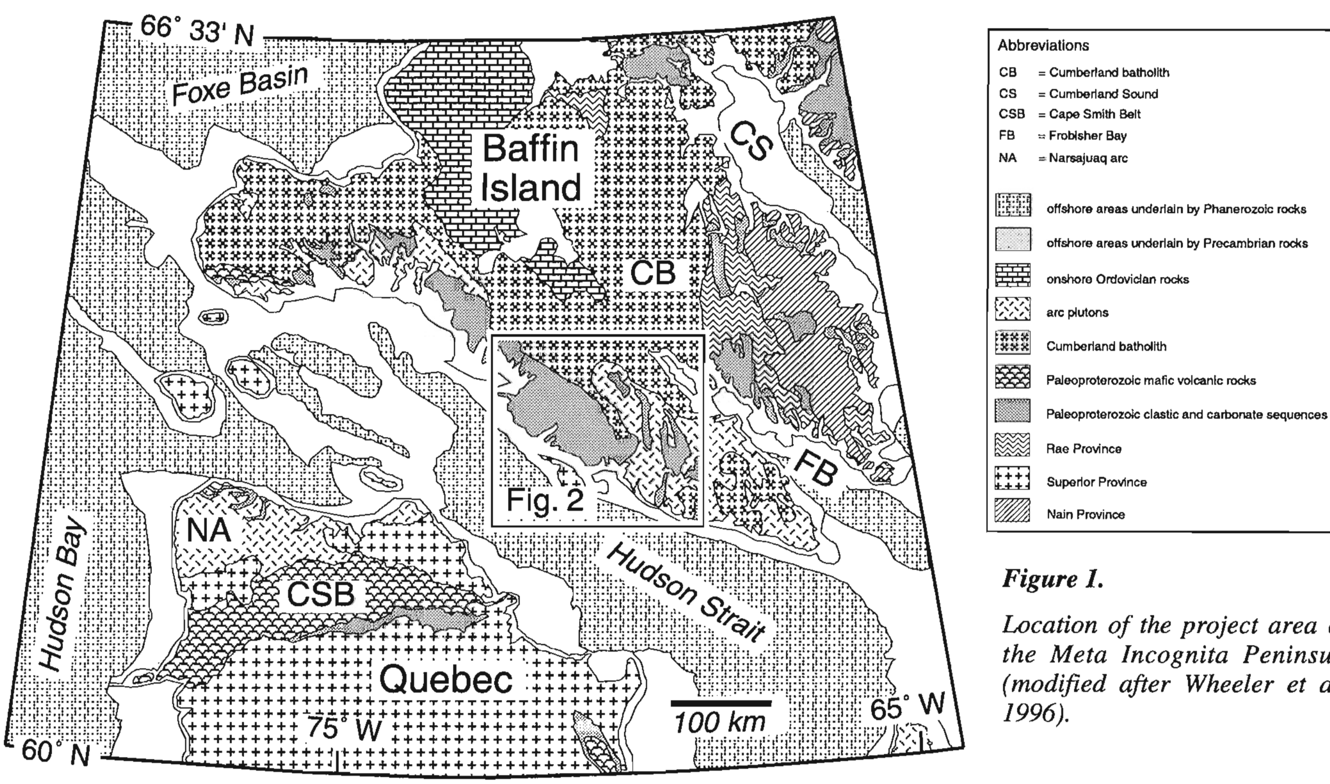

Figure 1.

Location of the project area on the Meta Incognita Peninsula (modified after Wheeler et al., 1996).

Quebec (St-Onge et al., 1992; Dunphy and Ludden, in press). The Lake Harbour Group, found in Level 3, tectonically overlies Level 2 and includes marble, psammite, and semipelite intruded by mafic and locally layered mafic-ultramafic sills (Scott et al., 1997). The youngest detrital zircons in the Lake Harbour Group are 1.93 Ga, whereas the group is cut by the 1.86 Ga Cumberland batholith (Scott and Gauthier, 1996; Scott, 1997). Along the antiformal hinge zone of the crossfold, Lake Harbour Group supracrustal units are preserved within Level 3 structural basins or klippen that result from the interference of the two regional fold sets (Fig. 2). In contrast, on the northwest and southeast limbs of the antiform, Lake Harbour Group rocks occur within kilometre-scale panels that are bounded by thrust faults (cf. Scott et al., 1997, and below). The dominantly monzogranitic to tonalitic gneiss mapped in Level 3 is informally referred to as the Ramsay River orthogneiss (Fig. 2). It is dated at ca. 1.95 Ga (Scott and Wodicka, in press) and is interpreted to be imbricated with units of the Lake Harbour Group. Both the Lake Harbour Group and the Ramsay River orthogneiss are intruded by monzogranite plutons of the Cumberland batholith (Fig. 2) dated at ca. 1.86-1.85 Ga (Jackson et al., 1990; Wodicka and Scott, 1997; Scott, in press).

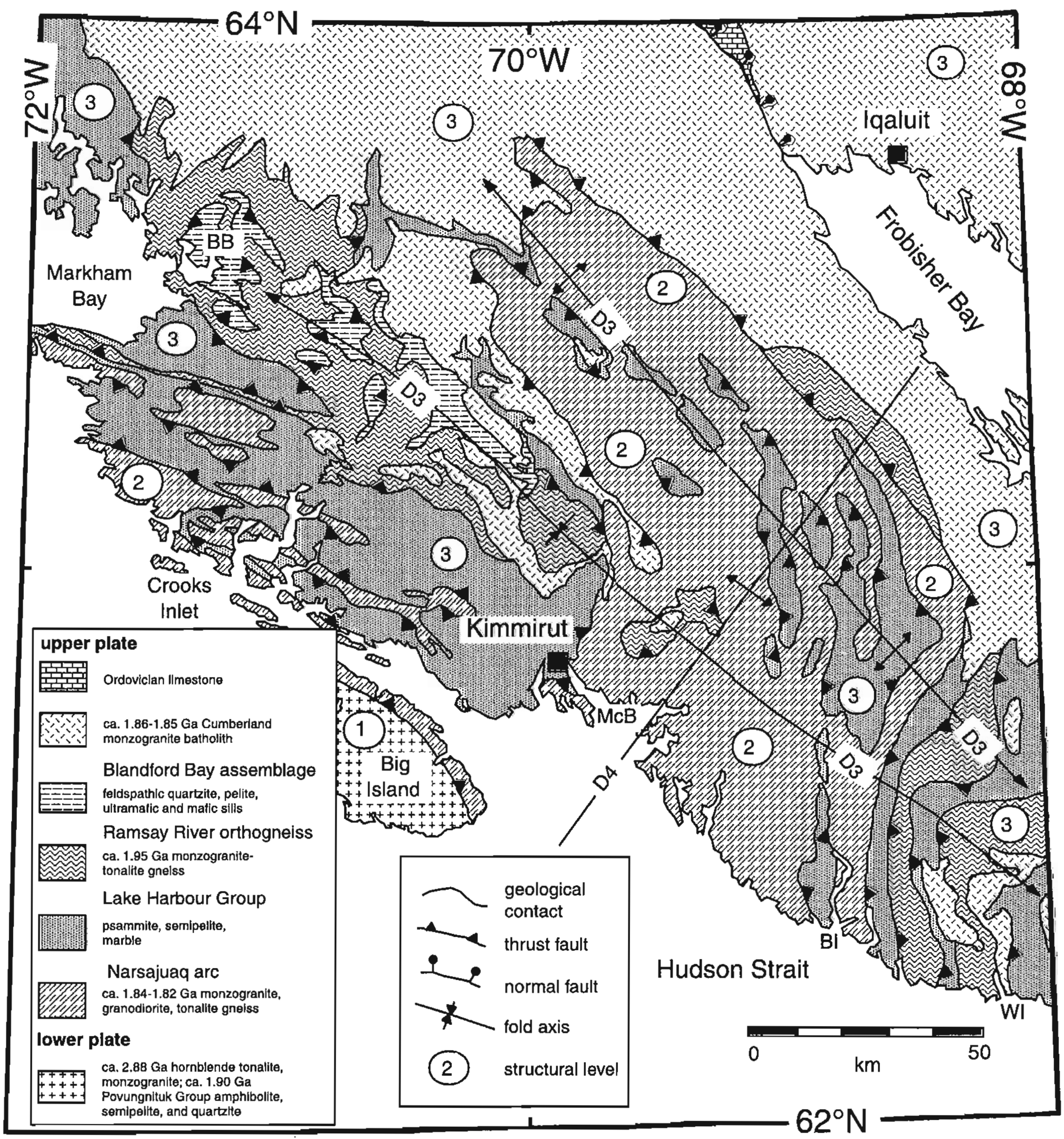

Figure 2. Generalized geology of the project area. BB=Blandford Bay, BI= Barrier Inlet, McB=McKellar Bay, WI=Wight Inlet.

Table 1. Deformation-metamorphism framework for project area

	Lower plate		Upper plate			
Structural level [5,14]	Archean basement -1-	Povungnituk Group -1-	Narsajuaq arc -2-	Lake Harbour Group -3-	Ramsay River orthogneiss -3-	Blandford Bay assemblage -3-
Age (Ga)						
3.22–2.74[1,2,3,4,5]	Granulite-facies arc plutonism, deformation, development of compositional layering					
>2.04–1.92[1,6]		Accumulation of rift-fill clastic and volcanic rocks				
ca. 1.95[7]					Granulite-facies (?) arc plutonism, deformation, development of compositional layering	
<1.93, >1.86[8,9,10]				Deposition of platformal clastic and carbonate units (basement uncertain), emplacement of mafic and ultramafic sills		Deposition of clastic units (basement unknown), emplacement of mafic and ultramafic sills
ca. 1.87 (?)[11]	D$_1$	D$_1$				
	basal shear zone deformation	SW-directed thrusting and folding (Cape Smith Belt), basal shear zone deformation				
	M$_1$	M$_1$				
	retrogression of granulite-facies assemblages, development of mineral foliation	prograde metamorphism, development of mineral foliation				
>1.86[10]				D$_1$	D$_1$	D$_1$
				(?) SW-directed thrusting and folding	imbrication	imbrication
1.86–1.85[5,12,13]				emplacement of Cumberland batholith	emplacement of Cumberland batholith	emplacement of Cumberland batholith
ca. 1.84[5,9]				M$_1$	M$_1$	M$_1$
				prograde upper amphibolite facies metamorphism, development of mineral foliation	retrogression of granulite-facies assemblages	prograde upper amphibolite facies metamorphism, development of mineral foliation
1.84–1.82[4,5,7,9]			D$_1$/M$_1$			
			Granulite-facies arc plutonism, deformation, development of compositional layering			
1.82–1.79[3,5,7,9,10,11]	D$_2$	D$_2$	D$_2$	D$_2$	D$_2$	D$_2$
	SW-directed basement imbrication	SW-directed thrusting	Accretion to Superior margin, imbrication, and recumbent folding		Accretion to Narsajuaq arc, SW-directed thrusting and recumbent folding	
	M$_2$	M$_2$	M$_2$	M$_2$	M$_2$	M$_2$
	retrogression of granulite-facies assemblages, foliation development	prograde upper amphibolite facies metamorphism, foliation development	retrogression of granulite-facies assemblages, foliation development		retrogression of upper amphibolite and granulite facies assemblages, foliation development	
ca. 1.79–1.78[5,9]	emplacement of postaccretion syenogranite	emplacement of postaccretion syenogranite	emplacement of postaccretion syenogranite	emplacement of posttectonic syenite		
ca. 1.76[1,9,11]	D$_3$	D$_3$	D$_3$	D$_3$	D$_3$	D$_3$
			SW-vergent folding about NW axes, cleavage development, emplacement of syenogranite pegmatite			
<1.76[11]	D$_4$	D$_4$	D$_4$	D$_4$	D$_4$	D$_4$
			upright folding about NNE axes			

(1) Parrish (1989)
(2) St-Onge et al. (1992)
(3) Scott and St-Onge (1995)
(4) Lucas and St-Onge (1995)
(5) Wodicka and Scott (1997)
(6) Machado et al. (1993)
(7) Scott and Wodicka (in press)
(8) Scott and Gauthier (1996)
(9) Scott (1997)
(10) Scott et al. (1997)
(11) Lucas and St-Onge (1992)
(12) Jackson et al. (1990)
(13) Scott (in press)
(14) St-Onge et al. (in press)

DESCRIPTION OF THE TECTONIC ELEMENTS

Narsajuaq arc orthogneiss

Several types of orthopyroxene-bearing, compositionally layered metaplutonic rocks (i.e. layered monzogranite-granodiorite-tonalite gneiss; monzogranite gneiss) occur at the lowest structural levels exposed along the southeast coast of the project area (Fig. 2; St-Onge et al., 1998a, b, c). These rocks are in physical continuity with and/or are lithologically similar to plutonic rocks in the Kimmirut area and the north shore of Big Island (Fig. 2) that have been dated at between 1.84-1.82 Ga and correlated by Scott (1997) and Wodicka and Scott (1997) with similar units in the 1.86-1.82 Ga Narsajuaq arc of northern Quebec (St-Onge et al., 1992; Dunphy and Ludden, in press).

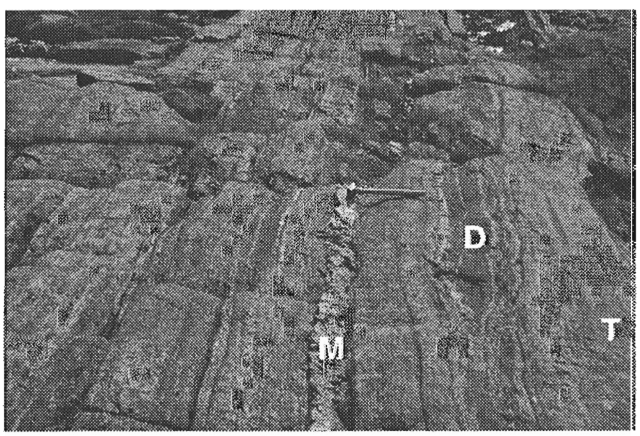

Figure 3. Layered monzogranite-granodiorite-tonalite gneiss (Narsajuaq arc) east of Kimmirut. T= tonalitic layers; D=quartz dioritic layers; M=monzogranitic layers. Hammer is 35 cm long.

Figure 4. Quartz diorite dyke (dark) in monzogranite-granodiorite-tonalite gneiss (Narsajuaq arc) south of McKellar Bay. Hammer is 35 cm long.

Layered monzogranite-granodiorite-tonalite gneiss

Crosscutting field relationships indicate that the oldest Narsajuaq arc plutonic unit in the project area (Fig. 2) is a layered, fine- to medium-grained, grey to buff orthopyroxene-biotite±hornblende±garnet tonalitic orthogneiss with subordinate grey orthopyroxene-biotite±hornblende granodiorite layers and pink monzogranite sheets and veins (Fig. 3). Compositional layering in the orthogneiss is typically a few centimetres in thickness and is laterally continuous for several tens of metres. Lenses, layers, and locally discordant dykes (Fig. 4) of dark hornblende-biotite-clinopyroxene±orthopyroxene quartz diorite, up to several metres thick, commonly form an integral component of the orthogneiss. The tonalitic, granodioritic, and quartz-dioritic components are crosscut by concordant (Fig. 3) to discordant (Fig. 5) veins of medium-grained orthopyroxene-biotite±hornblende monzogranite and by rare coarse-grained hornblende-biotite±orthopyroxene syenogranite. Grey anorthosite layers (Fig. 6) up to several tens of metres thick and over 1 km in strike length are part of the monzogranite-granodiorite-tonalite gneiss unit about 40 km northeast of McKellar Bay (Fig. 2).

Figure 5. Quartz diorite dyke (dark) cut by monzogranite (light) (Narsajuaq arc) south of McKellar Bay. Hammer is 35 cm long.

Figure 6. *Anorthosite layer (Narsajuaq arc) 40 km northeast of McKellar Bay. Hammer is 35 cm long.*

Monzogranite gneiss

Large areas of Narsajuaq arc (Fig. 2) are underlain by medium-grained orthopyroxene-biotite±hornblende monzogranite gneiss that intrudes the layered tonalite-monzogranite gneiss described above. These rocks weather light grey to pink and are composed of variously foliated layers <10 cm thick that differ principally in biotite content. Coarse-grained and locally megacrystic layers can reach 100 m in thickness. Hornblende-clinopyroxene-orthopyroxene-biotite quartz diorite layers are common.

Lake Harbour Group

The marble, psammite, and semipelite in the eastern portion of the project area are along strike from, or lithologically similar to, rocks of the Lake Harbour Group examined previously (St-Onge et al., 1996a; Scott et al., 1997). Two lithologically and geographically distinct sequences were recognized within these supracrustal rocks. Along the southern coastal inlets and river valleys between Barrier Inlet and 68°W (Fig. 2), the Lake Harbour Group comprises interlayered garnetiferous psammite, semipelite, and pelite (minor orthoquartzite) overlain by prominent, laterally continuous to boudined bands of pale grey to white marble and calcsilicate rocks ("Kimmirut sequence" of Scott et al., 1997). Inland, exposures of the Lake Harbour Group are dominated by garnetiferous psammite interlayered with semipelite and pelite and are essentially devoid of marble and calcsilicate rocks ("Markham Bay sequence" of Scott et al., 1997). Both sequences are intruded by generally concordant sheets of mafic to ultramafic rocks.

Psammite, semipelite, pelite, and orthoquartzite

Compositional layers within the psammite range from centimetres to tens of centimetres thick and can be traced for up to hundreds of metres along strike. They are defined by variations in the modal abundance of quartz, biotite, lilac garnet, cordierite, sillimanite, and granitic melt pods (Fig. 7). Garnet±cordierite±sillimanite pelite typically occurs as thin layers within garnet-biotite semipelite, the latter generally subordinate within the psammite. The psammite and semipelite are generally rusty weathering and characterized by trace amounts of disseminated graphite, pyrite, and chalcopyrite. The orthoquartzite occurs as discrete layers with total thicknesses of several metres. It often contains graphite, locally contains minor plagioclase, and is strongly recrystallized. Primary sedimentary features such as crossbedding are only rarely preserved within the siliciclastic rocks. White monzogranite, rich in lilac garnet, is a ubiquitous constituent within the siliciclastic package, occurring as concordant layers or pods less than 0.5 m thick (Fig. 8). Locally, it outcrops as discrete tabular bodies several metres thick.

Marble and calcsilicate rocks

Most of the calcareous rocks are medium grained to coarse grained and are locally characterized by compositional layering defined by varied modal proportions of calcite, forsterite, humite, diopside, tremolite, phlogopite, spinel, and wollastonite. Individual layers range from centimetres to metres in thickness and can be traced for tens of metres along strike.

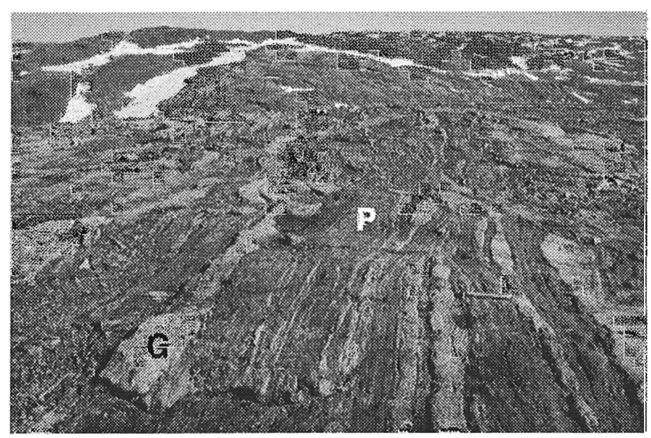

Figure 7. *Psammite (P) with granitic veins (G) (Lake Harbour Group) east of Wight Inlet. Hammer is 35 cm long.*

Figure 8. *Garnet-biotite-granitic melt±cordierite psammite (Lake Harbour Group) north of Kimmirut. Pen is 15 cm long.*

Calcsilicate rocks are commonly interlayered with siliciclastic rocks and generally associated with marble. Thicknesses of individual calcareous rock sequences typically range from about 1 km north of Kimmirut to about 200 m in the Wight Inlet area (Fig. 2). Individual marble units can be traced from 5 to 25 km along strike. No primary structures were observed in the calcareous rocks.

Mafic and ultramafic rocks

Generally concordant sheets of medium- to coarse-grained mafic to ultramafic rocks occur within both sequences of the Lake Harbour Group (St-Onge et al., 1998a, b, c). Individual bodies are typically 10 to 20 m thick, although some reach a few hundred metres in thickness, and extend up to several kilometres along strike. Metagabbroic textures (Fig. 9) and compositional layering defined by variations in modal abundance of clinopyroxene, orthopyroxene, hornblende, and plagioclase are commonly preserved in the mafic bodies. The concordant nature, tabular shape, and sharp contacts of these bodies suggest that they are sills. Several ultramafic bodies, either clinopyroxene-orthopyroxene±hornblende metapyroxenite or olivine-clinopyroxene-orthopyroxene metaperidotite, were observed (St-Onge et al., 1998a, b, c). In one locality, a metadunite sill several hundred metres in strike length (St-Onge et al., 1998b) is characterized by chromite seams several millimetres thick.

Ramsay River orthogneiss

Buff- to pink-weathering layered orthopyroxene-biotite± hornblende dominantly monzogranite-tonalite orthogneiss (Fig. 10) occurs on both limbs of the northeast-trending Kimmirut-Frobisher Bay antiform (Fig. 2). The orthogneiss in the eastern portion of the project area is along strike from orthogneiss that is intruded by the Cumberland batholith (see below; Fig. 2) in the Frobisher Bay area and that is correlated with metaplutonic gneiss mapped on the northwestern limb of the antiform (Scott et al., 1997) and dated by Scott and Wodicka (in press) at ca. 1.95 Ga. In most outcrops examined in the eastern region, the monzogranite-tonalite gneiss is interlayered with subordinate, boudined, and discontinuous layers of quartz diorite. All components of the gneiss are crosscut by veins of white to pink biotite monzogranite and syenogranite that range from well foliated to relatively massive and from a few centimetres to more than 10 m in thickness. Similarities in rock type, mineral assemblage, and strain state suggest that the monzogranite and syenogranite veins are related to and possibly comagmatic with plutons of the Cumberland batholith (see below) that intrude this unit in the Wight Inlet area (Fig. 2).

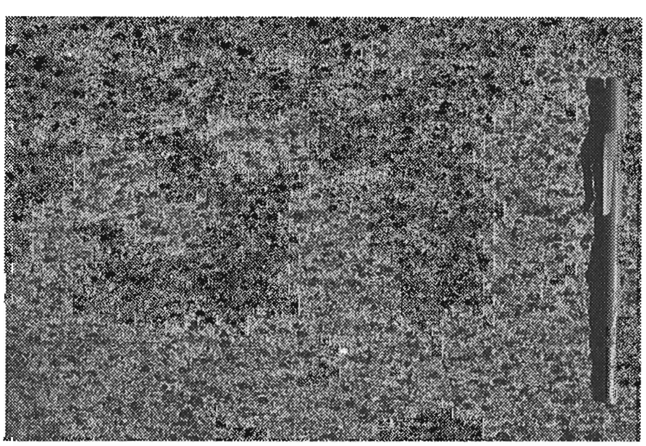

Figure 9. Metagabbro (Lake Harbour Group) northeast of Wight Inlet. Pen is 15 cm long.

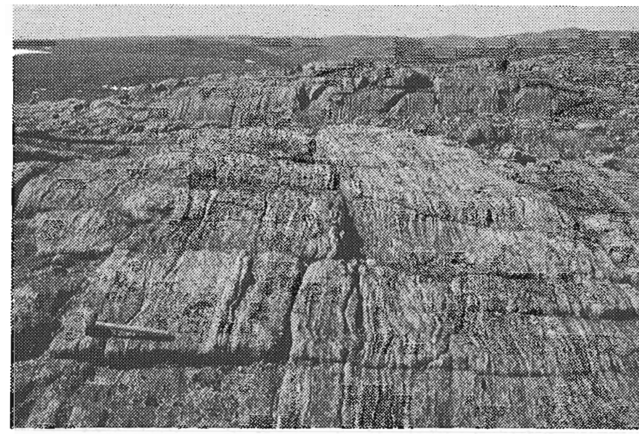

Figure 10. Monzogranite-tonalite orthogneiss (Ramsay River orthogneiss) north of Wight Inlet. Hammer is 35 cm long.

The orthogneiss may represent the stratigraphic basement to the Lake Harbour Group (1.93-1.86 Ga; Table 1). This, however, is difficult to determine in the field as all observed contacts between orthogneiss and supracrustal units are tectonic. The age of the orthogneiss and its spatial association with the younger Lake Harbour Group, both restricted to Level 3 (Fig. 2), suggest that a primary stratigraphic link is possible.

Cumberland batholith

Coarse- to medium-grained massive to foliated metaplutonic rocks in the northern and eastern portions of the McKellar Bay-Wight Inlet-Frobisher Bay area occur along strike from and are continuous with extensive regions underlain by the Cumberland batholith (Fig. 2; Blackadar, 1967; Jackson and Taylor, 1972; Scott et al., 1997; St-Onge et al., 1997b, c). The continuity of plutonic rocks suggests that plutonic rocks in the eastern portion of the project area are also part of the 1.86-1.85 Ga batholith (Jackson et al., 1990; Wodicka and Scott, 1997; Scott, in press).

The principal rock type mapped in the southeastern Cumberland batholith is a tan- to pink-weathering massive to weakly foliated orthopyroxene-biotite monzogranite. Along a number of well exposed contacts, monzogranite truncates Ramsay River orthogneiss and Lake Harbour Group host rocks (Fig. 11), indicating that intrusion followed the initial

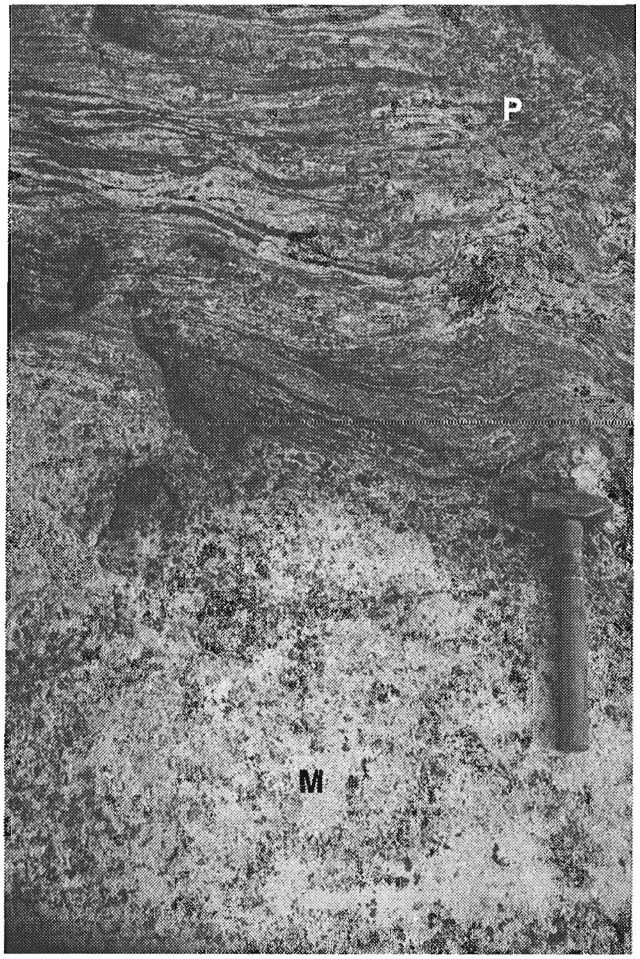

Figure 11. Cumberland batholith monzogranite (M) intrusive into Lake Harbour Group psammite (P) northwest of Wight Inlet. Hammer is 35 cm long.

juxtaposition of the orthogneiss and supracrustal units (see below). In the southern parts of the area, isolated kilometre-scale plutons of pink orthopyroxene-biotite monzogranite (Fig. 2; St-Onge et al., 1998b, c), one of which has been dated at 1.85 Ga (Wodicka and Scott, 1997), are interpreted to be part of the Cumberland magmatic system.

DEFORMATION AND METAMORPHISM

The completion of systematic regional mapping, the re-examination of key outcrops in previously mapped areas, and new geochronological data (Wodicka and Scott, 1997; Scott and Wodicka, in press) have facilitated the development of a comprehensive structural and metamorphic framework for the entire project area (Table 1). Deformation and metamorphism are polyphase, with at least three regional episodes of compression and one thermal event common to all tectonostratigraphic units (Table 1; Scott et al., 1997). The tectonothermal evolution is described in the following paragraphs, using the deformation-metamorphism framework outlined in Table 1. Age references are given in Table 1.

Pre-D_1 and D_1 deformation and metamorphism (Level 1)

The oldest deformation structures and mineral assemblages recognized in the project area are found in the Level 1 Archean orthogneiss on Big Island (Fig. 1, 2), which is correlated with the Superior Province in northern Quebec (St-Onge et al., 1996a). In northern Quebec, plutonism, concomitant granulite-facies metamorphism, and deformation range in age from 3.22 to 2.74 Ga (Table 1). The accumulation of the >2.04-1.92 Ga (Table 1) Povungnituk Group on this orthogneiss is interpreted to record Paleoproterozoic rifting of the northern Superior Province (St-Onge and Lucas, 1990, and references therein). Lucas and St-Onge (1992) defined D_1 (regular sequence) thrusting deformation and associated M_1 prograde metamorphism of the Povungnituk Group rocks in the Cape Smith Belt as an event that predated the Narsajuaq arc and may have been initiated by ca. 1.87 Ga. D_1/M_1 deformation structures and assemblages have not been recognized on Big Island.

D_1 deformation and M_1 metamorphism (Level 2)

On southern Baffin island, the age of arc plutonism, M_1 granulite-facies metamorphism, D_1 deformation, and the development of compositional layering in the metaplutonic rocks of the Narsajuaq arc (Lucas and St-Onge, 1995) is bracketed at between 1.84 and 1.82 Ga (Table 1). In northern Quebec, the age of plutonism and D_1/M_1 deformation structures and assemblages is bracketed at between 1.86 and 1.82 Ga (Lucas and St-Onge, 1992).

D_1 deformation and M_1 metamorphism (Level 3)

Crosscutting field relations (St-Onge et al., 1997a, b) indicate that early map-scale D_1 imbrication of the Ramsay River orthogneiss, the Lake Harbour Group, and the Blandford Bay assemblage within Level 3 (Scott et al., 1997) predates emplacement of the 1.86-1.85 Ga Cumberland batholith (Table 1). Prograde M_1 metamorphism of the Lake Harbour Group (Fig. 8) and Blandford Bay assemblage, and retrogression of granulite-facies assemblages in the Ramsay River orthogneiss, are constrained at ca. 1.84 Ga (Table 1).

D_2 deformation and M_2 metamorphism

The D_2 deformational event is defined as the oldest compressional deformation event that affects all tectonostratigraphic elements in the project area (Table 1). It involves (1) accretion of the imbricated Lake Harbour Group, Blandford Bay assemblage, and Ramsay River orthogneiss package (Level 3) to the metaplutonic rocks of the Narsajuaq arc (Level 2); (2) accretion of the Narsajuaq arc (Level 2) to the northern margin of the Superior Province (Level 1); and (3) imbrication of Povungnituk Group and Archean basement units (Level 1). The D_2 event is bracketed (Table 1) between the youngest (1.82 Ga) dated unit in the Narsajuaq arc and the age of emplacement (1.79 Ga) of a postaccretion syenogranite dyke. The presence of numerous repetitions and truncations of distinct tectonostratigraphic units and the overall ramp-flat fault geometry of the D_2 structures (Scott et al., 1997; St-Onge et al., 1997a, b; St-Onge et al., 1998a, b, c) suggest that juxtaposition of the units occurred along a system of southwest-verging thrust faults. These thrusts are commonly associated with development of mylonitic fabrics over thicknesses of metres to tens of metres (Fig. 12). In addition, D_2 thrust faulting was accompanied by outcrop-scale (Fig. 13) to map-scale recumbent folding (St-Onge et al., 1998a, b). In detail, the recumbent folds deform D_2 thrust faults and the principal foliation/gneissosity and are themselves cut by younger D_2 faults. The recumbent folds deform D_1/M_1 fabrics in rocks of levels 2 and 3.

D_2 deformation is characterized by a distinct M_2 metamorphic event involving retrogression of granulite facies and upper amphibolite facies assemblages in the Archean basement, Narsajuaq arc, and Lake Harbour Group (Wodicka and Scott, 1997), and growth of thermal-peak mineral assemblages in the Povungnituk Group (cf. Lucas and St-Onge, 1992). In the hinge zone of the D_2 recumbent folds (Fig. 13), growth of retrograde M_2 sillimanite-biotite-quartz at the expense of M_1 garnet±cordierite (Fig. 14) in psammite of the Lake Harbour Group led to the progressive development of a new schistose D_2 axial planar fabric (Fig. 15).

Massive syenogranite dykes and syenite plugs, which are discordant to the principal deformation fabrics in host rocks of all three structural levels, were emplaced ca. 1.79-1.78 Ga (Table 1). This age range provides a lower bracket for the age of the D_2 accretion event on southern Baffin Island. In addition, the documentation of 2.84 Ga zircon inheritance in a syenite north of Kimmirut (Fig. 2; Scott, 1997) suggests that the Superior Province basement extended at least that far north beneath rocks of levels 2 and 3 (Scott, 1997; St-Onge et al., in press).

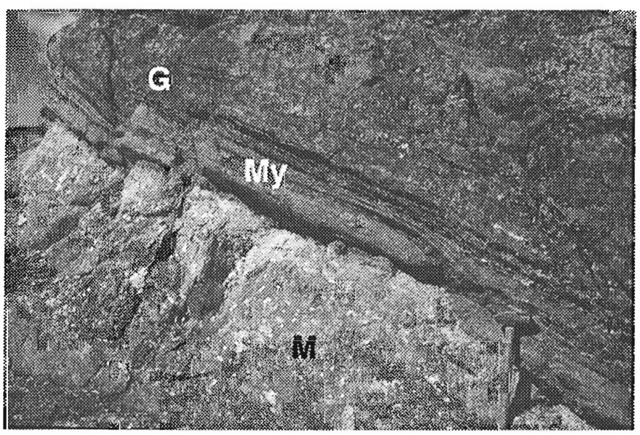

Figure 12. D_2 thrust contact between layered monzogranite-granodiorite-tonalite gneiss (G) (Narsajuaq arc, hanging wall) and marble (M) (Lake Harbour Group, footwall), west of Barrier Inlet. Note the development of a D_2 mylonitic fabric (My) in the orthogneiss above fault. Hammer is 35 cm long.

Figure 14. M_2 sillimanite-biotite assemblage with relict M_1 garnet in psammite (Lake Harbour Group), northeast of Kimmirut. Pen is 15 cm long.

Figure 13. D_2 recumbent fold of M_1 compositional fabric in a psammite (Lake Harbour Group), northeast of Kimmirut. Fold hinges highlighted with arrows. Pen cap is 4 cm long.

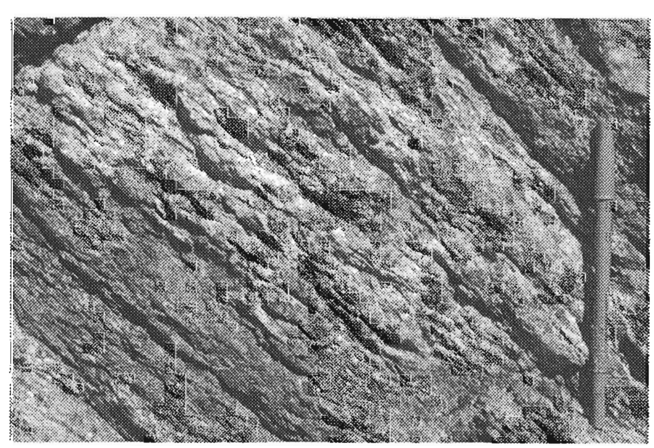

Figure 15. M_2 sillimanite-biotite assemblage defining schistose D_2 fabric in psammite (Lake Harbour Group), northeast of Kimmirut. Pen is 15 cm long.

D_3 deformation

Both D_1 and D_2 fault and fold structures have been reoriented by northwest-trending D_3 folds. The D_3 folds range from metre scale (Fig. 16) to map scale (Fig. 2; St-Onge et al., 1998a, b, c) and display a consistent southwest-verging asymmetry. The D_3 folding is evident at map scale from the large synform cored by Level 3 units northwest of Kimmirut and the northwest-striking antiform cored by Level 2 units southwest of Frobisher Bay (Fig. 2). The numerous klippen of Lake Harbour Group rocks north and east of Kimmirut (Fig. 2; St-Onge et al., 1998a, b, c) are second-order refolded D_3 synforms. D_3 folding in northern Quebec occurred at ca. 1.76 Ga (Table 1; Lucas and St-Onge, 1992).

D_4 deformation

Upright refolding (Fig. 17) of all structural elements about north-northeast-trending axes generated the large D_4 cross-fold antiform that dominates the map pattern between Kimmirut and Frobisher Bay (Fig. 2). D_4 refolding of D_3 synformal keels created the series of klippen of Level 3 units (Fig. 2) along the D_4 antiformal hinge zone. The interference of D_3 and D_4 folds is what generated sufficient structural relief in the area to allow the study of the architecture of the South Baffin orogenic belt and its three principal structural levels at the present erosion surface. D_4 folding in northern Quebec occurred between 1.76 and 1.74 Ga (Table 1; Lucas and St-Onge, 1992).

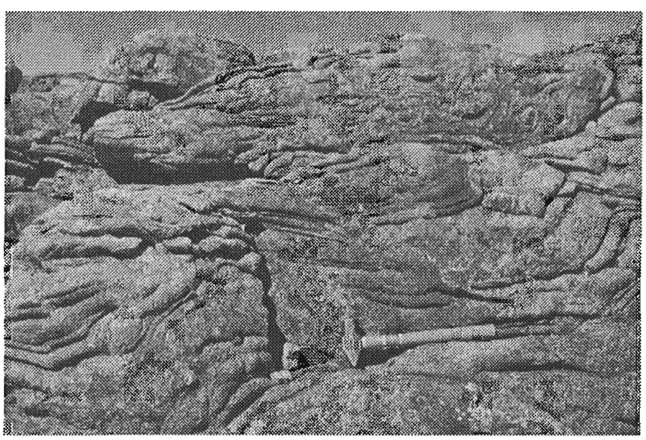

***Figure 16.** D_3 southwest-verging folds of psammite (Lake Harbour Group) northeast of Kimmirut. Hammer is 35 cm long.*

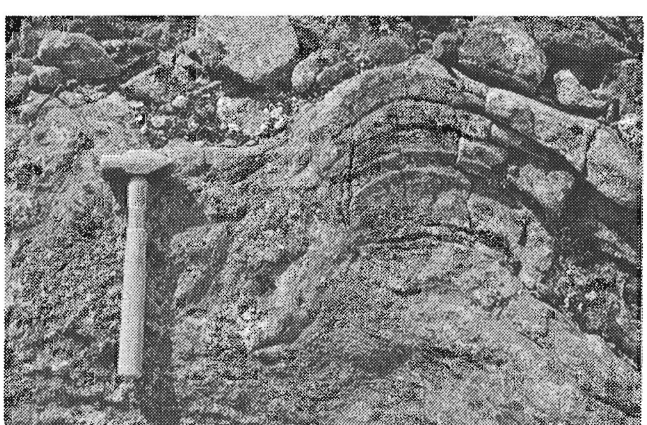

***Figure 17.** D_4 upright fold of psammite (Lake Harbour Group) northeast of Kimmirut. Hammer is 35 cm long.*

ECONOMIC POTENTIAL

Mafic and ultramafic sills in siliciclastic rocks of the Lake Harbour Group in the McKellar Bay-Wight Inlet-Frobisher Bay area may present conditions favourable for the formation of magmatic Cu-Ni sulphide mineralization. The largest sills are indicated on the 1:100 000 maps of St-Onge et al. (1998a, b, c). Serpentinized ultramafic rocks have been identified in a number of localities in the map area, some of which may provide material suitable as carving stone.

ACKNOWLEDGMENTS

We thank the Polar Continental Shelf Project for logistical support. Greg Brown, Olga Ijewliw, Sarah McMullen, Liza Piper, Jasen Robillard, and Liz Turner are thanked for independent mapping. Debbie Guilfoyle did an outstanding job as camp cook and manager. Tom McMahon and Louis-Claude Bourgeault (Huisson Aviation) provided efficient transportation. Reg Theriault is thanked for critically reviewing the manuscript. This is PCSP/ÉPCP Contribution No. 024-97.

REFERENCES

Blackadar, R.G.
1967: Geological reconnaissance, southern Baffin Island, District of Franklin; Geological Survey of Canada, Paper 66-47, 32 p.

Dunphy, J.M. and Ludden, J.N.
in press: Petrological and geochemical characteristics of a Paleoproterozoic magmatic arc (Narsajuaq terrane, Ungava Orogen, Canada) and comparisons to Superior Province granitoids; Precambrian Research.

Hanmer, S., St-Onge, M.R. and Scott, D.J.
1996a: Structural geology of the Meta Incognita thrust belt, south Baffin Island, Northwest Territories; in Current Research 1996-C; Geological Survey of Canada, p. 73-81.
1996b: Geology, White Strait, District of Franklin, Northwest Territories; Geological Survey of Canada, Open File 3192 (scale 1:100 000).

Jackson, G.D. and Taylor, F.C.
1972: Correlation of major Aphebian rock units in the northeastern Canadian Shield; Canadian Journal of Earth Sciences, v. 9, p. 1650-1669.

Jackson, G.D., Hunt, P.A., Loveridge, W.D., and Parrish, R.R.
1990: Reconnaissance geochronology of Baffin Island, N.W.T.; in Radiogenic Age and Isotopic Studies: Report 3; Geological Survey of Canada, Paper 89-2, p. 123-148.

Lewry, J.F. and Stauffer, M.R.
1990: The early Proterozoic Trans-Hudson Orogen of North America; Geological Association of Canada, Special Paper, v. 37, 505 p.

Lucas, S.B. and St-Onge, M.R.
1992: Terrane accretion in the internal zone of the Ungava Orogen, northern Quebec. Part 2: Structural and metamorphic history; Canadian Journal of Earth Sciences, v. 29, p. 765-782.

Lucas, S.B. and St-Onge, M.R. (cont.)
1995: Syn-tectonic magmatism and the development of compositional layering, Ungava Orogen (northern Quebec, Canada); Journal of Structural Geology, v. 17, p. 475-491.

Lucas, S.B., St-Onge, M.R., Parrish, R.R., and Dunphy, J.M.
1992: Long-lived continent-ocean interaction in the Early Proterozoic Ungava Orogen, northern Quebec, Canada; Geology, v. 20, p. 113-116.

Machado, N., David, J., Scott, D.J., Lamothe, D., Philippe, S., and Gariépy, C.
1993: U-Pb geochronology of the western Cape Smith Belt, Canada: new insights on the age of initial rifting and arc magmatism; Precambrian Research, v. 63, p. 211-224.

Parrish, R.R.
1989: U-Pb geochronology of the Cape Smith Belt and Sugluk block; Geoscience Canada, v. 16, p. 126-130.

Scott, D.J.
1997: Geology, U-Pb and Pb-Pb geochronology of the Lake Harbour area, southern Baffin Island: Implications for the Paleoproterozoic tectonic evolution of NE Laurentia; Canadian Journal of Earth Sciences, v. 34, p. 140-155.
in press: U-Pb geochronology of the eastern Hall Peninsula, southern Baffin Island, Canada: A northern link between the Archean of West Greenland and the Paleoproterozoic Torngat Orogen of northern Labrador; Precambrian Research.

Scott, D.J. and Gauthier, G.
1996: Comparison of TIMS (U-Pb) and laser ablation microprobe ICP-MS (Pb) techniques for age determination of detrital zircons from Paleoproterozoic metasedimentary rocks from northeastern Laurentia, Canada, with tectonic implications; Chemical Geology, v. 131, p. 127-142.

Scott, D.J. and St-Onge, M.R.
1995: Constraints on Pb closure temperature in titanite based on rocks from the Ungava orogen, Canada: Implications for U-Pb geochronology and P-T-t path determinations; Geology, v. 23, p. 1123-1126.

Scott, D.J. and Wodicka, N.
in press: A second report on the U-Pb geochronology of the Meta Incognita Peninsula, southern Baffin Island, Northwest Territories; in Radiogenic Age and Isotopic Studies, Report 11; Geological Survey of Canada, Current Research 1998-F.

Scott, D.J., Helmstaedt, H., and Bickle, M.J.
1992: Purtuniq ophiolite, Cape Smith Belt, northern Quebec, Canada: a reconstructed section of Early Proterozoic oceanic crust; Geology, v. 20, p. 173-176.

Scott, D.J., St-Onge, M.R., and Hanmer, S.
1996: Geology, Frobisher Bay, District of Franklin, Northwest Territories; Geological Survey of Canada, Open File 3193 (scale 1:100 000).

Scott, D.J., St-Onge, M.R., Wodicka, N., and Hanmer, S.
1997: Geology of the Markham Bay-Crooks Inlet area, southern Baffin Island, Northwest Territories; in Current Research 1997-C; Geological Survey of Canada, p. 157-166.

St-Onge, M.R. and Lucas, S.B.
1990: Evolution of the Cape Smith Belt: Early Proterozoic continental underthrusting, ophiolite obduction and thick-skinned folding; in The early Proterozoic Trans-Hudson Orogen of North America, (ed.) J.F. Lewry and M.R. Stauffer; Geological Association of Canada, Special Paper, v. 37, p. 313-351.

St-Onge, M.R., Lucas, S.B., and Parrish, R.R.
1992: Terrane accretion in the internal zone of the Ungava orogen, northern Quebec. Part 1: Tectonostratigraphic assemblages and their tectonic implications; Canadian Journal of Earth Sciences, v. 29, p. 746-764.

St-Onge, M.R., Hanmer, S., and Scott, D.J.
1996a: Geology of the Meta Incognita Peninsula, south Baffin Island: tectonostratigraphic units and regional correlations; in Current Research, 1996-C; Geological Survey of Canada, p. 63-72.
1996b: Geology, Soper River, District of Franklin, Northwest Territories; Geological Survey of Canada, Open File 3191 (scale 1:100 000).

St-Onge, M.R., Hanmer, S., Scott, D.J., and Wodicka, N.
1997a: Geology, Crooks Inlet, District of Franklin, Northwest Territories; Geological Survey of Canada, Open File 3397 (scale 1:100 000).
1997b: Geology, Blandford Bay, District of Franklin, Northwest Territories; Geological Survey of Canada, Open File 3398 (scale 1:100 000).
1997c: Geology, Hone River, District of Franklin, Northwest Territories; Geological Survey of Canada, Open File 3399 (scale 1:100 000).

St-Onge, M.R., Lucas, S.B., Scott, D.J., and Wodicka, N.
1997d: Tectonostratigraphic record and crustal architecture of an arc-continent collision zone: new views from the Ungava-Baffin segment of the Paleoproterozoic Trans-Hudson Orogen, Canada; Terra Nova, v. 9, p. 354.
in press: Lower plate crystalline basement involvement during protracted crustal convergence, Trans-Hudson Orogen (Quebec-Baffin segment), Canada; Precambrian Research.

St-Onge, M.R., Scott, D.J., and Wodicka, N.
1998a: Geology, Hidden Bay, District of Franklin, Northwest Territories; Geological Survey of Canada, Open File Map 3536 (scale 1:100 000).
1998b: Geology, McKellar Bay, District of Franklin, Northwest Territories; Geological Survey of Canada, Open File Map 3537 (scale 1:100 000).
1998c: Geology, Wight Inlet, District of Franklin, Northwest Territories; Geological Survey of Canada, Open file Map 3538 (scale 1:100 000).

Wheeler, J.O., Hoffman, P.F., Card, K.D., Davidson, A., Sanford, B.V., Okulitch, A.V., and Roest, W.R.
1996: Geological Map of Canada; Geological Survey of Canada, Map 1860A (scale 1:5 000 000.

Wodicka, N. and Scott, D.J.
1997: A preliminary report on the U-Pb geochronology of the Meta Incognita Peninsula, southern Baffin Island, Northwest Territories; in Current Research 1997-C; Geological Survey of Canada, p. 167-178.

Geological Survey of Canada Project 960006

Progress report: Precambrian geology, Angikuni Lake area, District of Keewatin, Northwest Territories[1]

L.B. Aspler[2], J.R. Chiarenzelli[3], K.B. Powis[4], and B.L. Cousens[5]
Continental Geoscience Division, Ottawa

Aspler, L.B., Chiarenzelli, J.R., Powis, K.B., and Cousens, B.L., 1998: Progress report: Precambrian geology, Angikuni Lake area, District of Keewatin, Northwest Territories; in Current Research 1998-C, Geological Survey of Canada, p. 55-66.

Abstract: Near Angikuni Lake, greenschist-grade remnants of ca. 2.68 Ga mafic to felsic volcanic, siliciclastic, and carbonate sequences were deposited in shallow water on transitional, if not continental, crust. Initial isotopic and geochemical data indicate that the volcanics are mantle-derived tholeiites, consistent with back-arc basin deposition. Amphibolite-grade granitic to gabbroic gneiss complexes formed during ca. 2.61 Ga plutonism and structural disruption of the supracrustal rocks, and are not basement. To the east, a northeast-trending, near-vertical, strike-lineated, dextral, mylonitic shear zone juxtaposes greenschist supracrustal rocks against amphibolite gneisses. It may be kinematically linked to a northwest-trending, shallowly north-dipping, dip-lineated, north-side-down shear zone to the southwest. Both shear zones and synkinematic tholeiitic plutonic rocks represent a distributed Snowbird tectonic zone, likely formed in an intracontinental setting late in the evolution of the Ennadai-Rankin greenstone belt. Paleoproterozoic Dubawnt Supergroup outliers outcrop across the area and define two northeast-trending sub-basins.

Résumé : À proximité du lac Angikuni, des vestiges métamorphisés au faciès des schistes verts de séquences carbonatées, silicoclastiques et volcaniques mafiques à felsiques datant d'environ 2,68 Ga ont été déposés en eau peu profonde sur une croûte intermédiaire, voire continentale. Les données isotopiques et géochimiques préliminaires indiquent que les roches volcaniques sont des tholéiites mantelliques, ce qui est compatible avec un dépôt en bassin d'arrière-arc. Des complexes gneissiques granitiques à gabbroïques du faciès des amphibolites se sont formés il y a environ 2,61 Ga au cours d'un épisode de plutonisme et de perturbation structurale des roches supracrustales et ne font pas partie du socle. À l'est, une zone de cisaillement dextre mylonitique de direction nord-est, quasi verticale et à linéation dans le sens de la direction, juxtapose des roches supracrustales du faciès des schistes verts contre des gneiss à amphiboles. Cette zone est peut-être liée cinématiquement à une zone de cisaillement au sud-ouest dont le côté nord a été abaissé, la direction est nord-ouest, le faible pendage est vers le nord et la linéation est dans le sens du pendage. Les deux zones de cisaillement et les roches plutoniques tholéiitiques syncinématiques représentent la zone tectonique de Snowbird, qui s'est vraisemblablement formée dans un milieu intracontinental au cours d'une phase tardive de l'évolution de la ceinture de roches vertes d'Ennadai-Rankin. Des buttes témoins du supergroupe paléoprotérozoïque de Dubawnt affleurent dans l'ensemble de la région et définissent deux sous-bassins de direction nord-est.

[1] Contribution to the Western Churchill NATMAP Project
[2] 23 Newton Street, Ottawa, Ontario K1S 2S6
[3] Environmental Research Center, State University of New York at Oswego, Oswego, New York, USA 13126
[4] Department of Geology, University of Ottawa, Ottawa, Ontario K1N 6N5
[5] Department of Earth Sciences, Carleton University, Ottawa, Ontario K1S 5B6

INTRODUCTION

Modern integrated study is needed to test provisional paleogeographic and tectonic models for the western Churchill Province and to evaluate if the Rae and Hearne provinces were parts of a Neoarchean supercontinent (Fig. 1; Aspler and Chiarenzelli, 1996; in press). Herein we report preliminary geological, geochemical, isotopic, and geochronologic results from a multiyear project based on 1:50 000 scale mapping near the western flank of the Hearne Province, in the Angikuni Lake area (Fig. 2). This work is a component of the Western Churchill NATMAP Project and compliments studies in other parts of the Ennadai-Rankin greenstone belt (Fig. 2) near Kaminak Lake (Hanmer et al., 1998 a, b) and Yathkyed Lake (Relf et al., 1998).

Building on work by Blake (1980), Tella and Eade (1985) and Eade (1986), the present study is directed toward 1) addressing uncertainties in the configuration of Mesoarchean basement, the depositional setting, age, and tectonostratigraphy of Neoarchean supracrustal rocks, and the record of Neoarchean plutonic, metamorphic, and structural events; 2) evaluating the significance of the boundary between the Hearne and Rae provinces (Snowbird tectonic zone); and 3) determining the nature of Paleoproterozoic crustal reactivation during development of Baker Lake Basin (Figs. 1, 2).

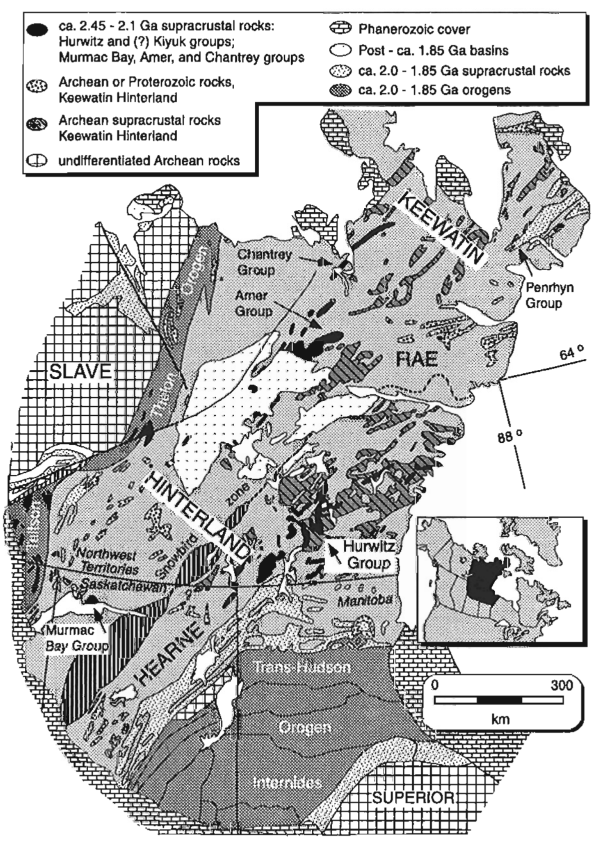

Figure 1. Regional setting: Rae and Hearne provinces and Snowbird tectonic zone (ornamented with vertical black and white stripes) (after Hoffman, 1989).

Below we describe Neoarchean supracrustal, plutonic, and metamorphic rocks in the Angikuni Lake area in terms of five lithostructural domains (Fig. 3). Paleoproterozoic continental siliciclastic and volcanogenic rocks of the Baker Lake Group (Dubawnt Supergroup), and related lamprophyre dykes and syenitic stocks, are exposed in small outliers across these domains and in two northeast-trending sub-basins in the northern part of the area (Figs. 2, 3).

ARCHEAN LITHOSTRUCTURAL DOMAINS

Archean map units define five fault-bounded lithostructural domains (Fig. 3; numbered I to V from east to west). Domain I is characterized by extensive areas of greenschist-grade supracrustal rocks, including mafic volcanic flows and biotitic psammite, both of which are cut by large granitic bodies. Domain II is an upper amphibolite-grade granite, gabbro, orthogneiss, and paragneiss complex containing only isolated slivers of readily recognizable supracrustal rocks. Domain III contains a greenschist-grade supracrustal assemblage including mafic and felsic volcanogenic rocks, microbial laminate and stromatolite-bearing dolostone and pelite, and quartz pebble conglomerate, sandstone, and pelite. Domain IV consists of granite and granitic gneiss. Domain V is a granitic gneiss complex that forms part of a regional-scale domal structure.

Domain I

On the east side of Angikuni Lake, greenschist-facies mafic volcanic rocks are exposed in three near-vertical, northeast-trending panels that are separated by coarse-grained, foliated, hornblende leucogranite sills (Fig. 3). Sparse, but consistent, top indicators suggest that the panels originally formed a single northwest-younging sequence. The volcanic rocks are cut by numerous thin (<10 m), likely synvolcanic, gabbro dykes and sills; in the central panel, a large gabbro body, ca. 1.5 km across (Fig. 3) may represent a feeder stock. Subaqueous sheet flows, pillow lavas, and tuffs are predominant. Layering in the sheet flows is manifested by centimetre-scale chilled margins spaced several decimetres to metres apart (Fig. 4). In three-dimensional exposures, the layering defines laterally continuous, parallel-sided, tabular sheets, similar to modern seafloor non-pillowed flows (e.g. Ballard et al.; 1979; Holcomb et. al., 1988; Tribble, 1991). Subaqueous sheet deposition is indicated by thick chilled margins and interbedding with local pillow lavas; local millimetre-scale amygdules imply relatively shallow water. Consistent with shallow-water deposition is a lens within mafic rocks in the northern panel consisting of cross-stratified, carbonate-cemented arkose; polymictic, framework-intact conglomerate (with mafic volcanic, felsic volcanic and sparse granitic clasts); and microbial laminated dolostone (Fig. 3). Effusive volcanism with high rates of extrusion is shown by the predominance of sheet flows relative to pillow lavas (e.g. Gregg and Fink, 1995). However, abundant, thinly laminated tuffs, locally with lapilli fragments, demonstrate periodic explosive volcanism.

A section of biotite-muscovite±garnet psammite and quartzofeldspathic paragneiss appears to underlie the mafic volcanic rocks in the eastern panel. Primary structures are not preserved, but these rocks appear to have originated as immature arenites. They are intruded on the south by a large, well foliated muscovite-biotite±hornblende leucogranite pluton (Fig. 3). Bedding and cleavage in the supracrustal rocks wrap around the nose of this pluton (Fig. 3). Within the pluton are narrow (<1 km) screens of mafic volcanic flows and biotitic paragneiss containing discordant and foliation-parallel granitic sheets.

Major-element geochemistry of nine samples indicates that the volcanic rocks range in composition from basalt to andesite and dacite, all of which plot within the tholeiitic field (Fig. 5 a). These rocks define a tholeiitic titanium-enrichment trend (Fig. 5 b).

Domain I-II Contact: dextral ductile shear zone

Domain I is bounded on the west by an approximately 0.5 km wide, near-vertical, upper amphibolite-grade mylonitic shear zone (Fig. 3). Along most of the shear zone, mineral and stretching lineations plunge shallowly (5-15°), but at its southern extent, lineations are steeper (30-50°). Kinematic indicators are consistently dextral (e.g. winged porphyroclasts, rotated porphyroclasts, asymmetric pull-aparts, shear bands, rotated axial surfaces of minor folds; Fig. 6 and see Figure 4 in Aspler and Chiarenzelli, 1997). The trace of the shear zone is sigmoidal, defining a restraining bend: it is north-northeast-trending at its northern and southern extremities and north-northwest-trending in its central portion (Fig. 3). The bend is likely original because appropriately oriented cross folds are lacking. Mafic rocks of Domain I display strong strain gradients as the shear zone is approached (progressive development of pervasive fabric and stretching

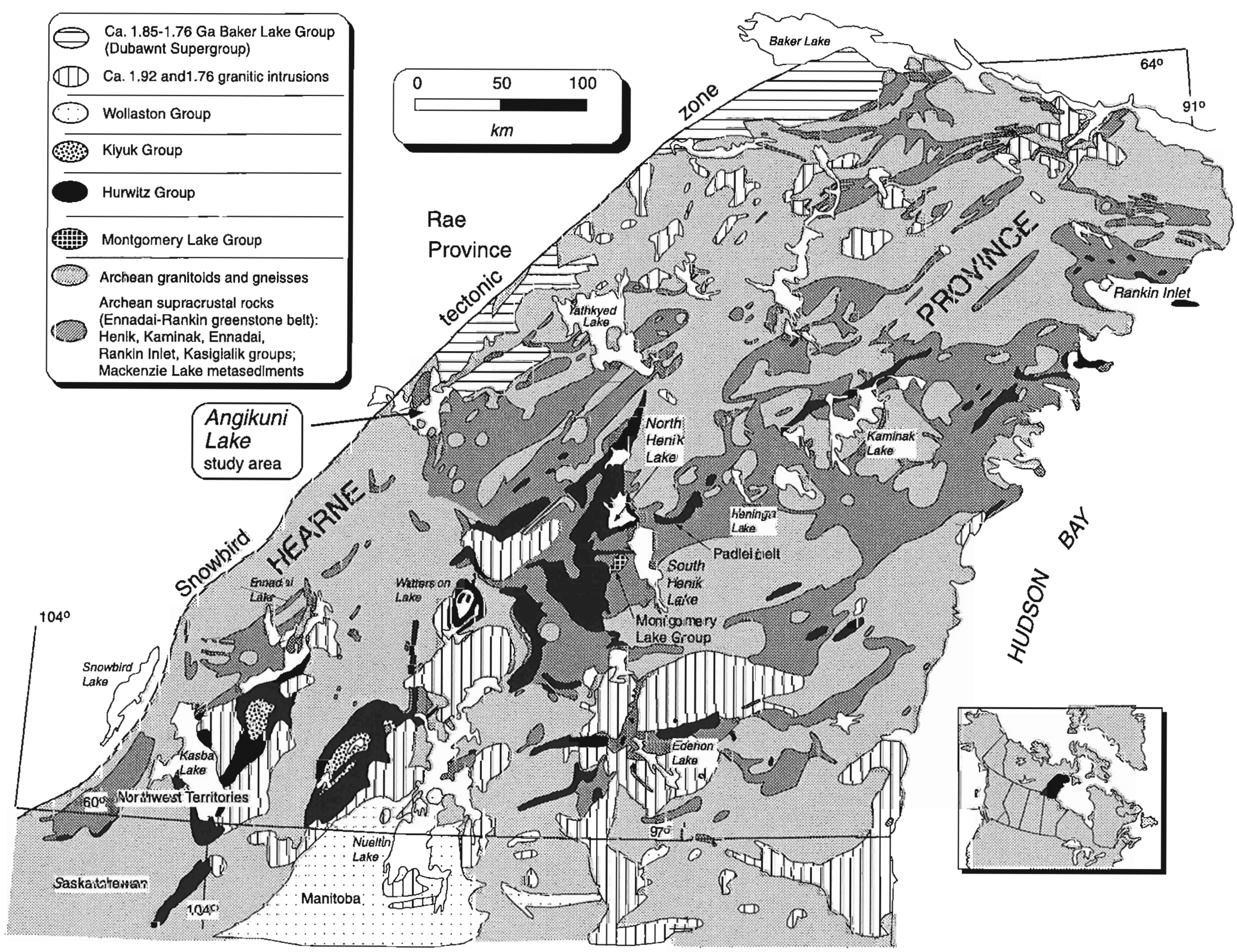

Figure 2. Location of study area, simplified geology of the Hearne Province, Northwest Territories.

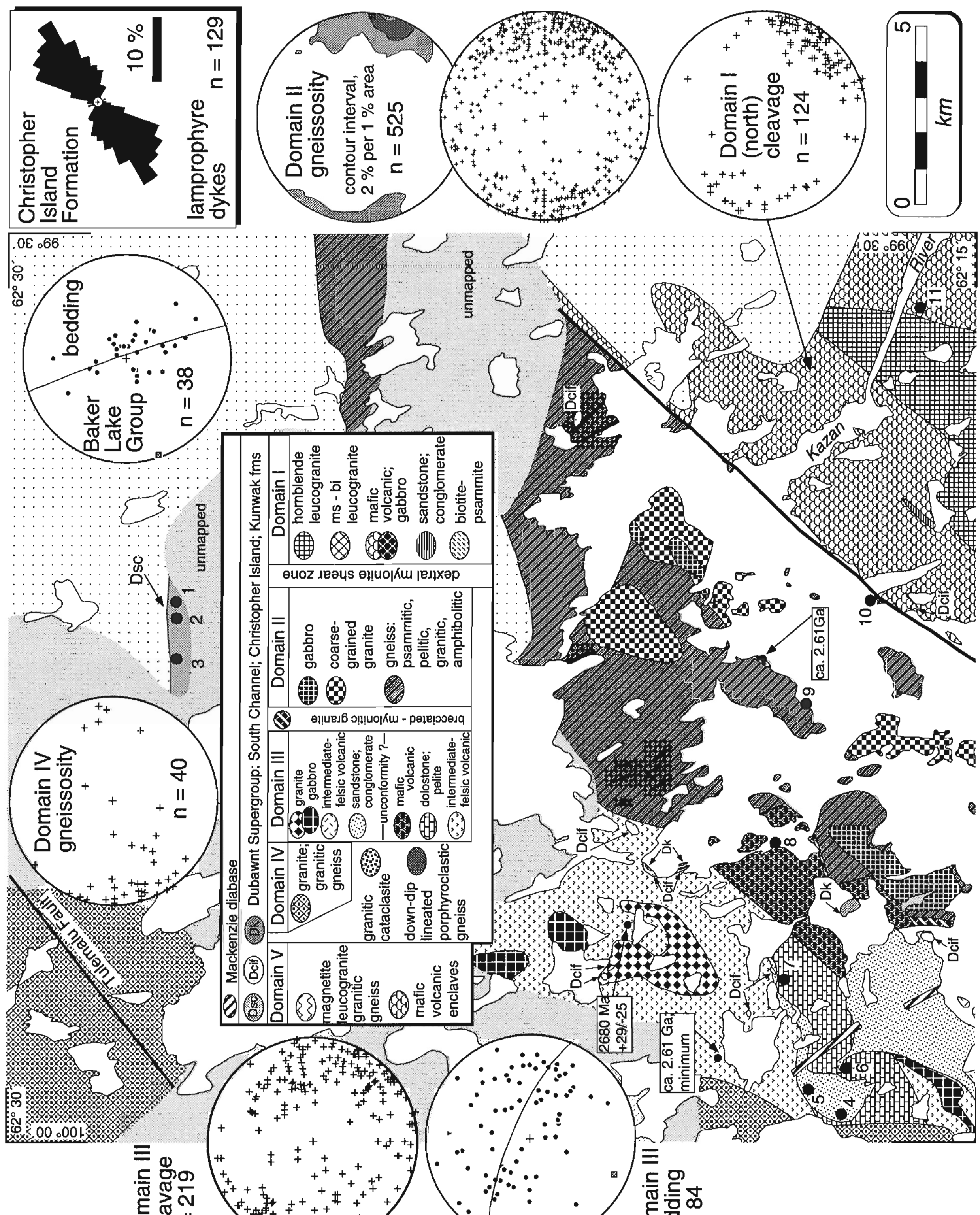
Christopher Island Formation
lamprophyre dykes
10 %
n = 129
Domain II gneissosity
contour interval, 2 % per 1 % area
n = 525
Domain I (north) cleavage
n = 124
0
5
km
Baker Lake Group bedding
n = 38
62° 30'
99° 30'
100° 00'
62° 15'
Domain IV gneissosity
n = 40
Domain III cleavage
n = 219
Domain III bedding
n = 84
Tulemalu Fault
Dsc
unmapped
Mackenzie diabase
Dsc Dcif Dk Dubawnt Supergroup: South Channel; Christopher Island; Kunwak fms
Domain V
magnetite leucogranite granitic gneiss
mafic volcanic enclaves
Domain IV
granite; granitic gneiss
granitic cataclasite
down-dip lineated porphyroclastic gneiss
Domain III
granite
gabbro
intermediate-felsic volcanic
sandstone; conglomerate
—unconformity ?—
mafic volcanic
dolostone; pelite
intermediate-felsic volcanic
brecciated - mylonitic granite
Domain II
gabbro
coarse-grained granite
gneiss: psammitic, pelitic, granitic, amphibolitic
dextral mylonite shear zone
Domain I
hornblende leucogranite
ms - bi leucogranite
mafic volcanic; gabbro
sandstone; conglomerate
biotite-psammite
Dcif
Dk
Kazan
River
ca. 2.61Ga
2680 Ma +29/-25
ca. 2.61 Ga minimum
1
2
3
4
5
6
7
8
9
10
11

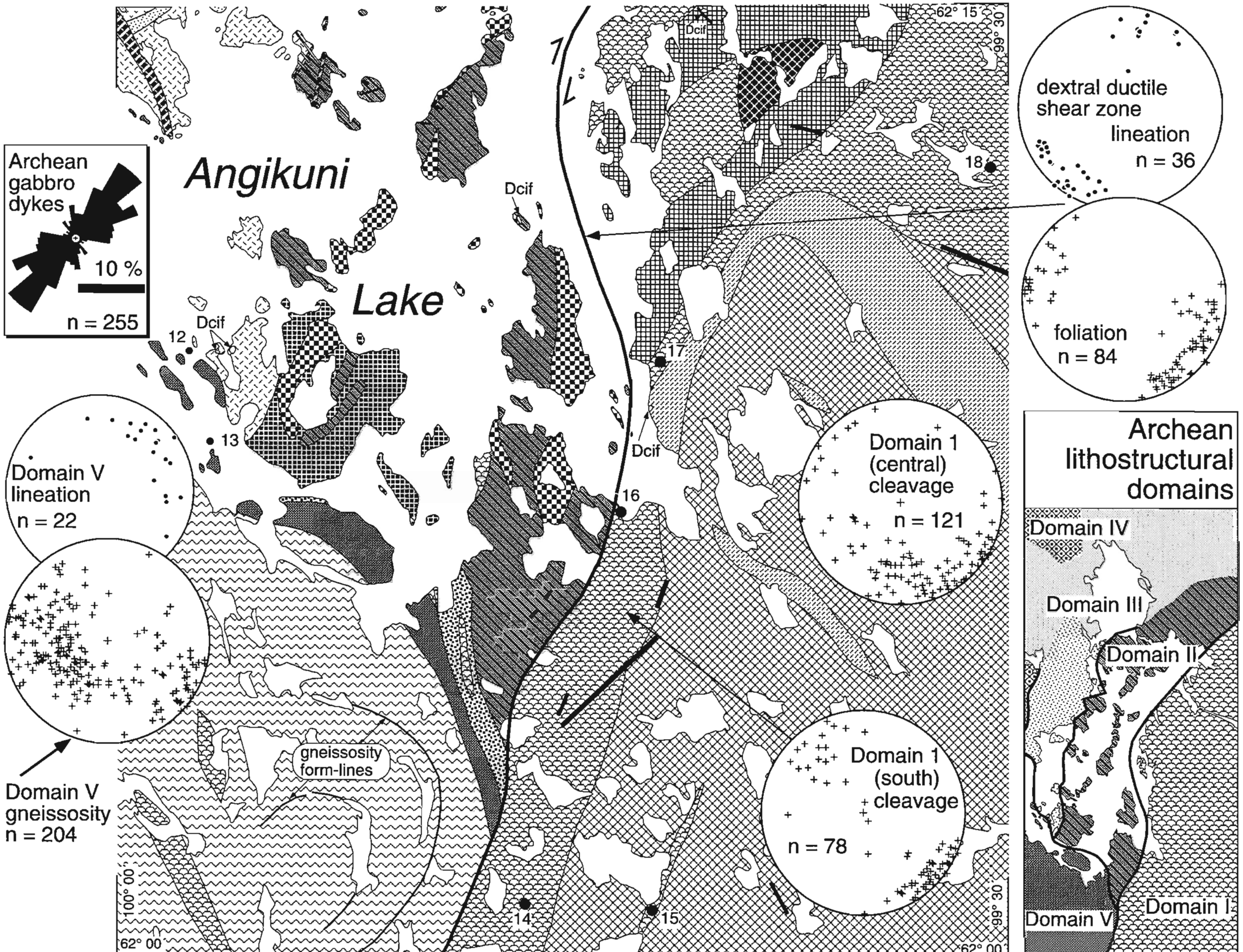

Figure 3. Simplified geological map, Angikuni Lake area. Numbered sites refer to gossans in Table 1. Domain III geochronology from Loveridge et al. (1988); Domain II geochronology from W.J. Davis (unpublished data).

lineation; development of isoclinal folds). Similarly, plutonic rocks of Domain II develop mylonitic textures, and within the shear zone, variably oriented foliations in gneisses become straight and concordant with the shear zone boundaries. A suite of intrusive bodies, with a full range of composition from gabbro to granite, occurs within the shear zone. These bodies contain the mylonitic fabric and are locally transposed along the shear zone, but are also locally discordant (see Figure 6 b in Aspler and Chiarenzelli, 1997) and are thus syntectonic. The shear zone displays evidence of a post-ductile brittle history in the form of local breccia zones and quartz stockwork veins.

Domain II: upper amphibolite-grade granite-gabbro-orthogneiss-paragneiss complex

Supracrustal gneisses are the oldest components of Domain II. These occur within plutonic rocks and gneisses, and range in scale from mappable screens to metre- scale layers to isolated, partially assimilated xenoliths. Psammitic gneiss with a granoblastic texture, consisting of plagioclase-quartz-hornblende±bitotite and clinopyroxene, is particularly common in the eastern part of the domain. Amphibolite gneiss is more prominent on the western margin. The psammitic gneiss likely originated as felsic to intermediate tuffs or immature arenites, although some may have been equigranular tonalitic intrusive bodies. Some of the amphibolitic layers

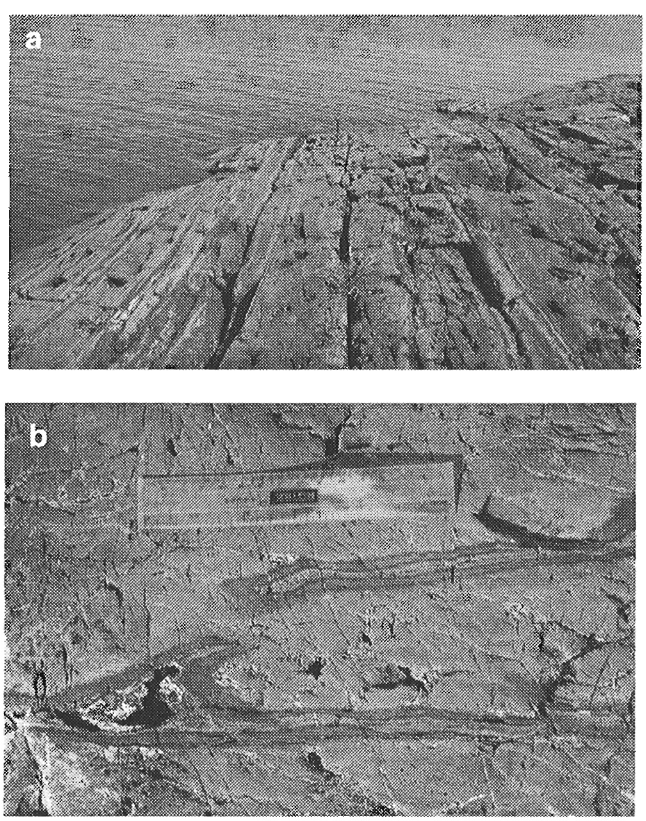

***Figure 4.** Domain I. **a)** Flow-layered mafic volcanic rocks. **b)** Breached chilled margin in layered mafic flows.*

retain diabasic textures and likely represent transposed dykes; others may have a mafic volcanic protolith. Mixed pelitic and psammitic gneiss, with (primary (?)) layering defined by alternating garnet-rich and garnet-poor zones define local lenses.

Multiple generations of tonalitic to granitic neosome occur in the paragneiss and range from foliation-parallel lenses to cross-cutting injections. Zones in which partially assimilated enclaves are engulfed by leucosomal material grade to granitic orthogneiss with decreasing enclave abundance. Granitic orthogneiss, with a gneissosity defined by mafic restite and aligned phenocrysts, outcrops throughout

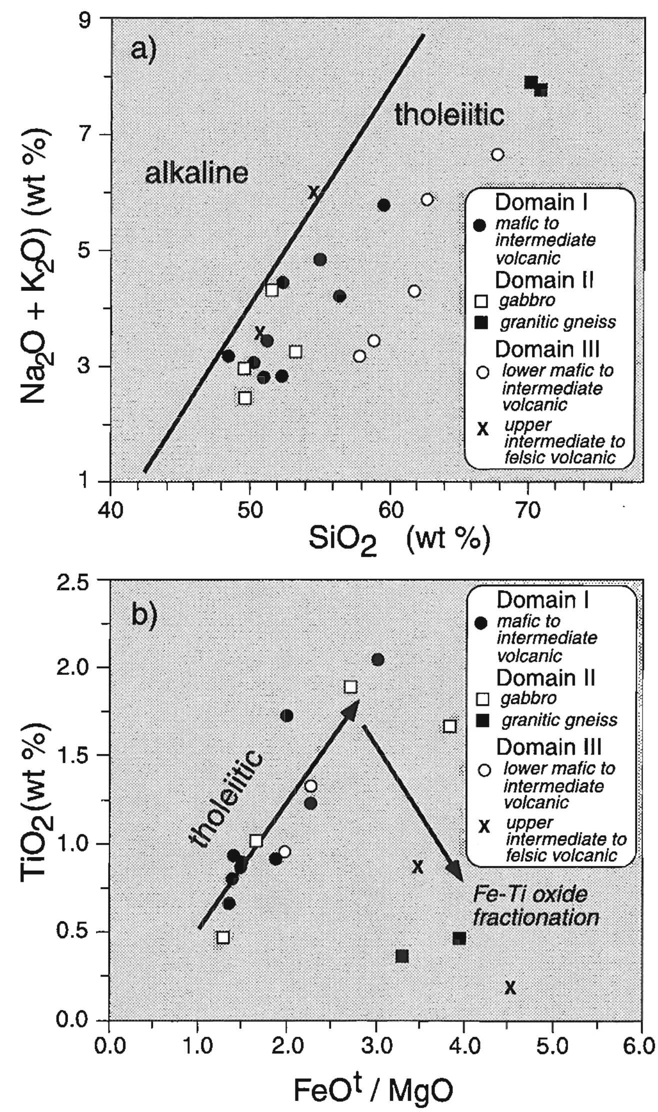

***Figure 5.** Preliminary geochemistry plots. **a)** Tholeiitic-alkaline boundary from MacDonald and Katsura (1964). **b)** Arrows show general titanium-enrichment trend. Three samples from Domain III have been omitted from 5B because of high dolomite contents and uncertainties in calcium-magnesium partitioning. Complete data available from B.L. Cousens.*

the domain. Mafic restite lenses locally contain coarse orthopyroxene that appears to be the product of prograde reactions from hornblende. Complex interference between granitic neosome and enclaves yields outcrops in which gneissosity defines swirly patterns.

Felsic plutonic rocks range in composition from granite to quartz monzonite. Coarse-grained granite, containing potassium feldspar phenocrysts up to 10 cm, forms map-scale lozenges that are enveloped by anastomosing zones of gneiss (Fig. 3). The granites cross-cut granitic, psammitic, and amphibolitic gneiss, but also contain mylonitic and protomylonitic fabrics (Fig. 7) and hence are syntectonic. These fabrics are subparallel to, and intensify toward, the shear zone separating domains I and II and the zone of porphyroclastic gneiss at the northern margin of Domain V. A coarse-grained syntectonic granite, sampled close to the shear zone between domains I and II (Fig. 3), has yielded a preliminary U-Pb zircon age of ca. 2.61 Ga (W.J. Davis, unpublished data), providing the first limit on the age of metamorphism and ductile strain in the region.

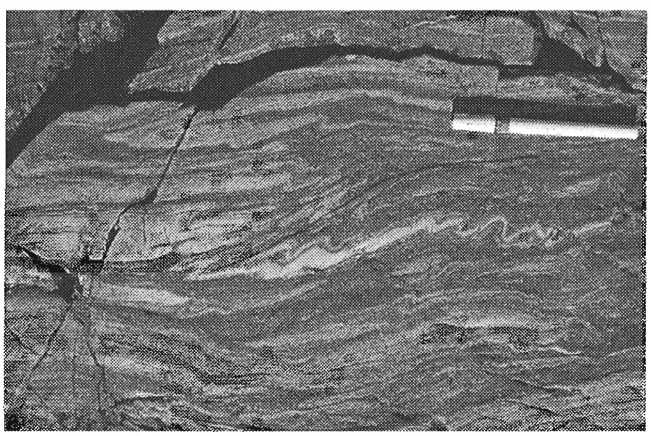

Figure 6. Shear zone separating domains I and II. Folded mylonitic granite and amphibolite. The tighter folds display axial surface traces that are clockwise relative to the more open folds, indicating dextral shear.

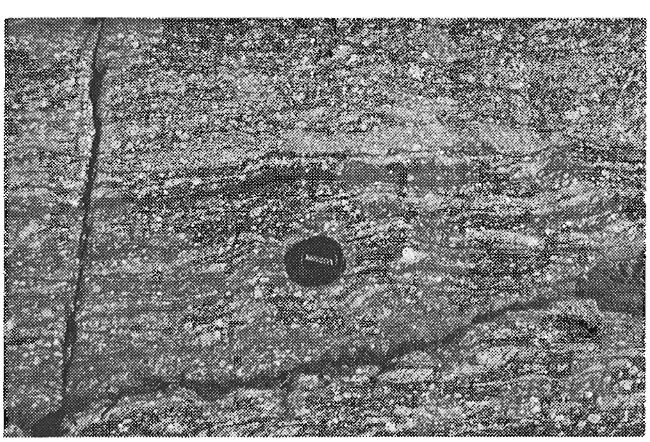

Figure 7. Domain II, protomylonitic coarse-grained granite; dextral shear bands from upper left to lower right.

Most outcrops of Domain II are cut by variably deformed, metamorphosed, and oriented gabbroic dykes that range in width from a few centimetres to about 200 m. The dykes are particularly abundant adjacent to several kilometre-scale gabbro plutons scattered across Domain II (Fig. 3). Border zones of these plutons consist of slightly rotated blocks of gneiss and granite engulfed by gabbro. Although the gabbros cut layering in host gneiss and granite, they commonly contain an internal fabric, and are locally transposed into the gneissic layering. In addition, they are cut by leucosomal pods injected from the host gneiss, and mylonitized equivalents are found within the shear zones separating domains I and II, and at the northern margin of Domain V. Thus, the gabbros are considered syntectonic.

The high dispersion of gneissosity trends in Domain II (Fig. 3) is attributed to host rock-neosome interference, deflection around variably oriented gabbro and granitic bodies, and rotation of gneiss and granitic blocks adjacent to the gabbroic plutons.

Four gabbros and two granitic gneisses from Domain II plot in the tholeiitic field on a $Na_2O + K_2O/SiO_2$ diagram (Fig. 5 a). The gabbros undergo titanium enrichment followed by iron-titanium oxide fractionation (Fig. 5 b).

Domain II-III boundary

In contrast to the straight mylonite zone separating Domains I and II, the boundary between amphibolite-grade rocks of Domain II and greenschist-grade supracrustal rocks of Domain III is irregular and marked by short fault segments (several km) with north, northwest, and northeast trends (Fig. 3). Some of these faults define near-vertical, narrow (to 300 m) zones of greenschist-facies, granitic cataclasite in which granitic and mylonitic granite are cut by millimetre-scale chloritic veinlets. Similar zones of granitic cataclasite are also found within both domains. They truncate structures and gabbro dikes in domains II and III, but at several localities, gabbro bodies were observed crosscutting granitic cataclasite.

Domain III: greenschist-facies supracrustal assemblage

Two unconformity-bounded (?) sequences are exposed in Domain III. The lower sequence consists of three subunits: 1) intermediate to felsic volcanic rocks; 2) interbedded microbial laminates (locally stromatolitic: see Figure 7 in Aspler and Chiarenzelli, 1997), pelites and carbonate-rich, intermediate to felsic volcanic rocks; and 3) carbonate-altered mafic (in part ultramafic ?) volcanic rocks. Interfingering of component rock types indicates that these subunits are conformable, but we remain uncertain of their stratigraphic order. Top indicators in the middle carbonate-pelite unit suggest that it overlies the intermediate to felsic volcanic unit and underlies the mafic volcanic unit. Loveridge et al. (1988) reported U-Pb zircon ages from what we presume to be the lowest unit (Fig. 3) of 2680+29/-25 Ma (containing ca. 3.04 Ga xenocrystic zircon; Eade, 1986) and ca. 2.61 Ga

Table 1. Geochemistry of grab samples from gossans. All analyses are ICP by Acme Analytical Laboratories Ltd., Vancouver.

Site	Sample	Element / Detection Limit / Lithology	Au 2 ppb	Ag 0.3 ppm	Pt 1 ppb	Pd 1 ppb	Cu 1 ppm	Pb 3 ppm	Zn 1 ppm	Ni 1 ppm	Cr 1 ppm	V 1 ppm	Mo 1 ppm	Fe 0.01 %	Mn 2 ppm	Co 1 ppm	As 2 ppm	Hg 1 ppm	W 2 ppm	Mg 0.01 %	Sb 2 ppm	U 5 ppm
1	97-25-23	sulphide veins	< 2	0.3			16	31	5	4	10	3	1	1.93	27	2	5	<1	2	0.04	< 3	< 8
2	97-25-24	in South Channel	< 2	< 0.3			10	19	6	6	12	3	5	1.53	21	7	2	<1	4	0.04	< 3	< 8
3	97-25-27	Formation arkose	< 2	< 0.3			15	6	4	6	14	5	2	1.32	52	3	< 2	<1	2	0.01	< 3	< 8
4	96-43-31	pyritic quartz	14	0.4	2	1	195	19	43	598	496	155	4	22.55	1116	40	259	2	4	0.79	31	< 5
5	96-43-37	pebble	8	< 0.3	3	5	192	21	34	565	274	62	5	17.39	414	90	383	< 1	3	0.48	< 2	< 5
6	96-43-44	conglomerate	5	< 0.3	5	3	117	11	36	641	1088	116	2	20.04	553	79	55	1	< 2	0.58	< 2	< 5
7	97-51-13	sulphide-carbonate altered mafic volcanic	< 2	1.5			180	46	5	1781	1166	< 3	< 1	32.16	576	194	151	< 1	< 2	0.33	< 3	< 5
8	96-33-14a	sulphides in quartz	7	< 0.3			521	30	1014	477	89	14	4	13.03	386	62	9	< 1	< 2	1.69	4	< 5
8	96-33-14b	veins and lenses in mafic	1	< 0.3			251	26	193	126	32	23	5	14.99	614	38	< 2	2	2	1.57	6	< 5
9	96-31-20b	Cu sulphides in late	45	3.2			12267	109	78	53	21	1	5	11.84	27	39	21	< 1	7	0.1	< 2	< 5
10	96-29-3 b	quartz veins	< 2	18.3			54301	43	25	17	32	64	1	6.53	573	14	3	< 1	3	0.55	< 3	< 8
11	97-56-27	sulphides in iron formation	< 2	< 0.3			342	6	50	63	26	101	1	8.16	628	41	< 2	< 1	3	0.31	< 3	< 8
12	97-17-24	disseminated sulphides in felsic volcanic	< 2	< 0.3			69	14	43	23	34	62	6	5.14	222	5	< 2	< 1	5	0.94	< 3	< 8
13	97-17-38	disseminated sulphides in tonalitic gneiss	< 2	< 0.3			14	< 3	25	190	212	98	< 1	7.14	176	52	< 2	< 1	3	2.65	< 3	< 8
14	97-22-9	sulphides in quartz veins in felsic volcanic	< 2	< 0.3			54	10	7	42	18	2	2	3.59	25	119	30	< 1	7	0.02	< 3	< 8
15	97-22-3	disseminated sulphides	< 2	2.4			1972	31	83	403	91	102	3	15.20	355	332	26	< 1	2	1.58	< 3	< 8
16	97-32-1	in mafic volcanic	< 2	< 0.3			1253	16	45	185	142	39	3	11.94	286	68	140	< 1	3	0.48	< 3	< 8
17	97-15-20 c	sulphide veins in	< 2	0.4			109	37	91	34	33	67	2	9.71	380	11	69	< 1	13	0.79	< 3	< 8
18	97-27-27	mafic volcanic	< 2	< 0.3			81	9	108	59	25	34	4	5.86	361	30	< 2	< 1	6	0.98	< 3	< 8

(minimum age; originally reported as 2643 Ma in Eade, 1986). Northwest of Angikuni Lake, the felsic volcanic rocks are cut by a small anorthositic gabbro pluton, and a granitic pluton which displays cataclastic textures.

At the base of the upper sequence is a subunit of interlayered subarkose and framework-intact quartz pebble conglomerate (Fig. 8). Metre-scale mudstone interbeds are common. In view of the paucity of mudrocks in pre-vegetative continental deposits, mixing of mature arenites and conglomerates with mudstones suggests shallow subaqueous, rather than subaerial, deposition. The conglomerate contains clasts derived from reworking of older quartz-rich sandstones. Basal beds of quartz pebble conglomerate are pyritic and yield high nickel, chromium and vanadium, and detectable platinum and palladium values (Table 1) signifying erosion of an ultramafic source. Samarium-neodymium isotopic study of a mudrock interbed yields an initial eNd value of - 2.0 ± 0.8 (assuming a mantle eNd value of +3 at 2680 Ma), suggesting that it includes detritus derived from significantly older (hundreds of Ma) crust. Tentatively, we interpret that the lower contact of this subunit is an unconformity because 1) the abrupt appearance of quartz pebble conglomerate above mafic and felsic volcanic rocks requires a period of intense weathering; 2) the unit appears to cut out lower sequence stratigraphy ; and 3) the unit appears to be distributed as outliers (Fig. 3; paleolow-infills ?). Sparse top determinations suggest that this siliciclastic subunit is overlain by a second sequence of felsic volcanic rocks. These contain abundant pyroclastic breccia, plagioclase crystal tuff, graded ash beds, dolomite-cemented sandstone, and pelite (see Figure 8 in Aspler and Chiarenzelli, 1997).

The lower and upper sequences are folded together. Folds are open, with steeply dipping, northeast-trending axial surfaces and shallow plunges to the northeast and southwest. A kilometre-scale north-trending zone of brecciated to mylonitic granite, such as described above for the Domain II-III boundary, cuts across Domain III stratigraphy near the western limit of mapping (Fig. 3).

***Figure 8.** Domain III , clast-supported quartz pebble conglomerate.*

Six volcanic samples from Domain III plot within the tholeiitic field on a $Na_2O + K_2O/SiO_2$ diagram; one mafic dyke plots just above the alkaline-tholeiite boundary (Fig. 5 a). Although the data are sparse, titanium enrichment (upper sequence) and abundant iron-titanium oxide fractionation (lower sequence) may be indicated (Fig. 5 b). Positive initial e_{Nd} values from the lower sequence (felsic volcanic: + 2.7 ± 0.8; mafic dyke + 3.8 ± 0.8; assuming mantle e_{Nd} value of +3 at 2680 Ma) indicate mantle derivation and minimal contamination by older crust.

Domain IV: granite-granitic gneiss

Domain IV consists of granites and granitic gneisses that are separated from supracrustal rocks of Domain III by a northeast-trending faulted/intrusive contact similar to the zones of granitic breccia that separate domains II and III. Granitic cataclasites are also common within the Domain. In the northwest corner of the map area, both lithologies and northwest-trending fabrics in Domain IV continue across the putative northeast trace of the Snowbird tectonic zone ('Tulemalu Fault' Fig. 3; after Eade, 1986) without truncation or deflection. Apparently, in this area, strain along the Snowbird zone is distributed and not confined to a single linear structural element.

Domain V

Domain V consists of well foliated magnetite leucogranite and granitic gneiss with rare slivers of mafic volcanic rock. Foliation trajectories define a gently northeast-plunging domal structure (Fig. 3). This domal structure appears to extend at least 15 km west of the limit of this year's mapping. Unlike other gneissic domains in the area, the central portion of Domain V is devoid of gabbroic intrusions.

The northern margin of Domain V is a northwest-trending curvilinear shear zone. The shear zone displays shallow to moderate (ca. 15-60°) northeast dips and a down-dip stretching direction defined by isoclinal fold hinges and mineral lineations (Fig. 3). It truncates the southern extent of domains II and III and appears to merge with the dextral ductile shear zone that separates domains I and II, suggesting kinematic linkage between the two. Sparse indicators suggest north-side-down movement. The shear zone consists of interlayered porphyroclastic granitic gneiss (Fig. 9), mylonitic amphibolite gneiss and magnetite leucogranite, apparently derived from protoliths in domains II and V. In addition, discontinuous ribbons of granitic cataclasite occur along the length of the shear zone; some were originally mapped as fragmental felsic volcanic rocks. This cataclasite is commonly non-foliated and consists of granite and mylonitic granite fragments cut and separated by variably oriented, narrow (millimetre-scale and less), chloritic veinlets, and irregular zones of pseudotachylite (Fig. 10). These rocks represent coherent (non-dilational) cataclastic flow and reflect passage through the brittle-ductile transition, such as described from the Great Slave Lake Shear Zone (Hanmer, 1989).

BAKER LAKE BASIN

Paleoproterozoic (ca. 1.85 Ga) rocks of Baker Lake Basin (Dubawnt Supergroup) define two northeast-trending sub-basins in northern Angikuni Lake (Fig. 3). In the northern sub-basin, the Angikuni (unmapped; Blake, 1980) and South Channel formations form local wedges beneath an extensive Christopher Island Formation blanket; in the southern sub-basin, only the Christopher Island Formation is exposed. The Angikuni Formation consists of arkosic redbeds and mud-cracked pelites, and probably represents fluvial and lacustrine sedimentation (Blake, 1980). The South Channel Formation (Donaldson, 1965) comprises framework-intact, polymictic (basement-derived) conglomerate, granulestone, pebbly sandstone and arkose (Fig. 11 a) and is likely a fluvial deposit. The Christopher Island Formation consists of minette flows, volcanic breccias, and local interbeds of framework-intact conglomerate and cross stratified arkose (Fig. 11b).

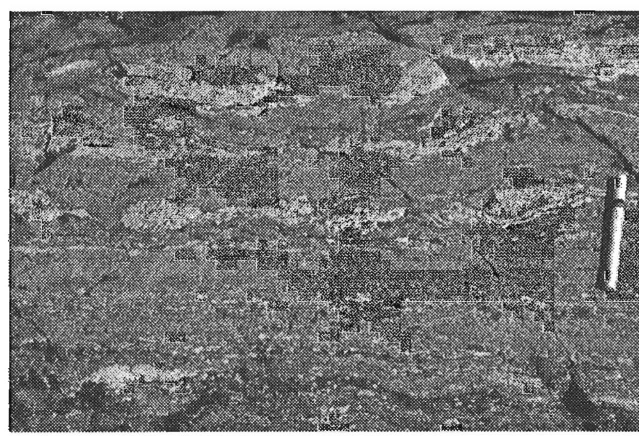

Figure 9. *Domain IV. Porphyroclastic gneiss with coarse-grained granitic dykes dismembered in a tonalitic host.*

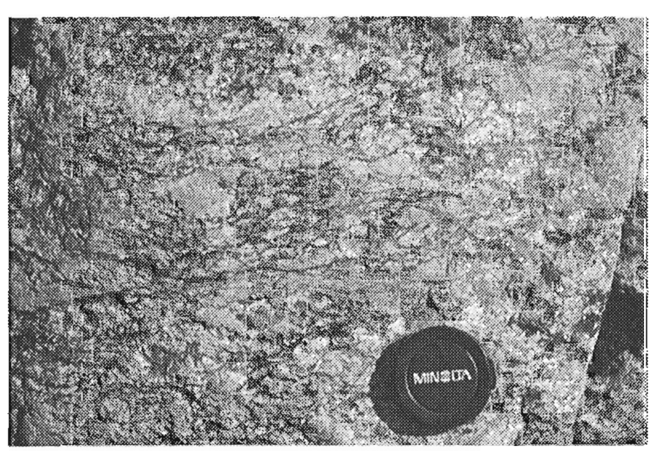

Figure 10. *Northern boundary of Domain V, weakly foliated granitic cataclasite.*

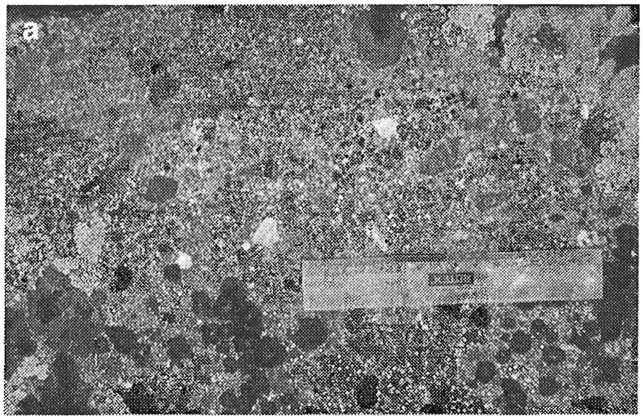

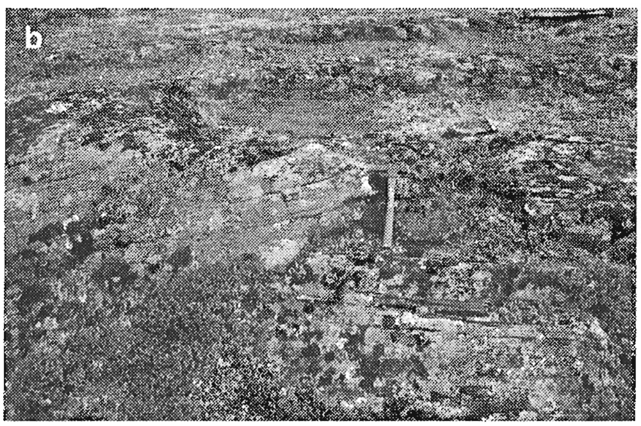

Figure 11. Baker Lake Group. ***a)*** *South Channel Formation, polymictic pebble conglomerate truncating parallel stratified heavy mineral layers in arkose.* ***b)*** *Christopher Island Formation, metre-scale planar cross-stratified arkose.*

In central and southern Angikuni Lake, small (several tens of metres) outliers of Christopher Island Formation and polymictic open-framework conglomerate and redbed arkose of the Kunwak Formation are scattered across the Archean domains described above. The outliers form surface veneers, and fill paleolows in the sub-Baker Lake paleotopography. Paleojoints in subjacent basement, up to 1 m wide and infilled by Baker Lake Group rocks, are locally exposed. Lamprophyre dykes, likely feeders to the Christopher island flows, occur throughout the region, and display strong northeast trends (Fig. 3). Small Martell Syenite (Donaldson, 1965) stocks are also common. Although the Baker Lake Group has not been dated directly, a syenitic pluton possibly comagmatic with lower Baker Lake Group rocks has a U-Pb age of 1850 +30/-10 (Tella et al., 1985).

GOSSANS

Analytical results from 18 gossans are presented in Table 1. Gossans 9 and 10, with high copper values (12,267 and 54,301 ppm), are from chalcopyrite-pyrite-bearing quartz veins that are part of late, post-ductile deformation, brittle stockworks. Gossan 9 has elevated gold values (45 ppb), whereas gossan 10 has elevated silver values (18.3 ppm). Gossans 4, 5, and 6 (gossans 1, 2, and 3 in Aspler and Chiarenzelli, 1997) are in quartz pebble conglomerates at the base of the sandstone-conglomerate sequence that appears to unconformably overlie volcanic and carbonate rocks in Domain III. They have abundant matrix pyrite (presumably paleoplacer) and display slightly elevated gold values (14, 8, 5 ppb respectively) and detectable platinum and palladium, in addition to high nickel, chromium, and vanadium values. A mafic (ultramafic ?) flow from Domain III (Gossan 7), extensively replaced by carbonate, has high nickel (1781 ppm) and chromium (1166 ppm).

DISCUSSION

Mesoarchean basement and Neoarchean paleogeography

Neoarchean supracrustal sequences in the Rae Province, with prominent shallow-water quartz arenites and ultramafic rocks, have been interpreted as rift or passive margin prism deposits (Schau and Ashton, 1988; Chandler et al., 1993) formed during extension of a Mesoarchean basement terrane called 'Nunavutia' by Schau and Ashton (1988). However, the full extent of Mesoarchean basement in the Hearne Province is unclear. Isolated exposures are known from the southern part of the region, within about 100 km north of the Northwest Territories border, near Snowbird Lake (Hanmer et al., 1995), between Kasba and Nueltin lakes (Loveridge et al., 1988), and near Edehon Lake (Loveridge et al., 1988; see Figure 13 in Aspler and Chiarenzelli, 1996). From an initial transect in the Angikuni Lake area, Aspler and Chiarenzelli (1997) questioned if the plutonic-gneissic domains that contain isolated paragneiss remnants (e.g. Domain II) could conceivably be basement to low-grade areas with extensive supracrustal rocks (e.g. domains I and III) or if the high-grade domains are entirely younger than, and developed at the expense of, the low-grade domains. Abundant intrusive relationships mapped during this year's work, and the difference in age between the supracrustal (ca. 2.68 Ga) and granitic (ca. 2.61 Ga) rocks indicate that supracrustal remnants in Domain II were likely derived from volcano-sedimentary units better preserved in domains I and III that were disrupted during plutonism and deformation.

Neoarchean supracrustal rocks in the Angikuni area were deposited in shallow water. In particular, the microbial laminates and stromatolites indicate photic depths (<100 m) and the mud-matrix-deficient sandstone-conglomerate unit demonstrates deposition within the realm of wave and current reworking. Reworked quartz arenite clasts in quartz pebble conglomerates with high nickel, chromium, and vanadium values suggest erosion of quartz arenite-ultramafic sequences in the Rae Province, and the initial e_{Nd} value of -2.0 ± 0.8 from a mudrock interbed demonstrates derivation from significantly older crust (although not neccessarily first cycle). This indicates subaerial exposure of a continental hinterland at the time of sedimentation. Although Mesoarchean basement has not been documented in the Angikuni area, shallow-water rocks derived from a continental hinterland imply deposition on, or close to, continental crust. This is in contrast to shallow-water deposits in the central part of the Ennadai-Rankin greenstone belt, which formed aprons surrounding felsic volcanic edifices in an ensimatic setting (Aspler and Chiarenzelli, 1996). Furthermore, a ca. 3.04 Ga xenocrystic zircon from a 2.68 Ga volcanic sample in Domain III (Eade, 1986; Loveridge et al., 1988) suggests subjacent Mesoarchean at the time of extrusion.

Tectonic setting of volcanism

At least two models for Rae-Hearne tectonic evolution are possible: collapsed back arc basin and merging island arcs. In the initial stages of both models, the Rae Province is considered the continental hinterland to an ensimatic central Hearne Province (Aspler and Chiarenzelli, 1996). Initial geochemical data indicate that volcanic rocks in the Angikuni Lake area follow tholeiitic differentiation trends, inconsistent with a subduction-related origin. Positive initial e_{Nd} values from two samples in Domain III indicate mantle derivation consistent with a back arc setting. We await rare earth element data to determine if these rocks represent continental or oceanic tholeiites.

Snowbird tectonic zone

Mapping in Domain IV documents that rocks and northwest-trending structures continue undeflected across the putative trace of the Snowbird tectonic zone in the northwest corner of the map area. A reconnaissance traverse to the northwest arm of Angikuni Lake, ca. 15 km west of this year's mapping, revealed porphyroclastic granitic rocks, gneisses, and granitic cataclasites remarkably similar to those observed in the map area. We suggest that the Snowbird zone, at the latitude of the present mapping, forms a distributed branching network, rather than being confined to a single linear element, and that it extends across the Angikuni Lake area, at least to the western edge of Domain I. The preliminary age of plutonism and ductile strain (ca. 2.61 Ga), and the preliminary geochemistry (syntectonic gabbroic rocks with tholeiitic titanium-enrichment trends) from Domain II support intracontinental movement along the Snowbird zone, late in the evolution of the Ennadai-Rankin greenstone belt, such as inferred by Hanmer et al. (1995) for the segment of the zone near the Saskatchewan - NWT border.

Baker Lake Basin

Thick sections of volcanogenic and fanglomerate rocks in Baker Lake Basin require active faulting at ca. 1.85 Ga. Contacts between Baker Lake Group rocks and basement mapped this summer failed to reveal evidence of syndepositional or postdepositional faulting, even though the shear zone separating domains I and II is close to, and parallels, the western boundary of the eastern Baker Lake sub-basin (Fig. 3). Testing for a genetic relationship (if any) between the shear zone, particularly its brittle history, and subsidence of the Baker Lake sub-basins will continue to be an important focus of future work. However, it could be that these sub-basins, similar to isolated pockets of Baker Lake Group farther south, represent thermal subsidence beyond the limits of active faulting, and that the syndepositional faults remain buried.

ACKNOWLEDGMENTS

This project is funded by the Northwest Territories Geology Division, Indian Affairs and Northern Development Canada (Yellowknife), with support from the Geological Survey of Canada. G., L. and S. Gurke (Treeline Lodge, Nueltin Lake) provided efficient logistics and pilot G. Clark (Jackson Air Services) flew safe camp moves. R. Bromecker (WMC International Ltd.) generously shared helicopter hours and ideas regarding economic geology. We thank J.A. Donaldson and S. Hanmer for instruction and discussion during field visits, and S. Hanmer, S. Lucas and C. Relf for constructive critical comments.

REFERENCES

Aspler, L.B. and Chiarenzelli, J.R.
1996: Stratigraphy, sedimentology and physical volcanology of the Henik Group, central Ennadai-Rankin greenstone belt, Northwest Territories, Canada: Late Archean paleogeography of the Hearne Province and tectonic implications; Precambrian Research, v. 77, p. 59-89.
1997: A preliminary transect across east-central Angikuni Lake, District of Keewatin, Northwest Territories; in Current Research 1997-C; Geological Survey of Canada, p. 133-143.
in press: Two Neoarchean supercontinents ?: evidence from the Paleoproterozoic; Sedimentary Geology.

Ballard, R.D., Holcomb, R.T., and van Andel, T.H.
1979: The Galapagos Rift at 86° W: 3. Sheet flows, collapse pits, and lava lakes of the Rift valley; Journal of Geophysical Research, v. 84, p. 5407-5422.

Blake, D.H.
1980: Volcanic rocks of the Paleohelikian Dubawnt Group in the Baker Lake -Angikuni Lake area, District of Keewatin, N.W.T.; Geological Survey of Canada, Bulletin 309, 39p.

Chandler, F.W., Jefferson, C.W., Nacha, S., Smith, J.E.M., Fitzhenry, K., and Powis, K.
1993: Progress on geology and resource assessment of the Archean Prince Albert Group, Laughland Lake area, Northwest Territories; Geological Survey of Canada, Paper 93-1C, p. 209-219.

Donaldson, J.A.
1965: The Dubawnt Group, Districts of Keewatin and Mackenzie; Geological Survey of Canada, Paper 64-20, 11p.

Eade, K.E.
1986: Precambrian geology of the Tulemalu Lake-Yathkyed Lake area, District of Keewatin; Geological Survey of Canada, Paper 84-11, 31 p.

Gregg, T.K.P. and Fink, J.H.
1995: Quantification of submarine lava-flow morphology through analog experiments; Geology, v. 23, p. 73-76.

Hanmer, S.
1989: Initiation of cataclastic flow in a mylonite zone; Journal of Structural Geology, v. 11, p. 751-762.

Hanmer, S., Peterson, T.D., Sandeman, H.A.I., Rainbird, R.H., and Ryan, J.J.
1998a: Geology of the Kaminak greenstone belt from Padlei to Quartzite Lake, Kivalliq Region, Northwest Territories; in Current Research 1998-C; Geological Survey of Canada.

Hanmer, S., Rainbird, R.H., Sandeman, H.A.I., Peterson, T.D., and Ryan, J.J.
1998b: Field contributions to thematic studies related to the Kaminak greenstone belt, Kivalliq Region, Northwest Territories; in Current Research 1998-C; Geological Survey of Canada.

Hanmer, S., Williams, M., and Kopf, C.
1995: Striding-Athabasca mylonite zone: Implications for the Archean and Early Proterozoic tectonics of the western Canadian Shield; Canadian Journal of Earth Sciences, v. 32, p. 178-196.

Hoffman, P.F.
1989: Precambrian geology and tectonic history of North America; in The Geology of North America—an Overview, Vol. A, The Geology of North America, (eds) A.W. Bally and A.R. Palmer; Geological Society of America, p. 447-511.

Holcomb, R.T., Moore, J.G., Lipman, P.W., and Belderson, R.H.
1988: Voluminous submarine lava flows from Hawaiian volcanoes; Geology, v. 16, p. 400-404.

Loveridge, W.D., Eade, K.E., and Sullivan, R.W.
1988: Geochronological studies from Precambrian rocks from the southern District of Keewatin; Geological Survey of Canada, Paper 88-18, 36p.

MacDonald, G.A. and Katsura, T.
1964: Chemical composition of Hawaiian lavas; Journal of Petrology, v. 5, p. 82-135.

Relf, C., Irwin, D., MacLachlan, K., and Mills, A.
1998: New insights into the geology of the Yathkyed Lake greenstone belt, western Churchill Province, Northwest Territories; in Current Research 1998-C; Geological Survey of Canada.

Schau, M. and Ashton, K.E.
1988: The Archean Prince Albert Group, northeastern Canada: evidence for crustal extension within a 2.9 Ga continent; Geological Society of America Abstracts With Program, v. 20, p. A50.

Tella, S., and Eade, K.E.
1985: Geology, Kamilukuak Lake, District of Keewatin, Northwest Territories; Geological Survey of Canada, Map 1629A, scale 1:250,000.

Tella, S., Heywood, W.W., and Loveridge, W.D.
1985: A U-Pb age from a quartz syenite intrusion, Amer Lake, District of Keewatin; a part of the Churchill structural province; Geological Survey of Canada, Paper, 85-1B, p. 367-370.

Tribble, G.W.
1991: Underwater observations of active lava flows from Kilauea volcano, Hawaii; Geology, v. 19, p. 633-636.

New insights into the geology of the Yathkyed Lake greenstone belt, western Churchill Province, Northwest Territories[1]

C. Relf[2], D. Irwin[3], K. MacLachlan[4], and A. Mills[3]
Continental Geoscience Division

Relf, C., Irwin, D., MacLachlan, K., and Mills, A., 1998: New insights into the geology of the Yathkyed Lake greenstone belt, western Churchill Province, Northwest Territories: in Current Research 1998-C; Geological Survey of Canada, p. 67-75.

Abstract: The Archean Yathkyed greenstone belt comprises a northwest-dipping package of metavolcanic and metasedimentary rocks exposed along the southeast side of Yathkyed Lake. Southeastward-younging indicators suggest that the belt is regionally overturned. Along the northwest side of the belt, a unit previously mapped as mixed gneiss and migmatite was subdivided into amphibolite (interpreted as high-grade mafic volcanic rocks), and paragneiss (high-grade sedimentary rocks) intruded by various granitoids, effectively doubling the width of the greenstone belt from previous maps.

The Yathkyed belt is bounded along its southeastern margin by the Tyrrell shear zone. Kinematic indicators along the zone record reverse displacement followed by normal-dextral movement. The tectonic significance of the shear zone and its relationship to regionally developed fabrics are unclear. Regional overturning of the supracrustal package and the occurrence of the shear zone at the highest exposed stratigraphic level suggest the possibility of a thrust nappe.

Résumé : La ceinture de roches vertes archéenne de Yathkyed (Province de Churchill occidentale, T.N.-O.) comprend une masse de roches métavolcaniques et métasédimentaires à pendage nord-ouest qui affleure le long de la rive sud du lac Yathkyed. La présence d'indicateurs de plus en plus jeunes vers le sud-est laisse supposer que la ceinture est régionalement renversée. Le long du flanc nord-ouest de la ceinture, une unité antérieurement cartographiée comme un mélange de gneiss et de migmatites a été subdivisée; elle comprend maintenant des amphibolites (interprétées comme des volcanites mafiques très métamorphisées) et des paragneiss (roches sédimentaires très métamorphisées) recoupés par divers granitoïdes, doublant ainsi la largeur de la ceinture de roches vertes par rapport à ce qui avait été cartographié auparavant.

La bordure sud-est de la ceinture de Yathkyed correspond à la zone de cisaillement de Tyrrell. Les indicateurs cinématiques observés le long de la zone de cisaillement indiquent qu'il y a eu des mouvements d'abord inverses puis normaux (dextres). La signification tectonique de la zone de cisaillement et ses rapports avec les fabriques caractéristiques de la région n'ont pas été déterminés avec certitude. Le renversement régional de la masse supracrustale et la présence de la zone de cisaillement au niveau stratigraphique le plus élevé (en affleurement) permettent de supposer qu'il s'agit peut-être d'une nappe de charriage.

[1] Contribution to the Western Churchill NATMAP Project

[2] Northwest Territories Geology Division, Department of Indian Affairs and Northern Development, Box 1500, Yellowknife, Northwest Territories X1A 2R3
[3] Department of Resources, Wildlife, and Economic Development, Government of the Northwest Territories, Box 1320, Yellowknife, Northwest Territories X1A 2L9
[4] Department of Earth Sciences, Memorial University of Newfoundland, St. John's, Newfoundland A1B 3X5

INTRODUCTION

During the 1997 field season, 1:50 000 scale bedrock mapping was carried out in the Yathkyed Lake area, about 300 km west-southwest of Rankin Inlet in the Kivaliq region of the Northwest Territories. The project, funded by the Department of Resources, Wildlife, and Economic Development, Government of the Northwest Territories, is part of a multi-year mapping project initiated by Relf (1996) to better understand the geology of the Yathkyed Lake greenstone belt, determine the area's mineral potential, and test whether rocks comprising the Yathkyed belt are contiguous with those of the Kaminak greenstone belt to the east. This project is a contribution to the Western Churchill NATMAP Project, and has benefited from field visits by Geological Survey of Canada colleagues. Ongoing support through geochemical, geochronological, and thermobarometric studies will further benefit the project.

Previous geological mapping, exploration work, and geophysical data from the area helped define several questions that focused 1997 mapping efforts. Although 1:250 000 bedrock mapping (Eade, 1985, 1986) had delineated the volcanic belt, little was known about the regional younging direction of the belt, its internal stratigraphic (tectonostratigraphic?) relations, or the nature of surrounding granitoids and gneisses. One of the questions that originally sparked interest in the map area was the significance of a linear aeromagnetic anomaly along the southeast margin of the Yathkyed greenstone belt (Geological Survey of Canada, 1981). This anomaly has a signature similar to, although weaker than, the positive linear anomaly associated with the Snowbird Tectonic Zone, suggesting the possibility of a tectonic contact between the volcanic belt and adjacent granitoids southeast of the belt. Numerous iron-formations, hosted by both volcanic and sedimentary rocks southwest of Tyrrell Arm on Yathkyed Lake, were the target of exploration efforts in the late 1980s, although most of the claims on this ground were subsequently dropped. As part of this project, seventy-five samples were collected for assay analysis, in order to help evaluate the mineral potential of the study area. These data will be compiled in a mineral showings database being created as part of the Western Churchill NATMAP Project.

REGIONAL GEOLOGICAL SETTING

The current project focuses on a northeast-trending belt of supracrustal rocks in the Yathkyed Lake area (Fig. 1). The belt comprises Archean metavolcanic and metasedimentary rocks, intruded by syntectonic to late tectonic granitoids, and is unconformably overlain by Paleoproterozoic sedimentary rocks of the Hurwitz Group.

One of the highlights of the 1997 mapping was the identification of a shear zone bounding the southeastern margin of the supracrustal belt (Fig. 2). The shear zone, informally named the Tyrrell shear zone after Tyrrell Arm on Yathkyed Lake, may have important implications for regional contact relations in the western Churchill Province. Another highlight of mapping was the delineation of a package of high-grade supracrustal rocks through an area previously mapped as largely undifferentiated gneisses and migmatites. The supracrustal package comprises mixed volcanic rocks, numerous gossans, sedimentary rocks, and ultramafic xenoliths of uncertain origin, and at present has unknown mineral potential. Geochemical studies underway at the Geological Survey of Canada will test whether this supracrustal package could represent high-grade equivalents of rocks of the Yathkyed greenstone belt.

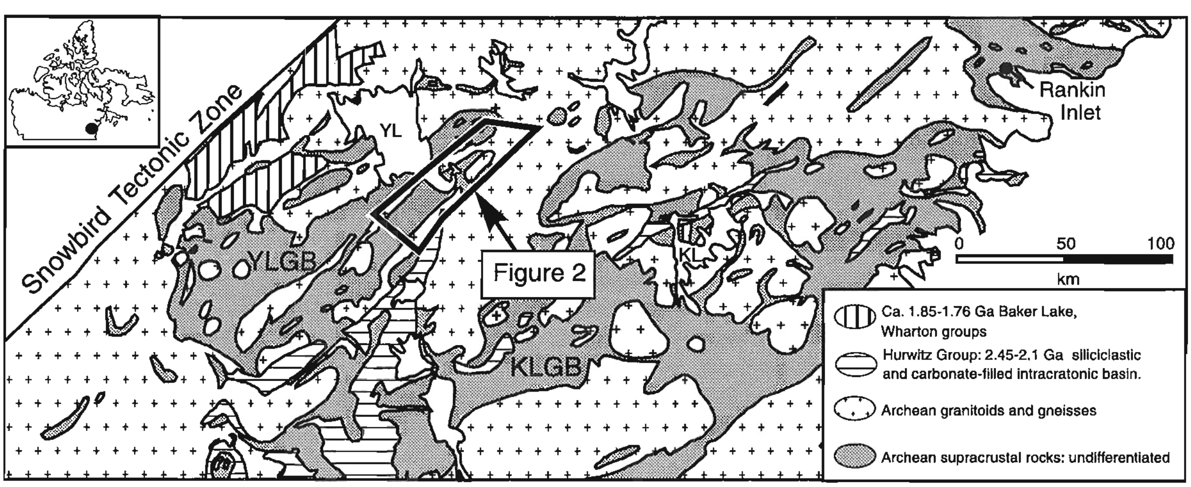

Figure 1. *Simplified geology of part of the western Churchill Province, showing location of map area. KL = Kaminak Lake; YL = Yathkyed Lake; KLGB = Kaminak Lake greenstone belt; YLGB = Yathkyed Lake greenstone belt. Figure modified after Aspler and Chairenzelli, 1996.*

MAP UNITS

Archean rocks

Volcanic rocks

The Yathkyed greenstone belt comprises a moderately to steeply northwest-dipping belt of pillowed mafic flows, with minor plagioclase-phyric flows or sills, volcaniclastic sedimentary rocks and rare felsic volcanic rocks. Younging directions in pillows are rarely preserved, although the few top determinations noted indicate consistent younging towards the southeast. The northwest dip of the belt, coupled with the apparent regional southeastward younging, suggests that it may represent an overturned panel. Volcaniclastic sedimentary rocks make up less than 10 per cent of the volcanic package and are typically characterized by alternating biotite- and chlorite- or hornblende-rich layers about 1-5 cm thick. The presence of biotite indicates a different bulk composition than that of the pillowed flows, suggesting that these rocks are not simply highly strained pillowed flows. Elsewhere, banded

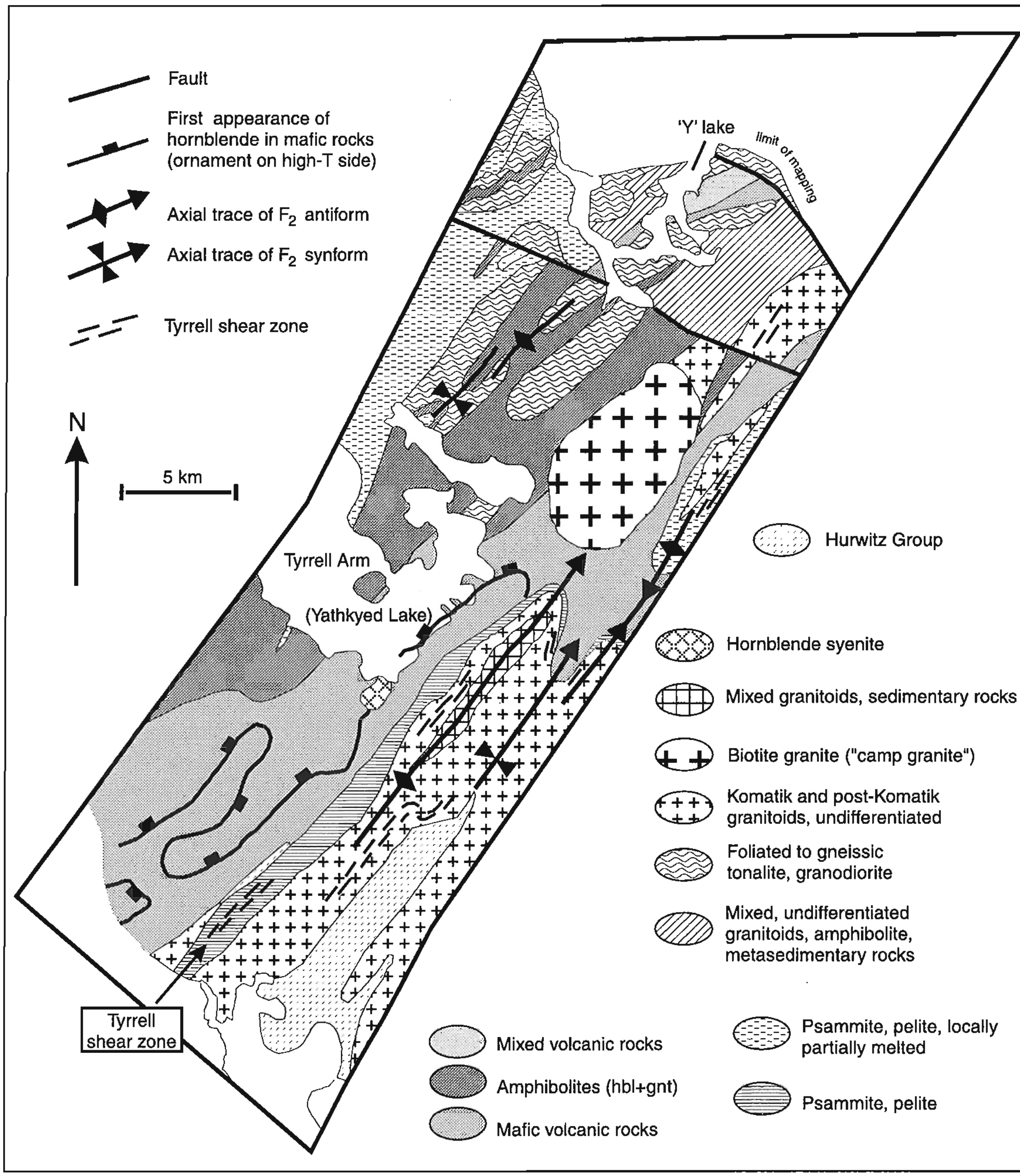

Figure 2. *Simplified geology of the northern Yathkyed Lake greenstone belt.*

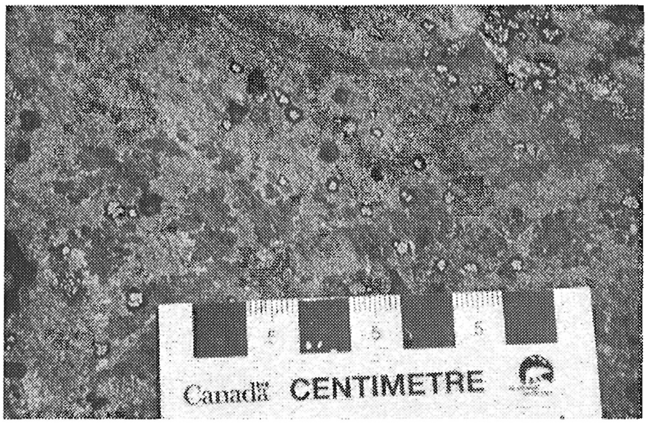

Figure 3. Cordierite-rich intermediate volcanic rock, commonly referred to as "dalmatianite". See text for description.

mafic rocks lacking biotite may be intensely flattened pillows. Felsic rocks were recognized in only a few outcrops. In the south and central parts of the map area, thinly bedded (up to 2 cm) felsic tuffs or volcaniclastic sedimentary rocks are locally associated with iron-formation. The felsic units are typically less than 10 m thick.

In the northern part of the map area, a package of mixed, dominantly mafic to intermediate volcanic rocks was recognized. It comprises fragmental volcaniclastic rocks characterized by felsic to intermediate clasts up to 10 cm, thinly bedded (1-5 cm) sedimentary rocks with mafic components, minor polymictic conglomerate (debris flow?), and fuchsitic felsic tuffs. Numerous gossans occur within this package, and cordierite-rich rocks of intermediate composition ('dalmatianite') were observed locally (Fig. 3). Individual units within this mixed package are typically too thin or discontinuous to be mapped out at the current map scale, and therefore the rocks are grouped into a single map unit comprising mixed volcanic rocks.

Sedimentary rocks

Sedimentary rocks in the map area are dominated by psammites and semipelites to pelites. Primary sedimentary features are best preserved within greenschist facies rocks in the southeastern part of the area. Here, graded bedding and local crossbeds indicate southeastward younging, suggesting that the sedimentary rocks stratigraphically overlie, yet structurally underlie, the volcanic rocks to the northwest. Locally chlorite-rich beds and the presence of euhedral to subhedral plagioclase clasts suggest detritus from a volcanic source. In the western and northern parts of the map area, metamorphic grade is higher, and primary structures are not as well preserved, although bedding can still be recognized locally.

Ultramafic rocks

Two outcrops of ultramafic rocks were identified in the map area. Both are small (~3 x 10 m) and are associated with a mixed unit of granitoids and hornblende-grade mafic volcanic rocks in the northern half of the study area. The unit consists of massive actinolite with minor talc and/or sericite, and has an unknown origin.

Granitoids

Several phases of granitoids, ranging from tonalitic orthogneiss to late two-mica pegmatite, intrude supracrustal rocks in the study area. In the field, at least five distinct units can be distinguished, although at the map scale, two of the granitoids are grouped as a single mappable unit.

Early tonalite

The earliest granitoid unit ranges in composition from biotite tonalite to granodiorite, and is strongly foliated to gneissic. It is typically grey on weathered and fresh surfaces, and locally contains up to 15 per cent biotite. It outcrops mainly in the northern part of the map area, but may be correlative with strongly foliated biotite tonalite xenoliths preserved locally in some of the younger granitoids throughout the map area.

The early tonalite occurs as foliation-parallel lenses and plutons, and is folded along with the volcanic rocks about northeast-trending folds, suggesting that it was emplaced relatively early in the area's geological history. The tonalite contains variably flattened enclaves of amphibolite and metasedimentary rocks. Locally, layering in the enclaves is transected by the tonalite, although more commonly, the foliation in enclaves parallels that in the surrounding tonalite, perhaps reflecting transposition.

Komatik granite

The Komatik granite consists of massive to moderately foliated pink-weathering biotite monzogranite to syenogranite. Grain size varies from medium to pegmatitic.This unit locally intrudes the early tonalite in centimetre-wide veins along the foliation, imparting a gneissic appearance. Much of the northern part of the area, previously mapped as gneisses (Eade, 1985), has been reinterpreted as mixed granitoids comprising these 'injection gneisses'.

In addition to the intrusive component of injection gneisses, the Komatik granite defines small mappable plutons, particularly along the southeastern margin of the supracrustal belt. South of Tyrrell Arm, the Komatik granite intrudes metasedimentary rocks in foliation-parallel sheets up to hundreds of metres wide. Locally these sheets define discreet plutons, whereas elsewhere they comprise part of a mixed unit with the sedimentary rocks (see below).

Post-Komatik granites

Post-Komatik granitoids include a unit of white-weathering, coarse to pegmatitic two-mica monzogranite to syenogranite. Garnet and/or tourmaline occur locally as accessory minerals. This unit is associated with high-grade metasedimentary rocks in the 'Y' lake area, where it is interpreted to be a product of anatectic melting of the sedimentary rocks. Southeast of Tyrrell Arm, this unit, along with the Komatik granite, pervasively intrudes low-grade metasedimentary rocks. Crosscutting relations indicate that this granite is younger than the Komatik unit, although both appear to be variably deformed in the Tyrrell shear zone.

A second post-Komatik granitoid occurs along the southeastern edge of the Yathkyed belt and is spatially associated with the Tyrrell shear zone. It comprises numerous foliation-parallel veins up to several tens of centimetres wide that are locally mylonitized. These veins weather white and comprise coarse (locally pegmatitic) tonalite to monzogranite with little or no accessory mica. Texturally, the unit is very similar to the late, locally pegmatitic, monzogranite described above, although it lacks the accessory mineral assemblage that distinguishes the monzogranite. Crosscutting relations with the monzogranite are unclear, and therefore the two units are grouped as a single unit on the 1:50 000 map (D. Irwin and C. Relf, unpubl. data, 1997).

The youngest post-Komatik unit is a pink-weathering, massive biotite monzogranite that is locally K-spar megacrystic. Informally named the 'camp granite', it defines a pluton about 8 x 12 km in the north half of the map area. Where the contact between the camp granite and surrounding country rock is exposed, the camp granite clearly crosscuts the foliation in the adjacent units, suggesting a post-tectonic age for the pluton. However, the pluton is slightly elongate parallel to the regional foliation (aspect ratio of ~1:1.5 in map view), suggesting that it may have been emplaced late during regional northwest-southeast shortening.

Mixed sedimentary rocks and granitoids

Where the Komatik and post-Komatik granitoids intrude sedimentary rocks along the southeastern margin of the Yathkyed belt, they are locally mixed in roughly equal proportions with the sedimentary rocks, imparting a migmatitic appearance. The host rocks are mainly psammites and semipelites, and contain millimetre-sized biotite porphyroblasts, attesting to a relatively low metamorphic grade. The migmatitic texture is therefore intrusive in origin, although where the unit is deformed in the Tyrrell shear zone, it superficially resembles a foliated anatectic migmatite.

Late Archean/Proterozoic rocks

Diabase dykes

Although most of the diabase dykes in the map area are Proterozoic, a few may be late Archean. On the southeast side of 'Y' lake, several fragments of a boudinaged, medium- to coarse-grained northwest-trending diabase dyke were mapped. The dyke contains metamorphic hornblende and is crosscut by pegmatitic granite veins. If the pegmatite veins are related to the surrounding granitoids, then the diabase is likely Archean. However, the crosscutting veins may be late Proterozoic (1.75 Ga Nueltin suite; Loveridge et al., 1987), in which case the diabase could be part of the ca. 2.19 Ga Tulemalu swarm (LeCheminant et al., 1997). Several other northwest- to west-striking diabase dykes with textures similar to those of the dyke described above, but lacking the crosscutting pegmatite, were mapped. They are tentatively interpreted to be correlative, on the basis of their compositional and textural similarities.

Hornblende syenite

A massive, K-feldspar megacrystic to pegmatitic hornblende±biotite syenite defines a small (2 km in diameter) pluton on the south shore of Tyrrell Arm. The core of the pluton is coarse grained and locally K-feldspar megacrystic, with a medium-grained margin within about 200 m of its contact with the country rocks. The age of this pluton is uncertain. It crosscuts the foliation in the volcanic belt, and is generally massive, except along its margins where a moderate (synchronous with emplacement?) foliation is developed. It may be correlative with the ca. 1.84 Ga Martell syenite of the Dubwant Group (Donaldson, 1965), although it is cut by a diabase dyke tentatively correlated with the ca. 2.19 Ga Tulemalu swarm (see above). Alternatively, it could be related to an older (possibly Archean), locally foliated hornblende syenite exposed east of Tulemalu Lake (Eade, 1985). The unit was sampled for U-Pb zircon geochronology.

Proterozoic rocks

Hurwitz Group

Shallow-water sedimentary rocks of the Hurwitz Group unconformably overlie Archean rocks in the southern part of the map area. The sedimentary rocks were correlated with the Watterson and Tavani formations by Eade (1985) and include quartz-rich subarkose, calc-silicate schist, minor dolostone, and quartz-pebble conglomerate. The subarkose weathers white to buff, contains up to about 10 per cent feldspar and lithic fragments, and is characterized by beds typically 1 to 30 cm thick. In the northern part of the exposed Hurwitz Group, carbonate-rich sedimentary rocks are locally interbedded with the subarkose. They include dolostone beds up to 15 cm thick, and calc-silicate schists dominated by the assemblage tremolite/actinolite-dolomite-quartz. The latter may represent metamorphic conditions as high as upper greenschist facies. A single occurrence of quartz-pebble conglomerate with subarkose is found in a narrow outlier west of the main Hurwitz Group outlier (Fig. 2). The conglomerate is less than 4 m thick and consists of white quartz cobbles in a matrix of white-weathering subarkose.

In the Yathkyed Lake area, bedding in the Hurwitz Group dips moderately to steeply, and metamorphic grade is atypically high. Eade (1986) suggested that Archean rocks immediately southeast of here were tectonically and thermally reworked during a Paleoproterozoic orogenic event, which must also have affected the Hurwitz Group. Near the southern part of the map area, a pegmatitic granite dyke cuts Hurwitz Group subarkose, and was sampled for U-Pb dating.

Diabase dykes

Proterozoic diabase dykes of the ca. 2.45 Ga Kaminak swarm (Heaman, 1994) and the ca. 1267 Ma Mackenzie swarm (LeCheminant and Heaman, 1989) were recognized in the study area. The Kaminak dykes are distinguished by their north-northeast strike and the presence of plagioclase megacrysts up to 5 cm. The Mackenzie diabase dykes strike northwest, are commonly magnetic, and are characterized by their ophitic texture and rubbly weathered texture.

Minette dykes

Minette dykes occur locally throughout the map area and are characterized by abundant biotite phenocrysts and a distinctive brown weathered surface. Most have a relatively fresh appearance, and are interpreted to be associated with the Christopher Island Formation (Peterson and Rainbird, 1990).

In addition to the Christopher Island minettes, several foliated minette dykes were found in the map area. They are recrystallized and locally appear to be altered, and therefore may be older than the Christopher Island dykes. Similar dykes have been described elsewhere (e.g. Relf, 1995).

STRUCTURAL ELEMENTS

Rocks in the Yathkyed Lake area preserve evidence of a complex Archean deformational history, characterized by an early event that produced a bedding-parallel foliation and resulted in overturning of the supracrustal package, followed by late upright folding that produced shallowly northeast-plunging folds and associated cleavage. Displacement along the Tyrrell shear zone apparently involved early, dominantly reverse movement, followed by later, oblique (normal) dextral shearing. Although no direct evidence exists to link the regional folding and cleavage-forming events with movement along the shear zone, field relations suggest that the early foliation may be coeval with reverse displacement along the Tyrrell shear zone. Samples were collected for U-Pb analyses to bracket the timing of the different structural elements and events.

Regionally developed folds, foliations

Throughout most of the map area, a single foliation, designated S_{main}, is preserved in Archean supracrustal rocks. S_{main} is defined by the alignment of metamorphic minerals, and is generally parallel to bedding. Correlation of S_{main} from outcrop to outcrop was assumed during mapping, although two foliations are preserved locally below the hornblende isograd and it is commonly unclear which fabric corresponds to S_{main}.

Where two foliations are preserved, the earlier foliation (S_1) is a layer-parallel penetrative fabric overprinted by a tightly spaced, steeply northwest-dipping cleavage (S_2). Such overprinting was observed only in the hinge zones of open to tight Z-asymmetrical folds (F_2); elsewhere the two fabrics are likely transposed into a single foliation. Most F_2 folds plunge shallowly to moderately (20-50°) northeast, with fewer southwest plunges. The shallow plunge of F_2 folds suggests that S_1 was shallowly dipping before D_2. In addition to bedding and S_1, F_2 folds deform, and therefore postdate, the hornblende isograd preserved in mafic rocks.

Rocks of the Hurwitz Group preserve a moderately to steeply dipping, near-bedding-parallel foliation that strikes northeast (030-040°). A weak, gently north-plunging mineral lineation is locally associated with the foliation. The foliation preserved in the Hurwitz Group is generally parallel to and indistinguishable from S_{main} in the underlying Archean rocks. However, S_{main} is cut locally by granitoid veins of presumed Archean age, distinguishing it from the Proterozoic foliation. Rather than attributing the parallelism to coincidence, it is suggested that either Proterozoic shortening reoriented pre-existing Archean fabrics into their present orientation, or the orientation of Proterozoic fabrics was controlled by the pre-existing Archean anisotropy.

The Tyrrell shear zone

The Tyrrell shear zone is a northeast-striking, northwest-dipping zone of high strain locally up to 2 km wide, within which mylonites 1-50 m wide anastomose between less strained augen. The mylonites occur within the mixed granitoids and intrusive migmatites along the southeastern margin of the supracrustal belt, and range from protomylonite with well preserved, asymmetrical porphyroclasts, to ribbon ultramylonites. A strong stretching lineation with a variable but typically shallow (20-30°) northward plunge is associated with the mylonites.

Shear sense indicators, including asymmetrical sigma-type porphyroclasts, shear bands, foliation fish, and, less commonly, C-S fabrics indicate predominantly dextral movement with a component of normal displacement (Fig. 4). However, in a few outcrops, asymmetrical folds, C-S fabrics, back-rotated pull-aparts and a dip-parallel extension recorded by isoclinal fold axes record an episode of reverse displacement along the shear zone. In one outcrop, reverse shear sense indicators are overprinted by dextral indicators, providing evidence for the relative timing of the two shearing events.

The tectonic significance of the shear zone is not entirely clear, although its regional setting is intriguing. Younging indicators within the Yathkyed belt suggest that the supracrustal package is an overturned southeastward-younging panel. Early reverse shearing along the structural base of the panel may represent a thrusting event with the volcano-sedimentary package the overturned limb of a nappe emplaced southeastward (present coordinates). If so, the early foliation (S_1) may be coeval with nappe emplacement.

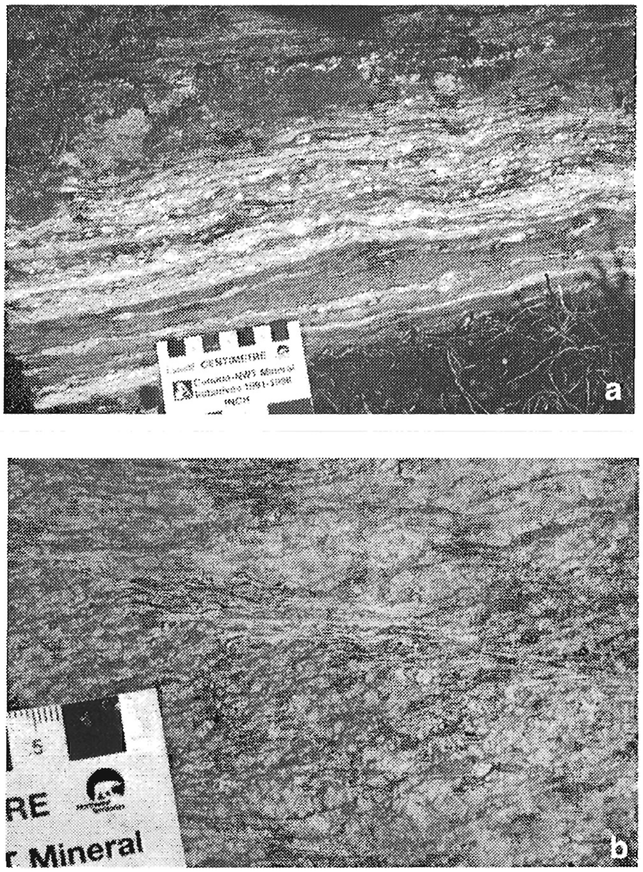

Figure 4. Dextral shear bands in mylonites along the Tyrrell shear zone: (a) mixed sedimentary rocks and granitoids; (b) Komatik granite.

If the Tyrrell shear zone is an Archean thrust fault, it may represent an important tectonic contact, and the Yathkyed greenstone belt may have a history distinct from the adjacent Kaminak belt to the southeast, against which it is juxtaposed. Ongoing geochemical and geochronological studies will test this possibility.

The significance of subsequent dextral-normal shearing is less clear. It may be related to uplift of the Nowyak metamorphic core complex 60 km to the southwest, where a thick panel of mixed amphibolites, pelites, and granite was unroofed from depths of about 30 km by slip along a gently north-dipping detachment (Labelle, 1997; Relf et al., 1997). The direction of maximum extension during this event was approximately north-south (subhorizontal), consistent with the instantaneous extension direction during late, dextral-normal displacement along the Tyrrell shear zone. The bulk of crustal extension related to formation of the Nowyak complex is interpreted to have occurred around ca. 2.64 Ga (B. Davis, unpubl. data, 1997). U-Pb dating of the Tyrrell shear zone by one of the authors (KM) will determine whether dextral shearing was coeval with crustal extension recorded to the southwest.

In several outcrops, mylonites and their associated lineations are deformed by tight, northeast-trending, upright folds with wavelengths of metres to tens of metres. These folds are correlated with map-scale F_2 folds on the basis of their orientation. This relationship requires that F_2 postdated shearing.

METAMORPHISM

Metamorphic grade in the map area ranges from greenschist to upper amphibolite facies. The lowest grade rocks occur in the southeast and are characterized by chlorite in mafic volcanic rocks, and phyllites with millimetre-scale biotite porphyroblasts in sedimentary rocks. Towards the west and northwest, mafic volcanic rocks preserve a hornblende-in isograd, which is folded about, and therefore predates, northeast-trending F_2 folds. The assemblages hornblende+garnet and hornblende+epidote+garnet were observed locally within the hornblende zone. Occurrences of these assemblages are uncommon, and are interpreted to reflect variations in bulk composition, rather than changes in metamorphic grade. Locally garnets within amphibolites are rimmed by fine-grained plagioclase, documenting uplift following garnet growth. A second, higher grade, zone was distinguished in the map area northwest of the hornblende isograd. It is not defined by the growth of new metamorphic minerals, but rather is characterized by a transition from hornblende-rich schists to layered amphibolites, locally with a gneissic texture. It is mapped as a separate unit on Figure 2, although the amphibolites and mafic gneisses are interpreted to be simply high-grade equivalents of the mafic volcanic rocks. Geochemical analyses are underway to compare the trace element compositions of the amphibolites with lower grade mafic volcanic rocks of theYathkyed belt.

The highest grade rocks in the map area occur along the southwest side of Tyrrell Arm. Amphibolites here locally contain a brown-weathered mineral tentatively identified as orthopyroxene, suggesting uppermost amphibolite to granulite facies. Petrographic studies will identify mineral assemblages to better establish peak metamorphic conditions.

On the west side of 'Y' lake, supracrustal rocks occur both as discreet mappable panels, and as enclaves, metres to tens of metres long within both foliated to gneissic tonalite and Komatik granite. Metasedimentary enclaves locally contain the assemblages biotite+garnet+sillimanite, biotite+garnet+cordierite, and biotite+garnet+sillimanite+cordierite. Where garnet and cordierite coexist, garnet seems to be breaking down to cordierite, indicating uplift and decompression. Small (millimetre scale) foliation-parallel lenses of white two-mica granite occur within the high-grade metasedimentary rocks, and are interpreted as locally-derived, anatectic melt. Where these lenses coalesce into coherent granitoid veins, they locally contain accessory garnet±tourmaline, attesting to their crustal origin.

MINERAL POTENTIAL

The preponderance of mafic volcanic flows through much of the supracrustal section suggests a depositional environment poorly suited to VMS-type mineralization. However, in the northern part of the map area, east of 'Y' lake, the package of mixed volcanic rocks includes volcaniclastic rocks with felsic to intermediate bulk compositions and, within this package, several stratabound gossans were mapped. Many of these gossans have significant strike lengths (hundreds of metres) and, in one locality, cordierite occurs within intermediate volcanic rocks adjacent to a gossan (Fig. 3). The cordierite-rich unit is commonly referred to as dalmatianite, and has been interpreted elsewhere to form by metamorphism of Na-Ca-K-depleted rocks in alteration zones related to VMS-type base metal deposits (e.g. Millenbach deposit, Quebec, Knuckey et al., 1982; Geco deposit, Ontario, Friesen et al., 1982). The presence of dalmatianite may indicate unrecognized base metal potential in the area. Three assay samples collected from stratabound gossans yielded Zn values up to 0.44 per cent and Cu values to 0.23 per cent.

Iron formation is fairly common throughout the southern part of the map area, and can be identified on regional aeromagnetic maps by its magnetic signature (Geological Survey of Canada, unpub. aeromag. data, 1997). Individual iron-formations locally makes useful marker beds and can be used to trace map-scale folds of bedding over several kilometres. Locally, individual silicate-rich beds within the iron-formation preserve sulphide overgrowths (pyrite, pyrrhotite) on amphibole (grunerite?). An assay sample of one such bed yielded 1379 ppb Au.

Rusty quartz veins, commonly with malachite staining and/or a few per cent pyrite, occur throughout the map area in a variety of host rocks. Where they are hosted by the Komatik granite, they are locally vuggy and contain up to 20 per cent pyrite (Fig. 5). In such cases, the rocks bear a striking resemblance to the 'yellow granite' 60 km to the southwest (Relf et al., 1997), although occurrences of pyrite-rich granite in the study area are small and isolated. The highest Au value from a quartz vein (868 ppb) came from a rusty pyrite+chalcopyrite-bearing vein in a gabbro near the southeast end of Tyrrell Arm.

SUMMARY

Mapping in the Yathkyed Lake area distinguished amphibolites, high-grade metasedimentary rocks, and various granitoids in an area previously mapped as undifferentiated migmatites and gneisses, thereby expanding the mapped width of the Yathkyed greenstone belt significantly. Along the southeastern margin of the belt, the Tyrrell shear zone records early reverse (thrust?) displacement followed by oblique strike-slip movement associated with extension. The shear zone could have important implications for the tectonic history of the Western Churchill Province.

Figure 5. *Pyrite in vuggy granite; similar appearance to 'yellow granite' of Relf et al. (1997).*

The mineral potential of the belt seems to be diverse, with a range of possible deposit settings represented. Iron formation is abundant in the southern half of the map area, and locally records evidence for sulphide (and Au?) replacement of silicate minerals. In the northern part of the study area, a distinct unit of mixed fragmental volcanic and volcaniclastic rocks, locally with stratabound gossans and rare dalmatianite, suggest VMS potential. Finally, fractured sulphidized portions of the Komatik granite share compositional and textural similarities with the yellow granite of Relf et al. (1997) and may prove to have gold potential.

ACKNOWLEDGMENTS

The authors would like to thank colleagues at the Geological Survey of Canada for informative discussions in the field and shared logistics. Larry Aspler is also thanked for numerous consultations about the Hurwitz Group. The Polar Continental Shelf Project provided helicopter support, and M&T Enterprises is thanked for their expediting services. This manuscript benefited from critical reviews by Simon Hanmer (GSC), Steve Goff (Geology Division, Department of Indian Affairs and Northern Development), and Larry Aspler.

REFERENCES

Aspler, L.B. and Chairenzelli, J.R.
1996: Geological compilation of the Hearne Province, south-central District of Keewatin; EGS Open File 1996-02, Northwest Territories Geology Division, Department of Indian Affairs and Northern Development, Yellowknife.

Donaldson, J.A.
1965: The Dubawnt Group, Districts of Keewatin and Mackenzie; Geological Survey of Canada, Paper 64-20, 11 p.

Eade, K.E.
1985: Geology, Tulemalu Lake–Yathkyed Lake, District of Keewatin, Northwest Territories; Geological Survey of Canada, Map 1064A (scale 1:250 000).
1986: Precambrian geology of the Tulemalu Lake–athkyed Lake area, District of Keewatin; Geological Survey of Canada, Paper 84-11, 31 p.

Friesen, R.G., Pierce, G.A., and Weeks, R.M.
1982: Geology of the Geco base metal deposit; in Precambrian Sulphide Deposits, H.S. Robinson Memorial Volume, (ed.) R.W. Hutchison, C.D. Spence, and J.M Franklin; Geological Association of Canada Special Paper 25, p. 343-363.

Geological Survey of Canada
1981: Magnetic anomaly map of the Dubwant River area; Geological Survey of Canada, Map 1567A (scale 1:1 000 000).

Heaman, L.M.
1994: 2.45 Ga global mafic magmatism: Earth's oldest plume?; in Eighth International Conference on Geochronology, Cosmochronology, and Isotope Geology, (ed.) M.A. Lauphere, G.B. Dalrymple, and B.D. Turrin; U.S. Geological Survey Circular 1107, p. 132.

Knuckey, M.J., Comba, C.D.A., and Riverin, G.
1982: Structure, metal zoning, and alteration at the Millenbach Deposit, Noranda, Québec; in Precambrian Sulphide Deposits, H.S. Robinson Memorial Volume, (ed.) R.W. Hutchison, C.D. Spence, and J.M Franklin; Geological Association of Canada Special Paper 25, p. 255-317.

Labelle, A.
1997: Structural and metamorphic history of the Nowyak shear zone, Western Churchill Province, NWT; B.Sc. Thesis, Carleton University, Ottawa, Ontario, 56 p.

LeCheminant, A.N. and Heaman, L.H.
1989: Mackenzie igneous events, Canada: Middle Proterozoic hot spot magmatism associated with ocean opening; Earth and Planetary Science Letter, v. 96, p. 38-48.

LeCheminant, A.N., Buchan, K.L., van Breemen, O., and Heaman, L.H.
1997: Paleoproterozoic continental break-up and reassembly: Evidence from 2.19 Ga diabase dyke swarms in the Slave and western Chruchill Provinces, Canada; Geological Association of Canada/Mineralogical Association of Canada Annual Meeting, Program with Abstracts, p. A86.

Loveridge, W.D., Eade, K.E., and Roddick, J.C.
1987: A U-Pb age on zircon from a granite pluton, Kamilukuak Lake area, District of Keewatin; in Radiogenic Age and Isotopic Studies, Report 1; Geological Survey of Canada, Paper 87-2, p. 67-71.

Peterson, T.D. and Rainbird, R.H.
1990: Preliminary report on the geology of northwestern Dubwant Lake area, District of Keewatin; in Current Research, Part C; Geological Survey of Canada, Paper 90-1C, p. 69-79.

Relf, C.
1995: Geological Map of the Snug Lake area, District of Keewatin, 55 L/8; EGS Open File 1995-15, Northwest Territories Geology Division, Department of Indian Affairs and Northern Development, Yellowknife (1:50 000 cale map and accompanying notes).
1996: Geology of the Nowyak Lake area, parts of NTS 65 G/9, 15, 16; 65 H/13; 65 I/4 and 65 J/1; EGS Open File 1996-19, Northwest Territories Geology Division, Department of Indian Affairs and Northern development, Yellowknife (scale 1:50 000).

Relf, C., Scott, C., Lépine, I., and Labelle, A.
1997: Geology and deformation history of the Nowyak Lake area, western Churchill Province, Northwest Territories; in Current Research 1997-C, Geological Survey of Canada, p. 71-79.

Tella, S., Roddick, J.C., and van Breemen, O.
1995: U-Pb zircon age for a volcanic suite in the Rankin Inlet Group, Rankin Inlet map area, District of Keewatin, Northwest Territories; in Radiogenic Age and Isotopic Studies: Report 9; Geological Survey of Canada, Current Research 1995-F, p. 11-15.

Field contributions to thematic studies related to the Kaminak greenstone belt, Kivalliq Region, Northwest Territories[1]

S. Hanmer, R.H. Rainbird, H.A. Sandeman, T.D. Peterson, and J.J. Ryan[2]
Continental Geoscience Division, Ottawa

Hanmer, S., Rainbird, R.H., Sandeman, H.A., Peterson, T.D., and Ryan., J.J., 1998: Field contributions to thematic studies related to the Kaminak greenstone belt, Kivalliq Region, Northwest Territories; in Current Research 1998-C; Geological Survey of Canada, p. 77-84.

Abstract: It is not possible to discriminate between single and multiple cycle stratigraphic models for the Archean Kaminak Group on the basis of fieldwork alone. However, facies associations in volcano-sedimentary rocks suggest that parts of the belt formed in an intra-arc depositional environment. In the Kaminak Group, regional deformation and metamorphism are Late Archean in age and have been influenced by the emplacement of major plutons. Most silicification and stratigraphically controlled carbonatization predates regional deformation. Some carbonatization and most sericitization is structurally controlled. The Mackenzie Lake sediments (*sensu lato*) represent two sequences: a Kaminak Group basement, and a cover of younger quartz arenites and conglomerates (Mackenzie Lake sediments *sensu stricto*). The Paleoproterozoic Hurwitz Group sits unconformably on a basement of Archean granitoids and Kaminak Group volcanic rocks. Paleoproterozoic reworking is confined to discontinuous chlorite alteration and quartz veining, with local cleavage, adjacent to the Hurwitz Group.

Résumé : Il n'est pas possible de départager sur la seule base des travaux de terrain les modèles stratigraphiques à cycle unique et ceux à cycles multiples pour le Groupe de Kaminak de l'Archéen. Toutefois, les associations de faciès dans les roches volcano-sédimentaires laissent supposer que certaines parties de la ceinture se sont formées dans un milieu de dépôt intra-arc. Dans le Groupe de Kaminak, la déformation et le métamorphisme régionaux datent de l'Archéen tardif et ont été influencés par la mise en place de plutons principaux. La plus grande partie de la silicification et de la carbonatisation contrôlée par la stratigraphie est antérieure à la déformation régionale. Une partie de la carbonatisation et la plus grande partie de la séricitisation ont été contrôlées par la structure. Les roches sédimentaires de Mackenzie Lake (sensu lato) représentent deux séquences : le socle du Groupe de Kaminak et une couverture de quartzarénites et de conglomérats plus jeunes (roches sédimentaires de Mackenzie Lake sensu stricto). Le Groupe paléoprotérozoïque de Hurwitz repose en discordance sur un socle de granitoïdes archéens et de roches volcaniques du Groupe de Kaminak. Le remaniement paléoprotérozoïque se limite à une altération chloritique discontinue et à un remplissage filonien de quartz, avec clivage local à proximité du Groupe de Hurwitz.

[1] Contribution to the Western Churchill NATMAP Project
[2] Department of Geology, University of New Brunswick, Fredericton, New Brunswick E3B 5A3

INTRODUCTION

The Western Churchill NATMAP Project is a collaborative, multidisciplinary initiative involving the Geological Survey of Canada (GSC), the Government of the Northwest Territories (GNWT), and Indian and Northern Affairs Canada (INAC). The first phase of the GSC's three year field program was initiated in June 1997 to investigate the geology of parts of the Eskimo Point (NTS 55E), Tavani (NTS 55K), Kaminak Lake (NTS 55L), Henik Lakes (65H) and Ferguson Lake (NTS 65I) map areas (Fig. 1), with particular emphasis on establishing the stratigraphy and tectonic setting of the Archean Kaminak greenstone belt. Bedrock mapping was undertaken between Padlei and Quartzite Lake (Fig. 1) at various scales, depending on the extent of outcrop. Previous work in the area includes bedrock mapping at 1:250 000 scale by Davidson (1970a, b) and Bell (1971), 1:100 000 by Park and Ralser (1992), and 1:50 000 by Irwin (1994, 1995, 1996, 1997) and Relf (1995). Fieldwork in the present study was divided between upgrading the geoscience knowledge base in the areas of recent detailed mapping north and east of Kaminak Lake (Fig. 1), and new mapping in adjacent areas to the south and west.

A number of strategic topics were identified either for systematic or pilot field study in the initial NATMAP project proposal. These include (i) the evaluation of existing tectonostratigraphic models for the Archean Kaminak Group, (ii) the nature of gneisses and plutonic rocks between the Kaminak greenstone belt and other greenstone belts to the north, (iii) the stratigraphic significance of the Mackenzie Lake sediments, and (iv) the potential for Paleoproterozoic reworking of greenstone belt rocks. In addition, we were able to make observations pertinent to some of the principal alteration zones and mineral prospects in the area. In this report, we present the results of field investigations relating to these topics. In a companion contribution (Hanmer et al., 1998), we present a systematic overview of the lithological and structural characteristics of the Kaminak Group and associated plutonic rocks.

ARCHEAN TECTONOSTRATIGRAPHIC MODELS

Although Davidson (1970a, p. 7) noted that "the inherently variable nature of the assemblage from place to place precludes precise correlation", he identified a relatively simple stratigraphy in the Kaminak Group. From oldest to youngest, the sequence comprised (i) mafic to intermediate flows and breccias, chiefly andesitic, (ii) intermediate to felsic flows, tuffs and breccias, and (iii) siliciclastic sediments with iron-formations. In the Tavani map area to the east, Park and Ralser (1992) adopted a similar tri-partite stratigraphy which they referred to as the Atungag, Akliqnaktuk, and Evitaruktuk formations. The mafic Atungag Formation and the mafic to felsic Akliqnaktuk Formation were interpreted as oceanic crust upon which an island arc had been built.

In the Henik Lakes map area to the southwest, Aspler and Chiarenzelli (1996) proposed a four-fold stratigraphy with (i) siliciclastic sediments at the base, overlain by (ii) mixed sedimentary and volcanic rocks with iron-formations, (iii) a mafic volcanic/gabbro sill complex, and (iv) more siliciclastic sediments. They interpreted the succession as a volcanic plateau prograding over a sedimentary basin in a deep oceanic regime, either in a back-arc basin setting, or associated with progressively accreted arcs.

In contrast to the foregoing single cycle models, Ridler and Shilts (1974) proposed a stratigraphic sequence comprising four complete and one incomplete mafic to felsic cycles, associated with stratigraphically intercalated metalliferous exhalite horizons. Their model predicted that the volcanic cycles and exhalites should young from west to east along the length of the Kaminak Belt. The available geochronological data (U-Pb, zircon) are not incompatible with Ridler and Shilt's (1974) model: 2697 ± 1.4 Ma at Spi Lake, 2692 ± 3 Ma in northeast Kaminak Lake, and 2681 ± 3 Ma at Quartzite Lake (Mortensen and Thorpe, 1987; Patterson and Heaman, 1990).

The discontinuous nature of map units in the Kaminak Group does not allow elaboration of a robust stratigraphy based upon field observation alone (Hanmer et al., 1998). Therefore, evaluation of the foregoing stratigraphic models, and discrimination between single and multiple volcanic cycles, must await petrological and geochronological studies currently underway. However, the sedimentary units described in our companion paper (Hanmer et al., 1998), particularly those from the Quartzite Lake area (Fig. 1), are similar to those described for modern intra-arc basins, where they are considered as part of the volcanic arc platform (Smith and Landis, 1995). Intra-arc basins are characterized by thick accumulations of volcanic and volcaniclastic material deposited in and around volcanic edifices of variable composition. The edifices are flanked by extensive, subaerial to subaqueous debris aprons composed of immature epiclastic sediment gravity flow and flood deposits, intercalated with both coarse and fine pyroclastic deposits and lava flows. Finer grained deposits, such as distal turbidites, tend to be rarer than in fore-arc or back-arc basins, where the direct affects of volcanism are less evident. We favour an intra-arc setting as a preliminary working model, at least for parts of the Kaminak Group in the Heninga-Carr-Kaminak-Quartzite corridor (Fig. 1). The nature of the inferred arc (e.g. oceanic, continental, or transitional) will be investigated through ongoing geochemical and tracer isotope studies.

METASEDIMENTS NORTH OF HENINGA-QUARTZITE LAKES AREA

North of the Heninga-Carr-Kaminak-Quartzite corridor, homogeneous semipelites and subordinate, fine grained, featureless amphibolite are part of the Kaminak Group (Davidson, 1970a; see Fig. 1). They differ from the volcano-sedimentary rocks to the south because the mafic to siliciclastic rock ratio is very much lower, and the metamorphic grade is higher. Biotite-muscovite semipelite contains restricted,

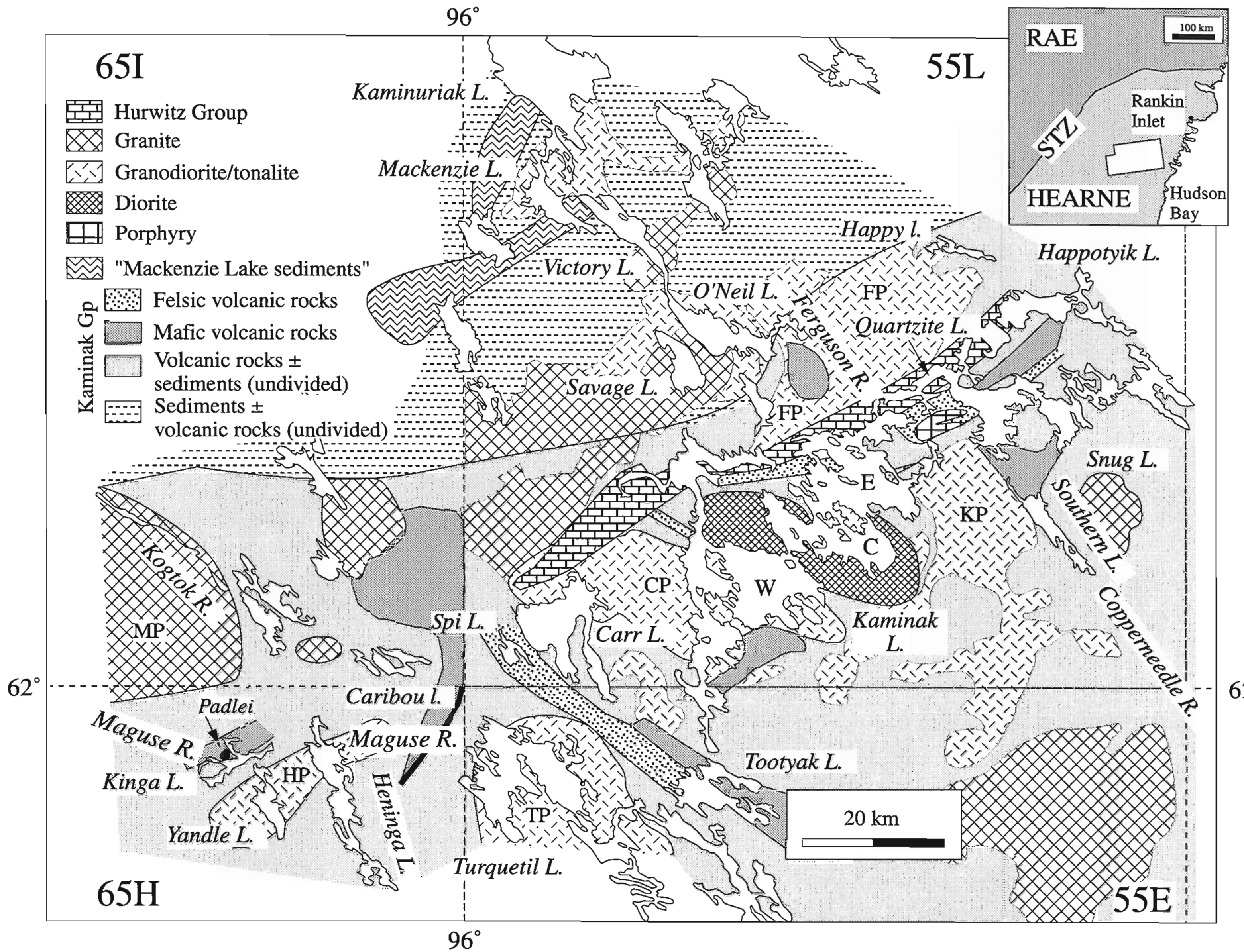

Figure 1. Sketch map of locations referred to in the text. Major Archean plutons are indicated, and a generalized line separates mainly volcanic rocks from mainly clastic sediments. "Felsic" units may include "bimodal" volcanic rocks. Symbols "E", "C", and "W" are east, central, and western Kaminak Lake, respectively. Other abbreviations are Carr (CP), Ferguson (FP), Heninga (HP), Kaminak (KP), Maguse (MP), and Turquetil (TP) plutons. Heavy solid line is Turquetil gold prospect.

local horizons of pelite which may contain subsets of the metamorphic assemblage garnet-cordierite-staurolite-kyanite (see Davidson, 1970a). Between Kaminak and Victory lakes (Fig. 1) there are no signs of anatexis. However, semipelite east of the Kogtok River carries concordant granitic leucosome, apparently derived by incipient *in situ* melting, and sillimanite was found at one locality. Very rarely, amphibolite may be garnet-bearing. These metamorphosed rocks are cut by the Maguse pluton (Fig. 1; cf. Bell, 1971), a medium- to coarse-grained, poorly foliated to isotropic, equigranular granite. On its northern side, veins of the Maguse pluton crosscut dioritic orthogneisses and a mixed granite, paragneiss, and diatexite association. Allowing for their extremely poor exposure, the supracrustal components of these higher grade rocks appear to be continuous with the Kaminak Group west of Turquetil Lake (Fig. 1). Granite exposed west of O'Neil Lake resembles the Maguse pluton and includes rafts and xenoliths of semipelite.

Kaminak Group sediments (?)

In the Kaminak Lake area, Davidson (1970a) mapped and defined the Kaminak Group as an assemblage of volcanic rocks, flanked to the north by siliciclastic sediments. However, the stratigraphic identity of siliciclastic metasediments north of Happy lake is uncertain (Davidson, 1970a; Irwin, 1997). The pelites and semipelites do not preserve bedding, except where they are interlayered with quartzite. The quartzites are up to several metres thick, spaced at 10-100 cm intervals, and contain rare calcareous interlayers. A penetrative, layer-parallel schistosity is deformed by tight, steeply plunging folds. The metamorphic assemblage biotite-muscovite-garnet-staurolite-kyanite in pelites, and kyanite in quartzites, appears to have been stable throughout the deformation history. In several places, quartzite preserves alternating, 5 cm thick planar beds of otherwise featureless white and grey sandstone (Fig. 2). The resemblance of this particular lithology to parts of the Kinga Formation of the Hurwitz Group led Irwin (1997) to propose a Paleoproterozoic age for the quartzite, but he considered the age of the semipelites and pelites to be unconstrained. However, calc-silicate rock, semipelite, micaceous quartzite and possible quartz arenite form isolated narrow layers (<2 m) within banded amphibolites which are accepted as part of the Kaminak Group (Davidson, 1970a; Irwin, 1997). Moreover, Irwin (1997) has mapped pelites with minor garnet and kyanite intercalated with these same mafic rocks. If this intercalation is primary, then we suggest that the entire sedimentary package is part of the Kaminak Group. However, we cannot exclude the possibility that the banded nature of the amphibolites could represent structurally transposed primary features (see Hanmer et al., 1998), thereby implying tectonic intercalation, possibly of Archean and Paleoproterozoic rocks. Geochronological studies are underway to test these possibilities.

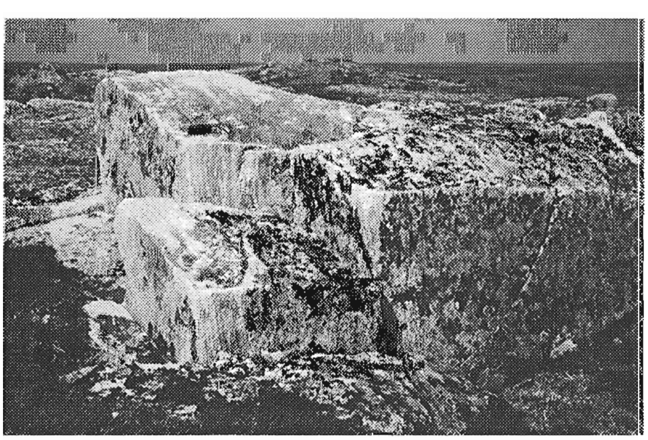

Figure 2. Vertically bedded quartzite north of Happy lake. GSC 1997-68E

Although richer in pelite and quartz arenite, these rocks are similar to semipelitic, locally garnet-cordierite-staurolite rocks mapped by Davidson (1970a) from Kaminak Lake to Victory Lake as part of the Kaminak Group. They also resemble the semipelites and quartz arenites associated with the Mackenzie Lake sediments (see below).

Mackenzie Lake sediments

Southwest of Kaminuriak Lake (Fig. 1), a package of arenites and conglomerates, plus "higher grade equivalents" injected by granite, were mapped by Davidson (1970a) and Bell (1971) as the "Mackenzie Lake sediments" (*sensu lato* herein). The stratigraphic significance of the Mackenzie Lake sediments, i.e. their potential correlation with Archean or Paleoproterozoic rocks, has remained controversial (see Aspler and Chiarenzelli, 1996).

Our field study indicates that the arenites and conglomerates constitute a subordinate component of the map unit as represented by the earlier workers. These rocks include quartzites, arkosic arenites, quartz pebble conglomerates, framework supported conglomerates, and pebble-lag conglomerates, exposed in the southern half of Mackenzie Lake (Fig. 1), and extending southwest to the edge of the Kaminak Lake map sheet. Trough crossbedding, outlined by heavy mineral bands, occurs in the quartzites and in feldspathic arenites interbedded with pebble-lag conglomerates. The latter form channel fills with erosional bases. Clasts in the conglomerates are subangular to well-rounded cobbles and pebbles, principally composed of tonalite, granodiorite and granite (Fig. 3). Scattered smaller clasts of "actinolite rock" may represent metamorphosed impure limestone, or ultramafic rock. The quartzites are either interbedded with quartz pebble conglomerate, or form a thick plane-bedded unit running southwest from the southern end of Mackenzie Lake. Soft-sediment deformation structures, in association with the coarse clastic sediments, may be indicative of nearby active tectonism. The facies association and unidirectional crossbedding suggest alluvial deposition. These deposits resemble late Archean molasse deposits seen in other Canadian greenstone belts (e.g. Jackson Lake Formation, Slave craton or Temiskaming Group, Superior Province). Diagnostic metamorphic mineral assemblages are lacking, but the arenites contain biotite and the quartzites locally carry sillimanite after kyanite.

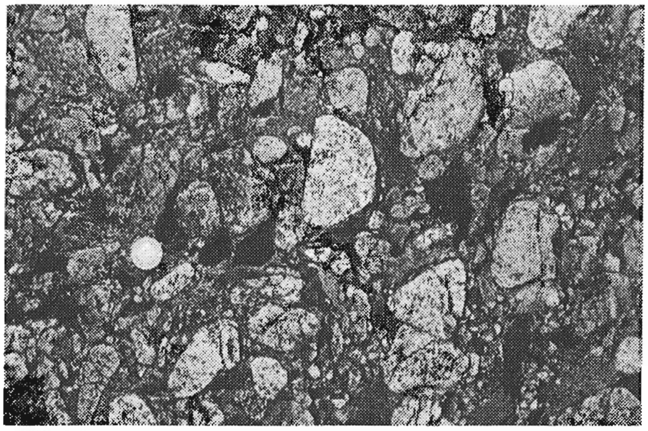

Figure 3. Subangular to rounded granite to tonalite pebbles in conglomerate, Mackenzie Lake sediments (sensu stricto), east side of Mackenzie Lake. Dark clasts are "actinolite rock". GSC 1997-68J

The volumetrically predominant lithological association within the major part of the "Mackenzie Lake sediments" (*sensu lato*) is composed of leucogranite sheets pervasively intruded into homogeneous semipelite with local amphibolite layers, and restricted occurrences of quartz arenite and calc-silicate rock. This association extends southwest from Kaminuriak Lake into the eastern quarter of the Ferguson Lake map area (Fig. 1). Except for its schistosity, the semipelite and amphibolite are generally featureless; they do not preserve primary layering. The quartz arenite is locally a quartzite, and the calc-silicate is represented by thin layers of plagioclase rock with subordinate green amphibole and minor quartz. These metasediments are concordantly injected by biotite leucogranite sheets which comprise at least 70% of the outcrop. They are more appropriately mapped as granite, charged with screens of wall rock.

We suggest that the "Mackenzie Lake sediments" (*sensu lato*) comprise two rock packages of different age. The quartzites and conglomerates, for which the name Mackenzie Lake sediments (*sensu stricto*) should be retained, are folded about upright, northeast-trending, first generation folds with an axial planar cleavage. However, the semipelites, arenites, and granite sheets contain a strong, layer-parallel cleavage. This cleavage is relatively flat lying at the latitude of Kaminuriak Lake (dips <10°), where it carries a north-trending extension lineation, but is progressively folded about the same folds which deform the quartzites and conglomerates at the latitude of southern Mackenzie Lake. Accordingly, we suggest that quartzites and conglomerates are younger than, and may unconformably overly the older rock package. Combining the foregoing with our preceding observations on the siliciclastic sediments of the Kaminak Group, we suggest that the Mackenzie Lake sediments (*sensu stricto*) represent a post-Kaminak Group sequence. Potential correlation with the Hurwitz Group will be tested by geochronological studies.

HURWITZ GROUP BASAL UNCONFORMITY

An unconformity between the folded and cleaved Hurwitz Group (Davidson, 1970a) and its underlying basement was identified northeast of Carr Lake (Fig. 1). The contact relationship typically places the basal Maguse Member of the Kinga Formation above granitoid or Kaminak Group volcanic rocks. At the northwestern end of Kaminak Lake, the interface is recognizable as a sericite-quartz schist, foliated subparallel to the unconformity. However, in an embayment along the unconformity, the rocks are less strained and a possible regolith produced by primary chemical weathering of a granodiorite protolith is preserved. Regolith alteration is sericite after kaolinite and plagioclase, and iron chlorite after biotite-hornblende. Protolith texture is preserved, but the degree of alteration increases upward (i.e. toward the unconformity) suggesting that it resulted from gravity driven rainwater-rock interaction. The contact zone between the regolith and the overlying Maguse Member is diffuse, and is composed of subrounded blocks of both altered and fresh granodiorite in a matrix of poorly sorted arkose. The transition zone is 1-3 m thick and passes upward into a distinctive jasper- and quartz-pebble conglomerate interbedded with arkose. The rock is sericite-rich, presumably due to incorporation of regolithic material, and has a distinctive greenish colour. Sericite alteration, produced by low grade K-metasomatism of kaolinite after initial chemical breakdown of feldspars, is a typical feature of Precambrian paleosols (Rainbird et al., 1990). Therefore, the sericite-quartz schist along this interface, outside of the protected embayment, is considered to represent the deformed equivalent of the transition zone.

Other segments of intact unconformity at the base of the Hurwitz Group occur along strike to the northeast and southwest, beyond our study area (Park and Ralser, 1992; Aspler and Chiarenzelli, 1997). The Carr Lake unconformity pins the Hurwitz Group in this middle section of its regional outcrop extent, thereby eliminating the possibility of significant Paleoproterozoic displacements between basement and cover. Localized deformation adjacent to the Hurwitz Group likely indicates strain incompatibility or partitioning at the basement-cover contact during Paleoproterozoic shortening.

ALTERATION AND MINERALIZATION

Volcanic and volcaniclastic rocks of the Kaminak Group are extensively altered, especially along the north side of Kaminak Lake and around Quartzite Lake (Fig. 1). Alteration around Spi Lake is less extensive, and alteration west of Turquetil Lake appears to be focused in a fault zone. The local aspects of the alteration comprise variable components of silicification, carbonatization, and sericitization.

Silicification

Silicification is the most extensive, and locally pervasive, form of alteration. It is most commonly seen in volcaniclastic conglomerates and breccias, but also occurs in massive and pillowed intermediate flows. In some cases, silicification is selective, preferentially affecting either the matrix, or the clasts, but generally the silicified matrix carries a well developed tectonic fabric, indicating that the alteration is early.

Stratigraphically controlled carbonatization

Carbonatization is typically more localized than silicification. To illustrate stratigraphically controlled alteration, we describe a distinctive, coarse clastic sedimentary unit immediately southeast of Quartzite Lake (Fig. 1). It is about 30-40 m thick and is composed of boulder to granule conglomerates overlain by crossbedded lithic arenite. Conglomerates are mostly clast supported, with poor to moderate sorting. The framework is almost exclusively composed of felsic volcanic rocks, and the matrix is lithic arenite. The conglomerate is overlain by medium-to coarse-grained lithic arenite with well preserved, small-scale trough crossbedding, to large scale wave-ripple crosslamination (Fig. 4). Local intraformational disconformities and large tilted blocks of strata indicate syndepositional tectonism. The distinguishing feature of this unit is partial to almost complete replacement by recessive, brown-weathering ankeritic dolomite (Fig. 4). Generally, replacement is controlled by grain size and is most pervasive in finer grained material, such as conglomerate matrix, and therefore most likely occurred during diagenesis. Similar, carbonate-altered lithic arenites were mapped in the northwest corner of Kaminak Lake, as well as northwest of Tootyak Lake (Fig. 1).

Structurally controlled carbonatization

Structural control of carbonate replacement in massive volcanic and volcaniclastic rocks begins by infiltration along a network of penetrative, macroscopically nondilated fractures (Fig. 5A). Progressive replacement can be traced into massive, featureless, fine grained brown carbonate, with a few isolated volcanic relics (Fig. 5B). Where massive carbonate replaces cleaved volcanic rocks, the alteration is clearly later than most of the S_1 cleavage forming event. However, in places, the main mass of carbonate may be cut by folded carbonate veins.

Sericitization

Sericitization may be penetrative and pervasive. Localized, concordant zones of sericitized volcanic and volcaniclastic rock, up to several tens of metres thick, are well cleaved, steeply lineated, buff weathering, and silky to the touch. Accordingly, the alteration either predates or accompanies cleavage formation.

At some localities, sericitization is localized in narrow, regularly spaced (5-10 cm), foliation-parallel bands. Progressive sericitization begins by infiltration and replacement along macroscopically closed, anastomosing fractures aligned subparallel to S_1. Replacement of the volcanic wall rock adjacent to the fractures produces sericite-rich bands, up to 5 mm thick, whose geometry reflects that of the initial fracture array. Within the sericite bands, a penetrative (sericite-quartz?) foliation is developed (Fig. 6). In all cases, the sericite

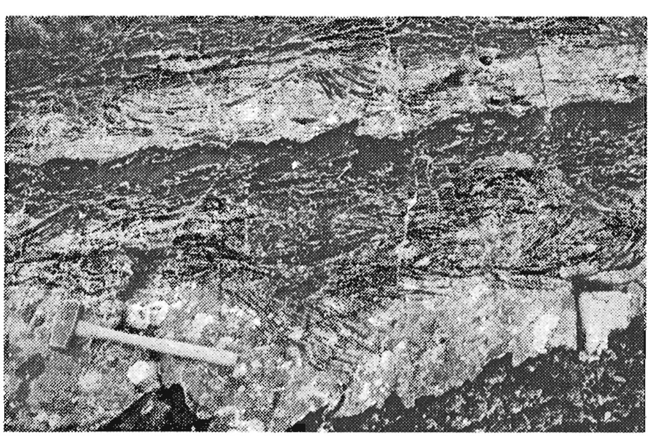

Figure 4. Trough crossbedded arenite with extensive carbonate replacement (dark recessive areas), southeast of Quartzite Lake. GSC 1997-68M

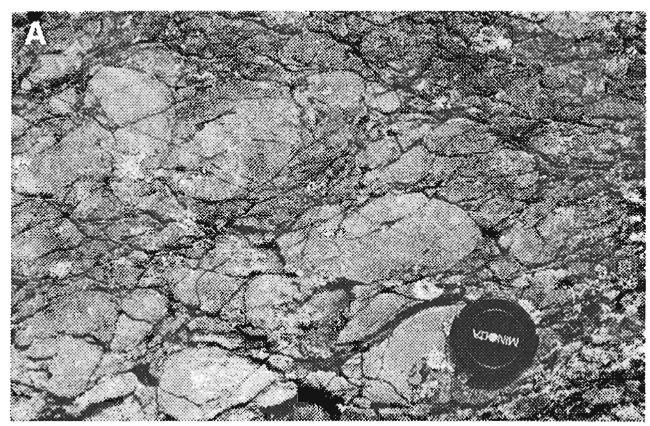

Figure 5. *Progressive carbonate replacement can occur by infiltration along fractures (**A**), eventually resulting in a featureless, fine grained, brown carbonate rock with isolated volcanic relics (**B**), northwest of Turquetil Lake. A) GSC1997-68Z; B) GSC 1997-68Y*

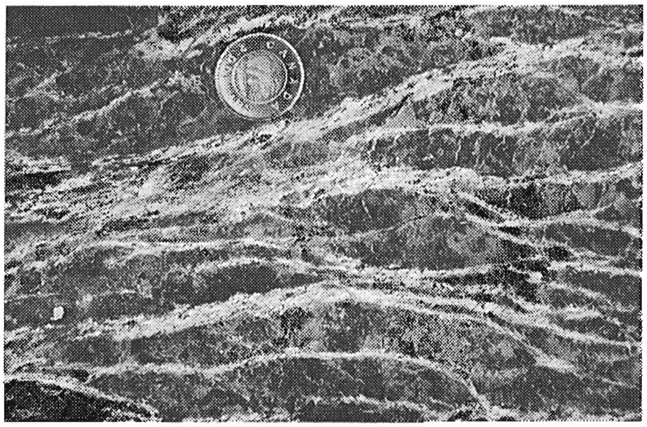

Figure 6. Sericite bands in brown carbonate rock west of Turquetil Lake. Note internal, anticlockwise foliation within bands, and thin quartz veinlets in the intervening lithons (upper right). GSC 1997-68AA

foliation is internal to the bands, and makes a uniform, anticlockwise angle (10-15°) with their boundaries. An extension lineation marked by sericite aggregates and elongate chlorite grains is always steeply pitching to vertically plunging. These observations indicate that the sericite alteration is localized by initial fracturing, and subsequently deformed by dextral shear. However, displacements along both the initial fractures and the evolved sericite bands must be minimal in order to avoid dilation and brecciation in the former, and to preserve the internal obliquity of the foliation in the latter.

Exhalite or alteration?

At the Turquetil gold prospect, west of Turquetil Lake (Fig. 1), precleavage (S_1) silicification is overprinted by postcleavage carbonatization in a zone about 500 m wide, which is in turn overprinted by spaced sericite bands as described above. There, sericitization is clearly a postcleavage process. The carbonate lithons between sericite bands are cut by steeply dipping quartz veinlets (<1 mm thick), which do not themselves cut the sericite bands, suggesting that the two are contemporaneous (Fig. 6). The horizontal extension implied by the quartz veinlets is perpendicular to the steeply plunging sericite extension lineation. However, late decimetre-scale quartz veins cut across the sericite bands, and are perpendicular to the lineation. These observations suggest that switching of the 'X' and 'Y' principal axes of strain occurred during the later stages of the progressive deformation. The observations presented here do not support an exhalite model for the Turquetil alteration zone, described by Ridler and Shilts (1974) as "Larder Lake" type.

AGE OF DEFORMATION AND METAMORPHISM

By mapping the distribution of Kaminak dykes (ca. 2.45 Ga; Heaman, 1994) which crosscut the Kaminak Group, but are absent from the Hurwitz Group, Davidson (1970a) and Bell (1971) established that regional deformation and metamorphism in the Kaminak Group occurred in the late Archean. More detailed mapping by Irwin (1994, 1995, 1996, 1997) and Relf (1995) showed that (i) layer-parallel S_1 foliation tends to mirror the outlines of the main tonalite and granodiorite plutons at the eastern end of Kaminak Lake, and (ii) the hornblende isograd tends to be hot-side towards the same plutons. We have mapped similar relationships with respect to the Heninga pluton (Fig. 1; new name) at Heninga Lake. However, at both the map and the outcrop scale, the major plutons are clearly crosscutting to both S_1 and isograds (see Hanmer et al., 1998). Along the southern part of Kaminak Lake, mafic to intermediate volcanic rocks, pelites and psammites locally contain synkinematic metamorphic garnet adjacent to the central Kaminak diorite suite and the Carr pluton (Fig. 1; Hanmer et al., 1998). These observations suggest that the granitoid plutons have influenced the deformation and metamorphism of their wall rocks, and that they are, at least in part, contemporaneous with S_1. However, it remains uncertain to what degree wall rock deformation and the formation of steeply dipping and plunging fabric elements were controlled by pluton emplacement (cf. Paterson and Tobisch, 1988).

One of the syntectonic plutons (Kaminak; Fig. 1) has been dated at ca. 2.7 Ga (Cavell et al., 1992), placing a preliminary upper age limit on regional Archean deformation and metamorphism. However, this does not constrain the age of localized shear zones, such as the Turquetil alteration zone. There, the identical orientations of the upright S_1 and the steeply plunging extension lineation, both within the alteration zone and its unaltered wall rock, strongly suggest that they are contemporaneous and Archean in age. On the other hand, chlorite alteration and shear zones developed in the Ferguson pluton (Fig. 1) just north of the Hurwitz Group at Kaminak Lake (Hanmer et al., 1998), and similar alteration associated with extensive quartz veining adjacent to the Hurwitz Group at Kinga Lake, are the best examples of Paleoproterozoic reworking of the Archean basement noted in the Heninga-Carr-Kaminak-Quartzite lakes corridor. Further north, a single metamorphosed Kaminak dyke with a wall-parallel foliation was observed at the north end of O'Neil Lake (Fig. 1). This location corresponds to the approximate southern limit of regional scale folding affecting the potentially Paleoproterozoic Mackenzie Lake sediments and their inferred Archean basement.

SUMMARY

Locally, the Kaminak Group appears to contain evidence for an intra-arc volcano-sedimentary environment. Regional deformation and metamorphism in the Kaminak Group is late Archean, and has been, at least in part, influenced by the emplacement of major granitoid plutons. In the Kaminak Group, stratigraphically controlled carbonatization and most silicification is pretectonic; some carbonatization and most sericitization is structurally controlled.

The "Mackenzie Lake sediments" represent two sequences: a potential Kaminak Group basement and a possible cover of younger quartz arenites and conglomerates. The

Paleoproterozoic Hurwitz Group sits unconformably on Archean basement. Paleoproterozoic reworking is confined to discontinuous chlorite alteration and quartz veining, with local cleavage, adjacent to the Hurwitz Group.

ACKNOWLEDGMENTS

We are grateful to Yannick Beaudoin, Nora Brown, Thomas Hadlari, and Chris Hemmingway for their excellent and enthusiastic assistance in the field, and to Laura Adams, our splendid and very patient cook. This work could not have been undertaken without the generous support of the Polar Continental Shelf Project. Huisson helicopters provided superb service throughout the summer, in particular pilots Rhéal Marchand and Terry Halton, and engineer James Ross. We benefited from visits (long and short term) by Larry Aspler, Rob Berman, Roy Cooper, Bill Davis, Steve Goff, Doug Irwin, John Kerswill, Isabelle McMartin, Carolyn Relf, and Subhas Tella. Welcome participation by representatives, and in some cases helicopters, from Nunavut Tunngavik Inc., Cameco Corporation, WMC International Ltd, Comaplex Minerals Corp., and Phelps Dodge Corporation made for a very successful end of season field workshop. The manuscript was critically read by Subhas Tella and Steve Lucas.

REFERENCES

Aspler, L.B. and Chiarenzelli, J.R.

1996: Stratigraphy, sedimentology and physical volcanology of the Henik Group, central Ennadai-Rankin greenstone belt, Northwest Territories, Canada: late-Archean paleogeography of the Hearne Province and tectonic implications; Precambrian Research, v. 77, p. 59-89.

1997: Archean and Proterozoic geology of the North Henik Lake area, District of Keewatin, Northwest Territories; in Current Research 1997-C Geological Survey of Canada, p. 145-155.

Bell, R.T.

1971: Geology of Henik Lakes (east half) and Ferguson Lake (east half) map-areas, District of Keewatin; Geological Survey of Canada, Paper 70-61, 31 p.

Cavell, P.A., Wijbrans, J.R., and Baadsgaard, H.

1992: Archean magmatism in the Kaminak Lake area, District of Keewatin, Northwest Territories: ages of the carbonatite-bearing alkaline complex and some host granitoid rocks; Canadian Journal of Earth Sciences, v. 29, p. 896-908.

Davidson, A.

1970a: Precambrian geology, Kaminak Lake map-area, District of Keewatin (55L); Geological Survey of Canada, Paper 69-51, 27 p.

1970b: Eskimo Point and Dawson Inlet map-areas (north halves), District of Keewatin, 55E and 55F (north parts); Geological Survey of Canada, Paper 70-27, 21 p.

Hanmer, S., Peterson, T.D., Sandeman, H.A.I., Rainbird, R.H., and Ryan, J.J.

1998: Geology of the Kaminak greenstone belt from Padlei to Quartzite Lake, Kivalliq Region, Nunavut (Northwest Territories); in Current Research 1998-C; Geological Survey of Canada.

Heaman, L.M.

1994: 2.45 Ga global mafic magmatism: Earth's oldest superplume?; in 8th International Conference on Geochronology, Cosmology and Isotope Geology, (ed.) M.A. Lanphere, G.B. Dalrymple, and B.D. Turrin; United States Geological Survey, p. 132.

Irwin, D.A.

1994: Mineral occurrences and preliminary geology of the Kaminak-Carr Lakes area, District of Keewatin (parts of 55L/3, 4, 5 and 6); Northwest Territories Geological Mapping Division, Map EGS 1994-03, scale 1:50 000.

1995: Mineral occurrences and preliminary geology of the Kaminak-Quartzite Lakes area, District of Keewatin (south-central 55L); Northwest Territories Geological Mapping Division, Map EGS 1995-05, scale 1:50 000.

1996: Geology and mineral occurrences of the Southern Lake area, District of Keewatin (55L/1); Northwest Territories Geological Mapping Division, Map EGS 1996-06, scale 1:50 000.

1997: Geology and mineral occurrences of the Happy Lake area, District of Keewatin (parts of 55L/9 and 10); Northwest Territories Geological Mapping Division, Map EGS 1997-00, scale 1:50 000.

Mortensen, J.K. and Thorpe, R.I.

1987: U-Pb zircon ages of felsic volcanic rocks in the Kaminak Lake area, District of Keewatin; in Radiogenic Age and Isotope Studies: Report 1; Geological Survey of Canada, Paper 87-2, p. 123-128.

Park, A.F. and Ralser, S.

1992: Precambrian geology of the southwestern part of the Tavani map area, District of Keewatin, Northwest Territories; Geological Survey of Canada, Bulletin 416, p. 81.

Paterson, S.R. and Tobisch, O.T.

1988: Using pluton ages to date regional deformations: problems with commonly used criteria; Geology, v. 16, p. 1108-1111.

Patterson, J.G. and Heaman, L.M.

1990: Geochronological constraints on the depositional age of the Hurwitz Group; Geological Association of Canada-Mineralogical Association of Canada, Program with Abstracts, v. 5, p. A102.

Rainbird, R.H., Nesbitt, H.W., and Donaldson, J.A.

1990: Formation and diagenesis of a sub-Huronian saprolith: comparison with a modern weathering profile; Journal of Geology, v. 98, p. 801-822.

Relf, C.

1995: Geological map of the Snug Lake area, District of Keewatin, (55L/8); Northwest Territories Geological Mapping Division, Map EGS 1995-00, scale 1:50 000.

Ridler, R.H. and Shilts, W.W.

1974: Exploration for Archean polymetallic sulphide deposits in permafrost terrains; an integrated geological-geochemical technique; Kaminak Lake area, District of Keewatin; Geological Survey of Canada, Paper 73-34, 33 p.

Smith, G.A. and Landis, C.A.

1995: Intra-arc basins; in Tectonics of Sedimentary Basins, (ed.) C.J. Busby and R.V. Ingersoll; Blackwell Scientific, p. 263-298.

Geological Survey of Canada Project 970006

Geology of the Kaminak greenstone belt from Padlei to Quartzite Lake, Kivalliq Region, Northwest Territories[1]

S. Hanmer, T.D. Peterson, H.A. Sandeman, R.H. Rainbird, and J.J. Ryan[2]
Continental Geoscience Division, Ottawa

Hanmer, S., Peterson, T.D., Sandeman, H.A., Rainbird, R.H., and Ryan, J.J., 1998: Geology of the Kaminak greenstone belt from Padlei to Quartzite Lake, Kivalliq Region, Northwest Territories; in Current Research 1998-C; Geological Survey of Canada, p. 85-94.

Abstract: Within a corridor spanning Heninga, Carr, Kaminak, and Quartzite lakes, the Archean Kaminak greenstone belt (western Churchill Province, Northwest Territories) is composed of discontinuous segments of volcanic and volcaniclastic rocks. These range in composition from mafic to felsic, with an important intermediate component, and are accompanied by voluminous debris flows and siliciclastic rocks (Kaminak Group). These supracrustal rocks are cut by large synvolcanic to late syntectonic diorite to granodiorite plutons. The principal map-scale deformation structure is a layer-parallel S_1 foliation with a steeply plunging extension lineation. Post-S_1 deformation structures are discontinuous, and therefore are difficult to correlate at map scale. The Kaminak Group appears to contain the remnants of a magmatic arc.

Résumé : À l'intérieur d'un corridor comprenant les lacs Heninga, Carr, Kaminak et Quartzite, la ceinture de roches vertes archéenne de Kaminak (partie ouest de la Province de Churchill, Territoires du Nord-Ouest) comporte des segments discontinus de roches volcaniques et volcanoclastiques dont la composition varie de mafique à felsique, avec une importante composante intermédiaire. Ces roches sont accompagnées de coulées de débris et de roches silicoclastiques volumineuses (Groupe de Kaminak). Ces roches supracrustales sont recoupées par de vastes plutons dioritiques à granodioritiques synvolcaniques et syntectoniques tardifs. La principale structure de déformation d'échelle cartographique est une foliation S_1 parallèle à la stratification accompagnée d'une linéation d'extension à fort plongement. Les structures de déformation postérieures à S_1 étant discontinues, il est difficile de les corréler à l'échelle cartographique. Le Groupe de Kaminak semble renfermer les vestiges d'un arc magmatique.

[1] Contribution to the Western Churchill NATMAP Project

[2] Department of Geology, University of New Brunswick, Fredericton, New Brunswick E3B 5A3

INTRODUCTION

The Western Churchill NATMAP Project involves the Geological Survey of Canada (GSC), the Government of the Northwest Territories (GNWT), and Indian and Northern Affairs Canada (INAC). The first phase of the GSC's three year field program was initiated in June 1997 to investigate the geology of parts of the Eskimo Point (NTS 55E), Kaminak Lake (NTS 55L), Henik Lakes (65H), and Ferguson Lake (NTS 65I) map areas (Fig. 1), with particular emphasis on establishing the stratigraphy and tectonic setting of the Archean Kaminak greenstone belt. Bedrock mapping was undertaken between Padlei and Quartzite Lake (Fig. 1) at various scales. Previous work in the area includes bedrock mapping at 1:250 000 scale by Davidson (1970a, b) and Bell (1971), and 1:50 000 by Irwin (1994, 1995, 1996, 1997) and Relf (1995). Fieldwork in the present study was divided between upgrading the geoscience knowledge base in the areas of recent detailed mapping north and east of Kaminak Lake (Fig. 1), and new mapping in adjacent areas to the south and west. The new map data were compiled at 1:125 000 scale to allow for the uneven distribution of outcrop, and to integrate with the compilation scale employed by the Government of the Northwest Territories (D.A. Irwin, unpub. map manuscript, 1997). In this report, we present a systematic overview of the lithological and structural characteristics of the Archean Kaminak Group and associated plutonic rocks within a corridor spanning Heninga, Carr, Kaminak, and Quartzite lakes (Fig. 1). In a second contribution (Hanmer et al., 1998), we present results of some of the strategically focused topics investigated during our fieldwork.

Geological overview

The Kaminak greenstone belt is a 500 km long segment of the "Ennadai-Rankin greenstone belt" from Pistol Bay on the Hudson Bay coast to west of Henik Lakes (see Miller and Tella, 1995; Aspler and Chiarenzelli, 1996). In the Kaminak Lake area, Davidson (1970a) mapped and defined the Kaminak Group as an assemblage of volcanic rocks, flanked to the north by clastic sedimentary rocks.

Field determination of the compositions of volcanic and volcaniclastic rocks was based on colour and phenocryst content. At low metamorphic grade (chlorite-albite), black to dark green rocks±plagioclase phenocrysts were called mafic, grey-green to grey rocks±plagioclase and/or hornblende phenocrysts were termed intermediate, and light grey, cream to white rocks±potassium feldspar and/or quartz phenocrysts were mapped as felsic. However, locally pervasive silicification, or the growth of metamorphic minerals made such field determinations difficult in some areas. Segments of distinct lithological associations, described below, can be traced over tens of kilometres along strike, but are invariably truncated by large plutons, and inferred faults. The highly discontinuous map pattern obscures the relative age of lithological packages.

Intrusive rocks (Fig. 1) are broadly grouped as synvolcanic, syntectonic, and post-tectonic. Synvolcanic intrusions include dykes, sills, and plutons, typically ranging from gabbro to diorite. These are commonly spatially associated with the mafic to intermediate volcanic rocks of the Kaminak Group. Syntectonic intrusions are the most widespread, forming three large, compositionally variable plutons (Kaminak batholith of Davidson, 1970a). Post-tectonic plutons include the 2659 ±5 Ma Kaminak Lake alkaline complex (see Cavell et al., 1992). The plutonic rocks are rarely foliated, except adjacent to the intrusive contacts of some synvolcanic and syntectonic plutons. We shall focus here on the synvolcanic and syntectonic intrusions.

KAMINAK GROUP

Mafic volcanic rocks

Homogeneous, massive mafic flows occur southeast of Tootyak Lake, and north and south of west Kaminak Lake (Fig. 1). They are fine grained, black and generally featureless, except for local, small plagioclase phenocrysts, and minor interflow shales. However, similar looking rocks adjacent to the granitoid pluton at Heninga Lake (Fig. 1) may be amphibole-bearing hornfels derived from volcanic rocks of intermediate composition.

Pillow lavas

Mafic to intermediate pillowed flows occur throughout the study area. However, particularly thick panels (up to 10 km) occur between Heninga and Turquetil lakes, north and south of Kaminak Lake, northeast of Quartzite Lake, and east of Southern Lake and the Copperneedle River (Fig. 1). Pillows vary in length from 10 cm to 3 m. Flow top breccias occur locally and interpillow hyaloclastite is rare (Fig. 2). Selvages are less than 2 cm thick, even on the largest pillows. Vesicles and quartz-filled amygdales can be very large, exceeding 4-5 cm in length. Locally, stratigraphic younging is readily determined from lower surface keels and convex upper pillow surfaces (Fig. 2). However, the frequency of unambiguous younging criteria is only high enough to be structurally and stratigraphically significant in a few places, such as west of Turquetil Lake and northeast of Quartzite Lake (Fig. 1).

Intermediate massive flows, gabbros, and layered rocks

Massive intermediate flows form relatively voluminous tracts, such as north of Caribou lake, and south of the Copperneedle River (Fig. 1). However, they are also commonly interlayered with intermediate pillow lavas, or with intermediate volcanic arenites and breccias. They are slightly coarser grained than their mafic equivalents, and are commonly finely plagioclase-phyric and/or amygdaloidal. The interiors of thicker flows (>5 m) tend to be coarser than the margins, and could be confused with microgabbro sills which also occur in the same outcrops. Without amygdales, or feldspar and/or hornblende phenocrysts, field identification of cleaved massive flows is difficult. For example, northeast of Quartzite Lake (Fig. 1), panels of oppositely younging intermediate pillow lavas in a 10 km thick homocline are separated by cleaved "intermediate massive flows". We interpret

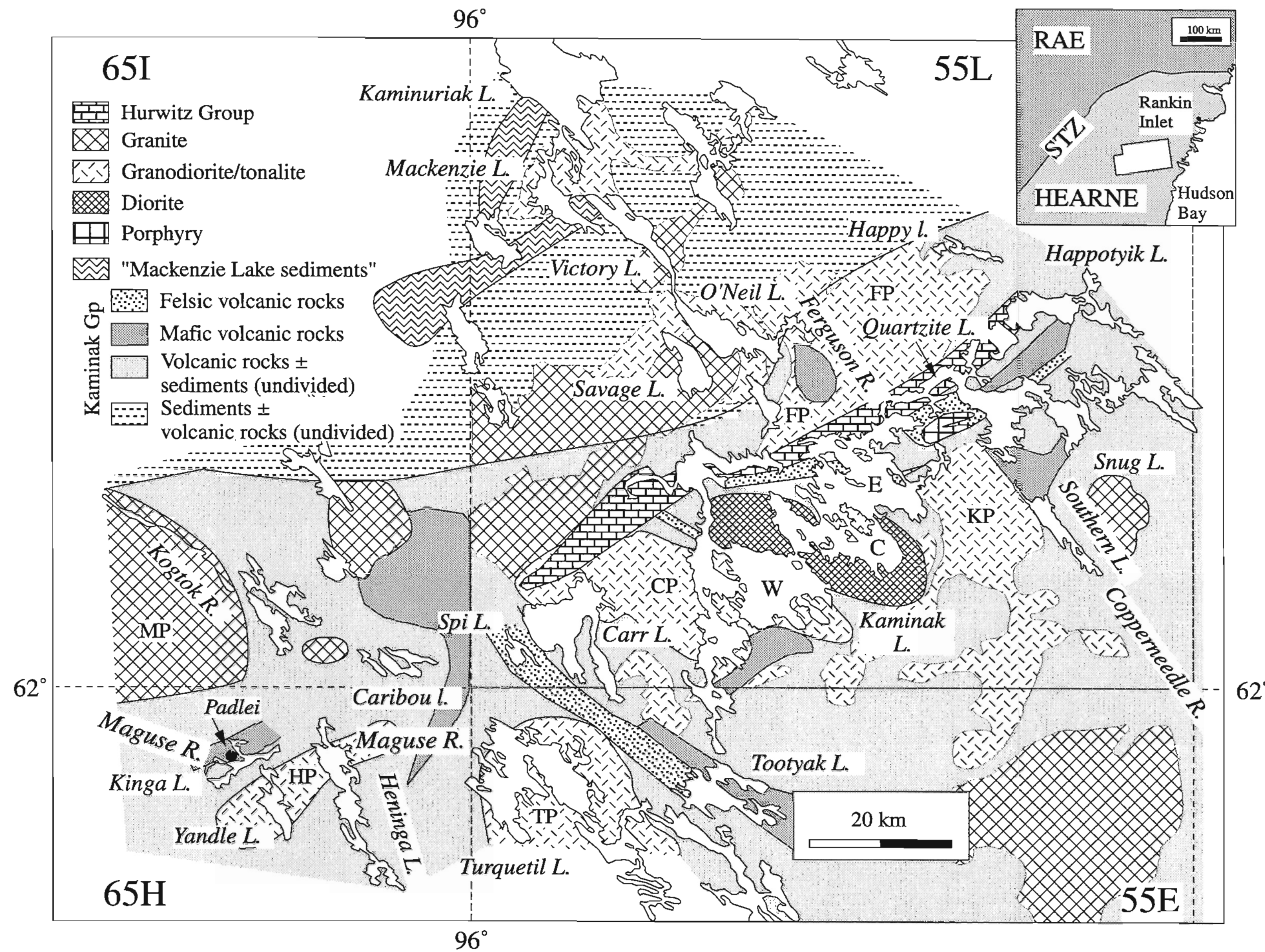

Figure 1. *Sketch map of locations referred to in the text. Major Archean plutons are indicated, and a generalized line separates mainly volcanic rocks from mainly clastic sediments. "Felsic" units may include "bimodal" volcanic rocks. Symbols "E", "C", "W" are east, central, and western Kaminak Lake, respectively. Other abbreviations are Carr (CP), Ferguson (FP), Heninga (HP), Kaminak (KP), Maguse (MP), and Turquetil (TP) plutons.*

the latter as strongly cleaved pillow lavas in sheared-out isoclinal fold closures, although no evidence for strain gradients and transposition was observed in outcrop.

Enigmatic mafic to intermediate, fine grained banded rocks are widespread (Fig. 3), but are particularly extensive south and east of Southern Lake, and north of Happy lake (Fig. 1). The banding is usually manifested by variation in the proportion of light (albite or plagioclase) and dark (chlorite or amphibole) minerals on a 1-2 cm scale. In the first two locations, the layering is visibly derived by the structural transposition of intermediate pillow lavas and their dark selvages. A strain gradient can be readily demonstrated just south of Southern Lake within the structure mapped by Irwin (1996) as the Southern Lake shear zone. However, in other occurrences there are few indications as to their origin, and the banding could be primary, possibly originally bedding.

Felsic volcanic rocks

Map-scale units of felsic volcanic rocks are well developed between Kaminak and Quartzite lakes (Fig. 1). Banded, quartz- and K-feldspar-phyric rhyolites form autoclastic breccias (Fig. 4) along the northwestern margin of a 10 km by 5 km quartz-feldspar porphyry body. We interpret these rocks to represent a large felsic dome. The dome is mantled by a carapace of felsic breccias and fine grained quartz-phyric rhyolite. The former comprise angular rhyolite fragments, 2-20 cm in diameter, set in a matrix of similar composition. The latter are fine grained, homogeneous layers, sometimes with feldspar phenocrysts, which are commonly difficult to identify as either flows or sediments. The felsic volcanic rocks are overlain by coarse volcaniclastic rocks, which we interpret as locally reworked flows and pyroclastic detritus (see below).

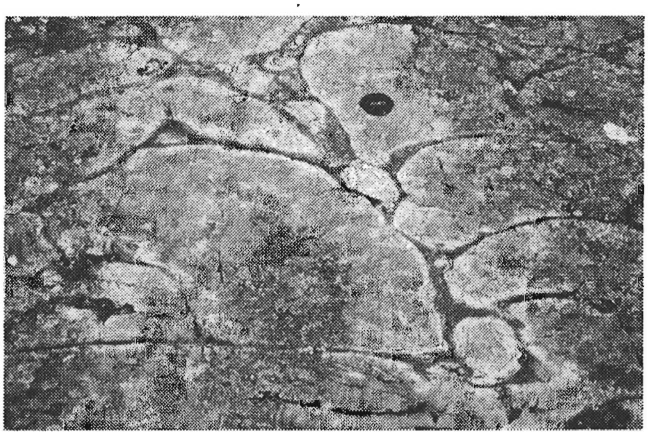

Figure 2. Pillowed flow, younging to top, west of Turquetil Lake. Note interpillow hyaloclastite. GSC 1997-68X

"Bimodal" volcanic rocks

Although isolated, thin horizons of sedimentary rock locally occur within mafic to intermediate volcanic rocks throughout the study area, a distinct lithological association with relatively high proportions of felsic versus intermediate to mafic materials (1:2 to 1:3) occurs from Spi Lake to Tootyak Lake, and in a number of areas along the northern side of Kaminak Lake between Carr and Quartzite lakes (Fig. 1). In general, the intermediate to mafic rocks range from pillow lavas, massive flows, and gabbro sills to volcanic breccias and volcaniclastic arenites. Interspersed within them are 5 m to 1 km thick bands of felsic volcanic rocks similar to those described in the preceding section. This "bimodal" assemblage is associated with abundant magnetite-chert-carbonate banded iron-formations southwest of the Kam deposit, central Kaminak Lake, and magnetite-hematite-chert facies iron-formation northwest of Tootyak Lake (Fig. 1; see below).

Volcaniclastic rocks: pyroclastic or epiclastic?

Large volumes of volcanic breccia, conglomerate and arenite occur throughout the study area, particularly between Heninga and Turquetil lakes, south of west Kaminak Lake, and at Quartzite Lake (Fig. 1). The volcanic arenites are composed of variable proportions of small (<5 mm) fragments of feldspar crystals set in a fine grained, grey-green intermediate matrix. The conglomerates and breccias are composed of

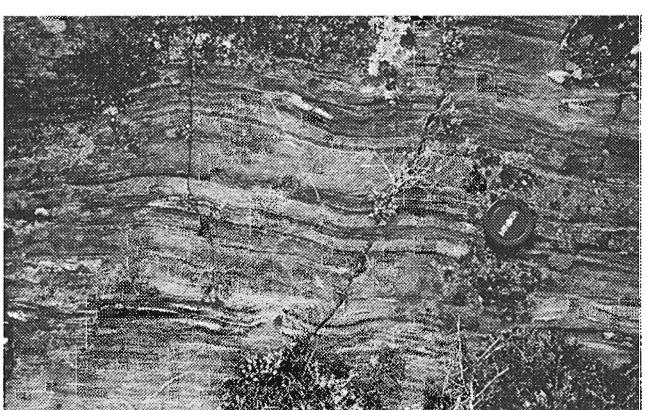

Figure 3. Banded mafic rocks west of Tootyak Lake; in many cases the origin of banding is unconstrained. GSC 1997-68B

Figure 4. Felsic autoclastic breccia northeast Kaminak Lake. GSC 1997-68V

mafic to felsic volcanic rock fragments, locally with quartz arenite and jasper clasts, set in a fine grained, grey-green intermediate matrix (Fig. 5). In some cases, the matrix is volcanic arenite. Angular fragments and rounded clasts may either be intimately associated, or mutually exclusive. The breccias and conglomerates may be monomicitic or heterolithic (compare Fig. 5 and 6). Rare plutonic clasts of leucodiorite to tonalite appear to be derived from subvolcanic intrusions (see below). In lichen covered inland outcrops, it is difficult to discern the primary features of these rocks, beyond their fragmental nature. However, more comprehensive descriptions were obtained from shoreline exposures, particularly at Quartzite Lake.

Conglomerates exposed on the west side of Quartzite Lake occur in units at least 50 m thick. They comprise poorly sorted, massive breccia/conglomerate (Fig. 7), composed mainly of subangular to rounded clasts of plagioclase-phyric felsic, and vesicular intermediate volcanic rock, quartz-feldspar porphyry, and clasts of disseminated sulphide (mainly pyrite). Clasts range up to 1 m in length, and may constitute at least 50% of the rock volume. The matrix is a

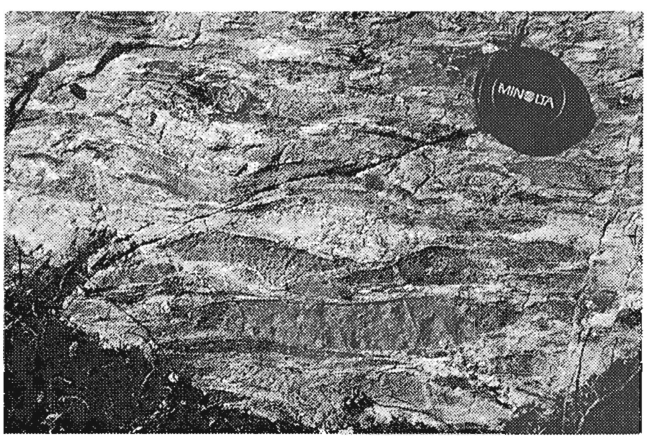

Figure 5. *Cleaved heterolithic intermediate breccia south of west Kaminak Lake. GSC 1997-68A*

Figure 6. *Cleaved monomictic felsic conglomerate west of Turquetil Lake. GSC 1997-68S*

Figure 7. *Conglomerate with clasts of felsic and vesicular intermediate volcanic rock, set in a matrix of equivalent composition, west side Quartzite Lake. GSC 1997-68D*

coarse lithic arenite composed of finer grained equivalents of the framework materials. In some cases, where the matrix is a dark green, fine grained arenite, mafic volcanic clasts are difficult to distinguish because of their dark colour and diffuse boundaries.

The lack of obvious bedding, the coarse grain size, and overall textural immaturity of the conglomerate, combined with recognition of local source-rock types in the principal clast populations, suggest that these rocks were derived from a nearby volcanic edifice composed of both mafic and felsic volcanic components, and were deposited as subaqueous debris flows. Lack of evidence for welding, and absence of interlayered fine grained material (e.g. ash) and bomb sags, would argue against primary pyroclastic deposition. However, away from shoreline exposures, diagnostic depositional criteria are generally hidden by the extensive lichen cover; it is therefore possible that significant volumes of crystal, lapilli, and lithic tuff may be present.

Quartz arenite and iron-formation

Within the Heninga-Carr-Kaminak-Quartzite lake corridor (Fig. 1), quartz arenites are volumetrically minor. Thin, laterally discontinuous siliceous beds occur episodically throughout the volcanic sequences, and clasts occur locally within the conglomerates described above. They comprise white to light grey, featureless horizons, rarely exceeding 2-3 m in thickness. In the field it is difficult to determine whether these rocks are quartzose epiclastic sediments, silicified tuffs, or recrystallized cherts. However, thick accumulations of siliciclastic sandstone occur at Quartzite Lake, and southeast of Savage Lake (Fig. 1).

North of the Heninga-Carr-Kaminak-Quartzite lake corridor, homogeneous and featureless semipelites of the Kaminak Group (Davidson, 1970a) are spatially associated with volumetrically subordinate amphibolites (Fig. 1) and a variety of granitoid plutonic rocks (see below).

Quartzite Lake sediments

The best exposed package of relatively mature clastic rocks occurs at Quartzite Lake (Fig. 1). Texturally mature polymictic conglomerate (Fig. 8), associated with coarse sandstones and sandstone/siltstone rhythmites, occurs in a well exposed, >500 m thick section, briefly described by Davidson (1970a, p. 8). Stratigraphically, it overlies (conformably?) a thick package (>500 m) of rhyolite which, in turn, overlies the conglomerate/breccia debris flows described above. The conglomerate, which dominates the lowermost 150 m of the section, is framework supported and composed of subangular to well-rounded clasts, up to 25 cm in diameter. Bedding is well defined by sandy lenses and interlayers, and by pebble imbrication which indicates westerly transport. Normal grading is the most common sedimentary structure, but reverse grading and low-angle crossbedding also are preserved. Clast types include felsic (70%) and mafic (20%) volcanic rocks, plus arenite and vein quartz (10%). The matrix is medium- to coarse-grained lithic arenite, dominated by felsic volcanic detritus.

Figure 8. *Texturally mature, polymictic conglomerate, east side Quartzite Lake. GSC 1997-68N*

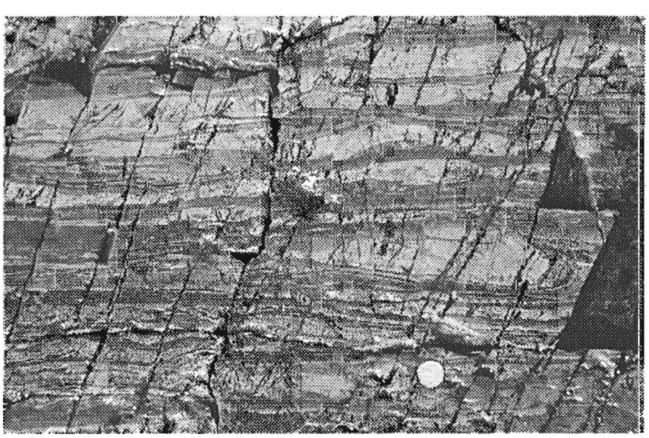

Figure 9. *Rhythmically interlayered mudstone and fine grained sandstone, east side Quartzite Lake. GSC 1997-68O*

In the middle of the section are two units, about 25 and 50 m thick, of rhythmically interlayered mudstone and fine grained sandstone (Fig. 9). Sandstone layers are tabular, wavy, and lenticular (starved ripples), varying in thickness from a few millimetres up to 10 cm. Thicker layers are tabular and normally graded, commonly with flames or ball-and-pillow structure developed along basal bed surfaces. Intervening fine grained layers are dark, thinly laminated mudstone and siltstone. Taken together, preliminary analysis of all the lithofacies and their associations points to a submarine fan to alluvial origin for most of the coarse grained section. Finer grained siltstone/sandstone lithofacies are probably deeper water turbidites.

Iron-formations

Banded iron-formation occurs southwest of Kaminak Lake (Fig. 1), where it is associated with fine grained, argillaceous, clastic sedimentary rocks within thick sequences of massive to pillowed mafic to intermediate volcanic rocks. The distribution of these rocks is clearly defined by pronounced linear anomalies in the regional aeromagnetic field (Geological Survey of Canada, 1987). The key feature of the iron-formations is the presence of very fine grained magnetite and both pigmentary and nonpigmentary hematite. Oxide layers exhibit very thin, rhythmic, parallel lamination, with no tractional sedimentary structures, attesting to deposition in quiet water (Fig. 10). In the northern part of west Kaminak Lake, ankerite interlayers occur with the oxide layers, chert, and possible felsic tuff. North of Tootyak Lake (Fig. 1), iron oxide is interbedded with 10-40 cm thick, normally graded beds of felsic lithic arenite. Some beds contain 5-50 cm rip-ups of

Figure 10. *Banded iron-formation, north of Tootyak Lake. Light bands are either tuffs or cherts and felsic lithic arenite. GSC 1997-68P*

iron oxide rhythmite, confirming their origin as gravity flows. Other potential indicators of slope instability include synsedimentary folds and clastic dykes.

The iron-formations display many attributes of the Algoma type (Gross, 1996). Depositional environments for these deposits are varied, but features described above indicate deposition in a quiet water basinal setting, below storm wave base (>100 m). Intercalated felsic volcaniclastic sediments, tuffs, and magmatic dykes indicate proximity to an active volcanic arc.

Savage Lake sediments

Normally graded, lithic arenite-siltstone rhythmites outcrop between Savage and Kaminak lakes (Fig. 1). Average bed thickness is 20-30 cm, with a maximum of 1 m. These rocks are similar to the turbidites at Quartzite Lake, without the coarser grained lithofacies. The section has an apparent thickness greater than 3 km, but stratigraphic reversals suggest that it is thickened by isoclinal folding. Davidson (1970a) suggested that these sediments may overlie the volcanic rocks of the Kaminak Group, though their contact relations remain unconstrained.

PLUTONIC ROCKS

Synvolcanic granitoids

Equigranular microgabbro commonly occurs as sheets in the volcanic and volcaniclastic rocks of the Kaminak Group. Crosscutting relationships between the gabbro and host volcanic rocks are rarely preserved, and thus these sheets are interpreted as synvolcanic intrusions.

The central part of Kaminak Lake (Fig. 1) is underlain by at least four texturally distinct units of diorite: (i) medium- to fine-grained, equigranular, hornblende leucodiorite, (ii) plagioclase-phyric to megacrystic diorite, (iii) hornblende oikocrystic (<3 cm) diorite, and (iv) intimately admixed components of all three. We refer to them collectively as the central Kaminak diorite suite (new name). Locally, these diorite units appear to both intrude and grade into adjacent hypabyssal and extrusive units of the Kaminak Group. They commonly contain abundant centimeter- to metre-scale xenoliths of locally derived supracrustal rocks. These include mafic to silicic volcanic and sedimentary rocks that have been deformed into foliated schlieren and hornfelsed, lending a gneissose appearance to the diorite. Rarely, the diorites crosscut a medium- to coarse-grained, probably synvolcanic biotite tonalite, but more typically they are themselves crosscut by silicic granitoids. The diorites are also crosscut by intermediate dykes with chilled margins, apparently similar in composition to parts of the Kaminak Group (Fig. 11). This suggests that volcanism continued subsequent to intrusion of the diorites.

Syntectonic granitoids

Granitoids constituting the Kaminak batholith occur as three distinct composite plutons, out cropping in the eastern, northern, and southwestern parts of Kaminak Lake. These three

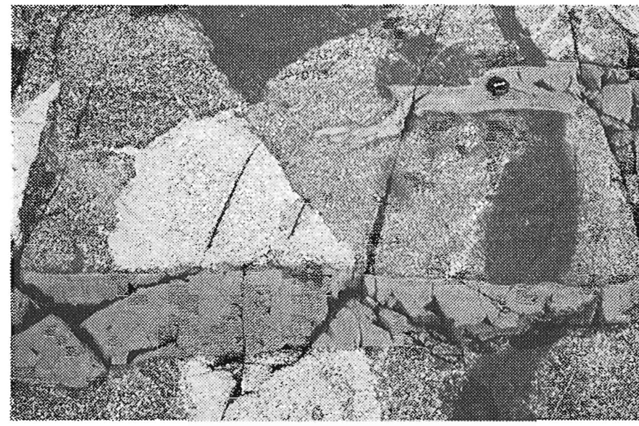

Figure 11. *Diorite cut by both leucodiorite mafic diorite, and by intermediate dykes, central Kaminak Lake. GSC 1997-68G*

plutons are distinct in composition and field character, and are herein referred to as the Kaminak, Ferguson, and Carr plutons, respectively (Fig. 1; new names).

The Kaminak pluton ranges in composition from granodiorite to gabbro, but is predominantly medium grained, hornblende-biotite granodiorite to tonalite. Hornblende grains, up to 10 mm, locally lend a porphyritic aspect to the rock. The pluton has a disruptive, net-vein contact along its northeastern margin, where it incorporates rafts and blocks of volcanic rocks of the Kaminak Group. In contrast, its western margin is characterized by hornfelsed, highly strained, banded metavolcanic rocks. There, variably deformed veins emanating from the pluton suggest that the wall rock was deformed as a consequence of the pluton emplacement. To the south and east, tonalite of the Kaminak pluton intrudes slightly older, probably comagmatic, quartz diorite, diorite, and rare gabbro. Cavell et al. (1992) obtained a moderately well constrained U-Pb zircon age of 2700 ±11 Ma for the Kaminak pluton.

The Ferguson pluton, out cropping north of central Kaminak Lake (Fig. 1), is similarly diverse in composition, ranging from rare gabbro through quartz diorite, to predominantly tonalite and locally granodiorite. In general, tonalite underlies the western part of the pluton, whereas mafic end-members prevail to the east. On the east side of the Ferguson River (Fig. 1), quartz diorite and diorite, with inclusions of mafic supracrustal rocks in a medium grained, biotite-hornblende tonalite, are more common. The pluton is extensively altered and plutonic textures are poorly preserved. For example, the tonalite is characterized by a fine grained chloritic matrix, surrounding quartz, plagioclase, and variable potassium feldspar, even where it is not significantly deformed. The original magmatic biotite and hornblende are only locally preserved. In addition, the pluton is cut by numerous, spaced (about 50 m), 045-080° trending, narrow chloritic shear zones. The spatial association of this alteration and retrograde metamorphism with the deformed Paleoproterozoic Hurwitz Group raises the possibility that it may postdate the Hurwitz Group.

The Carr pluton ranges from diorite to syenogranite and is characterized by at least five distinct plutonic phases. Incipiently to well foliated, medium- to coarse-grained biotite tonalite, with blue quartz phenocrysts, is locally associated with a medium grained diorite to hornblende quartz diorite. Diffuse, gradational contacts, mechanical incorporation of potassium feldspar and quartz phenocrysts from the tonalite into the diorite, and hornblende reaction coronas around incorporated quartz grains, are indicative of magma co-mingling/mixing relationships. The tonalite and diorite are crosscut by veins and dykes of a fine- to medium-grained biotite monzogranite that occurs as an extensive, coherent unit along the southern margin of the pluton. Locally, the biotite monzogranite appears to grade laterally into a medium grained, biotite monzonite. The central and major component of the Carr pluton comprises a homogeneous, medium grained, biotite-hornblende granodiorite. On the northern and southern margins of the pluton veins and dykes of granitoid intrude the country rock, although the northern contact has subsequently been faulted. The western contact is not exposed, and may underlie Carr Lake (Fig. 1). However, tonalite mapped on the western shore of Carr Lake, and occurring as clasts in the Spi Lake conglomerate (Miller and Tella, 1995), may be equivalent to the Carr pluton. The eastern margin of the pluton is distinct and comprises a series of margin-parallel, schlieren zones alternating with clean tonalite and granodiorite that, over a distance of about 4 km, pass into the central Kaminak diorite suite.

STRUCTURE AND METAMORPHISM

Within the Kaminak Group, compositional layering varies from centimetre-scale banding to packages of homogeneous pillow lavas, tens to hundreds of metres thick. Most outcrop scale lithological contacts are interpreted as bedding (S_0), or bedding-parallel sills. Smaller scale banding, for example in mafic to intermediate rocks of uncertain parentage, may either be primary or tectonometamorphic in origin (Fig. 3). Except for some outcrops of pillowed flows (Fig. 2), felsic lavas (Fig. 4), and some silicified volcanic rocks, the supracrustal lithologies of the Kaminak Group exhibit a variably developed layer-parallel foliation (Fig. 5 and 6). For the most part, this fabric is developed in lower greenschist facies chlorite-albite±sericite mineral assemblages. The foliation is axial planar to rare, small scale (<50 cm) intrafolial folds of layering. Although we recognize that it could represent a composite tectonic fabric, we refer to this early foliation as S_1.

The strike of S_1 and S_0 varies from 045-135°, with steep to vertical dips. A steeply pitching lineation is regionally developed on S_1 (Fig. 12), but its intensity is variable. Although the lineation is best developed in sheared zones of alteration (Hanmer et al., 1998), this association is not exclusive. The lineation is composite. In places, it is clearly an extension lineation defined by elongate quartz-sericite aggregates, locally highlighted by aligned chlorite crystals. Elsewhere, it is a fine crenulation of S_1. These two facets of the lineation are not mutually exclusive.

The S_1 foliation is locally deformed by structures which, with few exceptions, are only developed at a small scale (<50 cm). Isolated, asymmetrical folds (Fig. 13), and oblique crenulation cleavage parallel to their axial planes (Fig. 14), are heterogeneously distributed, but not necessarily together. Most folds are steeply plunging, and coaxial with the lineation described above. Locally, similar asymmetrical folds plunge more moderately (about 45°). The lineation parallel to these fold axes is always of the crenulation or intersection type. The lineation parallel to the steeply plunging folds may be either an extension or a crenulation lineation. Very locally, moderately plunging kink folds are seen to deform the lineation, for example in northeast Kaminak Lake (Fig. 1). Most importantly, the development of the steeply plunging/pitching lineation is independent of the presence of macroscopic folding. These observations suggest that, in general, the steep extension lineation is an L_1 structure, contemporaneous with the development of S_1. The crenulation component of the lineation is probably younger, and in places is demonstrably contemporaneous with post-S_1 folds to which it is coaxial. Rarely, vertical, 1-5 cm spaced asymmetrical shear bands cut

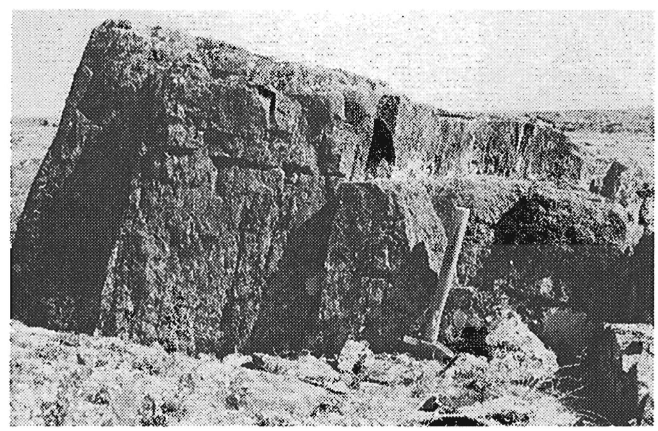

***Figure 12.** Steeply pitching extension lineation (L_1) on vertical S_1 cleavage surfaces, west of Turquetil Lake. GSC 1997-68F*

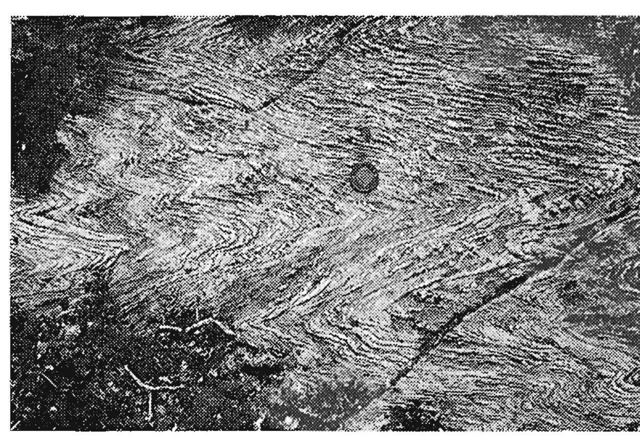

***Figure 13.** Vertically plunging fold pair ('Z' asymmetry) deforming S_1 in quartzite, north of Happy lake. GSC 1997-68H*

Figure 14. Oblique post-S_1 crenulation cleavage west of Quartzite Lake; does not extend beyond the volume illustrated here. GSC 1997-681

across the upright S_1 foliation. It is possible that microscopic-scale shear bands could be responsible for the steeply plunging crenulation lineation in some places.

We concur with Davidson (1970a), who noted that the discontinuous preservation of the Kaminak Group stratigraphy make it difficult to map out major folds. Of the few map-scale folds proposed by earlier workers, we could only confirm the post-S_1 fold mapped by Relf (1995) on the southeast side of Quartzite Lake. The arcuate structure south of Southern Lake, illustrated by Irwin (1996) as a post-S_1 fold, is a dip-lineated, banded amphibolite with synkinematic intrusive sheets of tonalite and granodiorite. Although it appears to represent a curvilinear band of transposed pillowed flows, the absence of parasitic folding of the amphibolite layering or an axial planar fabric anywhere in the arc is incompatible with a fold origin for the map-scale geometry. Nonetheless, the presence of younging reversals in pillowed flows north of Quartzite Lake, and in turbidites southeast of Savage Lake, suggests that the Kaminak Group is isoclinally folded on a wavelength of several kilometres. However, the relative age of these structures remains unconstrained. The only other extensive occurrence of abundant, unequivocal younging criteria is the thick homoclinal package of pillowed flows flanked on either side by intermediate volcaniclastic rocks and massive flows, west of Turquetil Lake and north of the Maguse River (Fig. 1). There, the pillows all young to the southeast and demonstrate the absence of folding. Thus, the question of whether the Kaminak Group is extensively isoclinally folded, either by F_1 or post-S_1 folds, remains unresolved.

SUMMARY

The discontinuous nature of map units in the Kaminak Group does not allow elaboration of a robust stratigraphy based upon field observation alone. Nevertheless, the abundance of intermediate to felsic extrusive lithologies, and the high proportion of volcaniclastic rocks, much of which may represent subaqueous reworking of material eroded from volcanic edifices, suggests that the Kaminak Group contains the remains of a calc-alkaline magmatic arc.

ACKNOWLEDGMENTS

We are grateful to Yannick Beaudoin, Nora Brown, Thomas Hadlari, and Chris Hemmingway for their excellent and enthusiastic assistance in the field, and to Laura Adams, our splendid and very patient cook. Please see Hanmer et al. (1998) for more comprehensive acknowledgments. The manuscript was critically read by Subhas Tella and Steve Lucas.

REFERENCES

Aspler, L.B. and Chiarenzelli, J.R.
1996: Stratigraphy, sedimentology and physical volcanology of the Henik Group, central Ennadai-Rankin greenstone belt, Northwest Territories, Canada: late-Archean paleogeography of the Hearne Province and tectonic implications; Precambrian Research, v. 77, p. 59-89.

Bell, R.T.
1971: Geology of Henik Lakes (east half) and Ferguson Lake (east half) map-areas, District of Keewatin; Geological Survey of Canada, Paper 70-61, 31 p.

Cavell, P.A., Wijbrans, J.R., and Baadsgaard, H.
1992: Archean magmatism in the Kaminak Lake area, District of Keewatin, Northwest Territories: ages of the carbonatite-bearing alkaline complex and some host granitoid rocks; Canadian Journal of Earth Sciences, v. 29, p. 896-908.

Davidson, A.
1970a: Precambrian geology, Kaminak Lake map-area, District of Keewatin (55L); Geological Survey of Canada, Paper 69-51, 27 p.
1970b: Eskimo Point and Dawson Inlet map-areas (north halves), District of Keewatin, 55e and 55f (north parts); Geological Survey of Canada, Paper 70-27, 21 p.

Geological Survey of Canada
1987: Magnetic Anomaly Map of Canada; Geological Survey of Canada, Map 1255A, scale 1:5 000 000.

Gross, G.A.
1966: Algoma-type iron formation; in Geology of Canadian Mineral Deposit Types, (ed.) O.R. Eckstrand, W.D. Sinclair, and R.I. Thorpe; Geological Survey of Canada, Geology of Canada, no. 8, p. 66-73 (also Geological Society of America, The Geology of North America, v. P-1).

Hanmer, S., Rainbird, R.H., Sandeman, H.A.I., Peterson, T.D., and Ryan, J.J.
1998: Field contributions to thematic studies related to the Kaminak greenstone belt, Kivalliq Region, Northwest Territories; in Current Research 1997-C; Geological Survey of Canada.

Irwin, D. A.
1994: Mineral occurrences and preliminary geology of the Kaminak-Carr Lakes area, District of Keewatin (parts of 55L/3, 4, 5 and 6); Northwest Territories Geological Mapping Division, Map EGS 1994-03, scale 1:50 000.
1995: Mineral occurrences and preliminary geology of the Kaminak-Quartzite Lakes area, District of Keewatin (south-central 55L); Northwest Territories Geological Mapping Division, Map EGS 1995-05, scale 1:50 000.
1996: Geology and mineral occurrences of the Southern Lake area, District of Keewatin (55L/1); Northwest Territories Geological Mapping Division, Map EGS 1996-06, scale 1:50 000.
1997: Geology and mineral occurrences of the Happy Lake area, District of Keewatin (parts of 55L/9 and 10); Northwest Territories Geological Mapping Division, Map EGS 1997-00, scale 1:50 000.

Miller, A.R. and Tella, S.
1995: Stratigraphic setting of semiconformable alteration in the Spi Lake area, Kaminak greenstone belt, Churchill Province, Northwest Territories; in Current Research 1995-C; Geological Survey of Canada, p. 175-186.

Relf, C.
1995: Geological map of the Snug Lake area, District of Keewatin, (55L/8); Northwest Territories Geological Mapping Division, Map EGS 1995-00, scale 1:50 000.

Geological Survey of Canada Project 970006

Preliminary report on the geology and tectonic history of the Trans-Hudson Orogen in the northwestern Reindeer Zone, Saskatchewan

D. Corrigan[1], R.O. Maxeiner[2], A. Bashforth[3], and S.B. Lucas
Continental Geoscience Division

Corrigan, D., Maxeiner, R.O., Bashforth, A., and Lucas, S.B., 1998: Preliminary report on the geology and tectonic history of the Trans-Hudson Orogen in the northwestern Reindeer Zone, Saskatchewan; in Current Research, Part C; Geological Survey of Canada, Paper 98-1C, p. 95-106.

Abstract: The La Ronge Domain in the northwestern Reindeer Zone comprises island arc supracrustal rocks (Central Metavolcanic Belt) and flanking sedimentary basins (Crew Lake and MacLean Lake belts) intruded by plutons of predominantly intermediate composition. The Rottenstone Domain flanks these assemblages to the northwest and consists mainly of their high-grade equivalents. To the southeast, the Central Metavolcanic Belt was thrust over younger terrestrial to shallow marine metasedimentary rocks (McLennan Group) after the emplacement of small ultramafic-mafic plutons and dykes, but prior to the regional emplacement of granitic to leucotonalitic plutons. The McLennan Group, which sat unconformably on the La Ronge Domain prior to thrust deformation, grades southerly into greywacke-turbidite of the Kisseynew Domain. We infer deepening of the paleo'Kisseynew' sedimentary basin towards the south, and predict similar deposition ages for the McLennan and Kisseynew sequences. All units record polyphase, nearly coaxial deformation and lower- to middle-amphibolite facies metamorphic conditions.

Résumé : Le Domaine de La Ronge dans le nord-ouest de la Zone de Reindeer comprend des roches supracrustales d'arc insulaire (Ceinture métavolcanique centrale) et des bassins sédimentaires inter-arc (ceintures de Crew Lake et de MacLean Lake) que recoupent des plutons de composition intermédiaire. Le Domaine de Rottenstone longe cet assemblage au nord-ouest et comporte surtout des équivalents plus fortement métamorphisés de l'assemblage. Au sud-ouest, la Ceinture métavolcanique centrale et une partie de la Ceinture de MacLean Lake ont été chevauchées par-dessus des roches métasédimentaires plus jeunes, d'origine terrestre à épicontinentale, du Groupe de McLennan après la mise en place de filons et dykes ultramafiques-mafiques et avant la mise en place de plutons de granite et de leucotonalite. Le Groupe de McLennan, qui avant le chevauchement recouvrait en discordance le Domaine de La Ronge, passe vers le sud à des grauwackes-turbidites du Domaine de Kisseynew. Nous concluons qu'il y a eu approfondissement vers le sud du paléobassin sédimentaire du Domaine de Kisseynew, et nous prévoyons que les séquences du Groupe de McLennan et du Domaine de Kisseynew ont un âge de sédimentation comparable. Toutes les unités témoignent de déformation polyphasée et presque coaxiale et de conditions métamorphiques équivalant au sous-faciès et au faciès intermédiaire des amphibolites.

[1] 5-55 Impasse de la Roseraie, Hull, Quebec, J9A 2S7
[2] Saskatchewan Energy and Mines, Regina, Saskatchewan S4P 4V4
[3] Department of Earth Sciences, Memorial University, St. John's, Newfoundland A1B 3X5

INTRODUCTION

In Saskatchewan and Manitoba, the southeastern Reindeer Zone segment of the Trans-Hudson Orogen (Fig. 1) has been the focus of recent government geoscience programs (e.g., NATMAP Shield Margin Project) as well as the LITHOPROBE Trans-Hudson Orogen Transect. Whereas our understanding of the geology and tectonic history of the area has advanced substantially (e.g., Stern et al., 1993; Lucas et al., 1996), the geology and geochronology of the northwestern Reindeer Zone are less well known. To improve understanding of the northwestern Reindeer Zone, the Geological Survey of Canada, in conjunction with Saskatchewan Energy and Mines, launched a mapping initiative in 1997. The long-term objective of the project is to map a transect along Reindeer Lake from the northern flank of the Kisseynew Domain to the Peter Lake Domain, which may represent the most internal basement inlier of the Hearne Province (Lewry et al., 1990) (Fig. 1). The long-term objective of Saskatchewan Energy and Mine is to provide 1:20 000 scale coverage of the La Ronge-Lynn Lake Domain. In 1997, we mapped a 700 km² area at 1:20 000 (Corrigan et al., 1997; Maxeiner, 1977) and 1:50 000 (this study) scales, providing a complete transect of the La Ronge Domain. Results are summarized below.

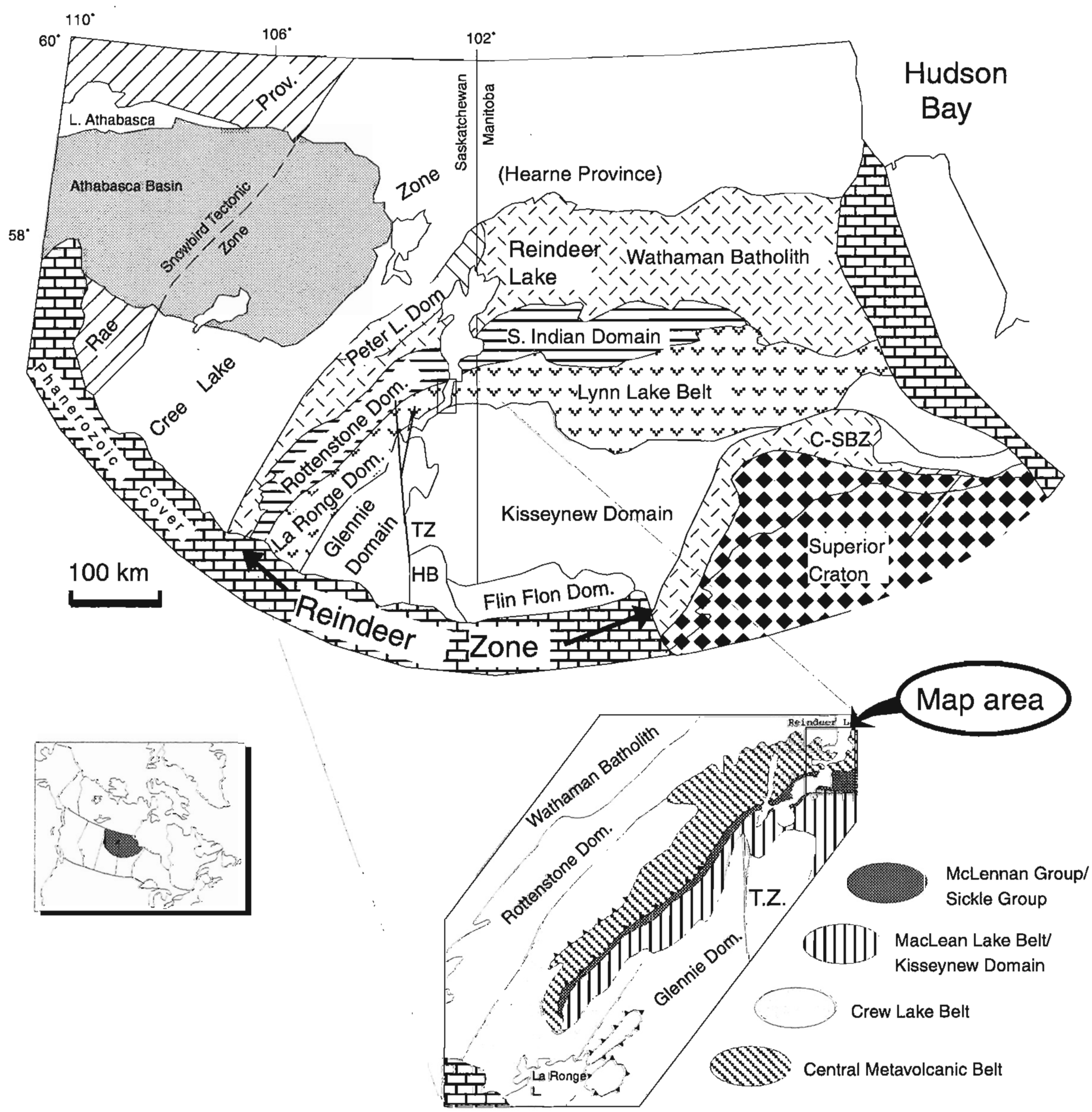

Figure 1. Simplified map of the Trans-Hudson Orogen in Saskatchewan and Manitoba showing major lithotectonic domains and the map location along Reindeer Lake. HB=Hansen Block; TZ=Tabbernor fault zone. Modified after Lewry et al. (1990).

GEOLOGICAL FRAMEWORK

The northwestern Reindeer Zone consists of a number of tectonostratigraphic belts that were accreted to the Archean Hearne Province during Paleoproterozoic collision (e.g., Lewry et al., 1990). In Saskatchewan and Manitoba they form a northwest-dipping homoclinal stack, comprising from lower to upper structural levels (i.e., southeast to northwest) the Kisseynew Domain, the La Ronge-Lynn Lake Domain, the Rottenstone-Southern Indian Domain, the Wathaman-Chipeywan Batholith, and the Peter Lake Domain (Fig. 1). The La Ronge Domain forms the central part of the area investigated in 1997. It is bounded to the south by the Kisseynew Domain (Gilboy, 1980), which consists of a turbidite sequence deposited at 1.85-1.84 Ga (Ansdell et al., 1995; David et al., 1996), and to the north by the Rottenstone Domain, a variously migmatized zone of tonalite-trondhjemite intrusions and minor psammitic to psammopelitic metasedimentary rocks that is of uncertain origin and age (see Johnston and Thomas, 1984). Its southwestern and central segments (Fig. 1) comprise 1882-1876 Ma volcanic and minor sedimentary rocks and 1874-1855 Ma plutonic rocks (Bickford et al., 1986) of the Central Metavolcanic Belt. These rocks have been interpreted as a volcano-sedimentary assemblage formed in an ensimatic island-arc setting, transitional into an ensialic setting (e.g. Thomas et al., 1987; Watters, and Pearce 1987; Thomas, 1993).

The Central Metavolcanic Belt is stratigraphically intercalated with and overlain by metasedimentary rocks of the MacLean Lake and Crew Lake belts (Thomas, 1993). The MacLean Lake Belt is found southeast of the Central Metavolcanic Belt (Fig. 1). In the southwestern La Ronge Domain, it comprises meta-arkoses of the McLennan Group and a mixed assemblage of pelitic to conglomeratic and in part calcareous metasedimentary rocks and minor hornblendic gneiss of the MacLean Lake "gneisses" (e.g. Thomas, 1993). The McLennan Group is interpreted to unconformably overlie MacLean Lake gneiss and the Central Metavolcanic Belt (Thomas, 1993). However, along much of its length southwest of Reindeer Lake, it has been overthrust along the McLennan Lake tectonic zone by the Central Metavolcanic Belt (Fig. 1) (Lewry et al., 1990). Recent detrital U-Pb zircon studies and geological investigations suggest that parts of the MacLean Lake gneiss may be as young as 1.85-1.84 Ga (Ansdell and Yang, 1995; Ansdell et al., 1995), forming part of a younger sedimentary assemblage that includes McLennan Group arkosic sedimentary rocks (Maxeiner and Sibbald, 1995). Several field studies, however, seem to confirm that some sedimentary rocks of MacLean Lake gneiss affinity are synvolcanic with respect to the Central Metavolcanic Belt (e.g., Thomas, 1993; Maxeiner, 1997). The Crew Lake Belt is northwest of and structurally above the Central Metavolcanic Belt and comprises predominantly psammitic to pelitic assemblages with subordinate intercalated hornblendic gneiss and amphibolite, all intruded by large granitoid plutons. The transition between the Central Metavolcanic Belt and the Crew Lake Belt is marked by intercalated pelitic material, carbonate rocks, calc-silicate, quartzite, iron-formation, and fine-grained volcaniclastic rocks (Thomas, 1993). In the northeast, rocks of the Crew Lake Belt seem to grade into rocks of the Rottenstone Domain with an increase in the melt component (Lewry et al., 1990, and references therein).

LA RONGE DOMAIN

Central Metavolcanic Belt

In the map area (Fig. 2), supracrustal rocks of the Central Metavolcanic Belt are divided into two longitudinal belts, the Lawrence Point and Reed Lake volcanic belts (Maxeiner, 1997; Corrigan et al., 1997). The Lawrence Point volcanic belt is found at the structural base of the Central Metavolcanic Belt and comprises highly deformed metabasites (Fig. 3) intercalated with minor intermediate and felsic volcanogenic rocks, altered volcanogenic and epiclastic rocks, and ferruginous psammites. The Reed Lake Belt is found at higher structural levels and is composed mainly of intermediate volcanic and volcaniclastic rocks (Fig. 4) interlayered with minor mafic and felsic volcanic rocks, cordierite-anthophyllite-garnet schist, metapelite, and minor ultramafic rocks. Both belts contain layer-parallel granodioritic and gabbroic intrusions, and are separated by the Butler Island Pluton (Fig. 2), which consists of predominantly homogeneous massive to locally extremely lineated diorite to quartz diorite. A compositionally and texturally similar intrusion, the Milton Island Pluton (Fig. 2), intrudes at a shallow angle along the north flank of the Reed Lake volcanic belt. Scattered throughout the Lawrence Point volcanic belt (but only rarely in the Reed Lake belt) are metre- to kilometre-scale, tectonically disrupted intrusions of layered to massive ultramafic-mafic rock (Fig. 5), including actinolite schist, serpentinite, and pyroxenite. A more detailed description of the Central Metavolcanic Belt is given in Corrigan et al. (1997) and Maxeiner (1997).

Metasedimentary assemblages

Two separate regionally extensive assemblages of psammitic to pelitic gneiss occur west of Fraser Bay (Barb Lake metasedimentary assemblage; Maxeiner, 1997) and on and northeast of Milton Island (Milton Island metasedimentary assemblage; Corrigan et al., 1997) on Reindeer Lake (Fig. 2). Their affinity is uncertain, but they seem to be similar both in character and structural position to rocks of the Crew Lake Belt in the southwestern and central La Ronge Domain (Harper, 1986; Thomas, 1993). The Milton Island metasedimentary assemblage consists of a relatively homogeneous package of psammitic to pelitic gneiss in the core of a map-scale synform opening towards the north-northeast (Fig. 2). Ubiquitous quartz-rich and quartz-plagioclase-rich leucosomes (Fig. 6) form layer-parallel segregations separated from the paleosome by thin biotite-rich selvages. Characteristic bluish-green apatite occurs locally in the leucosomes. To the south, near the contact with the Reed Lake volcanic belt, muscovite is stable in the metamorphic assemblage, but its abundance decreases progressively towards the north, concomitant with an increase in the proportion of melt, which locally forms up to 40 per cent of the rock volume. Northeast

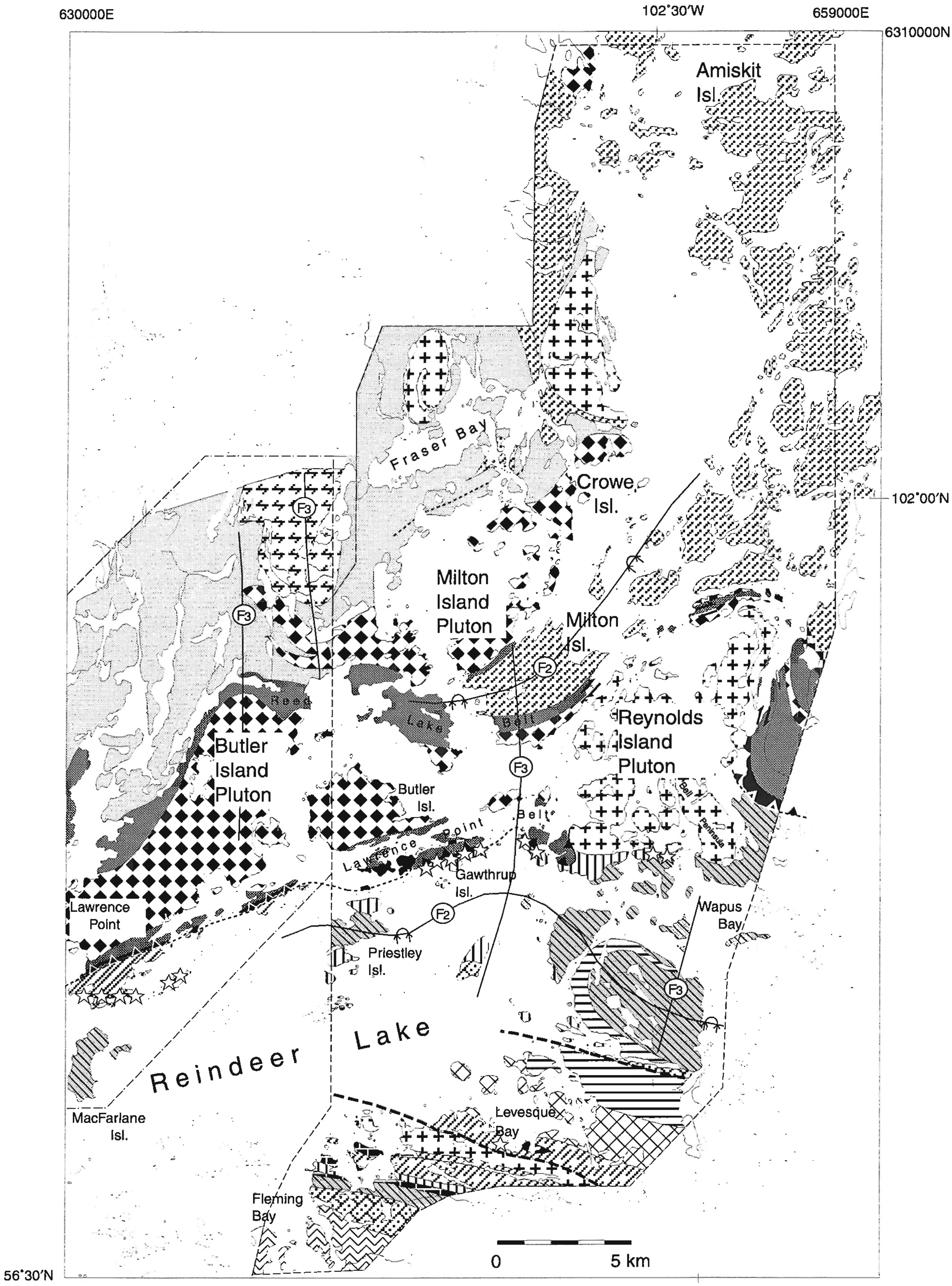

Figure 2. Geological map of the Reindeer Lake area showing major lithologies, based on mapping in the summer of 1997 (area outlined with dashed line), and area mapped at 1:20 000 scale by Maxeiner (1997) (dash-dot line).

Figure 3. Highly deformed mafic tectonite in Lawrence Point volcanic belt. Light coloured bands are stretched calc-silicate pods. View looking west. Bottom of photograph is approximately 1 m wide. (GSC 1997-70A)

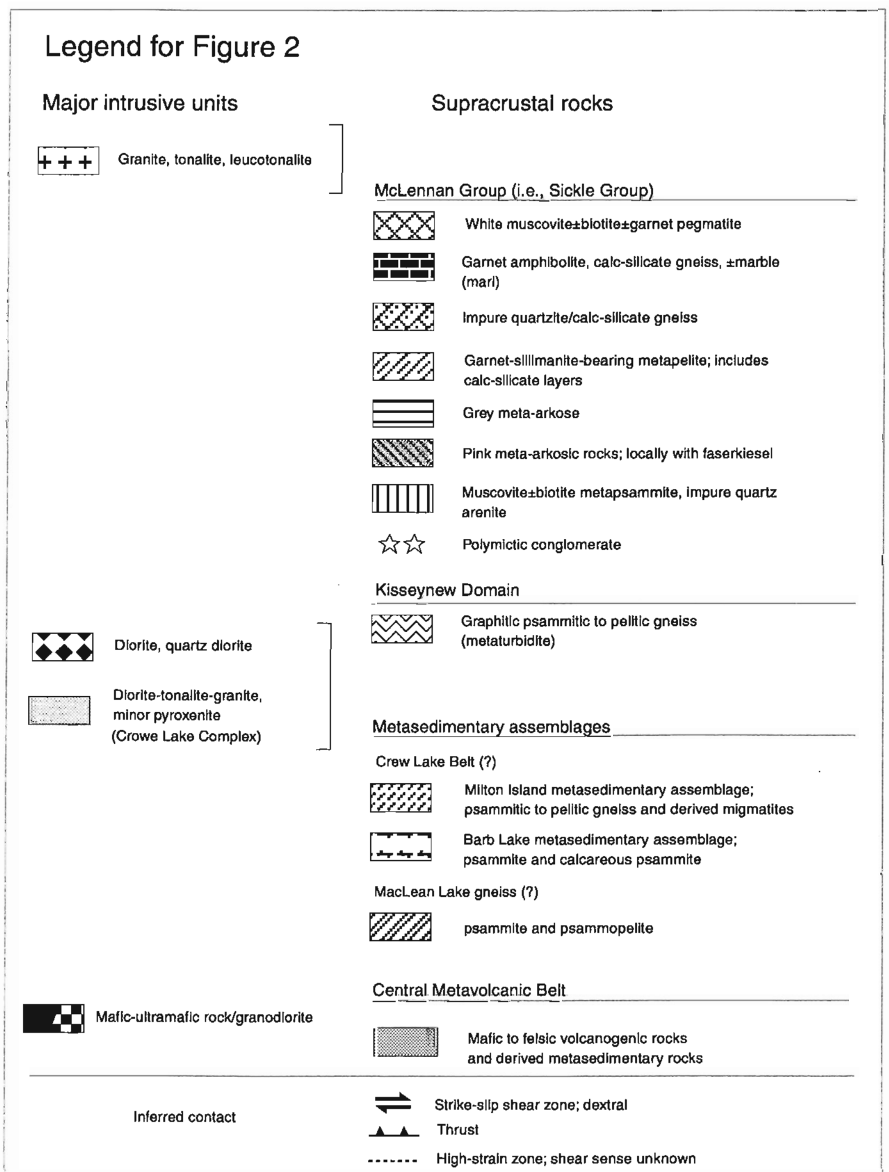

of the Reynolds Island Pluton (Fig. 2), volcanic rocks of the Reed Lake belt are structurally overlain by volcaniclastic and calc-silicate rocks that seem to grade into the Milton Island metasedimentary assemblage.

The Barb Lake metasedimentary assemblage is within the core of a northeast-plunging, north-trending regional synform (Fig. 2) and comprises psammitic and calcareous psammitic rocks containing variable amounts of injected, and in part locally derived, granitic and leucotonalitic melt material. The psammitic phase of the Barb Lake metasedimentary assemblage resembles the Milton Island unit, and may be equivalent. Both are intruded by the Crowe Island Complex and Milton Island Pluton, and are thus older than these intrusions.

A distinct easterly thinning wedge of metasedimentary rocks, interpreted as part of the MacLean Lake gneiss (Maxeiner, 1997), extends from Lawrence Point to immediately west of Priestley Island (Fig. 2). It consists of psammitic to psammopelitic gneiss (greywacke-turbidite) intercalated with calcareous psammopelite, and is intruded by feldspar porphyry and ultramafic to mafic dykes. It is flanked to the north by the Lawrence Point volcanic belt, and to the south by polymictic conglomerate of the McLennan Group. Both its lower and upper contacts are tectonic.

McLENNAN GROUP

Structurally below the Lawrence Point volcanic belt, polymictic conglomerate forms a narrow unit extending from MacFarlane Island to the west margin of the Reynolds Island Pluton (Fig. 2); thin slivers of the unit were also found at comparable structural levels east of the pluton, and in the bottom of Levesque Bay (Fig. 2). The conglomerate contains matrix-supported clasts of volcanic, sedimentary, and plutonic origin that have been ductilely deformed into elongate lenses up to 30 cm long (Fig. 7). Some clasts are texturally and compositionally similar to rocks in the Central Metavolcanic Belt, suggesting a provenance from that source. Down structural section, clast sizes generally decrease, and the polymictic conglomerate becomes interlayered with and finally grades into grey muscovite±biotite±fibrolite+magnetite-bearing metapsammites and impure quartz arenites. These observations suggest that the younging direction is towards the south, down structural section. In the western part of the map area, the conglomerate is structurally overlain by MacLean Lake gneiss. However, it is in contact with rocks of the Central Metavolcanic Belt towards the east, suggesting apparent map-scale overturned angular unconformity with rocks to the north (Fig. 2).

Pink meta-arkoses occur in a wide belt south of the grey metapsammite/impure quartz arenite assemblage. Primary structures such as crossbeds, gritty layers with quartz granules, and lag deposits are locally preserved. Potassium feldspar predominates over plagioclase and is accompanied by up to 30 per cent quartz, and generally less than 5 per cent biotite. Fibrolite-bearing faserkiesel up to 30 cm long are common (Fig. 8). One outcrop on the north shore of Priestly Island (Fig. 2) has well preserved crossbeds (Fig. 9) indicating top-to-the-south younging, which agree with younging directions inferred from the conglomerate, although northward younging in other outcrops (Sibbald, 1977; Maxeiner, 1997) indicates that the package is folded and overturned (see below). Grey magnetite-bearing biotite-rich arkose occurs to the south and structurally below the pink arkose (Fig. 2). The transition between the two is gradual and reflects a reduction of potassium feldspar content at the expense of plagioclase, and an increase in the amount of biotite. Both the pink and grey arkoses contain diopside-rich calc-silicate layers, which become progressively more abundant and thicker towards the south. Garnet first appears in a sillimanite-garnet-biotite metapelite that contains distinctive laminated quartz- and

Figure 4. *Dacitic to andesitic tuff breccia on west shore of Milton Island, Reed Lake belt. (GSC 1997-62I)*

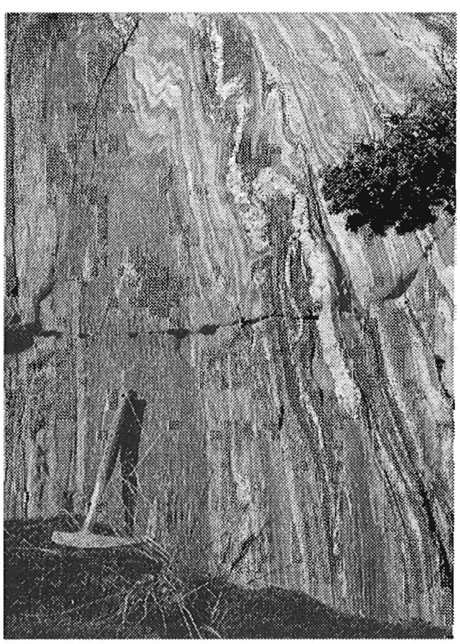

Figure 5. *Highly-strained and asymmetrically folded layered ultramafic-mafic tectonite in Duck Lake high-strain zone. Dark layers are composed of actinolite schist and pale layers are plagioclase-rich. Steep cliff section looking west. (GSC 1997-62Z)*

Figure 6. *Folded D_1 leucosomes in Milton Island metasedimentary rocks (i.e., possible Crew Lake Belt equivalent) showing thin biotite selvages; eastern tip of Milton Island. Knife is 20 cm long. (GSC 1997-62J)*

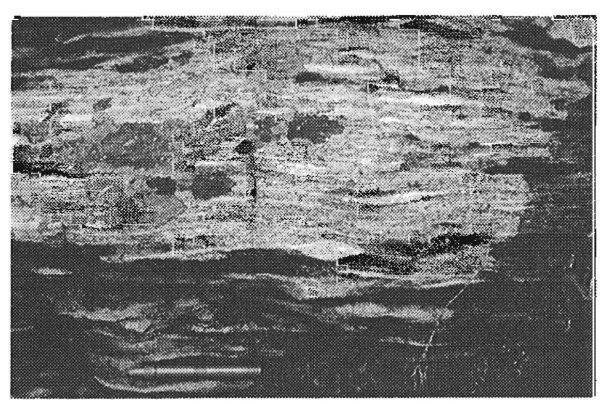

Figure 7. *Highly strained polymictic conglomerate on island about 1 km west of Reynolds Island Pluton. Granitoid and fine-grained feldspathic clasts (metavolcanic?) are the most visible, while more intermediate to mafic clasts of composition similar to that of the matrix are more difficult to differentiate from the matrix. (GSC 1997-62HH)*

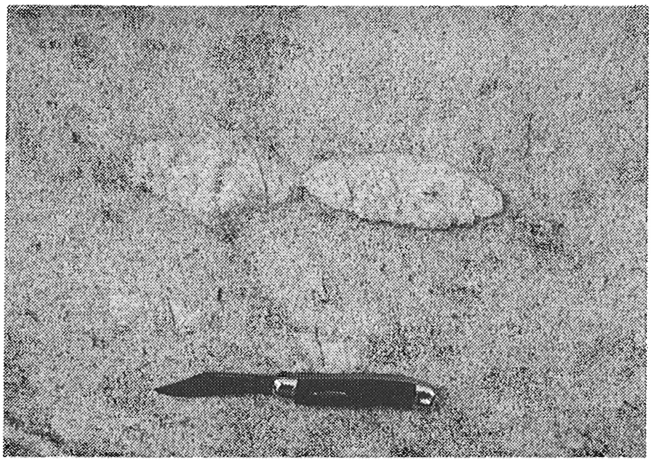

Figure 8. Fibrolite-muscovite-magnetite faserkiesel in McLennan Group arkose. (GSC 1997-62H)

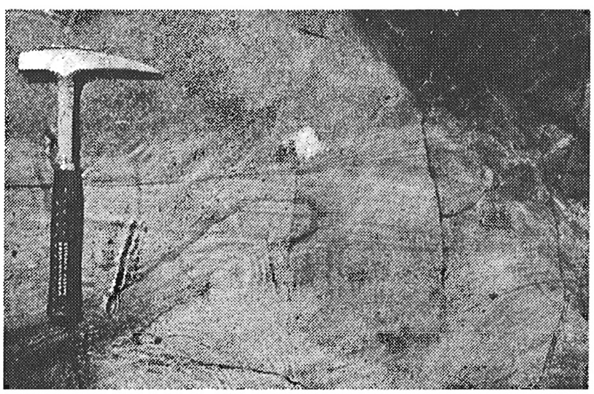

Figure 9. Crossbedded arkose, McLennan Group, Priestly Island. Photo looking south showing younging in this direction. (GSC 1997-62G)

diopside-rich bands up to 1 m thick (metapelite/calc-silicate unit; Fig. 2) and is separated from the grey arkose by a thick, low-strain zone dominated by late muscovite±garnet-bearing pegmatite.

McLENNAN GROUP TO KISSEYNEW DOMAIN TRANSITION

South of the pelite/calc-silicate unit described above lies a concordant map unit composed of garnet amphibolite that contains distinctive light green diopside-plagioclase-scapolite-rich bands and streaks. Garnets are generally rimmed by, or more commonly replaced by, plagioclase, suggesting postmetamorphic peak decompression. This unit is structurally underlain along most of its length by ferruginous metapsammite and locally by diopside-bearing marble. The ferruginous metasedimentary rocks are rusty and friable, and contain massive sulphide horizons up to 20 cm thick, consisting predominantly of pyrrhotite with minor pyrite. The amphibolite layer has been interpreted as marking the northern boundary of the Kisseynew Domain and hence of the northernmost extent of the Burntwood Suite (Johnston and Thomas, 1984). However, in the map area, it is juxtaposed to the south with more of the pelite/calc-silicate unit, which is itself flanked to the south by a pink faserkiesel-bearing arkose unit that is identical to the one mapped further north along Wapus Bay and Priestly Island (Fig. 2). These observations suggest that the amphibolite/calc-silicate unit does not represent the transition into a new unit, but forms an integral part of the McLennan Group, as do the rocks immediately south.

Further south, the pink arkose grades into a white massive to laminated metasedimentary unit composed of alternating quartz-rich and calc-silicate-rich bands, which is structurally underlain by a graphite-bearing biotite-rich psammitic to pelitic rock unit resembling metaturbidite. The transition between the two units occurs over about 1 km. Graphite occurs as small- to medium-sized disseminated flakes in the matrix, and as coarse-grained crystals (up to 1 cm diameter) in leucosomes and pegmatitic segregations. This unit fits descriptions of Burntwood Suite (Gilboy, 1980) and may therefore form the northernmost extent of the Kisseynew Domain (Fig. 2). Intrusive rocks in the McLennan Group consist of tectonically disrupted and folded ultramafic dykes, elongate tonalitic sheets, and pegmatite.

ROTTENSTONE DOMAIN

A large plutonic complex covering most of the northwestern part of the map area (Fig. 2) consists of an older dioritic phase cut by tonalite, granodiorite, granite, and aplite. All phases are medium grained and variously foliated. Some outcrops are dominated by diorite, tonalite, or granite, with tonalite forming the most abundant magmatic type. The overall appearance, however, is that of a weakly foliated to well banded orthogneiss (Fig. 10). Rare pyroxenite occurs as disrupted pods in the less mafic phases. This map unit, previously named the "Crowe Island agmatite" (Stauffer et al., 1979) and interpreted as part of the Rottenstone Domain (Johnston and Thomas, 1984), has been renamed the 'Crowe Island Complex' (Corrigan et al., 1997).

Field relationships observed on the well exposed shore of Crowe Island suggest that the dioritic phase may be contiguous with the Milton Island Pluton. Along its southeastern margin, the Crowe Island Complex hosts a large raft of strongly lineated intermediate metavolcanic tuff-breccia that resembles some of the metavolcanic rocks observed in the Reed Lake volcanic belt. Another supracrustal screen up to 1 km long is found northwest of Crowe Island. It contains a heterogeneous assemblage of sillimanite-K-feldspar-bearing pelite, grey biotite gneiss, and laminated quartzitic/calc-silicate gneiss that resemble rocks occurring at the structural top of the Central Metavolcanic Belt northeast of the Reynolds Island Pluton, near the contact with the Milton Island metasedimentary assemblage. A large raft of highly migmatitic Milton Island metasedimentary assemblage has also been observed within the Crowe Island Complex on a small island east of Crowe Island (Fig. 2). The Crowe Island Complex is thus

Figure 10. Deformed granitic veins in layered diorite-tonalite from the Crowe Island Complex, southwest of Fraser Bay. (GSC 1997-62V)

interpreted to be of an age similar to that of the Milton Island and Butler Island plutons, as it shares the same field relationships with supracrustal rocks. Consequently, rocks shown as belonging to the Rottenstone Domain on existing compilation maps seem to be higher grade equivalents of La Ronge Domain supracrustal and plutonic rocks.

DEFORMATION, METAMORPHISM, AND HIGH-STRAIN ZONES

At least four episodes of ductile deformation have been identified in the Butler Island area (Table 1). The first, D_{-1}, is restricted to supracrustal rocks of the Central Metavolcanic Belt and has been observed only in supracrustal xenoliths in the Butler Island Pluton. In contrast, we define D_1 as the first deformation event of regional scale to affect all lithological units, including those of the McLennan Group.

D_{-1} deformation

Supracrustal xenoliths are common in the Butler Island diorite. They locally show an older layer-parallel foliation (S_0=S_{-1}) that is stronger than and misoriented with respect to the fabric in the diorite. However, this early fabric is difficult

Table 1. Outline of relative chronological order of major protolith formation and tectonometamorphic events in the map area. See text for explanations.

Deformation event	Central Metavolcanic Belt	McLennan Group
D_3	Large-scale north-northeast-trending open to close upright folds; local development of low-grade cleavage	
D_2	Regional deformation coaxial to D_1; tightening of F_1 folds, crenulation of S_1 sillimanite and muscovite; development of S_2 axial-planar cleavage outlined by new growth of sillimanite and muscovite in metapelitic rocks	
	Reynolds Island Pluton and related granitic and leucotonalitic intrusions	
D_1	Folding; production of strong S_0= S_1 fabric; growth of actinolite, sillimanite, biotite, muscovite. Production of stromatic leucosomes in psammites and pelites Thrusting of CMB over McLennan Group	
	Ultramafic-mafic intrusions	
		Deposition of McLennan Group
	Butler Island diorite Milton Island diorite Crowe Island Complex	
D_{-1}	Layer-parallel schistosity	
	Volcanism and contemporaneous sedimentation; deposition of Milton Island metasedimentary rocks	

to differentiate from fabrics formed subsequently during D_1, since these later fabrics also formed parallel to S_0. Therefore, we restrict D_{-1} to those fabrics observed in xenoliths. Feldspar porphyry dykes in the Lawrence Point belt also postdate D_{-1}, as they cut the earliest fabric in metasedimentary rocks. Deposition of the McLennan Group must also have postdated D_{-1}, as neither Butler Island-type intrusions nor feldspar porphyry dykes are found within it.

D_1 deformation

The D_1 deformational event is responsible for the regionally developed S_0=S_1 foliation. Small-scale F_1 folds likely formed during this event but are not easily recognizable due to the strong and apparently coplanar D_2 overprint. Metamorphic minerals outlining S_1 seem to have formed at moderate metamorphic conditions (lower to middle amphibolite facies), as suggested by the development of leucosomes in Milton Island metasedimentary rocks (Fig. 6) and of a strong amphibolite-facies mineral lineation in the Butler Island and Milton Island plutons, as well as in supracrustal rocks of the

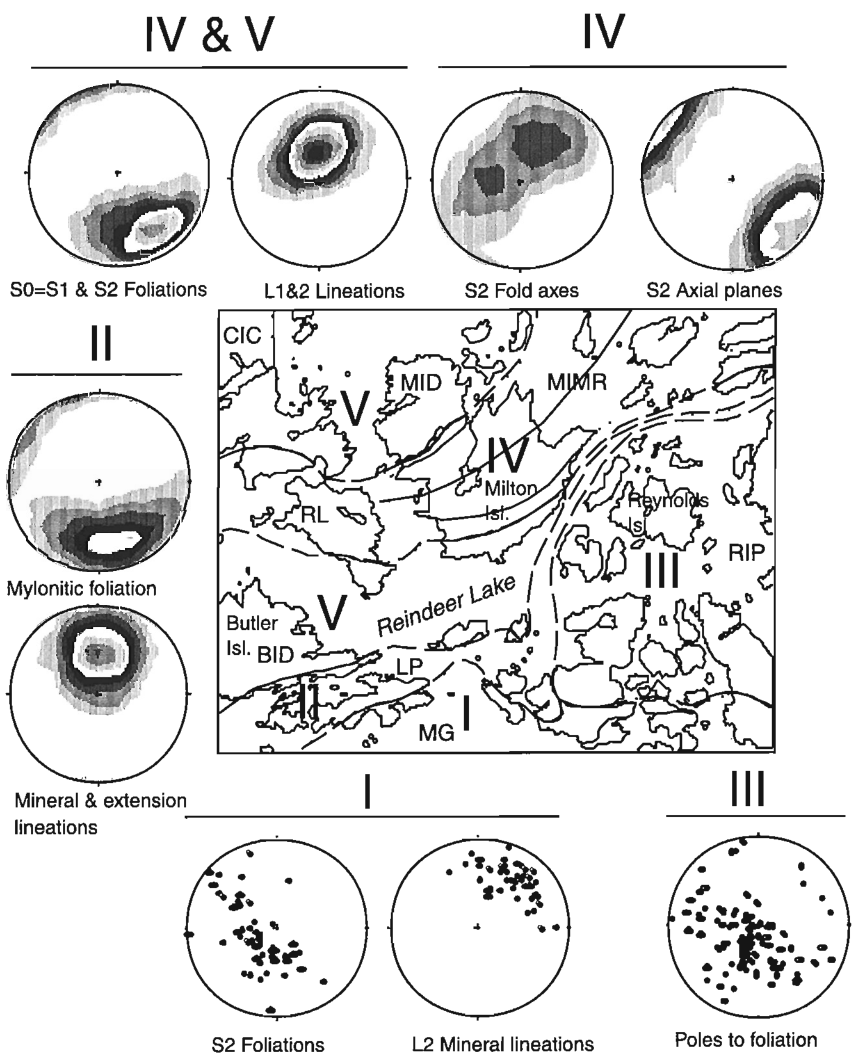

__Figure 11.__ Simplified map showing structural domains I to V and associated equal-area lower hemisphere stereographic projections of structural elements. Planar measurements are plotted as poles. See text for explanations. BID=Butler Island diorite: CIC=Crowe Island Complex: LP=Lawrence Point volcanic belt: MID=Milton Island diorite: MIMR=Milton Island metasedimentary rocks: MG=McLennan Group: RIP=Reynolds Island Pluton: RL=Reed Lake volcanic belt.

Central Metavolcanic Belt. A well developed layer-parallel fabric outlined by biotite and/or muscovite is also observed in some of the McLennan Group rocks.

During D_1, a zone of high strain, informally referred to as the Duck Lake high-strain zone (Maxeiner 1997), was localized within the base of the Central Metavolcanic Belt and in the structural top of the McLennan Group (see Fig. 4; mafic tectonite). Mineral lineations associated with this fabric are down dip (Fig. 11; group II) and are defined by high-grade metamorphic assemblages, such as hornblende and actinolite in mafic tectonites, and sillimanite in metasedimentary rocks. A widespread L>S fabric in the Butler Island and Milton Island plutons likely resulted from this deformational event, as suggested by parallelism with extension and mineral lineations developed in the shear zone and in the diorite (Fig. 11; group V). Moreover, mylonitic fabrics developed at the southern margin of the Butler Island Pluton are also parallel to those developed in the mylonitized supracrustal rocks of the Central Metavolcanic Belt, suggesting that they are contemporaneous. Unequivocal shear-sense indicators were not observed, but the old-over-young structural relationship is best explained by southward thrusting. The relative age of thrusting is constrained by the Butler Island Pluton, which was reworked along its structural base during this event, and by the Reynolds Island Pluton, which crosscuts the high-strain zone.

D_2 deformation

During D_2, S_0=S_1 fabrics were deformed into tight to isoclinal, northerly dipping, recumbent folds. The trend and plunge of F_2 fold axes in the Milton Island metasedimentary assemblage form a scatter of points from the northeast to the southwest quadrants (Fig. 11; group IV) on a stereonet. This suggests that F_2 folds were noncylindrical to begin with, or that they were refolded during F_3, or both. Mineral lineations in the same structural domain are parallel to fold axes and follow a similar path. S_2 axial-planar surfaces are subparallel to the long limbs of tight to isoclinal folds, generally dip northwest (Fig. 11; groups IV and V), and are particularly well developed in the core of a regional F_2 fold within the Milton Island metasedimentary assemblage (Fig. 2). Some high-grade metamorphic minerals are parallel to S_1, but a second generation is axial planar to F_2 folds and define the main S_2 foliation. Thus, metamorphic conditions during D_2 were possibly as high as those during D_1. In McLennan Group arkose, muscovite-fibrolite faserkiesel knots are common and grow slightly oblique to the S_0=S_1 plane along the long limbs of folds, and parallel to the S_2 axial-planar cleavage in fold hinges. S_2 surfaces wrap around the Reynolds Island Pluton, which may have behaved as a rigid buttress during D_2. This structural relationship also infers that the Reynolds Island Pluton predates D_2.

A few high-strain zones plain 100 m thick have been mapped within the metasedimentary rocks of the McLennan Group and at the base of an tonalite sheet that intrudes these rocks. Shear-sense indicators at different locations show either transtensional (oblique dextral) or transpressional (oblique sinistral) displacement, suggesting that both types of movement may have occurred at different times along the same system of shear zones. Some high-strain zones accommodated intense flattening strain, as suggested by the near-coaxial folding of pegmatite veins (Fig. 12). These shear zones transposed fabrics developed during D_1, and must therefore postdate that event. They are oriented parallel to the S_2 foliation and to the axial plane of F_2 folds, suggesting that they were developed during D_2. However, the random orientation of metamorphic minerals within some shear planes suggests that peak temperature conditions outlasted D_2 deformation.

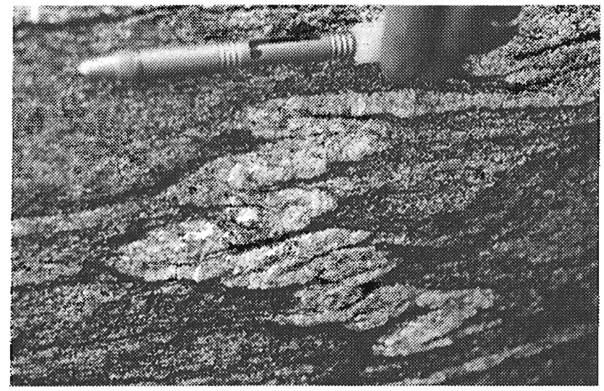

Figure 12. *Symmetrical tight folds outlined by pegmatite in tonalite intruding McLennan Group metasedimentary rocks, Levesque Bay. (GSC 1997-70C)*

D_3 deformation

A third deformational event (D_3) folded earlier structures about gently northeast-plunging axes, forming map-scale open folds. In the McLennan Group, plots of poles of S_2 foliations on a stereographic projection show a wide dispersion along a great circle with a pole plunging shallowly to the north-northeast, which is compatible with the observation on the geological map and in the field of large-scale upright open folds trending approximately NNE (Fig. 11; group I). F_3 folding postdates the emplacement of the Reynolds Island Pluton, as shown by the tightening of structures around the pluton during F_3, and the development of north-northeast-striking and steeply dipping crenulation cleavages defined by new growth of muscovite and chlorite in folded rocks adjacent to the pluton.

DISCUSSION

Understanding the tectonic history of the northwestern Reindeer Zone hinges on the recognition of distinct lithotectonic packages, the nature of their mutual boundaries, their ages, and their deformation histories compared to absolute and relative ages of igneous events. Our observations support the suggestion that the Crew Lake Belt grades into part of the Rottenstone Domain, proposed by Lewry et al. (1990 and references therein). Thus, the La Ronge Domain may extend further northeast and potentially form part of the accreted margin into which the Wathaman Batholith was emplaced. The apparent increase in metamorphic grade towards the northwest suggests that tectonic exhumation was greater in that direction, consistent with southward thrusting.

Mapping in 1997 has shown that polymictic conglomerate, which forms the stratigraphic base of the McLennan Group, grades into progressively more arkosic, pelitic, and calc-silicic protoliths towards the south, suggesting deepening of a sedimentary basin in that direction. It also implies that the McLennan Group stratigraphy is inverted below the leading edge of the Central Metavolcanic Belt. The different lithofacies observed in the McLennan Group match descriptions of the Sickle Group in Manitoba (Zwanzig, 1990) and support the contention that they are equivalent (e.g., Lewry et al., 1990). Graphitic metasedimentary rocks in the southern part of the map area match descriptions of the Burntwood Suite, also found in Manitoba, suggesting that they may also be equivalent. Preliminary field observations suggest that the transition between the McLennan Group and Kisseynew Domain is mainly a facies change and no first-order structural break exists between McLennan/Sickle groups and Burntwood Suite, although the overall sequence is imbricated by D_2 faults. Thus, the age of the Sickle Group is likely similar to that of the McLennan Group and possibly that of the Kisseynew Domain (Burntwood Group) (see Ansdell and Yang, 1995). This model suggests that the McLennan Group represents fluvial to littoral sediments deposited in the Central Metavolcanic Belt during opening of the Kisseynew Basin, and that lithological and temporal equivalents may exist along the southeast margin of the Kisseynew Domain, in the Flin Flon and Glennie domains (i.e., Missi Group; cf. Ansdell et al., 1995).

In order to test the above observations and models, we have undertaken systematic sampling of plutons, metasedimentary and metavolcanic rocks, and pegmatite and feldspar porphyry dykes that could constrain the age of magmatism, sedimentation, deformation, and metamorphism throughout the Reindeer Lake transect. We have also sampled metamorphic rocks in order to evaluate quantitative pressure and temperature conditions of metamorphism across the transect. Geochemical and tracer isotope studies will also be initiated on selected plutons and pegmatite dykes in order to provide constraints on the tectonomagmatic environment and the nature of the lower crust underneath the northwestern Reindeer Zone.

ACKNOWLEDGMENTS

The capable and cheerful assistance provided by Mojgan Adibpour and Gillian Royle is gratefully acknowledged. The crew at Osprey Wings, Missinipe, provided excellent air service. Visits in the field, observations, and discussions with Dave MacDougall, Tom Sibbald, Bruno Lafrance (SEM), and Kevin Ansdell (University of Saskatchewan) were greatly appreciated. Review by Marc St-Onge resulted in significant improvements to the paper.

REFERENCES

Ansdell, K.M. and Yang, H.
1995: Detrital zircons in the McLennan Group meta-arkoses and MacLean Lake Belt, western Trans-Hudson Orogen; in Report of 1995 Trans-Hudson Orogen Transect Meeting, (ed.) Z. Hajnal and J. Lewry; Lithoprobe Report no. 48, p.190-197.

Ansdell, K.M., Lucas, S.B., Connors, K., and Stern, R.A.
1995: Kisseynew metasedimentary gneiss belt, Trans-Hudson orogen (Canada): Back-arc origin and collision inversion; Geology, v. 23, p. 1039-1043.

Bickford, M.E., Van Schmus, W.R., Macdonald, R., Lewry, J.F., and Pearson, J.G.
1986: U-Pb zircon geochronology project for the Trans-Hudson: Current sampling and recent results; in Summary of Investigations 1986; Saskatchewan Geological Survey, Saskatchewan Energy and Mines, Miscellaneous Report 86-4, p. 101-107.

Corrigan D., Bashforth, A., and Lucas, S.
1997: Geology and structural evolution of the La Ronge-Lynn Lake Belt in the Butler Island area (parts of 64D/9 and 64D/10), Reindeer Lake; in Summary of Investigations 1997; Saskatchewan Geological Survey, Saskatchewan Energy and Mines, Miscellaneous Report 97-4.

David, J., Bailes, A.H., and Machado, N.
1996: Evolution of the Snow Lake portion of the Paleoproterozoic Flin Flon and Kisseynew belts, Trans-Hudson Orogen, Manitoba, Canada; Precambrian Research, v. 80, p. 107-124.

Gilboy, C.F.
1980: Geology of the Reindeer Lake south (southeast) area (NTS area 64D-SE); Saskatchewan Department of Mineral Resources, Report 198, 62 p.

Harper, C.T.
1986: Bedrock geological mapping, Windrum Lake area (part of NTS 64D-4, 73P-16 and 74A-1); in Summary of Investigations 1986; Saskatchewan Geological Survey, Saskatchewan Energy and Mines, Miscellaneous Report 86-4, p. 8-17.

Johnston, W.G.Q. and Thomas, M.W.
1984: Compilation bedrock geology series, Reindeer Lake south, NTS area 64D; Saskatchewan Energy and Mines, Report 230, 1:250 000 scale map with marginal notes.

Lewry, J.F., Thomas, D.J., MacDonald, R., and Chiarenzelli, J.
1990: Structural relations in accreted terranes of the Trans-Hudson Orogen, Saskatchewan: telescoping in a collisional regime?; in The Early Proterozoic Trans-Hudson Orogen of North America, (ed.) J.F. Lewry and M.R. Stauffer; Geological Association of Canada, Special Paper 37, p. 75-94.

Lucas, S.B., Stern, R.A., Syme, E.C., Reilly, B.A., and Thomas, D.J.
1996: Intraoceanic tectonics and the development of continental crust: 1.92–1.84 Ga evolution of the Flin Flon Belt, Canada; Geological Society of America Bulletin, v. 108, p. 602-629.

Maxeiner, R.O.,
1997: Geology of the Lawrence Bay (Reindeer Lake) area, northern La Ronge Domain; in Summary of Investigations 1997; Saskatchewan Geological Survey, Saskatchewan Energy and Mines, Miscellaneous Report 97-4.

Maxeiner, R.O. and Sibbald, T.I.I.
1995: Controversial rocks in the Hebden-MacKay lakes area, southern La Ronge Domain; in Summary of Investigations 1995; Saskatchewan Geological Survey, Saskatchewan Energy and Mines, Miscellaneous Report 95-4, p. 79-86.

Sibbald, T.I.I.
1977: The geology of the Milton Island area (west half); Saskatchewan Department of Mineral Resources, Report 153, 38 p.

Stauffer, M.R., Langford, F.F., Coleman, L.C., and Mossman, D.J.
1979: Geology of the area around Amiskit Island, Reindeer Lake (part of NTS area 64D-N.E.); Saskatchewan Department of Mineral Resources, Report 191, 21 p.

Stern, R.A., Lucas, S.B., Syme, E.C., Bailes, A.H., Thomas, D.J., Leclair, A.D., and Hulbert, L.
1993: Geochronological studies in the NATMAP Shield Margin Project area, Flin Flon Domain: Results for 1992 (1993); in Radiogenic Age and Isotopic Studies Report 7; Geological Survey of Canada, Paper 93-2, p. 59-70.

Thomas, D.J.
1993: Geology of the Star Lake-Otter Lake portion of the Central Metavolcanic Belt, La Ronge Domain; Saskatchewan Energy and Mines, Report 236, 132 p.

Thomas, D.J., , Watters, B.R., and Harper, C.T.
1987: The character of early Proterozoic plutonism in the Central Metavolcanic Belt, northern Saskatchewan; Geological Association of Canada/Mineralogical Association of Canada, Joint Annual Meeting, Saskatoon, Program with Abstracts, v. 12, p. 95.

Watters, B.R. and Pearce, J.A.
1987: Metavolcanic rocks of the La Ronge belt in the Churchill Province, Saskatchewan: Geochemical evidence for a volcanic arc origin; in Geochemistry and Mineralization of Proterozoic Volcanic Suites, Geological Society of London, Special Publication 33, p. 67-182.

Zwanzig, H.V.
1990: Kisseynew Gneiss Belt in Manitoba: stratigraphy, structure, and tectonic evolution; in The Early Proterozoic Trans-Hudson Orogen of North America, (ed.) J.F. Lewry and M.R. Stauffer; Geological Association of Canada, Special Paper 37, p. 95-120.

Geological Survey of Canada Project 910035

Some notes on the assemblage boundaries and internal structure of the Uchi-Confederation greenstone belt, northwestern Ontario[1]

C.R. van Staal
Continental Geoscience Division

van Staal, C.R., 1998: Some notes on the assemblage boundaries and internal structure of the Uchi-Confederation greenstone belt, northwestern Ontario; in Current Research 1998-C; Geological Survey of Canada, p. 107-114.

Abstract: The Uchi-Confederation greenstone belt, which spans at least 220 million years of Archean evolution (2960-2740 Ma), comprises three distinct lithotectonic assemblages: Balmer, Woman and Confederation, the amalgamation and orogenic history of which are not well understood. All three assemblages have been affected by at least two distinct phases of ductile deformation (D_1 and D_2). F_1 structures were at least in part overturned folds, because the younger, moderately to steeply plunging F_2 structures are locally downward facing. Tight, regional folds defined on the basis of younging reversals and trending (sub)parallel to the assemblage boundaries may be F_1 structures. None of the assemblage boundaries, however, is characterized by a continuous D_1 high-strain zone and no evidence for D_1-related accretionary structures (e.g. thrusts) near the assemblage boundaries has been found so far.

The Woman-Confederation assemblage boundary is characterized by a narrow, late syn- to post-D_2 sinistral shear zone.

Résumé : La zone de roches vertes d'Uchi-Confederation, qui couvre au moins 220 millions d'années d'évolution archéenne (2 960-2 740 Ma), comprend trois assemblages lithotectoniques distincts, ceux de Balmer, de Woman et de Confederation, dont la formation et l'évolution orogénique sont mal comprises. Les trois assemblages ont subi au moins deux phases distinctes de déformation ductile (D_1 et D_2). Les plis P_1 étaient au moins en partie déversés, car les plis P_2, plus jeunes, plongent modérément à fortement et, localement, font face vers le bas. Des plis régionaux serrés, définis selon l'observation de séquences en position renversée et le parallélisme (ou quasi-parallélisme) entre l'orientation des plis et les limites entre les assemblages, sont peut-être associés à P_1. Toutefois, aucune des limites entre les assemblages n'est caractérisée par la présence d'une zone à forte déformation continue D_1 et l'on n'a pas encore trouvé d'indices de structures d'accrétion (par ex. des chevauchements) liées à D_1 près de ces mêmes limites.

La limite entre les assemblages de Woman et de Confederation est marquée par la présence d'une étroite zone de cisaillement senestre, associée à l'intervalle entre la fin de D_2 et le début de la déformation postérieure à D_2.

[1] Contribution to the Western Superior NATMAP Project

INTRODUCTION

This paper reports on a three-week reconaissance study of the Uchi-Confederation greenstone belt of northwestern Ontario (Figs. 1, 2) to investigate whether this region is suitable for detailed structural analysis. This project, which forms part of the Western Superior NATMAP Project, was originally proposed by P.C. Thurston of the Ontario Geological Survey to better understand the assembly and orogenic history of the three distinct lithotectonic assemblages: Balmer (ca. 2960 Ma), Woman (ca. 2840 Ma), and Confederation (ca. 2740 Ma; Nunes and Thurston, 1980; Wallace et al., 1986) that make up this greenstone belt. The nature and timing of interaction between these three assemblages, which are separated from each other by large time intervals, has a direct bearing on the tectonic history of the Uchi Subprovince and the western Superior Province in general (Stott and Corfu, 1991), a theme central to the Western Superior NATMAP Project. Another problem is that recent U-Pb age determinations of silicic volcanic rocks in the eastern part of the greenstone belt (2739-2735 Ma; Noble,1989) have shown that the simple synclinal geometry of Goodwin (1967), Pryslak (1970), Thurston and Fryer (1983), and Thurston (1985) is not viable in that none of the older assemblages seem to occur east of the proposed synclinal axis (Fig. 2).

TECTONIC ASSEMBLAGES

Goodwin (1967), Pryslak (1970, 1971a,b), Thurston (1985) and Thurston and Fryer (1983) recognized three distinct, homoclinal volcanic cycles in the Uchi-Confederation greenstone belt, each with basal basalts overlain by intermediate and felsic volcanic rocks towards the top. Stott and Corfu (1991) subsequently reinterpreted the cycles as lithotectonic assemblages, although they recognized that the boundary between the Balmer and Woman assemblages is not a fault, but a tectonized disconformity.

Balmer assemblage

The Balmer assemblage (equivalent to cycle 1 of Thurston and Fryer, 1983) occurs adjacent to the Trout Lake batholith, which is dominated in the map area by foliated tonalites and granodiorites of the Narrow Lake phase (ca. 2838 Ma, Noble, 1989). The Narrow Lake phase intrudes the Balmer assemblage along its eastern boundary (Noble, 1989), indicating that this assemblage is older than 2838 Ma.

The Balmer assemblage mainly consists of pillowed and massive, locally amygdular flows, commonly interlayered with narrow diabase and gabbroic sills. Pillow facing

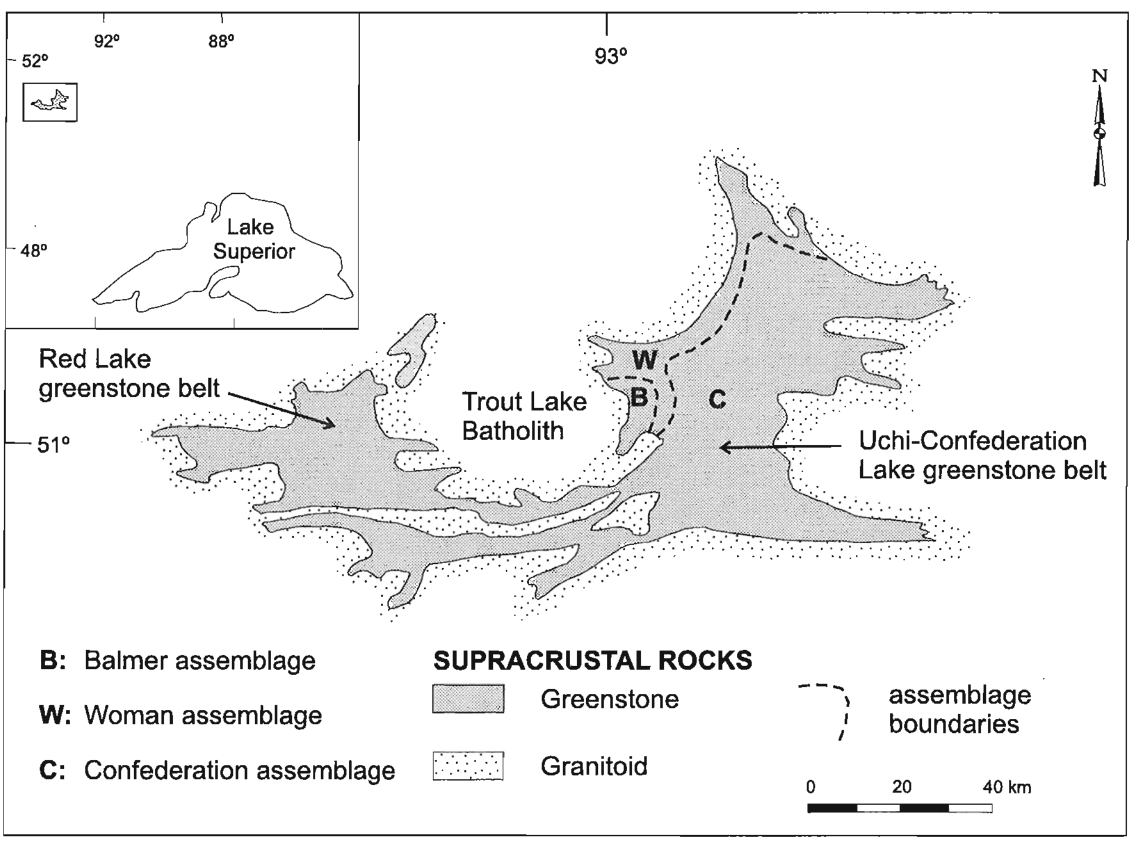

__Figure 1.__ Simplified outline of the Uchi-Confederation greenstone belt with its assemblage boundaries, Trout Lake Batholith and its continuation into the Red Lake greenstone belt (modified from Ontario Geological Survey, 1992).

directions were observed neither by Pryslak (1971a,b) or the present author; hence the internal facing direction of the Balmer assemblage is unknown in this area. Fragmental basalts occur near the eastern boundary with the Woman assemblage and are in turn capped by andesitic to dacitic (Thurston and Fryer, 1983), graded lapilli tuff and/or tuffaceous sandstone, containing crystal and pumaceous fragments. The volcaniclastic rocks young consistently towards the Woman assemblage, although bedding is commonly overturned (Fig. 2). A narrow sheet of moderate to highly strained quartz-feldspar-phyric or aphyric dacite/rhyolite locally marks the top of the Balmer assemblage and thus the boundary with the adjacent Woman assemblage. Near the east end of the southernmost part of Narrow Lake (Fig. 2), this felsite is altered to a highly foliated sericite schist and is associated with banded iron formation and sulphide-bearing graphitic argillite. Further west on Narrow Lake, the top of the Balmer assemblage is marked by highly strained pillow basalt interlayered with calcareous material.

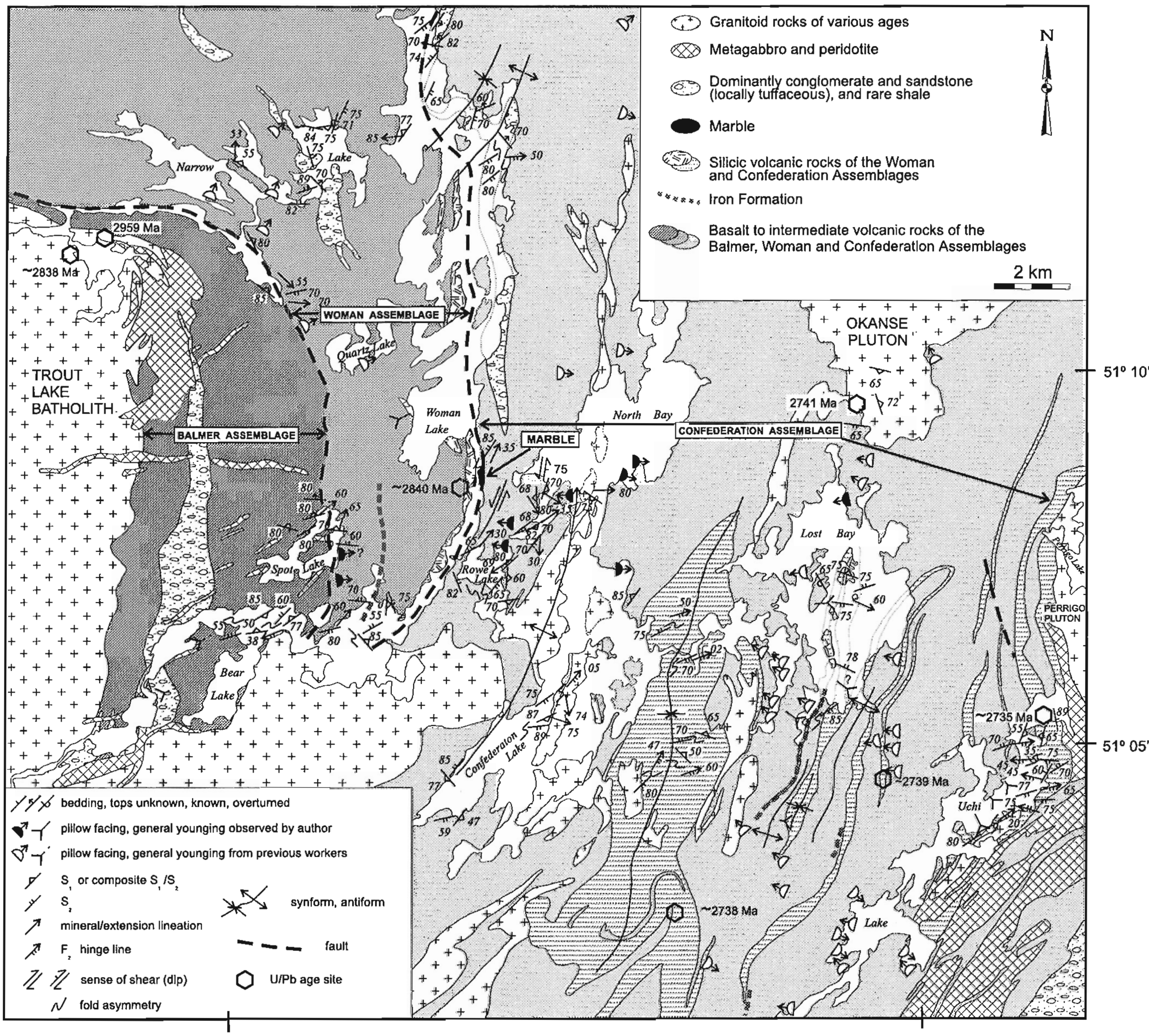

Figure 2. Geology of the Uchi-Confederation greenstone belt, modified from Pryslak (1971a,b) and Thurston (1980b, 1985) with additions by the author. Stippled boundaries represent inferred structural continuity of important units beneath the lakes.

The age of the Balmer assemblage was determined from a sample of a small unit of felsic lithic tuff, which anomalously occurs at the base of the assemblage near or at the contact with the Trout Lake batholith (Thurston, pers. comm., 1997). This tuff has yielded a U-Pb zircon age of ca. 2959 Ma (Nunes and Thurston, 1980). The author was unable to find this rock, but Schwerdtner (written comm., 1997) found a narrow zone of mylonitic quartz-phyric rock along the contact between the batholith and the Balmer assemblage a bit further to the west of the supposed sample locality. The contact relationships between the Balmer basalts and the dated felsic tuff are at present not well understood and hence the age of the Balmer basalts is uncertain.

The basalts of the Balmer assemblage typically are characterized by low high field strength (HFS) contents (Zr/Y<2, TiO_2< 0.76; Thurston and Fryer, 1983), whereas the Woman Lake assemblage basalts generally have slightly higher Zr/Y ratios (Zr/Y>2 and TiO_2>0.8) contents (in part based on unpublished analyses of K. Tomlinson).

Woman assemblage

The Woman assemblage (equivalent to cycle 2 of Thurston and Fryer, 1983) also shows a mafic to felsic cycle represented by mainly pillowed basalt flows and breccias, through intermediate, mainly fragmental volcanic and sedimentary rocks to rhyolitic ignimbrite (Thurston, 1980a), which is locally capped by stromatolitic marble. Rhyolite near the top of the assemblage has yielded a U-Pb age of ca. 2840 Ma (Wallace et al., 1986). Pillow facing directions have been observed in many locations (Thurston, 1985 and this paper) and together with the grading in tuffaceous rocks indicate an overall eastward younging direction (Fig. 2).

Confederation assemblage

The Confederation assemblage (equivalent to cycle 3 of Thurston and Fryer, 1983) is the unit studied most extensively during the summer of 1997. The internal stratigraphy is not a simple mafic to felsic cycle, as was originally proposed by Thurston and Fryer (1983). The 2739-2735 Ma U-Pb zircon dates of Noble (1989) on silicic volcanic rocks, combined

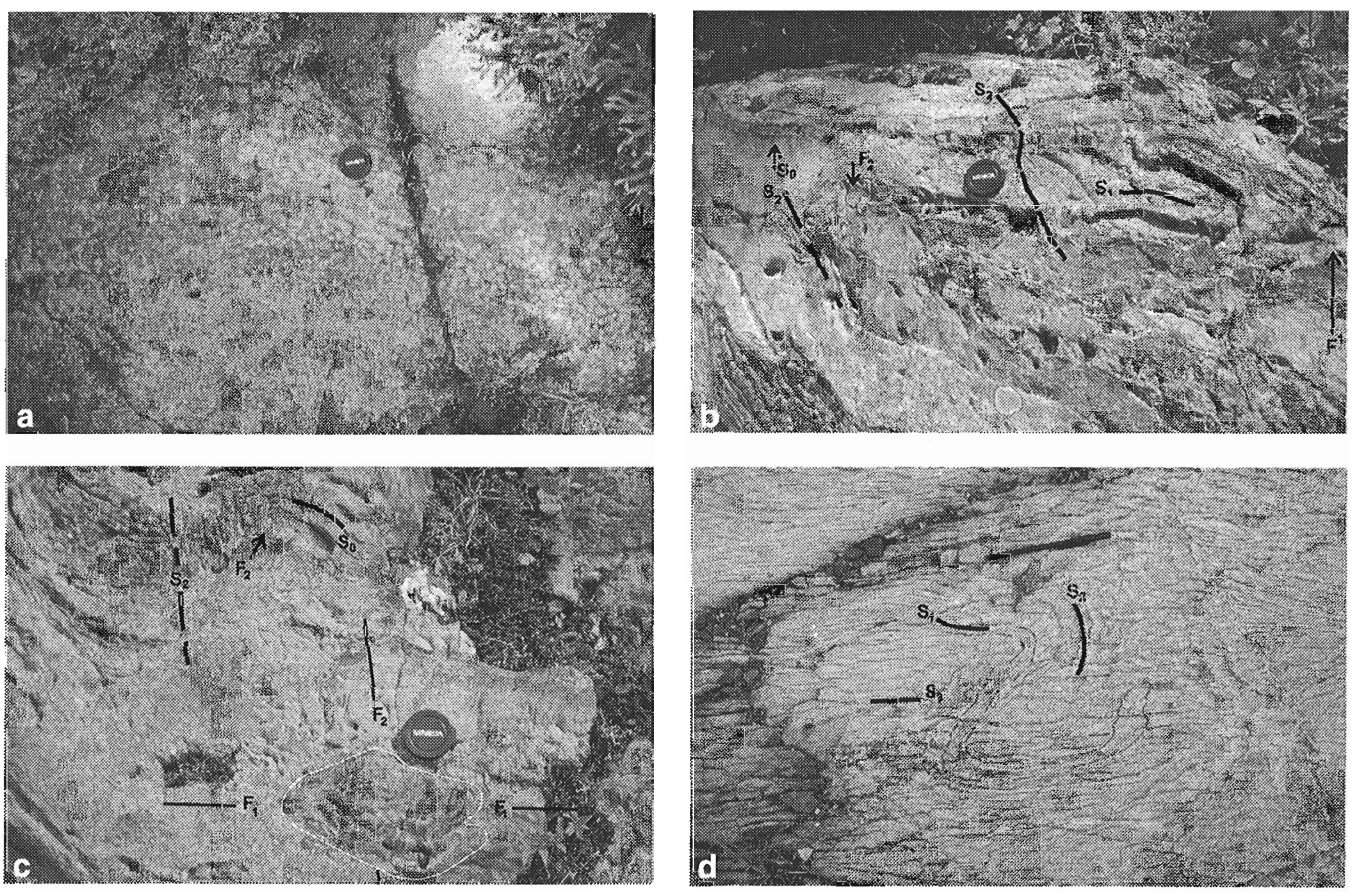

Figure 3. *a) Graded varioles in Confederation basalt; **b)** Z-shaped F_1 folds overprinted by S-shaped F_2 structures; **c)** Domal F_1 structure (highlighted in white) in the hinge area of a S-shaped F_2 fold. Trend of F_1 axial surface is at a high angle to F_2 axial surface; **d)** Three foliations (S_1, S_2, S_3 differentiated layerings) in strongly deformed felsic volcanic rocks near the South Bay massive sulphide deposit. A F_2 fold in S_1 is highlighted in black.*

with the present fieldwork, indicate a more complex stratigraphy, regardless of whether there is macroscopic folding or not (see below). The Confederation mafic rocks are characterized by a relatively high proportion of variolitic basalts. The varioles are locally graded (Fig. 3a). Pillow facing directions in adjacent outcrops suggest that the coarsest varioles occur at the top of flows, presumably due to coalescence of smaller varioles. The mafic rocks locally include sheeted dikes and trondhjemitic bodies.

Sedimentary rocks

Each of the three assemblages contains a separate unit of sedimentary rocks. The sedimentary units resemble one another lithologically and mainly consist of immature volcaniclastic, locally tuffaceous sandstones and conglomerates, related to emergence of volcanic edifices, either before or after amalgamation of the assemblages.

The conglomerate and sandstone in the Confederation assemblage near or at the Woman-Confederation boundary contain pumice, ignimbrite, basalt, vein quartz, and shale-chip pebbles and crystal fragments, possibly derived from the Balmer and/or Woman assemblages. Interlayered felsic tuffaceous beds suggest that these sediments were deposited coeval with silicic volcanism. A similar observation was made at Uchi Lake, where silicic volcanic rocks (ca. 2735 Ma, Noble, 1989) and minor basalts are interlayered with the sedimentary rocks.

STRUCTURAL HISTORY

The lack of small-scale markers (e.g. bedding) in the volcanic rocks hinders detailed structural analysis of the Uchi-Confederation greenstone belt. Future studies may have to rely on careful mapping of volcanic marker units. Deformation is markedly heterogeneous at all scales, but evidence for at least two foliations (S_1 and S_2), is preserved in most units (Fig. 2). Locally there is evidence for three generations of ductile structures (Fig. 3d). The two main foliations (S_1 and S_2) generally are subparallel, and in places of moderate to high strain, commonly form a composite cleavage (Fig. 4). Overprinting relationships between the two foliations are rarely preserved, particularly since refraction of S_2 on S_1 has been observed, which shows that apparent crenulation of one cleavage by another is not always a reliable criterion of their relative age (van Staal and Williams,1984). Overprinting relationships between associated folds in sedimentary and locally also volcanic rocks (Figs. 3b,c), confirm that S_1 and S_2 represent two different generations of structures, rather than a regional-scale S-C fabric. Where present, syntectonic quartz veins were used to separate S_1 and S_2 in the volcanic rocks, e.g., quartz veins that cut across S_1 but are folded by F_2. Small-scale F_1 folds are tight to isoclinal, steeply inclined structures, generally with shallow to moderate plunges (Fig. 3b). Steeply plunging hinge lines are rare. Where F_1 structures are overprinted by F_2 folds, F_1 folds are markedly non-cylindrical (Fig. 3c). Whether this is an original feature of F_1 folds, a result of F_2 overprint, or a combination of both is not clear at present. F_2 structures are open to tight, dominantly S-shaped folds with generally moderate to steep plunges (Fig. 4). F_2 hinge lines and L_2 intersection lineations are commonly parallel to the extension lineation (Fig. 4) defined by quartz ribbons, rods, extended fragments, amygdules, varioles, phenocrysts, and alignment of amphibole. Several F_2 folds are downward-facing structures, suggesting that F_1 folds were moderately overturned, and asymmetrical prior to F_2 folding. Not enough structural data is available at present to determine whether there is a consistent sense of overturning of F_1 structures.

Balmer-Woman assemblage boundary

The boundary between the Balmer and Woman assemblages is well outlined by a strong magnetic anomaly on aeromagnetic maps of the Ontario Geological Survey (Ontario Geological Survey, 1991a,b). The anomalies are presumably caused by iron formation interlayered with the Woman basalts. Iron formation, together with graphitic argillite, is exposed along this boundary at the southeasternmost shore of Narrow Lake. The position of the magnetic anomaly leaves no doubt that the enveloping surface of the Balmer-Woman boundary as interpreted by the Ontario Geological Survey geologists (Ontario Geological Survey, 1992) is basically correct. This observation is important, as all foliations and bedding in the Balmer rocks near Spot Lake and in several other places have an orientation at a high angle to this boundary, a relationship observed earlier by Crews and Schwerdtner (1997). The orientation of bedding and foliations at a high angle with respect to the enveloping surface, combined with the information on aeromagnetic maps, suggest the presence of numerous small tight, east-northeast-trending F_2 folds. The strike of S_2 shows some variation across the study area (Fig. 4), which may be due to fanning, deflection by shear zones, and/or overprinting by younger (D_3?) deformation. The significance of the latter deformation is poorly understood at present, but the presence of rare D_3 structures suggests that it is only of local significance. Significantly, S_2 appears to maintain its east to northeast strike, irrespective of whether the Woman and Balmer assemblages trend north-south or east-west; hence the relationship between S_2 and the enveloping surface to layering changes respectively from a high to a low angle. If these preliminary relationships are confirmed by further structural mapping, it suggests that the eastern part of the Trout Lake batholith and most of the study area (Fig. 1,2) is situated in the hinge area of a large, slightly S-shaped F_2 structure, which continues to the north. Consistent with such a geometry is a large S-shaped F_2 fold outlined by a band of sedimentary rocks that occurs immediately northeast of the Woman-Confederation boundary (Fig. 2). The Balmer-Woman boundary thus cannot have accommodated any significant differential translation between these two assemblages during D_2. D_1 high-strain zones not been observed at Spot Lake, suggesting that the Balmer-Woman boundary was not a structural dislocation during D_1. Phyllonites along this boundary at Narrow Lake suggest some movement here, but this appears to be of only local significance. Furthermore, the Balmer-Woman boundary is also cut at high angle by several gabbro sheets

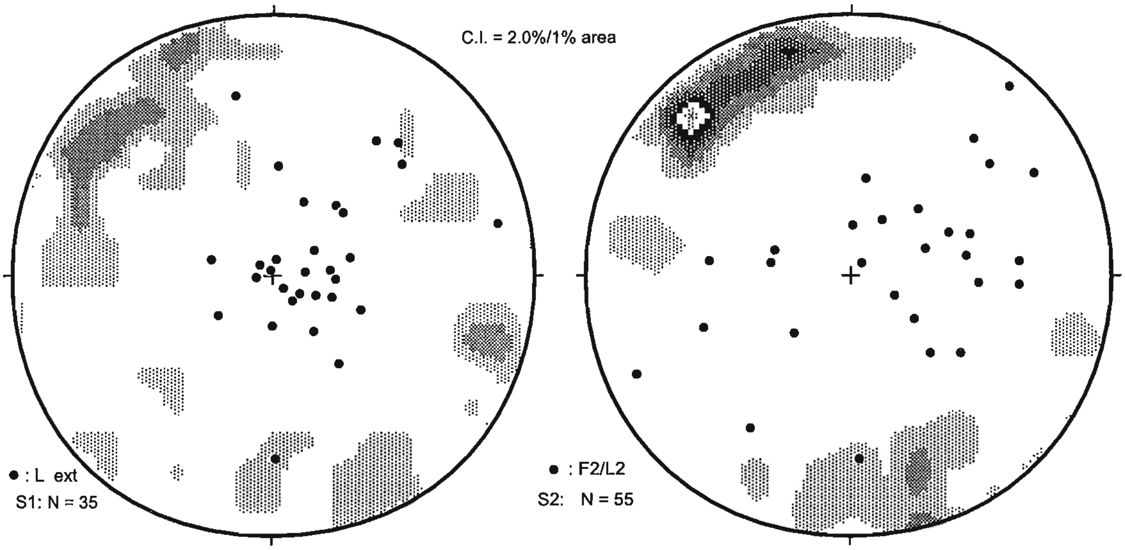

Figure 4. Lower hemisphere equal-area projections of the main structural elements.

(Pryslak, 1971a, Crews and Schwerdtner, 1997). These gabbro sheets are locally leucocratic and pegmatitic (and hence sampled for radiometric dating) and cut across the strike of the whole Balmer assemblage (Fig. 2), although they are locally deformed and metamorphosed. They are less abundant or absent in the adjacent Woman assemblage (Pryslak 1971a). In the Woman assemblage, gabbros are generally parallel to the strike of the internal units, suggesting that the 'cross' gabbros in the Balmer are feeders to the Woman basalts and gabbro sills. Such a relationship would support the interpretation of Stott and Corfu (1991) that the Woman assemblage disconformably overlies the Balmer assemblage.

Structure of the Woman assemblage and Woman-Confederation boundary

Younging indicators in the Woman assemblage indicate an overall eastward younging direction (Fig. 2), despite the presence of small-scale folds (Fig. 2) and one or two well developed foliations. The first foliation is subparallel to layering or unit boundaries in the volcanic rocks, which suggests that the angle between layering and the enveloping surface to any existing large-scale F_1 folds in the volcanic rocks must be very small, i.e. such folds are asymmetrical. This is consistent with the characteristics of observed small-scale F_1 folds. The re-occurrence of Woman pillow basalts east of the intermediate volcanics in the northern part of Woman Lake (immediately north of map in Fig. 2) suggest that map-scale F_1 folds may occur within the Woman assemblage.

The Woman-Confederation assemblage boundary is best exposed in Woman Lake Narrows (Fig. 2). At the contact there is a narrow zone (<50m) of marble mylonite with numerous isolated hinges of attenuated S-shaped F_2 folds and shallowly north-plunging extension lineations. Individual folds in fold trains locally become progressively tighter along the curviplanar axial surface of the folds, such that the sense of rotation of S_2 suggests sinistral transcurrent ductile shear along this boundary, accompanied by a slight west-side-up vertical component. Shear bands and abundant brittle-ductile Riedel shears in a narrow (<50 m) mylonite zone developed in Confederation silicic volcanic rocks along the western shoreline of Rowe Lake (~500 m east of the assemblage boundary) also indicate mainly sinistral transcurrent shear, which appears to have continued from the ductile into the brittle field. Sinistral shear thus probably took place late syn- to post-D_2 folding and foliation formation. Crews and Schwerdtner (1997) also deduced sinistral shear along this boundary, although their movement picture is more complex, based on the assumption that sinistral shear indicators and the L-S fabric elements in the rocks outside the assemblage boundary zone formed contemporaneously. Particularly important to testing their hypothesis is the relative age of the extension/mineral lineations.

Internal geometry of the Confederation assemblage

Younging indicators in volcanic and sedimentary rocks show that the the Confederation assemblage is not one simple mafic to felsic cycle. Along the south shore of Lost Bay, basalt and intermediate pyroclastic and epiclastic rocks are overlain by a thin, but extensive layer of banded iron formation interlayered with graded, silicic epiclastic sedimentary rocks. The latter may be the stratigraphic equivalent of silicic pyroclastic and graded epiclastic rocks that occur along strike of the iron formation to the north on islands in Lost Bay (Fig. 2). This mafic to felsic cycle is stratigraphically overlain by little-strained, west-facing pillow basalts, including a narrow band of variolitic basaltic rocks; hence silicic volcanic rocks do not always occur at the top of the assemblage and are at least locally sandwiched between basalt units (cf. Thurston and Fryer, 1983). Thus the U-Pb ages of Noble (1989) on the silicic volcanic rocks (2739-2735 Ma, Fig. 2) also date the basalts and suggest that the whole Confederation assemblage was deposited in a few million years.

Further to the west, a syncline (South Bay syncline) cored by silicic volcanic rocks, which are host to the South Bay massive sulphide deposit, and a newly determined anticline (Confederation Lake anticline) cored by basalts, are indicated by the younging reversals (Fig. 2). Fold repetition of variolitic basalt, silicic volcanic rocks, and sedimentary rocks on the west limb of the proposed Confederation Lake anticline is consistent with this structural interpretation. The variolitic basalt is thus potentially a regional marker unit . The relative age of the South Bay syncline and Confederation Lake anticline is at present poorly constrained and requires more work. S_2 seems to cut across these structures at a low angle, which, if correct, suggests they are F_1 or as yet unrecognized, earlier structures. The relationships between S_1 and the large-scale folds are poorly understood at present, hence S_1 may also postdate formation of the large-scale folds. Repetition of silicic volcanic rocks and iron formation between Lost Bay and Uchi Lake may also be due to large-scale folds, which are tentatively outlined on Figure 2. The available younging indicators of Thurston (1980b) do not support such an interpretation. However, Thurston's (1980b) younging reversals indicate several large folds a bit further east along the western shore of Uchi Lake, suggesting that internal folding of the assemblage was widespread. More detailed mapping is necessary to understand the geometry of the Confederation assemblage.

SUMMARY AND CONCLUSIONS

This preliminary study supports earlier suggestions that the Balmer and Woman assemblages are related, i.e. the Balmer represents some kind of basement to the Woman assemblage; hence the assemblage concept needs critical re-examination in the Uchi Subprovince. Relative translation of these two assemblages with respect to one another along the Balmer-Woman boundary during D_1 or earlier cannot be ruled out, although this boundary does not coincide with a major ductile or brittle fault zone along most of its north-south contact. The apparent large age gap (ca. 120 Ma) between these two assemblages, without the presence of a major unconformity or fault, is puzzling at present. This large age difference may in part be due to inadequate dating of the Balmer assemblage, i.e it is not known at present whether the rocks dated by Nunes and Thurston (1980) are representative of the Balmer assemblage. The Balmer-Woman relationships are being investigated currently at the Geological Survey of Canada as part of the Western Superior NATMAP Project by U-Pb dating of the stitching 'cross' gabbros from Spot Lake and felsic volcanic rocks at the top of the Balmer assemblage.

The boundary between the Woman and Confederation assemblages is characterized by narrow fault zones, which mainly accommodated a late syn- to post-D_2 sinistral transcurrent motion. The original relationships between these two assemblages is therefore obscure. The presence of D_1 and D_2 structures in both assemblages suggest a linkage prior to D_2, provided D_1 in the Woman assemblage is the same event as D_1 in the Confederation assemblage. Concerning the latter, combined microstructural and radiometric age determination studies may solve this problem.

Regional-scale folds with axial surfaces trending (sub)parallel to the strike of the Uchi-Confederation greenstone belt are indicated by younging reversals in volcanic and sedimentary rocks. The relative age and exact geometry of these large-scale folds is poorly known at present. Downward-facing F_2 folds suggest that the earlier F_1 structures were overturned, at least locally, although so far no evidence for thrusting or early accretionary structures has been found. In general, understanding the D_1 and D_2 kinematics can be achieved only by detailed mapping of the geometry of the volcanic rocks in all three assemblages in conjunction with structural studies of the plutonic rocks (particularly the Trout Lake Batholith) and determining the relationship between structure and metamorphism.

ACKNOWLEDGMENTS

First of all, I am much indebted to P.C. Thurston of the Ontario Geological Survey who suggested this project and enthusiastically showed me around the Uchi-Confederation Greenstone Belt for several days, which significantly speeded up the process of becoming familiair with these Archean rocks. Field trips and discussions with F. Schwerdtner, J. Devaney and T. Skulski were helpful. K. Tomlinson provided access to her unpublished geochemical analyses of Woman assemblage basalts. The Ontario Geological Survey personnel in the Red Lake office generously provided logistical support, and the Kabeelo Lodge provided us with an excellent base camp and efficient air transportation. Last but not least, the professional field assistance by A. Lindsay is very much appreciated

Critically reviews by P.C. Thurston, W. Bleeker, J. Percival, F. Schwerdtner, and T. Skulski improved the paper.

REFERENCES

Crews, M. J. and Schwerdtner, W. M.

1997: Structural analysis at tectonic assemblage boundaries in western Confederation Lake (Birch-Uchi) Greenstone Belt, Red Lake Region, Northwest Ontario; in 1997 Lithoprobe Report, (ed) Harrap, R.M. and Helmstaedt, H.; Lithoprobe Secretariat, University of British Columbia

Goodwin, A. M.

1967: Volcanic studies in the Birch-Uchi Lakes Area of Ontario; Ontario Department of Mines, Miscellaneous Paper 6, 96p.

Noble, S. R.

1989: Geology, geochemistry and isotope geology of the Trout Lake Batholith and the Uchi-Confederation Lakes greenstone belt, northwestern Ontario, Canada; Ph. D thesis, University of Toronto, Toronto, Ontario, 288p.

Nunes, P. D. and Thurston, P.C.

1980: Two hundred and twenty million years of Archean evolution: a zircon U-Pb age stratigraphic study of the Uchi-Confederation Lakes Greenstone Belt; Canadian Journal of Earth Sciences, v. 17, p. 710-721.

Ontario Geological Survey
1991a: Airborne electromagnetic and total intensity magnetic survey, Birch-Uchi-Confederation area, Ontario Geological Survey, Map 81 626, scale 1:20 000.
1991b: Airborne electromagnetic and total intensity magnetic survey, Birch-Uchi-Confederation area, Ontario Geological Survey, Map 81 634, scale 1:20 000.
1992: Tectonic Assemblages of Ontario, west central sheet; Ontario Geological Survey, Map 2576, scale 1:1 000 000.

Pryslak, A. P.
1970: Mitchell Township, District of Kenora (Patricia Portion); Ontario Department of Mines and Northern Affairs, Preliminary Map p. 593.
1971a: Corless Township, District of Kenora (Patricia Portion); Ontario Department of Mines and Northern Affairs, Preliminary Map p. 634.
1971b: Knott Township, District of Kenora (Patricia Portion); Ontario Department of Mines and Northern Affairs, Preliminary Map p. 635.

Stott, G. M. and Corfu, F.
1991: Uchi Subprovince; in Geology of Ontario, Ontario Geological Survey, Special Volume 4, Part 1, p.145-238.

Thurston, P. C.
1980a: Subaerial volcanism in the Archean Uchi-Confederation volcanic belt; Precambrian Research, v. 12, p. 79-98.
1980b: Earngey and Birkett Townships; Ontario Geological Survey, Map 2428, scale 1:20 000.
1985: Physical volcanology and stratigraphy of the Confederation Lake area, District of Kenora (Patricia Portion); Ontario Geological Survey, Report 236, 117p.

Thurston, P. C. and Fryer, B. J.
1983: The geochemistry of repetitive cyclical volcanism from basalt through rhyolite in the Uchi-Confederation Greenstone Belt; Contributions to Mineralogy and Petrology, v. 83, p. 204-226.

Van Staal, C. R. and Williams, P. F.
1984: Structure, origin and concentration of the Brunswick no. 12 and no. 6 orebodies; Economic Geology, v. 79, p. 1669-1692.

Wallace, H., Thurston, P. C., and Corfu, F.
1986: Developments in stratigraphic correlation: Western Uchi Subprovince; in Volcanology and Mineral Deposits; Ontario Geological Survey, Miscellaneous Paper 129, p. 88-102.

Geological Survey of Canada Project 970014

Tectonostratigraphy of central Sturgeon Lake, Ontario: deposition and deformation of submarine tholeiites and emergent calc-alkaline volcano-sedimentary sequences[1]

M. Sanborn-Barrie, T. Skulski, and J.B. Whalen
Continental Geoscience Division, Ottawa

Sanborn-Barrie, M., Skulski, T., and Whalen, J.B., 1998: Tectonostratigraphy of central Sturgeon Lake, Ontario: deposition and deformation of submarine tholeiites and emergent calc-alkaline volcano-sedimentary sequences; in Current Research 1998-C; Geological Survey of Canada, p. 115-126.

Abstract: The Sturgeon Lake greenstone belt separates reworked vestiges of Mesoarchean continental basement of the central Wabigoon Subprovince (Superior Province) from 2.78-2.70 Ga submarine volcanic rocks of the western Wabigoon Subprovince to the west, and as such, may hold the key to unraveling the history of continent-ocean basin interaction. Its tectonostratigraphy may comprise quartz-rich clastic sedimentary rocks representative of ancient platformal cover; submarine, low-potassium tholeiitic basalts and thin felsic tuffs that correlate with 2.775 Ga sequences; calc-alkaline-dominated, upward-shoaling, volcano-sedimentary rocks that resemble 2.745-2.704 Ga volcanic rocks at Savant Lake and 2.735 Ga caldera deposits in the south; and post-2.718 Ga fluvial-clastic sedimentary rocks. The central part of the Sturgeon Lake belt is deformed by east-southeast-trending, moderately to shallowly plunging F_1 folds, which are locally refolded by northeast-trending, variably plunging F_2 folds. Northeast-striking high-strain zones may separate temporally distinct volcanic sequences or reflect strain localizaton across rheological boundaries.

Résumé : La ceinture de roches vertes de Sturgeon Lake sépare des vestiges remaniés du socle continental mésoarchéen de la partie centrale de la Sous-province de Wabigoon (Province du lac Supérieur) de roches volcaniques sous-marines (2,78-2,70 Ga) de la partie ouest de la sous-province, à l'ouest. À ce titre, elle constitue peut-être un élément-clé pour le dévoilement de l'histoire des interactions continent-bassin océanique. Sa tectonostratigraphie comprend notamment : des roches sédimentaires clastiques riches en quartz représentatives d'une ancienne couverture de plate-forme; des basaltes tholéiitiques à faible teneur en sodium et de minces tufs felsiques d'origine sous-marine qui sont en corrélation avec des séquences de 2,775 Ga; des roches volcano-sédimentaires à dominante calco-alcaline marquant une diminution de la profondeur du milieu vers le haut, qui ressemblent à des roches volcaniques (2,745-2,704 Ga) au lac Savant et à des dépôts de caldera (2,735 Ga) au sud; et des roches sédimentaires fluvioclastiques postérieures à 2,718 Ga. La partie centrale de la ceinture est déformée par des plis F_1 à direction est-sud-est et à plongement modéré à faible, qui sont replissés localement par des plis F_2 à direction nord-est et à plongement variable. Des zones de déformation intense à direction nord-est pourraient séparer des séquences volcaniques temporellement distinctes ou traduire la localisation des contraintes au travers de discontinuités rhéologiques.

[1] Contribution to the Western Superior NATMAP Project

INTRODUCTION

The central Wabigoon Subprovince (Fig. 1) contains vestiges of ca. 3.0 Ga basement with locally preserved Mesoarchean cover sequences, remnants of ca. 2.73 Ga greenstone belts, and widespread plutonic rocks of probable ca. 2.7 Ga age (Blackburn et al., 1991). The western Wabigoon Subprovince comprises ca. 2.78-2.72 Ga submarine volcano-sedimentary sequences, ca. 2.71-2.70 Ga clastic sediment-dominated cover, and a collage of synvolcanic to post-tectonic plutonic complexes. The nature, extent, and timing of interaction between an older, central Wabigoon protocraton, and the younger, granite-greenstone terranes are uncertain. This problem has direct bearing on understanding both the tectonic history of the western Superior Province and the setting within which its mineral deposits were formed. It is a central theme of the recently initiated Western Superior NATMAP project, a geoscience mapping partnership project involving the Ontario Geological Survey, the Manitoba Geological Services Branch, and the Geological Survey of Canada. In order to address this theme, a geological investigation was initiated in the Sturgeon Lake greenstone belt, a long-lived (ca. 2.78-2.70 Ga) supracrustal belt with rich mineral endowment that lies at the interface between the central and western Wabigoon Subprovince (Fig. 1).

The study combines structural and stratigraphic methods to unravel the internal geometry, chronology, and tectonic setting of the central Sturgeon Lake greenstone belt. Follow-up U-Pb geochronology will calibrate field observations and complement tracer geochemical methods (e.g. trace elements; Sm-Nd, Pb-Pb and O isotopes) aimed at detecting inheritance in the source regions of its supracrustal and plutonic rocks. This study complements ongoing NATMAP investigations in the central Wabigoon Subprovince (Percival, 1998) and LITHOPROBE seismic profiles through the Sturgeon Lake-Savant Lake area.

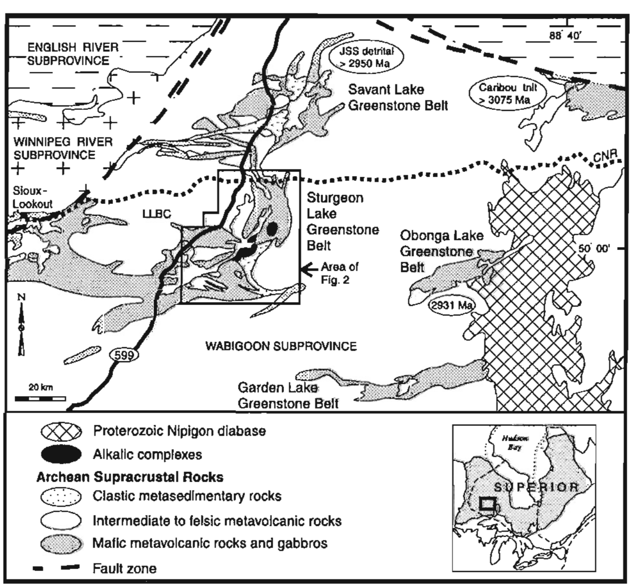

Figure 1. *Regional setting of the west-central Wabigoon Subprovince, Superior Province, showing dated occurrences of Mesoarchean crust.*

Six weeks of field mapping were conducted in the Sturgeon Lake area in 1997. New field results are integrated with existing data to establish a structural chronology, investigate the apparent disparity between the architecture of the contiguous Sturgeon and Savant Lake greenstone belts and to identify potential tectonostratigraphic correlations which will be tested with geochronological and geochemical methods.

PREVIOUS WORK

Comprehensive mapping (1:31 680) was conducted by N.F. Trowell (Trowell 1974; 1976; 1983a) concurrent with the discovery of base-metal mineralization in the Sturgeon Lake area. Previous geological investigations are summarized in these works. Detailed mapping of volcanic stratigraphy near the Mattabi deposit led to its interpretation as an Archean submarine caldera complex (Morton et al., 1991). The mine (caldera) stratigraphy is dated at 2735.5 ± 1.5 Ma (Davis et al., 1985), slightly older (see discussion in Davis et al., 1985) than the underlying 2733.8 ± 1.4 Ma Beidelman Bay intrusion (Davis and Trowell, 1982) and coeval with underlying, pre-caldera (Darkwater) strata. Overlying post-caldera rocks (South Shore cycle; Fig. 2) are dated at 2718 +2.7/-1.5 Ma (Davis and Trowell, 1982). Deformation of the eastern part of the massive sulphide camp was investigated by Dubé et al. (1989) and Koopman (1993) who delineated a major shallowly plunging fold with associated minor folds. The northern and western parts of the belt were re-examined in the early 1990s by Williams and Nacha (1991) and Robinson (1992), respectively.

LITHOLOGICAL UNITS

Metavolcanic Units

Trowell (1983b) subdivided metavolcanic rocks in the Sturgeon Lake area into seven volcanic cycles, each containing various proportions of older mafic and younger intermediate and felsic volcanic rocks. A simplified version of this nomenclature is tentatively adapted here (Fig. 2) pending ongoing investigations aimed in part at testing the validity of the volcanic cycle concept in the Sturgeon Lake area. Specifically, the Northeast Arm and Squaw Lake cycles of Trowell (1983b) are replaced by their northern, along-strike correlatives, the Beckington West and Beckington East cycles, respectively.

North Arm Cycle

Volcanic rocks of the North Arm cycle exposed west of Couture Lake (Fig. 2, 3) comprise east-southeast-facing pillowed and massive basalts cut by equigranular diabasic gabbro and tonalite of the Lewis Lake batholith. Pillowed basalts near the base of this cycle are low-potassium (0.13-0.38 K_2O%), low-titanium (0.63-1.38 TiO_2%) tholeiites (Fig. 4a), which are non-amygdaloidal and have flattened pillows up to 6 m in length (Trowell, 1983b). A transect across this apparently homoclinal sequence of basalts shows an up-section decrease in magnesium from relatively primitive basalts with 9% MgO to more iron-rich basalts with 4% MgO (Fig. 5). Overlying the mafic rocks is quartz-phyric felsic tuff, 1 to 30 m thick, which can be traced north of the map area where it is intercalated with thinly bedded graphitic and sulphidic siltstones (Trowell 1983b).

Beckington West Cycle

Metavolcanic rocks in the north-central part of the map area are part of the Beckington West cycle. Its lower part comprises east-facing massive and pillowed basalts and pillow breccia which show an up-section increase in the size and abundance of amygdules (cf. Trowell 1983b). Its upper part comprises calc-alkaline intermediate±felsic pyroclastic rocks and flows with minor intercalated tholeiitic basalts (Fig. 4a). Near Morgan Island, these consist of poorly sorted, poorly bedded, intermediate tuff breccia and lapilli tuff which are typically monolithic (Fig. 6a), and locally contain angular, vesicular andesitic blocks. Well bedded and well sorted quartz-feldspar phyric, heterolithic tuff±hypabyssal rocks occur northeast and southwest of Morgan Island, and are locally intercalated with epiclastic rocks. The Beckington West cycle is cut by dykes and sills of plagioclase-porphyritic diorite and gabbro, melanocratic gabbro, and tonalite.

Beckington East Cycle

Mafic rocks in the northeast part of the map area form part of the Beckington East cycle (Fig. 2 and 3) and are distinguished by highly vesicular and amygdaloidal, massive and pillowed basaltic flows, and hyaloclastic pillow breccia (Fig. 6b). The basalts are mainly calc-alkaline with low titanium contents (0.68-1.0 %), but include rare tholeiitic lavas (Fig. 4a). These are cut by sills and dykes of calc-alkaline gabbro including equigranular, melanocratic, and plagioclase megacrystic (2-3 cm) varieties.

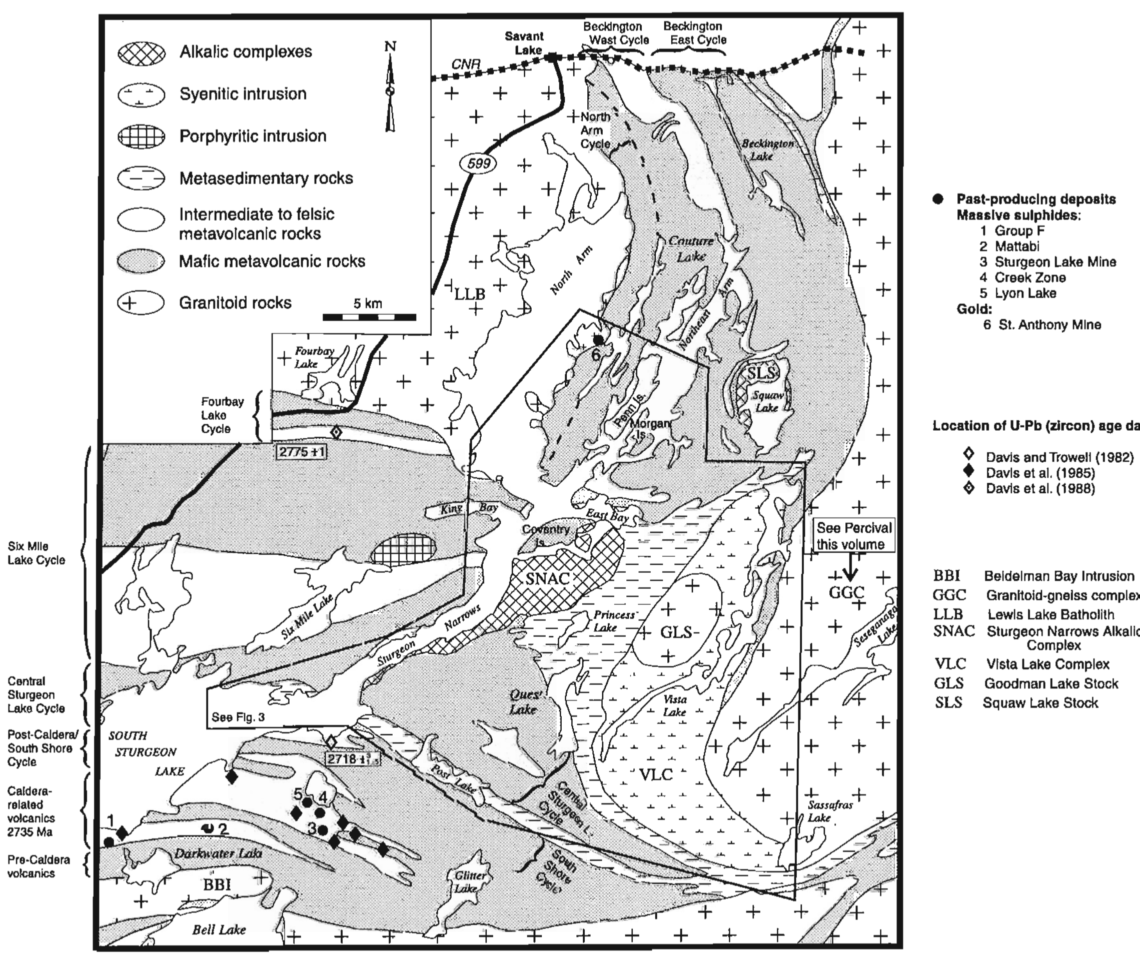

Figure 2. *Regional geology of the Sturgeon Lake greenstone belt, volcanic cycle nomenclature adapted from Trowell (1983b).*

Six Mile Lake Cycle

Mafic rocks of the lower Six Mile Lake cycle are exposed in the map area near King Bay (Fig. 2, 3). These consist of aphyric, non-vesicular, pillowed and massive, magnesian and iron-rich tholeiitic basalts (Beggs, 1975; Fig. 4a;), cut by diabase intrusions. Stratigraphically higher basalts contain a greater proportion of amygdules relative to those at the base of the cycle (Trowell, 1983b). The upper Six Mile Lake cycle is interpreted as a south-facing and eastward-thinning and -fining prism of pyroclastic rocks (Trowell, 1983a,b; Robinson, 1992). Its eastern extremity is exposed in central Sturgeon Narrows, where texturally diverse units include intermediate pyroclastic breccia, lapillistone, tuff, and epiclastic rocks.

Central Sturgeon Lake Cycle

The Central Sturgeon Lake cycle dominates the south part of the map area extending from Quest Lake to the northwest shore of Sturgeon Narrows (Fig. 2 and 3). Basal units on the shore of Sturgeon Narrows include chloritized, vesicular, and amygdular dykes and sills. Near Quest Lake, its basal unit comprises pillowed and massive amygdaloidal basalts, pillow breccia, flow breccia, and hyaloclastite. The lower part of the cycle includes both calc-alkaline low-titanium basalts (0.2-1.4 % TiO_2) and tholeiitic, high-titanium (0.58-2.47 % TiO_2) varieties (Fig. 4b). Some basalts of this cycle (i.e. on Mountain Island, just west of the map area), contain up to 11.9% MgO. A liquid corresponding to the composition of the 11.9% MgO primitive basalt, would be in equilibrium

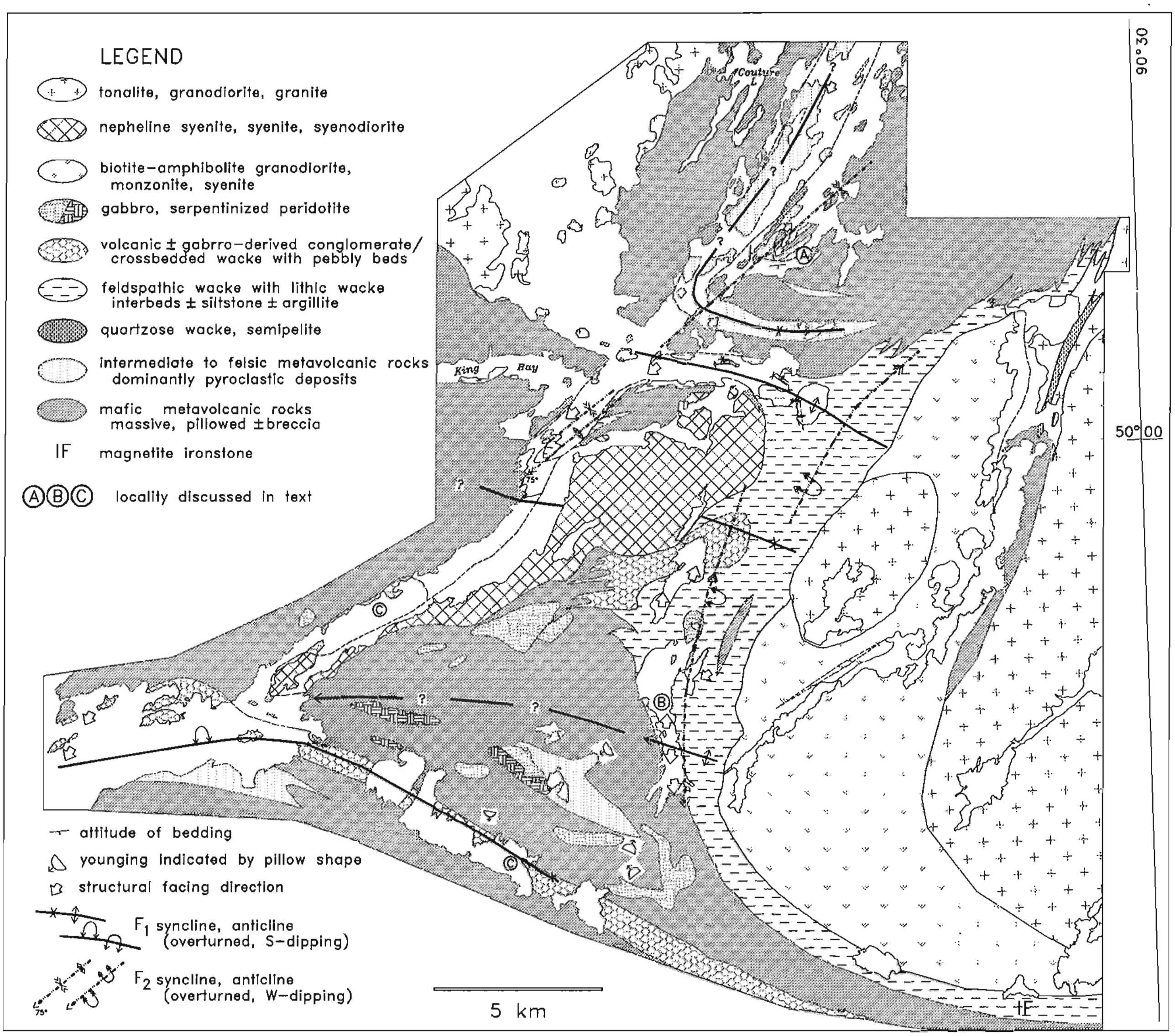

Figure 3. Geology of the central Sturgeon Lake area, modified from Trowell (1974, 1976, 1983a).

with an olivine of Fo_{86} composition (assuming $K_D{}^{Fe/Mg}$ oliv-liq = 0.3; Roeder and Emslie 1970; and XFe^{3+} = 0.0). These rocks are cut by gabbro and serpentinized peridotite (Fig. 3), the latter having Fe/Mg values appropriately low to contain Fo_{86} olivine, suggesting they may be cogenetic with the high-MgO basalts (Fig. 4b). Intermediate volcanic breccia and ferruginous wacke-siltstone overlie the mafic rocks west of Quest Lake (Trowell, 1983b).

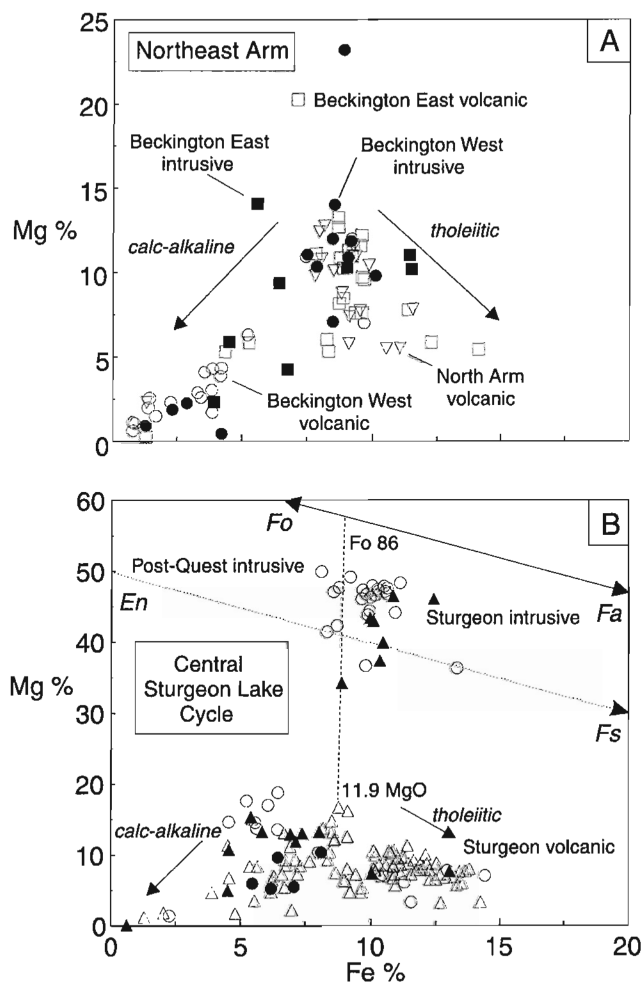

__Figure 4.__ Fe% versus Mg% (cation%) diagram of volcanic and intrusive rocks in the Sturgeon Lake belt (data from Trowell, 1983b; excludes pyroclastic, visibly altered, highly deformed, and samples with $S+CO_2+H_2O^+$ ≥5%, <95% totals >101%). __A)__ Northeast Arm area, North Arm cycle volcanic: open triangle; Beckington East cycle intrusive: filled square; volcanic: open square; Beckington West cycle intrusive: filled circle; volcanic: open circle. __B)__ Central Sturgeon Lake cycle (south Sturgeon Lake area volcanic: open triangle; intrusive: filled triangle; Post Lake area volcanic: solid circle; intrusive: open circle). Mineral endmembers are Fo: forsterite; Fa: fayalite; En: enstatite; and Fs: ferrosilite.

Metasedimentary Rocks

Clastic metasedimentary rocks occur at three main localities (Fig. 3), described from west to east. Relatively quartz-rich clastic metasedimentary rocks on Vista Lake form part of an approximately 500 m wide by 12 km long screen of supracrustal rock that defines the eastern margin of the greenstone belt (Fig. 2, 3). This screen divides plutonic rocks of the central Wabigoon granite-gneiss complex (Percival, 1998) from monzosyenitic rocks of the Vista Lake complex, and comprises foliated to gneissic, amphibolite-facies metasedimentary and mafic metavolcanic rocks in which primary structures are absent and tectonic layering is parallel to the supracrustal-intrusive contacts. Quartz wacke from this area is white-grey weathering (65% quartz) and is interlayered with metre-wide panels of strongly foliated, rusty-weathering lithic wacke (garnet-muscovite schist) and minor amphibolite.

A central sequence of clastic rocks extends from northern Sturgeon Narrows, through East Bay, to southeast of Quest Lake (Fig. 3). Kilometre-long screens of schistose wacke within the Vista Lake complex suggest they may have extended several kilometres further east. This elongate triangular exposure is dominated by well bedded, well graded feldspathic wacke (3 cm to 1 m thick beds) and interbedded lithic wacke (<4 cm thick beds). Thinly bedded siliceous siltstone occurs with feldspathic wacke along the west shore of Coveney Island, in East Bay, and on Princess Lake; these areas represent potentially lateral equivalents. Black argillaceous beds alternate with feldspathic and lithic wacke along the west shore of Quest Lake and East Bay. Magnetite ironstone interbanded with lithic wacke is restricted to the extreme southeast part of the map area (Fig. 3). Tectonically disrupted, thinly bedded cherts and associated graphitic beds occur in central East Bay.

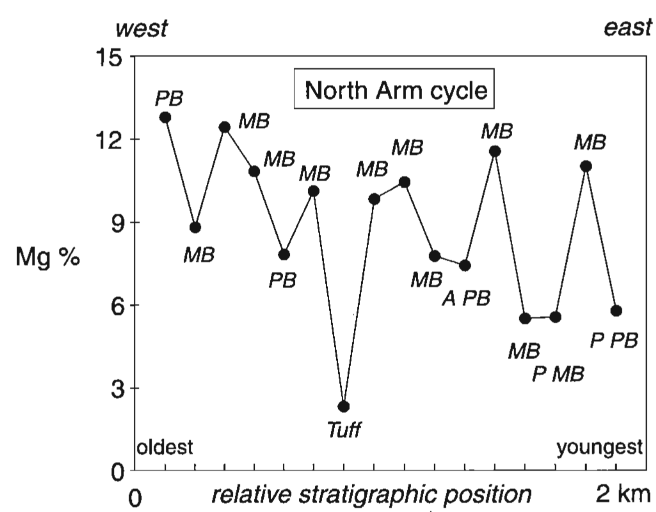

__Figure 5.__ Mg% (cation %) versus relative stratigraphic position for volcanic rocks collected across the North Arm cycle (data from Trowell, 1983b). Note non-linear horizontal scale.

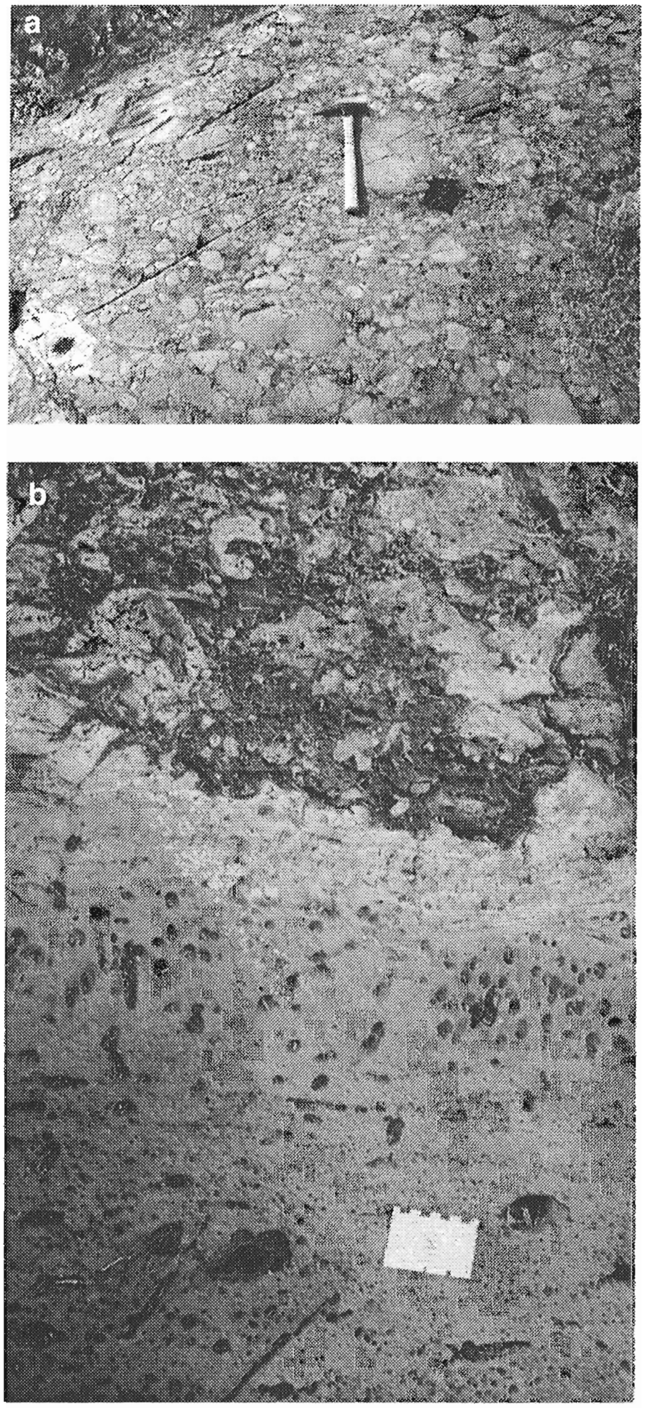

*Figure 6. **a)** Pyroclastic breccia of the upper Beckington West cycle (Morgan Island). **b)** Sectional view of upper part of Beckington East basalt flow. Fine vesicles in flow interior coalesce upsection (top) and are overlain by vesiculated hyaloclastite and pillow fragment flow top breccia.*

Although the central clastic sequence is internally folded, contact relationships and younging criteria at its margins and in surrounding metavolcanic rocks indicate overall westward-younging. It is interpreted to overlie basaltic to andesitic rocks of the Beckington cycles and be overlain to the west by westward-younging mafic metavolcanic rocks of the Central Sturgeon Lake cycle (Fig. 2). At several localities in the East Bay area, its basal contact was observed to consist of matrix-supported pebble conglomerate with angular mafic volcanic clasts in a relatively clean feldspathic wacke matrix. This basal unit reflects two source regions for these rocks: a minor component of directly underlying mafic rock and a significant contribution from a quartz-rich felsic volcanic and/or plutonic source. Rare pebble-conglomerate beds up-section contain clasts of fine-grained felsic volcanic and quartz-porphyritic granitoid/hypabyssal material.

A distinctive sequence of conglomeratic rocks and associated crossbedded wackes occur in the west half of the map area (Fig. 3). On the north shore of south Sturgeon Lake, poorly stratified, poorly graded, clast-supported conglomerate contains subrounded, pebble- to cobble-sized clasts of mafic metavolcanics and medium-grained gabbro. South of this mafic-derived conglomerate, island exposures are increasingly polymictic, with the appearance of clasts of fine-grained intermediate to felsic volcanic rock, chert, sulphide, and metasedimentary rock. Crossbedded feldspathic wacke occurs northeast and southeast of these conglomerates in Sturgeons Narrows and on Post Lake (localities C, Fig. 3). These white-weathering rocks display trough crossbedding (Fig. 7a) with foresets up to 1 m wide, and contain basal pebbly layers.

Clast-supported, mafic volcanic- and gabbro-derived conglomerate in the Princess Lake area (Fig. 7b) is texturally and compositionally similar to that on south Sturgeon Lake. These poorly bedded, ungraded deposits show a crude clast-size variation, from cobble- to boulder-sized clasts in the west to pebble-sized clasts in the east, which may reflect eastward younging. They are interpreted to overlie the central, west-younging clastic sequence, and the Central Sturgeon Lake volcanic rocks from which they appear to be derived.

Plutonic Rocks

The eastern part of the Sturgeon Lake belt is bound by the central Wabigoon granite-gneiss complex (Percival, 1998), which comprises foliated and gneissic granitoid rocks (Fig. 3). On Vista Lake, this complex consists of fine- to medium-grained, biotite tonalite gneiss containing flattened igneous and metasedimentary inclusions. On northeast Vista Lake, it consists of fine- to coarse-grained, equigranular, moderately to strongly foliated, mafic-poor, biotite tonalite to granodiorite. Some exposures contain xenoliths of strongly foliated and crenulated tonalite hosted by less deformed tonalite.

The Lewis Lake Batholith at the mouth of the North Arm of Sturgeon Lake consists of equigranular to quartz-porphyritic tonalite, gabbroic intrusive phases, and a variety of plutonic inclusions. This is transitional to coarse-grained hornblende porphyritic tonalite and medium- to coarse-grained hornblende+biotite quartz diorite to the northwest. Along Highway 599, variably foliated tonalite to quartz diorite occurs. Sheets, dykes, and stockwork veins of pink granitic aplite-pegmatite are important components locally.

The Vista Lake complex is a crescent-shaped pluton, 23 km by 7 km, that cuts the central Wabigoon granite-gneiss complex (Trowell 1976; 1983a, b; Fig. 3). It consists mainly of pink, medium- to coarse-grained, equigranular to potassium-feldspar porphyritic (1-1.5 cm), hornblende-biotite quartz monzonite to monzosyenite. Potassium-feldspar megacrystic (2-4 cm) variants are exposed on its north margin. The complex is moderately to strongly foliated and minor, aplite-pegmatite veins and dykes cut the foliation. Its central part contains a 5 by 0.3 km, northeast-trending roof pendant of strongly foliated quartz wacke.

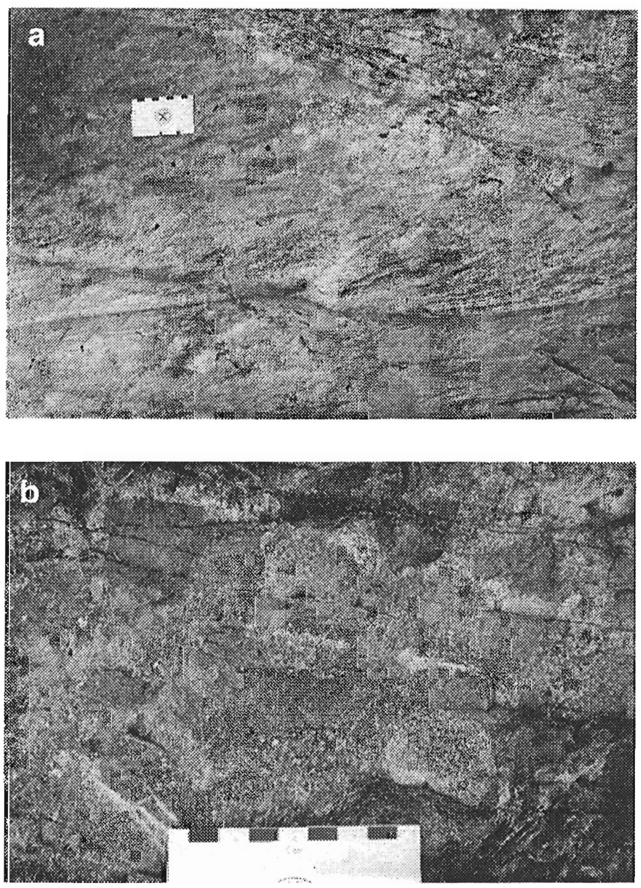

*Figure 7. **a)** Crossbedded feldspathic wacke from Sturgeon Narrows (locality C, Fig. 3). **b)** Mafic-derived conglomerate from Princess Lake showing subrounded gabbroic clasts in a clast-supported framework and chlorite-rich matrix. Pale coloured fenite veins are associated with the Sturgeon Narrows Alkalic Complex.*

The Sturgeon Narrows Alkaline complex is an elongate, tadpole-shaped body that occurs in the central part of the map area (Trowell, 1983a, b). It is dominated by coarse-grained nepheline syenite with well-aligned laths of 1-2 cm long potassium feldspar. Steeply dipping modal layering defined by a systematic, gradational change in the proportion of aegerine-augite was observed at several localities. The elongate, concordant shape of the pluton with respect to regional D_2 fabrics, potential S_2 foliation in its border phases, and folding of related syenitic dykes suggest the complex is late tectonic.

STRUCTURE AND METAMORPHISM

Structural elements within the map area are summarized in Figures 3 and 8. Tightly folded rocks with a pronounced foliation form two main corridors (Fig. 8; shaded areas) that transect the map area. These corridors are dominated by D_2 structures, whereas intervening panels, which may show lower strain, are dominated by D_1 structures. The resulting pattern is one of discrete lithological and structural domains within which reversals of younging are common. Reversals in structural facing (younging in the direction of axial plane cleavage) are less common. This architecture appears to contrast with other parts of the Sturgeon Lake belt, where consistently facing, homoclinal, conformable stratigraphic sequences are described (i.e. the east-facing Beckington Lake cycles of Trowell (1983b) and Williams and Nacha (1991); the south-facing Fourbay Lake and Six Mile Lake cycles of Trowell (1983b) and Robinson (1992); and the north-facing mine stratigraphy (Davis et al., 1985; Morton et al., 1991).

Most mineral assemblages are typical of greenschist-facies regional metamorphism, with an increase in grade to the east reflected by garnet and staurolite in metasedimentary rocks east of Quest Lake and hornblende±clinopyroxene in mafic rocks on Vista Lake. Lithic wacke throughout East Bay and Princess Lake contains up to 15% subhedral andalusite, 0.5 to 1 mm. Its presence may reflect slightly higher metamorphic grade and its spatial distribution suggests possible contact effects by the Sturgeon Narrows alkalic complex. A local S_2 foliation wraps around andalusite, indicating it grew prior to, or synchronous with, this foliation.

Folds

Two corridors of folded strata occur in the map area (Fig. 8, shaded areas). One of these is centered on Sturgeon Narrows, where interbedded metavolcanic and metasedimentary rocks are tightly to closely folded about south-southwest-trending, steeply northwest-dipping axial surfaces. Minor fold axes plunge steeply (70-80°) southwest, parallel to the elongation direction of clasts and fragments, and to the linear alignment of minerals in the axial planar foliation. This corridor extends into the Northeast Arm of Sturgeon Lake where macroscopic folds are less common (see Fig. 9), but the distribution of volcanic units and bedding orientations also define tight to close map-scale folds (Fig. 3). A second corridor of folded strata is centered on the central metasedimentary sequence,

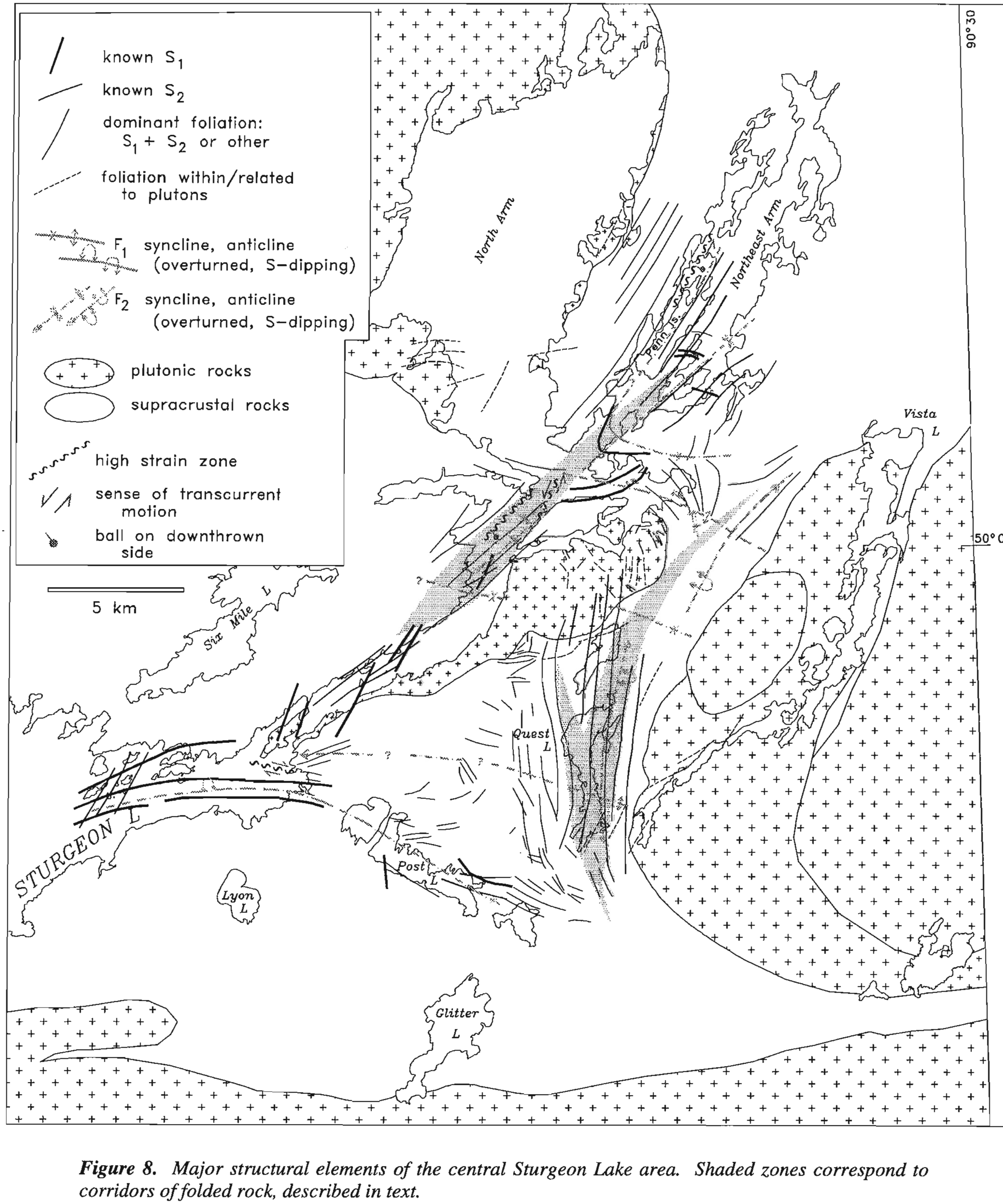

***Figure 8.** Major structural elements of the central Sturgeon Lake area. Shaded zones correspond to corridors of folded rock, described in text.*

particularly in the Quest Lake area. Here, tightly folded metasedimentary rocks have south-trending, steeply west-dipping axial surfaces. Minor folds plunge 30 to 70°, north and south.

Both fold corridors are characterized by a high degree of tectonic transposition, such that outcrop exposures are dominated by straight, strongly foliated layers where primary features such as grading may be obscured or obliterated. Invariably, tight, limbless, fold-hinge zones (≤metre scale) can be uncovered from these outcrops, and these generally contribute important younging and structural-facing criteria upon which the fold history of the study area is based.

Two generations of fold structures are recognized from both of these corridors. In the Northeast Arm area (locality A in Fig. 3), two outcrop-scale orthogonal fold sets are recognized (Fig. 9). One set consists of a paired syncline/anticline that plunges moderately (56°) south about northeast-trending (040°), steeply east-dipping axial surfaces (Fig. 9a, b). The geometry of this set corresponds to the fold style throughout

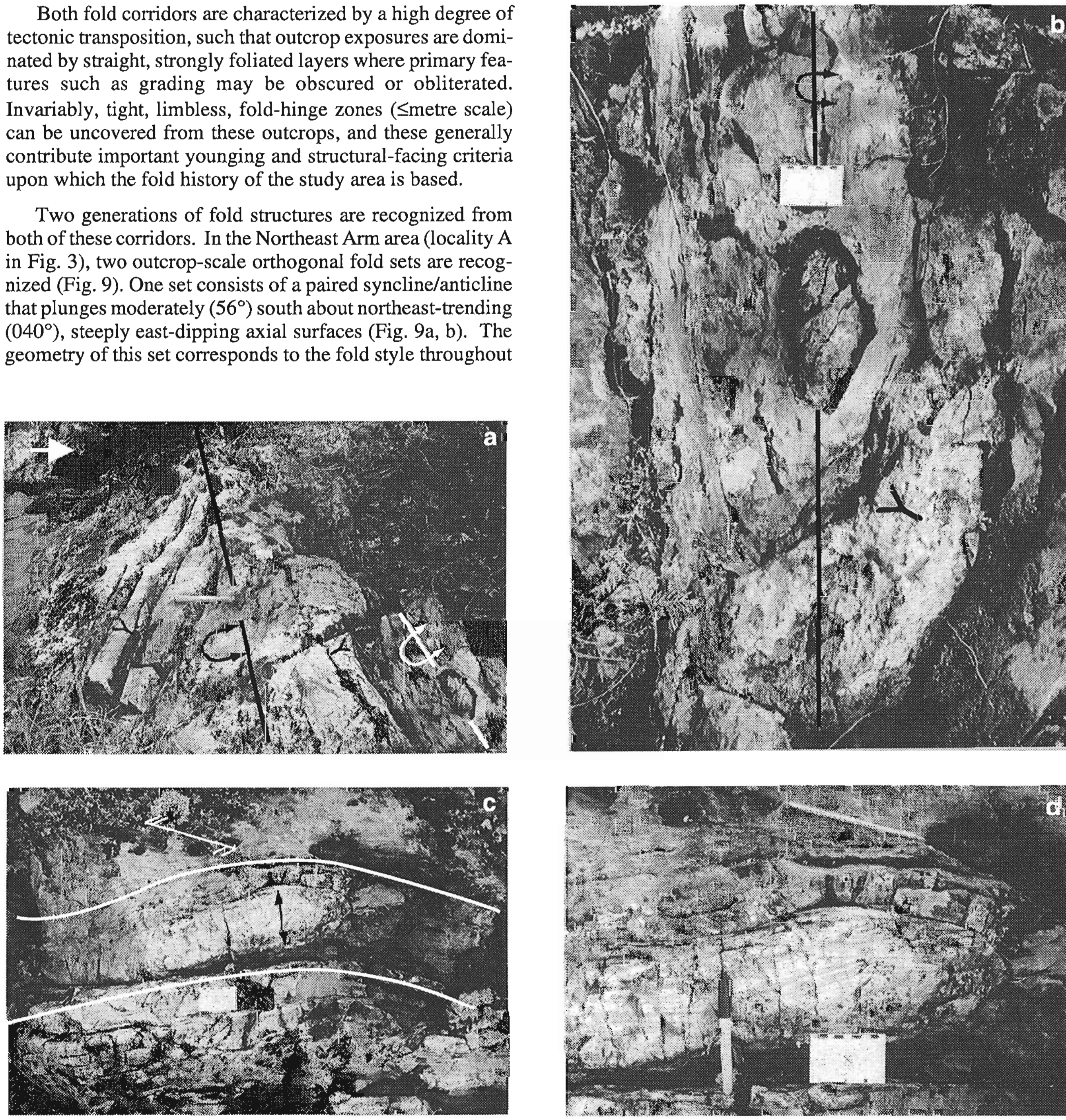

***Figure 9.** F_1 and F_2 folds in the Northeast Arm (locality A, Fig. 3). **a)** View northeast of steeply overturned, east-dipping F_2 syncline-anticline. Thick arrow indicates location of F_1 folds in c) and d). **b)** Detail of anticlinal hinge in a) showing domal geometry and attenuated northwest limb (left side of photo). **c)** Downplunge view (to east-southeast) of open F_1 folds showing axial planar cleavage (S_1) and transecting S_2 schistosity. **d)** Detail of fabrics in c), S_1 is parallel to marker pen, transecting S_2 is parallel to pencil.*

central Sturgeon Narrows, described above. The other fold set consists of moderately (50°) east-plunging, upright folds of metre-scale wavelength, whose subvertical axial surface (290/85) forms a 70° angle to the previously described fold set. The high angle made by axial surfaces of these two folds sets is reflected by locally developed domal geometry (Figure 9a,b), consistent with a Type 1 fold interference pattern. Both sets of folds have an associated axial planar cleavage. The relationship of these cleavages to the folds indicates their chronology of development, in that the northeast-trending cleavage (axial planar to the paired syncline/anticline) is not folded about the more open folds, but transects them (Fig. 9c, d). This establishes the more open, east-southeast-trending folds as F_1 and the steeply overturned, northeast-trending folds as F_2, a relationship confirmed by superposition of the northeast-trending schistosity (S_2) on the spaced east-southeast cleavage (S_1) at several localities. Continuity of the northeast-trending cleavage, and folds to which it is axial planar, southward through central Sturgeon Narrows indicates that folds throughout this corridor are F_2.

In the Quest Lake area, opposing structural facing, determined from relatively well preserved hinge zones of macroscopic folds, is used to identify the presence of a map-scale F_1 fold, whose anticlinal hinge is located at the change from north to south structural facing (locality B in Fig. 3). The presence of an east-southeast-trending, map-scale F_1 structure (Fig. 3), implies that the dominant folds observed throughout this corridor are F_2 structures. Superposition of F_2 folds on F_1 results in north-plunging F_2 folds on the north limb of the F_1 anticline and south-plunging F_2 folds on its south limb. Structural facing directions from other parts of the belt identify the location of several other, more cryptic, F_1 structures (Fig. 3).

Folds in the East Bay area (Fig. 3) are highly discordant to D_2 folds and fabrics and are interpreted as F_1, possibly modified by the Sturgeon Narrows alkalic complex (Fig. 3). Younging reversals in metasedimentary rocks on Post Lake (Fig. 3) define a syncline with an 110°-striking, steeply south-dipping axial surface. This structure may extend to south Sturgeon Lake where a syncline centered on conglomeratic rocks is defined on the basis of south-younging of conglomerate and bedding/cleavage relationships. Clasts in these units show pronounced elongation plunging 40-50° to the east-southeast, and may reflect a moderate eastward plunge to this fold which is geometrically compatible with F_1.

Foliation

The dominant foliation in the map area is a north- to north-northeast-striking, steeply dipping foliation which is axial planar to F_2 folds, and is designated S_2. This fabric is recognized throughout the Sturgeon Narrows-Northeast Arm and Quest Lake corridors (Fig. 8), and is locally developed in south Sturgeon Lake as a spaced, northeast-striking cleavage. North-striking foliation within the Sturgeon Narrows alkaline complex (Fig. 8) may represent the regional S_2 fabric.

S_1 fabric is less prominent, and mainly occurs across the south part of the map area, where it is manifest as a penetrative planar and linear shape fabric in conglomerates of south Sturgeon Lake and as a weakly developed schistosity in mafic metavolcanic rocks and mafic intrusions of the central Sturgeon Lake cycle (Fig. 8). East-striking foliation in East Bay may be a modified S_1 fabric. The single strong planar foliation in parts of the Northeast Arm may be a composite S_1 + S_2 fabric.

Shear Zones

Highly strained rocks occur at several localities in the Sturgeon Narrows-Northeast Arm corridor. These zones strike northeasterly, dip steeply, and contain steeply (mainly southwest) plunging mineral lineations. Their planar and linear elements parallel those of the dominant S_2 fabric in this region and, as such, are suspected to have developed, or been reactivated, during D_2.

Strain is mainly localized at the interface between intermediate metavolcanic rocks and mafic metavolcanic rocks (of the Beckington West and Six Mile Lake cycles; Fig. 8). This interface is characterized by a strong to intensely developed, northeast-striking, steeply dipping schistosity, defined mainly by chlorite in mafic rocks, and by muscovite in rocks of intermediate composition. Ferroan carbonate alteration is pervasive. This planar fabric is generally penetratively developed across widths greater than 10 m, but the extent of the zone and the relationship of units which it affects are obscured by lack of exposure. These rocks typically display weakly to moderately developed, steeply southwest-plunging mineral lineations and conjugate kink bands, less than 1 cm wide. The best exposure of high-strain rocks at the mafic/intermediate interface is on northwest Penn Island (Fig. 8). Here, chlorite schist contains epidotized pods and boudins of quartz±carbonate veins which display asymmetries consistent with sinistral, northwest-side-up movement (Fig. 10a). Chlorite schist is in contact with intermediate tuff which is not penetratively strained; instead, strain is localized in uniformly spaced (2-3 cm), parallel bands (Fig. 10b, c) which preferentially accommodated slip. At highest strains, these bands are completely transformed into muscovite (Fig. 10c), but locally a gradient between relatively low-strain host rock and proto-muscovite bands was recognized (Fig. 10b).

DISCUSSION

Mature clastic sediments at Vista Lake, submarine low-potassium tholeiites in the North Arm and shoaling-upward calc-alkaline volcano-sedimentary rocks in the central Sturgeon Lake greenstone belt reflect contrasting tectonic settings in its greater than 50 Ma history. The chemically mature (quartz-rich) nature of quartzose wacke from Vista Lake is lithologically comparable to that of the Jutten Sedimentary Sequence exposed in northeast Savant Lake

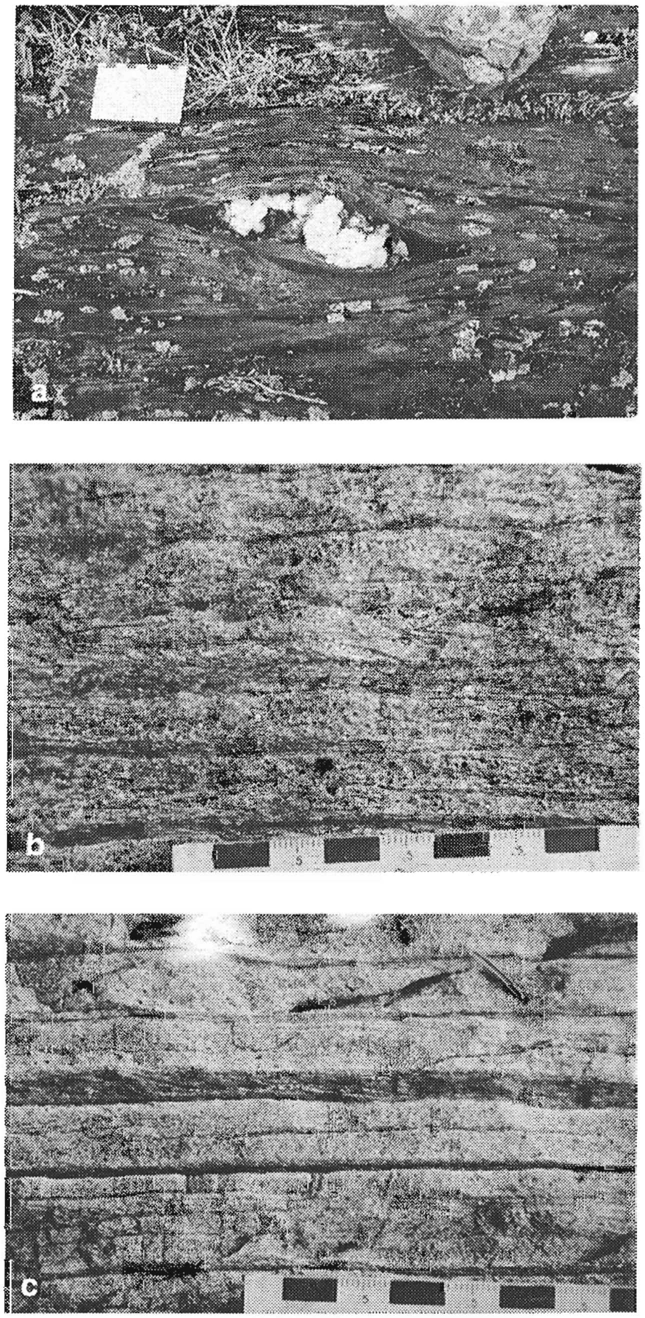

Figure 10. High-strain rocks at mafic/intermediate interface, west shore of Northeast Arm. ***a)*** *Chlorite schist with composite foliations and asymmetrical vein boudin consistent with sinistral, northwest-side-up movement across zone.* ***b)*** *Spaced deformation bands in dacite tuff with internal composite C-C' foliations consistent with sinistral shear.* ***c)*** *Higher strain state than b) showing more typical spaced muscovite bands which preferentially accommodated slip*

greenstone belt (Cortis et al., 1988; Sanborn-Barrie, 1990), which yielded detrital zircon ages older than 2.9 Ga (Davis and Moore, 1991). U-Pb dating of quartzose wacke and crosscutting granite from Vista Lake will bracket the age of sedimentation, and determine whether these also had a Mesoarchean provenance.

The oldest volcanic rocks in the map area may be submarine tholeiitic basalts of the North Arm cycle. This cycle is tentatively correlated with the Fourbay cycle (Trowell, 1983a) for which a zircon $^{207}Pb/^{206}Pb$ age of 2775 ± 1 Ma (Davis et al., 1988) was obtained on rhyolitic tuff near its top. This tuff underlies volcanic rocks correlated with the Handy Lake Volcanic Group. Accordingly, the 2775 Ma Fourbay sequence (and North Arm cycle?) may be correlative with Jutten volcanics of the Savant Lake belt to the north (Fig. 1). In order to test proposed correlations between the North Arm and Fourbay cycles, a sample of felsic crystal tuff from the North Arm cycle was collected for U-Pb dating.

The Beckington West, Beckington East, and Six Mile Lake cycles are upward-shoaling sequences dominated by calc-alkaline volcanic rocks. These 'cycles' may represent different volcanic centres of broadly similar age (cf. Trowell, 1983b, p. 61). Dating of rhyolite from the upper Beckington West cycle will test possible correlations with the 2745-2704 Ma Handy Lake Group to the north and 2735 Ma mine (caldera) stratigraphy to the south. Volcanic-derived clasts in basal conglomerates overlie the Beckington West and Six Mile Lake cycles, which coupled with local intercalation of sedimentary and pyroclastic rocks in Sturgeon Narrows, suggests that the Beckington West volcanics were locally emergent and flanked by a sedimentary apron.

The Central Sturgeon Lake cycle involved eruption of primitive tholeiitic basalts and intrusion of high-level ultramafic plutons. This was followed by erosion and deposition of mafic-derived conglomerates and associated crossbedded wackes in the west half of the map area. Felsic to intermediate volcanic rocks of the Central Sturgeon Lake cycle are likely to be correlative with the ca. 2718 Ma South Shore cycle (Fig. 2), since intermediate to felsic rocks of both cycles are disposed about an F_1 syncline at Post Lake (Fig. 8).

All supracrustal rocks appear to have been affected by two regional deformation events. D_1 is manifest as east-southeast-trending, moderate to shallow east-plunging folds (F_1) and locally developed axial plane cleavage. The F_1 fold style is consistent with a major 116°-trending, 16° east-southeast-plunging fold reported to have affected the Lyon Lake stratigraphy (Dubé et al., 1989) south of the map area. F_1 folds are superimposed, and refolded, by northeast-striking, variably plunging F_2 folds and associated penetrative axial planar S_2 foliation, prevalent in two corridors centered on Sturgeon Narrows and Quest Lake (Fig. 8, shaded areas). Although the possibility of refolded stratigraphy has been considered locally for these rocks (Trowell, 1976), previous workers have emphasized a layer-cake succession of consistently facing homoclinal panels. Our findings in the central part of the belt suggest that the structural history of the central Sturgeon Lake area is polyphase, not dissimilar to that of the Savant Lake greenstone belt, where initially northwest- to north-trending, shallowly plunging F_1 folds were modified by 050-070°-trending, steeply plunging F_2 folds with an associated penetrative axial-planar S_2 foliation (Sanborn-Barrie, 1990). The scope of our 1997 mapping did not reveal whether the central Sturgeon Lake belt is structurally unique, or whether these deformation styles are represented in other parts of the belt.

Discontinuous, northeast-striking high-strain zones through Sturgeon Narrows and the Northeast Arm may be parts of a continuous high-strain zone at the contact between mafic and intermediate volcanic rocks. They may express a fault across which distinct volcanic sequences have been juxtaposed, and/or may reflect localized D_2 strain in the contact region between two rheologically distinct units.

ACKNOWLEDGMENTS

We thank A. Lindsay, M. Radovanovic, and C. Sasseville for assistance in the field, and for some independent mapping (C. Sasseville). D. Davis, J.A. Percival, A. Smith and N.F. Trowell provided valuable information on aspects of Wabigoon geology. Digital data was provided by P.C. Thurston and J. Boyd (Ontario Ministry of Northern Development and Mines) and J. Harris (GSC). A. Mousseau ensured a comfortable and logistically unencumbered stay in central Sturgeon Lake. Reviews by J.A. Percival, C. van Staal, and S. Lucas are appreciated.

REFERENCES

Beggs, D.G.
1975: Petrology and geochemistry of Archean volcanic rocks north of Sturgeon Lake; M.Sc. thesis, University of Toronto, Toronto, Ontario.

Blackburn, C.E., Johns, G.W., Ayer, J., and Davis, D.W.
1991: Wabigoon Subprovince; in Geology of Ontario, (ed) P.C. Thurston, H.R. Williams, H.R. Sutcliffe, and G.M. Stott; Ontario Geological Survey, Special Volume 4, Part 1, p. 303-382.

Cortis A.L., Stott, G.M., Osmani, I.A., Atkinson, B., and Thurston, P.C.
1988: A geological re-evaluation of northwestern greenstone belts; in Summary of Field Work and Other Activities 1988; Ontario Geological Survey, Miscellaneous Paper 141, p.28-52.

Davis, D.W. and Moore, M.
1991: Geochronology in the western Superior Province; Jack Satterley Geochronology Summary Report - May 1991.

Davis, D.W. and Trowell, N.F.
1982: U-Pb zircon ages from the eastern Savant Lake-Crow Lake metavolcanic-metasedimentary belt, northwest Ontario; Canadian Journal of Earth Sciences, v. 19, p. 868-877.

Davis, D.W., Krogh, T.E., Hinzer, J., and Nakamura, E.
1985: Zircon dating of polycyclic volcanism at Sturgeon Lake and implications for base metal mineralization; Economic Geology, v. 80, p. 1942-1952.

Davis, D.W., Sutcliffe, R.H., and Trowell, N.F.
1988: Geochronological constraints on the tectonic evolution of a Late Archean greenstone belt, Wabigoon Subprovince, northwest Ontario, Canada; Precambrian Research, v. 39, p. 171-191.

Dubé, B., Koopman, E.R., Franklin, J.M., Poulsen, K.H., and Patterson, M.R.
1989: Preliminary study of the stratigraphic and structural controls of the Lyon Lake massive sulphide deposit, Wabigoon Subprovince, northwest Ontario; in Current Research, Part C; Geological Survey of Canada, Paper 89-1C, p. 275-284.

Koopman, E.R.
1993: Stratigraphy, structural geology, and structural controls of ore distribution of the Lyon Lake massive sulphide deposit, Sturgeon Lake, Ontario; M.Sc. thesis, Carleton University, Ottawa, Ontario, 170 p.

Morton, R.L., Walker, J.S., Hudak, G.J., and Franklin, J.M.
1991: The early development of an Archean submarine caldera complex with emphasis on the Mattabi ash-flow tuff and its relationship to the Mattabi massive sulphide deposit; Economic Geology, v. 86, p. 1002-1011.

Percival, J.A.
1998: Structural transect of the central Wabigoon Subprovince between the Sturgeon Lake and Obonga Lake greenstone belts, Ontario; in Current Research 1998-C; Geological Survey of Canada.

Robinson, D.J.
1992: Geology of the Six Mile Lake area; Ontario Geological Survey, Open File Report 5838, 93p.

Roeder, P. L. and Emslie, R.F.
1970: Olivine-liquid equilibrium; Contributions to Mineralogy and Petrology, v. 29, p. 275-289.

Sanborn-Barrie, M.
1990: Geology of the Savant Lake area; in Summary of Field Work and Other Activities 1990; Ontario Geological Survey, Miscellaneous Paper 151, p.22-30.

Trowell, N.F.
1974: Geology of the Glitter Lake area; Ontario Division of Mines, Geoscience Report 120, 31p.
1976: Geology of the Quest Lake area; Ontario Division of Mines, Geoscience Report 154, 60p.
1983a: Geology of the Squaw Lake-Sturgeon Lake area; Ontario Geological Survey, Report 227, 114p.
1983b: Geology of the Sturgeon Lake area; Ontario Geological Survey, Report 221, 97p.

Williams, H.R. and Nacha, S.M.
1991: Reassessment of the northern part of the Sturgeon Lake region; in Summary of Field Work and Other Activities 1991; Ontario Geological Survey, Miscellaneous Paper 157, p. 34-39.

Geological Survey of Canada Project 970014

Structural transect of the central Wabigoon subprovince between the Sturgeon Lake and Obonga Lake greenstone belts, Ontario[1]

John A. Percival
Continental Geoscience Division, Ottawa

Percival, J.A., 1998: Structural transect of the central Wabigoon subprovince between the Sturgeon Lake and Obonga Lake greenstone belts, Ontario; in Current Research 1998-C; Geological Survey of Canada, p. 127-136.

Abstract: The central Wabigoon region between the Sturgeon Lake and Obonga Lake greenstone belts is a complex granitoid terrane in which at least thirteen intrusive phases and five deformation events can be distinguished. The oldest unit, tonalite gneiss, has S_1 gneissosity and rarely preserved north-trending F_2 folds. The dominant rock types, biotite tonalite, biotite granodiorite, and hornblende-biotite granodiorite, carry the regionally dominant S_3 foliation and sporadic migmatitic layering. Map-scale F_4 folds are open to tight and upright, with gently east-northeast- or west-northwest-plunging hinges which have been warped by broad F_5 folds with easterly axial surfaces. The reconstructed structural stack comprises basal sheets of granodiorite and tonalite overlain by pods of syenite-monzodiorite and porphyritic granodiorite, the Sturgeon and Obonga supracrustal sequences, and uppermost tonalitic gneisses. The complex intrusive-deformation history of the granitoid terrane will be calibrated with geochronology to test geometric correlations with structures in adjacent greenstone belts.

Résumé : La partie centrale de la région de Wabigoon entre les ceintures de roches vertes de Sturgeon Lake et d'Obonga Lake est un terrane granitoïde complexe dans lequel on peut distinguer au moins treize phases intrusives et cinq épisodes de déformation. L'unité la plus ancienne, un gneiss tonalitique, se caractérise par une gneissosité S_1 et des plis F_2 de direction nord rarement conservés. Les lithotypes dominants, soit de la tonalite à biotite, de la granodiorite à biotite et de la granodiorite à hornblende-biotite, renferment la foliation S_3 régionalement dominante et un litage migmatitique sporadique. Les plis F_4 d'échelle cartographique sont ouverts à serrés et droits; leurs charnières, qui plongent doucement vers l'est-nord-est ou l'ouest-nord-ouest, ont été gauchies par de larges plis F_5 à surfaces axiales orientées vers l'est. L'empilement structural reconstitué comprend des couches de base de granodiorite et de tonalite que recouvrent des lentilles fusiformes de syénite-monzodiorite et de granodiorite porphyrique, les séquences supracrustales de Sturgeon et d'Obonga et des gneiss tonalitiques sommitaux. L'histoire complexe d'intrusion-déformation du terrane granitoïde sera étalonnée avec la géochronologie afin de tester les corrélations géométriques avec les structures des ceintures de roches vertes adjacentes.

[1] Contribution to the Western Superior NATMAP Project

INTRODUCTION

A NATMAP project has been initiated in the western Superior Province with the broad goal of establishing relationships between supracrustal sequences of 2.78-2.70 Ga and fragments of older (3-2.8 Ga) continental crust. Crust of both Mesoarchean and Neoarchean age occur in close proximity in the central Wabigoon subprovince, as well as at the northern and southern margins of the North Caribou terrane to the northwest (Thurston et al., 1991). Basal contacts of the 2.78-2.70 Ga sequences are exceedingly rarely preserved, owing mainly to emplacement of later intrusions. Therefore indirect means must be used to establish whether the volcanic rocks erupted through continental crust or were deposited in oceanic basins and subsequently tectonically juxtaposed. In addition to its significance for the tectonic history of the western Superior Province, distinction of the oceanic versus continental origin of volcanic rocks has important implications in assessing the mineral potential of supracrustal sequences.

The central Wabigoon region ("Wabigoon diapiric axis" of Edwards and Sutcliffe, 1980) has been postulated to represent ca. 3 Ga basement to adjacent, younger supracrustal belts (Thurston and Davis, 1985). Old rocks have been documented at widespread localities (Fig. 1): 1) near the northern margin of the Wabigoon subprovince, where the Caribou Lake greenstone belt is cut by 3.075 Ga tonalite (Davis et al., 1988); 2) south of the Obonga belt, where tonalite is 2.931 Ga (Tomlinson et al., 1996); and 3) near the southern margin of the Wabigoon subprovince, where the Lumby Lake belt and Marmion tonalite have ages of 3.0 Ga (Davis and Jackson, 1988). It is unclear whether the intervening parts of the central Wabigoon region also contain rocks of Mesoarchean age.

To assess this and related questions a transect was examined across the central Wabigoon region between the Sturgeon and Obonga greenstone belts during a three-week period. Specific objectives included: 1) elucidation of the regional structural geometry and chronology of the granitoid rocks, with particular attention to documenting "old" generations of structures; 2) comparison of the style and age of structures in the granitoid terrane with those in the Sturgeon-Savant and Obonga belts; and 3) comparison of the structural style of the Obonga belt with that of the possibly correlative Sturgeon belt.

GEOLOGICAL SETTING AND PREVIOUS STUDIES

The central Wabigoon region is underlain by a variety of granitoid rocks previously subdivided into foliated to gneissic and foliated to massive suites (Rogers, 1964; Sage et al., 1974). Geochronology is sparse, limited to U-Pb zircon ages of 2931 Ma on tonalite from south of the Obonga belt (D.W. Davis and M. Moore, unpub. rept., 1991), 2774 and 2697 Ma from tonalitic gneiss east of Harmon Lake (D.W. Davis, unpub. rept., 1989), and 2690 Ma from foliated tonalite south of Harmon Lake (D.W. Davis, pers. comm., 1997). Greenstone belts flank the western margin of the granitoid complex. In the north, the Savant Lake belt comprises three lithostratigraphic sequences, the Jutten (<2.94 Ga; Davis et al., 1988), Handy Lake (ca. 2730 Ma), and Savant Lake (<2705 Ma) groups (Sanborn-Barrie, 1990). Its polyphase folding history postdates the youngest strata and includes northwest-trending, upright F_1 folds and northeast-striking F_2 folds and S_2 cleavage. To the south in the Sturgeon Lake belt, the main volcanic sequences range

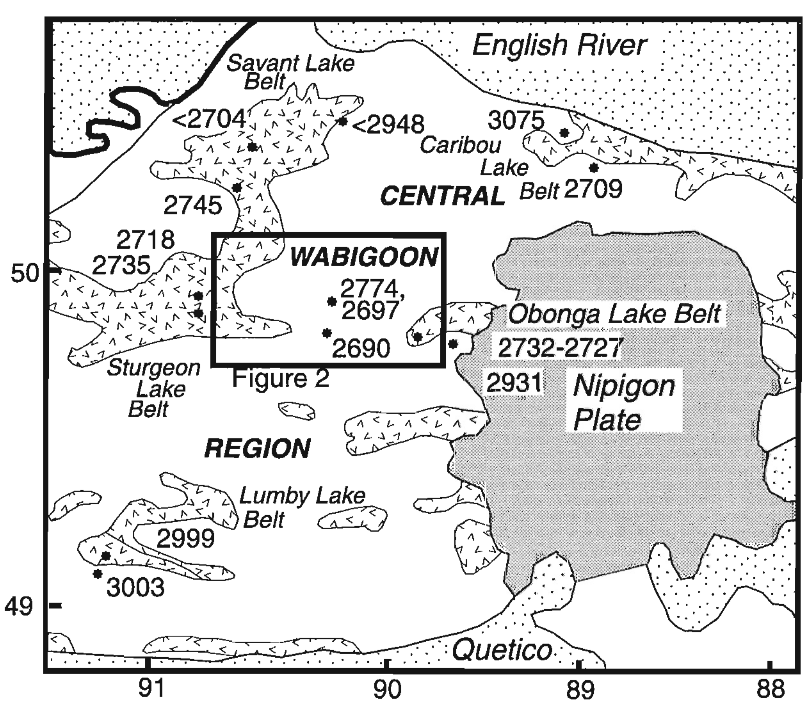

Figure 1.

General geological map of the central Wabigoon subprovince showing the distribution of greenstone belts, U-Pb zircon dates, and the study area (Fig. 2).

from 2745-2718 Ma (Davis et al., 1985) and probably correlate with the Handy Lake Group. Distinctly older (2775 Ma) mafic to felsic rocks of the Fourbay Lake cycle (Davis et al., 1988) may be correlative with the Jutten Group. Recent work (see Sanborn-Barrie et al., 1998) shows possibly younger sedimentary sequences and a similar polyphase deformation history to the Savant Lake belt. At the eastern margin of the granitoid complex is the Obonga Lake greenstone belt (Thurston, 1967), whose southern panel comprises a calc-alkaline arc sequence with an age of 2730 Ma (D.W. Davis and M. Moore, unpub. rept., 1991). Tectonic contacts have been postulated to separate this arc from ocean-floor basaltic rocks in adjacent panels to the north (Tomlinson et al., 1996).

STRUCTURAL-PLUTONIC SEQUENCE IN THE CENTRAL WABIGOON REGION

Virtually all granitoid rocks in the region are deformed to some extent; most are polydeformed (Fig. 2). The main penetrative fabric is a S_3 foliation, commonly accompanied by concordant granitic veins. D_1 and D_2 structures are preserved locally, marked by notably complex F_2-F_3 interference patterns. The S_3 foliation is deformed into map-scale upright F_4 folds with associated minor folds and rodding lineations. These are in turn affected by open F_5 warps. A summary of age relationships between major and minor intrusive units and deformation events is presented in Table 1.

Tonalitic gneiss is the oldest unit, recognized on the basis of unique and complex fold interference patterns. Where best preserved, the thinly-layered (S_1) biotite-quartz-plagioclase gneiss has concordant leucogranite and pegmatite veins, folded into moderately north-plunging F_2 folds (Fig. 3, 4). These structures are transected by mafic (Fig. 5) and tonalitic (Fig. 6) dykes involved in subsequent phases of deformation (D_3-D_5; Table 1), yielding common composite fabrics (e.g. Fig. 3-6).

Minor screens of supracrustal and associated rock occur within a few kilometres of greenstone belts, as concordant enclave trains adjacent to the Sturgeon belt and as on-strike extensions of the Obonga belt. These <200 m wide bodies of amphibolite and mafic gneiss (hornblende-plagioclase± clinopyroxene±garnet) display rare primary layering, pillows, local gossans and relict gabbroic textures. The internal foliation is generally parallel to the fabric of enclosing plutonic rocks. Rare north-trending folds of primary layering are assigned a D_2 age (Table 1).

Most of the remaining map units are relatively homogeneous plutonic bodies, with prominent S_3 foliation and sporadic S_3 gneissosity. The most common is biotite (10-15%) granodiorite, a medium grained, foliated rock which grades to migmatitic gneiss with up to 15% concordant granitic leucosome veins on a 1-3 mm scale. Biotite tonalite is more mafic (15-25% biotite), with similar textural characteristics, including migmatitic zones. Tonalite and granodiorite occur as intrusive sheets; crosscutting relationships were not observed. Foliated to gneissic biotite (5-10%) monzogranite is a relatively minor unit, forming younger, concordant, sub-map-scale bodies.

Two additional map units carry S_3 foliation without granitic leucosome, possibly a function of bulk composition or younger age. Hornblende-biotite granodiorite is homogeneous and medium grained, whereas porphyritic granodiorite (Fig. 7) contains up to 40% K-feldspar phenocrysts less than 2.5 cm long. Hornblende-biotite monzodiorite varies from foliated to massive and shows local gradational relationships to hornblende-bearing granodiorite.

The prominent regional foliation S_3, defined by mineral alignment and sporadic concordant leucosome, is variably developed in homogeneous plutonic rocks and older gneisses. Its attitude ranges from steep and concordant to the margin of the Sturgeon Lake belt, to subhorizontal (Fig. 2). Associated minor structures have not been recognized in homogeneous plutonic rocks, although F_3 folds are developed in older gneissic units (e.g. Fig. 4). In a few places, relics of the older gneissic layering are virtually transposed into S_3, making distinction of the two generations of structures in gneissic rocks hazardous. For this reason, Figure 2 shows large areas of undistinguished S_1/S_3 foliation. Judging by its subhorizontal orientation in the hinges of upright F_4 folds (see below), the S_3 fabric probably had subhorizontal attitudes. The association of the grain-scale S_3 foliation with concordant granitic leucosome veins and their regional extent suggest that the D_3 fabrics formed during metamorphism rather than as igneous flow lamination related to emplacement of the granitoid rocks.

Dykes of pegmatite discordant to S_3 foliation are ubiquitous throughout the region, and at least three ages have been recognized based on crosscutting relationships (pegmatite #2, #3, #4; Table 1). Where affected by outcrop-scale D_4 structures, pegmatite #2 dykes can be identified. These include coarse monzogranites with magnetite clusters up to 2 cm. Small (1-2 km) ovoid bodies of coarse leucogranite, some with abundant magnetite, are of similar relative age to the pegmatites and may be related.

Structures of D_4 age dominate the map pattern (Fig. 2) and the regional F_4 fold geometry is illustrated in cross-section in Figure 8. These open to close, upright folds generally plunge gently (10-20°) east-northeast. Associated minor structures include quartz rodding lineations (Fig. 9), spatially associated with F_4 hinge zones, asymmetric minor folds, and outcrop-scale ductile shear zones (Fig. 10). Gently-plunging rodding lineations are particularly well developed on ductile shear planes, indicating dominantly transcurrent motion. Where attitudes of minor fold hinges and rodding are measurable in close proximity on an outcrop, they are subparallel. In some fold limbs the shear zones appear sympathetic to the asymmetry of minor folds. In other locations they form conjugate sets indicating a horizontal north-northwest-south-southeast principal shortening direction consistent with the shortening vector inferred from F_4 folds. Some folds exhibit sheared limbs, both at outcrop and map scales. In the Wapikaimaski Lake area, steeply dipping fold limbs are characterized by ductile shear fabrics which involve pegmatite #2 dykes. Sinistral transcurrent movement is indicated by small-scale ductile shear zones, minor folds with consistent S-asymmetry, as well as C/S fabrics (Fig. 7) and rotated K-feldspar phenocrysts in porphyritic granodiorite. A subset

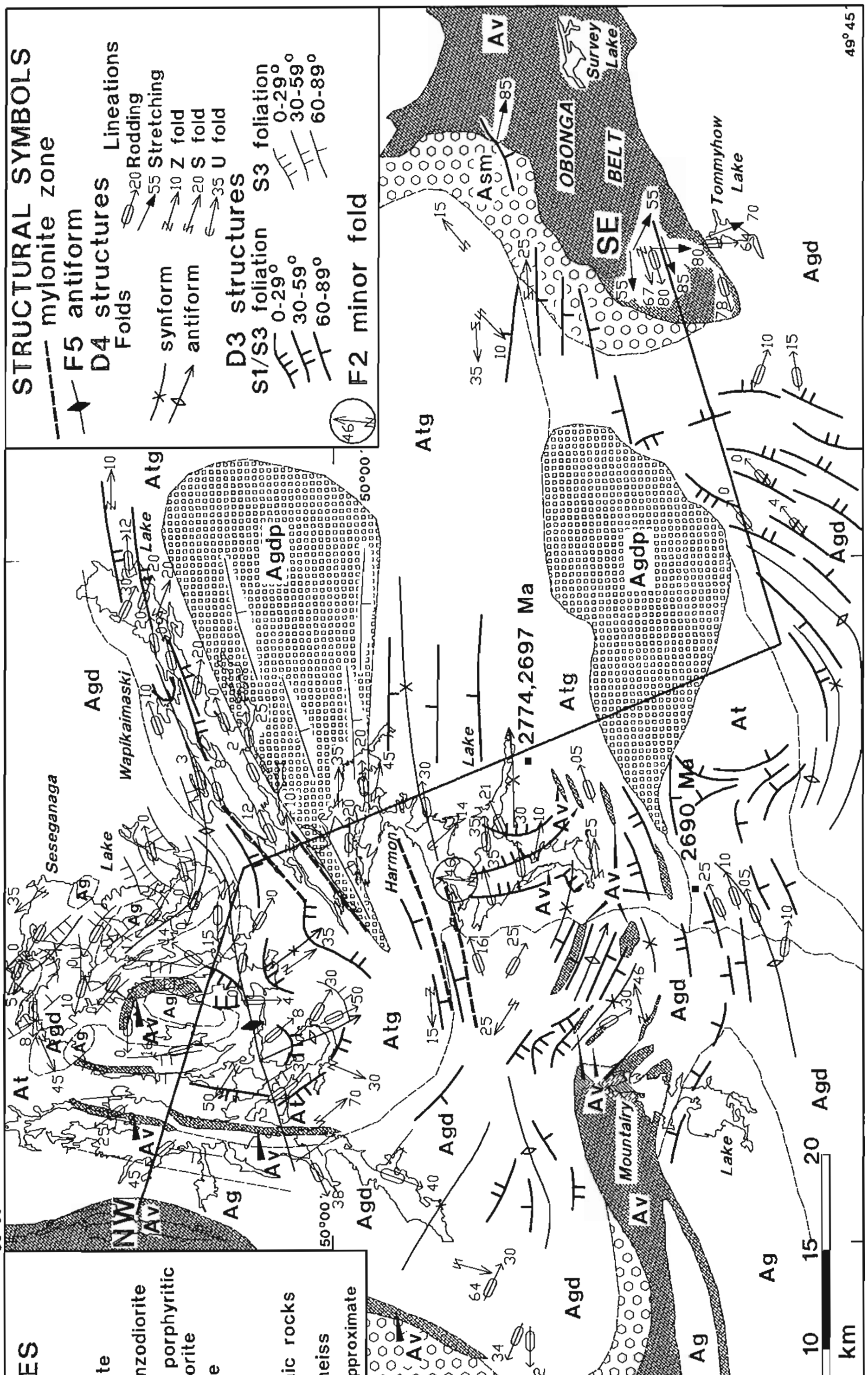

Figure 2. Summary geological map of the transect corridor showing major structural features. Representative structural measurements from the writer's 1997 field observations were augmented by Rogers' (1964) map. See Table 1 for a summary of chronological relationships and Figure 8 for a northwest-southeast cross-section.

of D_4 structures is associated with ductile shear zones showing normal displacement. A few kilometre-scale zones in the eastern Seseganaga Lake area are characterized by subhorizontal (<5° dip) foliation and horizontal rodding lineations (Fig. 2).

The map-scale D_4 structural geometry is an antiform-synform-antiform triplet, with a wavelength of about 30 km (Fig. 8). Major map-units appear as 5-10 km thick, laterally continuous tabular bodies on the flanks of the F_4 folds. A generalized vertical structural profile of the geometry following D_3 deformation extracted from Figure 8 has basal sheets of

Table 1. Summary of age relationships between intrusive and deformational events in the central Wabigoon region. Units in bold text correspond to major map units in Figure 2.

Intrusive unit	Deformation event	Style	Photograph	Age (Ma)
	D_5	Open E-W F_5 warps		
Pegmatite #4				
Pegmatite #3, aplite			Fig. 10	
Granite-basalt complex			Fig. 11	
	D_4	Upright ENE, NW F_4 folds; ductile shears; rodding lineations	Fig. 9	
Granite, Pegmatite #2				
K-feldspar porphyritic hornblende Granodiorite			Fig. 7	
Granitic veins				
	D_3	subhorizontal to subvertical penetrative S_3 foliation		
Biotite granodiorite				
Biotite tonalite				2690
Tonalite dykes			Fig. 6	
Mafic dykes			Fig. 5	
	D_2	N-trending F_2 folds	Fig. 4	
Pegmatite #1				
Supracrustal rocks				
	D_1	S_1 gneissosity	Fig. 3	2697
Tonalite gneiss				2774

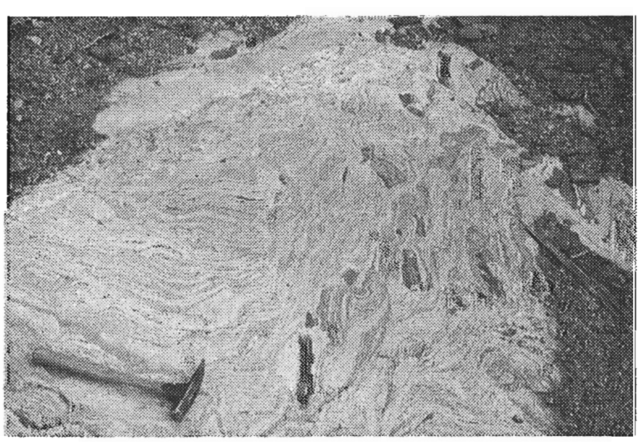

Figure 3. Refolded folds in tonalitic gneiss west of Harmon Lake. The S_1 gneissosity is deformed by F_2 and F_3 folds. Note pegmatite and tonalite dykes in the upper left corner of the photograph. Hammer is 30 cm long.

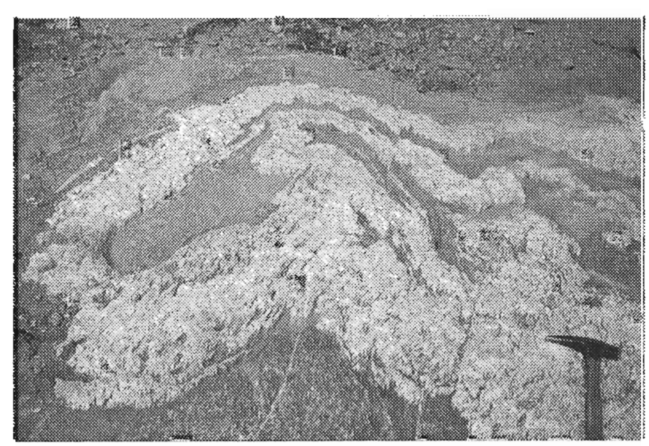

Figure 4. Refolded fold of pegmatite cutting dioritic gneiss west of Harmon Lake. The hammer handle, oriented east-west, lies parallel to a S_3 cleavage axial planar to F_3 folds. The F_2 fold defined by the pegmatite closes to the south (left).

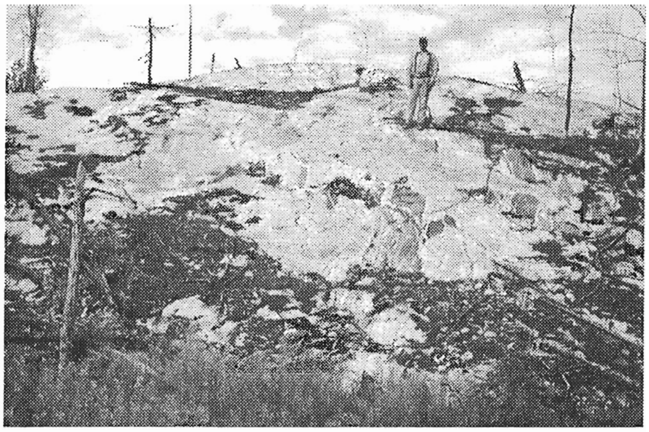

Figure 5. Complex gneissic outcrop in northern Harmon Lake showing steeply-dipping mafic screens in tonalitic gneiss. A train of mafic dyke boudins trends subhorizontally across the central part of the outcrop and is itself cut by a bifurcating dyke of monzogranite pegmatite.

Figure 6. Complex outcrop of tonalitic gneiss in central Harmon Lake showing cross-cutting relationships. A north-trending dyke of biotite tonalite (following the vertical axis of the photograph) cuts tonalite gneiss with prominent S_1 gneissosity and a north-plunging F_2 fold (15 cm pen lies parallel to F_2 axial trace). The dyke margin is warped by open F_5 folds and transected by a pegmatite dyke at the top of the frame.

granodiorite and tonalite, structurally overlain by porphyritic granodiorite and syenite-monzodiorite complexes. Structurally higher are the supracrustal rocks of the Sturgeon and Obonga belts and their possible continuations as screens and trains of mafic enclaves. The uppermost structural level is represented by tonalitic gneiss containing relics of the older (D_1, D_2) structural elements.

Several intrusive phases postdate D_4 structures. West of Harmon Lake, a 8 m wide granite dyke carries mafic enclaves which show evidence of magma mingling. The basaltic enclaves have massive, hornblende-porphyritic interiors and chilled margins with lobate-cuspate geometry, in contrast to shapes of country-rock xenoliths (Fig. 11). This dyke is cut by later aplite dykes which elsewhere commonly crosscut ductile D_4 shear zones (Fig. 10). In one location, two generations of granitic dykes (pegmatite #3, #4; Table 1) were observed to postdate D_4 shear zones.

At the map scale, an east-northeast-trending F_5 antiform in central Seseganaga Lake separates northwest-plunging F_4 folds to the north from southeast-plunging structures to the south. On the outcrop scale, open, east-trending warps with 2-5 m wavelengths deform S_1 (Fig. 6, 9) and S_3 foliations and L_4 lineations (Fig. 9) in domains with northerly trends. The temporal relation between pegmatite #3 and #4 dykes and the D_5 structures is uncertain.

High-strain zones occupying linear, northeast-striking valleys in the eastern Wapikaimaski Lake area (Fig. 2) affect all of the pegmatites and therefore represent the youngest ductile deformation events in the region. Although generally poorly exposed, these zones of steep mylonitic fabric appear to be relatively narrow (<30 m). Stretching lineations are not well developed. Z-shaped folds and offsets on microfractures in K-feldspar on horizontal exposures indicate a component of dextral transcurrent displacement.

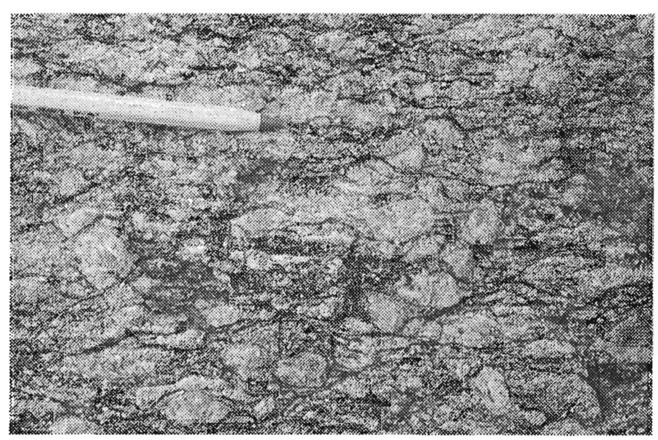

Figure 7. K-feldspar porphyritic granodiorite showing C-S fabric development in a D_3 sinistral high-strain zone, western Wapikaimaski Lake. Pen is 7 mm wide.

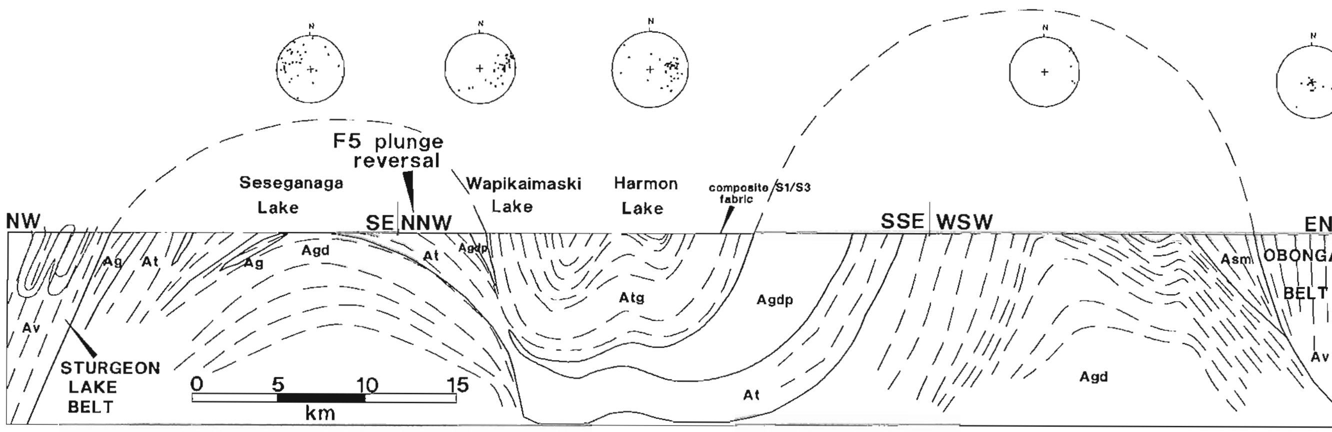

Figure 8. *Northwest-southeast vertical structural cross-section between the Sturgeon and Obonga belts. Although not a rigorous down-plunge projection, major F_4 folds, defined by S_3 foliation trajectories (dashed lines), plunge gently (stereonets are projections of L_4 rodding and minor fold axis lineations) approximately perpendicular to the plane of the section. The dashed line above the surface is the projection of the main contact between greenstones and granitoid rocks. This shows tonalitic gneisses in the Harmon Lake area to structurally overlie the greenstones, and sheets of younger granodiorite, tonalite, and syenite-monzodiorite as generally structurally lower in the section. Although the syenite-monzodiorite suite rocks carry a foliation concordant to regional S_3 and they are interpreted as tabular bodies, their intrusive form could equally as well be crescentic pod-like bodies as inferred by Schwerdtner et al. (1983). Generalized F_2 folds in the Sturgeon Lake belt from Sanborn-Barrie et al. (1998).*

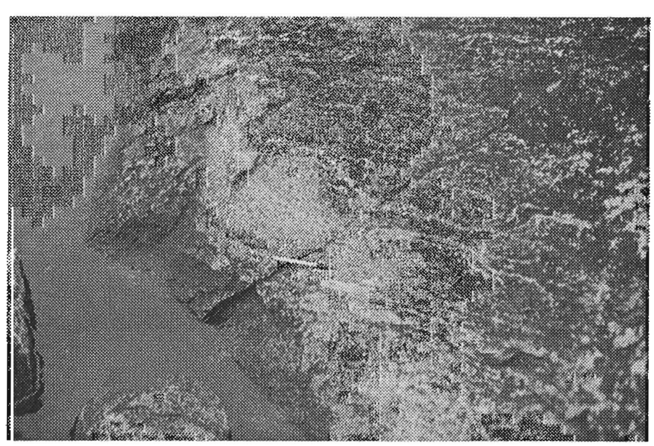

Figure 9. *Subhorizontal L_4 rodding lineation developed in migmatitic tonalite, western Seseganaga Lake. The deflection in trend is the result of open F_5 folds.*

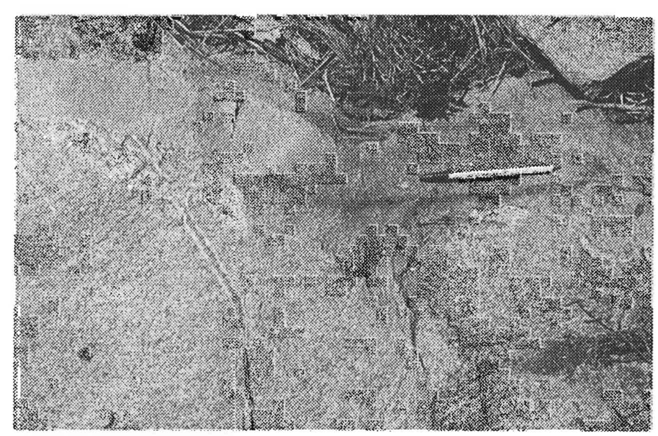

Figure 10. *Outcrop illustrating complex structural-intrusive relationships in biotite granodiorite. The relatively homogeneous rock carries a S_3 biotite-alignment foliation (subhorizontal in photograph) cut by a sinistral S_4 shear (vertical in photograph), itself cut by an aplite dyke. The aplite also cuts two older generations of monzogranite: a diffuse, coarse grained patch; and a younger, sharp-walled dyke whose relative ages with respect to the S_4 shear are not exposed.*

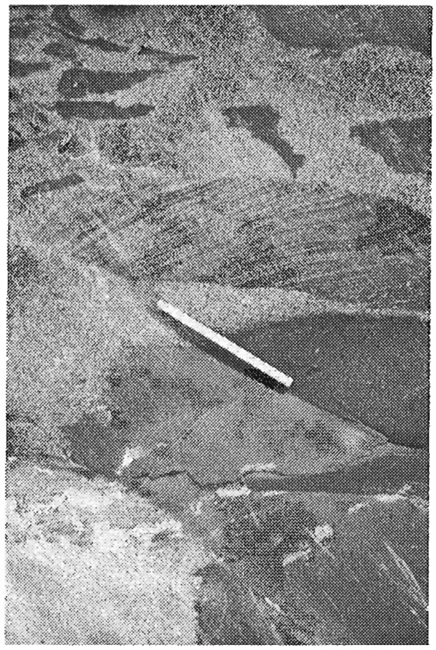

Figure 11. Granite-basalt complex west of Harmon Lake. This distinctive dyke shows evidence of magma mingling between the matrix of medium grained, biotite monzogranite and fine grained, hornblende-porphyritic basaltic enclaves with chilled, cuspate margins. The shapes and textures of basaltic enclaves contrast with those of country-rock mafic gneiss xenoliths.

Still younger brittle faults and fractures are sporadically developed in the eastern part of the region. Commonly epidote filled, these vertical zones trend east-southeast and display consistent dextral offset.

OBSERVATIONS ON THE WESTERN OBONGA BELT

The Obonga Lake greenstone belt is a linear east-striking zone of deformed supracrustal rocks (Thurston, 1967). Recent geochemical and geochronological studies have revealed considerable stratigraphic complexity in volcanic rocks that are partly equivalent in age (ca. 2730 Ma; D.W. Davis and M. Moore, unpub. rept., 1991; Tomlinson et al., 1996) to the calc-alkaline sequences of the Sturgeon-Savant belt. Plutonic rocks at the southern margin of the belt are considerably older (2931 Ma) than the supracrustals, although no unconformity is preserved (Cortis et al., 1988). Potential regional stratigraphic and structural correlations are hampered by a lack of geochronology and structural observations.

In the Tommyhow Lake area (Fig. 2), a high-strain zone forms the southern contact of the Obonga belt with homogeneous granodiorite to the south. The foliated granodiorite contains enclaves of strongly foliated gabbro, cut by straight-walled, fine grained, gabbro dykes with chill margins. These may be similar to those described by Cortis et al. (1988) as possible feeders to the volcanic pile. Strain increases over a 100 m wide zone in the granodiorite toward phyllonitic rocks of the southern Obonga belt. These fine grained phyllonites carry a steep down-dip lineation and shallow-plunging, north-verging folds suggesting south-over-north displacement. The southern 2 km of the belt is characterized by intense, locally mylonitic or phyllonitic cleavage and associated moderately to steeply plunging stretching and mineral lineations, as well as minor folds. Lithologically, the volcanic succession is dominated by homogeneous quartz-feldspar porphyry, with some intermediate pyroclastic rocks, minor greywacke-argillite, and gabbro. One pyroclastic breccia unit contains a heterogeneous 1-10 cm clast population dominated by felsic volcanic fragments but including gabbro with internal foliation discordant to the tectonic fabric in the matrix. This observation suggests that the basement to the calc-alkaline volcanic suite contained deformed gabbro, an abundant component of lithotectonic panels in the Obonga belt to the north (Tomlinson et al., 1996). Bedding is preserved locally in sedimentary units, where it is isoclinally folded about steeply plunging hinge lines and transposed into a strong, east-northeast-striking cleavage. Similar zones of intense cleavage development also occur internal to the belt. In central Survey Lake, a 200 m wide east-northeast-trending phyllonite zone has down-dip stretching lineations and narrow (10 m) marginal strain gradients to less deformed mafic and ultramafic protoliths. Its central corridor is a late fault breccia.

Near the northern margin of the Obonga belt, primary volcanic and sedimentary structures are locally preserved despite a strong cleavage-forming event and andalusite-grade metamorphism. Bedding is isoclinally folded about moderately to steeply plunging (55-75^{o}) hinges and is transposed parallel to east-northeast-striking cleavage. Late gabbroic rocks such as the Awkward Lake pluton (Thurston, 1967) are cut by thin, locally crenulated shear zones and appear much less deformed than the supracrustal units.

It is difficult to evaluate the precleavage (S_2?) history of the Obonga belt. It could host an earlier (D_1) set of structures like those documented through structural facing analysis in the Sturgeon-Savant belt (Sanborn-Barrie, 1990; Sanborn-Barrie et al., 1998). However, the intense degree of transposition into the east-northeast cleavage and associated obliteration of primary facing indicators makes similar treatment of parts of the Obonga belt virtually intractible.

DISCUSSION

The broad NATMAP objective of elucidating the relationship between supracrustal rocks and potential sialic basement can be partly addressed through correlation between structural elements of the Sturgeon-Savant belt and central Wabigoon region. The correlations presented in Table 2, based on similarities in style and orientation, represent a conceptual framework subject to geochronological testing. From this analysis it is apparent that the greenstone and granitoid domains have experienced a common polyphase deformation

Table 2. Correlation between structural elements of the Sturgeon-Savant greenstone belt and granitoid rocks of the central Wabigoon region.

Sturgeon-Savant			Central Wabigoon Region	
Event	**Style**		**Event**	**Style**
-	Open E-W warps of eastern margin	=	D_5	Open E-W warps
-	Regional S_2 trend variations	?	D_4	Upright, open to close folds; shear zones
D_2	F_2 folds, penetrative foliation: NE (Savant) to NNE (Sturgeon)	=	D_3	Penetrative grain-scale foliation; migmatitic layering
D_1	Upright F_1 folds: NNW (Savant) to WNW (Sturgeon)	=	D_2	Tight north-trending F_2 folds
D_0	Cryptic deformation in Jutten Group (pre-Savant Lake Group)	?	D_1	Gneissosity in tonalite gneiss

history which has obscured original relationships. Clearly, a challenge lies in deconvolving the structural record to establish the earliest, most cryptic linkages.

The clearest geometrical link between the two domains is provided by concordant, approximately 70° west-dipping fabrics (mainly S_2) along the eastern margin of the Sturgeon belt and the dominant foliation (S_3) in adjacent granitoid rocks west of Seseganaga Lake (Fig. 2). This map-scale observation is reflected at the outcrop scale, where the (S_2?) foliation in enclaves of supracrustal rock is concordant with the S_3 fabric in enclosing tonalite and granodiorite.

In terms of overall geometry, the structural cross-section (Fig. 8) illustrates a folded (F_4), sheet-like distribution of units, including supracrustal rocks. Reconstruction of the pre-F_4 geometry would produce subhorizontal attitudes not only for the S_3 fabric in the granitoid rocks, but also for S_2 and F_2 in the greenstone belts, with implied subsequent folding (equivalent to F_4 in the granitoid complex). Prominent regional variations in the trends of D_2 fabric elements within the Sturgeon-Savant belt (Table 2) might be attributed to such an event, although macroscopic folds postdating D_2 fabrics have not been recognized. Undulations of the interface between the Sturgeon-Savant greenstone belt and granitoids to the east (Fig. 1, 2) could represent open (about 30 km wavelength) warps about easterly axes corresponding to the east-trending F_5 warps recognized in the granitoid complex (Table 2).

The origin of the S_3 foliation of inferred initial subhorizontal orientation in the granitoid complex requires further discussion. Grain-scale biotite alignment is accompanied in some units by millimetre-scale granitic leucosome, suggesting that the fabrics developed during metamorphism and not in response to magmatic flow or emplacement-related processes. Similarly, superposition of S_3 on older ($D_{1,2}$) fabric elements in tonalite gneiss is consistent with a tectonic origin. Diapiric processes have been proposed for emplacement of the central Wabigoon granitoids (Edwards and Sutcliffe, 1980; Thurston and Davis, 1985) and some data from the Sturgeon-Obonga transect may support this hypothesis. The intense cleavage and strong vertical stretches recorded in the Obonga belt are consistent with predictions of high strain and vertical extension in a subsiding medium (Dixon and Summers, 1983). However, in the Sturgeon-Savant belt, the well preserved nature of primary features presents conflicting evidence. Within the granitoid complex, the dominant folds (F_4) have vertical, rather than horizontal axial surfaces, and are symmetrical (Fig. 8), as opposed to the cascading geometry expected at the flanks of a rising diapir. Most of the observed lineations relate to F_4 folds, and in any case do not correspond to the radial extension pattern expected in the core of a diapir. Folds related to the D_3 event would be more relevant, but these are rare and restricted to rocks with pre-existing heterogeneities. If the S_3 fabric formed through vertical shortening in the crest of a diapir, it has been subsequently folded.

Alternative mechanisms for producing subhorizontal fabrics include ductile horizontal extension (cf. Moser, 1994) and shear in nappe limbs or related contractional décollements. There is limited evidence for extensional deformation in eastern Seseganaga Lake, in the form of small-scale ductile normal faults. Their structural style resembles that of transcurrent D_4 shear zones, implying a D_4 age. However, the age of transcurrent faults relative to the normal shear zones was not directly observed, and the normal structures could be older. Evidence for nappe-like geometry is sparse and limited to map-scale observations. The reconstructed structural cross-section in Figure 8 places tonalitic gneiss structurally above supracrustal rock, as would be the case in the lower limb of a nappe if the gneisses were basement or a major thrust fault. A test of this model through consistency of fold asymmetry is hampered by the lack of F_3 structures in these dominantly homogeneous plutonic rocks. Schwerdtner (1990) cited consistently south or southeast-verging folds in support of a model of subhorizontal shear in the Rainy Lake area of the southwestern Wabigoon subprovince.

Correlation between structures predating the penetrative foliation (D_2 in greenstones; D_3 in granitoids) is highly speculative, as these are commonly cryptic owing to poor preservation. On the basis of the few F_2 folds observed in the granitoid gneisses, this set of north-trending structures could correspond to the map-scale northwest-trending F_1 folds of the Savant Lake area (Sanborn-Barrie, 1990) and west-northwest-trending F_1 folds of the central Sturgeon Lake belt (Sanborn-Barrie et al., 1998). A test of this hypothesis will be provided by the age of post-F_2 tonalitic dykes in the Harmon Lake area (e.g. Fig. 6), which should be younger than <2705 Ma, the minimum age for F_1 folds in the Savant belt. Still more speculative is correlation between even older structures. Early deformation of the Jutten Group (i.e. tilting) prior to deposition of the Y Ma Savant Lake Group, but older than the F_1 folds, has been inferred on the basis of angular unconformities ("D_0", Table 2; Sanborn-Barrie, 1990). However, the style and age of this event are unknown. Its possible correlation with the D_1 gneissosity of the central Wabigoon region (Table 2) will remain speculative until the ages of both events are known. Further analysis of the structural styles of deformation events, with resolution of their tectonic significance and relative and absolute ages where possible, will accompany future mapping.

ACKNOWLEDGMENTS

Christian Sasseville provided capable and thought-provoking field assistance. Jeff Harris produced GIS files for the region and contributed many field observations on Seseganaga Lake. Don Davis shared unpublished geochronological results on the Harmon Lake area. Perceptive reviews by Mary Sanborn-Barrie, Steve Lucas, and Cees van Staal helped clarify observations and interpretations.

REFERENCES

Cortis, A.L., Stott, G.M., Osmani, I.A., Atkinson, B., and Thurston, P.C.
1988: A geological re-evaluation of northwestern greenstone belts; in Summary of Field Work and Other Activities 1988; Ontario Geological Survey, Miscellaneous Paper 141, p. 25-52.

Davis, D.W. and Jackson, M.
1988: Geochronology of the Lumby Lake greenstone belt: A 3 Ga complex within the Wabigoon subprovince, northwest Ontario; Geological Society of America Bulletin, v. 100, p. 818-824.

Davis, D.W., Krogh, T.E., Hinzer, J., and Nakamura, E.
1985: Zircon dating of polycyclic volcanism at Sturgeon Lake and implications for base metal mineralization; Economic Geology, v. 80, p. 1942-1952.

Davis, D.W., Sutcliffe, R.H., and Trowell, N.F.
1988: Geochronological constraints on the tectonic evolution of a late Archean greenstone belt, Wabigoon subprovince, northwest Ontario; Precambrian Research, v. 39, p. 171-191.

Dixon, J.M. and Summers, J.M.
1983: Patterns of total and incremental strain in subsiding troughs: experimental centrifuged models of inter-diapir structures; Canadian Journal of Earth Sciences, v. 20, p. 1843-1861.

Edwards, G.R. and Sutcliffe, R.H.
1980: Archean granitoid terranes of the western Superior Province; Geological Association of Canada, Program with Abstracts, v. 5, p. 50.

Moser, D.M.
1994: The geology and structure of the mid-crustal Wawa gneiss domain: a key to understanding tectonic variation with depth and time in the late Archean Abitibi-Wawa orogen; Canadian Journal of Earth Sciences, v. 31, p. 1064-1080.

Rogers, D.P.
1964: Metionga Lake area; Ontario Department of Mines, Geological Report 24, 53 p.

Sage, R.P., Breaks, F.W., Stott, G.M., McWilliams, G.M., and Robertson, D.
1974: Operation Ignace-Armstrong; Obonga Lake-Lac des Iles sheet, District of Thunder Bay; Ontario Division of Mines, Preliminary Map P.963, scale 1 inch to 2 miles.

Sanborn-Barrie, M.
1990: Geology of the Savant Lake area; in Summary of Field Work and Other Activities 1990; Ontario Geological Survey, Miscellaneous Paper 151, p. 22-30.

Sanborn-Barrie, M., Skulski, T., and Whalen, J.B.
1998: Tectonostratigraphy of central Sturgeon Lake, Ontario: deposition and deformation of submarine tholeiites and emergent calc-alkaline volcano-sedimentary sequences; in Current Research 1998-C; Geological Survey of Canada.

Schwerdtner, W.M.
1990: Structural tests of diapir hypotheses in Archean crust of Ontario; Canadian Journal of Earth Sciences, v. 27, p. 387-402.

Schwerdtner, W.M., Stott, G.M., and Sutcliffe, R.H.
1983: Strain patterns of crescentic granitoid plutons in the Archean greenstone terrain of Ontario; Journal of Structural Geology, v. 5, p. 419-430.

Thurston, P.C.
1967: Obonga-Leigh Lakes area (west half), District of Thunder Bay; in Summary of Field Work, 1967, (ed.) E.G. Pye; Ontario Department of Mines, Miscellaneous Paper 11, p. 29-30.

Thurston, P.C. and Davis, D.W.
1985: The Wabigoon diapiric axis as a basement complex; in Summary of Field Work and Other Activities 1985; Ontario Geological Survey, Miscellaneous Paper 126, p. 138-141.

Thurston, P.C., Osmani, I.A., and Stone, D.
1991: Northwestern Superior Province: review and terrane analysis; in Geology of Ontario, (ed.) P.C. Thurston, H.R. Williams, R.H. Sutcliffe, and G.M. Stott; Ontario Geological Survey, Special Volume 4, Part 1, p. 81-144.

Tomlinson, K.Y., Thurston, P.C., Hughes, D.J., and Keays, R.R.
1996: The central Wabigoon region: petrogenesis of mafic-ultramafic rocks in the Steep Rock, Lumby Lake and Obonga Lake greenstone belts (continental rifting and drifting in the Archean); in Western Superior Transect Second Annual Workshop (ed.) R.M. Harrap and H. Helmstaedt; Lithoprobe Report 53, p. 65-73.

Geological Survey of Canada Project 970014

New observations on the French River alkaline syenite complex, Bigwood township, Ontario

K.L. Currie

Continental Geoscience Division, Ottawa

Currie, K.L., 1998: New observations on the French River alkaline syenite complex, Bigwood township, Ontario; in Current Research 1998-C; Geological Survey of Canada, p. 137-143.

Abstract: The French River alkaline syenite complex comprises two lenses of nepheline-bearing gneiss and associated peralkaline syenite within migmatitic biotite granite gneiss of the Britt Domain of the Grenville Province. The southern lens forms a shallow synform of biotite dominant gneiss about 4 km long and 800 m wide. The northern, amphibole-dominant lens forms part of the western limb of a synform. The equivalent horizon on the eastern limb is occupied by peralkaline amphibole syenite and garnet-pyroxene granulite, and the core of the synform is formed of megacrystic granite. Neither lens exhibits relicts of igneous texture. Both are associated with peralkaline syenite and appear to be structurally disconformable with surrounding gneiss. These data suggest that much of the nepheline gneiss may have formed by sodium metasomatism along low-angle fault planes with alkalies possibly derived from peralkaline syenite.

Résumé : Le complexe de syénite alcaline de French River comprend deux lentilles de gneiss néphélinique et de syénite hyperalcaline associée au sein de gneiss granitique migmatitique à biotite du Domaine de Britt de la Province de Grenville. La lentille sud se présente en synforme peu profonde de gneiss à biotite dominante d'environ 4 km de longueur et 800 m de largeur. La lentille nord, où domine l'amphibole, fait partie du flanc ouest d'une synforme. L'horizon équivalent sur le flanc est est constitué de syénite à amphibole hyperalcaline et de granulite à grenat-pyroxène, le noyau de la synforme étant constitué de granite mégacristallin. Aucune des deux lentilles ne présente de reliques de texture ignée. Les deux sont associées à des syénites hyperalcalines et semblent être en discordance structurale avec le gneiss environnant. Ces données laissent supposer qu'une bonne partie du gneiss néphélinique s'est formée par métasomatose sodique le long de plans de faille à faible pendage, les éléments alcalins provenant peut-être de la syénite hyperalcaline.

INTRODUCTION

Nepheline-bearing gneiss, which forms a minor but distinctive rock in the Grenville Province, has generated a quantity of literature disproportionate to its volume. The classic occurrences of the Haliburton-Bancroft region have drawn most attention, but nepheline gneiss also occurs close to the Grenville Front, including the French River alkali syenite complex (Hewitt, 1960). Occurrences in the Haliburton-Bancroft region form the subject of an ongoing debate on the relative importance of alkaline igneous intrusion versus metasomatism in their generation. In a recent contribution to this debate, Hanmer and McEachern (1992) proposed that much of the nepheline gneiss formed by action of metasomatising solutions channelled along a crustal-scale boundary. Currie and van Breemen (1996a, b) demonstrated major metasomatism associated with the Kipawa Syenite Complex, and noted that it marks both the Archean-Proterozoic contact and the base of far-travelled Grenville allochthons in a region a few kilometres south of the Grenville Front. These observations suggest that other nepheline-bearing metamorphic rocks need to be re-examined in order to determine the role of metasomatism in their formation, and the structural and tectonic significance of this metasomatism.

GEOLOGICAL SETTING

Bigwood Township lies within the northern part of the Britt Domain of the Grenville Province (Davidson et al., 1982; Culshaw et al., 1991), less than 20 km south of the Grenville Front Tectonic Zone, and about 70 km south-southeast of Sudbury. Nepheline gneiss and related rocks form a north-trending lens about 11 km long extending from the south shore of the French River to the northern boundary of Bigwood Township (Fig. 1). Nepheline was discovered by

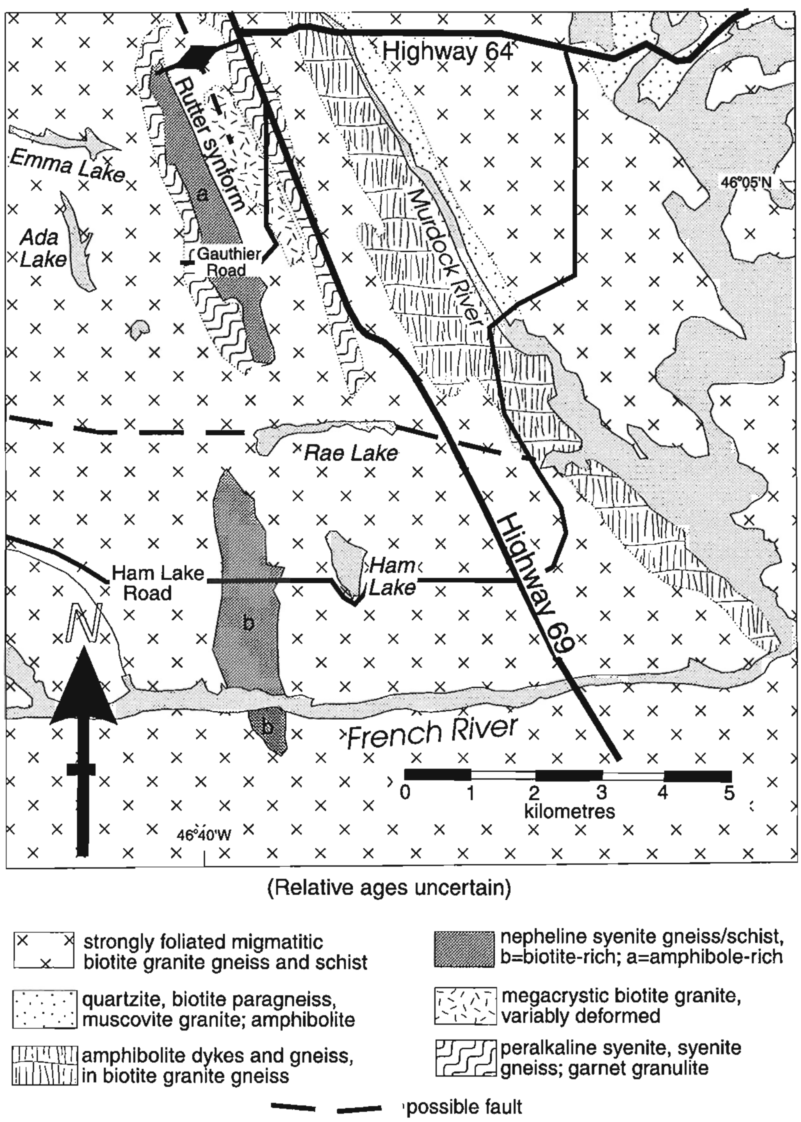

Figure 1. Geological sketch of the French River alkaline syenite complex and surrounding rocks(modified from Hewitt, 1960)

Quirke (1926), and the usual flurry of papers followed, as summarized by Hewitt (1960), who mapped the township at a scale of 1:15 840 as part of a summary study of nepheline-bearing rocks in the Grenville Province. Hewitt (1960) published several whole-rock chemical analyses of the rocks while Duke and Edgar (1977) published a limited number of mineral analyses. Little further work has been done on the nepheline gneiss despite relatively good exposure and easy access, probably because a plethora of linear swamps make it difficult to traverse across the body or to sample it in a systematic way.

Hewitt (1960) distinguished three major rock units in the vicinity of the gneiss, namely (1) a pervasive granite gneiss complex, (2) paragneiss, and (3) syenite gneiss (including the nepheline-bearing varieties). Hewitt also distinguished various granite sheets within the gneiss complex. The present study added several mappable lithologies to this list, namely (4) a mafic dyke complex, (5) a hornblende syenite-garnet granulite association, and (6) megacrystic granite.

Granite gneiss complex

The granite gneiss complex which underlies about 80% of Bigwood Township can be studied in hectare-scale exposures along Highway 69, in almost continuous outcrop in the gorge of the French River, and almost anywhere in between where it appears in abundant, glacially polished outcrops. In its typical form the complex consists of grey to pink, homogeneous quartz-microcline-plagioclase-biotite rock with colour index <25, foliated at millimetre scale but lacking segregation layering. Biotite occurs as fine, disseminated crystals and as polycrystalline spindles defining a pronounced lineation. The rock typically contains 10 to 30% of much coarser grey to pink leucogranite sheets 2 to 10 cm thick which exhibit little foliation and may be massive. Biotite is the common mafic mineral in the sheets, but amphibole, sometimes in large grains, is also abundant. Although generally concordant to the foliation, these sheets locally crosscut the host, and locally exhibit intricate folding including intrafolial folds and sheath folds. The most pervasive and systematic small structure is asymmetric folding indicating dextral south-over-north motion along gently south-dipping surfaces.

This foliated migmatitic unit contains a variety of enclaves ranging from metre-scale to mappable size. All map units described below are found as enclaves within the gneiss complex, although some are rare. In many cases the enclaves are difficult to detect among the monotonous gneisses, so that their numbers are probably larger than presently known.

Transposed mafic dykes

The most common enclaves within the granite gneiss complex are boudins or zones of mafic rocks, ranging in size from about 1 m by 10 m to a zone west of Murdock River, 800 m wide and 7 km long, in which 40% of the rock is mafic. The freshest mafic rocks comprise granoblastic, massive amphibole-plagioclase varieties, either as metre-scale boudins with surrounding foliation wrapping around them, or as partially transposed dykes still cutting the foliation at a low angle. Other types of mafic rock contain various amounts of quartz and potassium feldspar, as well as amphibole variously coated and replaced by biotite. Some occurrences have been reduced to centimetre-scale biotite-amphibole seams in the surrounding gneiss. All of the amphibolitic rocks contain seams or irregular veinlets and patches of granite.

Hewitt (1960) considered the zone west of Murdock River to be paragneiss. However traverses in this region found no trace of verifiable paragneiss, and most of the mafic rocks clearly represent transposed mafic dykes.

Paragneiss

Paragneiss occurs along both shores of the Murdock River in the form of quartzite and associated biotite gneiss which form a belt about 200 m wide and almost 10 km long. On the west side of the river, quartzite is in sharp conformable contact with overlying mafic rocks described above. East of the river quartzite rests on strongly deformed biotite gneiss, which in turn apparently rests on the granite gneiss complex, although the actual contact is not exposed. A few islands in the river, and a narrow zone exposed in a road cut on Highway 64, consist of mafic garnetiferous amphibolite.

The quartzite forms layers 2 to 15 cm thick, commonly slightly feldspathic and muscovitic, and separated by septa of biotite schist from 1 to 10 cm thick. A distinctive pink, coarse muscovite granite forms part of the sequence. The quartzite in general appears almost massive, but complex curving folds, commonly with steep northerly plunges, can be traced in a few locations. The biotite gneiss below the quartzite appears to have been strongly migmatized, but the granite layers have been reduced to strung-out porphyroclasts and boudins in a wavy matrix composed of quartz, feldspar, and abundant bioitite. Numerous quartz and pegmatite veins cut this matrix at high angles. These were the only crosscutting quartz and pegmatite veins observed in this region.

Red aplitic granite

Subdivision of granitic bodies within the granite gneiss complex could be made in several ways. I have generally followed the classification of Hewitt (1960) and distinguished red aplitic granite and granodiorite (termed by Hewitt (1960) the Rutter granodiorite), alkali syenite (lumped by Hewitt (1960) with the Rutter granodiorite), syenite gneiss associated with granulitic rocks (inaccurately termed by Hewitt (1960) "garnet syenite"), and megacrystic granite (a variety not distinguished by Hewitt (1960)). A fifth category, hornblende granite pegmatite sheets, is here included with the granite gneiss complex, again following Hewitt's (1960) classification.

Red aplitic granite forms numerous sheets and lenses within the granite gneiss complex, ranging up to 50 m wide and 400 m long. These rocks essentially consist of massive, granoblastic quartz and feldspar with only a few flakes of biotite. In general they form concordant sheets within the gneiss, but in detail most of them cut the foliation. They can be readily recognized by bright colour and lack of foliation. West of

Bigwood Township this rock forms large plutons. Hewitt (1960) grouped this rock with a peralkaline syenite surrounding the north end of the French River syenite complex, presumably because of similar red colour and lack of foliation, but the composition and mode of occurrence of the two units is quite different.

Megacrystic granite

A low-strain augen of almost undeformed megacrystic granite outcrops along Gauthier Road in a body almost 2 km long and 200 m wide. This rock consists of ovoid feldspars up to 3 cm long within a subgraphic intergrowth of quartz, feldspar, and amphibole. Pegmatoid lenses with feldspar crystals up to 10 cm long occur locally. At the western boundary with the gneiss complex foliation becomes progressively more intense across 10 m and the amphibole is replaced by biotite. Similar metre-scale high-strain zones occur within the low-strain augen. The eastern boundary is not well exposed, but at least 10 m of the granite gneiss complex occurs between the megacrystic granite and the syenite-granulite association described below. Megacrystic rocks similar or identical to this enclave were observed in kilometre-scale masses west of the map area.

Peralkaline quartz syenite

Red amphibole syenite fringes the northern end of the nepheline gneiss belt, extending south from the northern boundary of Bigwood Township for more than 5 km and locally reaching a width of 400 m. This lithology was not found south of Rae Lake. The rock is coarse grained, brick red, and consists of quartz, microcline, albite, amphibole, and minor biotite and magnetite. The rock lacks foliation, but exhibits a well-developed lineation defined by amphibole. Hewitt (1960) grouped this rock with the red aplitic granite, presumably on the basis of colour and lack of foliation, but a chemical analysis quoted by Hewitt (1960) shows that the syenite is strongly peralkaline (normative acmite 9.24%). The amphibole must therefore be an alkaline variety, not hornblende as reported by Hewitt (1960). Mineral analyses published by Duke and Edgar (1977) suggest that it may be an unusual silica-poor, potassium- and iron-rich variety (potassian taramite in the terminology of Commission on New Minerals and Mineral Names, 1997).

Syenite gneiss and granulite

Syenite gneiss and granulite outcrop in a belt 200 m wide and 5 km long extending from Highway 64 to Rae Lake. The western, or syenitic portion of this belt comprises white to pale pink, medium grained syenite gneiss, layered on a scale of 2 to 5 cm with granoblastic feldspar-rich layers separated by thinner layers composed of 40% weakly oriented amphibole and 60% granular feldspar. The texture and mineralogy strikingly resemble the northern part of the nepheline gneiss, but no nepheline was found in these rocks.

The eastern, or granulitic, part of the belt comprises coarsely granoblastic, lineated but unfoliated garnet- and pyroxene-bearing rocks with the greasy tan tinge typical of granulites. Many occurrences are pure L-tectonites with strong lineation defined by complex mafic clusters dominated by clusters of pyroxene prisms containing scattered equant granules of garnet. In salic varieties, garnet forms subhedral centimetre-scale porphyroblasts and minor biotite is present. Some mafic rocks also contain minor amphibole, presumably secondary after pyroxene.

Despite the striking difference in texture, the contact between the syenite gneiss and the garnet-pyroxene granulites is conformable and abruptly transitional. The sequence is abruptly truncated to the east by a linear swamp beyond which the granite gneiss complex reappears. Rare boudins of the granulitic rocks occur within the granite gneiss complex southeast of Rae Lake.

Hewitt (1960) referred to these rocks as "garnet syenite" which is not correct since the syenitic rocks do not contain garnet and the garnetiferous rocks are not syenitic.

Nepheline-bearing gneiss

Nepheline-bearing gneisses in Bigwood Township occur as a northern, amphibole- dominant lens, and a southern biotite-dominant lens, as noted by Hewitt (1960). Syenitic gneiss lacking nepheline is intimately associated with the nepheline-bearing varieties and is described with them.

The southern lens can be examined in almost continuous outcrop in the gorge of the French River, and in moderately good outcrop along the Ham Lake road. The rocks are grey, L>S tectonites exhibiting extreme rodding and lineation plunging about 15° to the southeast. A weak gneissosity defines a very shallow syncline with limb dips <20°. The lens terminates south of the French River where the plunge locally reverses. The rocks are medium grained, granoblastic, and friable, with the simple mineralogy plagioclase, nepheline, biotite, and commonly minor amphibole. Diffuse patch pegmatites occur sporadically with rounded pale orange nepheline up to 5 cm across, and scattered occurrences of grey corundum, yellow cancrinite, graphite, and a few flecks of sodalite. On both east and west sides, grey nepheline-bearing rocks at the base of the gneiss are interlayered at metre scale with pink to red nepheline-free syenite which commonly contains subequal amounts of amphibole and biotite. The red colour is a reliable indicator of the absence of nepheline in the rocks, while the presence of blue-grey spots of "nepheline weathering" is an equally reliable indicator of the presence of nepheline. The mixed zone of nepheline-bearing and nepheline-free rocks is about 5 to 10 m wide, below which the granite gneiss complex reappears. The upper part of the granite gneiss complex contains feldspar patch pegmatites up to 5 m in diametre which contain feldspar crystals up to 10 cm across. These pegmatites cut the foliation, and appear to be completely massive. Many examples contain seams or patches of deep red allanite as well as large amphibole crystals.

Amphibole is more abundant than biotite in the northern lens of nepheline-bearing gneiss, although biotite is commonly present in subordinate amount. The rocks, which display stronger foliation and much weaker lineation than the southern lens, dip moderately (45-65°) to the east and form part of the western limb of the Rutter syncline (Hewitt, 1960). The equivalent position on the eastern limb of this structure is occupied by the syenite gneiss-granulite association.

The nepheline-bearing gneiss of the northern lens forms coarse, granoblastic rocks typified by pale orange nepheline. Patch pegmatites with centimetre-scale nepheline are common but mineralogically simple. Like the southern lens, the northern lens is intercalated on a metre scale with red syenitic rocks which lack nepheline. At the northern end of the nepheline-bearing gneisses, the proportion of nepheline-bearing layers declines rapidly, and the complex reduces to a lens of red amphibole syenite about 800 m wide. This in turn grades by reduction of grain size, as well as increase in foliation and quartz content, into the granite gneiss complex. Along the east side of the northern lens, this contact is hidden by a narrow linear swamp which may mark the trace of a small fault.

Mineral analyses published by Duke and Edgar (1977) showed that biotite in the nepheline syenite approaches the lepidomelane-siderophyllite join, while the amphibole is an unusual silica-poor, potassium- and ferric iron-rich variety (potassian ferritaramite in the terminology of Commission on New Minerals and Mineral Names, 1997). All of the analyses (eight) are much richer in Na than hastingsite, the amphibole identified optically by Hewitt (1960).

STRUCTURE

Hewitt (1960) defined two major folds within Bigwood Township, namely the Rutter syncline and the Ham Lake syncline. Both of these folds are late, relatively simple structures superimposed on complex, poorly known, older folds. They are therefore better described as synforms. The Rutter synform is a well developed, open to close, gently south-plunging structure on the northern boundary of the township. There is no obvious axial plane cleavage. Farther south, the fold is poorly defined on Gauthier Road, where dips are generally steep (>60°). The dip reversal east of Highway 69 defines a structure of different style. The Rutter synform thus appears to be disconformable with its surroundings, as shown in Figure 2.

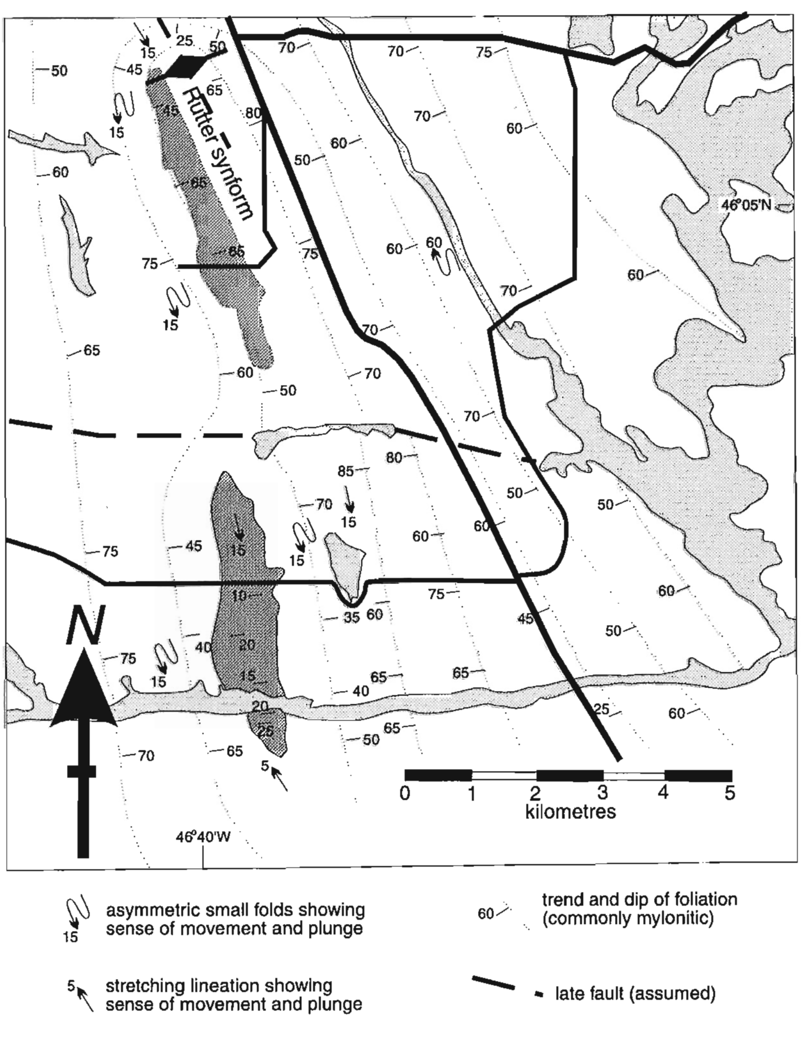

Figure 2.

Representative structural data for the Bigwood Township area. Note that both the shallow synform containing the southern nepheline syenite lens and the Rutter synform appear disconformable with their surroundings. Both are superimposed on steep east-dipping successions.

The Ham Lake synform contains an axial area about a kilometre across where foliation dips less than 25°. Within this area numerous small domes and basins can be recognized. The margins of the axial zone are abrupt, with dips increasing to steep or vertical within a few tens of metres. The eastern margin of the synform, exposed about 300 m east of the lake, displays dips steepening to 90° and passing through vertical, suggesting an overturned fold. Foliation within the southern lens of nepheline syenite defines a shallow synform. The underlying gneisses in this region exhibit a modest flattening of dip, but the axis of the Ham Lake synform lies to the east.

Complex small-scale folding of foliation and gneissosity, including recumbent isoclines and local sheath folds, which are older than the pervasive north-northwest-trending folds can be recognized locally, but no systematic study of these small structures has been made. They are all strongly overprinted and partially destroyed by the intense penetrative lineation which is the most prominent and pervasive structural feature of this region. In general this lineation plunges about 10° towards 150°, but local plunge reversals are present, particularly south of the French River and along Murdock River. According to current tectonic models, this lineation resulted from late, deep-seated southeast over northwest thrusting during final assembly of the Grenville Province (Davidson et al., 1982; Culshaw et al., 1991).

North-northwest-trending, post-lineation faults can be identified east of Ham Lake and in Murdock River. Both are marked by platy fissility and small amounts of crushed rock. In Murdock River local presence of steep north-plunging folds suggests sinistral motion on this feature. However in neither case was the amount of motion sufficient to juxtapose contrasting lithological packages.

The French River and parallel sets of lakes farther north lie in a very strong east-west joint set. Hewitt (1960) noted presence of smears of undeformed diabase in the French River gorge and along Murdock River. He deduced that these features were tensional, with little relative movement of opposite sides. Pseudotachylite veinlets occur along the French River just east of the margin of the nepheline gneiss, suggesting rapid, brittle deformation. Simple plots of foliation trends (Fig. 2) suggest that about a kilometre of dextral movement on the feature through Rae Lake would align synformal axes north and south of the lake, although the style of folds appears to be different.

Hewitt (1960) noted that the nepheline-bearing gneiss marked structural discontinuities with relatively steep dips below, and moderate dips within the nepheline-bearing gneiss and above. In the case of the northern lens, the rocks above the nepheline-bearing gneiss (megacrystic granite and garnet-pyroxene granulite) also exhibit much less penetrative deformation than those below (strongly foliated granite gneiss complex).

DISCUSSION

Mapping of the French River alkaline syenite complex reveals the following facts. (1) The southern lens of nepheline-bearing gneiss forms a thin, flat sheet, probably less than 100 m thick. (2) The northern lens lies on the west limb of a synform, with the stratigraphically equivalent position of the east limb occupied by syenite gneiss and granulites. (3) The core of the synform is mainly composed of megacrystic granite, an exotic lithology in this area. (4) Both bodies of nepheline-bearing gneiss are interleaved with red syenite along their margins. (5) Red colour and feldspathization signify alteration and replacement of nepheline. (6) All rock types (except nepheline-bearing varieties) are found as enclaves in the ubiquitous granite gneiss complex. (7) The nepheline-bearing gneiss forms tabular sheets which lie on, or close to, a transition from steep dips to moderate or low dips. All of these facts were noted by Hewitt (1960) without further comment. However, when considered as a group, they suggest the possibility that the nepheline-bearing gneisses mark a low-angle fault along which a syenite-granulite assemblage over-rode the granite gneiss complex. The large masses of syenite, granulite, and megacrystic granite to the west of Bigwood Township could have been part of this hypothetical assemblage, and enclaves of these lithologies in the ubiquitous granite gneiss complex may indicate tectonic mixing during and subsequent to the supposed juxtaposition. Such a scenario is, at present, entirely hypothetical in the absence of detailed structural studies, but it is compatible with what is known about the structure of the northern Britt Domain.

Even assuming such a scenario, why should nepheline-bearing gneiss form along the junction? It can readily be shown that given a sufficient source of sodium, metasomatic nepheline-bearing rocks will form during metamorphism. Consider the schematic reaction

$$\underset{\text{plagioclase}}{6\ CaAl_2Si_2O_8} + \underset{\text{biotite}}{5\ KAlFe_3Si_3O_{10}(OH)_2} + \underset{\text{quartz}}{12\ SiO_2} + 3\ O_2 + 9\ NaOH =$$

$$\underset{\text{nepheline}}{6\ NaAlSiO_4} + \underset{\text{K-feldspar}}{5\ KAlSi_3O_8} + \underset{\text{hastingsite}}{3\ NaCa_2Fe^{3}Fe^{2}{}_4Si_6Al_2O_{22}(OH)_2} + 2\ H_2O$$

Without attempting quantitative P-T analysis, this reaction is known to proceed to the right with increasing T at moderate P (transition from greenschist to amphibolite grade). Obviously, a necessary condition for such a reaction would be an adequate supply of Na. Such a supply could be furnished by reaction with trapped sea-water (Currie et al., 1986), with Na-rich strata such as evaporite beds (Ayrton, 1974) or with peralkaline igneous rocks (Curtis and Currie, 1981). Only the latter possibility seems at all plausible for the French River alkaline syenite complex, which is known to contain peralkaline syenite.

A metasomatic origin for the nepheline-bearing gneiss of the French River alkaline syenite complex remains highly speculative, but considerably more plausible than it appeared to Hewitt (1960) who rejected the possibility out of hand. Further structural, geochemical, and mineralogical studies are required to elucidate the origin of this complex body.

REFERENCES

Ayrton, S.
1974: Rifts, evaporites and the origin of certain alkaline rocks; Geologische Rundschau 63, p. 430-450.

Culshaw, N., Corrigan, D., Jamieson, R.A., Ketchum, J., Wallace, P., and Wodicka, N.
1991: Traverse of the Central Gneiss Belt, Grenville Province, Georgian Bay; Geological Association of Canada, Toronto meeting, Guidebook for Field trip B3, 32 p.

Currie, K.L. and van Breemen,O.
1996a: The origin of rare minerals in the Kipawa Syenite Complex, western Quebec; Canadian Mineralogist, v. 34, p. 435-451.
1996b: The Kipawa Syenite Complex - an unusual Archean-Proterozoic boundary marker in the Grenville Front Tectonic Zone of western Quebec; Geological Association of Canada Abstracts with Program, v. 21, p. A-20

Currie, K.L., Eby, G.N., and Gittins, J.
1986: The petrology of the Mont Saint Hilaire complex, southern Quebec - an alkaline gabbro-peralkaline syenite association; Lithos, v. 19, p. 67-83.

Curtis, L.W. and Currie, K.L.
1981: Geology and petrology of the Red Wine alkaline complex, central Labrador; Geological Survey of Canada, Bulletin 294, 61 p.

Davidson, A., Culshaw, N.G., and Nadeau, L.
1982: A tectono-metamorphic framework for part of the Grenville Province, Parry Sound region, Ontario; in Current Research, Part A;Geological Survey of Canada, Paper 82-1A, p. 175-190.

Duke, N.A. and Edgar, A.D.
1977: Petrology of the Blue Mountain and Bigwood felsic alkaline complexes of the Grenville Province of Ontario; Canadian Journal of Earth Sciences, v. 14, p. 514-538.

Hanmer, S. and McEachern, S.
1992: Kinematical and rheological evolution of a crustal-scale ductile thrust zone: Central Metasedimentary Belt, Grenville orogen, Ontario; Canadian Journal of Earth Sciences, v. 29, p. 1779-1790.

Hewitt, D.F.
1960: Nepheline syenite deposits of southern Ontario; Ontario Department of Mines, 69th Annual Report, pt. 8, p. 1-194, chapter IV, p. 163-188

Commission on New Minerals and Mineral Names
1997: Nomenclature of amphiboles: report of the Subcommittee on Amphiboles of the International Mineralogical Association, Commission on New Minerals and Mineral Names; Canadian Mineralogist, v. 35, p.219-246.

Quirke, T.T.
1926: Mineral deposits of the Rutter map-area, Sudbury District; Geological Survey of Canada Summary Report for 1924, pt. C, p. 89-95.

Geological Survey of Canada Project 680071

Questions of correlation across the Grenville Front east of Sudbury, Ontario

A. Davidson
Continental Geoscience Division, Ottawa

Davidson, A., 1998: Questions of correlation across the Grenville Front east of Sudbury, Ontario; in Current Research 1998-C; Geological Survey of Canada, p. 145-154.

Abstract: Intensely deformed and highly metamorphosed sedimentary and mafic igneous rocks southeast of the Grenville Front in the Sudbury area contrast strongly with the relatively simply folded, low-grade Huronian Supergroup and associated mafic intrusions in the adjacent Southern Province. Relict stratigraphy on the Grenville side of the front does not appear to correlate with any part of the well-known Huronian succession. It seems likely, however, that the mafic meta-igneous rocks are equivalent to anorthositic gabbro intrusions which occur at the base of the Huronian, and to Nipissing gabbro which intrudes it. If so, the metasedimentary rocks may represent distal facies of the Huronian Supergroup that have been tectonically transported northwestward during Grenvillian or earlier orogeny, or both.

Résumé : Les roches sédimentaires et ignées mafiques intensément déformées et métamorphisées au sud-est du front de Grenville dans la région de Sudbury contrastent fortement avec les roches déformées en plis relativement simples et peu métamorphisées du Supergroupe de Huronian et les intrusions mafiques associées dans la Province du Sud adjacente. La stratigraphie résiduelle du côté grenvillien du front ne semble pas être en corrélation avec une quelconque partie de la succession bien connue de Huronian. Il paraît toutefois vraisemblable que les roches méta-ignées mafiques sont équivalentes aux intrusions de gabbro anorthositiques qu'on trouve à la base du Supergroupe de Huronian, et au gabbro de Nipissing qui le recoupe. Si tel est le cas, les roches métasédimentaires représentent peut-être des faciès distaux du Supergroupe de Huronian qui ont été transportés tectoniquement vers le nord-ouest au cours de l'orogenèse grenvillienne ou d'une orogenèse antérieure, ou bien pendant ces deux épisodes.

INTRODUCTION

Rivers et al. (1989) coined the term "parautochthonous belt" for the northwest marginal part of the Grenville Province in which rocks southeast of the Grenville Front can be correlated with those in the adjacent, older provinces of the Canadian Shield. With few exceptions, superimposed high-grade metamorphism and intense deformation, compounded by relative uplift on the Grenville side, have made it difficult to correlate rock units directly, and the full extent of parautochthonous rocks can only be realized by less direct means (geophysical signature, geochronology). One of the more characteristic rock units in the Grenville foreland is the early Paleoproterozoic Huronian Supergroup in Ontario, a succession locally thicker than 12 km with a well-documented and continuous stratigraphy (see summaries in Card, 1978; Dressler, 1984a; Bennett et al., 1991). It has long been questioned why these rocks are not readily recognized southeast of the Grenville Front.

As shown on the regional geological compilation of Card and Lumbers (1977), rocks of the Huronian Supergroup and spatially associated intrusions of Nipissing gabbro (2.22 Ga; Corfu and Andrews, 1986; Noble and Lightfoot, 1993) underlie most of the immediate Grenville foreland in Ontario (Fig. 1). In the Cobalt Embayment northeast of Lake Wanapitei, little deformed and metamorphosed Huronian sedimentary rocks lie unconformably on Archean rocks of the Superior Province, which are exposed in erosional windows and along the Grenville Front to the northeast. Southwest of Lake Wanapitei, the Huronian rocks become increasingly deformed and variably metamorphosed within the Southern Province fold belt, where they are intruded, particularly near the Grenville Front, by granite plutons of two ages, late Paleoproterozoic (ca. 1.75 Ga) and early Mesoproterozoic (ca. 1.47 Ga).

The Grenville Province adjacent to this region is underlain by high-grade gneissic and migmatitic rocks of both supracrustal and plutonic parentage. Uranium-lead zircon dating and Nd isotopic studies have confirmed that Archean protoliths extend across the front east of Lake Wanapitei (Krogh, 1974; Dickin and McNutt, 1989), and that both ages of Proterozoic granitoid are represented in the orthogneiss units south of Sudbury (Davidson and van Breemen, 1994). In addition, anorthositic gabbro of the River Valley complex (Fig. 1) has been dated at 2.47 Ga (L.M. Heaman, pers. comm., 1994), the same age as obtained for mafic intrusions below the base of the Huronian Supergroup in the Southern Province west of Sudbury (Krogh et al., 1984).

On the basis that rocks both older and younger than the Huronian Supergroup occur on either side of the Grenville Front, it is perhaps surprising that the metasedimentary rocks in this part of the parautochthonous belt bear little or no resemblance, particularly with respect to details of stratigraphic order, to the Huronian Supergroup itself. Various explanations have been offered, among them high-grade metamorphism and metasomatism (Quirke and Collins, 1930), granitization (Phemister, 1961; Grant et al., 1962), and facies change coincident with the front (Lumbers, 1978). However, Frarey (1985, p. 34) was unable to substantiate Quirke and Collins' (1930) "... correlation of individual gneisses or associations of gneisses with known Huronian formations or sequences ..." in the Lake Panache area

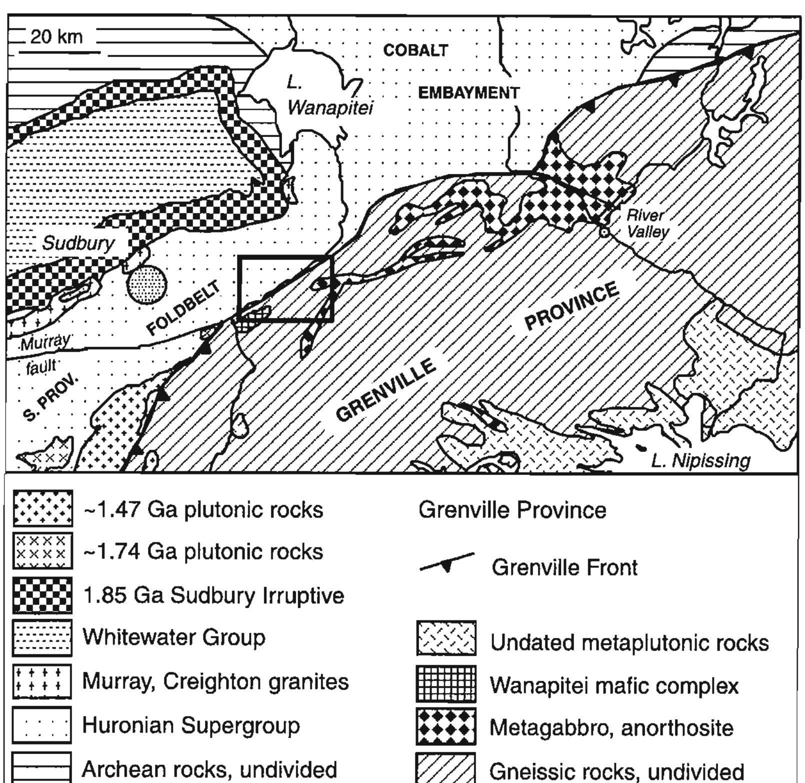

Figure 1.

Regional geological features in the area of the Grenville Front near Sudbury, Ontario. Box shows location of Figure 2.

southwest of Sudbury. Moreover, the granitized sedimentary rocks of Phemister (1961) and Grant et al. (1962) are certainly intrusive granite (Chief Lake batholith; Henderson, 1967; Davidson and Ketchum, 1993), and gneissic rocks interpreted by Lumbers to be coarse clastic facies equivalents to the Huronian are known to contain Archean pegmatite (Krogh, 1974), thus more likely correlative with the Pontiac Group of the Superior Province (Davidson, 1986).

This paper reports the results of detailed remapping on both sides of the Grenville Front east of Sudbury, aimed in part at addressing this question of correlation. The area between Coniston and Stinson summarized in Figure 2 lies within parts of areas mapped by Lumbers (1973, 1975) and Dressler (1987); it includes a small area east of Wahnapitae village formerly mapped in detail by Pearson (1962), and adjoins an area to the northeast (Street Township) recently mapped by Easton et al. (1996).

GRENVILLE FRONT EAST OF SUDBURY

From Coniston dam to Wahnapitae village (Fig. 2), the Grenville Front is coincident with the Wanapitei fault (Phemister, 1961; Davidson, 1992) and lies concealed beneath alluvial cover in a narrow, dry valley. Farther northeast, between Wahnapitae and the Stinson dam, it lies either in the bed of the Wanapitei River or crosses promontories on the south side of the river valley. Ultramylonite and cataclasite are locally exposed at the sides of this topographic lineament and along splays on the south side. Based on the attitude of their foliation, these faults are essentially vertical. Shear-sense indicators in these rocks imply relative uplift of the Grenville side of the fault.

Two and one half kilometres west of Coniston dam, this fault diverges from the Grenville Front and continues westward through Huronian Supergroup sedimentary rocks of the Southern Province, where it is known as the Murray fault (Davidson, 1992). Southwest of this divergence, the Grenville Front is a moderately southeast-dipping mylonite zone as much as 1 km wide, characterized by northwest-directed, thrust-sense displacement (Davidson and Ketchum, 1993). At the divergence, the Wanapitei-Murray fault truncates the Grenville Front mylonite zone and, to the east, metamorphic isograds that are parallel to the front in the Grenville Province (Davidson, 1997, Fig. 3).

ROCK UNITS

Southern Province

The Southern Province immediately north of the Wanapitei fault is underlain by crossbedded sandstone of the 2-3 km thick Mississagi Formation (unit 13; see legend of Figure 2 for all unit numbers) and large, crosscutting, elongate intrusions of Nipissing gabbro (unit 15). Some 3 km north of Wahnapitae village, polymictic conglomerate of the Bruce Formation (unit 14) overlies the Mississagi conformably in the core of a northeast-plunging syncline. Sandstone east of the Bruce conglomerate as far as the Stinson dam was assigned to the Serpent Formation by Dressler (1984c), but this could not be confirmed; all the sandstone in this area is typical of the Mississagi Formation. Metamorphic grade north of the Wanapitei fault probably does not exceed middle greenschist facies. Volumetrically minor units in this region include narrow, irregular biotite tonalite dykes of unknown age (but probably related to ca. 1.75 Ma plutonic rocks farther southwest (Davidson et al., 1992; Sullivan and Davidson, 1993; Davidson and van Breemen, 1994)), southeast-trending olivine diabase dykes of the Sudbury swarm (1.24 Ga; Krogh et al., 1987; Dudás et al., 1994), and east-trending diabase dykes of the Grenville swarm (0.6 Ga; Kamo et al., 1995).

Grenville Province

Bedrock in the adjacent Grenville Province is much more varied (Fig. 2), and quite evidently does not represent a more highly deformed and metamorphosed equivalent of the Mississagi Formation. The predominant rock units include various types of metasedimentary gneiss and schist, among them distinctive units of metaconglomerate (unit 2), kyanite schist (unit 5), quartz-rich metasandstone (unit 7) and minor marble and calc-silicate rock within biotite-hornblende-garnet gneiss (unit 3) and biotite-garnet gneiss and schist (units 4, 6). In most of these rocks, well-defined compositional layering is transposed bedding. Sill-like amphibolite bodies (unit 9) are present within this assemblage. Kilometre-scale masses of migmatitic granitoid gneiss (unit 1) (possibly slivers of Archean rock), cut by small, irregular, metamorphosed mafic dykes, lie close to the Wanapitei fault. They are either separated from the metasedimentary rocks by faults that splay into the Grenville Province or occur in the cores of antiforms.

South of the Wanapitei fault/Grenville Front between Coniston and Wahnapitae, metasedimentary rocks wrap around a 2 km by 5.5 km complex of metamorphosed mafic igneous rocks cut by granite dykes (unit 10, Fig. 2; Wanapitei complex; Rousell and Trevisiol, 1988). This complex has been interpreted as a tectonic lens derived from a formerly larger, layered igneous intrusion (Davidson and Ketchum, 1993). Farther east, south of the Stinson dam and Highway 17, elongate units of metamorphosed gabbro and anorthosite (unit 11) occur within the metasedimentary rocks.

All of the rocks are metamorphosed to upper amphibolite facies (kyanite and/or sillimanite with K-feldspar in pelitic rocks), are commonly coarse grained and variably migmatitic (Fig. 3A, B). Recognizable primary features, either sedimentary or igneous, are very rarely preserved, with the exception of a unit of metasedimentary gneiss (unit 2) close to the Grenville Front southeast of Stinson dam (Fig. 2) which contains metaconglomerate with relatively well-preserved clasts (Fig. 3C). Evidence for a conglomeratic protolith is also present in small, disconnected, non-migmatitic patches in otherwise highly migmatitic gneiss (unit 6) up to 3 km from the front (Fig. 3D). Despite the generally nonmigmatitic nature of thin bedded, quartzitic metasandstone units, however, sedimentary structures such as crossbedding have yet to be identified.

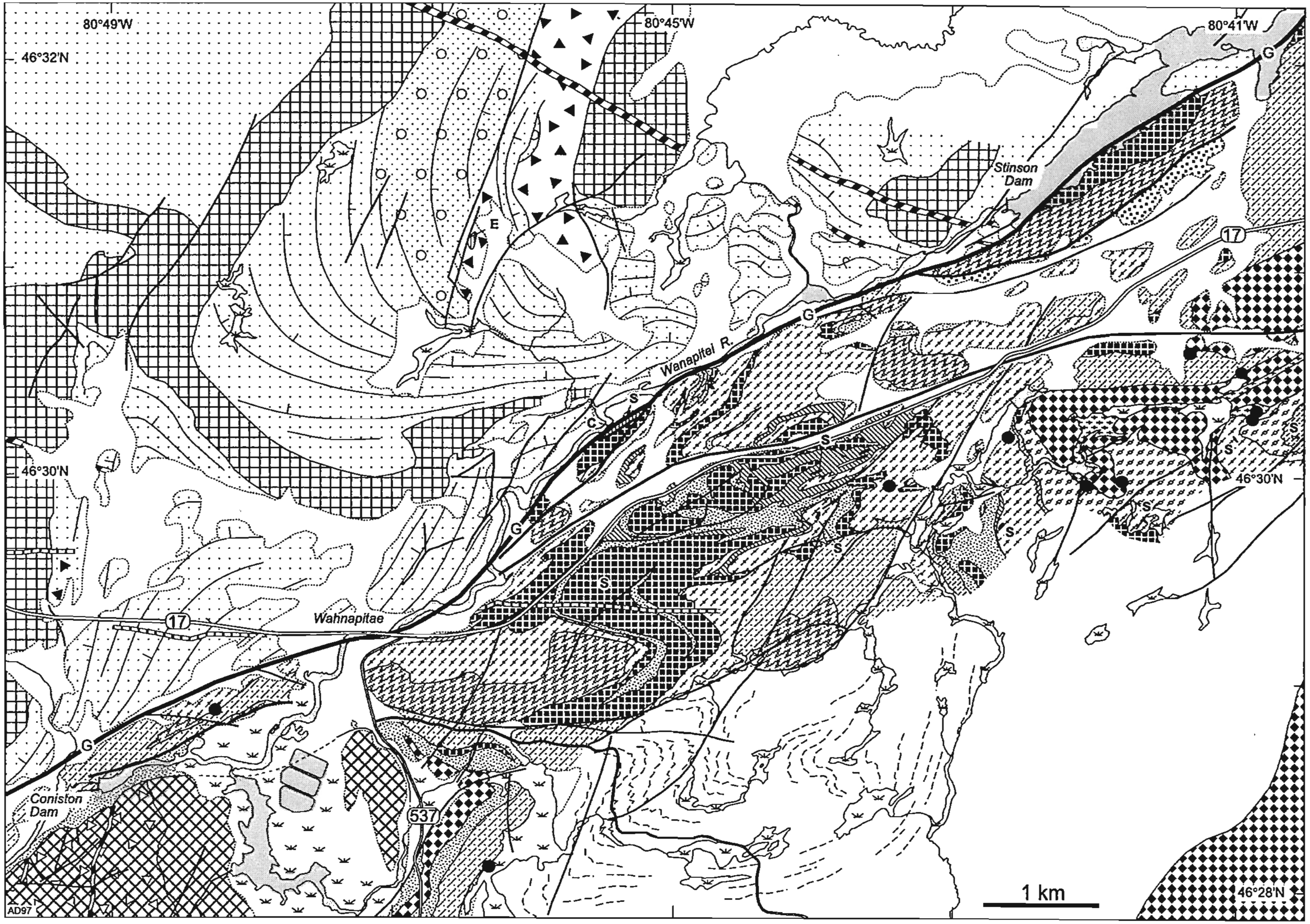

Figure 2. Detailed geology on either side of the Grenville Front (G) in the Wahnapitae area; "C" is fault sliver of marble and calc-silicate at the front. Broken lines at bottom indicate trend of layering from air photographs in unmapped area. Note that unit numbers in the legend do not imply stratigraphic order.

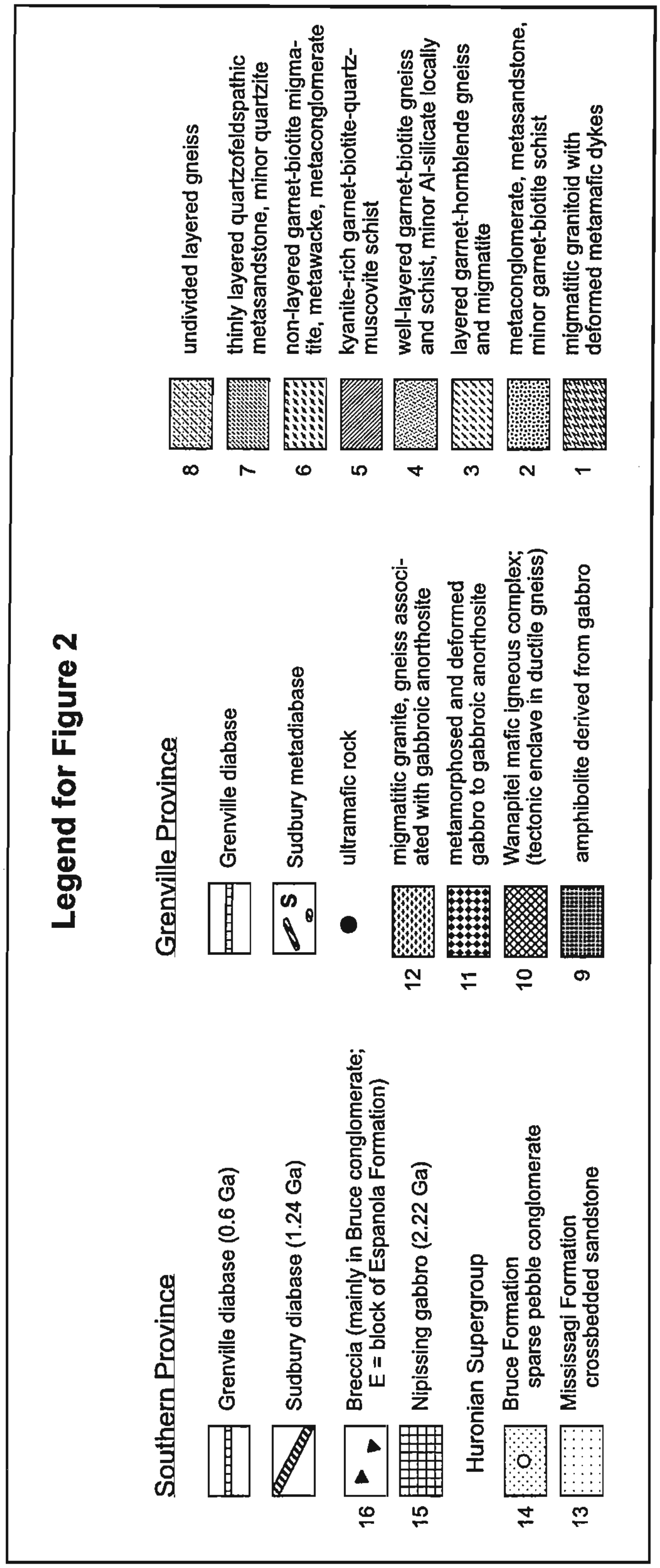

Scattered throughout this region are tectonically isolated pods of ultramafic rock composed of fine green amphibole enclosing centimetre-scale ovoids of orthopyroxene. As well, there are remnants of Sudbury dykes now represented by discontinuous dyke segments composed of coronitic metadiabase (Dudás et al., 1994), and at least two generations of pegmatite, distinguished by their relative state of deformation.

STRUCTURE

Southern Province

Structural styles on opposite sides of the Wanapitei fault/Grenville Front are fundamentally different and not related to one another. Beyond a few hundred metres north of the fault, primary sedimentary structures in Mississagi sandstone are preserved with very little distortion, everywhere allowing unequivocal determination of sedimentary facing direction. For the whole length of the segment of the Grenville Front illustrated in Figure 2, the Mississagi sandstone beds (50 cm to 2 m thick) dip moderately to steeply north away from the Wanapitei fault and face in the same direction. Bedding and fold-related cleavage, weakly developed in silty interbeds, are truncated at the contacts with massive Nipissing gabbro, itself showing no evidence of cleavage or folding. It thus seems likely that the fold pattern exhibited by the Mississagi at least in part predates emplacement of the Nipissing intrusions. The structure is relatively simple – broad, open folds cut by numerous small faults. Some of the faults, particularly those that cut the syncline cored by Bruce conglomerate, are associated with breccia (unit 16) which is now generally agreed to be related to the impact event that gave rise to the Sudbury Igneous Complex (1.85 Ga; Krogh et al., 1984; Dressler, 1984b), a mere 9 km from the Grenville Front at Wahnapitae. Both Sudbury and Grenville diabase dykes pass undisturbed across all these structures.

Approaching the Grenville Front from the north, bedding in the Mississagi Formation becomes thinner and turns abruptly into parallelism within 200 m of the Wanapitei fault. In the few exposures along the south side of the Wanapitei River, Mississagi sandstone is reduced to quartz-ultramylonite with very tight mesoscopic folds and well-developed subvertical lineation, parallel to fold axes. Surfaces of centimetre-scale, transposed and severely flattened beds are coated with fine muscovite. The closest exposures of Nipissing gabbro (200 to 400 m) are extensively fractured and contain small, chlorite-filled shears. Sudbury dykes are offset a few tens of metres along subsidiary faults and show evidence of internal cataclasis in the form of broken feldspar laths and networks of microfaults.

The zone of brittle-ductile deformation associated with the Wanapitei fault, intensifying southward within recognizable Southern Province rocks, is remarkably narrow (<100 m) compared with the extent of such deformation adjacent to the Grenville Front mylonite zone southwest of Coniston. The fault truncates structures on both sides (Fig. 2) and is the locus of an abrupt break in metamorphic grade; there is no obvious increase in grade in the Southern Province rocks along the fault, and the fault rocks themselves contain low-grade assemblages. All of these facts attest to a large component of vertical displacement along the Wanapitei fault at a late stage of Grenvillian orogeny, when the 'Grenville side' was sufficiently cool to have had no clearly discernible thermal effect on the rocks of the Southern Province.

Grenville Province

The region immediately south of the Wanapitei fault is cut by several late faults, characterized by ultramylonite and other brittle-ductile fault rocks, that divide the south wall into several narrow panels. Within the panel containing migmatitic granitoid (unit 1, Fig. 2) south of Stinson dam and also in the smaller occurrence 1.5 km northeast of Wahnapitae, early foliation and parallel leucosomes strike northwest and dip northeast. These are folded and dragged with sinistral sense into parallelism with the bounding mylonitic rocks. In the layered metasedimentary rocks, the youngest and most obvious folds plunge moderately to steeply east and are inclined to the north. Limb attitudes near the Grenville Front are nearly vertical, but change gradually to moderate southerly dip away from the front. All the rocks units outlining these folds are intensely folded internally at centimetre- to metre-scale, the youngest minor folds being parasitic to the predominant map-scale folds. At outcrop scale these folds are commonly seen to refold earlier minor folds (Fig. 4A, B). Nonfoliated leucosome is parallel to the axial planes of the youngest minor folds, and its formation thus appears to have accompanied or outlasted the latest deformation.

Notable examples of ductility contrast occur, particularly in the hinge areas of folds, between different rock types, such as kyanite schist and biotite-garnet gneiss (Fig. 4C) and metasedimentary gneiss and amphibolite (Fig. 4D). In the former example, kyanite schist locally intrudes across layering in the less ductile rocks; in the latter, amphibolite forms detached block or lenses with cut-off internal folds, commonly elongate parallel to the axial surfaces and invaded by a mixture of the adjacent rocks and deformed pegmatite. The extreme mobility of this ductile migmatite is such that around some fold noses it forms a carapace in which structure is decidedly chaotic. In all of this, it is remarkable that certain characteristic units of thinly bedded, quartz-rich metasandstone (Fig. 2),

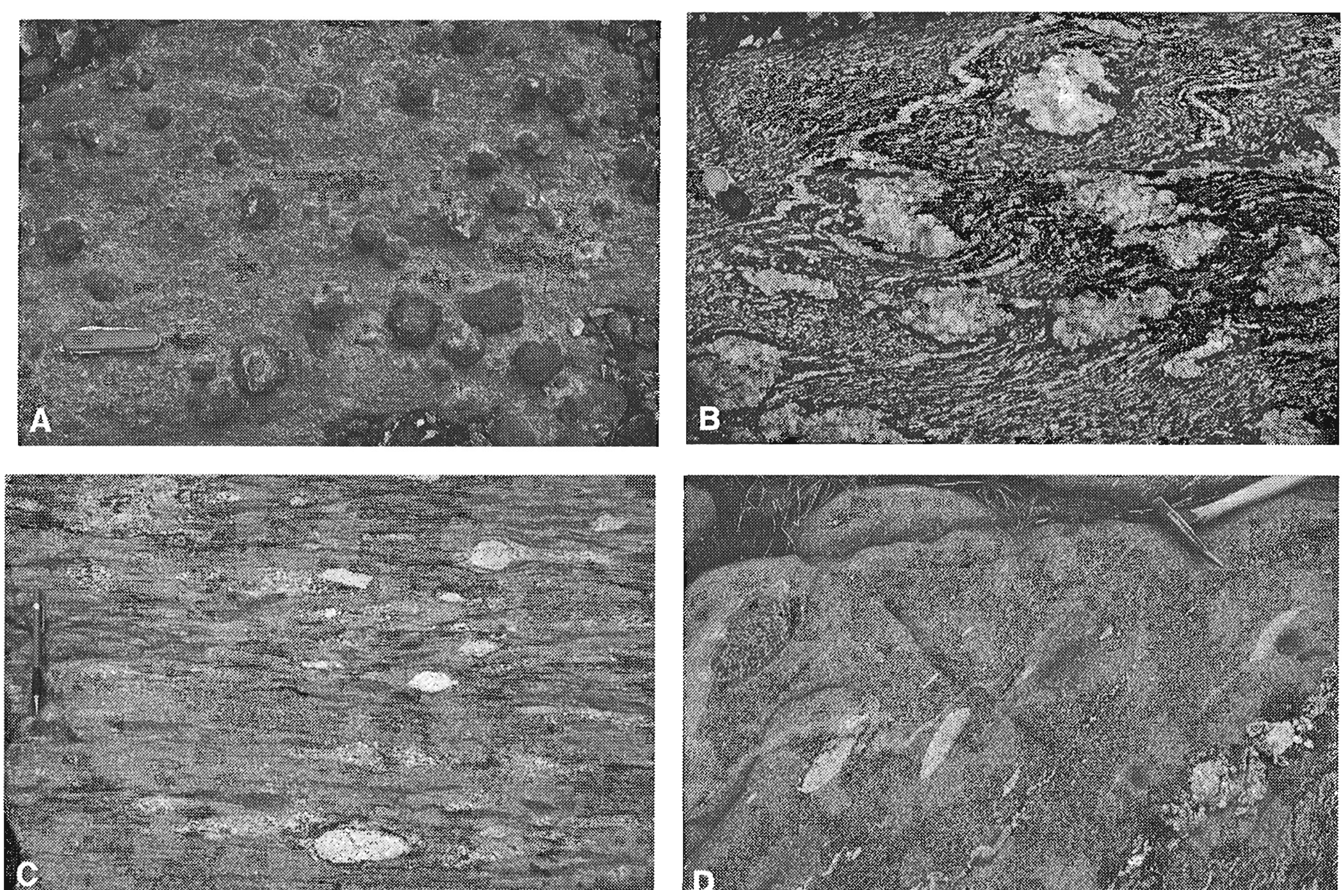

Figure 3. *A) garnet porphryoblasts in quartz-feldspar-biotite rock;* ***B)*** *leucosome in quartz-plagioclase-biotite-hornblende-garnet gneiss;* ***C), D)*** *metaconglomerate respectively 800 m and 3 km from the Grenville Front. Scales: pocket knife 9 cm, open hand lens 5 cm, pen 14 cm, hammer head 17 cm.*

even though exhibiting variable tectonic thinning, can be traced continuously for kilometres, making them valuable units for outlining the overall structure.

Despite continuous and relatively uncomplicated contacts with metasedimentary rocks, the gabbro-anorthosite units (Fig. 2) are internally intensely deformed. Nonfoliated relict igneous texture was noted in very few places. In less deformed parts, igneous layering, outlined by varying proportions of elongate metamorphic hornblende aggregates, is folded at mesoscopic scale, and the folds may be cut by thin metamafic dykes (Fig. 5A). Flattening of networks of mafic dykes in gabbroic anorthosite (Fig. 5B) can lead to development of an intensely striped, black-and-white gneiss, locally replete with small-scale folds (Fig. 5C).

The dominant east-plunging folds throughout the area refold earlier major folds. This is particularly evident in map patterns developed between amphibolite and gneiss east of Wahnapitae, and in the anorthositic gabbro unit south-southeast of Stinson dam, in which granitoid migmatite (unit 12, Fig. 2) forms the core of an earlier major fold. Through-going mylonitic fabric, so characteristic of the Grenville Front zone south of Coniston, is restricted to splays from the Wanapitei fault, which cut the youngest folds. The scattered, isolated remnants of Sudbury diabase dykes entirely wrapped by their country rocks, and perhaps also the ultramafic pods (Fig. 2), attest to a considerable amount of tectonic disruption in this area, provided that these were once continuous dykes. This appears to be at odds with the continuously traceable units within the relict stratigraphy of the enclosing metasedimentary rocks.

RELICT STRATIGRAPHY IN THE GRENVILLE PROVINCE

Several diagnostic metasedimentary units can be traced for considerable distances within the region immediately south of the Wanapitei fault. Among these is a fault-bounded unit containing metaconglomerate which has been traced for almost 3 km. Consistently on the south side of this conglomeratic unit is a dark grey biotite-quartz-feldspar schist with garnet porphyroblasts, which grades southward to a more feldspathic metasandstone, also with scattered garnet.

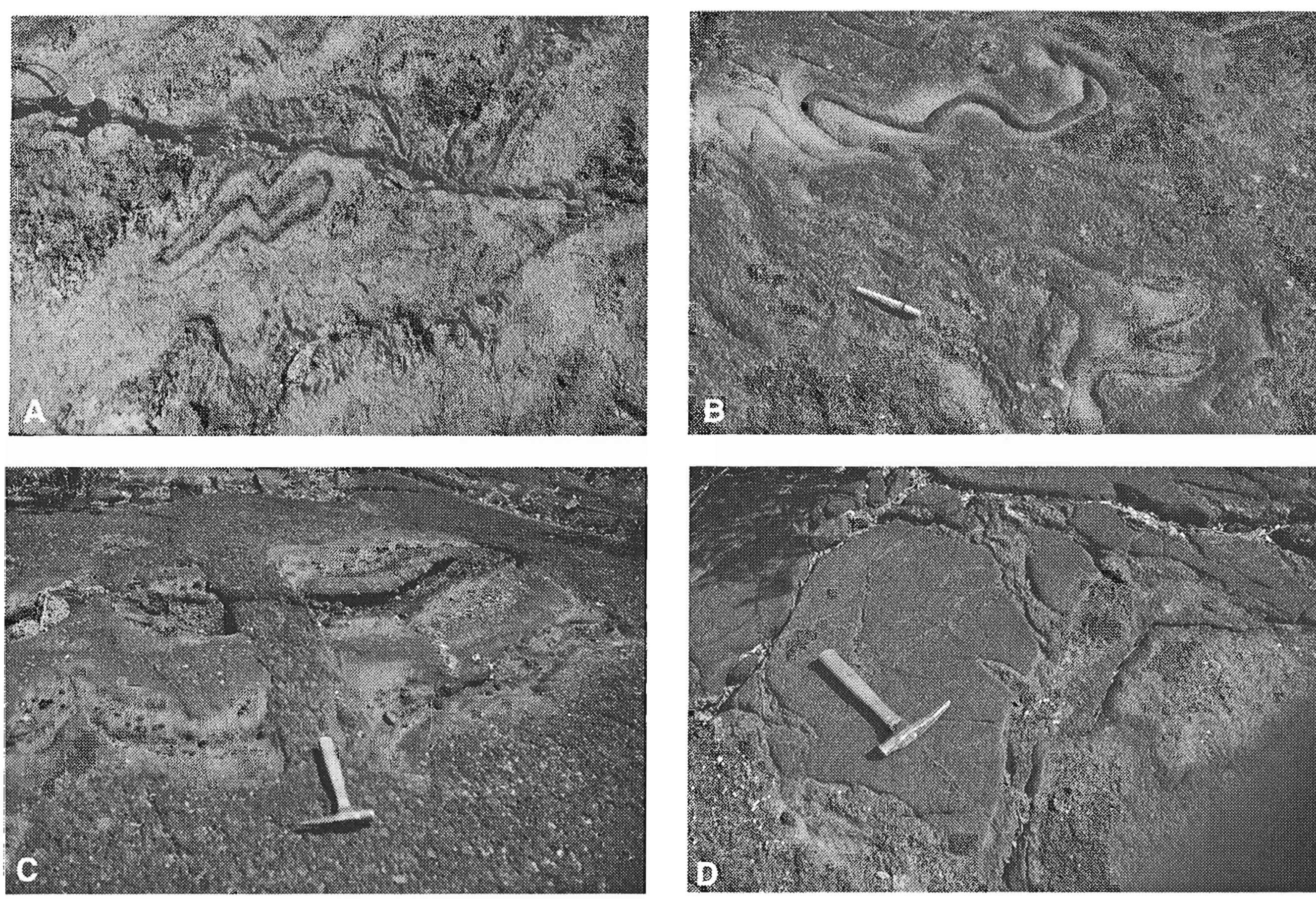

Figure 4. ***A), B)*** *refolded folds in metasedimentary rocks.* ***C)*** *'dykes' of remobilized kyanite schist cut relict bedding in quartz-feldspar-biotite-garnet rock.* ***D)*** *contact between amphibolite and metasedimentary rock.*

The region on either side of Highway 17 east of Wahnapitae contains a unit of coarse, kyanite-rich schist that has been explored for possible exploitation as a source of kyanite and was mapped in detail by Pearson (1962). This characteristic garnet-biotite-quartz-kyanite-muscovite schist is everywhere in contact with a thin (a few metres to less than a metre) but persistent unit of quartzite, which in turn is separated from a thick unit of layered and internally boudined quartz-plagioclase-garnet-biotite-hornblende gneiss by a thin unit of biotite schist with large (≤5 cm) garnet porphyroblasts (as in Fig. 3A). In areas of discontinuous outcrop, this diagnostic relict stratigraphy can be used to determine the respective limbs of major folds, even though there is no indication of facing direction.

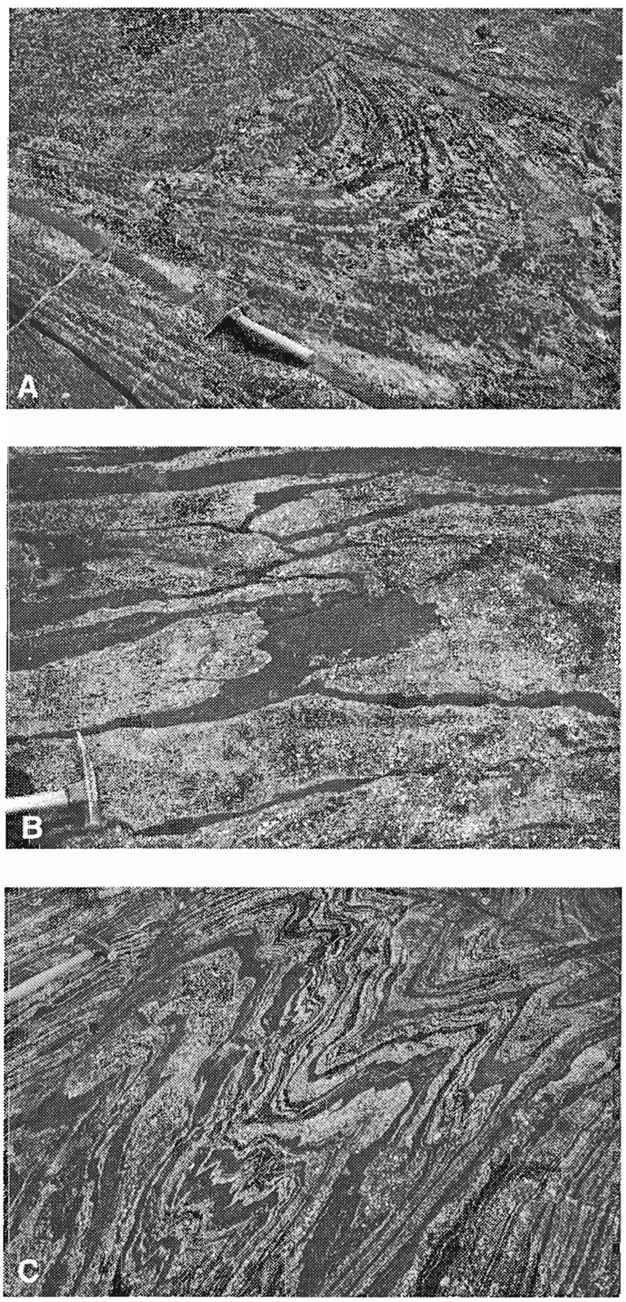

Figure 5. ***A)*** *fold in layered anorthositic metagabbro cut by mafic dyke.* ***B)*** *deformed dyke network in meta-anorthosite.* ***C)*** *intensely deformed and folded equivalent of B.*

In the southeast part of the area, south of Highway 17, elements of a similar relict stratigraphy have been recognized, involving the consistent position of a unit, no more than a few tens of metres thick, of thinly-bedded (centimetre-scale), metamorphosed quartz arenite with a characteristic reddish- to creamy brown-weathering surface. This nonmigmatitic unit is replete with mesoscopic folds, ranging from open to very tight parallel in shape. It lies adjacent to coarse, migmatitic biotite-garnet schist, lacking layering and several tens of metres thick, which in turn grades to layered biotite-garnet gneiss. On the opposing side it is in contact with garnet-hornblende gneiss.

A surprising find during this season's mapping was the exposure in roadcuts and in stripped outcrop in a sand pit of calcareous rocks (grossularite-diopside-plagioclase-scapolite gneiss and diopside-plagioclase marble) which have rarely been identified in natural outcrop in this area, presumably due to their more easily weathered nature. These are intimately interlayered with noncalcareous rocks, including kyanite-bearing and rusty quartz-rich rocks. The association of the calcareous rocks with quartz-plagioclase-garnet-biotite-hornblende gneiss suggests that the latter too is of calcareous sedimentary affinity. On earlier maps (e.g. Grant et al., 1962; Lumbers, 1975), garnet-hornblende gneiss had been included with amphibolite, presumed to be of igneous origin, and not distinguished as a separate metasedimentary unit.

POSSIBLE HURONIAN EQUIVALENCE

It is quite clear that the metasedimentary rocks south of the Wanapitei fault are not the deformed and metamorphosed equivalent of the Huronian strata that lie north of the fault. The rock types of the Mississagi Formation would be expected to give rise to a thick unit of interlayered quartz-rich gneiss and biotitic schist or gneiss, perhaps with garnet but unlikely to carry alumino-silicate minerals. If the metasedimentary rocks south of the fault are indeed correlative with the Huronian, they must then equate with part of the succession above or below the Mississagi. The assemblage in the Grenville Province includes calc-silicate rocks and minor marble. The only Huronian formation that carries appreciable calcareous rock is the Espanola Formation, part of the Quirke Lake Group that overlies the Mississagi Formation (Hough Lake Group). If this correlation is correct, then the calcareous metasedimentary rocks in the Grenville Province should have a unit of metaconglomerate on one side (Bruce Formation) and a thick unit of feldspathic quartz gneiss on the other (Serpent Formation); this is not the case – thick quartz-rich units are absent. The occurrence of kyanite-rich rocks on the Grenville side of the fault suggests correlation with either the Pecors Formation (stratigraphically below the Mississagi) or the McKim Formation (Elliot Lake Group), probably the only two formations in the Huronian succession aluminous enough to give rise to such a concentration of metamorphic kyanite. In the Huronian succession, these two units are separated by the Ramsey Lake conglomerate. However, in the Grenville the rocks associated with the kyanite schist do not match this succession.

Given that Nipissing gabbro is present as large sill-like bodies throughout the Huronian succession, it is tempting to equate the folded amphibolite bodies in the Grenville with this unit, as was suggested by Lumbers (1975, unit 14b). In addition, the anorthositic gabbro unit at the east side of the Figure 2 has been mapped continuously to the east-northeast to join with similar but less deformed rocks at River Valley (Fig. 1; see Card and Lumbers, 1977). Age-equivalent rocks in the Southern Province intrude Archean rocks at the base of the Huronian succession, and are considered to be related to overlying basaltic volcanic rocks of the Elliot Lake Group (Card, 1978). South of the front in the Wahnapitae area, however, rocks adjacent to the anorthositic gabbro are metasedimentary, and no evidence was found for association with metavolcanic rocks.

If the metasedimentary rocks in the Grenville Province south and east of Sudbury are indeed equivalent in age to the Huronian Supergroup, they do not correlate unit by unit with any part of the well known succession of Huronian groups and formations north of the front. It is certain that equivalents of the thick quartz-rich sandstone formations (Mississagi, Serpent, Lorrain, Bar River) are not present in this area. There is little evidence that the succession preserved in the Grenville Province has been either severely thinned (witness the locally preserved conglomerate clasts) or repeated by faulting. As such, one must either fall back on the suggestion of Lumbers (1978) that the present position of the Grenville Front coincides with a marked facies change or, preferably, postulate that the rocks represent a far-travelled package equivalent in age to the Huronian but developed in a distal part of the original depositional basin, emplaced tectonically against the Superior and Southern provinces. Alternatively, if the mafic rocks are not in fact correlative with the River Valley and Nipissing suites, the age of the enclosing metasedimentary rocks is unconstrained, and they may be altogether younger than the Huronian. Clearly, geochronology will play a critical role in solving this problem, provided that the mafic rocks in the Grenville Province retain isotopic evidence of their primary ages.

REFERENCES

Bennett, G., Dressler, B.O., and Robertson, J.A.
1991: The Huronian Supergroup and associated intrusive rocks; in Geology of Ontario, (ed.) P.C. Thurston, H.R. Williams, R.H. Sutcliffe and G.M. Stott; Ontario Geological Survey, Special Volume 4, pt. 1, p. 549-591.

Card, K.D.
1978: Geology of the Sudbury–Manitoulin area, Districts of Sudbury and Manitoulin; Ontario Geological Survey, Report 166, 238 p. and Map 2360, scale 1:126 720.

Card, K.D. and Lumbers, S.B.
1977: Sudbury–Cobalt; Ontario Geological Survey, Geological Compilation Series, Map 2361, scale 1:253 440.

Corfu, F. and Andrews, J.A.
1986: A U-Pb age for mineralized Nipissing diabase, Gowganda, Ontario; Canadian Journal of Earth Sciences, v. 23, p. 107-109.

Davidson, A.
1986: New interpretations in the southwestern Grenville Province; in The Grenville Province, (ed.) J.M. Moore, A. Davidson, and A.J. Baer; Geological Association of Canada, Special Paper 31, p. 61-74.
1992: Relationship between faults in the Southern Province and the Grenville Front southeast of Sudbury, Ontario; in Current Research, Part C; Geological Survey of Canada, Paper 92-1C, p. 121-127.
1997: New developments in Grenville Front geology, Sudbury area, Ontario; Institute on Lake Superior Geology, Field Trip Guidebook, v. 43, pt. 3, 38 p.

Davidson, A. and Ketchum, J.W.F.
1993: Grenville Front studies in the Sudbury region, Ontario; in Current Research, Part C; Geological Survey of Canada, Paper 93-1C, p. 271-278.

Davidson, A. and van Breemen, O.
1994: U-Pb ages of granites near the Grenville Front, Ontario; in Radiogenic Age and Isotopic Studies: Report 8; Geological Survey of Canada, Current Research 1994-F, p. 107-114.

Davidson, A., van Breemen, O., and Sullivan, R.W.
1992: Circa 1.75 Ga ages for plutonic rocks from the Southern Province and adjacent Grenville Province: what is the expression of the Penokean orogeny?; in Radiogenic Age and Isotopic Studies: Report 6; Geological Survey of Canada, Paper 92-2, p. 107-118.

Dickin, A.P. and McNutt, R.H.
1989: Nd model age mapping of the southeast margin of the Archean foreland in the Grenville Province of Ontario; Geology, v. 17, p. 299-302.

Dressler, B.O.
1984a: General geology of the Sudbury area; in The Geology and Ore Deposits of the Sudbury Structure, (ed.) E.G. Pye, A.J. Naldrett, and P.E. Giblin; Ontario Geological Survey, Special Volume 1, p. 57-82.
1984b: The effects of the Sudbury event and the intrusion of the Sudbury Igneous Complex on the footwall rocks of the Sudbury Structure; in The Geology and Ore Deposits of the Sudbury Structure, (ed.) E.G. Pye, A.J. Naldrett, and P.E. Giblin; Ontario Geological Survey, Special Volume 1, p. 97-136.
1984c: Sudbury geological compilation; Ontario Geological Survey, Map 2491, scale 1:50 000.
1987: Falconbridge Township, District of Sudbury; Ontario Geological Survey, Preliminary Map P.3067, scale 1:15 840.

Dudás, F.Ö., Davidson, A., and Bethune, K.M.
1994: Age of the Sudbury diabase dykes and their metamorphism in the Grenville Province; in Radiogenic Age and Isotopic Studies: Report 8; Geological Survey of Canada, Current Research 1994-F, p. 97-106.

Easton, R.M., Buckley, S.G., Lobanok, E., and James, R.S.
1996: Project unit 95-31. Grenville–Southern Province relationships in Street Township, District of Sudbury; in Summary of Field Work and Other Activities; Ontario Geological Survey, Miscellaneous Paper 166, p. 66-69.

Frarey, M.J.
1985: Proterozoic geology of the Lake Panache–Collins Inlet area, Ontario; Geological Survey of Canada, Paper 83-22 and Map 1593A, scale 1:50 000.

Grant, J.A., Pearson, W.J., Phemister, T.C., and Thomson, J.E.
1962: Geology of Broder, Dill, Neelon, and Dryden townships, District of Sudbury; in Ontario Department of Mines, Geological Report 9, p. 1-24.

Henderson, J.R.
1967: Structural and petrologic relations across the Grenville Province – Southern Province boundary, Sudbury District, Ontario; Ph.D. thesis, McMaster University, Hamilton, Ontario, 119 p.

Kamo, S.L., Krogh, T.E., and Kumarapeli, P.S.
1995: Age of the Grenville dyke swarm, Ontario–Quebec: implications for the timing of Iapetan rifting; Canadian Journal of Earth Sciences, v. 30, p. 273-280.

Krogh, T.E.
1974: Orogenic structural and metamorphic overprints: Archean intrusive and metamorphic rocks within a region of 1000 M.Y. deformation and migmatization; Carnegie Institution of Washington, Yearbook 73, p. 569-573.

Krogh, T.E., Corfu, F., Davis, D.W, Dunning, G.R., Heaman, L.M., Kamo, S.L., Machado, N., Greenhough, J.D., and Nakamura, N.
1987: Precise U-Pb isotopic ages of diabase dykes and mafic to ultramafic rocks using trace amounts of baddeleyite and zircon; in Mafic Dyke Swarms, (ed.) H.C. Halls and W.F. Fahrig; Geological Association of Canada, Special Paper 34, p. 147-152.

Krogh T.E., Davis, D.W., and Corfu, F.
1984: Precise U-Pb zircon and baddeleyite ages for the Sudbury area; in The Geology and Ore Deposits of the Sudbury Structure, (ed.) E.G. Pye, A.J. Naldrett, and P.E. Giblin; Ontario Geological Survey, Special Volume 1, p. 431-446.

Lumbers, S.B.
1973: River Valley area, districts of Nipissing and Sudbury; Ontario Division of Mines, Preliminary Map P.844, Geological Series, scale 1:63 360.
1975: Geology of the Burwash Area, Districts of Nipissing, Parry Sound and Sudbury, Ontario; Ontario Division of Mines, Geological Report 16, 158 p.

Lumbers, S.B. (cont.)
1978: Geology of the Grenville Front tectonic zone in Ontario; in Toronto '78, Field Trips Guidebook, (ed.) A.L. Currie and W.O. Mackasey; Geological Society of America–Geological Association of Canada–Mineralogical Association of Canada, p. 347-361.

Noble, S.R. and Lightfoot, P.C.
1993: U-Pb baddeleyite ages of the Kerns and Triangle Mountain intrusions, Nipissing diabase, Ontario; Canadian Journal of Earth Sciences, v. 30, p. 1424-1429.

Pearson, W.J.
1962: Kyanite occurrences in Dryden Township; in Ontario Department of Mines, Geological Report 9, p. 25-37.

Phemister, T.C.
1961: The boundary between the Timiskaming and Grenville subprovinces in the townships of Neelon, Dryden, Dill and Broder, District of Sudbury; Ontario Department of Mines, Preliminary Report 1961-5.

Quirke, T.T. and Collins, W.H.
1930: The Disappearance of the Huronian; Geological Survey of Canada, Memoir 160, 129 p.

Rivers, T., Martignole, J., Gower, C.F., and Davidson, A.
1989: New tectonic divisions of the Grenville Province, southeast Canadian Shield; Tectonics, v. 8, p. 63-84.

Rousell, D.H. and Trevisiol, D.D.
1988: Geology of the mineralized zone of the Wanapitei Complex, Grenville Front, Ontario; Mineralium Deposita, v. 23, p. 138-149.

Sullivan, R.W. and Davidson, A.
1993: Monazite age of 1747 Ma confirms post-Penokean age for the Eden Lake complex, Southern Province; in Radiogenic Age and Isotopic Studies: Report 7; Geological Survey of Canada, Paper 93-2, p. 45-48.

Geological Survey of Canada Project 760061

Sedimentology of the Oak Ridges Moraine, Humber River watershed, southern Ontario: a preliminary report[1]

H.A.J. Russell[2], D.R. Sharpe, and R.W.C. Arnott
Terrain Sciences Division, Ottawa

Russell, H.A.J., Sharpe, D.R., and Arnott, R.W.C., 1998: Sedimentology of the Oak Ridges Moraine, Humber River watershed, southern Ontario: a preliminary report; in Current Research 1998-C; Geological Survey of Canada, p. 155-166.

Abstract: The Oak Ridges Moraine is a 150 km long landform of regional significance for groundwater recharge. It crops out across 16% of the 900 km^2 Humber River watershed and its subsurface extent is poorly understood. Six lithofacies form much of the moraine in the study area and are discussed within the context of three sites. Architectural associations studied in outcrop are dominated by broad, shallow channels and scours, filled predominantly with medium sand and gravel facies. At two sites, drill core intersects the complete thickness of the moraine and consists mostly (~60-70%) of two lithofacies; graded fine sand-silt and small-scale cross-laminated fine sand-silt. At one of the two sites, gravel constitutes up to 30% of the moraine thickness. This study suggests that the moraine has been formed in an ice-supported environment by pulsating glaciofluvial flow discharging subaqueously in a glaciolacustrine environment.

Résumé : La Moraine d'Oak Ridges est une forme de terrain mesurant 150 kilomètres de longueur qui revêt une importance régionale pour l'alimentation des nappes souterraines. Elle affleure sur 16 % du territoire du bassin de drainage de la rivière Humber qui couvre une superficie de 900 kilomètres carrés; pour le moment, cependant, les connaissances sur son étendue sous terre sont limitées. Dans la région à l'étude, la moraine se compose principalement de six lithofaciès; le présent article décrit ces lithofaciès dans le contexte de trois sites. En affleurement, les associations structurales observées sont dominées par des chenaux et des traces d'affouillement larges et de faible profondeur, remplis pour la plupart de sable à grain moyen et de gravier. À deux sites, les forages ont recoupé l'épaisseur totale de la moraine qui consiste essentiellement en deux lithofaciès : l'un granoclassé et l'autre à petites laminations obliques, mais tous les deux faits de sables fins et de silts. À l'un des deux sites, du gravier s'observe sur 30 % de l'épaisseur de la moraine. Selon les données de cette étude, il semble que la moraine ait été formée dans un environnement dominé par les glaces, plus précisément par un cours d'eau glaciofluvial intermittent qui aboutissait par écoulement subaquatique dans un lac glaciaire.

[1] Contribution to the Oak Ridges Moraine NATMAP Project
[2] Department of Geology, University of Ottawa, Ottawa, Ontario K1N 6N5

INTRODUCTION

The Oak Ridges Moraine is the largest moraine in southern Ontario, extending eastward from the Niagara Escarpment for 160 km. It is the principal area of groundwater recharge for the Greater Toronto Area, the area of most intense groundwater use in Canada. The moraine forms the drainage divide east of the Niagara Escarpment for flow to Georgian Bay and Lake Ontario. Originating in the moraine, the Humber River drains a 900 km^2 watershed, located immediately east of the Niagara Escarpment, and flows southward from Mono Mills to Etobicoke on Lake Ontario (Fig. 1). With the exception of the surficial geology (White, 1973, 1975; Russell and White, 1997) little is known about the subsurface geology of the watershed and specifically the Oak Ridges Moraine. The one previous sedimentological study of the moraine in the area was a regional investigation (Duckworth, 1979) that focused on areas to the east where moraine sediments are better exposed in large aggregate pits (e.g. Stouffville). The small number of aggregate pits in the Humber River watershed has been a significant impediment to understanding the moraine sediments in this area. As a consequence, the western part of the moraine has been described from shallow roadside outcrops of 1-5 m depth (e.g. Russell and White, 1997).

Rationale and Approach

An understanding of the western end of the Oak Ridges Moraine is key to furthering knowledge of the formation of the moraine and the relationship between the Niagara Escarpment and ice-marginal positions responsible for ice-supported glaciolacustrine environments. Additionally, the high demand for groundwater in the Humber River watershed requires an improved hydrostratigraphic understanding, an understanding that can only be achieved through a complete basin analysis. This paper presents work in progress on the Oak Ridges Moraine area of the Humber River watershed.

The study involves both outcrop and drill-core studies using a lithofacies (Miall, 1978, 1996) and architectural (Miall, 1985, 1996) approach to completing a basin analysis (Potter and Pettijohn, 1963). A lithofacies summary and moraine architecture are discussed through examples from three sites: Gormley, GSC-Nob, and V4-158 (Fig. 1). These data provide the basis for the evaluation of a depositional model for the Oak Ridges Moraine.

Study Area

The Oak Ridges Moraine sediments crop out across 144 km^2 or 16% of the Humber River watershed (cf. Russell and White, 1997; Sharpe and Barnett, 1997) and physiographically

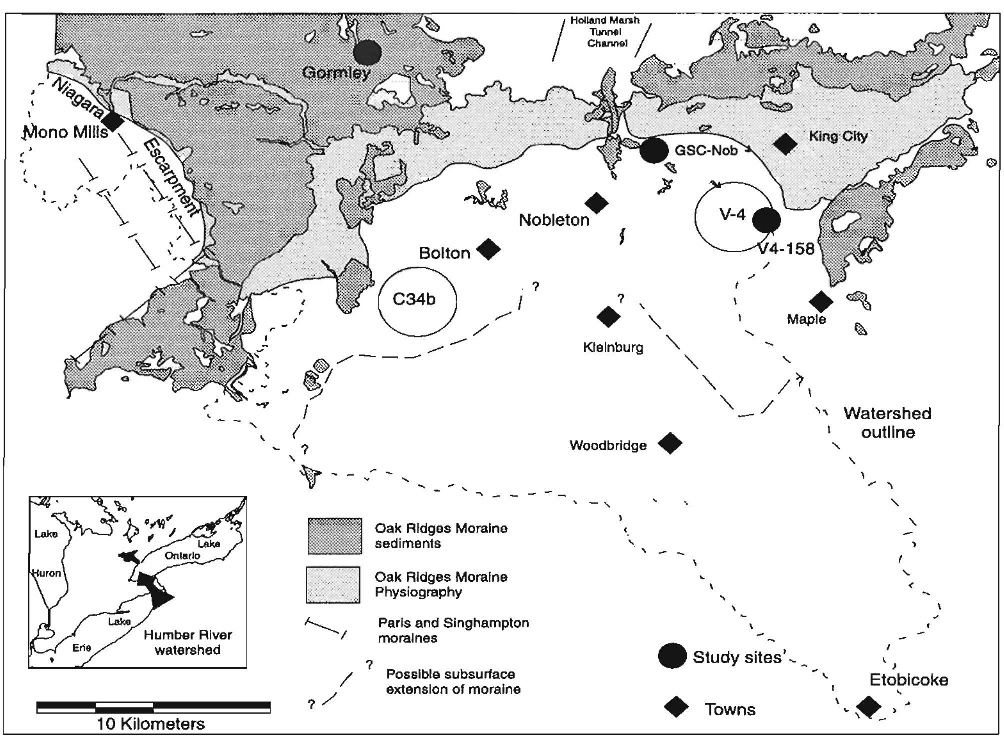

Figure 1. Humber River watershed and extent of Oak Ridges Moraine sediment outcrop and physiographic outline.

form 29% of the watershed (cf. Skinner and Moore, 1997). In the west, the moraine onlaps the Niagara Escarpment and associated Paris and Gibraltar moraines to an elevation of 400-420 m a.s.l. (cf. Russell and White, 1997). Shallow outcrops of the moraine are predominantly small-scale, cross-laminated, silty sand forming rhythmic packages of 20 to 60 cm thickness, capped by 0.5 to 2 cm clay strata (Russell and White, 1997). The subsurface extent of moraine sediments is poorly understood, but may extend south of the V-4 (King City) and C34b (Bolton) Interim Waste Association (IWA) sites (cf. Fenco-MacLaren Inc., 1994; Golder and Associates, 1994).

The moraine has traditionally been interpreted as an interlobate feature of glacial outwash origin with a strong glaciolacustrine component. The subsurface extent of the moraine has been poorly defined (Gwyn and Cowan, 1978; Eyles et al. 1985) prior to recent work identifying a regional unconformity (Sharpe et al., 1997) that truncates Newmarket Till and older geologic units forming an irregular channelized surface (Barnett, 1990; Sharpe et al., 1994, 1996; Pugin et al., 1996). Traditionally identified as ice-contact stratified drift (e.g. White, 1973), the moraine is composed predominantly of well-sorted, glaciofluvial-glaciolacustrine sediments interpreted as braided outwash (Duckworth, 1979), subaqueous fan (Paterson, 1995; Sharpe et al., 1996) or of a composite, esker-subaqueous fan-delta origin (Barnett, 1995). The hydrogeology of the moraine is poorly understood, largely due to a lack of attention to the moraine proper, as studies focus on the regional hydrostratigraphy (e.g. Howard et al., 1997). Detailed stream gauging and base-flow measurements have found the moraine to be the most significant source of base-flow for the Humber River (Hinton and Bowen, 1997).

SITES

Three sites are presented as being representative of the range of lithofacies and architectural associations of the western Oak Ridges Moraine. Each site is located in a different topographic and physiographic setting with respect to the moraine (Fig. 1). One site highlights the type of detailed information available from outcrop studies in aggregate pits (Gormley). Two sites illustrate the contribution drill core can provide where a complete sequence of moraine sediments are intercepted. As part of the IWA landfill investigations, a 159 m borehole (V4-159) was drilled to bedrock (121 m a.s.l.) southwest of King City (Fenco-MacLaren Inc., 1994). This hole was relogged during the autumn of 1994. The second borehole (GSC-Nob), was drilled northeast of Nobleton by the Geological Survey of Canada and intercepted bedrock at 192 m depth (67 m a.s.l.). The two boreholes are ~ 7 km apart (Fig. 1).

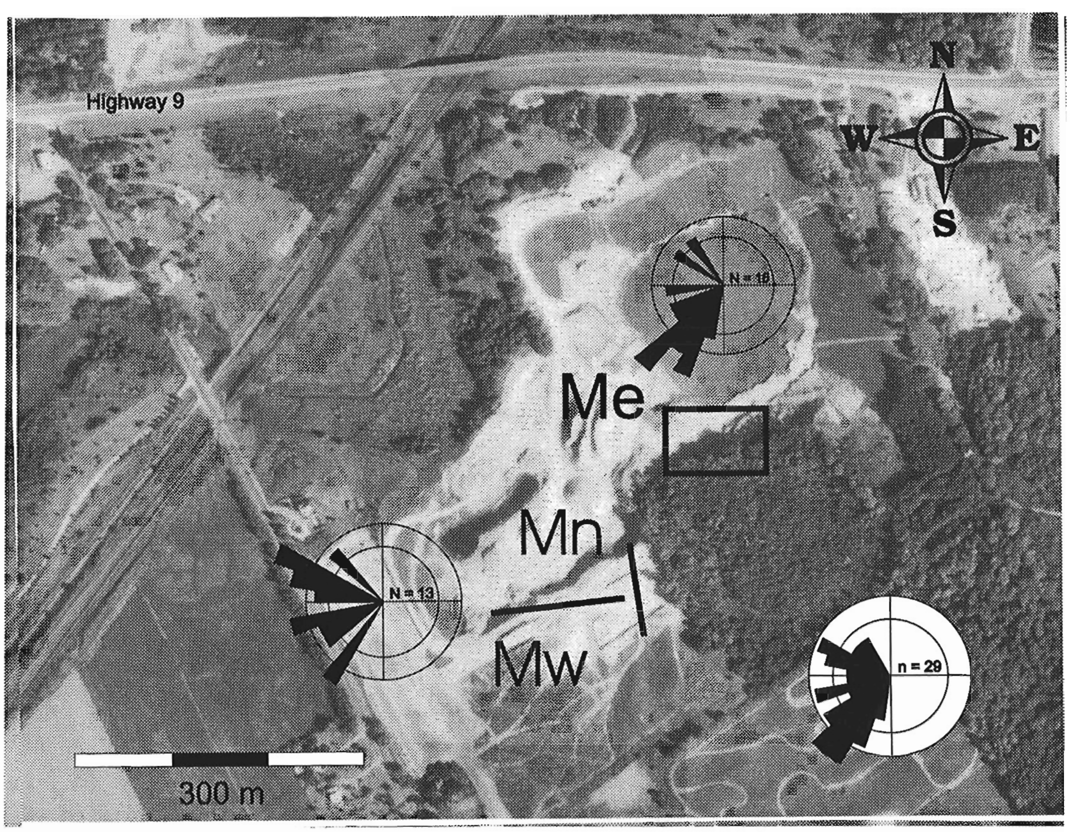

Figure 2. Location of outcrops Me, Mn, Mw at the Gormley aggregate excavation. Rose diagrams plotted in percent frequency, circles at 5 and 10% intervals (Nemec, 1988).

Gormley

This site is north of the Humber River Watershed and near the northern margin of moraine outcrop (Fig. 1). The pit has two areas of excavation: along the southern edge of the property (10-15 m high outcrops) and at the northeast corner of the property (a drag line operation that excavates to 15-20 m below the water table (Fig. 2)). Observations of sediment from the drag line indicate that below the water table the texture is similar to that being excavated from the faces.

The lithofacies cropping out at this site are predominantly gravel (facies G), medium - coarse sand (facies S) and small-scale, cross-laminated fine sand-silt (facies Sr) (Table 1). The pit outcrops are capped by a thin sequence of graded fine sand-silt (facies Sg). Four facies associations-architectural associations have been identified (Fig. 2) and are described according to selected sections from the accompanying photographic mosaics or line drawings. Sections Mn1 and Mn2 are both part of a larger architectural association composed of a stacked series of scour and/or channel fill (Fig. 3). Section Mw is located downflow from the Mn outcrop (Fig. 2). The architectural association (Fig. 4) is dominated by gently dipping cosets of planar-tabular, cross-stratified medium sand (subfacies Sp) and overlying channel fill of trough cross-stratified medium sand (subfacies St). The fourth section (Fig. 5), Me, is east of outcrop Mn and is composed of horizontal cosets of planar-tabular cross-stratified medium sand overlain by inclined gravel facies, that are, in turn, overlain by cross-stratified medium sand.

Outcrop Mn1

This section (Fig. 2,3) is dominated by diffusely stratified medium sand (facies Sd, Table 1), in-filling an ~3 m deep, ~20 m wide scour, into underlying quasi-planar-laminated medium sand (facies Sh) (Fig. 3a). The quasi-planar-laminated medium sand crops out at the northern extremity of the face. It is up to 3.5 m thick and composed of multiple bed sets, less than 40 cm thick, bounded by low-angle reactivation surfaces and interstratified with low-angle cross-stratification. Associated with this facies are sharp-based tabular strata of diffusely stratified medium sand (facies Sd), less than 20 cm thick, that are transitional downflow, and overlain by quasi-planar-laminated medium sand. The overlying diffusely stratified medium sand fills an irregular scour with gentle to steep slopes (Fig. 3a). Internally the fill has faint, secondary, scour surfaces. The sediment ranges from medium to coarse-medium sand with a minor amount of

Table 1. Summary of lithofacies and interpretation for the western Oak Ridges Moraine, Humber River Watershed. Coding modifed after Miall (1996).

Facies	Sub-facies	Facies code	Type section	Character	Interpretation
Diamicton		Di		sharp-based, massive to normal graded, <2 % oversized clasts	debris flow, direct glacial origin or basinal slumping
Gravel G		G	Mn2, Me	sharp-based, massive(Gm) and trough (Gt) cross-bedded, sandy pebble to pebble gravel, rare faults	channel sheets to dune cross-stratification
Medium-coarse sand S	Cross-bedded	Sp, St	Mw	sharp-based, planar-tabular (Sp) and trough (St) cross-stratified, medium to coarse sand, minor pebbly sand, rare convolute bedding	bed load transport, dune and transverse or longitudinal bars
	quasi-planar-laminated	Sh	Mn1	sharp-based, minor undulation,	high-flow velocity deposition
	Diffusely graded	Sd	Mn1	sharp-based, irregular scours, massive to bedded, amalgamated beds, sand intraclasts,	hyperconcentrated flow, traction carpet; hydraulic jump scouring and sedimentation
Small-scale cross-laminated fine sand-silt		Sr	V4, Nob	sharp-based, stoss-erosional to stoss-depositional, minor micro-faults, rare detrital organics	glaciolacustrine interchannel underflows
Graded fine sand-silt		Sg	V4, Nob	sharp-based, fining upward, micro-laminae to beds <5 cm thick, rare cross-laminae, minor bioturbation, rare detrital organics, minor deformation	glaciolacustrine underflow and turbidite sedimentation
Clay		Cl	V4	gradational, massive, minor silt partings,	glaciolacustrine suspension sedimentation

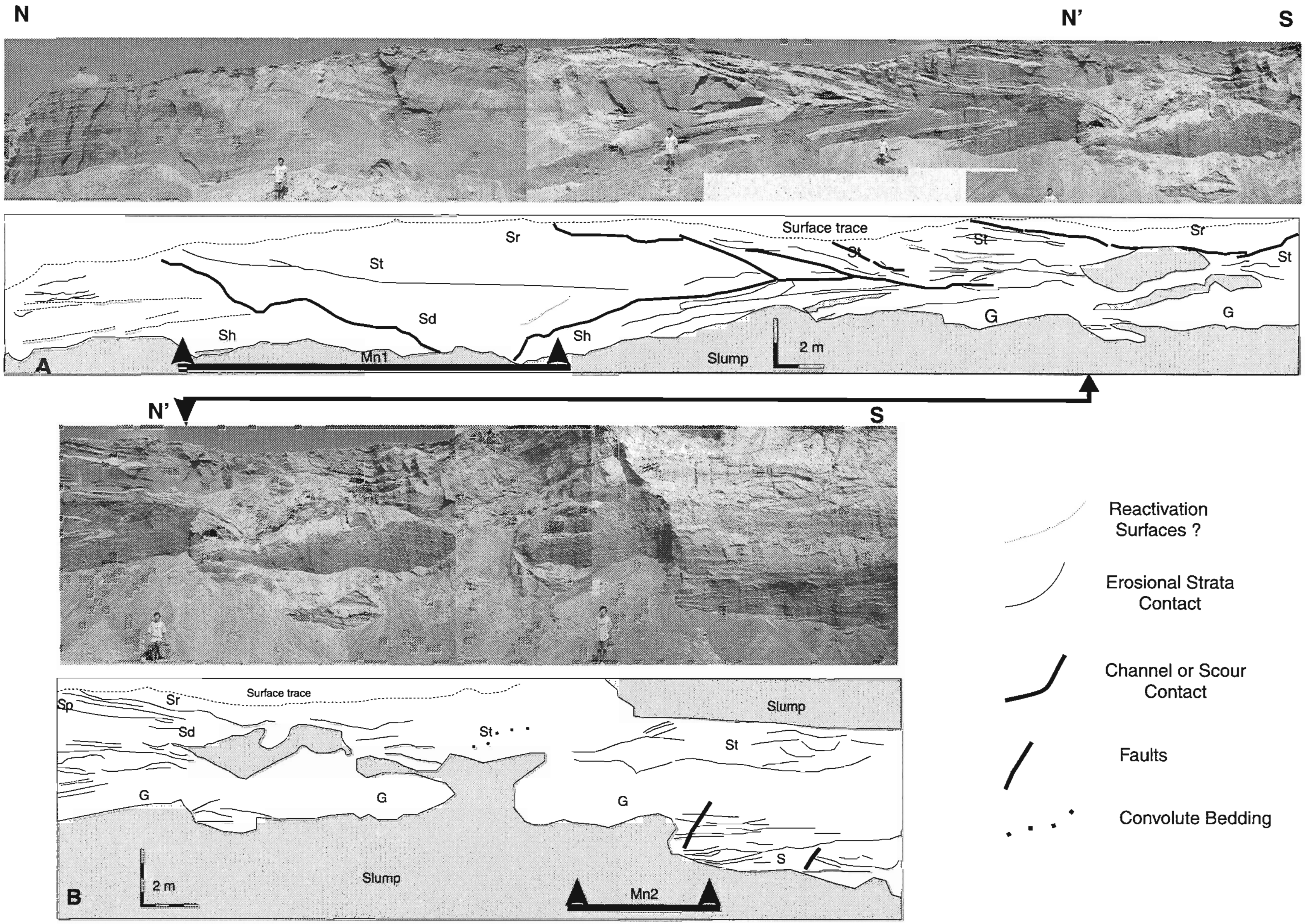

Figure 3. *Photo mosaic of outcrop Mn, Gormley aggregate site. Note diffusely bedded sand fill of scour and broad, shallow channels in upper part of face.*

pebbly sand in the lower part of the scour fill (Fig. 3a). The diffusely graded sand ranges from massive to faintly stratified, with strata thickness less than 10 cm and averaging ~5 cm. Stratification is more clearly defined toward the scour fill margins and upward in the fill. As observation of stratification was dependent upon wind enhancement, massive sediment may well be formed of amalgamated strata with similar dimensions as those observed. The diffusely stratified medium sand scour-fill is truncated by poorly exposed, overlying trough cross-stratified medium sand facies, and the sequence is capped by small-scale cross-laminated fine sand-silt (facies Sr, ripple-drift cross-laminae) (Fig. 3a).

Outcrop Mn2

Located ~20-25 m southeast of section Mn1, Mn2 is composed of three facies (Fig. 3b). At the base, medium-scale, cross-stratified, medium to coarse, and coarse pebbly sand are overlain by interbedded gravel and trough cross-stratified sand. The gravel facies ranges from graded, medium-scale, cross-bedded, bimodal, pebbly gravel to faintly horizontally bedded heterogeneous pebble gravel. The planar cross-bedded bimodal gravels form bed sets of 4-10 cm within cosets 25-30 cm thick. Foreset beds fine up-dip along the bedding plane, whereas bed sets fine upward normal to bedding. Individual bed sets are mantled by a fine silt-sand drape. Maximum pebble size is ~5 cm with a visually estimated average size ~1-2 cm. Thicker, less than 1.5 m, massive to faintly bedded to cross-bedded heterogenous sandy gravel occurs across the middle of the face. Locally the gravel fines upward to cross-stratified pebbly coarse sand. The gravel facies is overlain by poorly exposed planar and trough cross-stratified sand capped by small-scale cross-laminated fine sand. The central part of the outcrop between Mn1 and Mn2 is composed of broad, shallow channel fill of planar and trough cross-stratified medium sand. Strata are laterally discontinuous.

Outcrop Mw

This section crops out 50 m west of the Mn outcrop as a poorly exposed, ~6-8 m face, composed of two architectural associations (Fig. 4). The lower part of the face is predominantly planar-tabular, cross-stratified medium sand with a gentle dip toward the west. Coset are less than 50 cm thick, generally being 10-25 cm. Paleoflow directions are bimodal with a primary mode to the northwest and a secondary mode to the southeast (Fig. 2). The face contains multiple low-angle

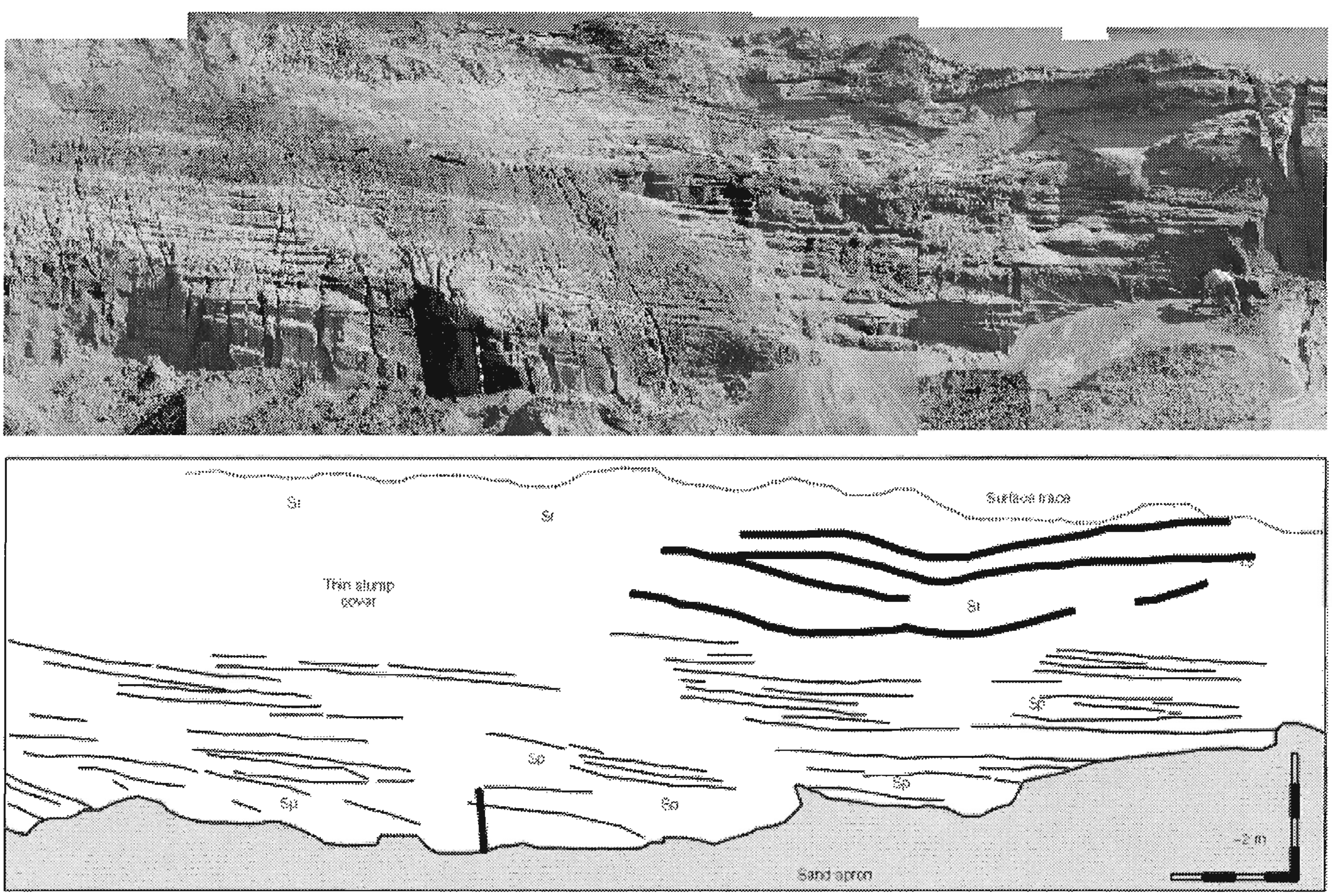

__Figure 4.__ Sketch from photo mosaic of outcrop Mw, Gormley aggregate site. Lower face predominately planar-tabular, cross-stratified medium sand overlain by shallow channels filled with trough cross-stratified medium sand and small-scale, cross-laminated fine sand. Symbol legend as for Figure 3.

erosional surfaces. The upper part of the section has stacked shallow scours (channels?) less than 10 m wide and 1-2 m deep, filled with poorly exposed cross-stratified medium sand and small-scale cross-laminated fine sand.

Outcrop Me

The most easterly outcrop is dominantly planar and trough cross-stratified medium to coarse sand, minor pebbly sand, and gravel (Fig. 2, 5). The lower part of the face is composed of horizontal cosets of medium-scale, planar-tabular, cross-stratified sand (subfacies Sp). The lower bed sets are less than 60 cm thick and form cosets greater than 4 m thick. Erosionally overlying this coset is dipping, heterogenous, sandy pebble gravel. The overlying cross-stratified medium sand rest on an erosional surface marked by a pebble lag or truncation of the underlying gravel (Fig. 5). This upper sequence is composed of two coset deposits. The lower 1-1.5 m thick coset comprises planar and trough, cross-stratified medium-coarse sand with bed sets 10-40 cm thick. The overlying 1-2 m thick coset is composed of trough cross-stratified pebbly sand with bed sets 20-40 cm thick. The upper part of the sequence has been truncated by excavation work, the fine sand and silt having been removed.

Nobleton Borehole

This borehole intercepted 54 m of Oak Ridges Moraine sediments resting unconformably on lower deposits (Sharpe et al., 1997), possible Thorncliffe, Scarborough, and Don Formation equivalents (Eyles et al., 1985) (Fig. 6). The lower contact of moraine sediments was not observed as no core recovery was obtained across the 194.5 to 201 m (a.s.l.) interval. The core is predominantly gravel (31%), small-scale cross-laminated fine sand-silt (20%) and graded fine sand-silt (43%) (Table 2). Core recovery from the gravel interval is low, but based on the drilling log and recovered sediment the 17 m interval is bedded with a number of graded sequences (Gorrell, pers. comm., 1997). With the incomplete recovery obtained, a coarse sand-granule gravel to cobble-pebble gravel facies was logged. Matrix sediment was generally not recovered; an exception being the upper 1.5 m transition from gravel to fine sand where an interbedded contact is present. Above ~223 m depth, there are two well defined fining-upward trends and a zone from 228-241 m a.s.l. with no distinct trend. Fining-upward trends are characterized by increasing clay facies, decreasing small-scale cross-laminated fine sand-silt facies, and decreasing bed thickness (Fig. 6). The diamicton (facies Di) occurs between 219-226 m a.s.l., as five thin, sharp-based, massive to normal graded beds with low oversized clast contents (<2%). The maximum bed thickness reported (1.52 m) represents the core-barrel length, beds thicker than this length have not been aggregated. Beds have been proportionately stretched to eliminate minor differences between reported drill depths and measured recovery (where <0.05 m/ 1.52 m). Eleven clay strata in the interval 221-233 m have an average thickness of 0.17 cm and spacing of 2.52 m.

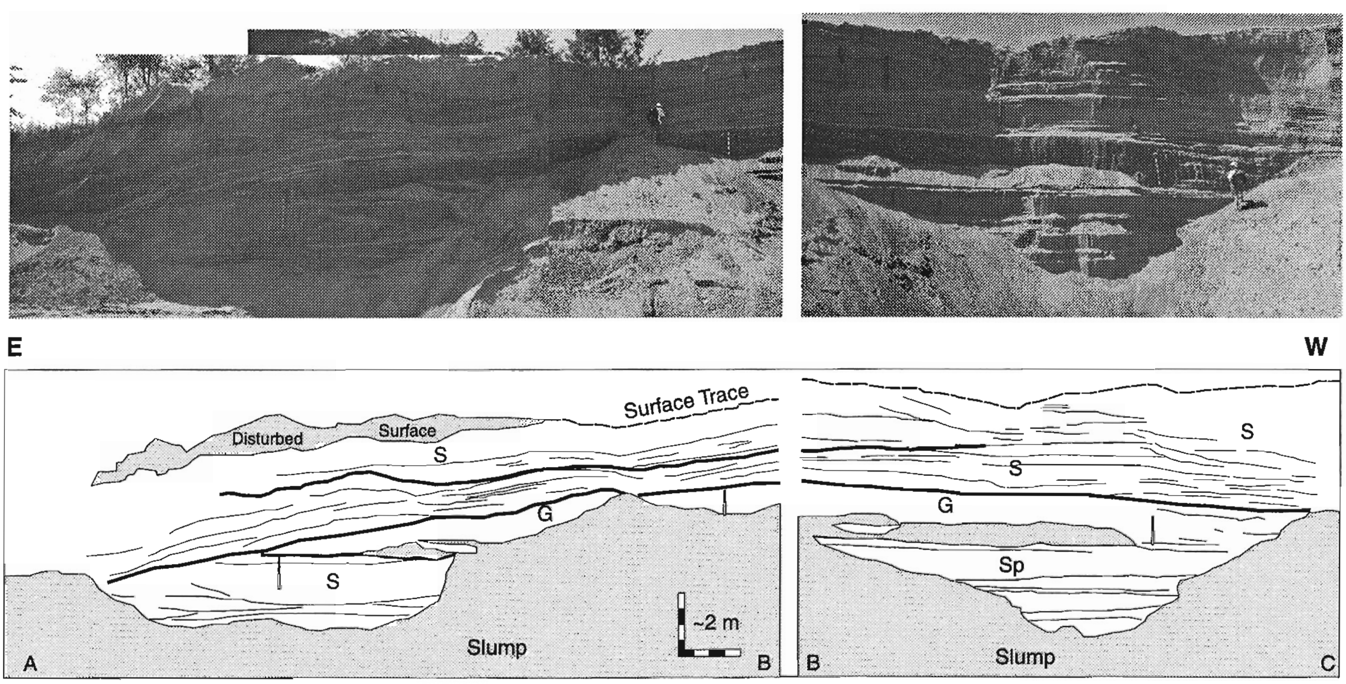

Figure 5. Sketch from photo mosaic of outcrop Me, Gormley aggregate site. Tripartite sequence of, i) planar cross-stratified medium to coarse sand, ii) cross-stratified gravel, iii) planar and trough, cross-stratified medium to pebbly medium sand. Symbol legend as for Figure 3. Letters B, B' indicate mismatched edges in the photo mosaic due to angular distortion.

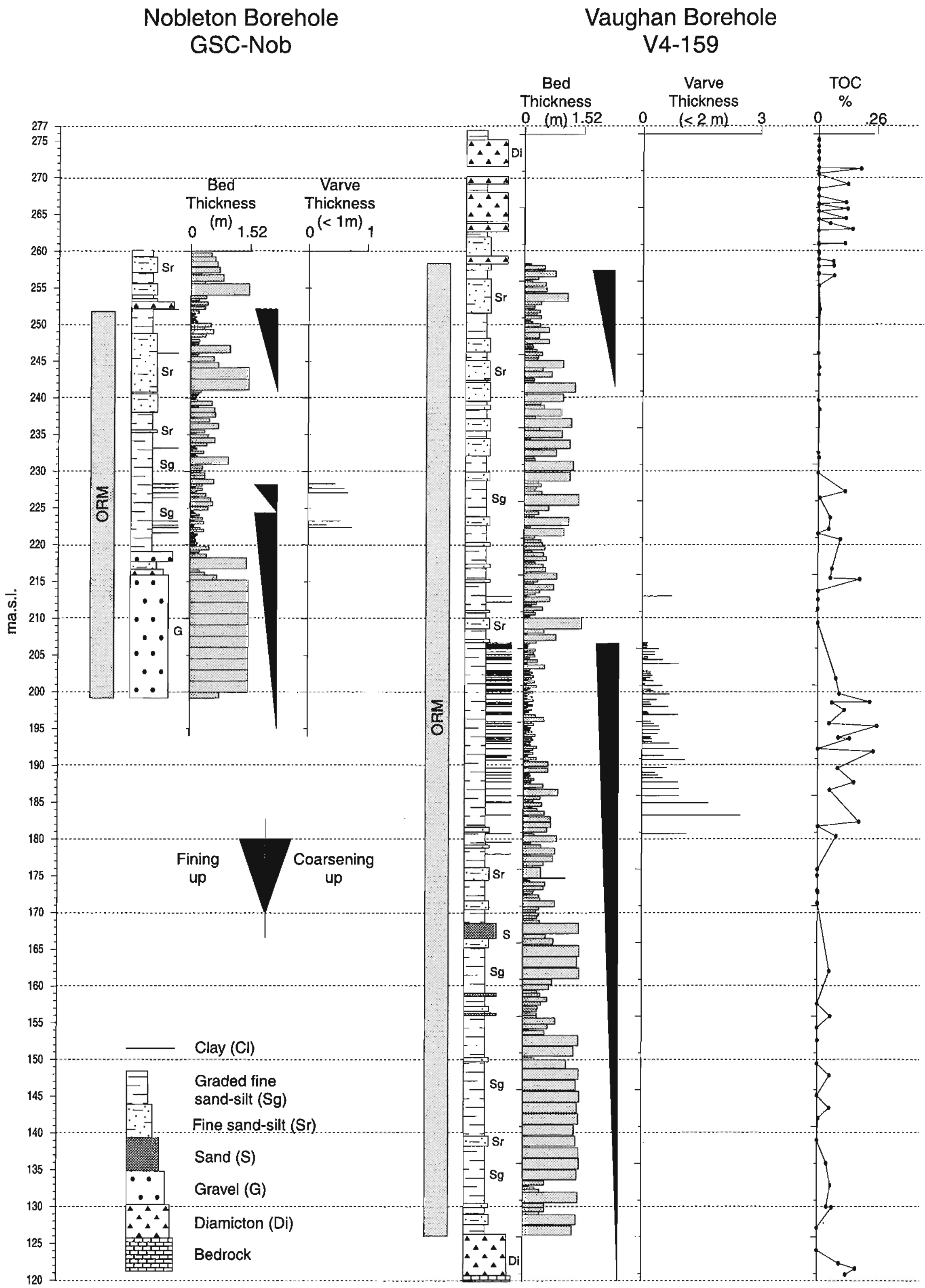

***Figure 6.** Simplified graphic log and accompanying graphs for boreholes GSC Nob and V4-158. Note predominance of facies Sr and Sg.*

Table 2. Lithofacies occurrence in Nobleton and V4/158 drill core for Oak Ridges Moraine.

Lithofacies	Nobleton %	V4/158 %
Diamicton	1.2	0.1
Gravel	32.7	0
Medium-coarse sand	0.7	2.1
Small scale cross-laminated fine sand-silt	21	20.4
Graded fine sand-silt	44	63
Clay	0.4	1.5
Missing	0	13

Vaughan Borehole

This borehole intercepted a 132.5 m sequence of Oak Ridges Moraine sediment (Fig. 6). The log reveals two general sequences, the upper one composed of multiple poorly defined cycles. Each sequence is dominated by graded fine sand-silt and small-scale, cross-laminated fine sand-silt (facies Sg and Sr) (Table 2). The lower sequence has a well defined fining-upward trend with thinning of bed thickness and increasing clay facies (Fig. 6). Thick lower beds in this hole are predominantly massive to graded, fine to medium-fine sand of the graded fine sand-silt facies (Table 1). The sequence is capped between 178 and 207 m a.s.l. by an interval of rhythmically bedded, graded fine sand-silt and clay facies (Fig. 5). Within this interval 62 clay facies strata occur with an average thickness of 0.03 m and average spacing of 1.19 m. Above 207 m a.s.l., the upper sequence is less clearly divided, with greater variability in strata thickness and increasing small-scale cross-laminated fine sand-silt (facies Sr). Above ~240 m a.s.l., graded fine sand-silt (facies Sg) increases with decreasing bed thickness. Analysis of 78 samples for total organic carbon yield maximum values of 0.26% with an average of 0.06 % (Fig. 6). The total organic carbon correlates with finer grained facies, specifically the clay facies. As for the Nobleton borehole, the maximum bed thicknesses are reported at 1.52 m. Additionally, many thin beds represent missing material (Table 2) as the measured recovery has not been proportioned over the total depth reported from drilling.

INTERPRETATION

The facies, facies assemblage, and architecture from the Gormley Pit indicate an environment of high-energy flow with abundant sediment transport as bedload (Todd, 1996). The facies present are commonly associated with fluvial (Miall, 1985), glaciofluvial (Church and Gilbert, 1975; Maizels, 1989), and esker-subaqueous-fan sedimentation (Rust, 1977; Cheel and Rust, 1986; Henderson, 1988; Gorrell and Shaw, 1991; Brennand 1994; Brennand and Shaw, 1994). The isolated occurrence of thin diamicton strata (facies Di) within a well-sorted sequence suggests these strata were deposited from minor plastic flows. Plastic flows (debris, liquified flows; Mulder and Cochonat, 1996) are a common element of a variety of deposits, ranging from fluvial-glaciofluvial (Maizels, 1989; Miall, 1996), subaqueous fans (Sharpe, 1988), to ice-proximal deposits (Lawson, 1981). In this setting the deposits are interpreted as forming from subglacial flow or basinal slope failure events (Mulder and Cochonat, 1996). The gravel facies is interpreted as being deposited from in-channel sheet flows and migrating dune bedforms (Miall, 1996). The two cross-stratified subfacies, planar and trough, represent deposition from traction sediment transport and migrating 2-D and 3-D dunes (Church and Gilbert, 1975; Miall, 1996). The cosets of this facies may be part of composite accreting bedforms (Fig. 5) (Miall, 1996). The stacked erosional channels (Fig. 3,4) are inferred to represent incision into the upper part of mega-bedforms deposited in front of a conduit mouth as the expanding flow lost competence. Such bedforms have been described in the area from tunnel channels (Shaw and Gorrell, 1991) and at grounding lines of Alaskan glaciers (Powell, 1990). The quasi-planar-laminated sands (subfacies Sh) were deposited under super-critical, upper-flow-regime conditions (Hand, 1974; Best, 1996). The diffusely stratified medium sand (facies Sd) is a common facies of subaqueous fans and considered characteristic of such environments (Rust 1988). This facies is generally associated with hyperconcentrated flows (Maizels, 1989; Gorrell and Shaw, 1991) and traction carpet sedimentation (Lowe, 1982; Sohn, 1997). In subaqueous fan settings two alternative interpretations have been invoked for similar facies. The interpretation of diffusely stratified medium sand facies has largely been based on the work of Lowe (1982) using liquefaction and high-density turbidity currents as a mechanism (Cheel and Rust, 1986; Rust, 1988). Alternatively, Gorrell and Shaw (1991) suggest an association with the intense scouring associated with hydraulic jumps. In this setting the underlying quasi-planar-laminated facies and lateral gravel facies support this interpretation. Where diffusely stratified sand (facies Sd) occurs as tabular strata laterally transitional to quasi-planar-laminated sand, stratification may have been suppressed by high rates of suspension sedimentation (Arnott and Hand, 1989).

The fine-grained, small-scale, cross-laminated and graded fine sand-silt (facies Sr and Sg) were deposited in lower energy subaqueous conditions. Small-scale, cross-laminated, fine sand-silt is characteristic of depositional environments where suspension sedimentation predominates over traction, forming rapidly aggrading beds (Jopling and Walker, 1968; Ashley et al., 1982). Such conditions are characteristic of density underflows, turbidity currents (Walker, 1992), and overbank sedimentation under expanding flow conditions (Harms et al., 1975). Both in drill core and in outcrop, small-scale, cross-laminated, fine sand-silt generally lack the corresponding divisions associated with the Bouma sequence. The graded fine sand-silt facies is more representative of distal turbidite deposits (Banerjee, 1973) with Bouma layers BCDE, BDE, and DE (Walker, 1992). The majority of graded fine sand-silt corresponds with BDE(t) or DE(t). Division E(h) is rarely associated with individual events of the graded fine sand-silt facies and where it clearly caps multiple, graded, fine sand-silt facies strata has been assigned to the clay facies.

The clay strata (facies Cl) are interpreted as forming from suspension sedimentation and recording a shutdown in sediment influx to the basin and suppression of turbulence in the water column. In glaciolacustirine environments such conditions are generally interpreted as representing sedimentation during seasons of no melt and surface ice cover (e.g. winter) (Banerjee, 1973; Gilbert, 1997).

DEPOSITIONAL MODEL

Recent studies have recognized the moraine as a composite regional landform of glaciofluvial-glaciolacustrine origin (Sharpe et al., 1994; Barnett, 1995; Paterson, 1995). As a positive-relief landform in a continental-glaciated landscape, the choice of depositional models is tightly constrained. The abrupt lateral moraine slopes and abrupt sediment facies and landform transitions combined with lacustrine sediments at elevations up to 420 m indicate deposition in an ice-supported environment (Chapman and Putnam, 1988; Barnett, 1995; Sharpe et al., 1997). The remaining question is whether the glaciofluvial deposits record predominantly subaerial, braided stream-deltaic outwash sedimentation or subglacial-subaqueous fan sedimentation at this site. The data presented here are interpreted as supporting a conduit-subaqueous fan environment on the basis of the thick basinal deposits of small-scale, cross-stratified, fine sand-silt; graded fine sand-silt; and clay facies and the fact that they overlie all the glaciofluvial deposits. Alternatively, various ice-marginal fluctuations and water-level variations can be invoked for braided-deltaic sedimentation. Features in the Gormley pit that may be interpreted for such fluctuations are channel foreset beds; however, such features are easily accommodated within a subaqueous fan model. Large composite bedforms recognized at the discharge point of marine tidewater glaciers (Powell, 1990) and in tunnel channels (Shaw and Gorrell, 1991) provide useful analogues. That architectural elements within the Gormley pit are related to mega-bedforms is supported by site Me. There the dipping gravel beds that climb over underlying planar-tabular, cross-stratified, medium sand are candidates for such bedforms, particularly in the absence of any deformation features suggesting ice let-down of the sediments (Fig. 5). The nonsteady, nonuniform discharge of glaciofluvial conduits provides a mechanism for the types of large scouring and channel incision present in the Gormley pit.

Using a conduit-subaqueous fan model, the moraine is inferred to have been built during two stages in this area. Stage one is recorded in the basinal sedimentation of the Vaughan site. Well constrained paleoflow control on this phase is unavailable but general facies relationships indicate a southwest flow (cf. Fenco-MacLaren Inc., 1994). This stage culminated in low-energy sedimentation recorded by the sequence of rhythmites in the middle of the V4-158 hole and above the gravel facies of the Nobleton borehole. In this event sequence the gravel sediments are inferred to be older deposits related to southward flow along the tunnel channels or part of the moraine package deposited by southward flow that has re-occupied the tunnel channel. As the deposits occur on a high shoulder of the subsurface continuation of the Holland Marsh tunnel channel (S. Pullan, GSC, pers. comm.) the first option (older) is preferred. In the absence of fossilized ice in tunnel channels or pre-moraine infilling, infilling of these basinal lows is a necessary first stage to permitting conduit flow axial to the moraine crest westward of these deeply scoured channels. The second stage involves both axial flow and lateral flow to the moraine ridge. Near-surface paleoflows east of the study area indicate strong axial flow (Duckworth, 1979; Paterson, 1995) whereas the Gormley pit indicates more lateral flow of a northern origin (Fig. 2). The elevation of the deposits and absence of evidence immediately up-flow of the Gormley site (cf. Russell and White, 1997) for braided outwash suggests an ice-proximal subaqueous environment.

SUMMARY

Three sites are reviewed as encompassing the range of lithofacies forming the western part of the Oak Ridges Moraine (Fig. 1). The facies assemblages and architecture are not unique to any one depositional system; however, interpreted in a regional glacial context, a subaqueous fan model of sedimentation is suggested. The facies assemblages can be separated into two packages. The first package is low-energy basinal facies of glaciolacustrine character, diamicton, small-scale, cross-laminated and graded fine sand-silt and clay lithofacies. The second package is coarser, medium-coarse sand and gravel facies (Table 2), that is frequently associated with broad, shallow channels and scours. This second package is more characteristic of channelized glaciofluvial processes. The moraine is predominately well sorted with little diamicton (Table 2). Deformation within the sediments is rare, with little to no evidence of significant letdown due to removal of ice support following sedimentation.

ACKNOWLEDGMENTS

This study was completed as part of the Oak Ridges Moraine NATMAP and hydrogeology program. Partial funding for H.A.J. Russell was provided by a NSERC operating grant to R.W.C. Arnott. Field assistance provided by D. Cummings, S. Dumas, and C. Helmer is gratefully acknowledged. Drilling supervision and site logging for GSC-Nob was done by G. Gorrell. Comments from M. Hinton and A. Blais helped improve various aspects of the paper.

REFERENCES

Arnott, W. R. C. and Hand, B. M.
1989: Bedforms, primary structures and grain fabric in the presence of suspended sediment rain; Journal of Sedimentary Petrology, v. 59, p. 1062-1069.

Ashley G.M., Southard, J. B., and Boothroyd, J. C.
1982: Deposition of climbing-ripple beds: a flume simulation; Sedimentology, v. 29, p. 67-79.

Banerjee, I.
1973: Part A: Sedimentology of Pleistocene glacial varves in Ontario, Canada; Geological Survey of Canada, Bulletin 226, 60p.

Barnett, P.J.
1990: Tunnel valleys: evidence of catastrophic release of subglacial meltwater, central-southern Ontario, Canada; in Abstracts with Programs, Northeastern Section; Geological Society of America, Syracuse, New York, p. 3.
1995: Project 92-19: geology of the Oak Ridges Moraine area, parts of Peterborough and Victoria counties and Durham and York Regional Municipalities, Ontario; in Summary of field work and other activities 1995; Ontario Geological Survey, Miscellaneous Paper 163, p. 155-160.

Brennand, T.A.
1994: Macroforms, large bedforms and rhythmic sedimentary sequences in subglacial eskers, south-central Ontario: implication for esker genesis and meltwater regime; Sedimentary Geology, v. 91, p. 9-55.

Brennand, T.A, and Shaw, J.
1994: Tunnel channels and associated landforms: their implication for ice sheet hydrology. Canadian Journal of Earth Sciences, v. 31, p. 502-522.

Best, J.
1996: The fluid dynamics of small-scale alluvial bedforms; in Advances in Fluvial Dynamics and Stratigraphy, (ed.), P.A. Carling and M.R. Dawson; Wiley, p. 67-125.

Chapman, L.J., and Putnam, D.F.
1988: The physiography of southern Ontario, 3rd edition; Ontario Geological Survey, Special Volume 2, 270 p.

Cheel, R.J. and Rust, B.R.
1986: Coarse grained facies of glacio-marine deposits near Ottawa, Canada; in Glacial, Glaciofluvial and Glaciolacustrine Systems, (ed.) R. Davidson-Arnott, W. Nickling, and F.D. Fahey, Geobooks, Norwich, England, p. 279-295.

Church, M. and Gilbert, R.
1975: Proglacial fluvial and lacustrine environmments; in Glaciofluvial and Glaciolacustrine Sedimentation, (ed.) A.V. Jopling and B.C. McDonald; Society of Economic Paleontologists and Mineralogists, Special Publication 23, p. 22-100.

Duckworth, P.B.
1979: The late depositional history of the western end of the Oak Ridges Moraine, Ontario; Canadian Journal of Earth Sciences, v. 16, p. 1094-1107.

Eyles, N., Clark, B.M., Kaye, B.G., Howard, K.W.F., and Eyles, C.H.
1985: The application of basin analysis techniques to glaciated terrains: an example from the Lake Ontario basin, Canada; Geoscience Canada, v. 12, p. 22-32.

Fenco-MacLaren Inc.
1994: IWA landfill site search, Metro/York region: Step 6 hydrogeological report sites V3B, V4A, V4D; Interim Waste Authority Report, prepared by M. Gomer, Fenco MacLaren Inc., January 1994.

Gilbert, R.
1997: Glacilacustrine environment of part of the Oak Ridges Moraine, southern Ontario; Géographie et physique Quaternaire, v. 51, p. 55-66.

Golder and Associates
1994: Peel region proposed landfill site C-34b: detailed assessment of the proposed site, appendix C- geology/hydrogeology; Interim Waste Authority Report, prepared by R. Blair, Golder Associates, November 1994.

Gorrell G. and Shaw, J.
1991: Deposition in an esker, bead and fan complex, Lanark, Ontario, Canada; Sedimentary Geology, v. 72, p. 285-314.

Gwyn, Q.H.J. and Cowan, W.R.
1978: The origin of the Oak Ridges and Orangeville moraines of southern Ontario; Canadian Geographer, no. XXII, v. 4, p. 345-351.

Hand, B. M.
1974: Supercritical flow in density currents; Journal of Sedimentary Petrology,v. 44, p. 637-648.

Harms, J.C., Southard, J.B., Spearing, D.R., and Walker, R.G.
1975: Depositional environments as interpreted from primary sedimentary structures and stratification sequences; Lecture notes for Short Course No. 2, Society of Economic Paleontologists and Mineralogists. 161 p.

Henderson, P. J.
1988: Sedimentation in an esker system influenced by bedrock topography near Kingston, Ontario; Canadian Journal of Earth Sciences, v. 25, p. 987-999.

Hinton, M. J. and Bowen, G. S.
1997: Stream baseflow surveys to identify regional groundwater discharge and chemistry in the Oak Ridges Moraine; Geological Association of Canada, Program with Abstracts, Ottawa '97, May 19-21, 1997, Ottawa, Ontario.

Howard, K. W. F., Eyles, N., Smart, P., Boyce, J., Gerber, R., Salvatori, S.L., and Doughty, M.
1997: The Oak Ridges Moraine of southern Ontario, a groundwater resource at risk; in Environmental Geology of Urban Areas, (ed) N. Eyles; Geological Association of Canada, p. 153-192.

Jopling, A.V. and Walker, R.G.
1968: Morphology and origin of ripple-drift cross-lamination, with examples from Pleistocene of Massachusetts; Journal of Sedimentary Petrology, v. 38, p. 971-984.

Lawson, D.E.
1981: Distinguishing characteristics of diamictons at the margin of Matanuska Glacier, Alaska; Annals of Glaciology, v. 2, p. 78-84.

Lowe, D.R.
1982: Sediment gravity flows II. Depostional models with special reference to the deposits of high-density turbidity currents; Journal of Sedimentary Petrology, v. 52, p. 279-297.

Maizels, J.
1989: Sedimentology, paleoflow dynamics and flood history of jokuhlaup deposits: paleohydrology of Holocene sediment sequences in southern Iceland sandur deposits; Journal of Sedimentary Research, v. 59, p. 204-223.

Miall, A.D.
1978: Lithofacies types and vertical profile models in braided river deposits: a summary; in Fluvial Sedimentology, (ed) A.D. Miall; Canadian Society of Petroleum Geology, Memoir 5, p. 597-604.
1985: Architecture-element analysis: a new method of facies analysis applied to fluvial deposits; Earth Science Reviews, v. 22, p. 261-308.
1996: The Geology of Fluvial Deposits; Springer-Verlag, Germany, 582 p.

Mulder, T. and Cochonat, P.
1996: Classification of offshore mass movements; Journal of Sedimentary Research, v. 66, p. 43-57.

Nemec, W.
1988: The shape of the rose; Sedimentary Geology, v. 59, p. 149-152.

Paterson, J.
1995: Sedimentology of the Bloomington fan complex, Oak Ridges Moraine, southern Ontario; M.Sc. thesis, Brock University, St. Catharines, Ontario.

Powell, R. D.
1990: Glacimarine processes at grounding-line fans and their growth to ice contact deltas; in Glacimarine Environments: Processes and Sediments, (ed.) J.A. Dowdeswell and J.D. Scourse; Geological Society of America, Special Publication 53, p. 53-73.

Potter, P.E. and Pettijohn, F.J.
1963: Paleocurrents and Basin Analysis; Springer-Verlag, Berlin, Germany, 296 p.

Pugin, A., Pullan, S.E., and Sharpe, D.R.
1996: Observations of tunnel channels in glacial sediments with shallow land-based seismic reflection; Annals of Glaciology, v. 22, p. 176-180.

Russell, H.A.J. and White, L.O.
1997: The surficial geology of the Bolton area, NTS 31M/13, southern Ontario; Geological Survey of Canada, Open File 3299, scale 1:50 000.

Rust, B.R.
1977: Mass flow deposits in a Quaternary succession near Ottawa, Canada, diagnostic criteria for subaqueous outwash; Canadian Journal of Earth Sciences, v. 14, p. 175-184.

Rust, B.R. (cont.)
1988: Ice-proximal deposits of the Champlain Sea at south Gloucester, near Ottawa, Canada; in The Late Quaternary Development of the Champlain Sea Basin, (ed) N.R. Gadd; Geological Association of Canada, Special Paper 35, p. 37-45.

Sharpe, D.R.
1988: Glaciomarine fan deposition in the Champlain Sea; in The Late Quaternary Development of the Champlain Sea Basin, (ed) N.R. Gadd; Geological Association of Canada, Special Paper 35, p. 63-82.

Sharpe, D.R. and Barnett, P.J.
1997: Surficial Geology of the Markham Area, NTS 30M/14, southern Ontario; Geological Survey of Canada, Open File 3300, scale 1:50 000.

Sharpe, D.R., Barnett, P.J., Brennand, T.A., Gorrell, G., and Russell, H.A.J
1997: Surficial geology of the Oak Ridges Moraine NATMAP Area, Ontario; Geological Survey of Canada, Open File 3456. Scale 1: 200 000.

Sharpe, D.R., Barnett, P.J., Dyke, L.D., Howard, K.W.F., Hunter, G.T., Gerber, R.E., Paterson, J., and Pullan, S.E.
1994: Quaternary geology and hydrogeology of the Oak Ridges Moraine area; Geological Association of Canada, Mineralogical Association of Canada, Joint Annual Meeting, Waterloo, 1994, Field Trip A7: Guidebook.

Sharpe, D.R., Dyke, L.D., Hinton, M.J., Pullan, S.E., Russell, H.A.J., Brennand, T.A., Barnett, P.J., and Pugin, A.
1996: Groundwater prospects in the Oak Ridges Moraine area, southern Ontario: application of regional geological models; in Current Research 1996-E; Geological Survey of Canada, p. 181-190.

Shaw, J. and Gorrell, G.
1991: Subglacially formed dunes with bimodal and graded gravel in the Trenton drumlin field, Ontario; Géographie et physique Quaternaire, v. 45, p. 21-34.

Skinner, H., and Moore, A.
1997: Digital elevation model of the Oak Ridges Moraine, southern Ontario (hillshade enhanced); Geological Survey of Canada and Ontario Ministry of Natural Resources, Open File 3297.

Sohn, Y.K.
1997: On traction-carpet sedimentation; Journal of Sedimentary Research, v.67, p. 502-509.

Todd, S.P.
1996: Process deduction from fluvial sedimentary strucutures; in Advances in Fluvial Dynamics and Stratigraphy, (ed,) P.A. Carling and M.R. Dawson, Wiley, p. 299-350.

Walker, R.G.
1992: Turbidites and submarine fans; in Facies Models - response to sea level change, (ed.) R.G. Walker and N.P. James; Geological Association of Canada, p. 239-264.

White, O.L.
1973: Bolton Quaternary Geology; Ontario Division of Mines, Geological Map 2275.
1975: Quaternary Geology of the Bolton area, southern Ontario; Ontario Division of Mines, Geological Report 117.

Geological Survey of Canada Project 930042

Data on the origin of the Kipawa syenite complex, northwestern Quebec

K.L. Currie
Continental Geoscience Division, Ottawa

Currie, K.L., 1998: Data on the origin of the Kipawa syenite complex, northwestern Quebec; in Current Research 1998-C; Geological Survey of Canada, p. 167-172.

Abstract: The Kipawa Syenite Complex forms a persistent, thin, folded layer within tectonized biotite-magnetite granite gneiss structurally overlain and underlain by metasedimentary rocks which in turn rest upon Archean plutonic rocks. Kataphorite+biotite (±aegirine) syenite comprises about 5% of the complex. The rest consists of distinctive granoblastic textured quartz syenite and granite characterized by large porphyroblasts and pods of hastingsite. Amphibole and biotite commonly show replacement by magnetite with formation of red oxidation spots. Observations suggest formation of the Kipawa Syenite Complex during amphibolite grade metamorphism by metasomatic fluids derived from a peralkaline igneous complex whose relics appear as lenses of nepheline syenite and as allochthonous blocks of igneous-textured aegirine melasyenite. This process occurred during a late stage of the assembly of the Superior and Grenville provinces (ca. 995 Ma), more than 100 Ma after emplacement of the host gneisses, and 40 Ma after emplacement of the alkaline complex.

Résumé : Le complexe syénitique de Kipawa constitue une couche persistante, mince et plissée au sein d'un gneiss granitique tectonisé à biotite-magnétite qui s'insère structuralement entre des roches métasédimentaires reposant à leur tour sur des roches plutoniques archéennes. Une syénite à kataphorite+biotite (±aegyrine) occupe environ 5 pour cent du complexe. Le reste se compose de syénite quartzique et de granite à texture granoblastique distinctive se caractérisant par de volumineux porphyroblastes et lentilles fusiformes de hastingsite. L'amphibole et la biotite sont souvent remplacées par de la magnétite, avec formation de taches d'oxydation rouges. Les observations laissent supposer que le complexe syénitique de Kipawa s'est formé au cours d'un épisode de métamorphisme au faciès des amphibolites par des fluides métasomatiques issus d'un complexe igné hyperalcalin dont les reliques se présentent sous forme de lentilles de syénite néphélinique et de blocs allochtones de syénite mélanocrate à aegyrine à texture ignée. Ce processus a eu lieu au cours d'une phase tardive de l'assemblage des provinces du lac Supérieur et de Grenville (vers 995 Ma), plus de 100 Ma après la mise en place des gneiss encaissants et 40 Ma après celle du complexe alcalin.

INTRODUCTION

The Kipawa Syenite Complex (Currie and van Breemen, 1996a, b) lies a few kilometres south of the Grenville Front, about 45 km east of Temiskaming, Quebec. The complex can be traced for more than 100 km around an anticline-syncline pair (Fig. 1) terminating in complex "fish-hook" folds at each end. The complex consists of numerous elongate lenses of granoblastic amphibole-biotite syenite, quartz syenite, and granite within a slightly migmatitic, strongly foliated biotite-magnetite granite gneiss. Some lenses contain minor amounts of nepheline-bearing gneiss (<1% of the volume of the complex) but most of the complex is nepheline-free or quartz-bearing, characterized by amphibole blastesis, coarse granoblastic texture, and blotchy red colouration due to late hematization. Syenite, and nepheline syenite where present, occur as lenses <50 m thick within quartz- and amphibole-bearing rocks which grade into the surrounding gneiss. Spectacular agpaitic metasomatic rocks occur on the margin of the complex (Tremblay-Clark and Kish, 1978; Currie and van Breemen, 1996a). New field and geochronological observations suggest that much of the syenite complex may also be of metasomatic origin.

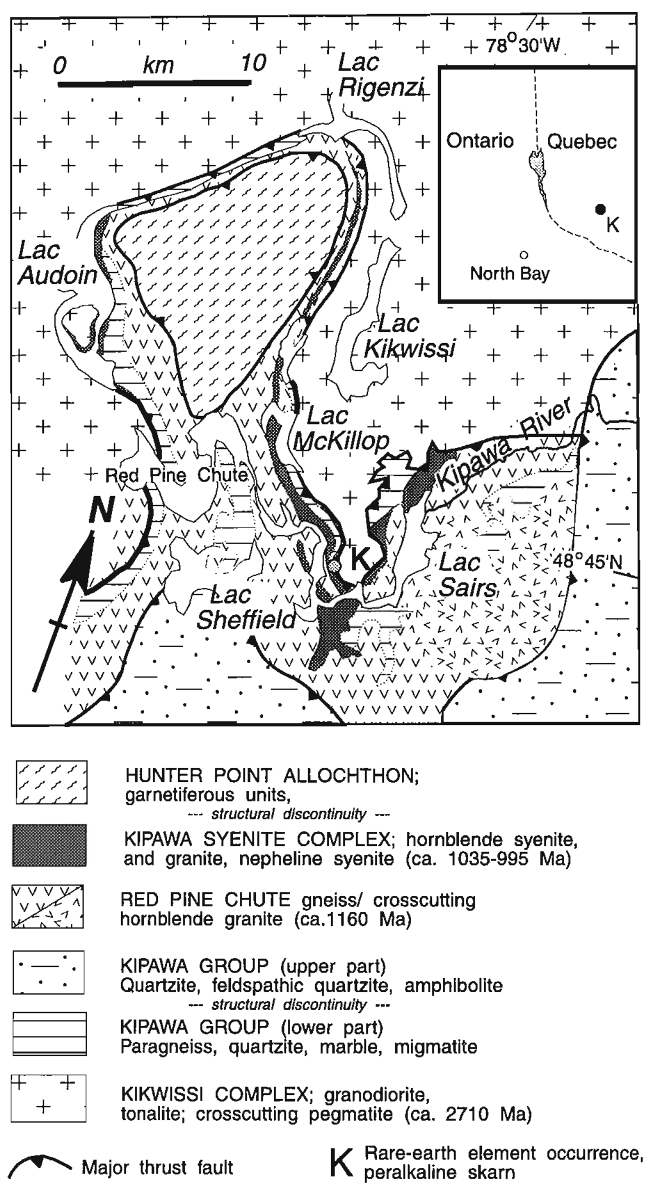

Figure 1. *Geological sketch of the Kipawa Syenite Complex.*

GEOLOGICAL SETTING

Geological mapping in this region rests on a remarkably precise reconnaisance survey by Lyall (1958), supplemented by subsequent work by Rive (1973) and Tremblay-Clark and Kish (1978). Currie and van Breemen (1996a) summarized and extended these findings based on extensive exploration work on a rare-earth element prospect (Allan, 1992). The rocks can be divided into five major units: the Kikwissi granitoid complex, the Kipawa Group of metasedimentary rock, the Red Pine Chute granite gneiss, the Kipawa Syenite Complex, and allochthonous garnetiferous rocks of the Hunter Point structure. Two minor, but stratigraphically critical units comprise mafic dykes, assumed to be part of the Sudbury swarm and amphibolitic gneiss.

The Kikwissi complex comprises weakly foliated to lineated white biotite tonalite to granodiorite with minor pink granite and pegmatite dykes. The rocks typically contain centimetre-scale aligned poikilitic spindles of biotite containing granules of epidote in a matrix of quartz and plagioclase with variable but minor amounts of perthitic microcline. Coarse, massive quartz-microcline-oligoclase-biotite pegmatite dykes cut cleanly across the foliation, and quartz veins of similar size and style also occur. Considerable variations in composition and style occur within the Kikwissi complex, but the complex clearly represents little-deformed igneous rocks. The assemblage biotite+epidote could represent retrogression of primary hornblende+plagioclase during cooling of the plutons. A preliminary U-Pb zircon age on the Kikwissi complex yielded an emplacement date of greater than 2710 Ma (Currie and van Breemen, 1996b). The Kikwissi complex appears as a large mass northeast of the Kipawa Syenite complex, extending well beyond the map boundaries, and also as small inliers, presumably structurally controlled, within other units of the complex.

Rive (1973) referred to the metasedimentary sequence overlying the Kikwissi complex as the Kipawa Group. Current mapping suggests that the Kipawa Group may be composite, with a lower portion below the Red Pine Chute gneiss, and an upper, possibly unrelated, portion above the gneiss. The lower portion comprises quartz-plagioclase-biotite gneiss (assumed to be metamorphosed greywacke and arkose), quartzite, and minor marble. Quartz-plagioclase-biotite gneiss rests with a sharp conformable contact on the Kikwissi complex, a contact interpreted as a metamorphosed unconformity (Currie and van Breemen, 1996b). The gneiss is mineralogically essentially identical to the Kikwissi complex, with the addition of minor muscovite. It exhibits strong centimetre-scale lamination, with alternating layers rich in quartz and biotite. Layers of biotite amphibolite up to 30 cm thick form about 5% of the unit, locally producing a rock with black and white stripes at centimetre scale. Like the Kikwissi complex, the gneiss is cut by pegmatite dykes and contains the assemblage biotite+epidote. The thickness of the unit varies from a few metres near Lac McKillop to almost 700 m along Lac Rigenzi. Much of this quartz-plagioclase-biotite gneiss unit appears to represent greywacke derived by erosion of the Kikwissi complex.

A unit of quartzite, quartz-muscovite gneiss, and migmatitic muscovite quartzite is interbedded with, and overlies, the quartz-biotite-plagioclase gneiss. Coarse granular quartzite layers with glassy, granoblastic quartz are common, but rarely exceed 30 cm in thickness. The rest of the rock is composed of granular quartz, muscovite, and deformed boudins of muscovite granite and pegmatite, with books of muscovite up to 5 cm across. Granite and pegmatite do not cut foliation which commonly wraps around metre-scale boudins of granitic rocks. Most outcrops are intricately folded, and appear to have flowed readily during deformation. Both sillimanite and kyanite have been reported from the upper part of this unit (Rive, 1973).

The upper part of the quartzite unit contains one or more layers of marble 1 to 2 m thick which are intricately folded on a metre-scale. Crystals of tremolite and diopside up to 10 cm long occur in coarse, friable calcite. All of the scattered occurrences of marble occur near the same structural level, and may represent relics of an originally more continuous layer. The apparent rarity of this rock type may result from some combination of easy erosion and tectonic thinning.

A fault separates the quartzite-marble layer from the Red Pine Chute gneiss. In drill core from the rare-earth element prospect, and in outcrop along Lac McKillop and northeast of Lac Audoin (Fig. 1) this contact is marked by a 1 to 2 m layer of straight gneiss or mylonite. In other places the contact is marked by narrow linear valleys. The relatively low grade of the mylonite may suggest that the fault is a late feature, and probably relatively minor.

Lyall (1958) and Rive (1973) included biotite-muscovite gneiss above the Red Pine Chute gneiss with the Kipawa Group. This gneiss varies from quartz-biotite-plagioclase gneiss similar to the lowest unit of the Kipawa Group through muscovite-quartz gneiss to thin layers of quartzite. The unit is migmatitic, locally with conformable layers of pink biotite granite, but more commonly the granitoid component cuts across the foliation in dykes or irregular masses. The most striking feature of the upper Kipawa Group is the local presence of sedimentary structure including crossbedding, heavy mineral lags, and metamorphosed graded bedding, now expressed by variation in proportions of biotite and muscovite. Although these palimpsests are rare and local, they form the only trace of original sedimentary structure in Kipawa region.

Although considerable parts of the Kipawa Group are migmatitic, garnet and amphibole are essentially absent. Sparse garnet occurs in the aureole of one pegmatite dyke, while amphibole occurs sparingly in rare amphibolite layers. By contrast, muscovite is ubiquitous. The age of the Kipawa Group is constrained between the age of the underlying Kikwissi Complex (2700 Ma) and the age of crosscutting mafic dykes thought to belong to the Sudbury swarm (emplaced at 1235 Ma; Dudas et al., 1994).

Mafic dykes

Rare metre-scale mafic dykes within the Kipawa Group exhibit sharp, locally crosscutting boundaries, preserved ophitic texture, relict clinopyroxene, and development of small metamorphic garnets. Two examples were found in the lower part of the Kipawa Group, and two more in the upper part. All bodies now lie more or less within the foliation of the surrounding gneiss, but crosscutting margins are locally preserved. The rocks consists of strongly zoned plagioclase, relict clinopyroxene rimmed by hornblende, accessory titanite and magnetite, and abundant microscopic garnet, commonly concentrated along fractures. On the basis of petrography and detailed geochemistry, K.M. Bethune (pers. comm., 1995) has positively identified one of these dykes as a member of the Sudbury swarm, emplaced at 1235 Ma (Dudas et al., 1994). Bodies of this type have not been found within the Red Pine Chute gneiss, Kipawa Syenite Complex, or units of the Hunter Point Structure. Lyall (1958) reported a crosscutting diabase dyke within the Kikwissi Complex, which may belong to this swarm, but this dyke was not examined in this study.

Red Pine Chute gneiss

The Red Pine Chute gneiss (Currie and van Breemen, 1996b) consists of migmatitic, strongly foliated, pink biotite granite laminated on millimetre scale. A granoblastic, rather fine-grained quartz-perthite-oligoclase matrix contains biotite as disseminated fine flakes, and more characteristically as narrow, diffuse schlieren a few millimetres thick and 1 to 2 cm long. Quartz-rich streaks of similar dimensions commonly give the rock a strong lineation. A highly characteristic mineral of the Red Pine Chute gneiss is magnetite, present either as flat plates, pseudomorphous after biotite, or as sparse equant porphyroblasts, up to 2 cm across, which cut the foliation. Both magnetite and biotite may be surrounded by red spots of hematite up to a centimetre in diametre, giving the rock an unmistakable red-spotted appearance.

The gneiss is migmatitic, especially in its upper parts, with development of 2 to 5 cm layers of coarse grained, leucocratic granite. These layers are perfectly concordant, and in many examples barely visible because they appear to be merely a coarsening of the grain size of the rock. However upon examination most layers prove to have a thin biotite selvage. Rarely these leucogranite layers follow northeast- or northwest-trending linear zones a few centimetres wide, and cut the foliation for up to a metre. The gneiss also contains several concordant layers of biotite amphibolite, particularly near the base. Like the granitoid portion, the margins of these layers exhibit a very strong foliation and lineation, with development of spindles of feldspar, but the central part of some of the amphibolite layers is less foliated, and locally preserves traces of ophitic texture.

The Red Pine Chute gneiss forms a continuous layer 1500 to 2000 m thick which can be traced for more than 100 km. It also appears in small isolated areas west of Red Pine Chute where the low dip and plunge of major structures produce numerous windows. The base of the gneiss appears to be faulted against the Kipawa Group, as noted above, although the displacement on this fault may be small. The top of the Red Pine Chute gneiss grades into the upper Kipawa Group by appearance of muscovite in the gneiss, and either increasing colour index, or loss of foliation where the gneiss passes into the almost massive granitic component of the upper Kipawa Group.

The upper contact of the Red Pine Chute gneiss is also marked by numerous tectonic blocks of unusual mafic syenite consisting of centimetre-scale, euhedral tablets of microcline in a finer grained matrix of aegirine. These blocks, many of which exceed 20 m in longest dimension, occur over a large area extending from Lac Sairs to west of Red Pine Chute (Fig. 1), everywhere at or near the upper margin of the Red Pine Chute gneiss. The gneissosity of the host is deflected around the blocks at angles of up to 90° to the regional strike. The central parts of the blocks exhibit igneous texture, but the marginal parts are moderately to strongly foliated, and zones of foliation up to a metre across may transect the blocks. In one block, south of Red Pine Chute, the foliated material passes transitionally into an amphibole- and quartz-bearing syenite very similar to amphibole quartz syenite of the Kipawa Syenite Complex. If all the blocks of mafic syenite originated in one body, a reasonable hypothesis given the unusual composition and texture of the blocks, the present separation of the blocks implies very large strains, exceeding 1000%, within the Red Pine Chute gneiss subsequent to the emplacement of the syenite.

Currie and van Breemen (1996b) reported an emplacement age for the Red Pine Chute gneiss of ca. 1160 Ma, noting that it displayed significant Archean inheritance, as well as some recent lead loss. If the mafic dykes in the Kipawa Group are correctly correlated with the Sudbury swarm, the Red Pine Chute gneiss postdates both dykes (1235 Ma) and the host Kipawa Group. The gneiss could have been emplaced as a sill within the Kipawa Group, and derived, in part at least, from Archean rocks like the Kikwissi Complex. However such derivation could not have taken place from any exposed parts of the Kikwissi Complex since the Archean rocks did not reach partial-melting temperatures. The strikingly regular fine foliation within the gneiss suggests strong planar deformation. The gneiss may therefore represent a major movement surface within the Kipawa Group. In this model, the Red Pine Chute gneiss would be a body emplaced along a fault surface, and subsequently further deformed. The melt parental to the Red Pine Chute gneiss could be derived from more southerly, presumably higher grade, parts of the Archean basement. Whatever model is adopted, the body parental to the mafic syenite blocks was emplaced within the Red Pine Chute gneiss, and hence must be younger than ca. 1160 Ma.

Hunter Point structure

The Hunter Point structure forms a north-northwest-trending, elliptical mass about 20 km long by 10 km wide. The base of the structure is marked by a spectacular zone of disruption including blocks of ophitic-textured garnet-pyroxene rocks, as well as innumerable metre-scale blocks and schlieren of hornblende-plagioclase-quartz gneiss which can be matched in the immediate surroundings. The least tectonized examples of garnet-pyroxene rocks contain no feldspar, although a trace of quartz may be present. Most blocks contain varying amounts of amphibole, and many are cut by irregular, ramifying granitoid veinlets. The edges of the blocks are invariably foliated, and in some case streaked out into the foliation, grading to mafic garnet gneiss indistinguishable from some layers in the surrounding host. Indares and Dunning (1997) reported a U-Pb age of 1403+14/-11 Ma from an eclogitic block at the same structural horizon located 30 km east of the Hunter Point structure.

The host of the garnet-pyroxene boudins consists of well-layered amphibolite gneiss with alternating amphibole- and plagioclase-rich layers on a scale of 1 to 10 cm. Subordinate quartz and biotite commonly occur in both layers, but garnet and potassium feldspar are absent. The thickness of the layers varies considerably from outcrop to outcrop, but within an outcrop layers are remarkably persistent and constant in thickness. Numerous reclined isoclinal small folds all exhibit south-over-north vergence, but in many outcrops this unit has been reduced to straight gneiss with millimetre-scale comminuted layers continuing ruler-straight for many metres.

The upper part of the amphibolite gneiss contains thin garnetiferous mafic layers, forming a transition to the upper unit of the Hunter Point structure which varies from amphibolitic through pelitic to locally granitic compositions, all richly garnetiferous. The rocks exhibit strong compositional layering on a scale of a few centimetres, and a strong lineation marked by spindles of quartz and feldspar up to a few centimetres long. In the pelitic parts of the complex these spindles also contain sillimanite. The gneissosity, and a small scale foliation superimposed upon it, is typically wavy, but small folds are sparse, although local boudined layers of marble about 10 cm thick and a few metres long do show metre-scale, gently south-plunging small folds. The garnets typical of this unit vary in size from 3 mm to 3 cm in diameter, but all are subhedral, apparently randomly distributed, and cut the foliation. An isolated occurrence of similar lithology occurs east of the mapped area along a major woods road (N814) 3 km southwest of the bridge over the Kipawa River. These rocks appear to form an outlier about 100 m in diameter resting on Kikwissi Complex.

Kipawa Syenite Complex

The Kipawa Syenite Complex forms a zone about 200 m thick within the Red Pine Chute gneiss, and extends more than 100 km from Lac Sairs to Lac Audoin, terminating abruptly at both ends in complex, polyphase folds. Most of the complex consists of brownish pink, coarsely granoblastic amphibole-biotite quartz syenite and syenite which grades imperceptibly to the enclosing host gneiss. In detail the complex consists of numerous elongate lenses at slightly varying tectonic levels within the host gneiss. The complex is characterized by porphyroblastic amphibole, commonly greater than 1 cm in largest dimension. Amphibole occurs both as single, subhedral porphyroblasts cutting the foliation, and as polycrystalline masses up to a metre long, commonly rimmed and veined by albite. These masses are mainly found within the syenite, but also in the surrounding rocks. The composition of the amphibole varies from steely blue kataphorite within the syenite to deep green hastingsite in the surrounding area (Currie and van Breemen, 1996a). The only specimens from the complex which do not contain amphibole are some nepheline-bearing rocks and the mafic syenite which both contain the assemblage biotite+aegirine. Biotite is also a ubiquitous constituent of the syenite, occurring as small, aligned flakes. Due to their granoblastic character, the rocks weather to fine, biotite-rich gravel. Aegirine occurs in about one quarter of specimens examined, but is difficult to recognize in hand specimen. Its presence does not appear to be reliably correlated with any other mineral. Feldspar consists of complex perthite coexisting with albite or oligoclase. Some specimens exhibit weak segregation into feldspar-rich and feldspar-poor layers. Quartz is commonly intersertal where present. Nepheline, in the few specimens containing it, forms large elliptical grains, slightly to moderately altered. In general terms the syenite complex mineralogically resembles its host, with the addition of amphibole porphyroblasts, a coarsening of grain size, and a loss of the fine foliation characteristic of the Red Pine Chute gneiss.

Currie and van Breemen (1996a) reported a U-Pb zircon age of 995+/-2 Ma for metasomatic agpaitic rocks on the margin of the syenite complex. A preliminary U-Pb zircon age on nepheline syenite suggests an emplacement age of about 1035 Ma (O. van Breemen, pers. comm., 1997). Both ages are significantly younger than the age of the Red Pine Chute gneiss (ca. 1160 Ma).

STRUCTURE

The complex fold structure of this region was discussed by Currie and van Breemen (1996a). Very large, open, north-trending folds control the large scale disposition of rock units, as recognized by Lyall (1958). These folds have low but variable plunges due to gentle northeast-trending warps. Local disposition of rock units is controlled by two earlier periods of isoclinal recumbent folds, as described by Currie and van Breemen (1996a). As a result, complex fold interference patterns abound in this region, some of which can be seen on map scale (e.g. at Ile à la Tortue and eastward; Fig. 1). All generations of folds, which appear to be present in all lithological units including the Hunter Point structure, can be explained by persistent south-over-north, low angle thrusting (Currie and van Breemen, 1996a).

Two major tectonic discontinuities can be recognized in this region, one at the base of the Hunter Point structure and the other within the Red Pine Chute gneiss. Both of these discontinuities are marked by extensive development of straight gneiss and mylonite, and decorated by numerous tectonic blocks of massive, igneous-textured rocks, garnet-pyroxene blocks in at the base of the Hunter Point structure and mafic syenite in the case of the Red Pine Chute gneiss. The base of the Hunter Point structure clearly cuts downward to the north across the upper Kipawa Group into the underlying Red Pine Chute gneiss.

Late faults in this region can be identified by strong planar fissility and development of local sheared rock. They tend to trend northeast or northwest and dip steeply. A few thin sheets of leucogranite within the Red Pine Chute gneiss lie in these orientations, and they may fill late faults with this orientation.

DISCUSSION

Field and geochronological evidence suggest that the Kipawa Group formed a cover, presumed to be of Proterozoic age, to late Archean basement of the Kikwissi Complex. Davidson (1995) interpreted the Hunter Point structure as correlative to part of the Britt domain of Ontario, in which 1.8-1.6 Ga gneisses and plutonic rocks form the host to voluminous ca. 1.45 Ga igneous rocks which are themselves highly deformed and metamorphosed. Restriction of the ca. 1.4 Ga mafic rocks to correlatives of the Hunter Point structure (Indares and Dunning, 1997), together with restriction of presumed Sudbury dyke equivalents in the underlying rocks, suggest that the Hunter Point structure was emplaced after emplacement of the mafic dykes which occurred at ca. 1235 Ma, presumably during an episode of extension. Emplacement of the Hunter Point structure may have been roughly contemporaneous with thrusting of the upper Kipawa Group over the lower Kipawa Group, and emplacement of the Red Pine Chute gneiss along the décollement, possibly as a synkinematic pluton, at ca. 1160 Ma. Observations suggest that the overthrust sheet was hot but relatively thin, since the steep inverted metamorphic gradient beneath the Red Pine Chute gneiss passes down from muscovite+sillimanite+potassium feldspar+quartz assemblages to biotite+epidote assemblages within a few tens of metres, although this transition may be tectonically attenuated.

Emplacement of nepheline syenite, and presumably of aegirine melasyenite, occurred more than 100 Ma after this episode at ca.1035 Ma. The original form of the alkaline complex cannot now be reconstructed, but it may have formed a sheet, or series of sheets near the top of the Red Pine Chute gneiss. General consideration of the petrology of alkaline complexes suggest that it was emplaced during a brief period of extension.

Subsequent to emplacement of this "proto-Kipawa" complex, northward thrusting recommenced, rejuvenating movement planes within the the Red Pine Chute gneiss and dismembering the alkaline complex. Final emplacement of the Hunter Point allochthon truncated the underlying stratigraphy, and imposed an inverted metamorphic gradient on the underlying rocks, as evidenced by the downward decrease in migmatization in the Red Pine Chute gneiss. A late stage in this process is dated by the 995 Ma U-Pb zircon age from massive agpaitic pegmatite (Currie and van Breemen, 1996a).

Evidence for major metasomatism within and below the Red Pine Chute gneiss during final tectonic assembly of this region has been presented by Currie and van Breemen (1996a), using a local spectacular development of agpaitic mineral assemblages. The ubiquitous presence of amphibole porphyroblasts and pods in and around the Kipawa Syenite Complex also testify to widespread metasomatism of a less spectacular kind. Mass balance considerations show that development of amphibole syenite from biotite granite is a plausible process during soda metasomatism. For example

$$3\ \underset{\text{plagioclase}}{CaAl_2Si_2O_8} + 4\ \underset{\text{biotite}}{KAlFe_3Si_3O_{10}(OH)_2} + 6\ NaOH + 15\ \underset{\text{quartz}}{SiO_2} =$$

$$3\ \underset{\text{kataphorite}}{Na_2CaAlFe_4Si_7AlO_{22}(OH)_2} + 4\ \underset{\text{K-feldspar}}{KAlSi_3O_8} + 4\ H_2O$$

Formation of kataphorite, typical of the syenite, would consume quartz and lead to rocks richer in potassium feldspar and poorer in calcic plagioclase. An analogous equation can be written for the hastingsitic amphibole typical of the quartz-bearing syenite. Operation of soda metasomatism in the Red Pine Chute gneiss is indicated by the presence of widespread peralkaline chemical compositions within the unit (Currie and van Breemen, 1996a). None of these considerations suggests the source of the metasomatising fluids, but an obvious possible source was the alkaline igneous complex indicated by the presence of nepheline syenite gneiss and mildly peralkaline aegirine syenite. The latter indicates that the complex was at least mildly peralkaline, and therefore a potential source of alkali metasomatism.

Coarse melasyenite appears to have resisted deformation better than many other rock types. Similar rocks in the Red Wine peralkaline complex of Labrador are the only portions to show relict igneous texture (Curtis and Currie, 1981). That complex also possesses an extended aureole of metasomatism developed during deformation. The source of the fluid carrier for metasomatism remains uncertain, but dehydration of the Kipawa Group during metamorphism could be a possible source.

The model suggested here bears considerable similarity to that proposed by Hanmer and McEachern (1992) for nepheline syenite in the Bancroft region. In the present case, the impermeable "lid", which these authors proposed to be a series of gabbro sheets, is supplied by the Hunter Point allochthon (which also includes numerous mafic sheets). These similarities suggest that nepheline syenite gneiss in highly deformed parts of the Grenville Province may tell as much about structure as they do about the petrology of alkaline rocks.

ACKNOWLEDGMENTS

I wish to acknowledge specifically the large and obvious debt which this work owes to the superb mapping by H.B. Lyall (1958). Conducted 40 years ago, at a time when modern ideas of structure and petrology had not been conceived, this painstakingly accurate recording of the lithologies remains the foundation for all serious geological work in this region.

REFERENCES

Allan, J.F.
1992: Geology and mineralisation of the Kipawa yttrium-zirconium property, Quebec; Exploration and Mining Geology, v. 1, p. 283-293.

Currie, K.L. and van Breemen, O.
1996a: The origin of rare minerals in the Kipawa Syenite Complex, western Quebec; Canadian Mineralogist, v. 34, p. 435-451.
1996b: The Kipawa Syenite Complex - an unusual Archean-Proterozoic boundary marker in the Grenville Front Tectonic Zone of western Quebec; Geological Association of Canada Abstracts with Program, v. 20, p. A-21.

Curtis, L.W. and Currie, K.L.
1981: Geology and petrology of the Red Wine alkaline complex, central Labrador; Geological Survey of Canada, Bulletin 294, 61 p.

Davidson, A.
1995: A review of the Grenville orogen in its North American type area; Journal of Australian Geology and Geophysics, v. 16, p. 3-24.

Dudas, F.Ö., Davidson, A., and Bethune, K.M.
1994: Age of the Sudbury diabase dikes and their metamorphism in the Grenville Province, Ontario; in Radiogenic Age and Isotopic Studies: Report 8; Geological Survey of Canada, Current Research 1994-F, p. 97-106.

Hanmer, S. and McEachern, S.
1992: Kinematical and rheological evolution of a crustal-scale ductile thrust zone: Central Metasedimentary Belt, Grenville orogen, Ontario; Canadian Journal of Earth Sciences, v. 29, p. 1779-1790.

Indares, A. and Dunning, G.
1997: Coronitic metagabbro and eclogite from the Grenville Province of western Quebec: interpretation of U-Pb geochronology and metamorphism; Canadian Journal of Earth Sciences, v. 34, p. 891-901.

Lyall, H.B.
1958: Preliminary report on the McLachlan-Booth area, Temiscamingue Electoral District; Quebec Department of Mines, Geological Survey Branch, Preliminary Report 391,8 p.

Rive, M.
1973: Géologie de la région des lacs Ogascanane et Sairs, Comté de Témiscamingue; Ministère des Richesses naturelles du Québec, Service de l'exploration geologique, Rapport Préliminaire 606, 13 p.

Tremblay-Clark, P. and Kish, L.
1978: Le district radioactif de Kipawa; Ministère des richesses naturelles du Québec, Service de l'exploration géologique, Direction générale des mines, Rapport préliminaire DPV-579, 28 p.

Geological Survey of Canada Project 680071

A note on the Obedjiwan nepheline syenite, central Quebec

K.L. Currie and J. Gittins[1]
Continental Geoscience Division, Ottawa

Currie, K.L. and Gittins, J., 1998: A note on the Obedjiwan nepheline syenite, central Quebec; in Current Research 1998-C; Geological Survey of Canada, p. 173-177.

Abstract: The Obedjiwan nepheline syenite forms two lenticular masses, one about 4 km by 2 km centred near 48°41′N, 74°56′W, and a smaller body 5 km to the northwest. Both bodies are coarse grained and weakly foliated, but show a strong lineation, and schlier-like areas of finer grain, interpreted as blastomylonitic. They have been substantially recrystallized, probably under amphibolite or granulite facies conditions. A pyroxene syenite outcropping around the periphery of the nepheline syenite forms part of a regional mafic gneiss complex hosting the nepheline syenite. The mechanical strength of the regional complex may be the reason why the nepheline syenite shows relatively little deformation, since migmatitic granite gneiss north of the complex is much more strongly deformed. These observations suggest that the Obedjiwan nepheline syenite is fairly typical of Proterozoic nepheline syenite bodies along the Grenville Front, and not anomalously undeformed and unmetamorphosed, as previously reported.

Résumé : La syénite néphélinique d'Obedjiwan se compose de deux masses lenticulaires. La première mesure environ 4 km sur 2 km et est centrée à proximité de 48° 41′ N, 74° 56′ W; la seconde, plus petite, est située à 5 km au nord-ouest. Les deux masses sont à grain grossier et faiblement foliées, mais elles présentent une linéation très accusée et des zones à grain plus fin à l'aspect de schlieren qui sont interprétées comme étant blastomylonitiques. Elles sont largement recristallisées, probablement au faciès des amphibolites ou des granulites. Une syénite à pyroxène affleure autour de la périphérie de la syénite néphélinique et fait partie d'un complexe gneissique mafique régional qui encaisse la syénite néphélinique. La déformation relativement faible de la syénite néphélinique pourrait être attribuable à la résistance mécanique du complexe régional; en effet, du gneiss granitique migmatitique situé au nord du complexe est beaucoup plus déformé. Ces observations laissent supposer que la syénite néphélinique d'Obedjiwan est passablement représentative des massifs de syénite néphélinique protérozoïques situés le long du front de Grenville et qu'il n'est pas exceptionnel qu'elle ne soit ni déformée ni métamorphisée, comme on l'a rapporté antérieurement.

[1] Department of Geology, University of Toronto, Toronto, Ontario M5S 1A1

INTRODUCTION

In the course of regional mapping during 1962, A.F. Laurin discovered two occurrences of nepheline syenite near the Attikamekh village of Obedjiwan in central Quebec (Laurin, 1965). He interpreted the main body to be a roughly circular mass about 7 km in diameter, centred on the north shore of the Gouin Reservoir near 48°41'N, 74°56'W (Fig. 1). A separate lenticular mass of nepheline syenite, about 2 km long by 400 m wide occurs 3 kilometers northwest of the main body. Gittins (1967), in a preliminary report on the nepheline syenite, remarked that much of the rock was very coarse grained (up to 1 cm grain size), and essentially massive, although weak foliation was locally present and lineation was pervasive. He noted that the main mass was composite, consisting of a central core of white to pink biotite-dominant nepheline syenite, and a surrounding area of brown to black pyroxene syenite. He interpreted all of the syenite to be essentially undeformed igneous rock. No further published work on the Obedjiwan nepheline syenite has appeared since this report.

The occurrence of an essentially undeformed, unmetamorphosed pluton of nepheline syenite within the northern part of the Grenville Province excited little remark in 1967. However subsequent mapping and dating have shown that all other plutons in this region were emplaced prior to final deformation and metamorphism at about 1000 Ma and are therefore deformed and metamorphosed to varying degrees. The Obedjiwan complex thus appears unusual, if not anomalous, particularly since it has yielded an unpublished U-Pb zircon date greater than 1020 Ma (M. Higgins, personal communication, 1997). The Obedjiwan complex was re-examined during 1997.

GEOLOGICAL SETTING

Obedjiwan can be reached via about 260 km of well maintained gravel roads from either Saint Felicien or La Tuque. The north shore of the Gouin Reservoir near Obedjiwan consists mainly of glacial till and boulder clay forming an almost flat surface punctuated by low drift ridges trending 180-190°, the direction of glacial transport indicated by striations on outcrops and well-defined glacial dispersion trains of boulders. Numerous spoil pits along roads and occasional landslip scars indicate that glacial deposits are commonly more than 2 m, and locally more than 10 m thick. Outcrop within this drift plain is almost nonexistent except for half a dozen small areas which have been excavated by road-building activity (Fig. 1). Steep, generally northeast-trending ridges rise above the glacial deposits, locally reaching heights of 200 m above the surroundings and exposing bedrock near their summits. In the Obedjiwan region these hills are spaced several kilometres apart, leaving the nature of the bedrock between them uncertain. Outcrop is also present in rapids on the major rivers. Gittins (1967) observed outcrop around the shore of Gouin Reservoir during a period of low water in 1965, but in 1997 water levels were high, and there was virtually no exposure along the shoreline.

Four major rock types were observed in the Obedjiwan region; (1) migmatitic, generally granitoid gneiss; (2) mafic metamorphic rocks, ranging from boudins of garnetiferous meta-gabbro to amphibolitic rocks; (3) pyroxene syenite; and (4) nepheline syenite. As noted above, few relationships between these rock types are exposed.

DESCRIPTION OF UNITS

Migmatitic granitoid gneiss outcrops in a small area northeast of the nepheline syenite and as a lenticle within mafic gneiss in rapids on Rivière Toussaint. According to the mapping of Laurin (1965), such gneiss underlies a large region north of the area examined this year. Outcrop consists of thinly laminated pink to grey biotite granite gneiss with millimetre-scale quartz-feldspar layers and intervening finer grained foliae containing fine bioitte. The layers are persistent at outcrop scale, but quite sinuous and locally folded on a scale of metres. One outcrop contains a decametre-scale boudin of ophitic-textured garnetiferous metagabbro. Metre-sized boulders of grey, generally granitic, biotite gneiss abound in the glacial overburden. Similar, but less foliated, pink granite gneiss boulders also form a component of the drift, as do more biotite-rich rocks with a coarser gneissosity. Presumably these erratics represent bedrock to the north of the nepheline syenite.

Mafic metamorphic rocks outcrop northwest of Obedjiwan, in the rapids of Rivière Toussaint, and west of the northern outlier of nepheline syenite. East and northeast of Obedjiwan, outside the area covered by Figure 1, they are a major component of the outcrop, but mafic rocks form only as a minor component (<10%) of the drift around Obedjiwan. Mafic rocks west and north of the Obedjiwan complex comprise medium grained, locally garnetiferous pyroxene-bearing amphibolitic gneiss. The rocks lack quartz, are relatively poor in plagioclase (15-30 volume per cent), and contain roughly equal amounts of weakly oriented olive amphibole and green clinopyroxene, with lesser amounts of biotite. Garnet, commonly in equant grains a few millimetres across, is sporadically present. Gneissosity is commonly weak and locally absent. Pyroxene in these rocks has recrystallized to form a blocky mosaic. Minor amounts of strongly foliated pink to grey granitoid gneiss are intercalated with the mafic rocks, and most outcrops also contain ramifying granitoid veinlets. A boudin approximately 20 m long by 10 m wide of massive, ophitic-textured, two-pyroxene gabbro with abundant pale pink garnet occurs within migmatitic granite gneiss 2 km north of the syenite complex. The outer part of the boudin contains millimetre-sized garnet interstitial to orthopyroxene and plagioclase. In the core of the boudin garnets up to a centimetre across are present, crosscutting other minerals. Gneissosity in the host wraps around the boudin, with deflections up to 70° from the regional northeasterly strike. This boudin strongly resembles metagabbro boudins south of the Grenville Front in western Quebec (Indares and Dunning, 1997).

Pyroxene syenite outcrops west and east of Obedjiwan on islands in Gouin Reservoir, in road cuts across a low ridge along the road just northeast of the village, and in the rapids of Rivière Toussaint several kilometres north of Obedjiwan. The weathering surface of the rock is pale pink to white with large grey feldspar crystals, but on fresh surface the colour varies from honey brown through deep brownish green to almost black. In some outcrops the syenite is coarse grained and massive, but in others strong foliation is present on a scale of centimetres. The rock contains biotite as well as pyroxene,

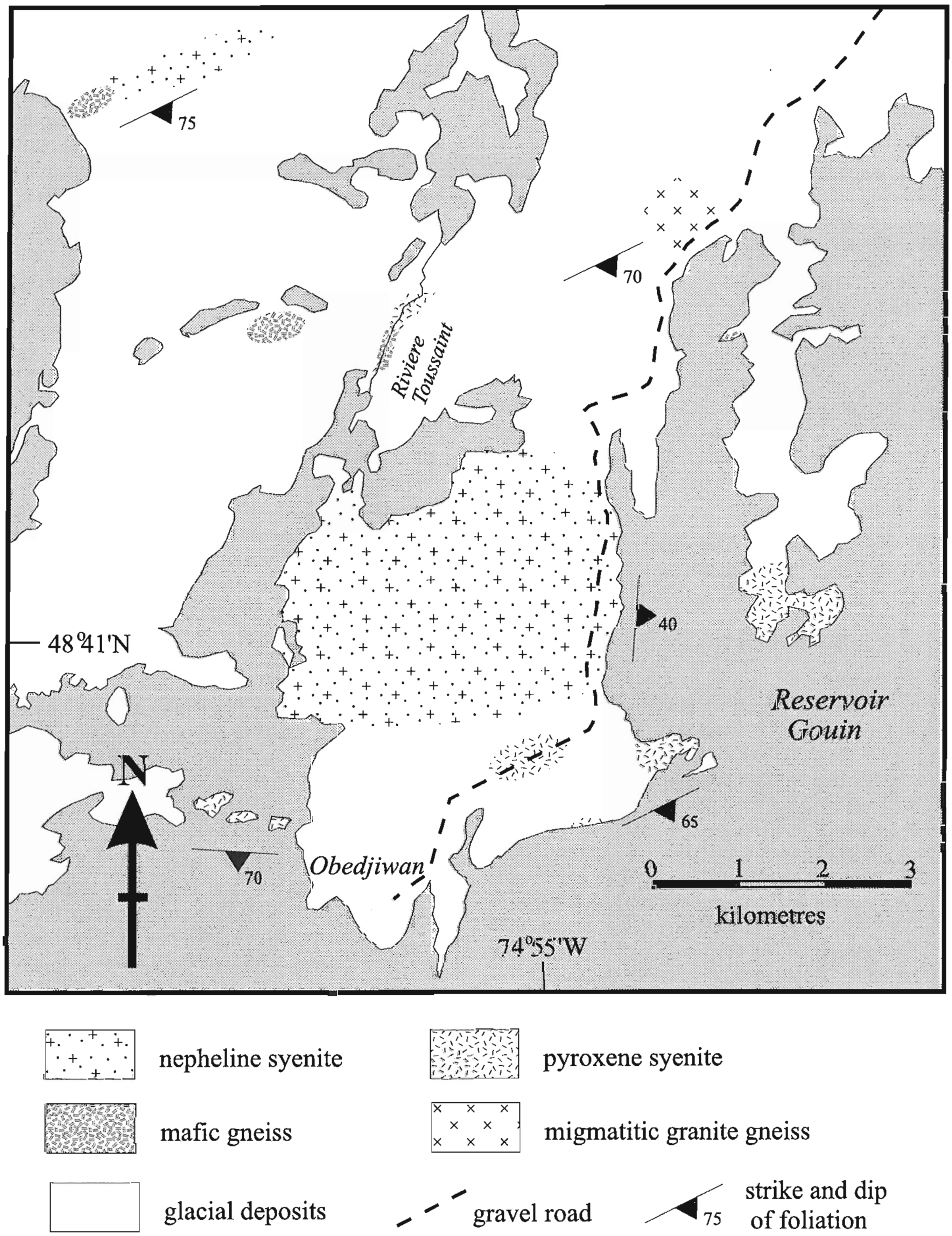

Figure 1. *Geological sketch of the Obedjiwan region, central Quebec. No bedrock outcrop occurs in the unpatterned areas. The nature of the bedrock in these areas remains uncertain.*

and there appears to be complete gradation to the mafic gneiss described above. Metre-scale schlieren of mafic pyroxene and biotite-bearing amphibolite are a common feature of the syenite. Gittins (1967) described the pyroxene syenite as consisting largely of crystals of fine perthite, with variable amounts of plagioclase, deep green clinopyroxene with brown exsolution lamellae of orthopyroxene, and varying amounts of ilmenite. Minor amounts of amphibole, biotite, and magnetite may be present. In thin section, this rock appears to be strongly recrystallized with mosaic clinopyroxene in an intricate sutured matrix of feldspar. Amphibole and biotite both appear to be developed by reactions involving pyroxene.

Preliminary electron microprobe analyses of pyroxene and biotite indicate that the pyroxene contains less than 25% of acmite component, while the biotite is extremely iron-rich, approaching lepidomelane.

Gittins (1967) believed the pyroxene syenite was confined to the Obedjiwan region, and therefore associated with the nepheline syenite, although he recognized that it probably resulted from reworking of the surrounding gneissic rocks. Cursory examination of road outcrops south of Gouin Reservoir between Gouin Dam and Parent show that pyroxene syenite occurs commonly as a component of a mafic granulite complex of regional extent. It therefore appears unlikely that the pyroxene syenite is genetically associated with the nepheline syenite.

Nepheline syenite is the best exposed rock type in the Obedjiwan region, outcropping on the prominent hills north of the village, in road cuts, on a few islands, and on the prominent ridge northwest of the main mass. Exposure of the main mass has been greatly enhanced by construction of logging roads.

Typically the nepheline syenite forms a very coarse grained, pale grey to pink rock dominated by aligned tablets of nepheline and perthitic feldspar up to a centimetre across. Depending on the degree of alignment, foliation may be present, although lineation is more common. The lineation is emphasized by streaks and spindles of biotite several tens of centimetres long in which biotite books reach 2 cm across. In thin section the biotite is commonly intergrown with green clinopyroxene, and less commonly minor hornblendic amphibole. The mafic aggregates clearly show evidence of deformation in the form of cuspate cross-sections, and, less commonly, internal slickensides. Foliation and degree of deformation increase gradually from south to north within the main body. The satellitic body northwest of the main body consists of very coarse grained (>1 cm), leucocratic rocks with no foliation and weak lineation. The colour of the rock varies from the pale grey typical of nepheline syenite to a rather patchy pink shade reminiscent of some granites. Gittins (1967) considered the pink material to be richer in potassium, although the immediate cause of the colour is alteration of nepheline.

Preliminary electron probe analyses indicate that the pyroxene of the nepheline syenite contains about 50% acmite component, but still has a substantially higher Mg number than pyroxene from the pyroxene syenite. The biotite is also much more magnesian than that in the pyroxene syenite with Mg numbers near 50.

Gittins (1967) drew attention to finer grained areas within the nepheline syenite which he considered to be dykes. A number of these bodies have now been more completely exposed by road construction. They consist of relatively fine grained (1-2 mm), uniform material which is in abruptly gradational, not intrusive, contact with its surroundings. The mineralogy appears to be identical to that of the surrounding rock, although the dykes consistently look darker because of their relatively fine grain size. In areas of good outcrop, the bodies can be seen to be schlier-like, elongated roughly along the gneissosity, and pinching out at the ends. Commonly the length appears to be 5-10 m, with widths up to 1 m.

The nepheline syenite also contains a number of patch pegmatites up to a metre across. Equant crystals of nepheline and feldspar up to 10 cm across occur together with minor amounts of biotite, clinopyroxene, orange cancrinite, and possibly corundum (Gittins, 1967). At least one of these bodies appears to be boudined into its surroundings, forming a "chain of beads" several metres long.

STRUCTURE

Due to the lack of outcrop, few firm statements can be made about the structure. In general, foliation in the host rocks of the nepheline syenite trends east-northeast and dips to the south at moderate to steep angles, but foliation is not strong. The pyroxene syenite locally shows strong, narrow shear zones trending parallel to foliation and dipping to the south at about 35°. Foliation within the main body of nepheline syenite generally parallels the margins of the body, and increases in intensity toward the margins. This pattern outlines a steeply south-plunging, pipe-like mass.

DISCUSSION

Investigations this year suggest that the topographic highs on which the nepheline syenite outcrops mark the edges of the nepheline syenite with considerable accuracy. Such a boundary can also be traced on the aeromagnetic map (Geological Survey of Canada, 1964) which shows a magnetic high over the central body, with a lesser high over the satellite, and some smaller highs over the pyroxene syenite. These criteria suggest that the main mass is an ovoid body about 4 km long and 2 km wide, elongated parallel to foliation in the country rocks. The boundaries drawn in Figure 1 are supported by observations of well-developed dispersion trains of clasts down-stream from these topographic highs, and the complete lack of nepheline syenite boulders in other regions.

Observations of the pyroxene syenite found in proximity to the nepheline syenite suggest that the two syenites are not directly genetically related. The following are among the observations leading to this conclusion. (1) The pyroxene syenite grades to syenitic gneiss, which in turn grades to mafic gneiss, suggesting that the pyroxene syenite forms part of a regional pyroxene-bearing gneiss complex. (2) Pyroxene in the syenite exhibits exsolution of orthopyroxene, a phenomena not observed in pyroxenes associated with nepheline syenite, and the pyroxene is associated with ilmenite, a mineral not observed in nepheline syenite. (3) Pyroxene syenite similar or identical to that at Obedjiwan is widespread south of Gouin Reservoir. (4) The compositions of pyroxene and biotite in the two rocks are incompatible with derivation of one from the other by magmatic processes.

These points suggest that the nepheline syenite at Obedjiwan was emplaced near the northern contact between a regional, relatively mafic, high-grade complex and a lower-grade, more deformed, migmatitic granite gneiss complex. Both nepheline syenite and the regional mafic gneiss complex (including pyroxene syenite) have been deformed and recrystallized, as shown by outcrop and thin section observations, but in neither case was the latest deformation severe, possibly because the two were mechanically stronger than the granite gneiss. The nepheline syenite appears to have deformed along the fine grained zones, which could also explain the pronounced lineation. Whatever the degree of deformation, subsequent annealing was sufficient to recrystallize clinopyroxene, suggesting amphibolite or granulite facies condition. The supposed unmetamorphosed, undeformed character of the Obedjiwan nepheline syenite is therefore fictitious, and the body exhibits many characteristics similar to those of other Proterozoic syenite complexes along the Grenville Front.

REFERENCES

Geological Survey of Canada
1964: Lac Marmette; Geological Survey of Canada, Map 1839G, scale 1:50 000.

Gittins, J.
1967: The Obedjiwan alkaline complex, Gouin Reservoir, Toussaint Township, Abitibi County, Quebec; Ministere des Richesses Naturelles, Quebec, DP27357.

Indares, A. and Dunning, G.F.
1997: Coronitic metagabbro and eclogite from the Grenville Province of western Quebec: interpretation of U-Pb geochronology and metamorphism; Canadian Journal of Earth Sciences, v. 34, p. 891-901.

Laurin, A.F.
1965: Gouin Reservoir basin, Abitibi East and Laviolette counties, a geological outline; Ministere des Richesses Naturelles, Quebec, Geological Report 130, 14 p.

Geological Survey of Canada Project 680071

Geochemistry and petrogenesis of the Lapeyrère gabbronorite, south-central Grenville Province, Quebec

L. Nadeau, P. Brouillette, and J. Bédard
GSC Quebec, Sainte-Foy

Nadeau, L., Brouillette, P., and Bédard, J., 1998: Geochemistry and petrogenesis of the Lapeyrère gabbronorite, south-central Grenville Province, Quebec: in Current Research 1998-C; Geological Survey of Canada, p. 179-188.

Abstract: The Lapeyrère gabbronorite is the largest of a number of post-collisional, mid-crustal gabbroic intrusions in Grenvillian terrain of the Portneuf-Mauricie region. These intrusions contain no significant amount of anorthosite and are 60-70 Ma younger than the much larger neighbouring Morin and Lac Saint-Jean anorthosite-mangerite-charnockite-granite complexes.

Whole-rock geochemistry shows unidirectional trends and large overlaps from 'hornblende-free' gabbronorite to 'pyroxene-free' hornblende-quartz-diorite and granodiorite, consistent with diversification from the same parent magma.

The flat distribution in heavy rare-earth elements and the low Ti/Y ratios of model liquids in equilibrium with the cumulate phases suggest extraction of gabbronorite parent magma from a shallow-mantle spinel-lherzolite reservoir, which contrasts with the deeper mantle-plume-related setting commonly invoked for anorthosite-mangerite-charnockite-granite magmatism. Partial melting in upper mantle reservoirs is consistent with intrusion of the Lapeyrère gabbronorite at the initial stage of orogenic collapse, following convective thinning of the lithospheric mantle.

Résumé : Un certain nombre d'intrusions gabbroïques d'origine mésozonale, postérieures à la collision, affleurent dans les terrains grenvilliens de la région de Portneuf-Mauricie. Ces intrusions, dont la gabbronorite de Lapeyrère est la plus grande, ne contiennent aucune quantité importante d'anorthosite et sont de 60 à 70 Ma plus jeunes que les complexes d'anorthosite-mangérite-charnockite-granite voisins beaucoup plus vastes de Morin et du Lac Saint-Jean.

La géochimie de roche entière révèle des tendances unidirectionnelles et des recoupements de la composition chimique, qui va des gabbronorites «sans hornblende» aux diorites et granodiorites «sans pyroxène», témoignant ainsi d'une diversification à partir d'un même magma parental.

La distribution plane des terres rares lourdes et le faible rapport Ti/Y des liquides modèles en équilibre dans les cumulats gabbronoritiques suggèrent que le magma parental provient d'un réservoir à lherzolite-spinelle dans le manteau supérieur, ce qui fait contraste avec les réservoirs plus profonds associés aux panaches mantelliques qui sont couramment proposés pour les magmas anorthositiques-mangéritiques-charnockitiques-granitiques. La fusion partielle dans les réservoirs du manteau supérieur aurait donné lieu à la mise en place de la gabbronorite de Lapeyrère au stade initial d'effondrement orogénique, après l'amincissement par convection du manteau lithosphérique.

INTRODUCTION

The study of the Lapeyrère gabbronorite was undertaken in order to characterize and better understand the petrogenesis and tectonic setting of late Grenvillian gabbroic intrusions in the Portneuf-Mauricie region, south-central Grenville Province (Fig. 1). These intrusions contain no significant amount of anorthosite and are 60-70 Ma younger than the much larger neighbouring Morin and Lac Saint-Jean anorthosite-mangerite-charnockite-granite complexes. They were emplaced after crustal thickening, but prior to late extensional denudation.

The Lapeyrère gabbronorite is the largest of these intrusions, outcropping over roughly 160 km². It stands out as a strong positive bull's-eye on the regional Bouguer anomaly map; there are no other comparable anomalies in the region. The field relationships, the internal structure of the body, and the petrography of the intrusive rock suite were described in detail by Nadeau and Brouillette (1997). Focus is placed here on the whole-rock geochemistry of the suite, and on the petrogenesis of the least fractionated rock type: the gabbronorite.

PETROGRAPHY

The Lapeyrère gabbronorite is composed largely of undeformed, pristine, medium- to coarse-grained gabbroic to dioritic plagioclase-rich rocks that contain 30 to 50 per cent mafic minerals (Fig. 2). Field and petrographic relationships suggest a continuous textural and compositional transition in the rock suite from 'dry' hornblende-free gabbronorite to 'hydrous' pyroxene-free hornblende-quartz-diorite, with more evolved monzonitic rocks occurring in minor amounts (see Table 1, Nadeau and Brouillette, 1997). Hornblende-gabbronorite and pyroxene-diorite represent abundant intermediate facies. This gradational transition is accompanied by associated increases in the amount of accessory quartz, Fe-Ti-oxides, biotite, apatite, and zircon.

The rocks of the Lapeyrère intrusion are typically very homogeneous at outcrop scale and in hand samples, except for a few small lenses of 'heterogeneous facies' quartz-dioritic to granodioritic rocks that locally contain and possibly grade into K-feldspar porphyritic monzonitic phases (Nadeau and Brouillette, 1997). Field and detailed petrographic examinations have shown that the rocks are cumulates (Fig. 3). A weak, pervasive igneous foliation is defined by the preferred orientation of prismatic plagioclase and pyroxene crystals; locally, the rocks are modally layered. Adcumulate and heteradcumulate textures are well preserved. Most samples contain cumulus plagioclase+orthopyroxene+clinopyroxene±Fe-Ti oxides. Light green hornblende, biotite, and Fe-Ti oxides are common intercumulus phases. Some of the more evolved dioritic rocks also

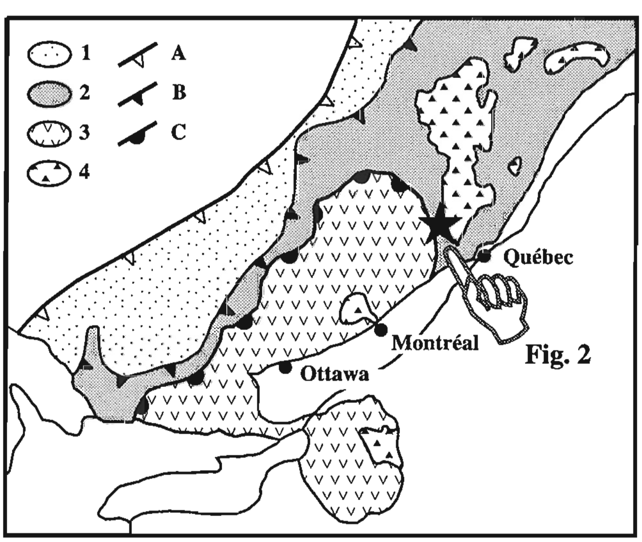

Figure 1. Location sketch map and tectonic subdivisions of the Grenville Orogen (modified from Rivers et al., 1989). Legend: (1) Parautochthonous belt; (2) Allochthonous polycyclic belt; (3) Allochthonous monocyclic bBelt; (4) Anorthosite-mangerite-charnockite-granite suite; (A) Grenville Front; (B) Allochthon boundary thrust; (C) Monocyclic belt boundary thrust.

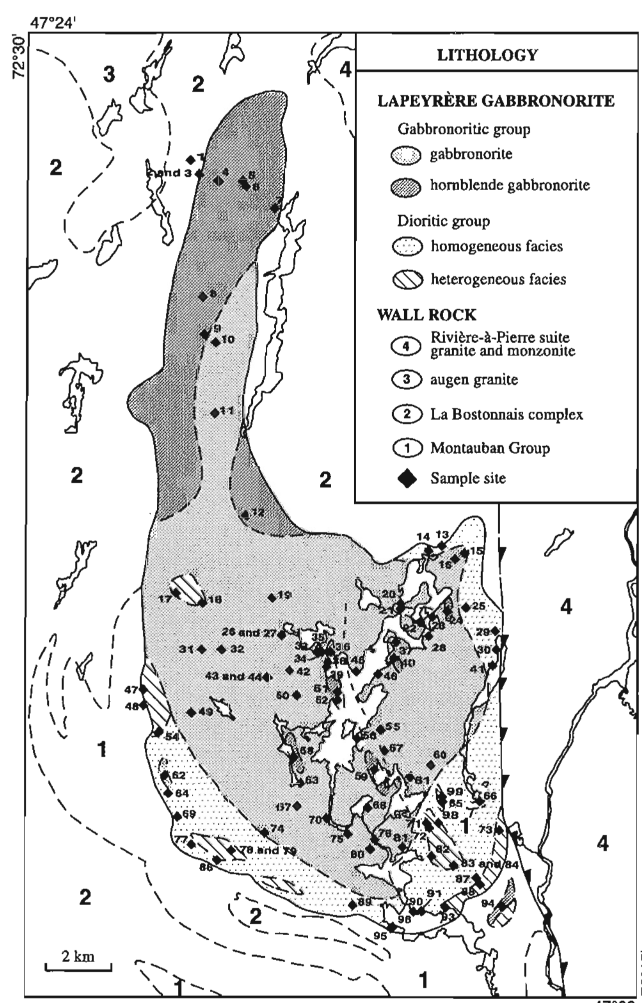

Figure 2. Geological sketch map of the Lapeyrère gabbronorite, and sample locations.

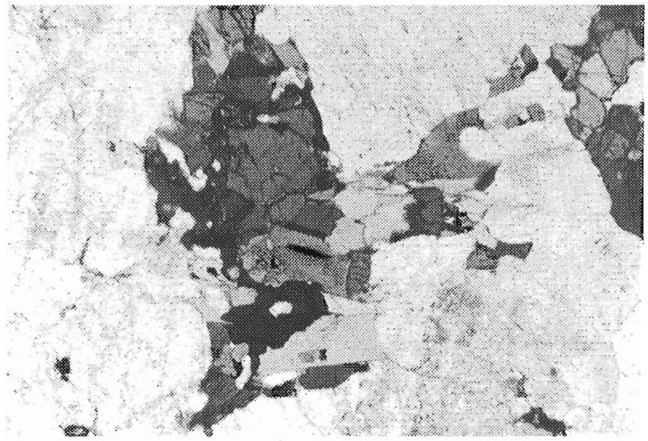

Figure 3. Typical example of intercumulus intergrowth of hornblende, biotite, Fe-Ti oxides, quartz, apatite, and zircon crystallized from interstitial melt trapped during consolidation (field = 2.5 mm).

contain equant, darker green hornblende that may be cumulus. The textural evidence implies that the bulk composition of these rocks does not correspond to magmatic liquids, hindering petrogenetic interpretation. No aphanitic or very fine-grained gabbro dykes were encountered during mapping. Only sample 2, a fine-grained homogeneous hypersthene-augite 'chilled' gabbronorite collected immediately adjacent the contact, may approach the composition of the intrusive magma. This sample was initially classified as dioritic on the basis of its optically determined plagioclase composition, which differs markedly from its normative composition close to An 60. Conversely, the anomalous composition of 'chilled' sample 3 (e.g. TiO_2, P_2O_5, Zr, ...) is by far too evolved to represent the composition of the parent magma.

GEOCHEMISTRY

Sampling and analytical methods

Forty-seven samples where selected for major- and trace-element analysis (Table 1; Fig. 2) on the basis of their textural homogeneity and representativeness of the outcrop area. None show field evidence of regional metamorphism, ductile deformation, or weathering. Sampling was designed in order to detect subtle internal zoning across the entire body and to provide a set of analyses representing all petrographically distinct lithologies of the suite. Modal counts were reported in Table 1 of Nadeau and Brouillette (1997).

Rock compositions are listed in Table 1. Rare earth elements (REE), Hf, Rb, Sc, Ta and Th were determined by instrumental neutron activation analysis. Major elements and trace elements were analyzed by X-ray fluorescence. Detection limits are given in Table 1. Analyses were performed at the geochemistry laboratory of the Quebec Geoscience Centre. All samples are consistently low in volatiles with average (H_2O+CO_2) equal to 0.24 wt.% and average totals of 99.94 wt.%. Plotted values have been recalculated volatile-free to 100%. Total iron has been expressed as FeO* using the conversion factor of Irvine and Baragar (1971).

Element mobility and contamination

The Lapeyrère gabbronorite was emplaced at mid-crustal level and was only slightly affected by late Grenvillian lower-amphibolite facies regional metamorphism. We emphasise that most of the rocks of the body are undeformed and exhibit original plutonic textures. Rare greenschist-facies veins may be present in some samples. Deformation effects are limited to undulose extinction and rare mechanical twins in plagioclase; recrystallization structures and granoblastic textures are absent. The homogeneity of most samples, together with the general absence of evidence for superimposed deformation and metamorphism, support the assumption that whole-rock geochemical signatures are essentially magmatic.

The possible extent of crustal contamination should be evaluated prior to discussing the significance of the distribution pattern and abundance of the trace elements. Continental crust is strongly enriched in zirconium. Therefore, elemental ratios including Zr can be used as tracers of crustal contamination. Table 2 shows that the gabbronorites have average whole-rock and model-liquid Zr/Y, Zr/Sm, Ti/Zr, and Ti/P ratios that are comparable to those of MORB, and markedly different from those of continental crust. Although the K/P ratio suggest a certain component of crustal contamination, the high coherence of incompatible trace-element data suggests that the mantle signature has been essentially preserved.

Major elements

Petrographic examination has shown that the samples analyzed are essentially plagioclase+orthopyroxene+clinopyroxene± hornblende±Fe-Ti oxides cumulates, with small components of trapped liquid now represented as either intergranular intergrowth of accessory minerals (Fig. 3) or thin amphibole rims or blebs on pyroxene. Therefore, given the cumulate nature of the rocks, major-element compositional variations cannot be discussed in terms of the models applied to lavas. Variation diagrams can however be useful for showing the absence of compositional gaps in the rock suite.

That gabbronorites are essentially mixtures of plagioclase and pyroxenes is well illustrated in the ACF diagram (Fig. 4), which also portrays the limited variability in their orthopyroxene/clinopyroxene ratio. Diorites were distinguished petrographically from the gabbronorites on the basis of optical determinations of the An(molar %) in plagioclase. The trend of decreasing An content in plagioclase from gabbronorites to diorites and granodiorites is also reflected on plots of Na_2O-CaO-(MgO+FeO) (Fig. 5). Calcium oxide was selected as abscissa on binary diagrams (Fig. 6), because variations in CaO are more or less systematic, with plagioclase-rich cumulates occurring at the high-CaO end and diorites and granodiorites spreading out towards the low-CaO end of the diagrams. Gabbronorite samples have average SiO_2 of 50.71 wt.% (46.96-54.90 wt.%), CaO of 9.73 wt.% (6.62-12.34),

Table 1. Major- and trace-element contents of representative samples from the Lapeyrère gabbronorite intrusion. All abundances in the model liquid are in ppm. Data: Mackenzie dyke swarm, Gibson et al. (1987); Columbia River flood basalts, Wilson (1989); OIB, E-MORB, and N-MORB, Sun and McDonough (1989). OIB = ocean-island basalt; XRF = X-ray fluorescence; INAA = instrumental neutron activation analysis.

	Element	SiO_2	TiO_2	Al_2O_3	Fe_2O_3	MnO	MgO	CaO	Na_2O	K_2O	P_2O_5				Cr
	Method	XRF	XRF	XRF	XRF	XRF	XRF	XRF	XRF	XRF	XRF				XRF
	Detection limit %wt/ppm	0.04	0.01	0.02	0.10	0.01	0.05	0.02	0.10	0.01	0.01	LOI	Total	Mg#	4
Sample site	Rock name														
11	gabbronorite	51.14	0.28	19.71	6.63	0.13	7.27	12.34	2.68	0.15	0.03	0.25	100.61	0.68	112
	model liquid		*8221*								*925*				*115*
26	gabbronorite	50.85	0.23	19.32	7.00	0.14	8.73	10.36	2.62	0.16	0.02	0.09	99.52	0.71	361
	model liquid		*6783*								*703*				*305*
31	gabbronorite	49.28	0.75	23.14	7.95	0.10	3.83	11.43	3.33	0.21	0.03	0.11	100.16	0.49	78
	model liquid		*12408*								*1027*				*94*
33	gabbronorite	48.96	1.16	21.19	10.50	0.12	4.64	10.12	3.43	0.26	0.06	0.00	100.44	0.47	72
	model liquid		*14693*								*1918*				*80*
37	gabbronorite	50.42	0.35	16.49	7.60	0.14	10.08	11.79	1.71	0.14	0.04	0.18	98.94	0.72	458
	model liquid		*9792*								*1212*				*413*
42	gabbronorite	49.17	1.05	21.66	10.03	0.12	4.50	10.29	3.53	0.22	0.04	-0.03	100.58	0.47	87
	model liquid		*15523*								*1500*				*109*
63	gabbronorite	50.18	0.61	16.16	11.56	0.14	8.30	10.07	2.41	0.18	0.02	0.53	100.16	0.59	117
	model liquid		*10160*								*790*				*81*
70	gabbronorite	51.75	0.53	21.22	7.23	0.10	4.25	10.36	3.49	0.32	0.04	0.19	99.48	0.54	112
	model liquid		*23173*								*1852*				*182*
76	gabbronorite	51.81	0.69	21.46	7.56	0.11	3.64	10.54	3.46	0.31	0.07	0.02	99.67	0.49	130
	model liquid		*24770*								*2578*				*187*
43	gabbronorite	53.09	0.25	19.10	7.64	0.12	7.04	10.15	2.83	0.18	0.02	-0.02	100.40	0.65	73
	model liquid		*9434*								*889*				*79*
16	qtz gabbronorite	51.37	0.37	18.78	7.82	0.14	7.85	10.63	2.63	0.31	0.05	0.09	100.04	0.67	247
	model liquid		*10140*								*1484*				*219*
48	qtz gabbronorite	54.90	1.05	16.80	10.20	0.18	3.50	7.83	4.05	0.75	0.45	0.53	100.24	0.40	-
	model liquid		*19114*								*7134*				-
49	qtz gabbronorite	51.52	0.36	21.87	7.75	0.13	5.27	9.92	3.20	0.57	0.06	0.05	100.70	0.57	104
	model liquid		*12172*								*2118*				*128*
5	hbl gabbronorite	51.83	0.22	21.33	6.06	0.09	5.39	10.49	3.05	0.22	0.03	0.17	98.88	0.64	49
	model liquid		*7816*								*1153*				*61*
7	hbl gabbronorite	49.87	1.31	18.41	11.23	0.16	4.74	9.84	3.57	0.46	0.28	0.09	99.96	0.46	101
	model liquid		*34920*								*7652*				*97*
55	hbl gabbronorite	47.55	0.76	17.23	10.15	0.14	10.98	9.90	1.95	0.17	0.09	0.38	99.30	0.68	1225
	model liquid		*12997*								*2269*				*697*
96	hbl gabbronorite	52.29	0.52	22.19	7.79	0.14	3.96	8.94	3.71	0.67	0.14	0.46	100.81	0.50	78
	model liquid		*11583*								*3870*				*74*
Mean whole rock		50.94	0.62	19.77	8.51	0.13	6.12	10.29	3.04	0.31	0.09	0.18	99.99	0.57	213
Mean model liquid			*14335*								*2298*				*183*
Mackenzie dykes swarm		*50.16*	*2.47*	*13.86*	*14.98*	*0.21*	*5.41*	*8.57*	*2.44*	*0.97*	*0.32*	*1.61*	*99.79*		*122*
Columbia River basalts		*50.60*	*2.33*	*14.34*	*13.49*	*0.21*	*5.20*	*8.80*	*2.70*	*1.15*	*0.45*	*1.08*	*99.32*		*86*
Ocean-island basalt		*49.20*	*2.57*	*12.80*		*0.17*	*10.00*	*10.8*	*2.12*	*0.51*	*0.25*				
E-type MORB		*51.20*	*1.69*	*16.00*		*0.16*	*6.90*	*11.5*	*2.74*	*0.43*	*0.15*				
N-type MORB		*50.40*	*1.36*	*15.20*		*0.18*	*8.96*	*11.4*	*2.3*	*0.09*	*0.14*				*346*
67	gabbronorite	53.89	0.20	22.08	6.30	0.10	5.38	10.10	3.27	0.21	0.03	-0.07	101.49	0.63	66
80	gabbronorite	50.57	0.91	21.55	9.11	0.09	3.79	10.03	3.57	0.27	0.04	0.02	99.95	0.45	53
59	hbl gabbronorite	48.27	1.91	16.82	13.26	0.19	5.34	9.93	2.85	0.27	0.91	-0.12	99.63	0.44	53
90	qtz gabbronorite	52.37	1.25	17.90	11.21	0.19	3.53	6.62	3.54	0.64	0.47	0.85	98.57	0.38	63
1	hbl gabbronorite	48.66	0.74	19.64	11.04	0.18	6.57	7.31	3.54	1.07	0.10	0.32	99.17	0.54	147
62	hbl gabbronorite	50.40	0.57	17.60	9.50	0.15	7.77	10.70	2.48	0.22	0.10	0.41	99.90	0.62	-
44	gabbronorite	50.33	0.57	7.58	15.87	0.28	16.10	8.05	0.98	0.07	0.02	-0.40	99.45	0.67	254
2	"chilled" gabbronorite	51.01	1.11	17.48	13.87	0.17	4.57	7.38	3.87	0.47	0.16	-0.41	99.68	0.40	98
3	"chilled" gabbronorite	46.98	3.32	16.15	15.57	0.20	4.51	7.76	3.51	0.94	0.69	0.21	99.84	0.36	92
91	px-diorite	53.72	1.15	18.94	10.42	0.17	3.12	7.44	3.62	0.69	0.35	-0.20	99.42	0.37	13
52	px-diorite	47.16	1.43	16.48	13.41	0.16	6.00	9.39	2.63	0.30	0.12	0.47	97.55	0.47	83
78	px-hbl diorite	49.63	1.75	20.52	11.52	0.23	3.52	8.60	3.81	0.56	0.70	-0.28	100.56	0.38	69
89	px-hbl diorite	54.20	1.12	16.30	10.60	0.19	5.96	7.70	3.58	0.77	0.37	-0.26	100.53	0.53	-
77	px-hbl qtz diorite	57.83	0.53	19.51	6.48	0.11	3.46	7.29	3.64	0.91	0.12	0.33	100.21	0.51	94
95	px-hbl qtz diorite	56.60	0.44	18.87	7.46	0.12	3.55	7.63	3.15	0.47	0.14	0.12	98.55	0.49	68
56	hbl diorite	46.20	1.54	16.90	13.72	0.14	5.14	9.77	2.61	0.46	0.08	0.60	97.16	0.43	54
79	hbl diorite	44.87	2.43	19.05	13.47	0.20	4.74	9.91	3.27	0.66	0.77	0.18	99.55	0.41	62
25	hbl-bt diorite	51.16	0.65	16.92	9.11	0.15	7.12	10.02	2.83	0.72	0.08	0.93	99.69	0.61	209
29	hbl-bt qtz diorite	51.44	1.28	20.39	8.19	0.14	3.52	7.52	4.61	1.10	0.30	0.81	99.30	0.46	117
83	hbl-bt qtz diorite	54.32	1.37	18.71	11.52	0.20	3.16	6.96	4.19	1.13	0.41	0.37	102.34	0.35	61
30	tonalite	60.39	0.85	16.76	5.74	0.12	2.95	6.17	3.72	0.96	0.21	0.78	98.65	0.50	138
17	opx granodiorite	61.60	0.77	18.40	6.54	0.12	1.49	5.59	4.48	0.93	0.19	0.22	100.33	0.31	-
86	hbl-bt granodiorite	64.07	0.55	18.14	5.19	0.09	0.81	4.28	4.28	2.42	0.18	1.02	101.03	0.24	60
73	granodiorite	59.13	0.85	18.02	6.46	0.11	3.89	5.50	4.10	0.80	0.23	1.45	100.54	0.54	110
66	qtz monzodiorite	74.34	0.19	14.06	2.47	0.02	0.19	1.21	2.42	6.05	0.06	0.25	101.26	0.13	69
47	qtz monzodiorite	68.10	0.43	15.40	4.37	0.06	0.53	3.00	3.94	3.30	0.08	0.46	99.67	0.19	-
84	qtz syenite	74.69	0.24	13.67	1.25	0.02	0.01	1.87	2.63	4.28	0.07	0.35	99.08	0.02	118
18	heterogenous rock	57.50	0.84	19.30	7.81	0.14	1.00	5.59	4.48	2.06	0.22	0.50	99.44	0.20	-
98	heterogenous rock	71.41	0.35	14.63	2.84	0.04	0.40	2.75	3.49	3.06	0.10	0.42	99.49	0.22	84
99	heterogenous rock	76.73	0.42	12.33	1.97	0.00	0.00	0.98	3.21	4.72	0.04	0.17	100.57	0.00	154

Ni XRF 3	Co XRF 2	Sc INAA 0.1	V XRF 5	Cu XRF 4	Zn XRF 5	Rb XRF 10	Sr XRF 3	Ba XRF 50	Ga XRF 2	Nb XRF 3	Zr XRF 3	Y XRF 4	Th INAA 0	La INAA 0.5	Ce INAA 2	Hf INAA 0.2	Nd INAA 2	Sm INAA 0.05	Eu INAA 0.1	Tb INAA 0.1	Yb INAA 0.2
119	35	36.3	122	62	54	< 10	355	< 50	17	< 3	21	10	<0.2	1.4	3	0.3	<2	0.87	0.6	0.2	1.2
145	69	116.6	570	328	167	-	210	-	89	0	122	52	-	10.5	19	1.7	-	5.27	1.9	1.3	6.3
143	40	24.7	93	53	60	< 10	341	< 50	17	< 3	18	5	<0.2	1.2	3	0.2	<2	0.62	0.5	0.2	0.9
164	75	73.1	422	286	177	-	186	-	92	0	110	25	-	11.0	29	1.2	-	3.87	1.7	1.0	4.5
23	40	22.8	279	39	63	< 10	484	< 50	28	< 3	27	7	<0.2	2.7	5	0.4	<2	1.00	0.7	0.2	0.9
27	89	90.2	928	233	225	-	226	-	169	0	173	45	-	21.1	43	2.2	-	7.05	2.5	1.5	5.7
36	48	22.6	389	64	76	11	405	136	22	< 3	25	11	0.3	2.5	5	0.4	<2	0.95	0.8	0.2	0.8
40	90	78.7	977	336	234	71	190	-	114	-	149	65	2.2	18.4	38	2.3	-	6.28	2.7	1.2	4.8
147	45	35.7	184	82	61	< 10	256	70	9	< 3	29	15	<0.2	3.0	6	0.5	<2	1.46	0.6	0.3	1.3
156	78	103.9	796	405	169	-	188	285	43	-	163	73	-	22.2	44	2.7	-	8.47	2.0	1.4	6.5
34	48	20.5	347	44	73	10	560	< 50	22	< 3	25	6	<0.2	1.3	3	0.2	<2	0.57	0.5	0.1	0.7
45	98	78.5	100	267	251	74	257	-	131	-	171	41	-	10.8	23	1.4	-	4.41	1.9	1.0	4.6
165	53	33.0	417	190	73	< 10	293	69	-	< 3	9	6	<0.2	1.1	2	<0.2	3	0.64	0.4	<0.1	0.6
135	74	84.7	118	930	172	-	198	285	-	-	58	31	-	11.5	24	-	24	4.26	1.5	-	3.2
46	36	19.0	217	44	54	< 10	420	91	20	< 3	20	6	0.3	2.0	4	0.2	<2	0.71	0.7	0.1	0.7
72	94	93.2	162	364	244	-	202	283	162	-	175	53	2.7	20.8	41	1.8	-	6.89	2.6	1.3	6.0
66	33	20.4	231	30	68	< 10	482	142	18	< 3	24	9	<0.2	3.7	8	0.3	5	1.19	1.1	0.2	0.7
113	88	87.2	141	206	286	-	234	422	125	-	168	60	-	31.3	65	2.3	43	8.93	3.9	1.7	5.0
22	27	26.0	121	77	63	10	361	89	-	< 3	5	6	<0.2	1.3	3	<0.2	<2	0.60	0.5	0.2	0.6
25	53	95.8	713	521	214	91	176	271	-	-	40	42	-	13.8	28	-	-	5.11	2.0	1.5	4.5
131	41	29.7	137	59	73	< 10	339	60	19	< 3	36	18	0.2	5.4	11	0.8	7	2.05	0.8	0.4	1.7
140	72	85.3	581	286	202	-	202	197	91	-	198	86	1.5	39.3	80	4.3	44	11.58	2.6	2.3	8.4
18	-	34.0	132	45	107	10	500	260	22	5	84	30	<0.2	17.0	36	-	<2	7.00	<0.1	-	-
-	-	79.1	387	140	-	36	321	639	68	19	279	94	-	62.9	132	-	-	23.71	-	-	-
54	40	21.0	166	45	74	14	378	136	23	< 3	29	14	0.5	8.7	17	0.6	10	2.11	0.9	0.4	1.9
73	88	79.0	917	279	265	100	244	533	140	-	194	87	4.2	71.7	143	3.8	76	15.00	3.3	2.9	11.9
-	21	20.8	97	38	129	< 10	382	84	-	< 3	5	5	<0.2	1.6	3	<0.2	<2	0.58	0.4	0.2	0.6
-	50	82.2	569	254	496	-	181	244	-	-	35	33	-	14.5	29	-	-	4.36	1.6	1.1	4.2
46	57	31.1	391	52	104	14	413	126	26	< 3	41	34	0.4	12.8	29	0.8	18	4.90	1.4	0.8	2.9
52	103	90.9	164	245	292	85	224	364	121	-	215	159	2.7	84.1	184	4.0	106	26.45	4.6	4.1	14.0
208	52	26.0	173	74	85	< 10	155	62	-	< 3	40	17	0.2	2.6	7	1.3	6	2.10	0.8	0.5	1.6
166	69	51.1	456	286	178	-	115	232	-	-	192	63	1.5	17.7	44	5.7	33	9.88	2.6	1.9	6.2
19	32	14.3	140	33	87	15	725	223	23	< 3	57	11	0.3	8.2	18	1.0	12	2.46	0.9	0.3	1.2
26	67	41.6	519	168	277	93	349	595	99	-	313	53	2.1	55.6	120	5.4	73	13.85	2.8	1.6	5.9
84	41	26	214	61	75	12	403	119	20		29	12	0.3	4.5	10	1	9	1.75	0.7	0.3	1.1
86	78	83	865	325	241	79	218	363	111		162	63	2.4	30.4	64	3	57	9.73	2.5	1.6	6.3
82			322			23	206	330		13	146	35	3.7		57	5.0	32	7.10	2.3	1.00	2.1
114		33.4				26	309	1590	22			36	3.6	24.7	53	6.5		6.70	2.6	1.2	3.6
						31	660	350		48	280	29	4.0	37.0	80	7.8	39	10.00	3.0	1.05	2.16
						5.04	155	57		8	73	20	0.6	6.3	1.5	2	9	2.6	0.9	0.53	2.37
177	50	40	2.62			0.56	90	6.3		2.3	74	28	0.12	2.5	7.5	2.1	7.3	2.63	1.02	0.67	3.05
-	20	18.0	78	51	50	< 10	483	92	-	< 3	-	4	<0.2	1.3	3	<0.2	2	0.47	0.5	0.1	0.4
-	31	19.0	247	43	79	< 10	513	105	-	< 3	-	4	<0.2	1.7	3	<0.2	<2	0.59	0.6	0.2	0.3
-	53	34.3	255	41	138	< 10	401	143	-	< 3	23	25	0.4	10.2	24	0.6	16	4.77	1.9	0.7	2.0
-	29	19.0	93	39	174	< 10	493	328	-	5	256	27	0.5	20.0	46	6.0	28	6.10	2.1	0.8	2.4
41	61	32.2	336	4	90	27	337	179	18	< 3	44	16	0.2	3.2	8	0.9	6	1.90	0.7	0.4	1.7
88	-	36.0	139	48	249	3	300	69	17	3	57	18	<0.2	4.0	14	-	<2	<0.05	<0.1	-	-
215	121	50.8	343	88	116	17	132	103	15	< 3	17	12	<0.2	0.9	3	0.4	<2	1.01	0.4	0.2	1.2
13	73	43.4	351	78	98	13	933	620	24	< 3	84	28	<0.2	3.7	11	1.7	11	3.53	1.2	0.8	3.0
33	86	24.9	435	37	143	15	738	1089	31	6	332	51	0.4	29.7	70	7.6	49	10.81	3.2	1.5	3.9
-	27	25.5	142	20	159	23	505	339	-	-	299	-	1.2	20.0	44	9.2	42	-	2.1	0.7	3.5
-	55	36.0	401	66	112	25	359	112	-	-	14	-	<0.2	2.9	6	<0.2	<2	1.53	0.8	0.4	1.1
5	47	22.0	105	13	142	13	783	219	22	6	78	33	0.2	18.2	44	1.6	34	7.10	2.4	1.0	2.8
138	-	26.0	77	22	144	7	40	255	23	6	-	180	<0.2	24.0	50	-	<2	7.00	<0.1	-	-
20	25	14.2	132	52	74	19	727	329	19	< 3	59	9	<0.2	9.0	19	1.5	11	2.29	0.7	0.3	0.8
-	16	16.7	123	26	78	13	586	215	-	-	23	-	0.2	6.7	14	0.6	10	1.66	0.8	0.2	0.9
-	55	36.6	486	65	109	18	346	129	-	-	17	-	0.3	3.1	7	<0.2	5	1.67	0.9	0.2	1.2
8	65	34.7	318	18	129	13	668	98	23	4	100	38	0.7	16.5	40	2.6	29	7.16	2.4	1.0	3.0
106	52	30.8	289	68	101	33	372	143	15	< 3	42	25	0.2	9.8	22	1.1	15	3.61	1.1	0.6	2.1
43	37	17.3	201	23	96	28	859	350	25	3	364	33	0.8	29.4	63	10.2	34	7.03	2.4	1.0	2.9
-	27	32.0	123	33	187	13	477	351	-	9	515	58	0.6	29.0	68	14.0	46	12.00	2.4	1.8	4.9
-	19	13.0	-	-	106	21	586	335	-	<3	124	16	1.9	16.0	35	3.0	17	3.50	1.2	0.4	1.5
3	-	19.0	44	12	121	6	370	349	24	8	440	26	<0.2	25.0	43	-	<2	5.00	<0.1	-	-
-	8	14.5	24	22	77	40	387	1660	-	7	333	38	3.4	41.8	81	11.7	40	8.35	2.8	1.2	3.3
-	19	15.1	105	25	105	25	579	320	-	-	82	-	0.6	16.6	34	2.5	18	4.19	1.3	0.4	2.2
-	-	1.9	12	18	34	84	209	1306	-	-	159	-	0.9	14.1	21	6.0	8	1.51	1.6	0.1	0.8
-	-	10.0	11	8	28	74	310	1500	21	6	330	16	<0.2	24.0	42	-	<2	7.00	<0.1	-	-
-	3	5.1	-	-	28	60	5	852	-	<3	<3	4	0.3	16.0	27	3.7	12	1.90	1.6	0.2	0.6
4	-	26.0	25	12	598	21	480	1400	27	10	660	28	<0.2	22.0	42	-	<2	<0.05	<0.1	-	-
-	5	3.8	-	-	31	66	260	3080	-	<3	168	17	0.6	17.0	33	4.8	17	3.40	2.2	0.4	1.2
-	3	1.4	-	-	35	62	145	1670	-	<3	358	12	0.4	21.0	30	11.0	11	1.90	1.9	0.2	0.6

and MgO of 5.82 wt.% (3.83-10.98 wt.%) with an average Mg# of 0.55 (0.38-0.72). The dioritic samples have higher average wt.% for SiO_2, K_2O, TiO_2, and P_2O_5, lower CaO and MgO, and comparable Na_2O, Al_2O_3, MnO, and FeO. Diorites and granodiorites have an average SiO_2 of 54.15 wt.% (44.87-64.07 wt.%), CaO of 7.58 wt.% (4.28-10.02 wt.%), and MgO of 3.89 wt.% (0.81-7.12 wt.%) with an average Mg# of 0.44 (0.24-0.61). The silica rich (68.10-76.70 wt.%) monzonitic and heterogeneous facies rocks plot as a distinct group on all diagrams and generally off the gabbronorite-diorite-granodiorite trend.

The fact that diorites and gabbronorites plot together on these diagrams suggests that the abundance of hornblende in the dioritic rocks was essentially controlled by the availability of deuteric water in the last stages of rock consolidation. The diagrams further emphasize the fact that there is no compositional gap between the gabbronorites, the diorites, and the granodiorites. Note that sample 44, by far the most mafic sample of the group, with over 73% modal pyroxene, plots off the composition field for other gabbronorite samples, which are dominated by cumulus plagioclase (see Table 1, Nadeau and Brouillette, 1977). The gabbronorites are markedly enriched in Al_2O_3 and deficient in TiO_2 and P_2O_5 (which is consistent woith their cumulate origin) compared to diabase dykes and basalts (Table 1). Finally, the large gap in composition that distinguishes the monzonitic and heterogeneous facies rocks suggests that these rocks are not directly related to the gabbronorite.

Calculation of model-liquid compositions

We used the equilibrium distribution method of Bédard (1994) to calculate the trace-element contents of liquids in equilibrium with the gabbronorites. This requires modal data, a well constrained set of partition coefficients, and an estimate of the trapped melt fraction. The modes used are from

Table 2. Average incompatible-element ratios for Lapeyrère gabbronorite whole rock and model liquid, oceanic basalts, and continental crust. Data: (1) Sun and McDonough (1989); (2) Wedepohl (1995); (3) Weave and Tarney (1984).

	Zr/Y	Zr/Sm	Ti/Zr	Ti/P	K/P
Lapeyrère (whole rock)	2.64	18	112	9.46	6.7
Lapeyrère (model liquid)	3.1	19.6	75	6.24	6
E-MORB (1)	2.64	28	110	9.67	1
N-MORB (1)	3.32	28	82	14.9	3.4
Ocean-island basalt (1)	9.66	28	55	6.37	4.4
Continental crust (2)	8.38	37.9	20	5.19	25
Continental crust (3)	15	51.2	17	4.34	21

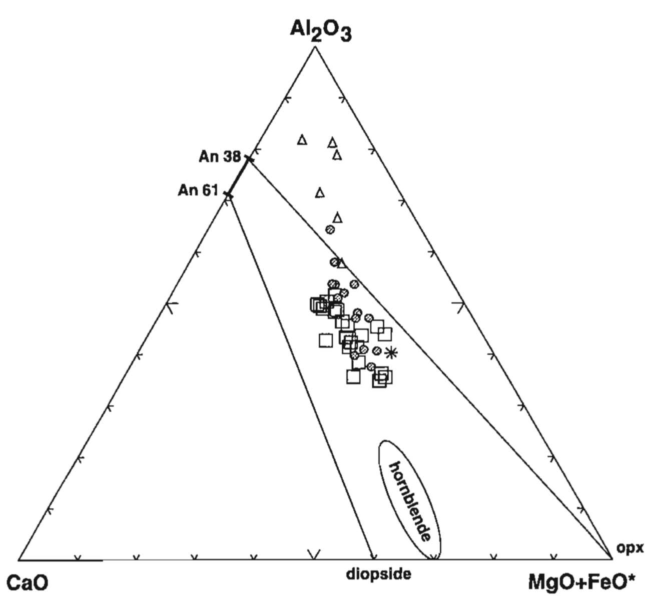

Figure 4. ACF diagram showing the variations in whole-rock composition in the Lapeyrère gabbronorite suite. Legend: square = gabbronoritic rock; closed circle = dioritic rock; asterisk = chilled margin; triangle = monzonititic and heterogeneous rocks.

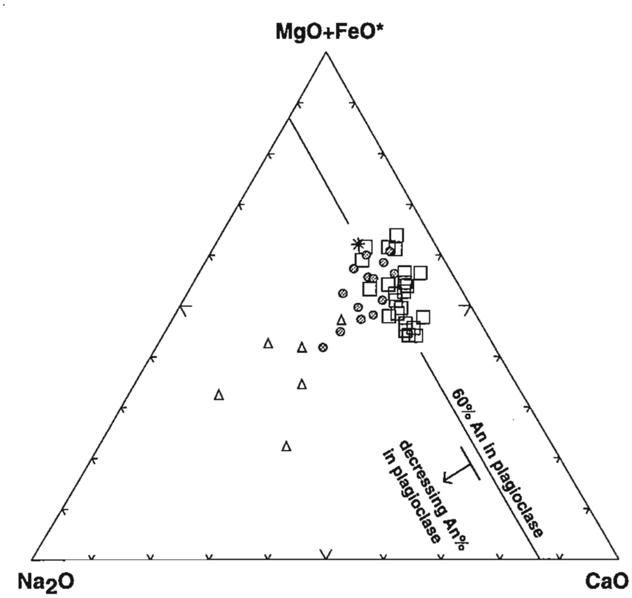

Figure 5. FNC diagram showing the variations in whole-rock composition in the Lapeyrère gabbronorite suite. Legend as in Figure 4.

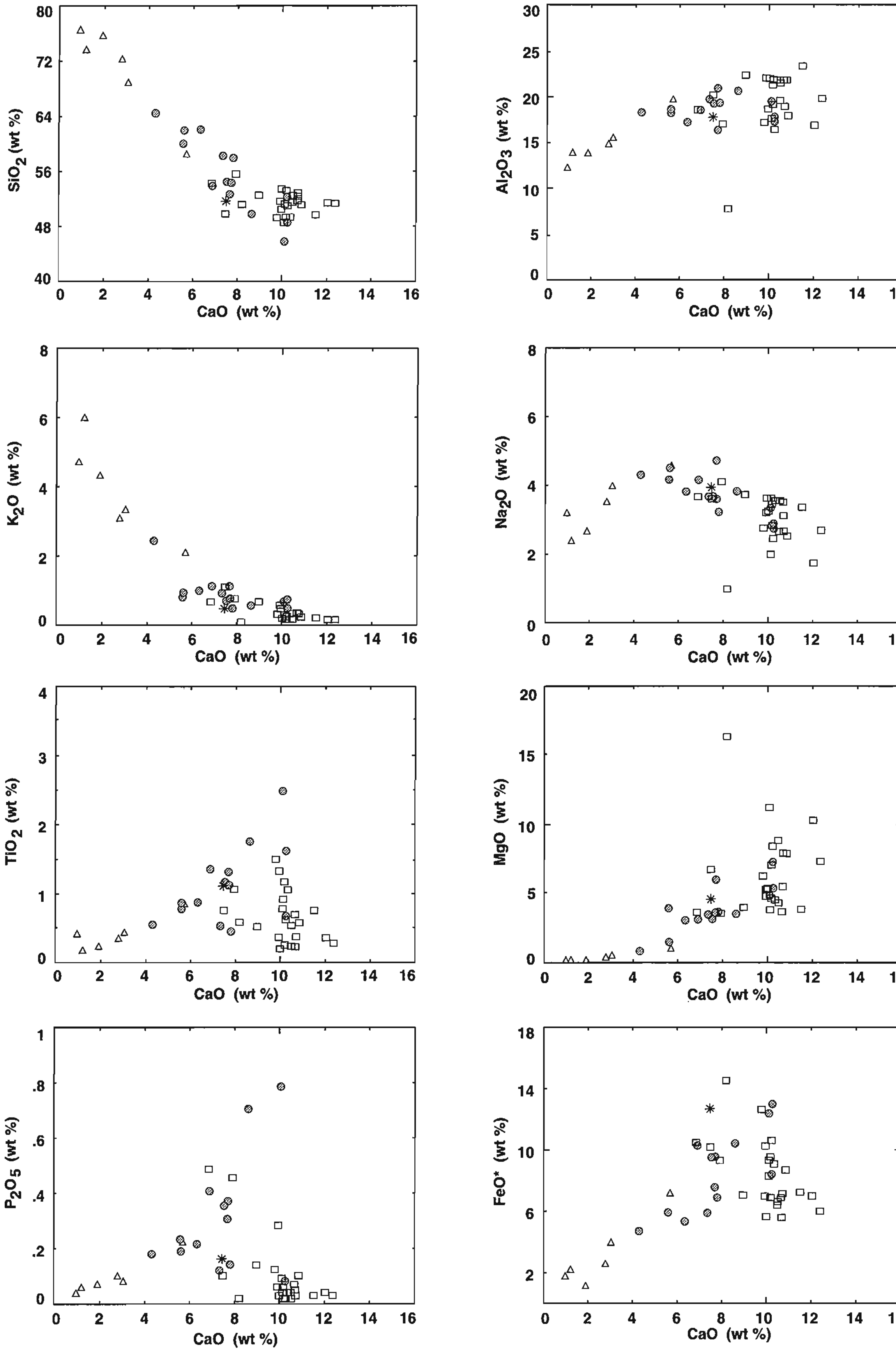

Figure 6. *Variation plots of CaO versus other major elements for the Lapeyrère gabbronorite suite. Legend as in Figure 4.*

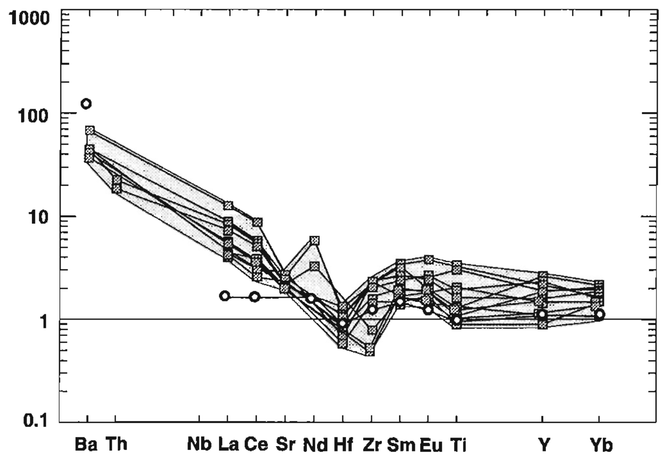

Figure 7. N-MORB normalized incompatible trace-element diagram of selected gabbronorite model liquids and of 'chilled' sample 2.

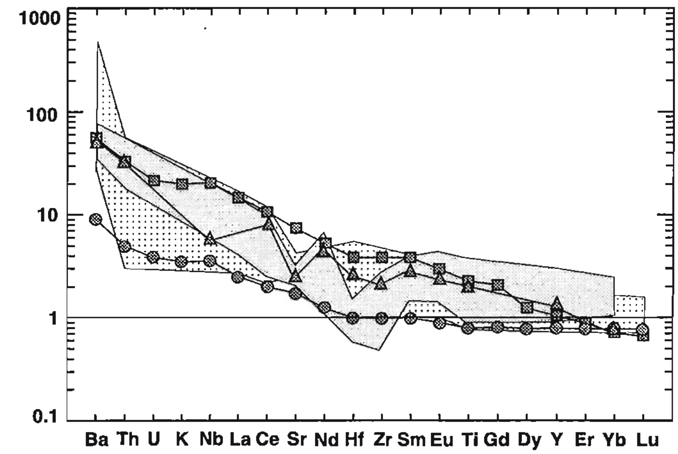

Figure 8. Comparative N-MORB normalized incompatible trace-element diagram. Legend: shaded field = Lapeyrère gabbronorite model iquid; dotted field = Columbia River flood basalts; triangle = Mackenzie dyke swarm; square = ocean-island basalt; circle = E-MORB. Data: N-MORB, E-MORB, and ocean-island basalt, Sun and McDonough (1989); Columbia River flood basalts, Basaltic Volcanism Study Project (1981); Mackenzie dyke swarm, Gibson et al. (1987).

the point-counts of Nadeau and Brouillette (1997). The proportion of cumulate/interstitial phases was estimated from textural data. The partition coefficient data set is broadly similar to the data set compiled by Halliday et al. (1995). Textural data imply that these rocks retain small proportions of melt, generally <10%. Backstripping of phases to correct for crystallization of the trapped melt fraction generally eliminated Fe-Ti-oxides, amphibole, or mica at trapped melt fractions <10%. Note that normalized REE patterns of model liquids closely resemble those of 'chilled' sample 2 (Fig. 7), which suggests that the model results are valid.

Transition metals (Ni, Cr, V, and Sc)

The gabbronorites contain modest and varied amounts of transition metals. The exceptionally high Ni an Cr values of samples 26, 37, and 55 are possibly due to trace amounts of sulphide or Cr-spinel. Values for Ni in the other gabbronorite samples range from below the detection limit to 165 ppm (average ~52 ppm), for an average of 60 ppm in model liquids. Likewise, whole-rock Cr values range from <10 ppm to 247 ppm (average ~97 ppm), with and average of 108 ppm in the model liquid. These values are comparable to those of the Columbia River flood basalts and Mackenzie dykes, but are inferior to N-MORB by factors of 1 to 3 (Table 1). Whole-rock V contents show the widest range, from 93 ppm to 417 ppm (average ~185 ppm), consistent with its moderate incompatibility and high sensitivity to redox conditions (Pearce, 1996). Values for Sc have a narrow range, from 14 ppm to 45 ppm (average ~21 ppm).

The generally low values for transition metals in the whole-rock data are consistent with the predominance of plagioclase as cumulate. In addition, the low Cr and Ni values in model liquids can be attributed to prior fractionation of olivine and/or pyroxene and/or spinels from the parent magma. Compared to the gabbronorites, the dioritic rocks are further depleted in these elements, which is consistent with generally decreasing Mg# of the whole-rock data (Table 1).

Incompatible trace elements

The extended REE pattern normalized to N-MORB (Fig. 7) of calculated model liquids have a negative slope with progressive enrichment from heavy rare earth elements, through high field strength elements (Zr/Y ~ 3.1) and light rare earth elements (La/Yb ~ 5.1), to large ion lithophile elements. Niobium contents are below the detection limit (<3 ppm), which suggests a Nb concentration significantly below values typical of ocean-island basalts (~48 ppm), as is also commonly the case for continental flood basalts (Wilson, 1989). Model-liquid zirconium values (~180 ppm) are intermediate between MORB (~74 ppm) and ocean-island basalt (~280 ppm), with modest Zr/Y ratios similar to N-MORB (~ 0.64) but different from ocean-island basalts (~ 9.66) and the Mackenzie dykes (~ 4.29) (Table 1). The melts in equilibrium with the gabbronorite are apparently not significantly enriched in Ti compared to MORB or high-Ti continental flood basalts such as the Mackenzie dykes and the Columbia River flood basalts.

The inferred Lapeyrère gabbronorite parental magma shows incompatible trace element and REE distribution and abundances that sem to be transitional between E-MORB and ocean-island basalt (Fig. 8), and shares similarities with low-Ti continental flood basalts and arc magmas. The field defined by the gabbronorite model liquids largely overlaps that of representative samples from the Columbia River flood basalts, which are taken as a type example of continental within-plate basalts. While the Columbia River flood basalts show a marked negative-slope HREE distribution with high Ti/Y ratio (Fig. 8), the Lapeyrère model liquids show a fairly flat HREE distribution, with significantly lower Ti/Y ratios and modest enrichment in Y and Yb relative to the Columbia River suite.

DISCUSSION

Parental magma

The Lapeyrère gabbronorite parental magma is generally similar to continental flood-basalt lavas, but has a flatter MREE-HREE segment (Fig. 8). The two are further distinguished from common within-plate basalts on the Ti-Zr-Y paleotectonic discrimination diagram (Fig. 9). Samples from the Lapeyrère gabbronorite do not plot in the within-plate basalt field, but fall in the MORB-volcanic-arc basalts fields. This result is peculiar, given that the Lapeyrère gabbronorite was intruded late in Grenvillian history into thickened continental crust. That some continental flood basalts plot in the field of MORB and volcanic-arc basalts in Ti-Zr-Y-space has long been recognized (Holm, 1982), so that the paleotectonic implications of this diagram must not be overemphasized. Nevertheless, the high Ti/Y ratio characteristic of most parental magmas of ocean-island and within-plate basalts is generally attributed to low-degree melting of deep-mantle garnet-lherzolite reservoirs. In contrast, low Ti/Y ratios typical of MORB and volcanic-arc basalts are commonly attributed to melting of shallow-mantle spinel-lherzolite reservoirs. This reflects the fact that, although Ti and Y have similar bulk distribution coefficients during partial melting of spinel-lherzolite, Y has a significantly higher bulk distribution coefficient for garnet, imparting high Ti/Y ratio to melts derived from garnet-lherzolites (Pearce and Parkinson, 1993). These relationships suggest that the petrogenesis of the Lapeyrère gabbronorite parental magma differs significantly from that of 'normal' plume-related within-plate basalts. The flat distribution of HREE and the low Ti/Y ratios of the Lapeyrère gabbronorite parental magma suggest extraction from a shallow-mantle spinel-lherzolite reservoir, rather than from a deep-mantle garnet-lherzolite reservoir from which plume-related magmas are extracted.

Tectonic implication

The distinctive geochemical signature of the Lapeyrère gabbronorite parental magma suggests that it is unlikely to have originated from a mantle reservoir and setting comparable to that of within-plate basalts and 'normal' continental flood basalts which, like gabbroic magmas of anorthosite-mangerite-charnockite-granite suites, are widely considered to be linked to deep mantle plumes (e.g. Ashwal, 1993). This further suggests that the Lapeyrère intrusion is unlikely to be related to anorthosite-mangerite-charnockite-granite magmatism, as was recently suggested for time-correlative intrusions in the region (Corrigan and Hanmer, 1997; Higgins and van Breemen, 1996). In continental settings, partial melting of spinel-lherzolite facies upper-mantle reservoirs is commonly attributed to thinning of the lithosphere (Wilson, 1993; Pearce, 1996). Following Grenvillian collision, the

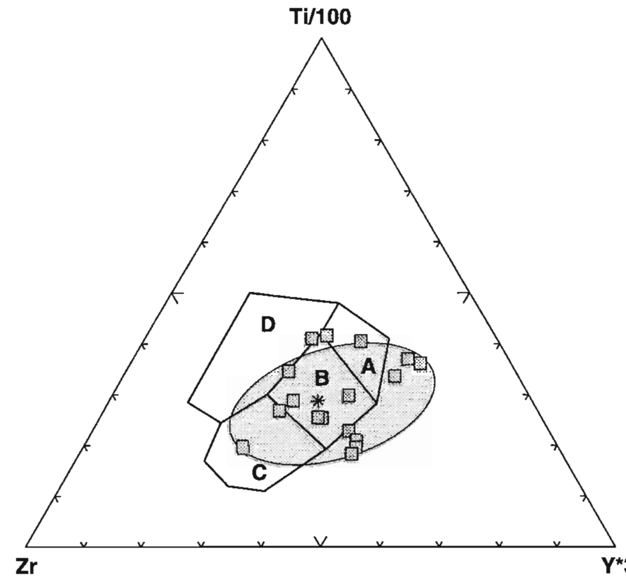

Figure 9. *Ti-Y-Zr discrimination diagram of Pearce and Cann (1973) showing the distribution of calculated gabbronorite model liquid for the Lapeyrère gabbronorite and 'chilled' sample 2. The diagram shows the 10 per cent probability ellipse for volcanic-arc basalts of Pearce (1996) and emphasizes the absence of data points in the within-plate basalts field.*

unstable overthickened crust is likely to have acted as a thermal blanket, setting up favourable conditions for subsequent thinning of the lithosphere, generation of melt in upper-mantle reservoirs, and gravitational collapse of the orogen. These conditions are consistent with emplacement of the Lapeyrère intrusion at the initial stage of post-collisional regional extension. Our petrogenetic model, which is based on the geochemistry of the Lapeyrère intrusion, provides further support to models that link post-collisional extension to convective thinning of the lithospheric mantle (e.g. Houseman et al., 1981; Corrigan and Hanmer, 1997).

ACKNOWLEDGMENTS

Susie Nantel, Claude Hébert, and Serge Perrault from the Ministère des Richesses naturelles du Québec are gratefully acknowledged for kindly providing field data and a large collection of samples and thin sections used in this study. Louise Corriveau is thanked for reviewing the manuscript.

REFERENCES

Ashwal, L.D.
1993: Anorthosites; Berlin, Springer-Verlag, 422 p.
Basaltic Volcanism Study Project
1981: Basaltic volcanism on the terrestrial planets; New York, Permagon Press, 1286 p.

Bédard, J.H.
1994: A procedure for calculating the equilibrium distribution of trace elements in the minerals of cumulate rocks, and the concentration of trace elements in the coexisting liquids; Chemical Geology, v. 118, p. 143-153.

Corrigan, D. and Hanmer, S.
1997: Anorthosites and related granitoids in the Grenville orogen: a product of convective thinning of the lithosphere?; Geology, v. 25, p. 61-64.

Gibson, I.L., Madhurendra, N.S., and Fahrig, W.F.
1987: The geochemistry of the Mackenzie Dyke Swarm, Canada; in Mafic dyke swarms, (ed.) H.C. Halls and W.F. Fahrig; Geological Association of Canada, Special Paper 34, p. 109-121.

Halliday, A.N., Lee, D.C., Tommasini, S., Davies, G.R., Paslick, C.R., Fitton, J.G., and James, D.E.
1995: Incompatible trace elements in OIB and MORB and source enrichment in the sub-oceanic mantle; Earth and Planetary Science Letters, v. 133(3-4), p. 379-395.

Higgins, M.D. and van Breemen, O.
1996: Three generations of anorthosite-mangerite-charnockite-granite (AMCG) magmatism, contact metamorphism and tectonism in the Saguenay-Lac-Saint-Jean region of the Grenville Province, Canada; Precambrian Research, v.79, p. 327-346

Holm, P.E.
1982: Non-recognition of continental tholeiites using the Ti-Y-Zr diagram; Contributions to Petrology and Mineralogy, v. 79, p. 308-310

Houseman, G., McKenzie, D., and Molnar, P.
1981: Convective instability of a thermal boundary layer and its relevance to the thermal evolution of continental convergent belts; Journal of Geophysical Research; v. 86, p. 6115-6132.

Irvine, T.N. and Baragar, W.R.A.
1971: A guide to the chemical classification of the common volcanic rocks; Canadian Journal of Earth Sciences, v. 8, p. 523-548

Nadeau, L. and Brouillette, P.
1997: Field relationships and petrology of the Lapeyrère gabbronorite, south-central Grenville Province, Quebec; in Current Research 1997-E; Geological Survey of Canada, p. 61-71

Pearce, J.A.
1996: A user's guide to basalt discrimination diagrams; in Trace Element Geochemistry of Volcanic Rocks: Applications for Massive Sulphide Exploration, (ed.) D.A. Wyman; Geological Association of Canada, short course notes, v. 12, p.79-113

Pearce, J.A. and Cann, J.R.
1973: Tectonic setting of basic volcanic rocks determined using trace element analyses; Earth and Planetary Science Letters, v. 19, p. 290-300

Pearce, J.A. and Parkinson, I.J.
1993: Trace element models for mantle melting: application to volcanic arc petrogenesis; in Magmatic Processes and Plate Tectonics, (ed.) H.M. Prichard, T. Alabaster, N.B.W. Harris, and C.R. Neary; Geological Society Special Publication no. 76, p.373-403

Rivers, T., Martignole, J., Gower, C.F., and Davidson, A.
1989: New tectonic divisions of the Grenville Province, southeast Canadian Shield; Tectonics, v. 8, p. 63-84.

Sun, S.S. and McDonough, W.F.
1989: Chemical and isotopic systematics of oceanic basalts: implications for mantle composition and processes; in Magmatism in the Ocean Basins; (ed.) A.D. Saunders and M.J. Norry; Geological Society Special Publication no. 42, p. 313-345

Wedepohl, K.H.
1995: The composition of the continental crust; Geochimica et Cosmochimica Acta, v. 59, p. 1217-1232.

Weave, B.L. and Tarney, J.
1984: Empirical approach to estimating the composition of the continental crust; Nature, v. 310, p. 575-577

Wilson, M.
1989: Igneous petrogenesis: a global tectonic approach; Unwin Hyman, London, 466 p.
1993: Geochemical signatures of oceanic and continental basalts; a key to mantle dynamics?; Journal of the Geological Society of London, v. 150, p. 977-990.

Geological Survey of Canada Project 920002QN

AUTHOR INDEX

Arnott, R.W.C. 155
Aspler, L.B. 55
(email: cy249@freenet.carleton.ca)
Bashforth, A. 95
Bédard, J. 179
Berrigan, M.E. 1
(email: mberriga@gsc.nrcan.gc.ca)
Bleeker, W. 1, 9
(email: wbleeker@gsc.nrcan.gc.ca)
Bretzlaff, R. 29
Brouillette, P. 179
Chiarenzelli, J.R. 55
(email: chiarenz@oswego.edu)
Cooper, R.V. 1
(email: rcooper@gsc.nrcan.gc.ca)
Corrigan, D. 95
(email: dcorrigan@gsc.nrcan.gc.ca)
Cousens, B.L. 55
(email: bcousens@ccs.carleton.ca)
Currie, K.L. 137, 167, 173
(email: kcurrie@gsc.nrcan.gc.ca)
Davidson, A. 145
Gittins, J. 173
Goff, S.P. 29
Hanmer, S. 77, 85
(email: shanmer@gsc.nrcan.gc.ca)
Hendry, K.A.B. 1
Irwin, D. 67
Jenner, G.A. 29
Kerr, D.E. 21
(email: dkerr@gsc.nrcan.gc.ca)
Kerswill, J.A. 29
(email: jkerswill@gsc.nrcan.gc.ca)
Ketchum, J. 9
Kjarsgaard, B.A. 29
(email: bkjarsga@gsc.nrcan.gc.ca)
Knight, R.D. 21
(email: rknight@gsc.nrcan.gc.ca)
Lucas, S.B. 43, 95
(email: slucas@gsc.nrcan.gc.ca)
MacLachlan, K. 67
Maxeiner, R.O. 95
Mills, A. 67
Nadeau, L. 179
Percival, J.A. 127
(email: joperciv@gsc.nrcan.gc.ca)
Peterson, T.D. 77, 85
(email: tpeterso@gsc.nrcan.gc.ca)
Powis, K.B. 55
Rainbird, R.H. 77, 85
(email: rrainbir@gsc.nrcan.gc.ca)
Relf, C. 67
Roest, W.R. 1
(email: roest@gsc.nrcan.gc.ca)
Russell, H.A.J. 155
(email: hrussell@gsc.nrcan.gc.ca)
Ryan, J.J. 77, 85
Samaras, C. 29
Sanborn-Barrie, M. 115
(email: msanborn@gsc.nrcan.gc.ca)
Sandeman, H.A. 77, 85
(email: hsandema@gsc.nrcan.gc.ca)
Scott, D.J. 43
(email: dscott@gsc.nrcan.gc.ca)
Sharpe, D.R. 155
(email: dsharpe@gsc.nrcan.gc.ca)
Skulski, T. 115
(email: tskulski@gsc.nrcan.gc.ca)
St-Onge, M.R. 43
(email: mstonge@gsc.nrcan.gc.ca)
van Staal, C.R. 107
(email: cvanstaa@gsc.nrcan.gc.ca)
Whalen, J.B. 115
(email: jwhalen@gsc.nrcan.gc.ca)
Wilkinson, L. 29
(email: lwilkin@gsc.nrcan.gc.ca)
Wodicka, N. 43
(email: nwodicka@gsc.nrcan.gc.ca)

NOTE TO CONTRIBUTORS

Submissions to the Discussion section of Current Research are welcome from both the staff of the Geological Survey of Canada and from the public. Discussions are limited to 6 double-spaced typewritten pages (about 1500 words) and are subject to review by the Chief Scientific Editor. Discussions are restricted to the scientific content of Geological Survey reports. General discussions concerning sector or government policy will not be accepted. All manuscripts must be computer word-processed on an IBM compatible system and must be submitted with a diskette using WordPerfect. Illustrations will be accepted only if, in the opinion of the editor, they are considered essential. In any case no redrafting will be undertaken and reproducible copy must accompany the original submissions. Discussion is limited to recent reports (not more than 2 years old) and may be in either English or French. Every effort is made to include both Discussion and Reply in the same issue. Current Research is published in January and July. Submissions should be sent to the Chief Scientific Editor, Geological Survey of Canada, 601 Booth Street, Ottawa K1A 0E8 Canada.

AVIS AUX AUTEURS D'ARTICLES

Nous encourageons tant le personnel de la Commission géologique que le grand public à nous faire parvenir des articles destinés à la section discussion de la publication Recherches en cours. Le texte doit comprendre au plus six pages dactylographiées à double interligne (environ 1500 mots), texte qui peut faire l'objet d'un réexamen par le rédacteur scientifique en chef. Les discussions doivent se limiter au contenu scientifique des rapports de la Commission géologique. Les discussions générales sur le Secteur ou les politiques gouvernementales ne seront pas acceptées. Le texte doit être soumis à un traitement de texte informatisé par un système IBM compatible et enregistré sur disquette WordPerfect. Les illustrations ne seront acceptées que dans la mesure où, selon l'opinion du rédacteur, elles seront considérées comme essentielles. Aucune retouche ne sera faite au texte et dans tous les cas, une copie qui puisse être reproduite doit accompagner le texte original. Les discussions en français ou en anglais doivent se limiter aux rapports récents (au plus de 2 ans). On s'efforcera de faire coïncider les articles destinés aux rubriques discussions et réponses dans le même numéro. La publication Recherches en cours paraît en janvier et en juillet. Les articles doivent être envoyés au rédacteur en chef scientifique, Commission géologique du Canada, 601, rue Booth, Ottawa K1A 0E8 Canada.

Geological Survey of Canada Current Research, is released twice a year, in January and July. The four parts published in January 1998 (Current Research 1998-A to D) are listed below.

Recherches en cours, une publication de la Commission géologique du Canada, est publiée deux fois par année, en janvier et en juillet. Les quatre parties publiées en janvier 1998 (Recherches en cours 1998-A à D) sont énumérées ci-dessous.

Part A:	Cordillera and Pacific Margin
Partie A:	Cordillère et marge du Pacifique
Part B:	Interior Plains and Arctic Canada
Partie B:	Plaines intérieures et région arctique du Canada
Part C:	Canadian Shield
Partie C:	Bouclier canadien
Part D:	Eastern Canada and national and general programs
Partie D:	Est du Canada et programmes nationaux et généraux